Advanced separation techniques for nuclear fuel reprocessing and radioactive waste treatment

Edited by Kenneth L. Nash and Gregg J. Lumetta

Advanced separation techniques for nuclear fuel reprocessing and radioactive waste treatment

Related titles:

Understanding and mitigating ageing in nuclear power plants: Materials and operational aspects of plant life management (PLiM)
(ISBN 978-1-84569-511-8)
Plant life management (PLiM) is a safety-based methodology for the management of nuclear power plants over their entire lifetime. It is used by plant operators and regulators to assess the condition of nuclear power plant, and to establish the technical and economic requirements for safe, long-term operation. This book critically reviews the fundamental ageing–degradation mechanisms that affect nuclear power plant structures, systems and components (SSC), along with relevant analysis and modelling methods and mitigation paths. Coverage of plant maintenance and replacement routes is extended through chapters on the development of advanced materials and components, as well as through reactor-type specific PLiM practices.

Handbook of advanced radioactive waste conditioning technologies
(ISBN 978-1-84569-626-9)
Conditioning technology is essential to the nuclear fuel cycle for the immobilisation and encapsulation of spent nuclear fuels and radioactive wastes, forming the initial engineer barrier required for radioactive waste transportation, storage and disposal. Long-term radiological safety is ensured through the performance and durability of conditioned waste, which advanced conditioning technologies and techniques continue to improve upon. This book provides a comprehensive and systematic reference on advanced radioactive waste conditioning technologies. Coverage includes fundamental science and safety criteria, treatment processes and immobilisation technologies, the development of specific types of waste form materials and systems, and performance and safety analysis.

Geological repository systems for safe disposal of spent nuclear fuels and radioactive waste
(ISBN 978-1-84569-542-2)
The long-term fate of spent nuclear fuel and radioactive waste materials is of critical importance to the nuclear industry. Long-term safety must be assured without active human oversight, based on the requirement that we do not pass the burden of nuclear waste onto future generations. Geological disposal systems and technology, utilising both natural geological barriers and engineered barrier systems, have therefore been developed to isolate spent nuclear fuel and radioactive materials from the human environment. This book critically reviews state-of-the-art technologies, scientific methods and engineering practices directly related to the design, operation and safety of geological repositories.

Details of these and other Woodhead Publishing books can be obtained by:

- visiting our web site at www.woodheadpublishing.com
- contacting Customer Services (e-mail: sales@woodheadpublishing.com; fax: +44 (0) 1223 832819; tel.: +44 (0) 1223 499140 ext. 130; address: Woodhead Publishing Limited, 80 High Street, Sawston, Cambridge CB22 3HJ, UK)

If you would like to receive information on forthcoming titles, please send your address details to: Francis Dodds (address, tel. and fax as above; e-mail: francis. dodds@woodheadpublishing.com). Please confirm which subject areas you are interested in.

Advanced separation techniques for nuclear fuel reprocessing and radioactive waste treatment

Edited by
Kenneth L. Nash and Gregg J. Lumetta

WP

WOODHEAD
PUBLISHING

Oxford   Cambridge   Philadelphia   New Delhi

Contents

v

S. Arm and C. Phillips, EnergySolutions, LLC, USA

S. A. Bryan, T. G. Levitskaia, A. J. Casella,
J. M. Peterson, A. M. Johnsen, A. M. Lines, and
E. M. Thomas, Pacific Northwest National Laboratory,
USA

K. M. Goff, G. L. Fredrickson and D. E. Vaden,
Idaho National Laboratory, USA

(* = main contact)

Editors

Professor Kenneth L. Nash
Chemistry Department
Washington State University
PO Box 644630
Pullman, WA 99164-4630
USA
E-mail: knash@wsu.edu

Dr Gregg J. Lumetta
Pacific Northwest National
    Laboratory
P.O. Box 999, MSIN P7-25
Richland, WA 99352
USA
E-mail: gregg.lumetta@pnl.gov

Chapter 1

Professor Kenneth L. Nash* and
    Jenifer C. Braley
Chemistry Department
Washington State University
PO Box 644630
Pullman, WA 99164-4630
USA
E-mail: knash@wsu.edu

Chapter 2

Dr Alena Paulenova
School of Nuclear Engineering and
    Radiation Sciences
Oregon State University
Corvallis, OR 97331
USA
E-mail: alena.paulenova@
    oregonstate.edu

Chapter 3

Dr S. Arm* and C. Phillips
EnergySolutions, LLC
Suite 240
2345 Stevens Drive
Richland, WA 99354
USA
E-mail: starm@energysolutions.com
cjphillips@energysolutions.com

Chapter 4

Samuel A. Bryan*, Tatiana G. Levitskaia, Amanda J. Casella, James M. Peterson, Amanda M. Johnsen, Amanda M. Lines, and Elizabeth M. Thomas
Pacific Northwest National Laboratory
PO Box 999
MSIN P7-25
Richland, WA 99352
USA
E-mail: Sam.Bryan@pnl.gov
Tatiana.Levitskaia@pnl.gov

Chapter 5

Dr K. Michael Goff*, Guy L. Fredrickson and DeeEarl Vaden
Idaho National Laboratory
Idaho Falls, ID 83415
USA
E-mail: mike.goff@inl.gov
Guy.Fredrickson@inl.gov
DeeEarl.Vaden@inl.gov

Chapter 6

Dr R. Scott Herbst*
Idaho National Laboratory
USA
E-mail: R.Herbst@inl.gov

Dr Pascal Baron
CEA
France
E-mail: baron.pascal@cea.fr

Dr Mikael Nilsson
Department of Chemical Engineering and Materials Science
University of California Irvine
USA
E-mail: nilssonm@uci.edu

Chapter 7

Dr Monica C. Regalbuto
Argonne National Laboratory
9700 South Cass Avenue
Argonne, ILL 60439-4837
USA
E-mail: regalbuto@anl.gov

Chapter 8

Emory D. Collins* and Guillermo D. Del Cul
Nuclear Science and Technology Division
Oak Ridge National Laboratory
One Bethel Valley Road
Oak Ridge, TN 37831-6152
USA
E-mail: collinsed@ornl.gov

Bruce A. Moyer
Chemical Sciences Division
Oak Ridge National Laboratory
One Bethel Valley Road
Oak Ridge, TN 37831-6119
USA

Chapter 9

Dr Valery N. Romanovsky*, Dr
 Igor V. Smirnov, Dr Vasily A.
 Babain and Dr Andrey Y.
 Shadrin
Khlopin Radium Institute
194021, 28
2nd Murinsky Avenue
St. Petersburg
Russia
E-mail: romanovski@khlopin.ru

Chapter 10

Tadafumi Koyama
Central Research Institute of
 Electric Power Industry
2-11-1 Iwado-kita
Komae
Tokyo 201-8511
Japan
E-mail: koyama@criepi.denken.
 or.jp

Chapter 11

Dr Clément Hill
Commissariat à l'Energie
 Atomique
France
E-mail: clement.hill@cea.fr

Chapter 12

Dr Dominique M. Warin
Commissariat à l'Energie
 Atomique et aux Energies
 Alternatives
CEA/Marcoule
Radiochemistry and Processes
 Department
France
E-mail: dominique.warin@cea.fr

Chapter 14

Professor Chien M. Wai
Department of Chemistry
University of Idaho
Moscow, ID 83844
USA
E-mail: cwai@uidaho.edu

Chapter 15

Professor (Evans) M. N. Chirwa
University of Pretoria
South Africa
E-mail: evans.chirwa@up.ac.za

Woodhead Publishing Series in Energy

Preface

As the 21st century unfolds, energy has become a theme underlying many of the challenges facing mankind. There is little doubt that standard of living closely correlates with the availability of energy resources. Raising the global standard of living will require providing power to those who currently do not have it. It is estimated that two billion people do not have access to electricity.[1] This represents 30% of the world population. Providing power to these people, while continuing to satisfy the needs of the developed world, represents an enormous challenge, especially in the face of the threat of global climate change and decreasing availability of "clean" fossil fuels. Fission-based nuclear power will play a vital role in meeting this challenge. Nuclear power provides reliable base-load power with virtually no greenhouse gas emissions (other than those associated with mining and construction operations). This power production technology is well established and has proven to be safe and reliable, although it will be essential to maintain the improvements that have been made in plant operational safety and efficiency over the past several decades. One aspect of nuclear power that still provides significant technical challenges is the management of irradiated nuclear fuel.

For the most part, the United States has pursued a "once through" fuel cycle policy in which the uranium passes once through the power reactor and the irradiated fuel is emplaced intact in a geologic repository. However, no geologic repository has been licensed and this policy is presently being re-evaluated. At present, the fate of irradiated fuel from commercial power production reactors in the US is uncertain. Partial recycling of the irradiated fuel has been practiced in a number of countries (e.g., France, the United Kingdom, Russia, and Japan). These operations allow recycling of fissile uranium and plutonium back into the fuel cycle as mixed oxide (MOx) fuel, but they still result in problematic long-lived transuranic elements in the high-level waste that must be disposed of in a repository. The presence of the transuranic elements in waste placed in a repository requires engineering of the repository to ensure safe performance for hundreds of thousands

of years. Ensuring repository performance over such a large span of time is beyond human experience. Because of this, there has been growing interest in closing the nuclear fuel cycle in a manner that allows long-lived radionuclides to be recycled back into the fuel cycle and thus to have little effect on repository design or performance. Under such scenarios, the integrity of the repository need only be ensured for hundreds of years, a time frame well within the horizon of recorded history.

The subject matter of this book is the separation science and technology underpinning the efforts to manage irradiated nuclear fuel, including an examination of progress towards achieving a closed fuel cycle. The book is organized into three parts. The first part is aimed at providing fundamental scientific and engineering information related to nuclear fuel cycle separations. The second part is devoted to describing standard and advanced technological solutions for application in nuclear fuel cycle separations. The third part reviews emerging and innovative separation and extraction techniques that are being pursued in the development of advanced nuclear fuel cycles.

Part I opens with two chapters summarizing fundamental actinide chemistry as it relates to the separation of these elements and also their behavior in the environment, and the physical and chemical properties of actinides in particular, i.e. the most critical type of element of concern in nuclear fuel reprocessing. This is followed by a chapter describing the nuclear engineering principles as they relate to aqueous separations. Chapters 4 and 5 discuss issues related to monitoring material flow through nuclear separation plants both for the purpose of process monitoring and control, and for safeguarding of special nuclear materials.

Part II of the book begins with Chapter 6 describing well-established technology for separating uranium and plutonium from dissolved irradiated fuel (i.e., the PUREX process). This chapter not only discusses the established PUREX methods, but also describes recent enhancements such as the recovery of a mixed uranium/plutonium product (the COEX™ process) and options for managing neptunium. This is followed by a chapter describing the recent work performed in the US on advanced alternatives to the PUREX process. Chapter 8 describes recent developments in the separation of fission products such as ^{137}Cs and ^{90}Sr from the dissolved irradiated fuel matrix. Taking this a step further, Chapter 9 discusses efforts to develop a single process that can extract and separate a number of radionuclides (actinides and fission products) together.

Part III of the book opens with Chapter 10 describing pyrochemical/electrochemical separations and engineering. Chapter 11 details the quest to design new separation materials that are highly specific for selected fuel components, coverage that is enhanced by Chapter 12, which reviews developments in the partitioning and transmutation of radioactive wastes.

The development of such highly selective separations media would greatly simplify implementation of the separations required for closing the fuel cycle. Finally, the book closes with three chapters that discuss separation methods that are somewhat different from the traditional liquid-liquid extraction methods. Firstly, Chapter 13 discusses the possibility of using solid-phase extraction methods in nuclear fuel separations; secondly, Chapter 14 explores the use of supercritical fluid extraction and ionic liquids in advanced fuel cycle separations; and thirdly, Chapter 15 details biological treatment and bioremediation processes of use in separations science and for the recovery of useful materials from radioactive wastes.

It is our hope that this book will provide a useful reference to scientists and engineers working in the field of nuclear fuel cycle separations. But perhaps more importantly, we hope that it will provide a starting point for the young scientists and engineers who will rise to meet the challenge of safely managing the nuclear fuel cycle in a sustainable manner, enabling safe expansion of this low-carbon means of electrical production to raise mankind's standard of living worldwide in the 21st century.

Finally, the editors and publisher would like to make a special dedication to Dr Troy Tranter, formerly of Idaho National Laboratory, USA, and author of Chapter 13 of this book, who sadly passed away in December 2010.

Reference

1. Rhodes, R.; Beller, D. The Need for Nuclear Power, *Foreign Affairs*, **2000**, 79, 30–44.

Gregg J. Lumetta
Pacific Northwest National Laboratory
P.O. Box 999, MSIN P7–22
Richland, WA 99352
USA
gregg.lumetta@pnl.gov (email)

Kenneth L. Nash
Washington State University
P.O. Box 644630
Pullman, WA 99164–4630
USA
knash@wsu.edu (email)

1

Chemistry of radioactive materials in the nuclear fuel cycle

K. L. NASH and J. C. BRALEY,
Washington State University, USA

Abstract: From the days of the Manhattan Project, the chemistry of actinides and selected fission products has shaped decisions on the handling of irradiated nuclear fuel. This chemistry is characterized by the diversity of the fission products, the rich redox chemistry of the light actinides, high radiation levels, concentrated nitric acid used to dissolve the fuel and the nuclear chemistry of both actinides and fission product lanthanides. This chapter introduces the actinide and fission product chemistry relevant to the nuclear fuel cycle, from the isolation of uranium from mined ores through reprocessing to management of the byproduct wastes. The important features of historically successful solvent extraction separations and alternative chemical processes are described. Finally, the role of nuclear energy as a source of primary power sans greenhouse gases is discussed.

Key words: nuclear fuel, actinide chemistry, solvent extraction, molten salts.

1.1 Introduction

Prior to the 1940s, the only radioactive elements on planet earth were those long-lived enough to have persisted since the condensation of the solar system (primarily $^{235,\ 238}$U, ^{232}Th, ^{40}K, ^{87}Rb), the short-lived isotopes linking actinides to their stable end-member lead or bismuth isotopes (Ra, Rn, Po ...), those created as a result of cosmic radiation in the upper atmosphere (^{36}Cl, ^{32}P, ^{14}C, ^{3}H ...) and the very small amounts of man-made isotopes that had been created in scientific research. That research and the activities of the ensuing Manhattan Project introduced to the terrestrial environment considerable amounts of both short- and long-lived new isotopes, including most significantly kilogram quantities of some transuranium elements. These activities also required the mining and processing of uranium ores, which increased the accessibility of uranium and its radioactive daughters to the biosphere. The subsequent activities of the Cold War increased the terrestrial abundance of some of these elements to thousands of kilograms. During the years of atmospheric testing of nuclear weapons, weapons tests released significant amounts of radioactive debris into the environment.

3

Since the institution of a ban on atmospheric testing of nuclear weapons, the only significant injection of anthropogenic radioactivity into the terrestrial environment occurred in the Chernobyl accident in 1986.

Though nuclear energy was first exploited for plutonium production for military purposes (and was in fact driven by the defense buildup of the Cold War), the production of electricity through the operation of fission reactors began in the early 1960s. The first nuclear reactors designed for electricity production were of a graphite-moderated, gas-cooled design in the United Kingdom. In the US, the first power reactors were designed for use in US Naval ships. The same design ultimately was adapted to stationary applications in water cooled and moderated reactors fueled with partially enriched uranium. The Canadian design utilized natural uranium or slightly enriched fuel with D_2O moderation and cooling. Each design has its advantages and limitations, but all produce a similar array of waste byproducts, hence offer similar constraints on the execution of the fuel cycle.

The use of high purity light water (H_2O) as a neutron moderator and coolant offers several advantages, starting with its reasonable price and favorable thermal properties. In the operation of a light water reactor, enriched uranium (3–5% ^{235}U, 97–95% ^{238}U) is partially consumed with the resulting creation of transuranium elements (in order of decreasing amounts, plutonium (Pu), neptunium (Np), americium (Am) and curium (Cm)), and fission products including varying amounts of all elements in the periodic table between zinc and erbium. The fission products include noble gases, halides, calcogenides, pnictides, geranium, tin, indium, second row transition metals, alkali metals, alkaline earths and about two-thirds of the lanthanide series. Post removal of the fuel from the reactor, the total uranium content is about 95.5% of the non-oxide mass. Plutonium isotopes account for about 0.9% of the heavy metal content. The isotopic distributions for uranium and plutonium post-irradiation are shown in Fig. 1.1. Weapons grade plutonium is defined as material containing at least 93% ^{239}Pu. Reactor grade plutonium is defined as material composed of more than 18% ^{240}Pu. The high
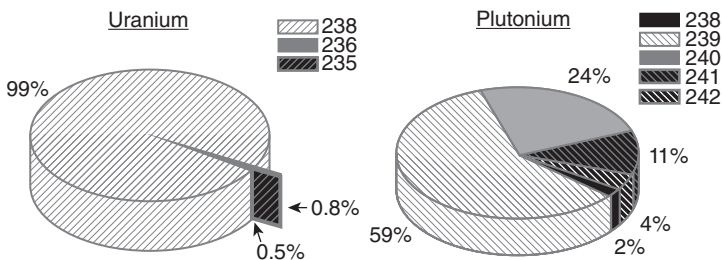
1.1 Isotopic ratios of uranium and plutonium from a light water reactor in used fuel when discharged from reactor.

neutron capture cross-section of ^{240}Pu aids in limiting the utility of plutonium with significant amounts ^{240}Pu from being used in a weapon. At discharge, used fuel also includes about 500 g/ton of ^{237}Np.

Though the mass of used fuel is predominantly uranium, the radioactivity of the actinide component is dominated on discharge by the plutonium and curium isotopes, the former based on mass, the latter on the short half-lives of the isotopes present. Most of these isotopes have longer half-lives than the majority of fission products, hence they tend to dominate the radiotoxicity of used fuel beyond about 500 years after discharge. In storage, the isotopic distribution of actinides in used fuel changes primarily from the decay of ^{242}Cm, ^{244}Cm, ^{241}Pu resulting in an increase in the ^{238}Pu, ^{240}Pu, and ^{241}Am content of the fuel, respectively. Though it represents only a minor component of used fuel on discharge, ^{241}Am content of the used fuel increases substantially as a result of ^{241}Pu decay; the dominant curium isotopes decay away in a relatively short time (resulting in a decrease in the total curies). The total radioactivity arising from the actinide isotopes is about 0.11 MCi/ton at discharge and 0.07 MCi/ton after ten years of decay storage (these figures and all subsequent product information are based on 33,000 MWd/t U burnup at a power density of 30 MW/t U and neutron flux of $2.92*10^{13}$ Ncm^{-2}s^{-1}, as described in [1]). As all actinide isotopes are radioactive, ultimately all decrease in concentration of spent fuel in storage, though clearly the long-lived isotopes decrease slowly. A summation of the radioactive properties of the important actinide isotopes present in used fuel is shown in Table 1.1.

Among the fission products, there are many short-lived and stable species. At discharge, the radioactive materials content of one ton of fuel is about 15 MCi, dominated by small amounts of very short-lived fission products. The most important fission product radionuclides in used fuel after about one year are ^{137}Cs (1230 g/ton of 30.1 year half-life in equilibrium with its radioactive ^{137m}Ba daughter – 0.21 MCi total), ^{90}Sr (543 g/ton of 28.5 year half life in equilibrium with its radioactive ^{90}Y daughter – 0.15 MCi total), ^{99}Tc (841 g/ton of 2.1×10^5 year half-life – 14 Ci total) and ^{129}I (229 g/ton of 1.57×10^7 year half-life – 0.04 Ci total). The latter two isotopes are of greater concern for their potential environmental mobility, their long half-lives and for their bioaccumulation possibilities than the numbers of curies present or the energetic characteristics of their emissions. The cesium/barium and strontium/yttrium isotopes dominate the dose, produce substantial amounts of heat and are the most radiotoxic materials in used fuel from shortly after discharge through several hundred years.

As noted above, rare earth elements are significant byproducts of fission. They represent about 40% of the mass of fission products and including measurable amounts of all lanthanides from lanthanum (La) through erbium (Er) plus moderate amounts of yttrium (Y), which exhibits chemistry similar

Table 1.1 Actinides in used nuclear fuel [1]

Isotope	$t_{1/2(yr)}$	Decay mode	Amount at discharge: g/ton, (Ci/ton)	After 10 years: g/ton, (Ci/ton)	Comment
^{234}U	2.44×10^5	α	122 (0.8)	204 (1.3)	daughter of ^{238}U
^{235}U	7.04×10^8	α	8,000 (0.02)	8,000 (0.02)	fissile
^{236}U	2.34×10^7	α	4,540 (0.29)	4,540 (0.29)	fertile
^{238}U	4.47×10^9	α	942,000 (0.32)	942,000 (0.32)	fertile
^{237}Np	2.14×10^6	α	482 (0.34) (+0.34 from ^{233}Pa)	483 (0.34) (+0.34 from ^{233}Pa)	daughter of ^{241}Am, in eq. With ^{233}Pa
^{238}Pu	87.8	α	84 (1.44×10^3)	88 (1.51×10^3)	daughter of ^{242}Cm
^{239}Pu	2.44×10^4	α	5,260 (3.22×10^2)	5260 (3.22×10^2)	fissile
^{240}Pu	6.54×10^3	α	2,160 (4.92×10^2)	2170 (4.94×10^2)	daughter of ^{244}Cm, parent of ^{236}U
^{241}Pu	14.9	β^-	1,000 (9.96×10^4)	632 (6.29×10^4)	decays to ^{241}Am
^{242}Pu	3.87×10^5	α	350 (1.34)	350 (1.34)	
^{241}Am	433	$\alpha\gamma$	44 (1.5×10^2)	412 (1.40×10^3)	daughter of ^{241}Pu
^{243}Am	7.4×10^3	$\alpha\gamma$	91 (1.81×10^1) (+1.81×10^1 from ^{239}Np)	91 (1.81×10^1) (+1.81×10^1 from ^{239}Np)	
^{242}Cm	0.45	α	6 (1.48×10^3)	0	parent of ^{238}Pu
^{244}Cm	18.1	α	31 (2.51×10^3)	21.2 (1.72×10^3)	parent of ^{240}Pu

to that of the lanthanides. The lanthanide composition of fuel irradiated as described above (33,000 MWd/t U at power density of 30 MW/t U and neutron flux of $2.92*10^{13}$ Ncm^{-2}s^{-1}) is shown in Fig. 1.2. [1] This is an important factor in the used fuel management equation, as several isotopes of these elements have thermal neutron capture cross-sections greater than those of the actinides, hence must be separated to enable any waste management scenario that includes transmutation of actinides by neutron capture. Figure 1.2 also contains the thermal neutron capture cross-sections and resonance integrals for important lanthanides and americium. In a light water reactor, transmutation (by fission) of Am isotopes will be virtually impossible in the presence of lanthanide isotopes. As will be noted below, the separation of fission product lanthanides from actinides can be a challenging obstacle to effective waste management.
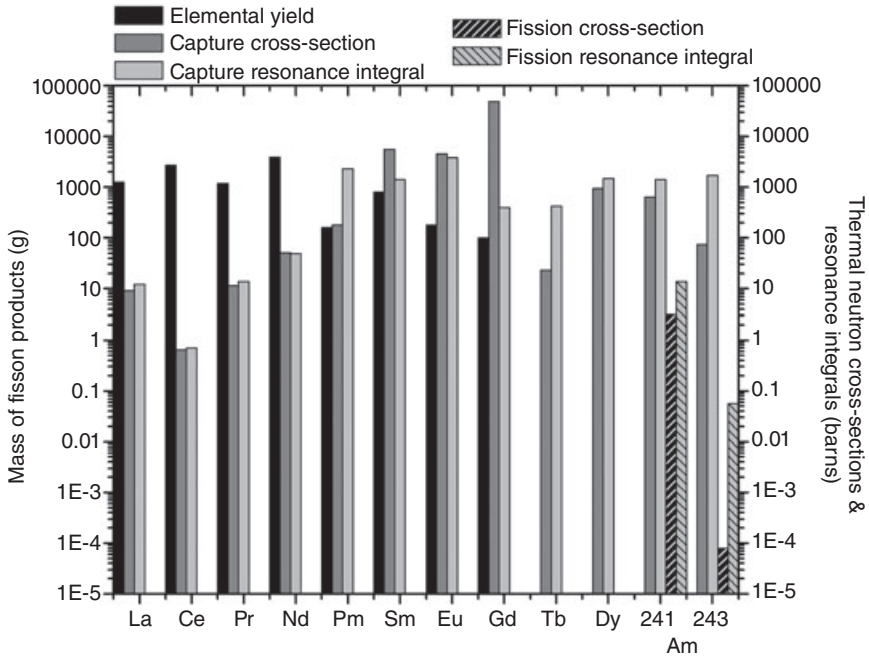
1.2 Significant lanthanide composition of spent fuel by mass after 33,000 MWd/t U burnup at a power density of 30 MW/t U and neutron flux of 2.92 * 10^{13} Ncm^{-2}s^{-1}. The neutron capture cross sections and resonance integrals for americium and additional lanthanides are also shown. [1]

As is true of all electricity production technologies based on fuel consumption, nuclear power systems operate within the framework of a fuel cycle that includes mining and preparation of the fuel, "combustion" with the generation of heat to power generators, and waste management. In a nuclear fuel cycle, uranium is mined, converted and isotopically altered before fuel elements are prepared, assembled into a critical mass and allowed to undergo controlled nuclear fission. Ultimately, the fuel must be replaced with a fresh load of fuel. Unlike power generation based on fossil fuels, the large majority of "waste" byproducts in nuclear fuel are retained within the fuel assemblies in a fission reactor.

Materials considered as waste in used fuel may simply be disposed of as waste (an open fuel cycle), or recycled to recover fuel for reuse and to improve waste management (a closed fuel cycle). Both waste management methods require the accepted use of a geological repository engineered to retain the majority of the most radiotoxic elements for an adequate time to protect the surrounding environment. An open fuel cycle focuses on permanent disposal of the fuel without concern about the additional energy

potential of the irradiated fuel. The closed fuel cycle focuses on recovering additional fuel value through either recycle of plutonium or recovery of fuel value and transmutation of troublesome isotopes. Both cost and complexity increase as additional processing is imposed, but with the advantage of extending the potential life of fuel supplies and a shorter time requirement for geologic isolation. The decision is one whose dimensions are defined by the need for power, supplies of resources, and the limits of safety.

In the following discussion, the basic chemistry that supports the decision-making process for these options will be discussed. The emphasis will be on the solution phase chemistry of actinides and important fission products, the former including uranium, thorium, neptunium, plutonium, americium and curium; the latter, cesium, strontium, iodine, technetium and the lanthanides. The interrelated features of the nuclear and radiochemistry, oxidation-reduction chemistry, solution chemistry (i.e., complexation and hydrolysis) media will be discussed.

1.2   Chemical features of important fission products and actinides

To effectively manage the recycle and disposal of the fission byproducts, the chemistry of the most challenging elements must be addressed in two different stages, during the recycling process (generally solution chemistry) and wastes produced from the recycling process (generally solid-state chemistry). Some nuclear and radiological features have been discussed in the previous section. In this section, the emphasis will be on discussing the essential features of the solution phase and solid-state chemistry of these elements, starting with the lightest, proceeding to the heaviest and emphasizing the aqueous chemistry that is of the greatest significance. The discussions of the chemistry start from the lightest elements to the heaviest.

1.2.1 ^{90}Sr/^{90}Y

Strontium is an alkaline earth element, existing either in the elemental state or as the divalent ion, the latter predominant in consideration of the nuclear fuel cycle. It forms insoluble phosphates and carbonates, is only weakly hydrolyzed, and in generally forms rather weak coordination complexes in aqueous and most organic media. Bonding in coordination compounds of Sr is mostly ionic in nature. Generally, strontium would be expected to follow barium in spent fuel processing and radioactive waste management. The daughter product of ^{90}Sr decay (^{90}Y, $t_{1/2}$ = 2.67 d) quickly comes to radioactive equilibrium with the ^{90}Sr parent and usually behaves chemically like a heavy lanthanide. Yttrium's chemistry will be discussed below with that of the lanthanides

1.2.2 ^{99}Tc

Technetium is a second row transition metal, d^5 in the elemental state, and a chemical analog of manganese. It exists in a multiplicity of oxidation states from +1 through +7 in solution. In the context of nuclear fuel cycle chemistry, the most important oxidations states are the tetra and heptavalent species. The most important Tc(IV) species is $TcO_{2(s)}$. Heptavalent technetium is present as the pertechnetate anion TcO_4^- in solution, chemically analogous to perrhenate (ReO_4^-) or perchlorate (ClO_4^-). In the solid state it exists as Tc_2O_7. Oxides of technetium can be volatilized during used fuel processing or waste glass preparation. Pertechnetate will co-extract with U(VI) in PUREX chemistry, thus potentially "contaminating" the primary product of PUREX extraction. As an anion, TcO_4^- is a species likely to be quite mobile in the environment, in essence able to travel with the solvent front if leaked from an underground storage facility. In the presence of chelating agents, a variety of Tc complexes are formed, as has been reported in selected underground waste tanks at the Hanford Site. [2,3]

1.2.3 ^{129}I

As a halide, iodine also can be found in a variety of oxidation states from −1 through +7. The most important species in used fuel processing and waste management are I^-, I_2 and IO_3^-. Volatility of I_2 is a concern in used fuel processing. In fact, volatilization and capture of the gas during fuel dissolution is a preferred method of isolating iodine in used fuel processing. Though the specific activity of ^{129}I is low, iodine will bioaccumulate in the thyroid (which regulates growth processes in mammals) hence represents a substantial hazard. Fortunately, this bioaccumulation can be reversed by isotopic dilution with natural iodide. Bioaccumulation and the mobility of anions and volatile I_2 are each important drivers for isolation of iodine. In the context of ultimate waste disposal, iodine is also of concern because it is not compatible with most of the solid materials being contemplated for high level waste isolation.

1.2.4 ^{137}Cs/^{137m}Ba

Cesium is the heaviest stable alkali metal, existing under most circumstances relevant to the nuclear fuel cycle as the weakly hydrated cation, Cs^+. As the largest of the un-reactive alkali metal cations, it is weakly hydrated and resistant to the formation of coordination complexes. Size-recognition phenomena have proven the most viable means of manipulating the speciation of Cs^+ for successful separations. Separation procedures have been developed around the use of crown ether or calixarene compounds, typically

large polyether species with molecular cavities designed to accept large cations of low charge. They can be isolated from solution using ion exchange materials, either organic or inorganic in nature. Cs^+ should be relatively mobile in the environment, though this ion is readily taken up by clays and other layered minerals with appropriate interlayer spacing to accept a large cation. Like $^{90}Sr/^{90}Y$, ^{137}Cs and ^{137m}Ba ($t_{1/2} = 2.55$ min) rapidly establish secular radioequilibrium, hence ^{137}Cs is always accompanied by ^{137m}Ba, which decays with a characteristic 661 kev gamma ray to produce stable ^{137}Ba.

1.2.5 Lanthanide fission products

The lanthanides from La through about Er are found in measurable amounts in used nuclear fuel (plus the chemically analogous yttrium), with maximum yields (by mass) of neodymium and cerium. Yttrium behaves chemically very much like a lanthanide and is in fact found in nature in association with lanthanide minerals. These elements exist in solution and in the solid state in the trivalent oxidation state, with the minor exceptions of tetravalent cerium (Ce^{4+}) and divalent europium (Eu^{2+}). Because the valence electrons are placed in relatively constricted 4f valence orbitals, which shield the increasing nuclear charge across the series poorly, the cations decrease in size (by about 20%) from La^{3+} to Lu^{3+}. [4] The bonding in coordination complexes appears to involve minimal covalent interactions. As a result, the coordination geometry of the complexes formed by the ions is usually dictated more by ligand steric constraints, by packing factors (in the solid state), and by rearrangement of the donor atoms in the ligands. In most situations, comparatively simple electrostatic models can be applied to correlate thermodynamic data describing lanthanide interactions with complexing agents or solvent molecules. This aspect of lanthanide chemistry has been discussed in detail by Choppin. [5] These cations are strongly hydrated, but comparatively weakly hydrolyzed, in part because of their comparatively large size (cation radii average about 100 pm). The pK_a values for the Ln^{3+} cations range from about 10 for La^{3+} to 7.8 for Lu^{3+}, with the corresponding pH for precipitation of $Ln(OH)_{3(s)}$ ranging from 7.8 for La^{3+} to about 6.7 for Lu^{3+}. The average primary hydration numbers for La^{3+} through Sm^{3+} are 9, for Gd^{3+} to Lu^{3+} the cations are octahydrates. Europium(III) represents the transition from hydration numbers of 9 to 8, exhibiting an average hydration number of 8.6. These metal ions form moderately stable soluble complexes with a wide variety of complexing agents. Complex stability typically increases across the series, but only occasionally in a linear fashion all of the way across the series. Lanthanide ions form insoluble oxides/hydroxides, fluorides, sulfides, carbonates, and phosphates, though most of these are readily dissolved in acidic solutions.

1.2.6 Actinides

As first suggested by Seaborg, the chemical features of the 5f elements lie between those of the d transition elements and the 4f lanthanides. [6] Certain features of the chemistry of the light members of the series (Ac through Am) bear resemblance to that of the 5d transition metals including the accessibility of a variety of oxidation states, the presence of oxo-ions, and some evidence for covalency in the bonding interactions of the cations with complexing agents. The trans-americium ions exist predominantly in the trivalent oxidation state and resemble in their chemistry the lanthanide ions. Seaborg was recognized with the Nobel Prize for this observation.

Actinium, the namesake of the series, exists only in the trivalent oxidation state in solution, exhibits chemistry similar to that of the lanthanides and transamericium elements, but is otherwise of little significance in the nuclear fuel cycle, except as a component of uranium mill tailings. Selected actinium isotopes could find important applications in nuclear medicine.

Thorium is a primordial element, existing in nature in a single long-lived isotope (^{232}Th) with minor amounts of short lived isotopes ^{234}Th, ^{231}Th, ^{230}Th and ^{228}Th present in thorium and uranium ores as radioactive decay daughters. It exists only in the tetravalent oxidation state (Th^{4+}), forms moderately strong complexes with a variety of chelating agents, is strongly hydrated and more readily hydrolyzed than the lanthanides. It forms insoluble oxides, fluorides and oxalates, and is often found in nature in association with lanthanide phosphate (monazite) ores. Thorium is not important in uranium-fueled nuclear energy systems, but is the fertile parent of ^{233}U in the thorium-uranium breeder reactor system. [7] In the absence of chelating agents, thorium has low mobility in the environment.

Protactinium can be found in solution in two oxidation states, the tetravalent (Pa^{4+}) and pentavalent PaO_2^+. The dioxocation is characterized by a bent O-Pa-O bond (distinguished from the heavier actinides in which the dioxocations are linear) and chemically more closely resembles its 5d congener Ta more strongly than it does its actinide neighbor uranium. The only isotope of Pa that is important in nuclear fuel systems is ^{233}Pa, both as a radioactive decay daughter of ^{237}Np and as an intermediate in the production of ^{233}U from ^{232}Th in the uranium-thorium breeder cycle.

Uranium is also a primordial element, present in native ores as a mix of isotopes (^{234}U, ^{235}U, ^{238}U). Uranium can be found in four oxidation states: trivalent (unstable in air), IV (the predominant species in the solid state), V (prone to disproportionation) and VI (stable and the predominant species found in solution in oxygenated environments). The pentavalent and hexavalent species exist under normal circumstances as substitution-inert linear dioxocations in which coordination chemistry with secondary ligands

is restricted principally to the equatorial region. The hexafluoride of U(VI) (UF_6) is a solid at room temperature, but readily volatilized at slightly elevated temperatures. UF_6 is used in isotope separation to enrich the ^{235}U content to prepare reactor fuel elements. The tetra- and hexavalent cations are moderately hydrated and strongly hydrolyzed, and form strong complexes with a variety of chelating agents. In oxic natural waters containing a representative concentration of dissolved CO_2, carbonate complexes, specifically the triscarbonato complex ion ($UO_2 (CO_3)_3^{4-}$), dominate the speciation of hexavalent uranium.

Neptunium is a man-made actinide that has no natural analog, though features of its chemistry resemble that of uranium and thorium. It can be found in all oxidation states from the tri- to heptavalent. The trivalent state (Np^{3+}) is unstable in water, readily oxidized to the tetravalent oxidation state. The tetravalent state (Np^{4+}) exhibits chemistry similar to that of U^{4+}/Th^{4+}. The pentavalent state (NpO_2^+) is under most circumstances the most redox-stable species, forming comparatively weak complexes with typical chelating agents and somewhat prone to precipitation as double salts with simple anions. The hexavalent state (NpO_2^{2+}) is a moderately strong oxidant exhibiting a general similarity to UO_2^{2+}. Np(VII) is prepared in strongly alkaline solutions, existing as the octahedral oxohydroxo anion ($NpO_4(OH)_2^{3-}$). Np(VII) is a strong oxidant in acidic solutions.

Plutonium is also a man-made actinide that can be prepared in the tri-through heptavalent oxidation states. Pu is unique in the periodic table in that the species Pu^{3+}, Pu^{4+}, PuO_2^+, and PuO_2^{2+} are of comparable redox stability in acidic solutions, thus allowing for the creation of acidic aqueous solutions containing all of these species simultaneously. The middle oxidation states are susceptible to disproportionation, though complexation in general tends to stabilize Pu^{4+} relative to the adjacent species. This feature of plutonium chemistry destabilizes Pu^{3+} in oxygenated ground waters, under which conditions Pu^{4+} is considered most stable in the solid state; in environmental pH aqueous media and in the absence of strong complexants, PuO_2^+ is considered the most stable species in solution. The tetravalent ion is strongly hydrolyzed and susceptible to the formation of hydrolytic polymers in mildly acidic aqueous solutions. Plutonium (III) and Pu^{4+} are the most important species in process chemistry, though PuO_2^{2+} has also been utilized in selected separations. Like Np(VII), heptavalent Pu can be prepared, though higher concentrations of base are needed to stabilize this species than are used for Np(VII).

Americium is the final actinide that can be found in multiple oxidation states in typical aqueous solutions. However, unlike U, Np, and Pu, oxidized Am species are very unstable, being readily reduced on contact with a variety of reducing agents, including organic compounds. Though Am^{3+} dominates the solution chemistry of Am in nuclear fuels processing, some

examples of process development schemes involving oxidized Am species have been suggested. Am (IV) can be stabilized in the solid state as the oxide (AmO_2) but is unstable in simple aqueous solutions.

Actinide ions heavier than Am are mainly stable in the trivalent oxidation state and exhibit chemistry similar to that of the lanthanides, except as noted in the next section. Aside from curium, these elements are unimportant in contemporary nuclear fuel cycles, though increased recycle of plutonium will increase production of Cm, Bk, and Cf isotopes. Each of these species behaves quite similarly to Am^{3+}.

1.2.7 Common features of actinide solution chemistry

Two basic features of actinide solution chemistry create essential and unavoidable complications in the discussion of the chemistry of these elements in the nuclear fuel cycle.

First, all are radioactive, though the specific activities vary over a wide range. The important consequence of this reality is that the chemistry of these species in both aqueous and organic solutions is significantly impacted by the effects of ionizing radiation on the surroundings. In aqueous media, this implies that an overriding consideration will be the effect of hydrogen peroxide (H_2O_2) on the chemistry of these systems. Both oxidizing and reducing radicals are created during the radiolysis of water, hence the redox state of the light actinides is not always reliably predicted by thermodynamic factors alone. In the environment, radiolysis is a very localized phenomenon, of comparatively low importance in actinide solution chemistry, but it cannot be neglected entirely. Regarding used fuel processing, radiolysis is severe with many contributing isotopes. This feature represents a dynamic contribution that, in the end, substantially impacts the accuracy of any predictions based on thermodynamic parameters.

The second complication regards the important need to separate trivalent actinides from fission product lanthanides. The actinides interact more strongly with ligand donor atoms "softer" than oxygen due to a slight enhancement in the covalency of the bonding of the actinides. This feature is exploited in every successful aqueous scheme for the separation of Am^{3+} and Cm^{3+} from lanthanides. This observation was first made by Diamond *et al.* in chloride-based cation exchange separations of the groups. [8]

1.3   Relevant actinide chemistry in the nuclear fuel cycle

Actinide chemistry in the nuclear fuel cycle begins with the extraction of uranium from minerals. The common mineral phases are oxides, carbonates, phosphates, silicates and vanadates. Uranium recovery is typically

accomplished by leaching extracted ore with sulfuric acid (sometimes with the addition of an oxidizing agent), nitric acid, or sodium carbonate after crushing and grinding of the ore. For uranium from basic minerals, precipitation of $Na_2U_2O_7$ is used for purification. From acid leaching processes, solvent extraction with organophosphorus or trialkylamine extraction agents selectively isolates U(VI) from the matrix. The recovered uranium is then stripped with acidic, neutral or basic solutions (depending on the extraction process employed) to allow further purification/processing and recycle of the extractant solution. Uranium can also be recovered from phosphate minerals using a somewhat more complex solvent extraction process. [9] Among the byproducts of environmental concern are mill tailing residues from uranium mining, containing most of the radioactive decay daughter activity, but also residual uranium.

The recovered uranium is then subjected to further processing to convert it to U_3O_8. This uranium is oxidized and converted to the fluoride with F_2, providing UF_6, to allow isotope enrichment. The enriched uranium stream is then sent to fuel fabrication while the residual UF_6 comprising isotopically depleted uranium (>99.7% ^{238}U) is stored for later treatment and disposal. Substantial amounts of such depleted uranium reserves are found in storage at various locations.

To prepare fuel, the enriched UF_6 is hydrolyzed,

$$UF_6 \text{ (g)} + 2\ H_2O \rightarrow UO_2F_2 + 4\ HF \text{ (aq)}$$
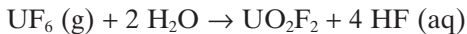
precipitated with ammonia,

$$2\ UO_2F_2 \text{ (aq)} + 6\ NH_4(OH) \text{ (aq)} \rightarrow (HN_4)_2U_2O_7 \text{ (s)} + NH_4F \text{ (aq)} + 3\ H_2O$$
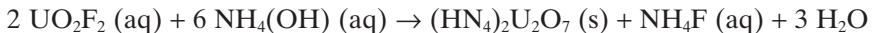
and the ammonium diuranate product reduced with H_2 and converted to UO_2. The "green" UO_2 is pressed and sintered at 1700°C in a dry H_2 atmosphere to give a material with a small oxygen excess (UO_{2+x}). The UO_{2+x} ceramic material is machined to the proper size and shape then "canned" in zirconium (or aluminum) fuel pellets which are used to prepare a fuel assembly. The enriched fuel is then used to create power through sustained fission chain reactions in a reactor, producing the mixture of fission and activation products described above.

In the single pass fuel cycle, the used fuel becomes the waste form upon its discharge from the reactor, ultimately destined for disposal in a geologic repository. As long as the used fuel remains dry and it is not altered through outside intrusion, this material can be expected to remain intact, particularly if the surroundings remain reducing. However, it cannot be ensured that water will *never* contact the waste package. Over the millennia that used fuel will remain radiotoxic, alterations in climate are expected to occur, including (with high probability) periods of wet conditions and of glaciation. When this occurs, alterations and potentially oxidation of the

used fuel should be expected to occur, which ultimately leads to the potential for mobilization of the radioactive materials from the fuel and migration to the biosphere.

The effects of radiation damage to the solid fuel contributes an increased friability of the predominantly UO_2 matrix, resulting ultimately in the conversion of the monolithic ceramic UO_2 to a more readily mobilized powder. Interfacial reactions in the thermal and radiolytic environment will ultimately lead to deterioration of the fuel cladding and eventually to contact between the water and the fuel matrix. At this point, leaching of the fuel components by water can result in the mobilization of radioactive materials from the waste package. The distance traveled by the components from the waste package will be governed by the chemistry of the isotopes, redox conditions, strength of the interactions between the solute components and surrounding mineral surfaces, water flow rate, temperature and radiation field strength.

As noted above, those species with the greatest potential for true solubility have the highest probability for significant migration from the repository. Technetium and iodine are of primary concern, followed by Np (in oxidizing conditions, but not in reducing environments) and Cs. Over time, alteration of the mineral phase or of the fuel matrix can either enhance or retard migration potential. In the case of direct disposal of fuel, the matrix is UO_2. The dissolution of spent fuel releases radioactive material to the water column. Whether waste migrates any substantial distance from the repository will be a complex function of the chemistry of the radionuclides and the nature of the surroundings.

Though such assumptions must be used with caution, the release of radioactive materials from the repository will be generally predicted based on thermodynamic models. Thermodynamic models are considered to be representative, as favorable thermodynamics are a necessary condition for there to be any migration. The validity of such an assumption will depend significantly on the completeness of the model and the ambient conditions. The complexity of the system, with many solid and fluid phase reactions to be taken into account, makes accurate predictions a formidable challenge. In addition, the constant alteration provided by radiolysis, thermal gradients, changes in ground water flow rates and alteration phases ultimately complicate the development of the models and could reduce the validity of thermodynamic model predictions. Colloid transport phenomena are a particular challenge to making accurate predictions of migration potential using thermodynamic modeling due to the substantial variety of colloids that can be created.

A similar range of phenomena and isotopes will be present in high level wastes from reprocessing as practiced today, except for the relative absence of uranium and plutonium isotopes. In a closed loop fuel cycle, uranium is

routed to low or intermediate level waste, plutonium is recycled to the preparation of mixed-oxide fuel (MOX). The matrix of high level waste glass from reprocessing is in most cases borosilicate glass, hence the leaching characteristics and mineral alteration products are expected to be different from fuel stored in cladding. For high level reprocessing wastes, the outer container is a welded stainless steel can (as opposed to zircalloy fuel cladding in direct disposal of fuel). In any disposal scenario, the tendency for radionuclides to migrate from the point of emplacement is dependent on the ambient conditions including temperature, water flow rate and redox conditions plus the contribution of engineered backfill materials. For actinide ions in general, it is expected that they should remain largely in the repository environment if the conditions remain reducing and intrusions are limited. The primary mechanism for long distance displacement that can be envisioned for most metallic radioactive species is probably colloid transport; ionic species of low charge (Cs^+, Rb^+, TcO_4^-, I^-, Br^-) would be expected to manifest significantly greater mobility and to transport as simple ions.

1.4　　Essential features of solvent extraction separations in the nuclear fuel cycle

Most effective separations are based on the phase transfer of the species of interest away from a diverse mixture. Distillation and precipitation are two examples of practical applications of phase transfer in separations. In solvent extraction, partitioning of the species of interest between two immiscible liquids is employed to accomplish the desired separation. Commonly used in organic chemistry, the difference in solubility of the selected species between the immiscible fluids forms the basis for the separation (Nernst partitioning). For metal ion separations, more complex interactions are typically required. The specific features of the application of both solvent extraction and pyrometallurgy (molten salts/molten metals) to the processing of used nuclear fuel have been discussed in detail elsewhere. [10]

Owing to the substantial differences in the polarity of the aqueous and organic solutions, there is, in general, minimal tendency for metal ions or their electroneutral salts to spontaneously partition into nonpolar media (like kerosene), particularly for polyvalent metal ions, which tend to have substantial hydration energies. For the transfer of metal ions or their polar salts into non-polar medium to occur, the presence of amphiphilic (featuring polar and non-polar regions, like surfactants) molecules is necessary. Such molecules can (and often do) aggregate in the bulk organic solutions to improve their compatibility with the typically low dielectric constant medium.

These same molecules tend, at the same time, to arrange themselves at the polar–non-polar fluid interface with the polar end penetrating significantly into the aqueous solution while the lipophilic portion of the molecule remains firmly in the organic side of the interface. If the interaction of the polar end of the extractant molecule with the cation is strong enough, it promotes dehydration of the metal cation, resulting in a substantial increase in entropy for the biphasic system, which can drive the phase transfer process. The extractant molecule can either simultaneously transfer a more weakly hydrated cation to the organic phase or facilitate the re-solvation of the anion needed to accompany the cation into the organic solution. Typically, once this interfacial transfer reaction is completed, the nascent metal complex completes the transfer to the bulk by completing the dehydration through selective solvation (or chelation) by lipophilic molecules present in the organic phase.

Two primary procedures for cation partitioning are possible: cation exchange or solvation of metal salts. The latter process can also exhibit considerable ability to support the partitioning of mineral acids into the organic phase. Under most circumstances in the processing of dissolved used fuel solutions, acidic conditions are maintained (to minimize the possibility for hydrolysis and precipitation of metal hydroxides). In some systems, the application of salting out agents has been required for efficient phase transfer. Under these conditions, the primary cation exchange reaction will involve H^+ exchange. A general example of the cation exchange reaction is:

$$M^{3+}_{aq} + 3\ HL_{org} = ML_{3org} + 3\ H^+_{aq}$$
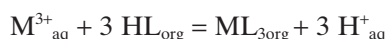
The alternative reaction of partitioning an electroneutral salt could be defined as,

$$M^{3+}_{aq} + 3\ X^-_{aq} + 2\ Y_{org} = MX_3Y_{2org}$$
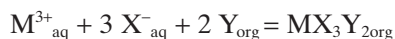
where X is the supporting anion in the aqueous phase and Y is the solvating extractant. A third process related to the ion solvation method arises in extraction systems based on the use of lipophilic tertiary amine or quaternary ammonium compounds, in which an anionic metal solvate coordination compound is extracted,

$$M^{3+}_{aq} + 4\ X^-_{aq} + HY^+_{org} = MX_4^- HY^+_{org}$$

The energetic details and kinetics of these systems can be quite different and selectivity can arise from a variety of different interactions.

Selectivity of solvent extraction processes can be altered through the introduction of water-soluble chelating agents. Complex equilibria can control these processes and multiple interactions between species in each phase are possible. Selectivity can arise from the nature of the extracting agent, the anions co-extracted by solvating or anion exchange reagents, the

chelating agents present in the aqueous phase or by changing the oxidation state of the extracted species relative to that of competing matrix ions. In many cases, classical solution chemistry provides useful guidance to the prediction of process efficiency, though supramolecular organization of solute or solvent molecules and the mutual miscibility of aqueous and organic phases can further alter system performance.

Solid-liquid separations based on organic or inorganic ion exchange materials can also be (and have been) employed as an alternative or complement to solvent extraction. In some instances, anion exchange has also proven an acceptable mode for conducting separations of nuclear materials. An advantage that accrues from the application of chromatographic methods like ion exchange is the large numbers of theoretical plates that can be achieved in such separations when conducted in column mode. If solvent extraction reagents are immobilized on solid support materials (extraction chromatography), the selectivity advantages and flexibility of solvent extraction can be augmented with multiplicity of re-equilibrations of chromatography. These solid-liquid separation methods have one particular limitation in the context of operating closed-loop fuel cycles in their batch-wise mode of operation, which differs from the continuous (or nearly so) operation that is possible in solvent extraction. Devices that employ easily replaceable ion exchange cartridges have been developed, though their application in a processing canyon (where remote operation and maintenance is required) might offer unique challenges in operations. In principle, solvent impregnated membranes could also be operated in a semi-continuous mode, though research to date on such methods applied to metal ion separations processes has revealed issues with the stability for membranes and the kinetics of mass transfer.

1.4.1 Multiphase formation in solvent extraction

In the operation of solvent extraction systems in the laboratory, where new reagents and processes are typically developed, conditions are typically maintained in a moderately idealized state. In particular, the effects of "loading", i.e., contacting aqueous solutions containing high concentrations of metal ions with extractant solutions targeting those metal ions, are typically not investigated until an advanced stage of process development is approached. In this limit, deviations from ideality are often observed. For example, a UO_2^{2+} extraction reaction having the following ideal stoichiometry,

$$UO_2^{2+} + 2\ NO_3^- + 2\ Ex = UO_2(NO_3)_2Ex_2$$

might adhere to this ideal stoichiometry through some range of concentrations, or more appropriately up to a solubility limit in the organic phase. At

higher concentrations of metal ions, the extraction stoichiometry might drop to

$$UO_2^{2+} + 2\ NO_3^- + 1\ Ex = UO_2(NO_3)_2 Ex$$

While the metal ion continues to partition, the possibility solute-molecule reorganization in the organic phase can occur leading to precipitation or to the separation of a third liquid phase (third phase formation).

In this metastable (though typically reversible) condition, the aqueous phase retains much of its essential character, while the organic phase will split into solute-poor (mainly diluent) and solute-rich (mainly extracted metal complex and excess extractant molecules) phases. This condition is at best an annoyance as a source of process upset and at worst a serious safety hazard in the operation of a reprocessing facility, as the unintentional formation of a critical mass of fissile material can occur with potentially disastrous consequences. Such phenomena are well known in solvent extraction of metal ions and mineral acids. The minimization of the potential for such an event to occur is addressed through appropriate alteration of diluent structures and mixtures of diluents, effective extractant design or by carefully designing process monitoring and control procedures to prevent overloading of extractant solutions. Recent research being conducted in the US and in particular in Europe have provided unique insights into the nature and driving force for such interactions. In the design of any facility or process that incorporates fissile materials, it is quite important to always consider these possibilities.

1.5　Behavior in molten salts/molten metals/ionic liquids/alternative media

In advanced fuel cycles, it is likely that fast spectrum, high temperature reactors will be utilized to transmute actinide isotopes that are inefficiently transmuted in light water moderated reactors. Many such reactors will utilize metallic fuels and electrometallurgical processing might become a practical alternative to aqueous processing methods like solvent extraction and ion exchange. The solution chemistry of actinides and fission products is significantly different in the molten salt/molten metal media used for such processing.

Dry processing (pyrometallurgy) has historically found use in electrolytic production of some metallic products, notably for refining very electropositive elements and strong reducing agents like alkali metals. Potassium and sodium metals were first prepared in 1807 by using melt electrolysis of respectively potash and soda. [11,12] Today melt electrolysis (alkali chloride) remains the only process for production of metallic sodium or lithium. Molten salt refining is also appropriate for aluminum, which is obtained by

electrolytic decomposition of aluminum oxide in molten cryolite (Hall-Héroult process). [13]

Pyrochemical processing involves dry chemical reactions at high temperature where reactions occur in solid, liquid and gas phases. Oxidation-reduction, volatilization (of halide or metal), slagging (melt refining, molten salt extraction, carbide slagging), liquid metal (melt refining, liquid metal extraction, liquation, precipitation), and electrolytic processes are the most common types. Implicit in this chemistry is the requirement of conducting separations operations when the metals or metal salts are in a fluid condition, which typically occurs only at moderate to high temperatures. A sub-category of such media are the so-called room temperature ionic liquids (RTILs) which by convention form molten salts below 100°C. This new category of materials would appear to offer the greatest promise for electrometallurgical partitioning, but is still quite new, thus most important details of metal ion coordination chemistry in these media are unknown.

Pyrometallurgy operates in a quite different manner from solvent extraction. Such dry processing offers some advantages, but also suffers limitations. The first significant attempts at actinide metal production in molten salts started with the Manhattan Project in the 1940s. [14] Significantly, Kolodney confirmed that uranium and plutonium could be electrodeposited from molten chlorides. [15] The literature on U and Pu electrorefining in molten salts has been reviewed by Willit *et al*. [16] Basic chemistry and technologies developed in Russia have been described by Bychkov and Skiba. [17] Molten alkali and alkaline-earth chlorides have been most extensively studied for plutonium conversion and separation. Three processes are in use thorough the world at significant scale-up: (i) DOR process (direct oxide reduction) which consists in PuO_2 reduction by calcium in Ca-based chloride salt, (ii) MSE process (molten salt extraction) for [241]Am removal from weapon-grade plutonium by $MgCl_2$ in alkali chloride salt, (iii) ER process (electrorefining) for high plutonium purification using molten alkali and/or alkaline earth chloride electrolyte. [18]

1.6   Interactions at interfaces significant to the nuclear fuel cycle

Interactions that occur at phase boundaries (in particular, liquid–liquid interfaces in solvent extraction, solid–liquid interfaces in used fuel dissolution, in the environment, in electrometallurgy and in the cleanup of wastes at the former nuclear weapons complex) by definition control the rates of materials transfer which in turn often governs the efficiency of the separation process. In solid-liquid separation systems, molecular motions on the solid side of the interface are generally limited while the fluid phase motions are quite dynamic. In liquid–liquid interfaces, both sides of the interface are

in a state of dynamic movement. At the interface, solute and solvent molecules reorder their relative structures to facilitate phase transfer. In solvent extraction, surface active molecules arrange themselves to assist in the transfer of polar species into the less polar regime represented by the organic phase. The organization of these molecules at the interface controls the rate of mass transfer. Such systems have been investigated, but the necessity of probing a dynamic interfacial zone of with dimensions of only a few molecular diameters hinders a complete understanding. Computational modeling studies have attempted to create a rational framework for advancing understanding of interfacial interactions, but progress is slow.

1.7   Future trends

At the beginning to the 21st century, the emergence of rapid modernization in the economies of China, India, Russia and Brazil, together representing a bit more than 30% of the global population, has increased demands for new supplies of energy. In addition, it is recognized that geometric growth of the human population on the planet could result in a 40% increase in the global population by 2050. Further, either depletion of fossil carbon resources or alteration of the global climate due to CO_2 emissions will also bring additional pressures for new power sources that do not emit substantial quantities of greenhouse gases. These factors taken together would appear to be primary drivers for a projected expansion of the effective utilization of existing energy sources.

The single pass nuclear fuel cycle, practiced by about two-thirds of the nuclear power generating economies globally, is quite wasteful of this resource, extracting only a few percent of the energy potential of uranium (and for the moment almost none of the energy potential of thorium). At present usage levels and patterns, it is estimated there is approximately a 50 year supply of uranium available in economically recoverable mineral resources. With the application of enhanced recovery systems for uranium mineral resources, this supply could be extended (with current usage patterns) to about 250 years. If the nuclear component of global energy production grows (as many are projecting), these estimates are far too optimistic. It will become increasingly important to more efficiently utilize this resource through the recycle of plutonium; first to light water reactors and ultimately to a fleet of fast spectrum reactors that are capable of "burning" actinides that do not readily undergo fission in light water reactors. This will require recycling and fabrication of fuels containing a larger proportion of heavier actinide isotopes. Another advantage gained by more extensive recycle of actinides for power production will be the potential for eliminating (or at least reducing the amount of) long lived radiotoxic actinides like Am, thus improving the viability of any geologic repositories that are constructed.

To further extend the potential of this resource, it makes sense to consider the potential (an effort for the moment being led by India) of the thorium-uranium breeder reactor cycle. As thorium is three to four times more abundant than uranium, the viability of fission powered electricity is further extended by taking this step.

1.8   References

1. Choppin, G.R., Rydberg, J., Liljenzin, J.O. *Nuclear Chemistry: Theory and Applications, First Edition* Oxford [Eng.]; New York: Pergamon Press, 1980 Appendix H, pp. 593–599.
2. Chamberlin, R.M., Ashley, K.R., Ball, J.R., Bauer, E., Bernard, J.G., Berning, D.E., Schroeder, N.C., Sylvester, P. *Radioanalytical Methods in the Discovery and Characterization of Non-pertechnetate (^{99}Tc) Species in Hanford Tank Wastes.* ACS Symposium Series (2004), 868 (Radioanalytical Methods in Interdisciplinary Research), 177–192.
3. Lukens, W.W., Shuh, D.K., Schroeder, N.C., Ashley, K.R. *Behavior of Technetium in Alkaline Solution: Identification of Non-pertechnetate Species in High-level Nuclear Waste Tanks at the Hanford Reservation.* ACS Symposium Series (2006), 943 (Nuclear Waste Management), 302–318.
4. Shannon, R.D., Prewitt, R.C.T. *Acta Crystallogr*. 1969 B25, 925.
5. Choppin, G.R. *J. Less Common Met.* 1984 100, 141
6. Seaborg, G.T., *Chem. Eng. News* 1945 23, 2192.
7. Sherrington, L. *Handbook of Solvent Extraction*; Lo, T.C., Baird, M.H.I., Hansen, C. Eds. John Wiley and Sons: New York, 1981, Chapter 25.6.
8. Diamond, R.M., Street, K., Jr., Seaborg, G.T., *J. Am. Chem. Soc.* 1954 76, 1461.
9. Musikas, C., Shulz, W.W. In *Principles and Practices of Solvent Extraction*; Rydberg, J., Musikas, C., Choppin, G.R., Eds. Marcel Dekker: New York, 1992, Chapter 11.
10. Nash, K.L., Madic, C., Mathur, J.N. and Lacquemont, J. Chapter 24: Actinide Separation Science and Technology in *The Chemistry of Actinides and Transactinide Elements*, Morss, L.R., Katz, J.J., Edelstein, N., Fuger, J., editors (International collaborative three volume summary of the current state of the art in actinide science and technology) (2004) pp. 2622–2798.
11. Davy, H. (1808) *Philosophical Transactions of the Royal Society*.
12. Siegfried, R. The Discovery of Potassium and Sodium, and the Problem of the Chemical Elements. *Isis* 1963 54, 247.
13. Grjotheim, K., Krohn, C., Malinovsky, M., Matiasovsky, K., Thonstad, J. *Aluminum Electrolysis: Fundamentals of the Hall-Heroult Process.* 2nd edn, 1982, 446.
14. Rhodes, R. *The Making of the Atomic Bomb.* New York: Simon & Shuster. 1986.
15. Kolodney, M. *J. Electrochem. Soc.* 1982 129, 2438.
16. Willit, J.L., Miller, W.E., Battles, J.E. *J. Nucl. Mater.* 1992 195, 229.
17. Bychkov, A.V., Skiba, O.V. *NATO Science Series, Series 2: Environmental Security*. 1999, 53 (Chemical Separation Technologies and Related Methods of Nuclear Waste Management), 71.
18. Moser, W.S., Navratil, J.D. 1983 *Review of Major Plutonium Pyrotechnical Technology*, Rocky Flats Plant Report RFP-3686.

2

Physical and chemical properties of actinides in nuclear fuel reprocessing

A. PAULENOVA, Oregon State University, USA

Abstract: This chapter provides a short insight into multifaceted chemistry of actinides. The chapter first reviews the unique features of the f-block elements and compares the lanthanide and actinide transition series. The chapter then discusses the coordination chemistry of actinides with hard- and soft-donor ligands, hydrolysis, redox reactions, and radiation effects. Kinetic and thermodynamic aspects of solution chemistry of actinides and their effect on their separation behaviour are discussed.

Key words: reactivity, speciation, complexation, disproportionation, radiolysis.

2.1   Introduction

There are more than 400 operating nuclear reactors around the world. They produce about 15% of the world's electricity, almost 24% of electricity in OECD countries, and 34% in the European Union (WNA, 2010). Nuclear power is the most environmentally benign way of producing electricity on a large scale. Without it most of the world would have to rely almost entirely on fossil fuels for a continuous, reliable supply of electricity. The use of electricity is continuously increasing; it is expected that global electricity demand will double from 2004 to 2030. It is also likely that the fraction of nuclear energy in the total energy produced will increase; therefore, it is essential that the expected need for increased supplies of nuclear fuel be addressed.

One of the unique characteristics of nuclear energy is that used fuel may be reprocessed to recover fissile and fertile materials to provide fresh fuel for existing and future nuclear power plants. Several European countries, Russia, and Japan have a policy of reprocessing used nuclear fuel, although government policies in many other countries have not yet addressed the various aspects of reprocessing (WNA, 2010). As early as the Manhattan Project (when the idea of reprocessing and closing the fuel cycle was first expressed), the principal motivation was the recovery of unfissioned uranium and plutonium from the used fuel elements. Such recycling results in some 25% more energy from the original amount of uranium in the

process, thus contributing to energy security. A second reason for reprocessing of used fuel is to reduce the volume of material to be disposed of as high-level waste to about one fifth of the volume of waste at discharge from the reactor. At the same time its radioactivity level is decreased such that after about 100 years the activity decreases much more rapidly than in used fuel itself (WNA, 2010). At the moment, only a few countries are reprocessing LWR used fuel (France, UK, Russia, and Japan) and other reactor fuel (India), with the largest reprocessing capacity existing in France at La Hague (WNA, 2010).

This multistep technology, spanning from mining, conversion, enrichment, fuel fabrication, burning during reactor operation, storage of irradiated fuel, reprocessing (separation, recycling), to conversion into a stable waste form and final disposal involves a highly sophisticated array of many chemical transformation processes. The chemistry of the nuclear fuel cycle is an example of interdisciplinary applied science; it demands a combination of inorganic, coordination, and environmental chemistry of actinides (and fission products). The chemistry of reprocessing is quite complex and includes many aspects of fundamental inorganic and physical chemistry: Complexation (coordination), redox reaction (thermodynamics and kinetics), acid-base equilibria, hydrolysis, and so on. The coordination chemistry of actinides with both hard- and soft-donor ligands plays a crucial role through the entire nuclear fuel cycle.

This chapter will provide a review of selected chemical and physicochemical properties of the actinide elements, their typical compounds and their ions in aqueous solutions. The f-block elements have many unique features, and comparison of similar species of the lanthanide and actinide transition series provides valuable insights into the chemistry of both series.

Since Mendeleyev's development of the modern concept of periodicity of elements, the table of elements has significantly changed. Numerous experiments confirmed the position of actinides in the periodic table as a 5f series of elements, first proposed by G. T. Seaborg (Seaborg *et al.*, 1949, pp. 1492–1524, 1978). Chemical behavior and electronic structural evidence established the actinides (Ac–Lr; atomic numbers $Z = 89$–103) as an inner transition series with actinium as the first member, analogous to the lanthanide transition series (La–Lu; $Z = 57$–71). Electronic configuration of elements may be significantly different in the gaseous atoms, in ions in solutions or solids, and in the metallic state. Comparing the electronic structures of lanthanides and actinides (Table 2.1), it can be seen that in the Ln^{3+} ions, 14 4f electrons are added in the sequence beginning with cerium ($Z = 58$). In the An-series, the addition of 14 5f electrons in the sequence from thorium ($Z = 90$) to lawrencium ($Z = 103$) is not as regular as in 4f series. While protactinium metal displays 5f electron character, as is expected for

Table 2.1 Electronic configurations of gaseous atoms of f-block elements (Edelstein, 2006)

Ln	Z	(Xe core)	An	Z	(Ra core)
La	57	$5d6s^2$	Ac	89	$6d\,7s^2$
Ce	58	$4f\,5d6s^2$	Th	90	$6d^27s^2$
Pr	59	$4f^36s^2$	Pa	91	$5f^26d7s^2$
Nd	60	$4f^46s^2$	U	92	$5f^36d7\,s^2$
Sm	61	$4f^56s^2$	Np	93	$5f^46d7s^2$
Pm	62	$4f^66s^2$	Pu	94	$5f^67s^2$
Eu	63	$4f^76s^2$	Am	95	$5f^77s^2$
Gd	64	$4f^75d6s^2$	Cm	96	$5f^76d7s^2$
Tb	65	$4f^96s^2$	Bk	97	$5f^97s^2$
Ho	66	$4f^{10}6s^2$	Cf	98	$5f^{10}7s^2$
Dy	67	$4f^{11}6s^2$	Es	99	$5f^{11}7s^2$
Er	68	$4f^{12}6s^2$	Fm	100	$5f^{12}7s^2$
Tm	69	$4f^{13}6s^2$	Md	101	$5f^{13}7s^2$
Yb	70	$4f^{14}6s^2$	No	102	$5f^{14}7s^2$
Lu	71	$4f^{14}5d6s^2$	Lr	103	$5f^{14}6d7s^2$ or $5f^{14}7s^27p$

the third member of an actinide series (Zachariasen, 1973; Fournier, 1976; Haire *et al.*, 2003), no compelling evidence exists to show that thorium metal, or thorium ions in solution or in any of its well-defined compounds, contain 5f electrons (Edelstein, 2006).

Both the similarities in and the differences between the actinide and lanthanide series have had great heuristic value in actinide element research (Edelstein, 2006). The metallic (zero valent) and 3+ ionic forms with half-filled f-electron shells, are of special interest because of the enhanced stability of this particular electron configuration. For example, curium ($Z = 96$) has seven 5f electrons in the elemental form and the 3+ oxidation state and magnetic, optical, and chemical properties that are remarkably similar to those of gadolinium ($Z = 64$) with seven 4f electrons.

The principal differences between the two transition series arise largely from the lower binding energies and less effective shielding by outer electrons of 5f as compared to 4f electrons. The 4f orbitals of lanthanides are deeply buried and completely screened by 5s and 5p electrons that causes 4f electrons to have limited importance in chemical bonding. The trivalent oxidation state is the most stable because it is formed by ionization of two 5s and one 5p electrons. On the other hand, the 5f orbitals have greater spatial extension, and penetrate the core. The energy differences between the 5f, 6d, 7s and 7p orbitals are relatively small; hence, multiple oxidation state are possible, and covalent bonding interaction with other atoms is possible.

2.2 Thermodynamic properties of compounds

In solutions, all 15 Ln-elements from La to Lu have a common 3+ oxidation state in which they behave chemically in a very similar manner, making their separation very difficult. Only Ce has a strongly oxidizing (but kinetically stable) tetravalent oxidation state. Uncommon divalent species of lanthanides (Morss, 1976, Hitchcock, 2008), can be prepared in dilute solution (or solid state) either by gamma irradiation, metallic reduction with alkaline earth metal or electrolysis; only Eu(II) demonstrates appreciable stability.

It is evident that the oxidation states of actinides in solutions are far more variable than those of the lanthanides, particularly in the first half of the series. Multiple oxidation states for the actinide ions are guaranteed by a close proximity of the energy levels of the 7s, 6d, and 5f electrons (Edelstein 2006). The rich chemistry of lighter actinides, from Pa to Am, due to their multiple oxidation states, hydrolytic behavior of their cations and strong coordination of organic ligands, is the most complex and intricate among all elements in the periodic table.

A summary of the oxidation states of actinides is shown in Table 2.2. The bold text indicates the most stable species. The most unstable oxidation states can be produced as transient species in solution by pulse radiolysis (Sullivan *et al.*, 1976a,b, 1982; Gordon *et al.*, 1978). They can also be stabilized by structural restrictions imposed in some of their solid coordination compounds (Albrecht-Schmitt, 2008, Edelman, 2006). All actinide divalent species (except for No) are of only transient stability, having only been observed in pulse radiolysis studies; Am(II), Cm(II), and Cf(II) have half-lives of the order of 5–20 ms. While trivalent species are typical for the transplutonium actinides, the lighter actinides are less stable in trivalent oxidation state – in acidic solutions, U(III) is oxidized by water, Np(III) is oxidized by dissolved oxygen in water, Pu(III) is stable, but easily oxidized to Pu(IV) by a variety of mild oxidants. Thorium and protactinium do not

Table 2.2 The oxidation states of the actinide elements. The most stable species are in **bold**, unstable are in *italic,* claimed but not important are in () (Edelstein, 2006)

Z	89	90	91	92	93	94	95	96	97	98	99	100	101	102	103
Element	Ac	Th	Pa	U	Np	Pu	Am	Cm	Bk	Cf	Es	Fm	Md	No	Lr
Oxidation state	**3**	*2*	*3*	3	3	3	*2*	**3**	**3**	*2*	*2*	2	2	2	**3**
		3	4	4	4	**4**	**3**	4	4	**3**	**3**	**3**	**3**	**3**	
		4	5	5	5	5	4	(5)		(4)	(4)				
				6	6	6	5	(6)							
					7	7	6								
						(8)	(7)								

even exhibit the trivalent state in solutions. Stable Th(III) has been reported only in organometalic compounds (Blake *et al.*, 2001).

The tetravalent species also can be considered transient, since a stable 4+ state is observed only for elements from thorium through plutonium and for berkelium. Tetravalent Am in aqueous media can be stabilized by very strong complexing agents like carbonate, phosphate or fluoride. If Am can be stabilized (even as a transient) in its various upper oxidation states, unique options are available for potential Am/Ln group separations (Nash, 2008; 2009). The quantitative oxidation of trivalent americium to the tetravalent state can be accomplished by strong oxidants using complexants such as lacunary heteropolyanions tungstophosphate and tungstosilicate which are specific for tetravalent species (Donnet *et al.*, 1998). Since tungstosilicate is a stronger complexing agent towards Am than tungstophosphate, quantitative generation of Am(VI) is possible with both polyanions. Nevertheless, it is easier to obtain Am(IV) with the tungstosilicate and easier to reach Am(VI) with tungstophosphate.

The 5+ oxidation state is well established for the elements protactinium through americium, and the 6+ state in the elements uranium through americium. The 4+ state in curium is confined to a few solid compounds, particularly CmO_2 and CmF_4, and appears to be present in a stable complex ion that exists in concentrated cesium fluoride solution. The Cf(IV) state is limited to the solid compounds CfO_2, CfF_4, a complex oxide $BaCfO_3$, and in tungstophosphate solutions; the oxidation of Cf(III) to Cf(IV) in strong carbonate solutions is a disputed topic (Frenkel *et al.*, 1986).

The 2+ oxidation state first appears at americium in a few solid compounds and then at californium in the second half of the series. The II oxidation state becomes increasingly stable in proceeding to nobelium. Md(II) and No(II) have been observed in aqueous solution and this appears to be the most stable oxidation state for nobelium. Am(II) has not only been encountered in solid compounds, but also in electrochemical and pulse radiolysis experiments in acetonitrile solution. The formation of Bk(IV) is associated with enhanced stability of the half-filled 5f configuration (5f7), and the No(II) state reflects the stability of the full 5f shell (5f14). The increase in the stability of the lower oxidation states of the heavier actinide elements relative to the lanthanides may be the result of stronger binding of the 5f (and 6d) electrons in the elements near the heavy end of the actinide series.

2.3   Speciation, complexation and reactivity in solution of actinides

The solution chemistry of the actinide elements has been investigated in both aqueous and selected organic solutions. The majority of the information available describes species found in aqueous solutions. Although

Table 2.3 Colors of actinide ions in aqueous solution (Edelstein, 2006)

Element	M^{3+}	M^{4+}	MO_2^+	MO_2^{2+}	$MO_4(OH)_2^{3-}$ (alkaline solution)
Actinium	Colorless				
Thorium		Colorless			
Protactinium		Colorless	Colorless		
Uranium	Red	Green	Unknown	Yellow	
Neptunium	Blue to purple	Yellow-green	Green	Pink to red	Dark green
Plutonium	Blue to violet	Tan to orange	Reddish-purple	Yellow to	Dark green
Americium	Pink or yellow	Unknown	Yellow	Rum-colored	
Curium	Pale green	Unknown			
Berkelium	Green	Yellow			
Californium	Green				

actinide cations can exist in a variety of oxidation states (2+ to 7+) in aqueous solution (Table 2.2), the most common for light actinides in aqueous acidic solutions are trivalent, tetravalent, pentavalent and hexavalent oxidation states. The stability of a particular oxidation state across the actinide series is quite variable, and for some actinides (Np, Pu) several oxidation states can coexist in the same solution. This is most evident for plutonium as there are small differences in the reduction potentials of Pu(III), Pu(IV), Pu(V), and Pu(VI) over a range of pH values (Choppin, Jensen, 2006).

2.3.1   Redox chemistry of actinides in solutions

The oxidation state of actinides is a primary determinant of their behavior in solutions. As an example, Table 2.3 and 2.4 summarize their color and stability in aqueous solutions.

   The trivalent oxidation state of f elements, which is so markedly stable in the lanthanides and heavier actinides, is not typical for Pu, Np and U. The ability of the light actinides to exhibit multiple oxidation states leads to their rich and complex redox chemistry. Comparison of the stability of their oxidation states (Table 2.4) which are supported by data on their standard reduction potentials at pH = 0 in different acids (Figs 2.1–2.2), can lead to interesting conclusions. For example, while uranium (III) can reduce water, U(IV) and Np(IV) can be stabilized in aqueous solution only under anaerobic conditions. U(III) exists at −0.631 V vs. saturated hydrogen electrode, indicating that U(III) liberates H_2 from water. Np(III) (0.155 V) is

Table 2.4 Stability of actinide ions in aqueous solution (usually acidic)

Z+	Ion	Stability
2+	No	Stable
	Md	Stable to water, but readily oxidized
3+	Ac	Stable
	U	Oxidizes to u^{4+}, reducing water (evolving h_2)
	Np	Stable to water, but easily oxidized by air
	Pu	Stable to water and air, but easily oxidized to pu^{4+}
	Am	Stable; can be oxidized with difficulty
	Cm	Stable
	Bk	Stable; can be oxidized to bk^{4+}
	Cf, Es, Fm, Lr	Stable
	No, Md	Stable, but rather easily reduced to 2+
4+	Th	Stable
	Pa	Stable to water, but readily oxidized
	U	Stable to water, but slowly oxidized by air to uo_2^{2+}
	Np	Stable to water, but slowly oxidized by air to npo_2^+
	Pu	Stable in concentrated acid, e.G. 6 M hno_3, but disproportionates to pu^{3+} and puo_2^{2+} at lower acidities
	Am	In solution only in presence of strong complexants
	Cm	In solution only in presence of strong complexants
	Bk	Marginally stable; easily reduced to bk^{3+}
5+	PaO_2^+	Stable, hydrolyses readily
	UO_2^+	Disproportionates to u^{4+} and uo_2^{2+}; most nearly stable at ph 2–4
	NpO_2^+	Stable; disproportionates only at high acidities
	PuO_2^+	Tends to disproportionate to pu^{4+} and puo_2^{2+} (ultimate products); most nearly stable at ph≈8
	AmO_2^+	Disproportionates in strong acid to am^{3+} and amo_2^{2+}; (as [241]am rapidly reduced at lower acidities by alpha-autoradiolysis)
6+	UO_2^{2+}	Stable; difficult to reduce
	NpO_2^{2+}	Stable; easy to reduce
	PuO_2^{2+}	Stable; easy to reduce; (as [239]pu slowly reduced by alpha-autoradiolysis)
	AmO_2^{2+}	Easy to reduce; (as [241]am isotope reduces fairly rapidly by alpha-autoradiolysis)
7+	$NpO_4(OH)_3^{2-}$	Observed only in alkaline solution
	$PuO_4(OH)_3^{2-}$	Observed only in alkaline solution; oxidizes water

still a strong reducing agent, but less so than hydrogen. Plutonium Pu(III) is stable at 0.982 V.

The reduction potentials for the four common oxidation states of plutonium (III–VI) under acidic conditions are all near 1 V. As a result, all four oxidation states can coexist in aqueous solutions (Newton, 1975). The

$$U(III) \xrightarrow{-0.631} U(IV) \;\text{—}\; U(V) \;\text{—}\; U(VI) \tag{1}$$
$$U(IV) \xrightarrow{0.327} U(VI)$$

$$Pu(III) \xrightarrow{0.982} Pu(IV) \;\text{—}\; Pu(V) \xrightarrow{0.925} Pu(VI) \tag{2}$$
$$Pu(IV) \xrightarrow{1.022} Pu(VI)$$

$$NpO_2^{2+} \xrightarrow{1.137} NpO_2^{+} \xrightarrow{0.739} Np(IV) \xrightarrow{0.155} Np(III) \tag{3}$$
$$NpO_2^{2+} \xrightarrow{0.938} Np(IV)$$
$$NpO_2^{+} \xrightarrow{0.447} Np(III)$$
$$NpO_2^{2+} \xrightarrow{0.677} Np(III)$$

$$\tag{4}$$
$$HNO_2 \xrightarrow{0.94} HNO_3$$
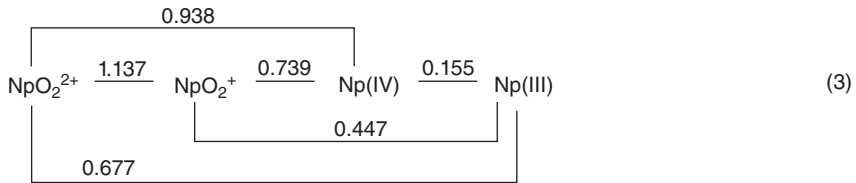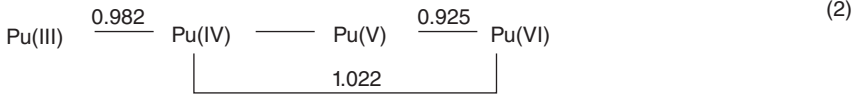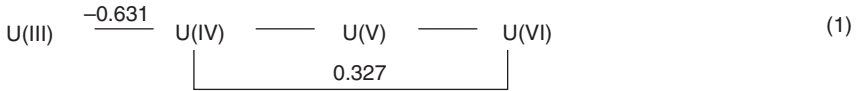
2.1 The scheme of standard redox potentials (in volts) for U, Pu, Np and 1 M HNO_2/HNO_3 (Miles, 1990; Drake, 1990).

equilibrium concentrations of plutonium species existing simultaneously will be determined by Equations 2.1 and 2.2.:

$$Pu^{4+} + PuO_2^{+} \leftrightarrow Pu^{3+} + PuO_2^{2+} \tag{2.1}$$

$$Pu^{4+} + 2H_2O \leftrightarrow Pu^{3+} + PuO_2^{+} + 4H^{+} \tag{2.2}$$

The equilibrium constant for Equation 2.2 is dependent on $[H^+]^4$, hence the position of this disproportionation equilibrium changes significantly with acidity.

The couples in which only an electron is transferred, e.g. Pu^{3+}/Pu^{4+} or NpO_2^{+}/NpO_2^{2+}, are electrochemically reversible and the redox reactions are rapid. Redox reactions that involve forming or rupturing of the actinide-oxygen bond, e.g. Np^{4+}/NpO_2^{+} and Pu^{4+}/PuO_2^{2+}, are not electrochemically reversible and have a slower reaction rate because of the barrier introduced by the subsequent reorganization of the solvent shell and also because some of these are two-electron reductions (Edelstein, 2006).

Disproportionation of neptunium is appreciable only for the Np(V) oxidation state, and the reaction is favored by high concentration of acid:

$$2NpO_2^{+} + 4H^{+} \leftrightarrow Np^{4+} + NpO_2^{2+} + 2H_2O \tag{2.3}$$
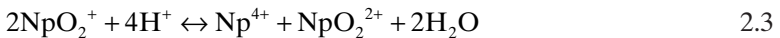
Table 2.5 summarizes the activation parameters of the An(V) disproportionation reaction in perchlorate medium $[H^+] = 1.0$ M at 25°C.

$$U^{3+} \xrightarrow{-0.553} U^{4+} \xrightarrow{\underset{0.447}{\overset{0.2673}{}}} UO_2^+ \xrightarrow{0.088} UO_2^{2+} \tag{5}$$

$$Np^{3+} \xrightarrow{0.219} Np^{4+} \xrightarrow{\underset{0.604}{\overset{0.882}{}}} NpO_2^+ \xrightarrow{1.159} NpO_2^{2+} \xrightarrow{2.04^*} NpO^{3+} \tag{6}$$

$$Pu^{3+} \xrightarrow{1.047} Pu^{4+} \xrightarrow{\underset{1.031}{\overset{0.983}{}}} PuO_2^+ \xrightarrow{0.936} PuO_2^{2+} \xrightarrow{2.31^*} PuO^{3+} \tag{7}$$

$$Am^{3+} \xrightarrow{\underset{2.62(11)}{}} Am^{4+} \xrightarrow{0.84} AmO_2^+ \xrightarrow{\underset{1.60(9)}{\overset{1.683(3)}{}}} AmO_2^{2+} \xrightarrow{2.5(2)^*} AmO^{3+} \tag{8}$$

$$Cm^{3+} \xrightarrow{3.0} Cm^{4+} \tag{9}$$
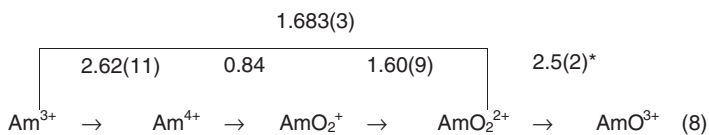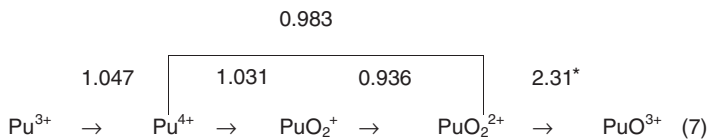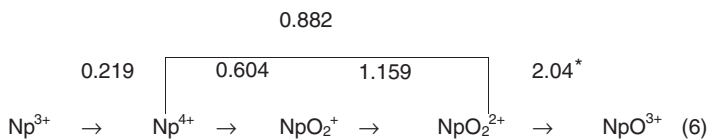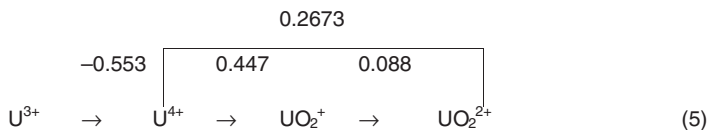
2.2 The scheme of standard redox potentials (in volts) for U, Pu, Np, Am and Cm in 1 M HCl or 1 M HClO$_4$ (*) (Edelstein, 2006).

Both the tetravalent and hexavalent cations, having higher effective cationic charge, are more strongly complexed by ligands, thus the disproportionation reaction will be accelerated toward completion by an addition of complexing agents. Obviously, the reproportionation reaction will be promoted by lower acidity of solution:

$$Np^{4+} + NpO_2^{2+} + 2H_2O \leftrightarrow 2NpO^{2+} + 4H^+ \tag{2.4}$$
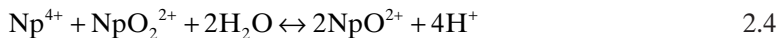
Examination of the redox potential diagrams of U, Pu and Np, compared with part of the nitrogen-potential diagram, leads to the conclusion that in

Table 2.5 Apparent second order rate constant and activation parameters for the disproportionation reaction (2.3) for actinyl ions An(V) in perchlorate medium, [H$^+$] = 1M at 25°C (Ahrland, 1986)

$2AnO_2^+ + 4H^+ \leftrightarrow An^{4+} + AnO_2^{2+} + 2 H_2O$			k	ΔG*	ΔH*	ΔS*
Ion	I(M)	n^a	M^{-1}s^{-1}	[kJmol^{-1}]	[kJmol^{-1}]	[JK^{-1}mol^{-1}]
UO_2^+	2	1	4×10^2	60	46	−46
NpO_2^+	2	2	9×10^{-9}	119	72	−159
PuO_2^+	1	1	3.6×10^{-3}	87	79	−24

n^a – acid dependence of the rate constant.

HNO_3 solution containing NO_2^-, only U(VI), Pu(IV), Pu(VI) and Np(VI) should be present; trivalent species are not stable (Miles, 1990; Drake, 1990). The oxidation of Np(V) by nitrate ion is favored by high HNO_3 and low HNO_2 concentrations, and conversely, at high concentrations of HNO_2, Np(VI) is rapidly reduced to Np(V) (Drake, 1990). Moulin found the rate of oxidation of Np(V) to be dependent on the [HNO_2]/[Np(V)] ratio and the nitrate concentration; the mechanism of oxidation starts with the proton activation of Np(V), followed by oxidation of activated species by nitrate (Moulin, 1978). The rate-limiting step of the overall oxidation of Np(V) is the formation of the activated species, except at very low concentrations of HNO_2, when oxidation of the activated species becomes comparatively slow (Siddall, Dukes, 1959).

Obviously, the role of the proton in redox processes is paramount, which is confirmed by the fact that the most dramatic changes in reduction potentials are observed with increase or decrease of acidity of aqueous solutions. For example, a change of medium from 1 molar acid to 10 molar base causes a change in redox potential of 2 V and makes possible the oxidation of Np(VI) to Np(VII), as seen in Equation 6 in Scheme 2 (Fig. 2.2). Np(VII) can in fact only be prepared in strongly basic solution; a similar effect is seen for Pu, though higher concentrations of base are required.

Generating unusual oxidation states opens new separation opportunities. For example, the typically trivalent Am, if oxidized to upper oxidation states, can be separated from lanthanides either as Am(VI) in a manner similar to other hexavalent actinides (e.g., PuO_2^{2+} or UO_2^{2+} by extraction with TBP) or, similarly to poorly extracted Np(V), pentavalent Am should be poorly extracted by most solvents, while Ln will be extracted by many extractants. Numerous candidates, including TRPO, CMPO's and diamides (malonamides, diglycolamides and even picolinamides) are all potential reagents (Nash, 2009).

The equilibria and variety of actinide species discussed above confirm the necessity of careful control of the conditions and oxidation state of the actinides in separation processes.

2.3.2 Coordination of actinide ions in solutions

The coordination chemistry of actinides in aqueous solutions can be split into two groups: lower oxidation state (di, tri and tetravalent) and higher oxidation state (penta, hexa- and heptavalent) ions.

The coordination number and geometry of their aqueous complexes is determined by the electronic configuration and steric size and shape of the ligands. While ionicity is the predominant characteristic of both lanthanide and actinide bonding (Choppin, 2002), an appreciable covalency, stronger in the actinide bonds, has been confirmed by many spectroscopic studies and attributed to the 6d orbital interactions with the ligands, which are significantly stronger than the 5f interactions (Clark, 2006).

The actinide ions are relatively large cations. Their ionic radii range from 0.112 to 0.095 nm for the trivalent and from 0.094 to 0.082 nm for tetravalent cations. The actinides are found to have high coordination numbers, from 6 to 14. For a majority of the actinides, the exact numbers of water molecules that are bound to the metal centers in the hydrated metal ions are still controversial; the uncertainty in the structures can be explained by the limited number of crystal structures that exist for their aquo complexes. This lack of data is related to the difficulty in crystallizing materials from aqueous solutions (Keogh, 2005).

Typical examples of coordination geometries for An^{3+} and An^{4+} are the Structures 2.1–2.6 for their octa- and nona-aquo ions $An(H_2O)_{8/9}^{3+/4+}$. Structures (2.1–2.3) are octa-coordinate with a cubic, square antiprism, and a bicapped trigonal prism arrangement of the ligands (water molecules), respectively. The nine-coordinate structure (2.4) is a tricapped trigonal prism. Higher coordination numbers are observed with multidentate ligands, such as carbonate and nitrate. Ten-coordinate species include, for example, anionic pentacarbonate species of tetravalent actinides (Structure 2.5) with an irregular geometry with two trans carbonate ligands at the axial sites and three nearly planar carbonate ligands in a pseudo-equatorial plane that is reminiscent of the structure of dioxocation complexes of hexavalent actinides. The hexanitrate anion $An(NO_3)_6^{2-}$ is extremely important in separation of actinides, for example plutonium, under conditions when other metals are in cationic form. Cation exchange resins have a strong affinity for the hexanitrato species $Pu(NO_3)_6^{2-}$. Structure 2.6 represents the coordination geometry for this anion, which has six bidentate nitrate ligands, giving the central Pu^{4+} ion a coordination number of 12. A single crystal XRD study (Spirlet *et al.*,1992) performed on $(NH_4)_2Pu(NO_3)_6$ confirmed

the structure (6) of the icosohedral $Pu(NO_3)_6^{2-}$ unit characterized by three mutually perpendicular planes formed by the trans NO_3^- groups giving virtual symmetry T_h. The twelve Pu–O bond distances average 2.487(6) angstroms (Clark, 2006).
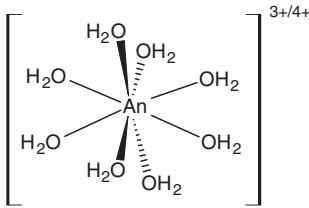
Structure 2.1
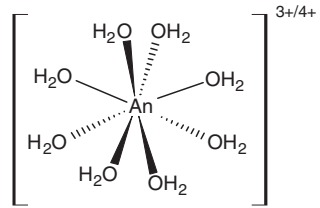
Structure 2.2
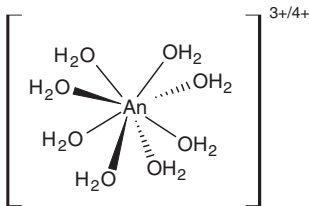
Structure 2.3
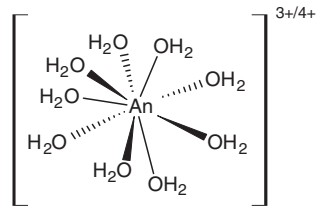
Structure 2.4
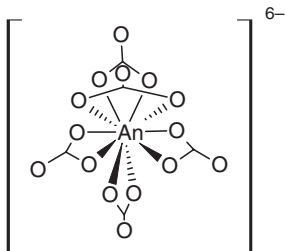
Structure 2.5
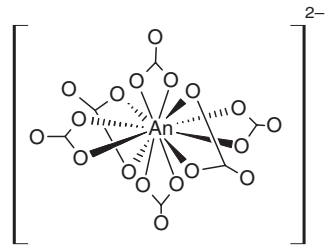
Structure 2.6

The structural chemistry of selected non-aqueous complexes of the tri- and tetravalent actinides is similar to their aqueous complexes (Keogh, 2005). Structures 2.7–2.8 show the geometry of $U(MeBH_3)_4$ (7) and $[\{U(N(CH_2CH_2NSiMe_3)_3)\}_2(\mu^2\text{-}\eta^2 : \eta^2\text{-}N_2)]$ (Structure 2.8), respectively.
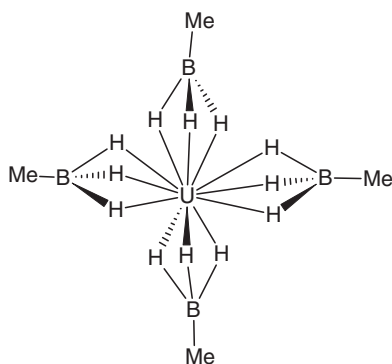
Structure 2.7
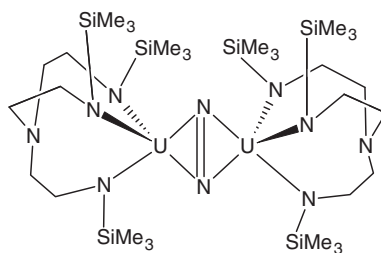
Structure 2.8

For the aqueous species of penta- and hexavalent actinides, the typical species includes the linear dioxo unit, $AnO_2^{+/2+}$, with two oxygen atoms positioned at 180° with an average M-O distance of 0.175–0.180 nm for hexavalent cations and 0.181–0.193 nm for pentavalent cations. All "secondary" ligands are coordinated in the perpendicular equatorial plane with typical M-X bond distances of 0.24–0.26 nm. The bonding for these ions has significant covalency with the axial An–O ligands, while the bonding for the majority of the ligands residing in the equatorial plane is primarily ionic (Keogh, 2005). As a result of this dual behavior (covalency and ionicity) of the trans dioxo ions, the linear dioxo unit is unperturbed (with the exception of bond distance changes) in all of the aqueous-based complexes. The coordination numbers of the central actinide cation are defined by the equatorial size of ligands and their electronic properties. The structures of a variety of aqueous-based coordination complexes have been observed (Structures 2.9–2.12). Compounds with tetragonal symmetry (D_{4h}) are represented by the complexes, $AnO_2Cl_4{}^{2-}$ (Structure 2.9) and $NpO_4(OH)_2{}^{3-}$ (Structure 2.10).
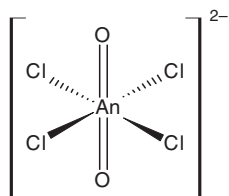
Structure 2.9
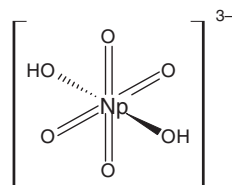
Structure 2.10
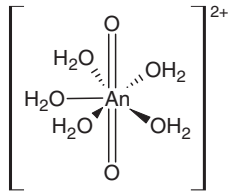
Structure 2.11
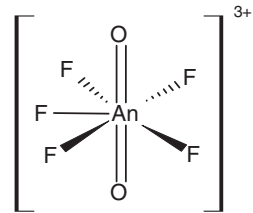
Structure 2.12

The penta-aqua ion (Structure 2.11) and pentafluoro complex (Structure 2.12) for the hexavalent actinides are seven-coordinate structures, prevalent in actinide chemistry, and are the highest coordination numbers achievable with all monodentate ligands; however, coordination complexes with eight atoms bound to the actinide are achievable. The most well-studied aquo ion of the actinides is $UO_2(H_2O)_5^{2+}$ (Structure 2.11). From EXAFS, structural data on the aquo ions have been obtained for the hexavalent ions, $AnO_2(H_2O)_5^{2+}$ (An = U–Am). For calibration purposes, the bond distance for the oxo ligands of the UO_2^{2+} species obtained from XAFS and single-crystal analyses show a nearly identical length. The bond An = O distance was found to be 0.176, 0.175; 0.174 and 0.18 nm for An(VI) = U, Np, Pu, and Am, respectively. The An–OH_2 distance for the same complexes was found to be 0.242, 0.242, 0.241 and 0.24 nm, respectively (Keogh, 2005). For neptunyl and plutonyl aqua ions of pentavalent Np and Pu, 4, 5 and 6 water ligands were identified by XAFS. The bond distances for both An = O (0.183 nm for both Np and Pu) and An–OH_2 (0.251 and 0.250, respectively) expand in the pentavalent ions in line with an increase in the ionic radii with the change in oxidation state.

Structures with 9–12 molecules of water have been proposed for tetravalent actinides in aqueous solutions. In general, the most accepted values for the number of H_2O molecules bound to the metal center are 10 for Th and 9 for U to Pu. The An–OH_2 distances in these ions range from 0.25 to 0.24 nm (Keogh, 2005). Trivalent plutonium with nine molecules of water (Matonic, 2001) was crystallized in a tricapped trigonal prismatic geometry.

2.3.3 Hydration and complexation of actinides

The thermodynamics of complexation between hard acid cation and hard ligands are often characterized by positive values of both the enthalpy and entropy changes (Choppin, 2004). The positive enthalpy values indicate a net decrease in bond strength for the system (including the solvent) going

from reactants to products. The positive reaction entropy overcomes this unfavorable enthalpic component to promote complex formation. Many lanthanide and actinide complexation reactions are considered to be "entropy-driven", since the entropy contribution from dehydration of cation is more significant than loss of entropy associated with the combination of the ion with another ligand. The observed overall changes reflect the sum of the contributions of dehydration and cation–ligand combination. It has been shown that for many of the hard–hard complexation systems, there is a linear correlation between the experimental values of enthalpy and entropy of complexation reaction, a so called "compensation effect" (Choppin, 2004).

The hydration of an actinide cation is a critical factor in the structural and chemical behavior of their complexes. During the complexation reaction, one or more water molecules in the hydration sphere of the metal cation are replaced with a ligand, donating electrons and electrostatic molecules to the central atom. Based on Pearson hard/soft acid/base theory, they are usually characterized as hard or soft donor-ligands. Actinides are "hard" Lewis acids and exhibit a strong preference for oxygen donor ligands. The complexation in aqueous solution many times involves substitution of the solvate waters with their metal—oxygen (ion-dipole) bond by a ligand (Choppin, 1971). The water expelling ligands can form either direct bonds with the metal cation in the first (inner) coordination sphere of the cation, creating a so called "inner-sphere complex", or, if they cannot displace the water from their inner coordination sphere, they stay directly bonded only to the primary hydration sphere of the metal cation. Such "outer sphere ligands" remain separated from direct contact with the metal ion by a molecule of water; such complexes have a very subtle influence on the behavior of the metal ion.

Actinide cations are known to form both outer and inner sphere complexes and, for labile complexes, it is often difficult to distinguish between these two types. Choppin proposed (Choppin, Strazik, 1965); (Ensor, Choppin, 1980) and (Khalili et al., 1988) the use of thermodynamic parameters of complexation (enthalpy and entropy) to help evaluate outer sphere vs. inner sphere complexation. Because the primary solvation sphere is minimally perturbed by the ligand in outer sphere complexes, little energy is spent on de-solvation and little disordering occurs. As a result, outer sphere complexation is often associated with usually near zero enthalpy and negative and near zero entropy. In contrast, the enthalpy for inner sphere complexation is determined by the relative balance of metal–ligand bond strength and the metal–water bonds broken; usually it is small and maybe slightly exothermic while the entropy for inner sphere complexes is usually positive because more water molecules are released than ligands complexed (Nash, Sullivan et al., 1986, 1991).

Predominantly outer sphere ligands include Cl^-, Br^-, I^-, ClO_3^-, NO_3^-, sulfonate, and trichloroacetate ligands, all with acid dissociation constant pK_a values <2. As the pK_a increases above 2, increasing predominance of inner sphere complexation is expected for carbonate/bicarbonate, sulfate, fluoride, and most carboxylate ligands (Choppin, 1998). Comparison of the thermodynamic parameters of nitrates and chlorides also reflect the intermediate character of the nitrate complexes (Choppin, Strazik, 1965; Choppin, Graffeo, 1965); a near zero entropy suggests that the nitrate is probably mainly monodenate with one water molecule displaced. Water coordination may induce changes in anion coordination mode and coordination number. Quantum mechanical calculations suggest that when the first coordination shell is saturated, the two types of binding modes become of similar energy, leading to different coordination numbers (CNs) and distributions of first and second shell water molecules. For instance, for $La(NO_3)_3(H_2O)_6$, CN ranges from 9 (3 monodentate nitrates + 6 water) to 10 (3 bidentate nitrates + 4 water) or 11 (3 bidentate nitrates + 5 water). Thus, at some point, adding water to the second or to the first shell becomes isoenergetic. As the cation becomes smaller, the preference for monodentate nitrate binding increases, due to avoided repulsions in the first coordination sphere (Dobler *et al.*, 2001).

Whether the U(VI)-nitrate complex is "outer sphere" or "inner sphere" is another question that is still open for debate (Rao, Tian, 2008). Earlier data on the complexation of U(VI) with nitrate at variable temperatures (10–40°C) appeared to suggest that the $UO_2NO_3^+$ complex was outer sphere (Ensor, Choppin, 1980; Khalili *et al.*, 1988). However, Rao's calorimetric data suggest that both the inner and outer sphere complexes may exist in the U(VI) nitrate system and the $UO_2NO_3^+$ complex has significant inner sphere character (Rao, Tian, 2008).

The structure of actinide complexes, when H_2O is replaced by the addition of the ligand, for example OH^-, F^-, CO_3^{2-}, tends to weaken the v_1 stretch of the $O = An = O$ and increase the $An = O$ distance. On transitioning between AnO_2^+ to An^{4+}: the loss of the linear dioxo unit in the lower valent complexes results in both a higher overall charge and a smaller radius of the cation, which combines to result in a slight decrease in the An–ligand bond distance (Keogh, 2005), and with a stronger metal–ligand interaction.

Experimental data on the size and structure of the hydration sphere of a metal ion are very important for understanding of metal complexation and the behavior of complexes in separation systems. They have been probed by several direct and indirect experimental methods. Recently, two reviews devoted to critical evaluation of results obtained for solution coordination chemistry of actinides by both direct, including X-ray and neutron diffraction, X-ray absorption fine structure (XAFS) measurements, luminescence decay, nuclear magnetic resonance (NMR) relaxation measure-

ments, and indirect methods such as compressibility, NMR exchange, and optical absorption spectroscopy, have been published (Choppin, Jensen, 2006; Szabo *et al.*, 2006) Theoretical and computational studies are also important in understanding the coordination geometry and coordination number (CN) of actinide ion hydrates (e.g., Spencer *et al.*, 1999; Hay *et al.*, 2000; Tsushima, Suzuki, 2000; Antonio *et al.*, 2001).

2.3.4   Hydration in concentrated solutions

As the electrolyte concentration increases, the number of water molecules in the secondary hydration sphere decreases. Consequently, there is a tightening of the bond between the metal cation and the hydrate waters in the inner sphere (Choppin, Jensen, 2006). Based on NMR studies of trivalent actinides and lanthanides, Choppin concluded that inner sphere complexation by perchlorate ions does not occur below approximately 8–10 M (Choppin, Labonne-Wall, 1997). Multiple equilibria for the uranyl chloride system ($UO_2Cl_2(H_2O)_2$, $UO_2Cl_3(H_2O)^-$, and $UO_2Cl_4^{2-}$) have been used for separation of uranium from its progeny or other metals. Since Th^{4+} does not form anionic chloride complexes, it is retained on cation-exchange resin while anionic chloride complexes of UO_2^{2+} pass through the column in the eluate. Alternatively, such anionic complexes can be retained on an anion-exchange column.

The hydration number of Eu(III) remains relatively constant in hydrochloric acid up to approximately 6–8 M, above which concentration it decreases. The same is true for the hydration number of Cm(III) in HCl, which begins a decline at about 5 M HCl. This difference between (Eu^{3+} and Cm^{3+}) reflects greater complexation of the actinide trivalent ion by the relatively soft anion Cl^-. The difference in chloride complexation has been used to provide efficient separation of trivalent actinides from trivalent actinides in concentrated HCl solutions by passage through columns of cation exchange resin since 1950s (Diamond *et al.*, 1954).

Nitrate complexes for tetravalent actinides, for example, Th^{4+} and Pu^{4+}, are extremely important in actinide separation and purification processes. Nitrate ions begin to form inner sphere complexes at lower concentrations than chloride anions; this observation is confirmed by the decreased hydration number of the cation even at relatively lower concentrations (Choppin, Jensen, 2006). However, since the oxygen atoms of the nitrate are hard donors, there is no evidence of any covalent enhancement in its bonding as is seen with the chloride anions for the trivalent actinide cations relative to the lanthanide cations (Choppin, Jensen, 2006). In separation and purification processes, the nitrate complexes of actinides are extremely important. Nitrate-nitric acid solution is the most common aqueous medium in nuclear separation processes. In the case of neutral extractants such as

tributylphosphate (TBP), carbamoyl methyl phosphine oxide (CMPO) or dipicolinamides (DPA) it provides nitrate units necessary to compensate the actinide cation charge to enable extraction. Nitrate complexation with hexavalent actinide ions is very weak and the determination of the formation constants for aqueous nitrate solution species is extremely difficult. Under aqueous conditions with high nitric acid concentrations, complexes of the form $AnO_2(NO_3)(H_2O)_x^+$, $AnO_2(NO_3)_2(H_2O)_2$, and $AnO_2(NO_3)_3^-$ (An = U, Np, Pu) are likely to be present. The limiting species in the nitrate series is the hexanitrato complex, $An(NO_3)_6^{2-}$ (Matonic *et al.*, 2002). The complexation of the Pa and Np pentavalent ions by nitrate is known; however, limited thermodynamic and structural data are available. The presumed stoichiometry for the Np(V) species is $NpO_2(NO_3)(H_2O)_x$. For protactinium, which easily hydrolyzes, mixed hydroxo/nitrato or oxo/nitrato complexes have been proposed.

Fluorides and chlorides are the best studied actinide-halide systems, and they are very important for the pyroprocessing and electrorefining processes.

Carboxylic acids are strongly bound to actinide ions. The primary binding mode for simple carboxylic acids is bidentate, while in polycarboxylic acid complexes, carboxylates tend toward monodentate coordination with the metal ion. The affinity of the low-valent actinides for these ligands increases with the denticity of the ligand, for example, ethylenediaminetetraacetate (EDTA) >>> acetate. For An^{4+}, the EDTA ligand is hexadentate with a twist conformation (a spiral conformation, wrapping around the metal ion, rather than encapsulating the metal ion in a central cavity in the manner of tripodal or macrobicyclic ligands). Diethylenetriamine-N,N,N′,N″,N″-pentaacetate (DTPA) has an even higher affinity for both An^{3+} and An^{4+} ions.

2.3.5   Structure and strength of complexes

As has been noted above, actinide ions in their common solution oxidation states (3+ to 6+) are all hard Lewis acids, and their bonds with aqueous ligands are predominantly ionic. Several decades ago it was observed that for a given ligand, the strength of actinide complexes increased with the "effective" cationic electrostatic charge of the actinide ions (Rao, Choppin 1984):

$$AnO_2^+ < An^{3+} < AnO_2^{2+} < An^{4+} \qquad\qquad 2.5$$
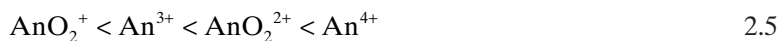
The effective cationic charges of both the actinyl(V) and actinyl(VI) ions, larger than their overall, formal charge, suggest that the oxygen atoms of both $O = An^{5/6} = O$ cations retain a partial negative charge and the bonds between the actinide cations and the ligands in the equatorial plane are

Table 2.6 Nominal, overall and effective cationic charge of actinides

Cationic charge	NpO_2^+	Am^{3+}, Pu^{3+}	UO_2^{2+}	Pu^{4+}, U^{4+}
Nominal	5+	3+	6+	4+
Overall (formal)	1+	3+	2+	4+
Effective	2.2+	3+	~3.2+	4+

considerably stronger than would be indicated by their formal charge of +1/+2. The values of the effective charge, determined experimentally (Choppin, Rao, 1984) have been confirmed by theoretical calculations (Walch, Ellis, 1976; Matsika, Pitzer, 2000), providing theoretical foundations for the observed behavior of actinides (Choppin, Jensen, 2006) (Table 2.6).

The thermodynamic bond strengths of actinide–ligand complexes are determined primarily by electrostatic attraction of metal and ligand modified by steric constraints; aside from the dioxocations, directed valence effects are generally not evident in actinide coordination compounds. The electrostatic attraction between an actinide cation and a ligand is proportional to the product of the effective charges of the metal and ligand divided by the actinide–ligand distance (Choppin, Jensen, 2006). The steric constraints may arise from the properties of the actinide cation (ion size and presence or absence of actinyl oxygen atoms) or of the ligand (number and spatial relationship of donor atoms, size of the chelate rings, and flexibility of ligand conformations).

If the interactions of ligands with both the actinide cation and proton are governed by the same (electrostatic) interactions, some properties of their metal complexes, such as the stability constant, stoichiometry or structure can often be predicted from the chemistry of their chemical analogs (related ligands or other metal ions of similar properties). Linear free energy correlations of structurally-similar complexes can be used to understand differences in coordination geometries for actinide complexes in solutions (Choppin, 1996; Choppin, Jensen, 2006; Paulenova, Clark, 2009). One can predict the relative strength of the metal complexes by comparison of the ligand affinity for a proton and metal cation. Gibbs free energy of a reaction is proportional to its equilibrium constant K:

$$\Delta G = -2.3 \, RT \log K \qquad\qquad 2.6$$

where R is the universal gas constant and T is the absolute temperature. The logarithmic constants for complex stability constant and the protonation of ligand can be used for correlating and interpreting observed values. Obviously, the ligand protonation constant can be expressed as a constant
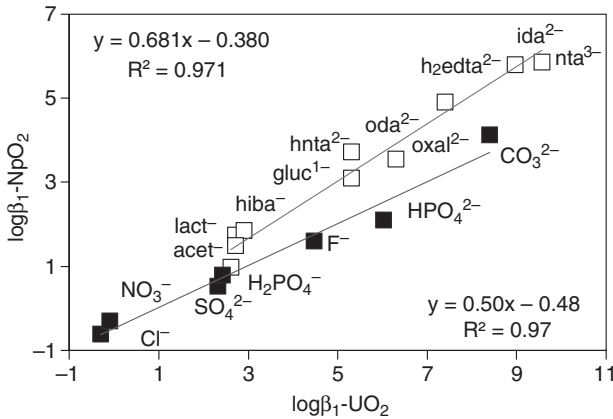
2.3 Correlation between the 1:1 stability constants for the neptunyl and uranyl cations with a variety of ligands. The linear relationships observed for inorganic ligands (black squares) and the organic ligands (open squares) suggests the same coordination geometry for the dioxo f-element cations.
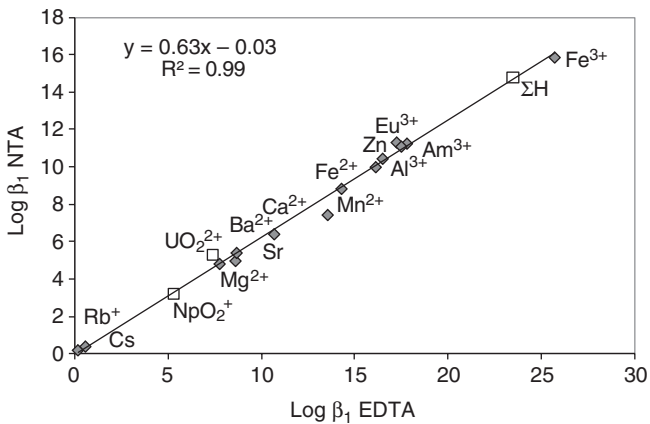
2.4 Correlation between log β_1 for NTA and EDTA with a variety of metal cations.

of the reverse process, ligand dissociation, and log k_H will be replaced with pK_a.

The next three thermodynamic correlations (Figs 2.3–2.5) are based on the assumption that the interactions between the ligand and cation are primarily electrostatic in nature. When the coordination chemistry of complexes is the same, linear correlations between stability constants are apparent. A comprehensive database of ligand pK_a values (Smith, Martell, 2006)
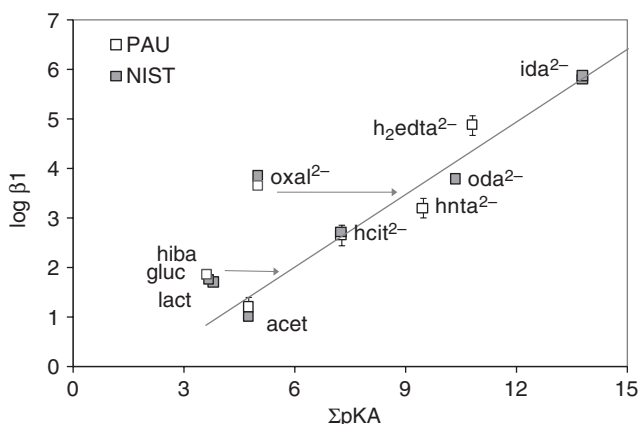
2.5 Correlation between log β1 and the sum of the protonation constants (ΣpK$_A$) for a variety of complexes with the uranyl cation.

was used in correlations below. Thermodynamic data for gluconate and oxalate ligands were measured at WSU (Paulenova, Clark, 2009).

A nearly ideal correlation between the 1:1 stability constants for the neptunyl and uranyl cations with a variety of organic and inorganic ligands confirms the same coordination geometry for both the di-oxo-linear structures of f-elements, and can be used (with caution) to predict the stability constants if one of constant for this pair is known.

Though the different structures of the $An^{3+/4+}$ cations and $An^{5+/6+}$ dioxocations should impose restrictions on the correlation of thermodynamic data, it is noteworthy that data for the actinyl cation (U(VI), Np(V)) complexes generally correlates well with corresponding data for complexes of aminocarboxylates with the simple, spherical cations (Paulenova, Clark, 2009). Although the coordination geometry for the dioxocations differs from the spherical cations, the correlation between the first stability constants (log) for NTA (nitrilotriacetic) and EDTA (ethylenediamine-N,N,N′,N′-tetra acetic) acids with a variety of metal cations is consistent for both NTA and EDTA. As displayed in Fig. 2.4., the formally monovalent cation NpO_2^+ lies half-way between the monovalent and divalent spherical cations, and the correlation is satisfactory also for uranyl cation.

The correlation between log β_1 and the sum of the protonation constants (ΣpK$_a$) for neptunyl complexes with different carboxylate ligands is displayed in Fig. 2.5. The hydroxy-monocarboxylates are correlated worse than aminocarboxylates, and lie between dicarboxylate (oxalate) and other carboxylate ligands. This is presumed to result from the strong donor effect of the oxygens present in the molecules of hydroxycarboxylates.

2.4   Irradiation effects

The effect of ionizing radiation caused either by photons or particles having sufficient energy to ionize the molecules of the medium is very important in process chemistry. It may involve photons with energies ranging from the first ionization energy of the medium (~10 eV) up to several MeV, as well as alpha and beta particles (electrons) generated by spent nuclear fuel decay. Whether in solid, solution, or gaseous states, the alpha, beta and gamma radiation interacts with the environment and affects the chemical speciation of the actinides because the result of the energy absorption is breaking or rearrangement of chemical bonds.

2.4.1   Radiation damage in solid state

As the energetic beta and alpha particles traverse through a crystalline medium, atoms are displaced from their stable lattice positions, forming Frenkel pairs (ion pairs, vacancy and interstitials). For example, the autoradiolysis in metallic ^{239}Pu ($T_{1/2} = 2.41 \times 10^4$ y) causes significant structural changes. When the ^{239}Pu atom decays, an α-particle with an kinetic energy of 5 MeV and the recoil nucleus of ^{235}U atom with an energy of 86 keV are created. In metallic Pu, the α-particle deposits its kinetic energy in approximately 10 μm, while for the heavier recoil atom it is only 12 nm. For each disintegration event, approximately 2600 ion pairs are formed, and over the course of 20 years, every atom in a piece of Pu metal changes its position. This property becomes critical when trying to predict the long-term behavior of Pu materials (Keogh, 2005). However, while metallic structures can undergo a significant degree of self-annealing (heating to a melting point and cooling over a long period of time), molecular complexes can suffer irreversible structural damage. A typical example would be autoradiolysis causing amorphization of crystalline compounds of relatively short-lived americium ^{241}Am ($T_{1/2} = 432.7$ y). As confirmed by the single crystal X-ray diffraction analysis, the intensity of the diffraction decreases with time. Visible damage of crystal lattice can be observed by opacity of originally clear crystal and increased solubility. Similar structural disordering in materials was observed after irradiation with high-energy electron beam. Electrons, being much smaller than alphas or heavy ions, penetrate deeper through the bulk of the irradiated crystal, and cause amorphization of the crystalline lattice. Uranophane and other uranium solid matrices (Douglas *et al.*, 2002; Utsunomia *et al.*, 2003), important for the development of radiation resistant waste forms have been studied using accelerated beams. Thermochemical investigation of stability of microporous and mesoporous materials such as frameworks in silica zeolites or selected metal-phosphates (Petrovic *et al.*, 1993; Hu *et al.*, 1995) is another example of material studies

for high-level nuclear waste immobilization (Navrotsky *et al.*, 2009; Weber *et al.*, 2009).

A material very resistant to radiation damage is glass, because it is a noncrystalline "solid" liquid. Though at an atomic level the same phenomena occur in glass, it is not appropriate to speak of dislocations in glass: the random structure of the glass allows it to accommodate foreign species throughout the sample (Sales, Boatner, 1984; Oelkers, Montel, 2008). Glasses have been intensely studied as the matrix for high active waste consisting of fission products and actinides (Ewing, Wang, 2002).

2.4.2 Radiolysis in aqueous solutions

Radiolysis in aqueous solutions has an entirely different effect than in solid materials; water molecules become either excited or ionized. The ionization event occurs on the time scale of an electronic transition ($<10^{-16}$ s) and the positive ion H_2O^+ is formed along with an electron; H_2O^+ reacts with another molecule of water ($<10^{-14}$ s), forming an $\cdot OH$ radical and H_3O^+. The electron, if liberated with sufficient kinetic energy, ionizes further water molecules until its energy falls below the ionization threshold of water (12.61 eV. Spending the rest of its energy on vibrational and rotational excitation of the water molecules, it becomes solvated ($<10^{-12}$ s) (Rydberg *et al.*, 2001).

The excited states of irradiated molecules of water dissociate to form radicals $\cdot O$, $H\cdot$, $\cdot OH$ and molecular H_2; this occurs on the same time scale as a molecular vibration, within 10^{-14}–10^{-13} s. The physical and physico-chemical (pre-thermal) processes are thus completed within 10^{-12} s, leaving the species in thermal equilibrium with the water (Rydberg *et al.*, 2001).

The radiolysis products, formed upon excitation and ionization of irradiated water molecules, are clustered in "spurs"; i.e. they are inhomogeneously distributed in the water and proceed to diffuse out of the spur volume. During this "spur diffusion" process, recombination reactions (equation 2.7) take place, leading to the formation of molecular or secondary radical products.

$$
\begin{aligned}
e^-_{aq} + e^-_{aq} &\rightarrow H_2 + 2OH^- & H\cdot + H\cdot &\rightarrow H_2 \\
e^-_{aq} + \cdot OH &\rightarrow OH^- + H_2O & \cdot OH + \cdot OH &\rightarrow H_2O_2 \\
e^-_{aq} + H_3O^+ &\rightarrow H\cdot + 2H_2O & \cdot OH + H\cdot &\rightarrow H_2O \\
e^-_{aq} + H\cdot &\rightarrow H_2 + OH^- & H_3O^+ + OH^- &\rightarrow 2H_2O_2
\end{aligned}
\qquad 2.7
$$
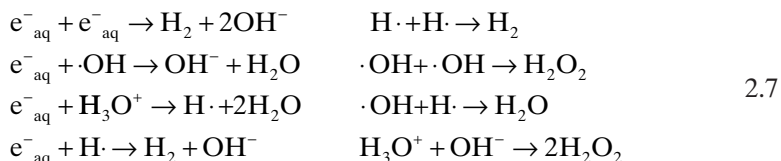
Alpha particles deposit their kinetic energy in a very short distance (38 μm in water for 5.3 MeV alphas; de Carvalho, 1952). Because of their higher charge, generally greater kinetic energy and greater mass, their linear energy transfer (LET) is much larger than the LET of photons or high energy electrons. As is shown in Table 2.7, the G-values (radiation product

Table 2.7 Radiation yields in irradiated neutral water G-values (ìmol/J) in irradiated neutral water (Rydberg, *et al.*, 2001)

Radiation	$-H_2O$	H_2	H_2O_2	e^-_{aq}	$H\bullet$	$\bullet OH$	$\bullet HO_2$
Gamma and fast electrons	0.43	0.047	0.073	0.28	0.062	0.28	0.0027
Alpha (12 MeV)	0.294	0.115	0.112	0.0044	0.028	0.056	0.007

yields) for the radical products are larger for the radiation with low LET whereas the yields of molecular products (H_2, H_2O_2) are larger for the high LET radiation. Hart estimated that about 88% of the radicals during alpha-radiolysis recombine to give molecular products, the proportion of free radicals in the product being only 12% (Hart, 1954).

In irradiated dilute aqueous solutions, practically all the energy absorbed is deposited in the water molecules and the observed post-irradiation chemical changes are the result of the reactions between the solutes and the products of the water radiolysis. With increasing solute concentrations, the direct radiolysis of the solute gradually can become more important. At higher concentrations, the solute may also be modified through direct inter-action with radiation in the spur.

Self-radiolysis may greatly affect the chemical equilibrium and speciation of actinides in their solutions. For example, in acidic solution of [239]Pu, the self-radiolysis results in changes of the oxidation state of PuO_2^{2+} which "degrades" by being reduced to Pu^{4+} at a rate of approximately 1.5% per day (Keogh, 2005). Intermediate Pu(V) is unstable in acidic solutions; it disproportionates to produce Pu^{4+} and Pu(VI). Equation 2.8 shows the radiolytic reductions in solutions of [239]Pu along with the reproportionation and disproportionation reactions.

$$
\begin{aligned}
&Pu^{4+} \rightsquigarrow Pu^{3+} \\
&PuO_2^{2+} \rightsquigarrow PuO_2^{+} \\
&Pu^{4+} + PuO_2^{+} \leftrightarrow Pu^{3+} + PuO_2^{2+} \\
&2PuO_2^{+} + 4H^{+} \leftrightarrow Pu^{4+} + PuO_2^{2+} + 2H_2O
\end{aligned}
\qquad 2.8
$$
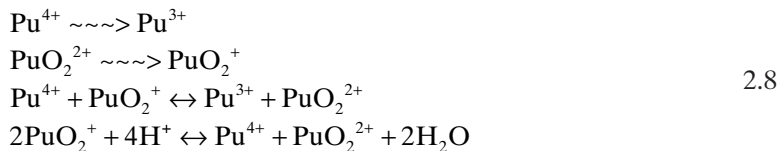
Hydrogen peroxide, produced by higher concentrations of [239]Pu in a suf-ficient amount, may decrease the concentration of tetravalent plutonium by forming a precipitate of plutonium peroxide (Rydberg *et al.*, 2001). To sta-bilize the concentration of Pu(IV) in processing, nitrite ions are added to the solution to scavenge the hydroxyl radicals formed by the radiolysis and thus eliminate the production of H_2O_2.

The effect of radiation on actinide containing materials and solutions can be altered by careful selection of different isotopes with varying half-lives

that can be used. In the case of the plutonium example given above, by using the ^{242}Pu isotope, which has a half-life 15.5 times longer than ^{239}Pu, solutions that show diminished radiation effects (for example, increased stability in a given oxidation state) can be created. In contrast, ^{238}Pu, which has an 87.7 year half-life and specific activity about 300 times greater than ^{239}Pu, is well suited for alpha-radiolysis studies.

The radiolytic reduction of Np(VI) to Np(V) by alpha self-radiation (of ^{237}Np) results with a relatively large radiation yield (G = 0.66 mol/microjoul), and does not vary with perchloric acid concentration within the limits investigated ($3.1 \times 10^{-9} sec^{-1}$ in 0.5–1.7 N HClO$_4$) (Cohen, Taylor, 1961; Zielen et al., 1958; Siddall, 1960). This high reduction yield is attributed to the high concentration of Np in irradiated solutions: the investigations of Pu and Am were never performed with concentrations higher than 10^{-2}M (Vladimirova, 1964). Gamma irradiation, typically studied with Co-60 source (with γ energy of 1.17 and 1.33 MeV) leads to either reduction of Np(VI) to Np(V) or oxidation of Np(IV) to Np(V) (which has a comparatively high stability to radiolysis) (Burney, Harbour,1974). Studies of beta-radiolysis using accelerated electron beams show an increasing yield of Np(V) in solutions of low acidities (0.01–0.7 M HClO$_4$); with increasing concentration of acid, the radiation yield of Np(V) drops (Burney, Harbour, 1974).

The most reactive water radiolysis species produced are the oxidizing hydroxyl radical (•OH), hydrogen peroxide (H$_2$O$_2$), reducing aqueous electrons (e$_{aq}^-$), and hydrogen atoms (H•), which are produced in equal amounts. The hydrated electron e$^-_{eq}$ is a strongly reducing species (E$_0$ = −2.9 V) whereas the hydrogen atom is a less powerful reductant (E$_0$ = −2.3 V) (Rydberg et al., 2001). The hydroxyl radical •OH is a strong oxidant (E$_0$ = 2.7 V in acidic and 1.8 V in basic solution) (Rydberg et al., 2001). Under the acidic, aerated conditions of the solvent extraction process, the aqueous electrons produced would be scavenged according to the fast reactions 2.9 and 2.10 (Mozumder, 1999; Mincher et al., 2009).

$$e^-_{aq} + H^+ \rightarrow H \cdot \qquad k = 2.3 \times 10^{10} M^{-1} s^{-1} \qquad\qquad 2.9$$

$$e^-_{aq} + O_2 \rightarrow \cdot O_2^- \qquad k = 1.9 \times 10^9 M^{-1} s^{-1} \qquad\qquad 2.10$$
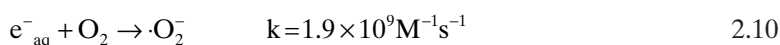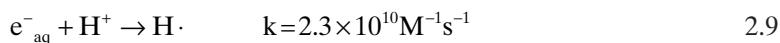
Process solutions of used nuclear fuel are quite concentrated. As noted above, with increasing solute concentrations, direct radiolysis of solutes can occur. Nitrate salts and nitric acid predominate in the process solutions; hence, the radiation chemistry of nitric acid in both the water and organic solvent media is very important. HNO$_3$ is distributed in both phases and its radiolytic degradation products have a huge influence on the separation processes.

The most important radiation product in irradiated solutions of nitric acid is nitrous acid (nitrite ion), since it directly affects the redox chemistry

Table 2.8 Radiation yields of nitrite for different concentrations of nitric acid and nitrate (Kazanijan, 1970)

$G(NO_2^-)$ mol/100 eV

HNO_3 (M)	Alpha	Beta	Gamma
0.01	–	–	1.1
0.1	0.51	1.4	1.6
1	1.3	2.5	2.6
5	1.8	1.9	2.2
10	2.8	1.8	1.9
8 M	–	–	2.2
$NaNO_3$ (M)	$G(NO_2^-)$ mol/100 eV (gamma)		
5 M	–	–	3.1
8 M	–	–	3.8

of Np and Pu. At lower acid concentrations, the nitrite yields from alpha irradiation are much lower than the yields from the gamma or beta irradiation but steadily increase with increasing HNO_3 concentration (Table 2.8, Kazanijan, 1970). The nitrite yields in HNO_3 below 1 M exhibit the same trend as has been observed in neutral nitrate solutions since water is absorbing most of the radiant energy and the nitrite yields are determined by the reaction of the radicals formed from the radiolysis of water via the following mechanism:

$$H \cdot + NO_3^- \rightarrow NO_2 + OH^- \qquad 2.11$$

$$2NO_2 + H_2O \rightarrow NO_2^- + NO_3^- + 2H^+ \qquad 2.12$$

$$\cdot OH + NO_2^- \rightarrow NO_2 + OH^- \qquad 2.13$$
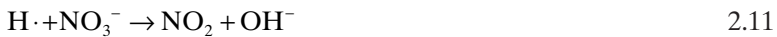
The nitrite yields from the solutions with $HNO_3 > 1$ M are different from those in neutral or low nitrate solutions. Increased concentration of nitrate leads to these reactions:

$$NO_3^- \sim\sim\sim> e^-_{aq} + \cdot NO_3 \qquad 2.14$$

$$NO_3^- \sim\sim\sim> NO_2^- + O \qquad 2.15$$

$$NO_3^- \sim\sim\sim> NO_2 + O + e^-_{aq} \qquad 2.16$$

The effect of the solution acidity, expressed by lower nitrite yields in acidic than in neutral solutions is caused by radiolytic decomposition of the undissociated nitric acid molecule (as well as the nitrate ion). Redlich *et al.* (1968) established that the undissociated acid fraction grows from 1% in 1 M to 48% in 10 M nitric acid; hence, the probability of the reaction in Equation 2.14 increases with increased concentration of nitric acid:

$$HNO_3 \rightarrow \cdot NO_2 + \cdot OH \qquad\qquad 2.17$$

The different trends for the high (alpha) and low (beta, gamma) linear energy transfer (LET) radiations can be explained by different yields of ionic and molecular radicals upon interaction with aqueous solutions. Radical combination to produce molecular products would be higher for alpha irradiation. The dimer (N_2O_4) or the H_2O_2 produced would have no effect on the net yield of nitrite.

Nitrous acid HNO_2 is a key redox controlling factor, affecting the speciation of neptunium and plutonium in the used nuclear fuel solutions. One of the most significant reactions in this complex system is the reduction of Np(VI) to unextractable Np(V) by nitrous acid; it is reversible, controlled by H^+-concentration. Nitrous acid also acts as a catalyst of oxidation of Np(V) by nitric acid back to Np(VI):

$$2NpO_2^{2+} + HNO_2 + H_2O \leftrightarrow 2NpO_2^+ + 2H^+ + HNO_3 \qquad 2.18$$
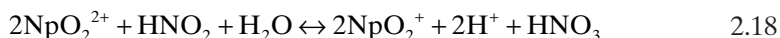
2.4.3 Radiolysis in organic solutions

PUREX process is the most mature solvent extraction separation process in use today. Its principles are described in a great detail in Chapter 6 of this book. PUREX was first implemented in the 1950s, thus its radiation chemistry is the best studied. In general, the PUREX solvent consists of 30 vol % n-tributylphosphate (TBP) in an alkane diluent. In this process, as in its advanced version, UREX (Uranium Extraction), a multistage usage of the solvent is expected. With each use it is exposed to the high radiation field arising from dissolved used nuclear fuel. Considering either the group separation design or the multistep UREX+ process, the PUREX/UREX is the starting process step and hence, TBP obtains the highest radiation dose possible during the processing. The aqueous phase initially contains all fission products, which emit strong beta and gamma radiation, and most of which are much shorter lived than actinides. It has long been recognized that the major products of TBP radiolysis are hydrogen, methane, and dibutylphosphoric acid (HDBP), with monobutylphosphoric acid (H2MBP) and phosphoric acid produced in lesser amounts, but increasing with prolonged exposure without cleanup. Dibutylphosphoric acid is a major radiolytic product with ion-exchange extraction properties (Egorov, 1986; Zilberman *et al.*, 2002). The radiation chemistry of TBP was recently reviewed (Mincher *et al.*, 2008; 2009).

Many of the extractants applied in the post-PUREX separation stages of advanced nuclear fuel cycle concepts are functionalized aromatic compounds. Their irradiation in the form of a nitric acid saturated organic solvent and in the presence of aqueous nitric acid may result in aromatic nitration reactions. This may lead to degradation or formation of different

bonds and, actually, new coordination chemistry between the metal of interest and the ligands. This may have adverse effects on solvent extraction. Dependent on the dose and LET of irradiation, different effects are possible. The degradation of ligand or extracted complexes doesn't have to be progressive. For extraction of Am^{3+} with diamidic dipicolinates, it was observed that extraction yields first increased with low radiation doses, then with increased dose significantly dropped (Lapka *et al.*, 2010). Stronger binding also may lead to difficulties in stripping, and in such a way, to lower separation yields than desired.

2.5   Future trends

It has been more than 65 years since the first reactors and huge chemical separation plants at Hanford were constructed. Since the first industrial-scale separations of Pu began in December 1944, fundamental studies of the chemistry, physics, and nuclear properties of Pu and other actinides have advanced understanding of their properties. Actinide studies also have had a significant influence on the development of all other aspects of chemistry, physics, and engineering. Additionally, from the very beginning, nuclear science and technology have been inextricably linked to the major political decisions that shaped history of the world and future global trends.

Advances in actinide chemistry will certainly drive (or at least inform) the development of future separation methods. An enhanced understanding of the properties, behavior, and interactions of actinides and fission products in both the environmental or irradiated fuel chemical matrices is just as essential today as the debated issues, such as whether to operate closed or open fuel cycle or opening of long-term radioactive waste repositories.

Both plutonium and neptunium have very rich redox chemistry. This redox chemistry is important in the processing of nuclear fuels and in waste management. Owing to similar redox potentials for Pu(III, IV, VI) and Np(IV–VI) and their pH-dependent solubility, a great variety of redox reactions are used in Pu and Np separation and purification processes and in analytical procedures in acid. Research on redox reactions is expanding into carbonate and alkaline media, chloride brines, taking into account the presence of other complexing agents (particularly carbonate/bicarbonate), inorganic Pu oligomers, and other low solubility or insoluble species (Zr-Mo). The comparative inaccessibility of the upper oxidation states of Am amplifies the difficulty of developing advanced closed loop fuel cycles to support actinide transmutation. Research into redox chemistry will continue as it opens the door for separation of other actinides (e.g., Am) in a higher oxidation state than the typical 3+. Physicochemical enhancement

of fuel dissolution processes (electrochemistry, microwave, photo-irradiation, H_2O_2 oxidation) is another fast-expanding area of investigation.

Experimental investigation of actinide chemistry is a quite complex task. The complexity arises from both the radioactive and toxic nature of plutonium and other actinides. However, recent advances in science offer new methods of investigation. For example, synchrotron studies have provided evidence for new solid oxide phases having stoichiometry previously believed not to exist. Since its development in the early 1970s, synchrotron-based X-ray absorption fine structure spectroscopy (XAFS) has proven to be a versatile probe for studying the local environments of cations in a variety of materials (Den Auwer *et al.*, 2000). The structural information provided by XAFS includes average interatomic distances and the number and chemical identities of neighbors within 5–6 Å of a selected cation; characterization of self-aggregation phenomena and micellar behavior of actinide complexes in extraction systems (Antonio *et al.*, 2008), and suggests new catalytic reactions for Pu materials and mechanistic pathways for important chemical changes.

Quadrupole ion trap mass spectrometry, Fourier transform ion cyclotron resonance mass spectrometry (FT-ICR-MS) and traveling wave ion mobility mass spectrometry offer new approaches for probing uniquely the vapor phase chemistry of f-elements and their complexes by controlling individual metal identities for subsequent exotic reactions with special reagents. Laser ablation studies with Pu have revealed unique oxide clusters in the gas phase. The multitude of clusters found with Pu contrasts with the scarcity of clusters observed for Ce (Gibson, Haire, 2001; Aubriet *et al.*, 2009). Sensitive high-temperature mass-spectrometric studies have provided evidence for the existence of a previously unknown gaseous molecule, which has been assigned as PuO_3 and even PuO_4. These volatile gaseous materials offer the prospect that they may also serve as precursors of other new solid phases. The best redox compatibility of Pu was shown for Ce-Pu and U-Pu clusters (Gibson, Haire, 2003).

Recent scientific investigations using advanced techniques and technologies offer unique scientific opportunities and challenges to elevate our knowledge and understanding of actinide chemistry to a new level. Future trends in fundamental chemistry of actinides will be focused on their physicochemical properties and behavior in different matrices: solid, gaseous, aqueous and non–aqueous liquid using modern equipment and techniques, supported by computational modeling methods. A better understanding of Pu behavior in these systems will be applicable to resolving current and future problems related to separations and processing, long-term stewardship, facility retirement, environmental restoration, waste form development, and waste site performance. Although the separation of plutonium

will remain controversial into the foreseeable future, research will continue to develop better separation methods (Hoffman, 2002).

From the very beginning, separations – precipitation/coprecipitation, ion-exchange, solvent extraction – have played a crucial role in the development of nuclear chemistry and discovery of transuranic elements. While the small-scale, laboratory analytical separations require very specific and efficient methods, the large-scale industrial technologies usually work quite well with less specific materials, but more robust process design. In process applications lower single-stage separation yields can be compensated by repeating steps, recycling of materials and a full or semi-automation of the processes. Such enhancements also result in a smaller volume of processing waste and are labor, time and cost-economical. Hence, the future development, will be focused on group separation technologies, with post-processing refinements and adjustments of properties of the desired products.

2.6   Sources of further information and advice

Fundamental chemistry of actinides has been reviewed a few times during the past decade. The benchmark book in recent years is *The Chemistry of the Actinide and Transactinide Elements*, a five-volume work edited by Norman M. Edelstein, Jean Fuger and Lester R. Morss, and published by Springer, 2006. The last, sixth volume was released in 2010. It is a contemporary and definitive compilation of chemical properties of all of the actinide elements, especially of the technologically important elements uranium and plutonium, as well as the transactinide elements. In addition to the comprehensive treatment of the chemical properties of each element, this book has specialized and definitive chapters on electronic theory, optical and laser fluorescence spectroscopy, X-ray absorption spectroscopy, organoactinide chemistry, thermodynamics, magnetic properties, the metals, coordination chemistry, separations, and trace analysis. Each chapter was written by a team of authors who are recognized experts in their specialty. All chapters represent the current state of research in the chemistry of these elements and related fields. It expounds on topics in actinide science that are undergoing rapid scientific developments and that are germane to the safe development of nuclear energy in the 21st century, from nuclear fuels to the environmental science and management of waste, and this text refers to this book several times, especially to Chapters 15, 23 and 24 (properties, solution chemistry and separations, respectively).

Organometallic and Coordination Chemistry of the Actinides (Springer, 2008), edited by T.E. Albrecht-Schmitt, pages presents critical reviews of the present position and future trends in modern chemical research concerned with chemical structure and bonding. It contains short and concise reports, each written by the world's renowned experts.

The book *Recent Advances in Actinide Science* edited by R. Alvarez, N.D. Bryan, and I.May (Royal Society of Chemistry, 2006), in six sections (Analysis, the Environment and Biotransformations; Coordination and Organometallic Chemistry; Heavy Elements; Nuclear Fuels, Materials and Waste Forms; Separation and Solution Chemistry; and Spectroscopy and Magnetism) covers more than 200 presentations from leading scientists, presented at the international conference "Actinides 2005" Conference, held at the University of Manchester, UK in July 2005.

Structural Chemistry of Inorganic Actinide Compounds (Elsevier, 2007, edited by Krivorichev, S.V., Burns, P.C. Tananaev, I.G.), is a collection of 13 reviews on structural and coordination chemistry of actinide compounds. Within the last decade, these compounds have attracted considerable attention because of their importance for radioactive waste management, catalysis, ion-exchange and absorption applications, etc. Synthetic and natural actinide compounds are also of great environmental concern as they form as a result of alteration of spent nuclear fuel and radioactive waste under Earth surface conditions, during burn-up of nuclear fuel in reactors, represent oxidation products of uranium mines and mine tailings, etc. The actinide compounds are also of considerable interest to material scientists due to the unique electronic properties of actinides that give rise to interesting physical properties controlled by the structural architecture of respective compounds.

Advances in Plutonium Chemistry, 1967–2000 (American Nuclear Society, 2002), is a multi-authored review of advances in plutonium chemistry from 1967 to 2000, documenting the advances in understanding of plutonium chemistry over the more than thirty years since the publication of J. M. Cleveland's *The Chemistry of Plutonium*. The book is written by internationally recognized experts in plutonium science, it addresses both the theoretical interpretations and fundamental properties of plutonium. The detailed technical content is framed together by an impressive and thoughtful summary by the senior editor, D. Hoffman.

The ACS Symposium Series contains high-quality, peer-reviewed books developed from the ACS technical divisions' symposia. Each volume is a collection of chapters carefully edited by an internationally recognized leader, and chapters are written by experts in the field as invited contributions, usually presented to their peers at the symposia of the ACS annual meetings. The series covers a broad range of chemistry topics. One of the recent volumes, *Separations for the Nuclear Fuel Cycle in the 21st Century* (Ed. Gregg J. Lumetta, Kenneth L. Nash, Sue B. Clark, and Judah I. Friese), released in 2006 as 933rd volume, is the proceedings from a symposium titled "Separations for the Nuclear Fuel Cycle" in the 21st century which was held in March 2004 and focused on assessing the current state-of-the art in nuclear separations science and technology, and on identifying R&D directions

required to enable nuclear separations to meet 21st century demands for waste minimization, environment protection, safety, and security. It was the fifth symposium series devoted to nuclear and radiochemistry. It covers the past 20 years between the previous proceedings, *Radioanalytical Methods in Interdisciplinary Research: Fundamentals in Cutting-Edge Applications*, volume 868 (released in 2003 and edited by C. A. Laue and K.L. Nash) and *Plutonium Chemistry* (Vol. 216; 1983; edited by W.T. Carnall and G. R. Choppin), *Transplutonium Elements – Production and Recovery* (Vol. 161; 1981; edited by J. D. Navratil and W. W. Schulz) and *Actinide Separations* (vol. 117, 1980, edited by J. D. Navratil and W. W. Schulz).

2.7   References

Ahrland, S., Solution chemistry and kinetics of ionic reactions, In: *Chemistry of the Actinide Elements*, 2nd Edn, vol. 2 (eds J. J. Katz, G. T. Seaborg, L. R. Morss), Chapman & Hall, New York (1986) 1480

Albrecht-Schmitt, T. E., Ed. Organometallic and coordination chemistry of the actinides, *Struct Bond* 127 (2008) 1–85

Antonio, M. R., Soderholm, L., Williams, C. W., Blaudeau, J. P., Bursten, B. E., *Radiochim. Acta* 89 (2001) 17

Antonio, M. R., Chiarizia, R., Gannaz, B., Berthon, L., Zorz, N., Hill, C., Cote, G., *Separ. Sci. Techn.* 43(9 & 10) (2008) 2572

Aubriet, F., Gaumet, J. J., de Jong, W. A., Groenewold, G. S., Gianotto, A. K., McIlwain, M. E., Van Stipdonk, M. J. Leavitt, C. M., *J. Phys. Chem. A.* 113 (2009) 6239

Blake, P. C., Edelstein, N. M., Hitchcock, P. B., Kot, W. K., Lappert, M. F., Shalimoff, G. V., Tian, S., *J. Organomet. Chem.* 636 (2001) 124

Burney, G. A., Harbour, R. M., *Radiochemistry of Neptunium*, National Academy of Sciences, Technical Information Center, US Atomic Energy Committee, 1974

Choppin, G. R., *IUPAC Journal* (1971) 1198

Choppin, G. R. Covalency in f-element bonds. *J. Alloys Compounds* 344 (2002) 55–5

Choppin, G. R., Complexation of Metal Ions, In: J. Rydber, M. Cox, C. Musikas, G. R. Choppin, *Solvent Extraction Principle and Practice*, Marcel Dekker, Inc., NY, Basel, 2004

Choppin, G. R., Graffeo, A. J., *lnorg. Chem.* 4 (9) (1965) 1254

Choppin, G. R., Jensen, M. P., Actinides in Solution: Complexation and Kinetics, In: *The Chemistry of the Actinides and Transactinides*, eds L. R. Morss, N. M. Edelstein and J. Fuger, Springer, 2006

Choppin, G. R., Labonne-Wall, N., *J. Radioanal. Nucl. Chem.* 221 (1997) 67

Choppin, G. R., Rao, L. F., *Radiochim. Acta.* 37 (1984) 143–6

Choppin, G. R., Strazik, W. F., *Inorg. Chem.* 4 (9) (1965) 1250

Choppin, G. R., Wong P. J., *Aquatic Geochemistry* 4 (1998) 77

Clark, D. L., Hecker, S. S., Jarvinen, G. D., Neu, M. P., Plutonium, In: *The Chemistry of the Actinides and Transactinides*, eds L. R. Morss, N. M., Edelstein and J. Fuger, Springer, 2006

Cohen, D., Taylor, J. C., *J. Inorg Nuclear Chem.* 22 (1961) 151

de Carvalho H. G., H. Yagoda, *Phys. Rev.* 88 (1952) 273–278

Den Auwer, C., Grigoriev, M., Madic, C., Presson, M. T., Nierlich, M., Thuery, P., David, F., Hubert, S., Drew, M. G. B., Hudson, M. J., Iveson, P. B., Russell, M. L., In: *Speciation, Techniques and Facilities for Radioactive Materials at Synchrotron Light Sources Workshop Proceedings*, Grenoble, France, 10–12 September 2000; Nuclear Energy Agency Organization for Economic Co-Operation and Development, 2000

Diamond, R. M., Street, K., Jr, Seaborg, G. T., *J. Am. Chem. Soc.* 76 (1954) 1461

Dobler, M., Guilbaud, P., Dedieu, A., Wipff, G., *New J. Chem.* 25 (2001) 1458

Donnet, L., Adnet, J. M., Faure, N., Bros, P., Brossard, P. H. Josso, F., The Development of the SESAME Process, Fifth Information Exchange Meeting on Actinide and Fission Product Partitioning and Transmutation, Belgium, Mol, 1998

Douglas, M., Clark, S. B., Utsunomiya, S., Ewing, R. C., *J. Nucl. Sci. Techn.* Supplement 3 (2002) 504

Drake, V. A. Extraction of Neptunium, *Science and Technology of Tributyl Phosphate* Volume III, Part II, eds. W. W. Schulz, J. D. Navratil, CRC Press (1990) p. 123

Edelmann, F. T., *Coordination Chemistry Reviews* 250 (2006) 2515

Edelstein, Thermodynamic of Actinides, In: *The Chemistry of the Actinides and Transactinides*, eds L. R. Morss, N. M. Edelstein and J. Fuger, Springer, 2006

Egorov, G. F., *Radiatsionnaya Khimiya Ekstraktsionnykh Sistem (Radiation Chemistry of Extraction Systems)*, Moscow: Energoatomizdat, 1986

Ensor, D. D., Choppin, G. R., *J. Inorg. Nucl. Chem.* 42 (1980) 1477

Ewing, R. C., Wang, L., *Reviews in Mineralogy and Geochemistry* 48 (2002) 673

Frenkel, V. Ya., Kulyako, Yu. M., Chistyakov, V. M., Lebedev, I. A., Myasoedov, B. F., Timofeev, G. A., Erin, E. A., *J. Radioanal. Nucl. Chem.* 104 (4) (1986) 191

Fournier, J. M., *J. Phys. Chem. Solids* 37 (1976) 235

Gibson, J. K., Haire, R. G., *J, Alloys Compounds* 322 (1–2) (2001) 143

Gibson, J. K., Haire, R. G., *Radiochimica Acta* 91 (2003) 441–448

Gibson, J. K., Haire, R. G., *J. Alloys Compounds* 363 (1–2) (2004) 115

Gordon, S., Mulac, W., Schmidt, K. H., Sjoblom, R. K., Sullivan, J. C. *Inorg. Chem.* 17 (1978) 294–296

Haire, R. G., Heathman, S., Idiri, M., Le Behan, T., Lindbaum, A., Rebizant, J., *Phys. Rev. B.* 67 (2003) 134101

Hart, E., *Radiation Res.* 1 (1954) 53

Hay, P. J., Martin, R. L., Schreckenbach, G., *J. Phys. Chem. A.* 104 (2000) 6259

Hitchcock, B., Lappert, M. F., Maron, L. D., Protchenko, V., *Angew. Chem.* 120 (8) (2008) 1510

Hoffman, D. C., Future directions, In: *Advances in Plutonium Chemistry* 1967–2000, ed. Hoffman, D. C., American Nuclear Society, Quantum Publishing Services, Inc., Bellingham, WA (2002) p. 308

Hu, Y., Navrotsky, A., Chen, C.-Y., Davis, M. E., *Chem. Mater.* 7 (10) (1995) 1816

Kazanijan, A. R., Miner, F. J., Brown, *et al.*, *Trans. Faraday Soc.* 66 (1970) 2192

Keogh, D. W., Actinides: inorganic and coordination chemistry. In: *Encyclopedia of Inorganic Chemistry*, eds. R. B., King, R. H., Crabtree, John Wiley & Sons, Chichester, England (2005) Vol. 1, p. 2

Khalili, F. I., Choppin, G. R., Rizkalla, E. N., *Inorg. Chim. Acta* 143 (1988) 131

Lapka, J. L., Paulenova, A., Wade, E. C., Effect of gamma-radiolysis on the synergistic extraction behavior of diamides of dipicolinic acid and chlorinated cobalt dicarbollide, In: *Proceedings of the 11th OECD NEA Information Exchange Meeting on Actinide and Fission Product Partitioning and Transmutation*, San Francisco, CA, 1–4 November (2010)

Matonic, J. H., Scott, B. L., Neu, M. P., *Inorg. Chem.* 40 (2001) 2638

Matonic, J. H., Neu, M. P. A., Enriquez, E., Paine, R. T., Scott, B. L., *J. Chem. Soc. Dalton Trans.* 11 (2002) 2328

Matsika, S., Pitzer, R. M., *J. Phys. Chem. A*. 104 (2000) 4064–8

Miles, J. H., Separation of plutonium and uranium, In: *Science and Technology of Tributyl Phosphate* Volume III, Part II, eds. W. W. Schulz, J. D. Navratil, CRC Press (1990) p. 123

Mincher, B. J., Modolo, G., Mezyk, S. P., *Solvent Extr. Ion. Exch.* 27 (2008) 72

Mincher, B. J., Elias, G., Martin, L. R., Mezyk, S. P., *J. Radioanal. Nucl. Chem.* 282 (2009) 645

Morss, L. R. Thermochemical properties of yttrium, lanthanum, and the lanthanide elements and Ions, *Chem. Rev*. 76 (1976) 827

Moulin, J. P., *Oxidation – Reduction Kinetics of Neptunium in Nitric Acid Solution*, Comm. a l'Energie At. Rep. CEA-R-4912, Fontenay-aux-Roses, France, 1978; INIS Atomindex, 451540

Mozumder, A., *Fundamentals of Radiation Chemistry*, Elsevier (1999) p. 392

Nash, K. L. Final Report, WSU 2008: Characterization Of Actinides In Simulated Alkaline Tank Waste Sludges and Leachates, Project Number DE-FG02-04ER63757 OSTI, 2008

Nash, K. L. Final Report, WSU 2009: Selective Separation of Trivalent Actinides from Lanthanides by Aqueous Processing with Introduction of Soft Donor Atoms, Project Number DE-FC07-05ID14644 OSTI, 2009

Nash, K. L., Sullivan, J. C., Kinetics and mechanisms of actinide redox and complexation reactions. In: *Advances in Inorganic and Bioinorganic Reaction Mechanisms*, ed. A. G. Sykes Academic Press, New York (1986) Vol. 5 p. 185

Nash, K. L., Sullivan, J. C., Kinetics of complexation and redox reactions of lanthanides in aqueous solutions, In: *Handbook on the Physics and Chemistry of Rare Earths*, eds K. A. Gschneidner, Jr., L. Eying, G. R. Choppin, G. H. Lander, Elsevier Science, Amsterdam (1991) Vol. 15 p. 287

Navrotsky, A., Trofymluk, O., Levchenko, A., *Chem. Rev.* 109 (9) (2009) 3885

Newton, T. W., ERDA Critical Review Series *The Kinetics of the Oxidation-Reduction Reactions of Uranium, Neptunium, Plutonium, and Americium in Aqueous Solutions* (TID-26506: NTIX, Springfield, VA (1975)

Oelkers, E. H., Montel, J.-M., *Elements* 4 (2008) 113

Paulenova, A., Clark, S. B., *Correlations of Thermodynamic Parameters for F-Elements with Organic Acids: Implications for Coordination Geometry*, Migration 2009, Kennewick, WA, September (2009)

Petrovic, I., Navrotsky, A., Davis, M. E., Zones, S. I., *Chem. Mater.* 5 (12) (1993) 1805

Rao, L. F., Choppin, G. R., Complexation of pentavalent and hexavalent actinides by fluoride. *Radiochim. Acta* 37 (1984) 143

Rao, L. F., Tian, G., *J. Chem. Thermodynamics* 40 (2008) 1001

Redlich, O., Duerst, R. W.,· Merbach, A., *J. Chem. Physics* 49 (1968) 2986

Rydberg, J., Liljenzin, J-O., Choppin, G. R., Radiation Effects on Matter, Chapter 7, In: *Radiochemistry and Nuclear Chemistry*, 3rd Edition, Elsevier, Amsterdam, 2001, p. 167

Sales, B. C., Boatner, L. A., *Science* 226 (1984) 45

Seaborg, G. T. (ed.) *Transuranium Elements. Benchmark Papers in Physical Chemistry and Chemical Physics*, vol. 1, Dowden, Hutchinson&Ross, Stroudsburg, PA (1978)

Seaborg, G. T., Katz, J. J., Manning, W. M. (eds) (1949) *The Transuranium Elements: Research Papers*, Natl. Nucl. En. Ser., Div. IV, 14B, McGrawHill, New York. p. 1492

Siddall, T. H. III, *J. Inorganic. Nucl. Chem.* 13 (1960) 151

Siddall, T. H., Dukes, E. K., *J. Am. Chem. Soc.* 81 (1959) 790

Smith, R. M., Martell, A. E., NIST Critically Selected Stability Constants of Metal Complexes Database; NIST Standard Reference Database 46; Version 8.0, NIST, Gaithersburg, MD, 2004

Spencer, S., Gagliardi, L., Handy, N. C., Ioannou, A. G., Skylaris, C. K., Willetts, A., Simper, A. M. *J. Phys. Chem. A*. 103 (1999) 1831–7

Spirlet M. R., Rebizant J., Apostolidis C., Kanellakopulos B., Dornberger E., *Acta Crystallogr. C* 48 (1992) 1161

Sullivan, J. C., Gordon, S., Mulac, W. A., Schmidt, K. H., Cohen, D., Sjoblom, R., *Inorg. Nucl. Chem. Lett.* 12 (1976a) 599–601

Sullivan, J. C., Gordon, S., Cohen, D., Mulac, W., Schmidt, K. H., *J. Phys.Chem.* 80 (1976b) 1684–6

Sullivan, J. C., Morss, L. R., Schmidt, K. H., Mulac, W. A., Gordon, S., *Inorg. Chem.* 22 (1982) 2338–9

Szabo, Z., Toraishi, T., Vallet, V., Grenthe, I., *Coordination Chemistry Reviews* 250 (2006) 784

Tsushima, S., Suzuki, A. J., *Mol. Struct.* (THEOCHEM) 529 (2000) 21

Utsunomiya, S., Wang, L. M., Douglas, M., Clark, S. B., Ewing, R. C., *American Mineralogist* 88 (2003) 159

Vladimirova, M. V., Alpha Radiolysis of Aqueous Solutions, *Russian Chem. Rev*. 33 (4) (1964) 212

Walch, P. F., Ellis, D. E., *J. Chem. Phys.* 65 (1976) 2387–92

Weber, W. J., Navrotsky, A., Stefanovsky, S., Vance, E. R., Vernaz, E., *MRS Bull.* 34 (2009) 46

World Nuclear Association, WNA Nuclear Century Outlook, downloadable at http://www.world-nuclear.org/outlook/clean_energy_need.html; World Nuclear Association, London, UK, 2010

Zachariasen, W. H., *J. Inorg. Nucl. Chem.* 35 (1973) 3487

Zielen, A. J., Sullivan, J. C., Cohen, D., *J. Inorg. Nucl. Chem.* 7 (1958) 378

Zilberman, B. Ya., Makarychev-Mikhailov, M. N., Saprykin, V. F., *Radiochemistry* 44 (3) (2002) 274

Chemical engineering for advanced aqueous radioactive materials separations

S. ARM and C. PHILLIPS, EnergySolutions, LLC, USA

Abstract: Almost every facet of chemical engineering is impacted when processing material with radioactive and fissile properties. Different containment concepts, passive or secure cells and canyons, have evolved in Europe and the USA, respectively, and have profoundly impacted equipment and processing concepts. The special features associated with filtration, ion exchange and solvent extraction processes and equipment are aimed at reducing maintenance requirements, simplifying operations and reducing plant footprint and height. Equipment materials considerations include corrosion resistance and special measures required to control criticality and radiation damage. Process intensification and transportable equipment and processes are the two important trends associated with chemical engineering for advanced aqueous radioactive material separations.

Key words: filtration, ion exchange, solvent extraction, reprocessing, radioactive waste processing.

3.1 Introduction

3.1.1 Overview of the need for radioactive materials separations

Aqueous processing of radioactive materials commenced in the USA in the late 1940s, when initially precipitation processes, and subsequently solvent extraction processes, were used to separate weapons grade plutonium from irradiated nuclear fuel. The process of choice for this Manhattan Project application evolved to be the PUREX solvent extraction process where a solvent consisting of tri-butyl phosphate dissolved in a hydrocarbon diluent is contacted with a solution of the dissolved nuclear fuel in nitric acid to extract uranium and plutonium, leaving the fission products and other transuranics in the aqueous high level waste stream. The uranium and plutonium were then separated in a further stage of solvent extraction by chemically manipulating the valence state of the plutonium so as to decrease it extractability into TBP. This processing scheme came to be known as reprocessing of used nuclear fuel (UNF).

The UK and France refined this basic PUREX process and constructed a second generation of reprocessing plants in the 1960s, and similar facilities

were constructed at various scales in Belgium, Germany, Japan, Russia, China and India. During the 1980s a third generation of civil reprocessing plants were designed and constructed in the UK and France and these incorporated significant improvements to plant chemistry and waste handling so as to reduce environmental discharges of radioactivity to essentially zero. They also were designed to reprocess higher burnup fuel (typically 40–50 GWD/ton) and to mix the non-weapons grade plutonium product with some of the uranium to produce mixed oxide (MOX) fuel for use in the world's Light Water Reactors. In the Thermal Oxide Reprocessing Plant (THORP) in the UK, and in the UP2-800 and UP3 facilities in France, "salt free" reagents are used so that nearly all wastes can be retained in their acid state, evaporated to small volumes and vitrified for long-term safe storage. In THORP, for example, over 99% of the radioactivity in the feed UNF is vitrified and almost all of the remaining 1% is encapsulated in cement. This developed PUREX technology has subsequently been used as the basis for the Rokkasho-Mura reprocessing plant in Japan, which is currently in hot commissioning.

This developed PUREX technology can be said to be the first stage of advanced aqueous processing of radioactive materials and this chapter will explain how nuclear chemical engineering has contributed to the success of these new facilities. In the late 1990s the US National Laboratories started development of a second stage of advanced aqueous processing of UNF. A major aim of this work was to avoid the separation of pure plutonium at any stage in the process so as to reduce the nuclear proliferation risk even further than had been achieved by the IAEA safeguarding of the second generation of reprocessing facilities. Plutonium was either kept with the fission products and other transuranics (the UREX process) or was left mixed with a proportion of the uranium (the NUEX process). Another major aim of this work was to develop new separation and waste handling processes that enabled the minor actinides (principally neptunium, americium and curium) to be kept out of the high level waste and instead to be transmuted by returning them to fast neutron spectrum reactors. This reduces the long-term heat load on the then proposed US national nuclear waste repository so as to extend its capacity.

In parallel with this development of reprocessing technologies, development has been ongoing in the US and Europe on processes and equipment to deal with the legacy wastes from the first and second generation of reprocessing plants. In the US the most pressing issue is the removal and treatment of millions of gallons of high level fission product waste currently stored under alkaline conditions in million gallon tanks at the nuclear reservations at Hanford, Washington and Savannah River, South Carolina. These wastes require cesium, strontium and transuranic removal for optimal management and filtration, ion exchange, and solvent extraction processes

have been developed for this purpose. A range of other waste treatment processes have been developed and are in use, including cement encapsulation, and simple compaction, and facility designs have ranged from permanent large-size concrete shielded cells and canyons to contain the processing equipment, through temporary transportable systems, depending on the amount of waste to be treated and the expected life of the facility.

3.1.2   Chemical engineering for radioactive material separations

Almost every facet of chemical engineering is impacted when processing material with radioactive and fissile properties. The radioactive properties impact plant operations and maintenance where minimizing the radiation dose to workers and the environment has led to the development of process equipment and concepts unique to nuclear chemical engineering. Criticality control is required to handle material with fissile properties, invoking equipment construction material and geometry considerations.

   The purpose of this chapter is to provide the reader with a broad overview of nuclear chemical engineering for aqueous radioactive material separations. It is not the intention here to provide an exhaustive description of every unit operation or facet of chemical engineering employed in processing radioactive material. Rather, the more common chemical engineering operations and equipment are described to exemplify the concepts and features unique to nuclear chemical engineering and on how chemical engineering is impacted by radioactive material properties. Wherever possible, reference is made to operating plant for examples.

   Nuclear chemical engineering for advanced aqueous radioactive material separations is a broad subject area. Different containment concepts, passive or secure cells and canyons, have evolved in Europe and the USA, respectively, and are discussed first, since they profoundly impact equipment and processing concepts. The special features associated with separations equipment are then described with reference to solid-liquid separation, ion exchange and solvent extraction unit operations. Equipment materials considerations not only include corrosion resistance but also the special measures required to control criticality and radiation damage. Finally, future trends in the aqueous processing of radioactive material are discussed.

3.2   Containment concepts

This section focuses on the containment of plant for processing radioactive material and provides necessary background for subsequent discussion on equipment. Plants processing radioactive material require significant biological shielding to protect workers and the environment from harmful

doses of radiation. Phillips (2007) has provided a comprehensive review of the use of the two main containment concepts: canyons and passive secure cells (PSCs). Radioactive material processing plants using PSCs and canyons as containment have been successfully built and operated in Europe and the USA.

Canyons are used with overhead and polar cranes within the enclosure, typically shielded windows in the walls, remote manipulators and similar equipment installed. These allow operations, maintenance work and the replacement of equipment to be carried out remotely. Canyons can be constructed with no windows and rely entirely on internal cameras, or they can have shielded windows for internal viewing on at least one side and many have windows on both sides. Lighting units in the cell walls allow bulbs to be replaced from outside the canyon. Canyons are typically used to contain predominately mechanical handling equipment that requires maintenance and physical control, although in the USA they are used also for chemical plant and equipment which is connected by removable pipe-work "jumpers" to allow remote removal and replacement of equipment items. A good example of a mechanical equipment canyon is the one containing Advanced Gas-cooled Reactor (AGR) UNF dismantling equipment at the Sellafield nuclear facility in the UK (Fig. 3.1). This canyon allows the
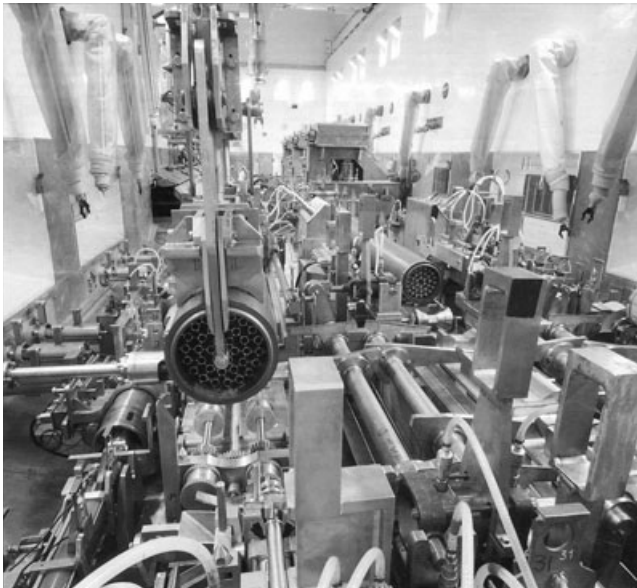
3.1 AGR UNF dismantling canyon, Sellafield, UK. Source: Nuclear Decommissioning Authority ("NDA"), copyright: Nuclear Decommissioning Authority ("NDA").

remote removal of individual fuel pins from the graphite containment prior to reprocessing.

PSCs are used, on the other hand, when the cell is to be employed predominately for process plant with mainly pipes, tanks, pumps, separation and filtration equipment. PSCs are located separately and linked by shielded pipe enclosures, they do not normally surround canyons. There are three types of PSC. Type 1 PSCs contain plant items with no maintainable moving parts, and the pipework, vessels and other process equipment are all welded and radiographed to nuclear standards. The use of Type 1 PSCs has led to the development of a range of liquid transfer and liquid redirection equipment plus measurement devices that have no moving parts and thus can be permanently installed in the cell for the facility lifetime (Phillips 2006). Type 2 PSCs contain plant items with slowly rotating or intermittently moveable parts, but all maintainable items such as motors and gearboxes are located outside the cell, with sealed through-cell-wall drives. Type 3 PSCs are a newer design, dating from the 1980s, in which all in-cell equipment items with moving parts that require maintenance are designed as removable modules.

With all PSCs, there is no expectation for cell entry, or manipulation of the equipment within it, during the life of the facility. Nevertheless access doors are usually provided and, because there are no pipework jumpers to spill small amounts of radioactive liquid when they are removed, the internal surfaces of PSCs remain uncontaminated. Therefore, the radiation levels in PSCs are usually very low after the process pipework is flushed.

The Enhanced Actinide Removal Plant (EARP) at Sellafield, UK provides a good example of the use of type 3 PSCs (Fig. 3.2). The housings for the equipment are permanently welded into the in-cell pipework, and the equipment modules can be withdrawn from these housings, through

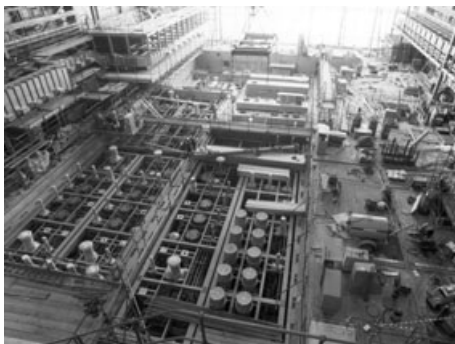*3.2* Type 3 PSCs under construction at EARP, Sellafield, UK. Source: Nuclear Decommissioning Authority ("NDA"), copyright: Nuclear Decommissioning Authority ("NDA").
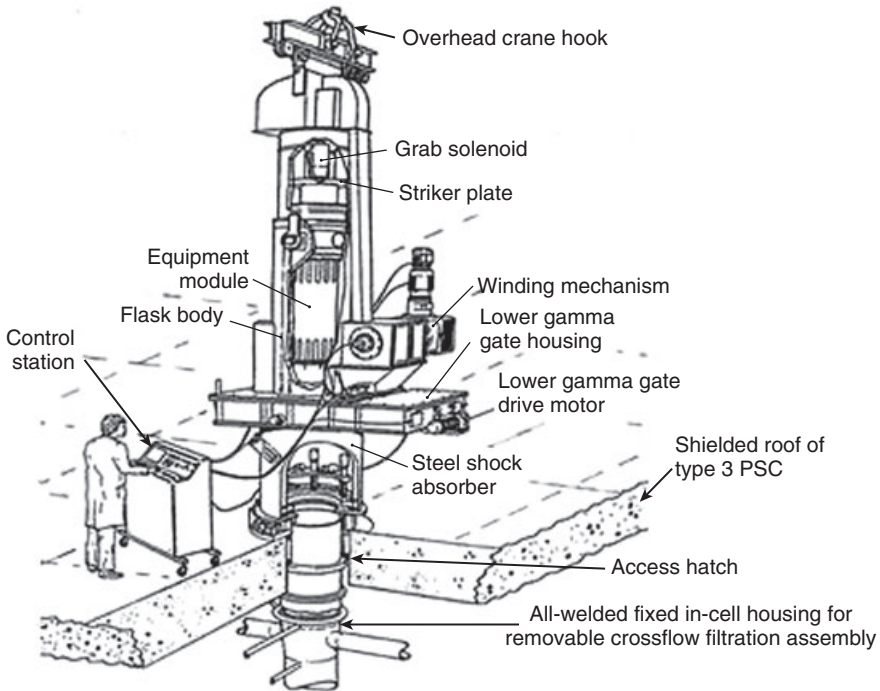
3.3 Type 3 PSC with flask in place on cell top. Source: Nuclear
Decommissioning Authority ("NDA"), copyright: Nuclear
Decommissioning Authority ("NDA").

removable hatches in the PSC roof, into shielded steel "flasks" (Fig. 3.3). The flasks are moved to a maintenance cell where the modules are repaired or prepared for disposal. The process is reversed to re-install the modules back into service in the PSC. Equipment modules can contain a wide range of process equipment including liquid pumps, valves, filter units, centrifugal contactors, and instruments. It is usual practice to keep a range of spare modules so that in the event of failure a replacement can be rapidly installed and plant downtime kept to a minimum.

3.3   Separations equipment

3.3.1 Solid-liquid separation

A variety of solid-liquid separation systems have been deployed in the nuclear industry for a range of purposes. Most systems have had their design adapted from standard chemical industry practice so as to facilitate their operation in hot cells or gloveboxes.

Centrifuges

Centrifuges are typically used to separate undissolved fission product particles and fuel cladding debris from the dissolved nuclear fuel prior to reprocessing. A typical unit, used in the Thermal Oxide Reprocessing Plant (THORP) at Sellafield in the UK, and similar to the units used at the La Hague nuclear site in France, is shown in Fig. 3.4. This has a rotating inner bowl that spins at several thousand rpm contained within an outer container. As was described in Section 3.2 on the Type 3 PSC, the outer
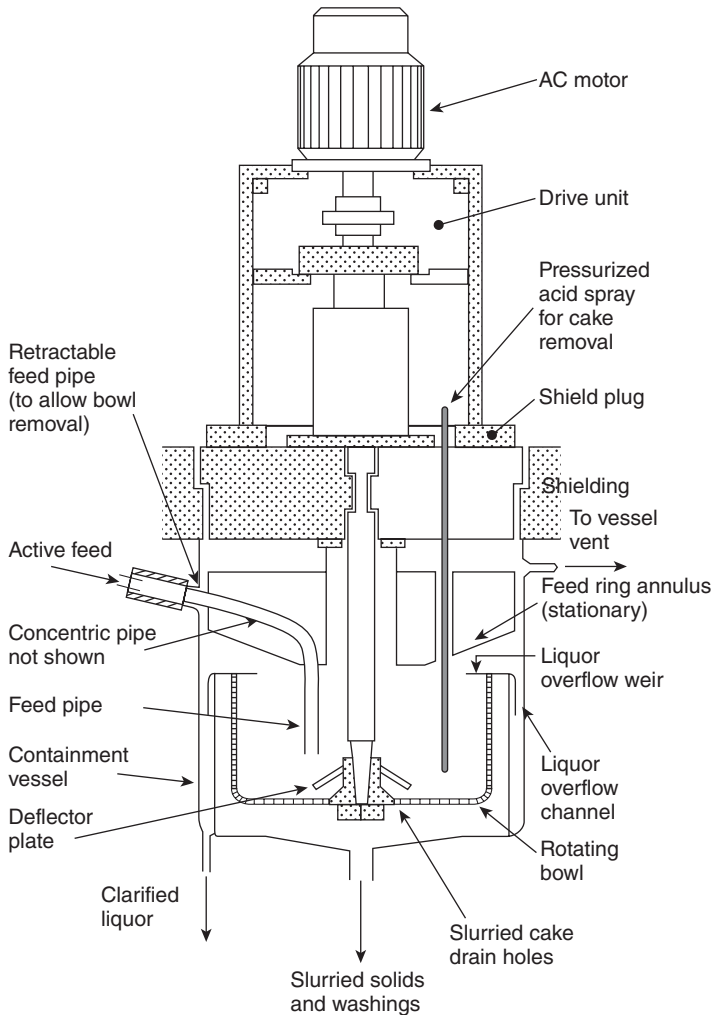
3.4 Solids removal centrifuge.

container is permanently welded into the in-cell pipework, while the inner bowl is suspended on a shaft from the cell top and can be withdrawn through a cell roof plug into a flask if this is ever needed. The motor and gearbox are located outside the cell and so can readily be maintained without breaking the cell containment.

This unit is operated "batch continuously" with the dissolved nuclear fuel solution ("dissolver liquor") being fed into the inner bowl for an extended period, with the clarified product overflowing from the top of the bowl, over a weir inside the outer container, so that it then flows from the bottom of the outer container to a receipt tank.

The removed solids progressively build up on the inner bowl wall and, when this layer reaches a set thickness, the feed of dissolved fuel is stopped and the centrifuge changed to solids recovery mode. In this mode, high pressure water jets from a spray lance inside the inner bowl remove the solids "cake" and slurry it from the bottom of the bowl into a separate receiving tank. Feed of the dissolved fuel is then restarted and the cycle is repeated. Two such centrifuges are usually operated together to provide continuous solids removal capability.

Rotary vacuum filters

Rotary vacuum filters are typically used to separate precipitated high value products such as plutonium oxalate from the "mother liquor". An example design of rotary vacuum filter, used routinely over many years at a number of reprocessing plants, is shown in Fig. 3.5.

In this application, plutonium nitrate solution is fed to the precipitator vessels and oxalic acid used to precipitate plutonium oxalate. The resulting slurry is fed via nozzles onto a filter table which is formed of a stainless steel fine mesh and which is rotated at a few rpm. The underside of this mesh table has a vacuum applied to it which draws the mother liquor away from the precipitated solids. As the table rotates the accumulated solids move under a wash station where they are washed with water, and then under a "scraper" system that removes them from the table and collects them in a screw feeder for transfer to the next process stage. By suitably balancing the slurry feed rate and the rotation speed of the table, continuous operation can be achieved. The unit is small and compact enough to be installed within a glovebox for radioactive contamination containment, but it is not suitable for in-cell use so is not used for materials emitting penetrating radiation.

Crossflow filtration

Although crossflow filtration is not a new technique, is it nevertheless one of the more recent applications of filtration used in radioactive processing
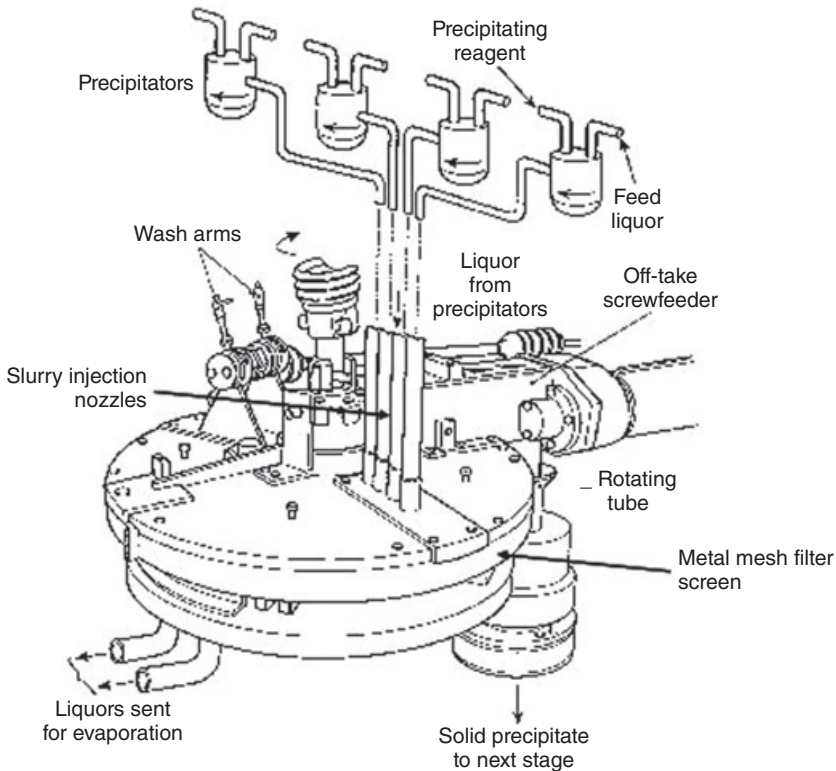
3.5 Rotary vacuum filter arrangement.

environments. Unlike the previous two filtration methods, which produce, in a single pass, solids which are essentially free of the mother liquor, cross-flow filtration produces a concentrated slurry of the solids within the original mother liquor. Successive additions of water or other process fluid and re-filtration steps are necessary to free the solids from the mother liquor.

Crossflow filtration recycles the solid-liquid slurry at high velocity (typically 4 to 5 m/sec) and moderate pressure through a bundle of several hundred parallel sintered stainless steel, or porous graphite, filter tubes, normally arranged in the manner of a shell and tube heat exchanger. The pore size can range from a few hundredths to a few tenths of a micron, depending on the particle size of the slurry. The tubes are typically 1 to 2 meters long and 5 to 6 mm internal diameter. Sintered stainless steel tubes are welded to the end plates to form the tube bundle, while graphite tubes are sealed with elastomer seals.

During each passage of the slurry through the tube bundle, some of the liquid in the feed slurry permeates the pores in the tube and flows into the

"shell side" of the filter unit, which is maintained at a lower pressure than the tube side. Smaller filter tube pore sizes are found to be capable of sustaining higher specific liquid flowrates (or flux) than larger ones. This is because they are less susceptible to blocking by the solid particles. As the slurry is recirculated through the tube bundle it becomes progressively more concentrated. When the desired concentration is reached the filtration is stopped and the concentrated slurry is mixed with water or other washing agent and the filtration cycle is then repeated. These cycles are repeated until the desired degree of separation of mother liquor from the solids is achieved.

Crossflow filtration has been developed and demonstrated for several nuclear waste processing plants that are under design and construction in the USA. At the Savannah River nuclear site in South Carolina, the Salt Waste Processing Facility will use crossflow filtration to treat high level waste from the tank farms prior to cesium-sodium separation and vitrification of the highly active constituents in the Defense Waste Processing Facility (Poirer, 2007). The high level waste is first mixed with mono-sodium titanate (MST) to sorb TRU elements in the waste, and then the MST and solids already present in the waste, are concentrated by crossflow filtration. At the Hanford nuclear reservation in Washington, the Waste Treatment Plant also will use crossflow filtration to concentrate high level waste sludge prior to vitrification (e.g. Geeting, 2006 and Peterson, 2007).

A highly successful nuclear application of crossflow filtration that has been in use since the early 1990s is the Enhanced Actinide Recovery Plant (EARP) at the Sellafield nuclear site in northwest England. In EARP, acidic, TRU-contaminated wastes arising from the "Magnox" reprocessing facility, and which also contain significant quantities of iron, are neutralized to cause the iron and TRUs to co-precipitate. The TRU-contaminated floc is sufficiently separated by crossflow filtration from the solution to facilitate discharge of the permeate to sea. In this application a modified form of filter bundle is used, with the floc inlet and outlet, and the permeate outlet positioned all at the same end of the bundle (Fig. 3.6).

Two stages of ultrafiltration are employed in EARP to optimize the pumping requirements. The de-watered floc required for immobilization and disposal is a thixotropic material with a viscosity of approximately 7 poise, which would require special pumps. Therefore, a two-stage ultrafiltration is employed. Up to 90% of the water is removed from the slurry in the first stage so that a standard pump can be employed to recirculate the slurry. De-watering is completed in a second stage on a smaller slurry volume that consequently uses smaller specialized pumps than if a single stage process were employed.

Backwashing and chemical cleaning with nitric acid removes any floc that is fouling the tubes. However, the membranes are expected to have a finite

Floc inlet→

Floc outlet→

Permeate→

770 membrane tubes

Shell

Tubeside

Shellside

(a)

(b)
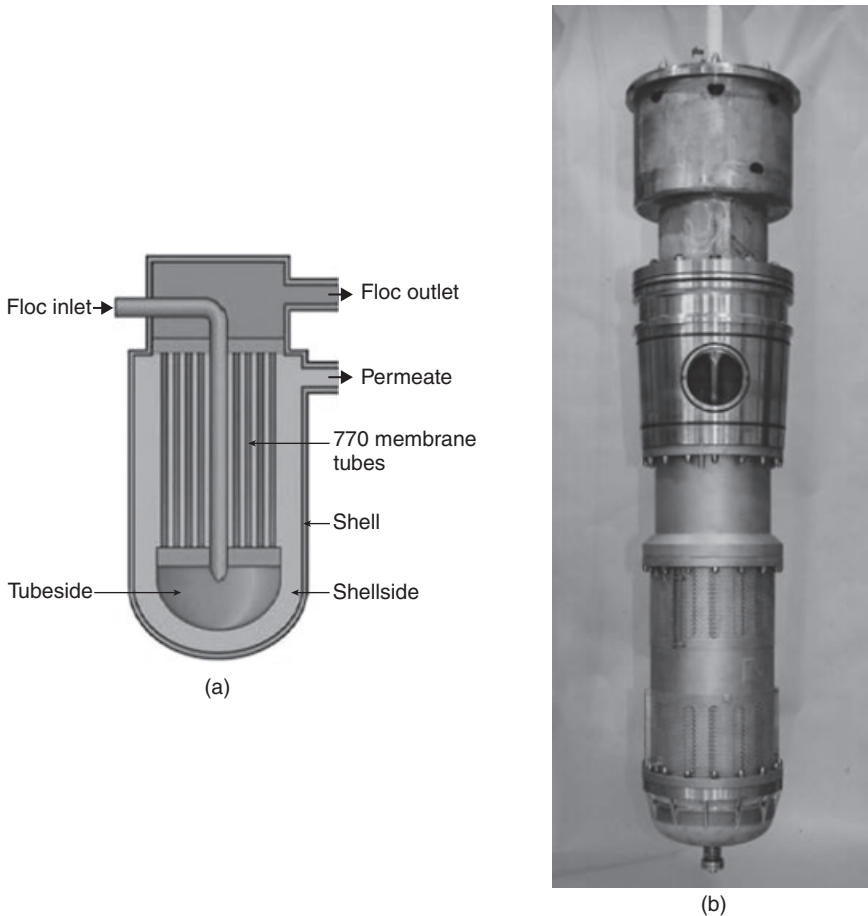
3.6 a and b Schematic representation and photograph of an EARP ultrafilter module. b Source: Nuclear Decommissioning Authority ("NDA"), copyright: Nuclear Decommissioning Authority ("NDA").

life through incomplete cleaning, mechanical damage, wear to the coating and possible blockage of the pores or the tubes themselves. Therefore, the EARP ultrafilter cartridges are specially designed for remote maintenance and replacement (Fig. 3.7), being contained in type 3 PSCs. A fixed housing is permanently built into the plant below the cell roof and thus within the biological shielding. The filter modules fit within these housings and all inlet and outlet ports and seals are incorporated into one plug unit in the module top. This is sealed to the housing by replaceable O-ring seals. When necessary, the complete module, complete with its O-ring seals, can be withdrawn from the housing into a flask positioned above the cell top, and

3.7 Remote replacement of an EARP ultrafilter module. Source: Nuclear Decommissioning Authority ("NDA"), copyright: Nuclear Decommissioning Authority ("NDA").

a replacement module installed into the housing by reversing the process. In EARP, nine modules of ultrafilters containing 800 membrane tubes are used for primary de-watering while two modules of 500 membrane tubes complete de-watering.

Intensified crossflow filtration

The "Spintek" filtration unit is an intensified form of crossflow filtation. Instead of a bundle of porous tubes, the Spintek unit has a series of circular, hollow porous plates made from sintered stainless steel, arranged in a stack on a central hollow post (Fig. 3.8).

The stack is contained within an outer housing into which the slurry to be concentrated is pumped. The stack of plates is spun to increase shear forces across the surface of the plates, and the supernatant from the slurry
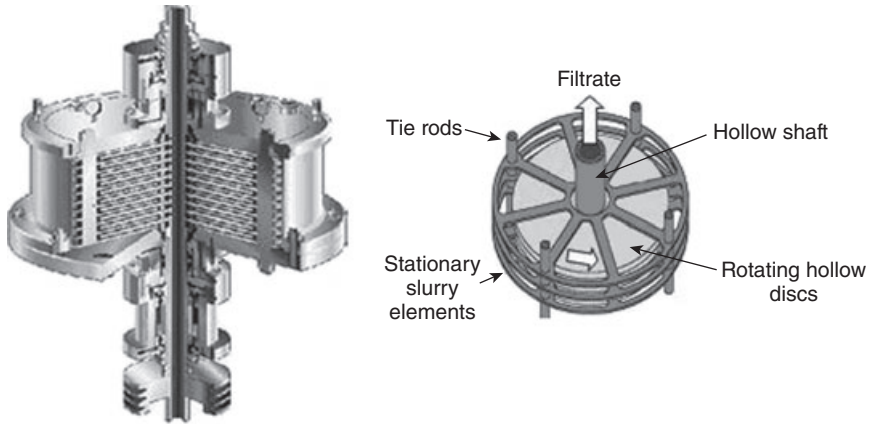
3.8 Spintek crossflow filtration unit.

passes into the center of the hollow plates and exits via the central post. The slurry is thus concentrated and can be recycled through the system until the desired degree of concentration is achieved. Because of the increased shear forces, typical fluxes achieved are some ten times higher than those in conventional crossflow filtration. The stack of plates can be removed for maintenance or replacement by withdrawing it from the top of the unit, and this arrangement is well suited to installation in a type 3 PSC. At present there has been no industrial plant application of this type of filter system, though it remains under active development (Herman, 2006).

3.3.2   Ion exchange

Ion exchange uses solid porous sorbents that have either anions or cations within the pores that are relatively loosely attached. The cations and anions can be exchanged for anions or cations in a solution that is passed through the ion exchange material. Contact between the solution and the ion exchange material is usually achieved within a column, with the solution flowing either upwards or downwards though the ion exchange bed. Ion exchange is typically employed for separating radionuclides at low concentrations from aqueous effluent streams from radioactive processing facilities, though it has also been used occasionally to carry out bulk separations. Ion exchange materials are categorized into three main types:

* Inorganic. These are typically naturally occurring zeolite and other alumino-silicate minerals with a well-defined crystal lattice structure. They can be selected so that only contaminants with a certain molecular size, that fit within the lattice, are sorbed.

- Organic. These are carbon-based polymeric materials, often known as "resins". They can be porous and sorb species themselves, or they can form a passive substrate that is coated with other materials which are chemically active.
- Specialist. These are inorganic or organic materials which contain "tailored" molecules, such as crown ethers. These molecules have a molecular structure which contains rings enclosing a space that is right-sized for the atoms or molecules of specific contaminating species. Such materials are thus highly specific for such species.

Each type of ion exchange material can also be anionic, capable of sorbing negative ions, or cationic, capable of sorbing positive ions from solution.

Ion exchange process operations fall into two categories.

Once-through

In a once-though ion exchange process, the solution to be decontaminated is passed continuously through the ion exchange bed until the bed becomes saturated with the sorbed contaminant. At this point the ion exchange material is replaced. A good example of an operating once through ion exchange plant is the Site Ion Exchange Effluent Plant (SIXEP) at the Sellafield site in the UK. SIXEP (Fig. 3.9) has been in successful hot operation since 1985 and is designed to remove radioactive cesium and strontium from water, routinely purged from the spent nuclear fuel storage basin.

The ion exchange material used is clinoptilolite, a naturally occurring zeolite that is quite specific for cesium and strontium. These species are sufficiently removed by the SIXEP process for the treated basin purge water to meet regulatory requirements for discharge to the ocean. The basin purge water is first filtered in sand filters before the ion exchange process so as to remove suspended solids and sludges that may otherwise block the ion exchange bed. The pressure vessels for both sand filter and ion exchange duties were produced to a common design to maximize operational flexibility.

The basin purge water feed is introduced to the ion exchange vessel top through a diffuser plate to prevent it channeling through the bed. The decontaminated product is collected through a number of stainless steel wedge wire strainers welded into the dished false bottom. Loaded ion exchange material is periodically discharged from the vessel by fluidizing it with water and then discharging it under pressure through the emptying pipe. A lower fluidizing ring is fitted with tangential spray nozzles used to produce a vortex action to assist emptying of the vessel contents, particularly the final residue. Two higher rings are fitted with radial spray nozzles to assist with breaking up the bed. It is important to discharge as much loaded ion exchange material as possible since any remaining in the column

3.9 The Site Ion Exchange Effluent Plant at Sellafield UK. Source: Nuclear Decommissioning Authority ("NDA"), copyright: Nuclear Decommissioning Authority ("NDA").

will contaminate the product during its subsequent operation after re-filling. Development work on the first SIXEP production vessels enabled the residue remaining in the vessel to be reduced to 0.1%, which was considered well within process requirements.

Sorption and elution

In sorption and elution ion exchange processes the feed solution to be decontaminated is passed through the ion exchange bed until a point somewhat before removal efficiency starts to fall. At this point, feed to the column terminated and the resin is eluted and regenerated to make it ready to process more feed solution. Continuous operation of a sorption and elution process is achieved by processing the feed through a series of columns. Here, the lead column is taken off-line and eluted when the
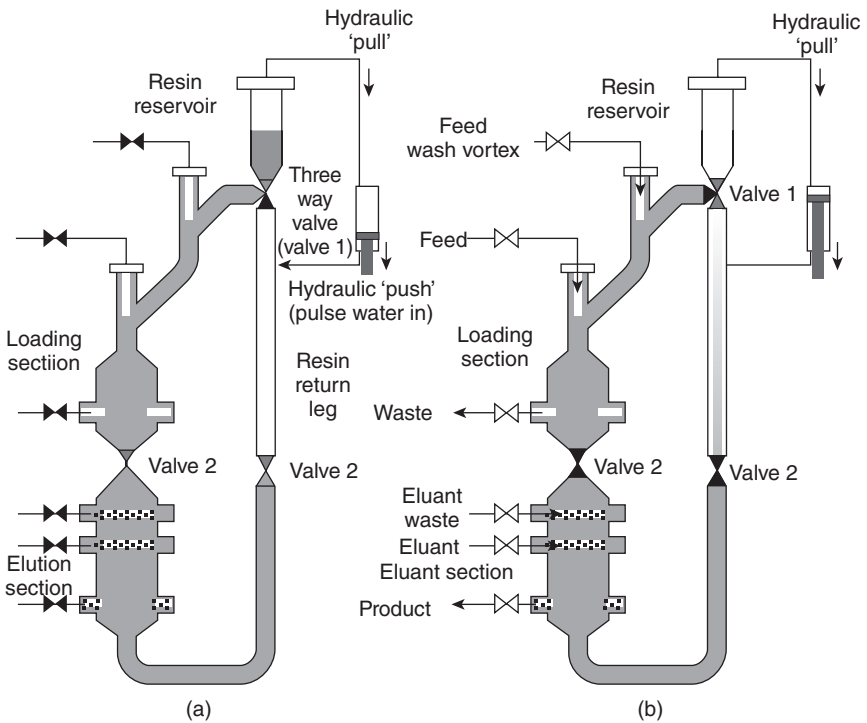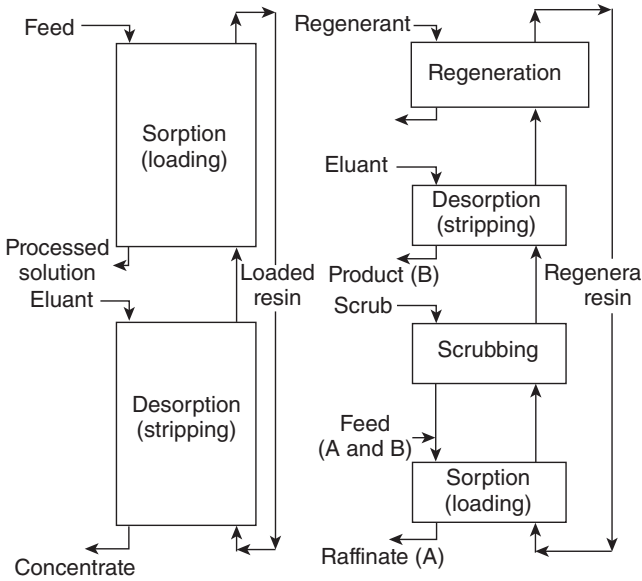
contaminant concentration in the product rises to a target value. Feed is then directed to the lag column, which becomes the lead column and a previously regenerated column is taken on-line into the lag position. A major factor affecting the number of columns is the mass transfer rate of contaminant ions. For a slow mass transfer rate, a large number of small columns may be preferable to maximize the quantity of contaminant loaded onto the lead column. However, system complexity increases with increasing number of columns since column positions are switched by means of valves.

The Higgins moving bed ion exchange system (Fig. 3.10) was an attempt to avoid such complexity. In this system, the ion exchange material is slurried and physically moved from one ion exchange column to another while it undergoes the sorption and desorption (or elution) cycles (a) or the full sorption, scrubbing, desorption and regeneration cycles (b). Though potentially elegant, this process has not seen service in any nuclear plant ion exchange application.

An example of the use of a non moving bed sorption and elution ion exchange process is in the waste treatment plant (WTP) currently under construction at the Hanford nuclear reservation in Washington, USA (Nash, 2005). In this process cesium is separated from a primarily mixed sodium-cesium alkaline feed solution to produce a low cesium, high sodium product solution which will be solidified and buried in engineered near-surface vaults. The ion exchange material used for this process was specially developed for the application and is highly specific for cesium (Fiskum, 2008). The resin is eluted with dilute nitric acid and regenerated with sodium hydroxide. Processing these solutions through the ion exchange bed also causes it to shrink and swell by up to 50%.

Ion exchange process design issues encountered on WTP included:

- Estimating required heights and diameters for the columns. The height determines how much of the resin capacity is utilized before the contaminant concentration in the effluent becomes unacceptable. The diameter mainly determines the liquid throughput for a given utilization of the resin capacity.
- Channeling of the liquid through the ion exchange bed. Larger diameter columns can suffer from channeling if the feed is not adequately distributed across the column cross-section. Channeling can be exacerbated by fissures in resin beds caused by it swelling and shrinking.
- Feed distributor design. A well-designed feed distribution device can mitigate channeling at least to some degree in a large diameter column.
- Deciding on upward or downward flow of liquid through the bed. Up-flow velocities are limited by the need to prevent fluidization of

Feed

Sorption
(loading)

Processed
solution

Eluant

Desorption
(stripping)

Concentrate

Loaded
resin

Regenerant

Regeneration

Eluant

Desorption
(stripping)

Product (B)
Scrub

Scrubbing

Feed
(A and B)

Sorption
(loading)

Raffinate (A)

Regenera
resin

Hydraulic
'pull'

Resin
reservoir

Three
way
valve
(valve 1)

Hydraulic 'push'
(pulse water in)

Loading
sectiion

Resin
return
leg

Valve 2   Valve 2

Elution
section

(a)

Hydraulic
'pull'

Feed
wash vortex

Resin
reservoir

Valve 1

Feed

Loading
section

Waste

Valve 2   Valve 2

Eluant
waste

Eluant

Eluant section

Product

(b)

3.10 Moving bed ion exchange system.

the ion exchange bed and possible loss of ion exchange material from the top of the column. However, down-flow elution of a column may cause higher concentrations of cesium to remain at its bottom when it is returned to the lag position. This phenomenon will then cause re-contamination of the decontaminated product from the lead column.

- Preventing progressive rise in pressure drop across the bed. Re-orientation of the ion exchange material, its degradation under acid and radiation conditions and the nature of the ion exchange particles (spheres, amorphous particles, crystals, etc.) all affect the tendency of the bed to pack down with time and thus increase the pressure drop across it. Eventually this phenomenon will make the process inoperable and re-orientation of the bed becomes necessary by fluidizing it.

3.3.3 Solvent extraction

Liquid-liquid solvent extraction processes have been widely used for aqueous radioactive material separations. These processes employ two immiscible liquid phases, aqueous and organic, to preferentially extract from one phase to the other the desired components of the feed. A solvent extraction cycle consists of up to four operations: extraction, scrubbing, stripping and washing, which are illustrated in Fig. 3.11 and exemplified by the reprocessing of UNF.

Reprocessing entails the separation of plutonium and unused uranium from the fission products and other transuranics in UNF. In this reprocessing application, the UNF is dissolved in nitric acid and the *aqueous* solution is mixed with an immiscible organic liquid or solvent to form a dispersion of aqueous or organic phase drops in the continuous other-phase. The solvent comprises the *extractant*, tri-butyl phosphate that will preferentially extract uranium and plutonium, dissolved in a *diluent*, which is typically a kerosene. The aqueous and organic phases are separated after adequate time mixing to ensure sufficient extraction of the desired species. A small quantity of fission products and other transuranics are inevitably extracted but these are separated from the organic phase in the scrub step by contacting it with a relatively small volume of dilute nitric acid. Uranium and plutonium are then stripped into dilute nitric acid by further contacts with the solvent. The solvent is finally washed of acidic degradation products by contacting it with sodium carbonate and dilute nitric acid to make it ready for further extraction.

In industrial practice, each step of the solvent extraction cycle step is repeated a number of times to achieve the desired separation of uranium and plutonium. The liquid phases are mixed and separated in process
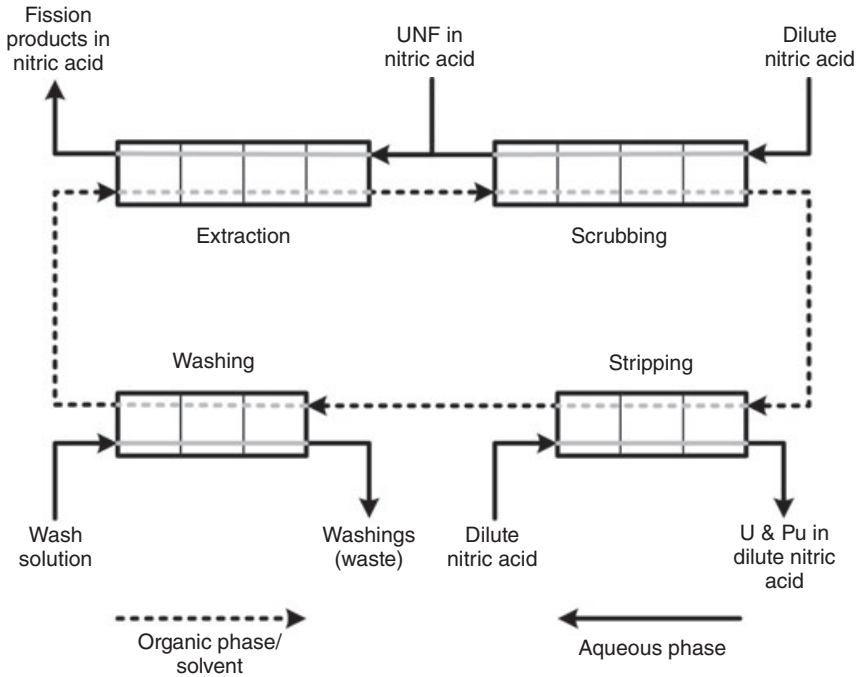
3.11 Typical solvent extraction cycle.

equipment collectively known as contactors. The cycle is additionally con-figured so the aqueous phase flows from contactor to contactor in the opposite direction to the organic phase, or counter-currently, to increase efficiency.

A wide range of contactors for solvent extraction have been used in general industry and these fall into two overall types: stage-wise and dif-ferential. Stage-wise contactors, typified by mixer-settlers, are composed of a number of discrete stages in which the two phases are mixed together and brought to chemical equilibrium before being physically separated and passed counter-currently to the adjacent stages. In differential contactors, the two phases do not reach equilibrium at any point in the contactor. Instead, mass transfer occurs throughout the unit driven by a continuous concentration gradient as the phases flow counter-currently. The phases are only separated as they exit the contactor.

For successful nuclear facility application, contactors must:

- develop sufficient interfacial area between the two phases to promote the desired transfer of the extractable components;
- facilitate counter-current flow of the two phases, while avoiding exces-sive entrainment of one phase in the other as they leave the contactor;

- have flexibility to operate over a range of phase flow rates, ratios and feed concentrations;
- be reasonably compact with low hold up of the process solutions;
- be mechanically reliable and/or easy to maintain.

Reliability is particularly important and a maintenance-free design with no moving parts within the hot cell is preferable. A low holdup of process solutions is important for nuclear applications, since this reduces the aqueous-solvent contact time and hence the degradation of the solvent by the radioactivity of the aqueous phase. It also facilitates designs that are safe by geometry from nuclear criticality at higher than very dilute concentrations of fissile material.

A summary of solvent extraction contactors that are currently in use, or that have been proposed, is shown in Table 3.1. It can be seen that, in the nuclear industry, only three types of contactor are in current use: mixer-settlers, pulsed perforated plate columns and centrifugal contactors.
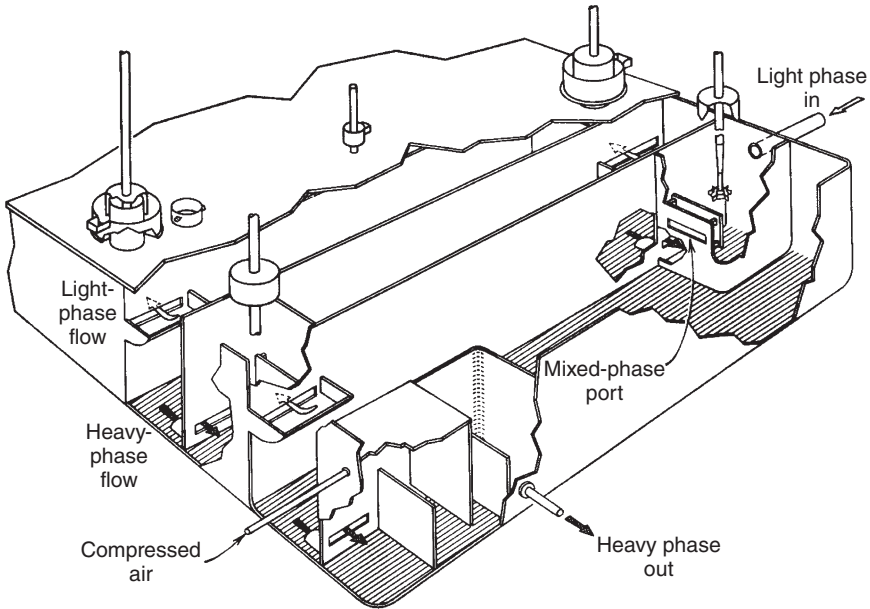
Mixer-settlers

Mixer-settlers are classed as stage-wise or equilibrium contactors because they manifest a step concentration profile as the aqueous and solvent phases pass from stage to stage. They consist of two compartments (Fig. 3.12):

- A mixer compartment where the two liquids are mixed to form a dispersion. Mixing is typically achieved by a mechanical impeller with the motor and gearbox mounted outside the biological shielding for ease of maintenance. Mass transfer is primarily achieved in the mixing compartment.
- A settler compartment where the two liquids are separated by gravity and exit through a system of weirs. The weir system can be designed for the separated liquids to flow to the succeeding contactor under gravity without the need for inter-stage pumping.

Mixer-settlers' continued application in nuclear facilities is warranted on the basis of their mechanical simplicity and industrial pedigree and their important chemical engineering attributes are summarized in Table 3.2. Mixer-settlers are well-established equipment for liquid-liquid extraction unit operations for processing radioactive material and are employed in currently operating commercial UNF recycling plants (e.g. THORP, Sellafield, UK; UP3, Cap La Hague, France; and the Rokkasho Reprocessing Plant, RRP, Rokkasho Mura, Japan) mainly for purifying uranium product streams in which the fissile material content is sufficiently low that nuclear criticality can never be reached even within the non-ever-safe geometry of these contactors.

Table 3.1 Summary of solvent extraction contactors

Contactor	Differential (D) or stage-wise (S)	Reliability	Flexibility	Ease of critically safe design	Size relative to capacity	Comments
Spray column	D	Excellent	Poor	Good	Large	
Packed column	D	Good	Poor	Good	Large	
Rotating disc column	D	Poor	Fair	Good	Medium	
Disk & Donut column	D	Excellent	Poor	Good	Medium	In use at La Hague, France
Rotary annular contactor	D	Fair	Fair	Good	Medium	Proposal only
Pulsed packed column	D	Good	Fair	Good	Medium	Packing tends to orientate with pulses
Pulsed perforated plate column	D	Excellent	Good	Good	Medium	In use at Sellafield, UK
Reciprocating plate column	D	Poor	Good	Good	Medium	
Raining bucket contactor	D	Fair	Poor	Poor	Large	Each phase dispersed alternately
Mixer-settler	S	Excellent	Fair	Poor	Large	In use at La Hague, France and Sellafield UK
Pump-mix mixer-settler	S	Good	Good	Poor	Medium	
Centrifugal contactor	S	Good	Good	Good	Small	In use at Savannah River USA
Static mixer	S	Excellent	Poor	Good	Small	Proposal only

3.12 Schematic of a typical mixer-settler configuration.

Table 3.2 Chemical engineering attributes of mixer-settlers (typical for a used nuclear fuel recycling plant throughput of 5 MTHM/year)

| Attribute	Value or description
Dimensions	12 m by 3 m by 2 m
Total liquid volume	60 m^3
Total liquid residence time	18 hours
Criticality safety	Not safe by geometry. This restricts mixer-settler application to processing solutions dilute in fissile material.
Design	Well-established using well-proven algorithms. One mixer-settler equivalent to one theoretical stage.
	Internal design details include aqueous and solvent weirs, mixed phase port, speed and design of impeller, aqueous off-take weir control system.
Operability	Contactor can be simply restarted without pre-flushing after minor shutdowns. Long residence time provides operators with a long time to respond to process malfunctions.

Pulsed perforated plate columns

Pulsed perforated plate columns are differential type liquid-liquid extraction contactors because they manifest continuous, rather than step, concentration profiles. These devices have been used for recycling used nuclear fuel since the Hanford PUREX plant was started up in 1955. All current commercial UNF recycling plants (THORP, UP3 and RRP) employing advanced PUREX separations technology use pulsed columns in three functions:

• Separation of uranium and plutonium from UNF.
• Separation of plutonium from uranium.
• Purification of the plutonium product.

A schematic of a typical industrial pulsed column used for processing used nuclear fuel is illustrated in Fig. 3.13. THORP pulsed columns are cylindrical and are filled with a series of horizontal perforated plates (Fig. 3.14), spaced at 2-inch intervals, and held together by a series of vertical tie-rods (Phillips, 1993a). In contrast, the La Hague plants use annular pulsed columns with inner and outer columns arranged concentrically. The plates, which in this case are rings, are spaced similarly to the ones in the cylindrical columns but are not perforated and alternately attached to the external and internal column walls. Some smaller cylindrical columns are also used and these are filled with alternating rings and discs, with the rings attached to the outer column wall and the disks carried on a central vertical tie-rod (Drain, 1997).

In all column contactors the more dense aqueous phase enters the column near the top while the less dense solvent phase enters through a pulse limb close to the bottom. A liquid-liquid dispersion is created as the phases flow counter-current through the plate perforations under the action of the periodic pulse applied to the solvent. This can be arranged to be a dispersion of aqueous drops falling through a continuous solvent layer, or it can be a dispersion of solvent drops rising through a continuous aqueous phase. In the former case, the phase separation interface is formed and held in the "bottom settler" at the base of the column while in the latter case this interface is in the top settler. Any solids in the aqueous phase feed will typically congregate at the liquid-liquid interface and be directed with the dispersed phase. Therefore, when extracting uranium and plutonium into solvent from an aqueous UNF feed, the aqueous phase is dispersed so that any solids will be directed to the bottom settler where the aqueous drops coalesce at the solvent/aqueous interface. Thus, contamination of the solvent containing the separated uranium and plutonium is avoided. The top settler provides sufficient freeboard for the solvent to exit the column free of aqueous phase entrainment.
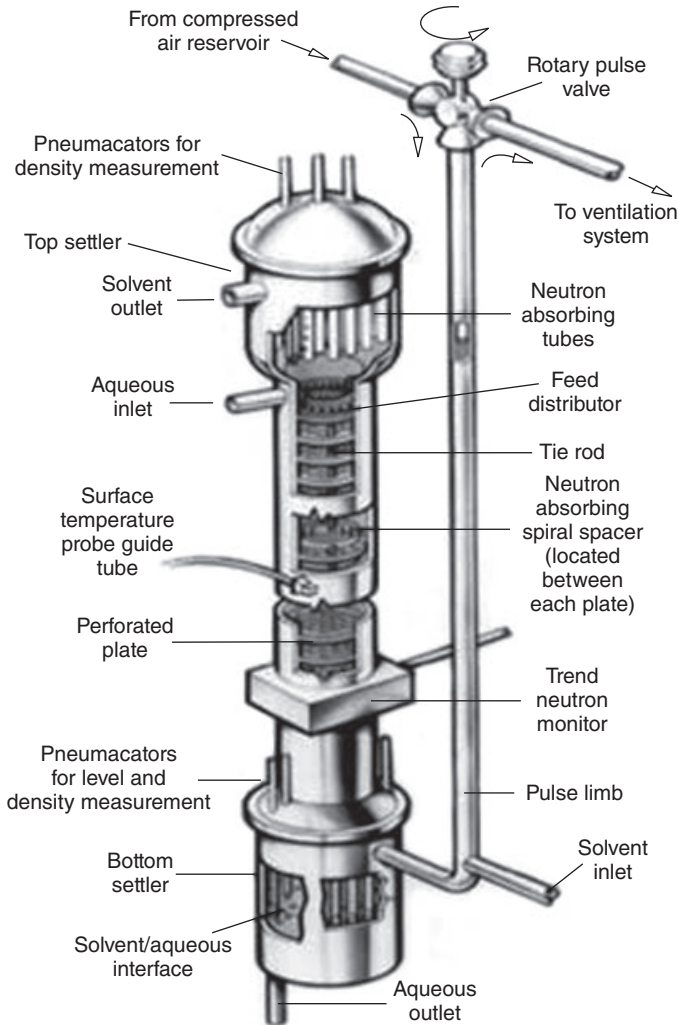
3.13 Schematic of a typical industrial pulsed column.

Pulsed columns are typically safe by geometry because of their high surface area to volume ratio. However, they can be fitted with special inserts made from a neutron absorbing material where high concentrations of fissile material must be processed. For example, the largest diameter THORP pulsed columns uses spacers made from the neutron absorber hafnium between the perforated plates and tubes filled with boron carbide in the top and bottom settlers (Phillips, 1993a). The inner space of annular pulsed columns is filled with boron concrete (Drain, 1997).
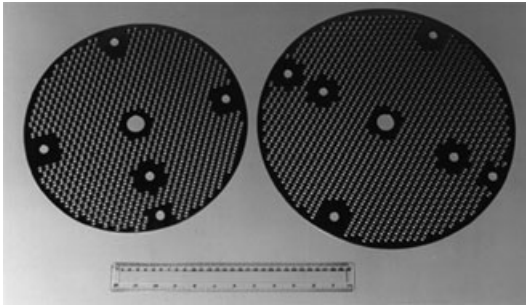
3.14 Pulsed column perforated plates. Source: Nuclear Decommissioning Authority ("NDA"), copyright: Nuclear Decommissioning Authority ("NDA").

There are two stable hydrodynamic operating regimes for pulsed columns. The mixer-settler operating regime manifests at low pulse frequencies and/ or amplitudes and flow rates when dispersion and coalescence entirely occurs between plates. At higher pulse frequencies and/or amplitudes and flow rates the mixer-settler regime transitions to the dispersive or emulsion regime where a continuous dispersion is established throughout the column's length. Drop sizes in the dispersion regime are typically 1–3 mm in a nitric acid – 30% tributyl phosphate systems with uranium and plutonium (Phillips, 1993b). At still higher pulse frequencies and/or amplitudes and flow rates, the dispersion becomes unstable, leading to gross wrong-phase entrainment in the products, a condition known as flooding. Pulsed columns are usually operated in the dispersive regime because the higher dispersed phase hold-up and higher interfacial area maximizes mass transfer efficiency and minimizes wrong-phase entrainment. However, they also provide good mass transfer performance when operating in the mixer-settler regime because the lower interfacial area is at least partially mitigated by the continuous coalescence and re-dispersion of the drops, which continually exposes a fresh interface for mass transfer.

Detection and control of the position of the bulk interface in the top settler for a continuous aqueous phase, or bottom settler for a continuous organic phase, is critical for stable pulsed column operation and hence good mass transfer performance. Interface detection and control is achieved in the THORP pulsed columns using equipment with no in-cell moving parts so that no in-cell maintenance is required through the life of the facility. Interface detection is achieved using air bubbler tubes ("pneumercators") to measure the relative densities of the two liquid phases above and below the interface and thus infer the interface position between the bubbler tubes (Phillips, 1993a). In solvent continuous columns, with the interface in the bottom settler, the pneumercator pressure signals are interfered with

Table 3.3 Chemical engineering attributes of pulsed columns (typical for a UNF recycling plant throughput of 5 MTHM/year)

Attribute	Value or description
Dimensions	12 m high by 0.3 m diameter
Total liquid volume	0.8 m^3
Total liquid residence time	15 minutes
Criticality safety	Typically safe by geometry and straightforward to add internal structures fabricated from neutron absorbing material. This makes pulsed columns attractive for processing radioactive material with high concentrations of fissile TRUs.
Design	Straightforward to define diameter, which governs achievable liquid throughputs, using standard algorithms. Height, which governs mass transfer performance, depends on liquid velocities and column diameter, which makes scale-up more challenging.
Operability	Reaction to off-normal events required within 10 s of minutes makes operator vigilance and/or auto controls required. Control via rate of aqueous phase off-take, but sophisticated measurement and control airlift systems needed. Does not perform well with extreme phase ratios.

by the large pulsing pressure applied. Rapid response pressure transducers and sophisticated signal processing are used to extract a reliable interface position signal from the pulse pressure wave "noise". Interface position control is accomplished using an air lift system (see below) to control the rate of aqueous phase removal from the bottom settler. The airlift is coupled with a fluidic pump to provide a constant submergence for the air lift air input. When such a constant submergence is provided, liquid flows from airlifts are stable and increase reproducibly with increasing air flow, making them excellent control devices.

Some important chemical engineering attributes of pulsed columns are provided in Table 3.3.

Centrifugal contactors

Centrifugal contactors are classed as stage-wise or equilibrium contactors because, like mixer-settlers, they manifest a step concentration profile as the aqueous and solvent phases pass from stage to stage. Also, like mixer-settlers, they consist of mixing and phase separation compartments. However, phase separation occurs under the action of centrifugal, rather

than gravitational forces, which leads to more compact processing units than mixer-settlers.

Various designs of centrifugal contactor have been developed and they are used extensively for small-scale process development tests (e.g. Leonard, 1997). Centrifugal contactors were used successfully in the first UNF reprocessing plant at the Savannah River Site but since then they have seen limited use. However, their compact size makes them ideal for processing solutions containing high concentrations of fissile material and Baron (2008) has described their recent industrial application to plutonium product purification in the UP2 UNF recycling plant at La Hague. In addition, their compact size also makes them amenable to modular processing unit concepts, such as the Modular Caustic Side Solvent Extraction Unit currently being used to separate cesium from radioactive wastes stored at the Savannah River Site (Poirier, 2008 and Geeting, 2008). Centrifugal contactors are being considered for future thermal and fast reactor UNF recycling plants (e.g. Balasubramanian, 1992, Washiya, 2004, Duan, 2005 and Law, 2006).

The centrifugal contactors receiving most recent attention have integral mixing and phase separation compartments and are more accurately referred to as annular centrifugal contactors. As shown in Fig. 3.15, the mixing compartment consists of an annulus bound by the outer housing and an internal rotor bowl that spins at several thousand revolutions per minute. The two liquid phases enter the annulus and are mixed as a result of the shear forces set up by the rotating rotor and the bottom vanes. The mixed phase is drawn from the annulus, between the rotor base and housing and into the rotor bowl. The phases separate as a result of the centrifugal forces and exit the rotor bowl over their respective weirs. Banks of centrifugal contactors are connected together in a similar manner as mixer-settlers to permit counter-current flow (Fig. 3.16).

Annular centrifugal contactor size is usually specified by the rotor diameter. Laboratory-scale units used for testing flowsheets typically have 2-cm diameter rotors with a throughput capacity of 40 mL/minute (Leonard, 1997). Units with 5-cm diameter rotors and throughputs up to 5 L/minute are used for engineering scale tests (e.g. Law, 2006). Industrial scale units with rotors of diameters from 12.5 cm are available. Clean-in-place capability has been incorporated into 12.5 cm units by adding to the rotor a hollow central shaft with spray nozzles that can effectively flush out solids (Garn, 2008).

Residence time in the mixing annulus is very short, of the order of seconds. However, the turbulent energy is sufficiently high that very small drops (fractions of a millimeter) are formed with a high interfacial area that provides for efficient mass transfer. Nonetheless, centrifugal contactors are generally not ideal for liquid-liquid systems exhibiting slow interfacial mass
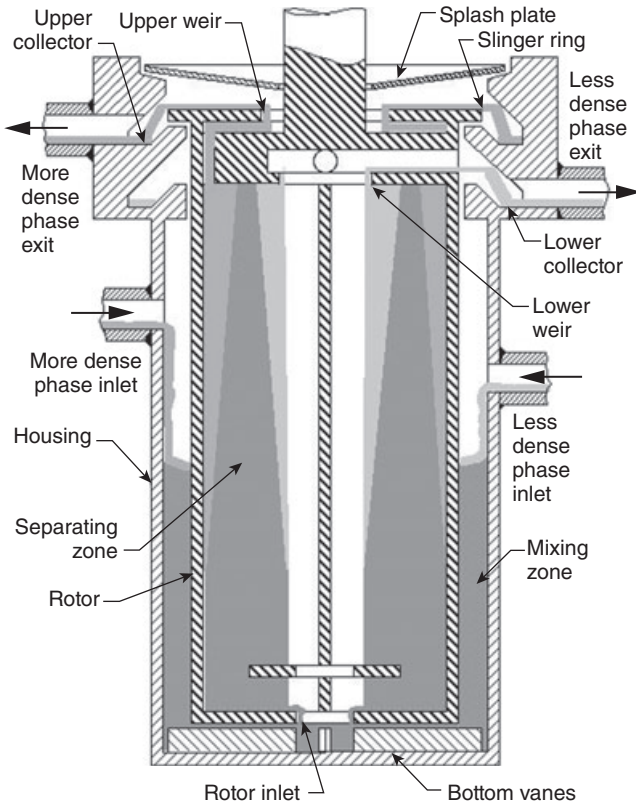
3.15 Schematic representation of an annular centrifugal contactor.
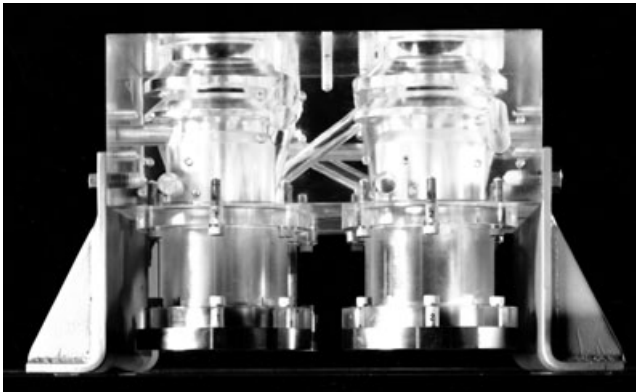
3.16 Bank of four centrifugal contactors (two in view) with Perspex housing showing inter-connections. Source: Nuclear Decommissioning Authority ("NDA"), copyright: Nuclear Decommissioning Authority ("NDA").

Table 3.4 Chemical engineering attributes of annular centrifugal contactors (typical for a UNF recycling plant throughput of 5 MTHM/year)

Attribute	Value or description
Dimensions	Contactor bank comprising 12 units each 20 cm diameter and 40 cm high
Total liquid volume	0.1 m^3
Total liquid residence time	2 minutes
Criticality safety	Safe by geometry on account of very low liquid hold-up. This makes centrifugal contactors attractive for processing radioactive material with high concentrations of fissile TRUs.
Design	Internal design, particularly of the weirs is critical for successful operation. Vendors use algorithms developed through testing and theoretical analysis.
Operability	Operator vigilance is critical and the only feasible reaction to off-normal events is shutdown due to the low residence time. Start-up, however, is consequently straightforward. Speed of centrifuge rotors and feed pump rate provide the main control parameters.

transfer. Wrong-phase entrainment is again a measure of hydraulic performance and Arm (2006) has shown entrainment first decreases and then increases with increasing rotor speed. This phenomenon is indicative of how mixing intensity and phase separation performance are related by the rotor speed. The larger drops formed at low rotor speeds are easier to separate, but this is counteracted by the fact that phase separation improves with increasing rotor speed. As the rotor speed increases, the drops become smaller and less easy to separate. Wrong-phase entrainment also increases with increasing flow rate because the mixed phase has less time to separate. Therefore, there is an optimum rotor speed and flow rate to minimize wrong-phase entrainment.

Some important chemical engineering attributes of annular centrifugal contactors are provided in Table 3.4.

3.4   Equipment materials considerations

3.4.1   Materials selection

The selection of a material for any chemical process plant is a complicated decision involving many parameters such as corrosion resistance, mechanical properties, availability and cost. What makes nuclear plant more demanding is the presence of radiation, particularly gamma, and of radioactive

contamination of surfaces, usually alpha radiation emitting particles, which need to be decontaminated either on a routine basis or at the end of their life. Not only must the materials perform their function for extended periods of time in non-maintainable areas but this performance has to be demonstrated. The application of the most common materials for nuclear process plant is described below.

3.4.2   Austentic stainless steels

Austenitic stainless steels are used extensively as the main material of construction for process vessels and pipework. Much effort has been expended in defining the operating limits of these steels. After many thousands of hours of laboratory testing and decades of plant experience, it has been possible to define realistic and predictable corrosion rates before and after welding, cold working and hot working. The main advantages of austenitic stainless steels are their inherently high resistance to corrosion in oxidizing media such as nitric acid and the relative ease with which they can be decontaminated. They also have excellent impact resistance down to sub-zero temperatures, they are readily available and are easy to fabricate and weld.

There are two main types of austenitic stainless steel used throughout a reprocessing plant (Baldev, 2006). The first is a special grade developed by British Nuclear Fuels Limited and the steel companies which has been given the name NAG (nitric acid grade) 18/10L (Merrill, 1990). NAG 18/10L is basically a 304L type stainless steel with reduced carbon levels and close control on residual elements to give improved corrosion resistance. Careful controls are also placed on the manufacturing and testing processes for this material and it can only be manufactured by a limited number of companies which have to meet stringent technical and quality assurance requirements. It is used on all high integrity nitric acid applications. The 304L grade is used for less arduous duties such as cladding, water jackets and low or non-active pipework and vessels.

3.4.3   Titanium and zirconium

There are certain types of evaporators which are too demanding for austenitic stainless steel. For these processes titanium and, more recently, zirconium are used (Baldev, 2006). These materials have an extremely high resistance to nitric acid corrosion (zirconium is virtually immune to corrosion in pure nitric acid). However, serious problems can arise in the presence of impurities such as fluorides, and great care is needed to ensure correct process chemistry. These materials are very expensive and can be difficult to fabricate without the necessary know-how, i.e. only companies with the relevant expertise are capable of manufacturing high integrity

plant and equipment in these materials. Zirconium, in the form of specially designed rings formed from strip, is used in packed columns to supply a large surface area on which condensation can occur. The older packing material, stainless steel, contributed significant quantities of iron to the process fluids even though their corrosion rate was very low and this iron, added to the process liquor, could enhance the corrosion of stainless steel vessels and pipework. Zirconium has virtually zero corrosion even in nitric acid vapor.

3.4.4 Polymers

Polymers are used for valve diaphragms, gaskets and seals, insulation and sheathing for electric cables, lubricants, greases, pneumatic pipes and adhesives. Certain processes are carried out in sealed gloveboxes – the transparent windows are usually polycarbonate, acrylic or PVC, sometimes leaded for extra shielding; seals for the windows can be fluoropolymers or specially formulated nitrile or EPDM seals. The "gloves" themselves are made from chlorosulphonated polyethylene.

   Much work has been carried out to characterize polymers for use in radiation areas. Of the common materials polythene, polyamides, polyimides, fluoroelastomers and, to a lesser extent, PEEK (polyetheretherketone) have been used in seals and bearings when radiation levels are low enough. For non-active or low active pipework, the commonest form of gasket is based on PTFE, which has now been used for many years with no difficulties. Unfortunately, PTFE is one of the least radiation-resistant polymers and cannot be used in high radiation areas. Indeed, there are no polymers available which will survive high radiation levels for protracted periods and they are usually avoided by the use of metal seals or inorganic materials such as graphite and, to a lesser extent, asbestos.

3.5   Future trends

For advanced aqueous processing of radioactive materials there are two clear future trends: process intensification for large-scale facilities with an expected long production life, and the increasing use of transportable equipment and processes for shorter-term waste cleanup requirements, which are geographically dispersed on a nuclear site or where the need for the facility is expected to be short term.

3.5.1 Process intensification

The need to construct canyons and passive secure cells with walls up to 18 inches thick for radiation shielding and containment provides a strong

incentive to reduce the size of the processing equipment so that the canyon and cell sizes can be reduced to the minimum. This downward pressure on equipment sizes has existed since the start of reprocessing of UNF and continues to be a significant influence on plant design. Typical examples of this are the trend in solids-liquid separation from dead end filtration methods through crossflow filtration to the Spintek compact rotary filtration unit. The key is the supply of greater energy so that liquid throughputs are retained in smaller equipment.

A similar trend can be seen with the solvent extraction contactors in reprocessing facilities. Some early reprocessing facilities used packed, unpulsed columns as their solvent extraction contactors. At the first generation "BUTEX" facility at the Sellafield site in the UK, for example, these columns had to be some 90 to 100 feet in height to provide the required mass transfer performance. The resulting passive secure cell was thus very tall and expensive to construct and operate. The replacement "MAGNOX" reprocessing plant at Sellafield used mixer-settlers instead of packed columns, with energy supplied via the mechanical stirrers in the mixing compartments. The facility was thus much less tall and more economical to construct and operate (Fig. 3.17). This trend continued with the use of pulsed perforated plate columns for the third generation THORP facility at Sellafield. These columns have a significant energy input via the pulse and are therefore much more efficient for mass transfer. At about 30 feet in height, they are a third of the height of the BUTEX plant columns, allowing the cells that contain them to be much smaller.

For future reprocessing facilities it is expected that significant use will be made of centrifugal contactors which have a large energy input via the high

3.17 The MAGNOX reprocessing plant at Sellafield, UK. Source: Nuclear Decommissioning Authority ("NDA"), copyright: Nuclear Decommissioning Authority ("NDA").

speed rotor, are thus extremely compact units and will further reduce plant footprints and hence capital costs.

The main constraint on process intensification is the continuing need for buffer tanks between unit processes. These are necessary in most plants to ensure that perturbations in one unit process do not adversely affect the operation of precursor or successor units. In addition they are often needed if sampling and analysis of an intermediate product is needed before it can be allowed to go forward to the next unit process. In these cases, buffer tank size is set by considerations of analysis turn-round times, and operator reaction times to off-normal events, and can dominate the size of the overall plants when other equipment is intensified.

3.5.2 Transportable equipment and processes

Transportable radioactive waste processing facilities can be an attractive alternative to the building of large facilities with fixed canyons or PSCs. Transportable facilities are particularly attractive when processing is expected to be complete within short timescales, when it is advantageous to be able to move the processing equipment within a facility or amongst a series of geographically disperse waste treatment sites, or when the extensive decommissioning and clean-up of a large fixed facility is considered undesirable. Phillips (2008) has produced comprehensive review of transportable processing systems.

Transportable processing equipment is typically constructed within standard steel ISO-containers, or similar sized spaceframes, and includes portable ventilation and off-gas equipment added as required. The ISO-containers are shielded and confined as necessary by the addition of steel shielding and confinements to the outside of the containers. Alternatively the ISO-containers are placed within separately constructed concrete enclosures that do not come into contact with any radioactive material and thus do not themselves require any radioactive decommissioning at mission end.

Within the shielded confinements maximum use is made of systems that greatly minimize the use of moving parts, substituting these with non-moving process equipment and instruments based on fluidics and compressed air. Additionally, use is made of "through-wall" drives where moving parts are located outside the shielded ISO-container, with only a shaft drive penetrating the shielding and connecting with the in-container processing equipment. These design provisions enable the placement of most mechanical items and instruments requiring maintenance outside the shielding and thus accessible, and ensure that there is no need for personnel to enter the shielded parts of the containers during the life of the system. The Mobile Solidification System (MOSS, Fig. 3.18) is a typical system developed for

3.18 MOSS transportable waste grouting unit.

use at the Hanford, WA nuclear reservation for the transfer, conditioning and solidification of radioactive sludges from the reservation's K-Basins, previously used for the underwater storage of UNF.

3.6   Sources of further information and advice

Further information on nuclear chemical engineering is available from meetings of major professional societies and publications. In the USA, the American Nuclear Society (ANS) holds two meetings every year in the Spring and Fall. The latter meeting currently provides a focus for nuclear chemical engineering topics and their proceedings are published. The Nuclear Engineering Division of the American Institute of Chemical Engineers regularly organizes sessions at bi-annual meetings in the Spring and Fall.

A noteworthy conference is GLOBAL, which focuses entirely on advanced nuclear fuel cycles and systems with published proceedings and which is held every two years in different nations each time. The International Solvent Extraction Conference has a strong nuclear chemical engineering component to its programming and is held every three years again in different venues each time. In the USA, the Waste Management Conference is held every year in Tucson, Arizona and includes topics covering waste processing and UNF reprocessing. In France, the Commissariat a l'Energie Atomique organizes their ATALANTE series of conferences, which have

been held every four years since 2000. They also cover advanced fuel cycles and systems topics and their proceedings are published on the internet.

There are three journals, which routinely publish papers describing advances in the separations field of nuclear chemical engineering:

- *Nuclear Technology*, which is published by the ANS;
- *Separation Science and Technology*, published by the Taylor and Francis Group;
- *Solvent Extraction and Ion Exchange*, also published by the Taylor and Francis Group.

As already stated, most nuclear chemical engineering unit operations are adapted from standard industrial practice and so standard chemical engineering texts are appropriate. However, there are a number of noteworthy texts specifically covering nuclear chemical engineering:

- *Nuclear Chemical Engineering* (Benedict, 1981)
- *Engineering for Nuclear Fuel Reprocessing* (Long, 1978).
- *Chemical Separation Technologies and Related Methods of Nuclear Waste Management: Applications, Problems and Research Needs* (Choppin, 1999).
- *The Nuclear Fuel Cycle: From Ore to Wastes* (Wilson, 1996)
- *Nuclear Energy: An Introduction to the Concepts, Systems, and Applications of Nuclear Processes* (Murray, 2001).

Although some of these texts are over two decades old, the principles and subject matter described in them remain equally applicable for the advanced nuclear engineering concepts being considered today for the 21st century.

3.7   References

Arm, S, Jenkins, J (2006), "Haze formation and behavior in liquid-liquid extraction processes", *Separations for the Nuclear Fuel Cycle in the 21st Century*, ACS symposium series 933, American Chemical Society, Washington, DC, USA.

Balasubramanian, G (1992), "Advancements in fuel reprocessing technology to close the fast breeder reactor fuel cycle", *Mineral Processing and Extractive Metallurgy Review*, 9, 305–312.

Baldev, R, Mudali, U (2006), "Materials development and corrosion problems in nuclear fuel reprocessing plants", *Progress in Nuclear Energy*, 48, 283–313.

Baron, P, Dinh, B, Duhamet, J, Drain, F, Meze, F, Lavenu, A (2008), "Plutonium purification cycle in centrifugal extractors: from flowsheet design to industrial operation", *Solvent Extraction: Fundamentals to Industrial Applications. Proceedings of ISEC 2008 International Solvent Extraction Conference Volume 1*, Quebec, Canada, Canadian Institute of Mining, Metallurgy and Petroleum, 587–592.

Benedict, M, Pigford, T, Levi, H (1981), *Nuclear Chemical Engineering*, McGraw-Hill.

Choppin, G, Khankhasayev, M (1999), *Chemical Separation Technologies and Related Methods of Nuclear Waste Management: Applications, Problems, and Research Needs*, Springer.

Drain, F, Miquel, P, Moulin, J, Alexandre, D, Kniebihli, B, Boullis, B, Baron, P (1997), "Uranium/plutonium separation in annular pulsed column", Global '97, Yoko-hama, Japan.

Duan, W, Song, C, Wu, Q, Zhou, X, Zhou, J (2005), "Development and performance of a new annular centrifugal contactor for semi-industrial scale", *Separation Science and Technology*, 40(9), 1871–1883.

Fiskum, S, Arm, S, Steele, M, Thorson, M (2008), "Spherical resorcinol formaldehyde performance testing with Hanford tank waste", *Solvent Extraction and Ion Exchange*, 26, 435–452.

Garn, T, Meikrantz, D, Mann, N, Law, J, Todd, T (2008), "Hydraulic and clean-in-place evaluations for a 12.5 cm annular centrifugal contactor at the INL", *Solvent Extraction: Fundamentals to Industrial Applications. Proceedings of ISEC 2008 International Solvent Extraction Conference Volume 1*, Quebec, Canada, Canadian Institute of Mining, Metallurgy and Petroleum, 733–738.

Geeting, J, Hallen, R, Peterson, R (2006), "Ultrafilter conditions for high-level waste sludge processing", *Separation Science and Technology*, 41(11), 2313–2324.

Geeting, M, Brass, E, Brown, S, Campbell, S (2008), "Scale-up of caustic-side solvent extraction process for removal of cesium at Savannah River Site", *Separation Science and Technology*, 43, 2786–2796.

Herman, D, Poirer, M, Fink, S (2006), "Washing simulated radioactive sludge with a full-scale rotary microfilter", American Institute of Chemical Engineers Annual Meeting, San Francisco, California, USA.

Law, J, Meikrantz, Garn, T, Mann, N, Herbst, S, Todd, T (2006), "The testing of com-mercially available engineering and plant scale annular centrifugal contactors for the processing of spent nuclear fuel", 15th Pacific Basin Nuclear Conference, Sydney, Australia.

Leonard, R, Chamberlain, D, Conner, C (1997), "Centrifugal contactors for labora-tory-scale solvent extraction tests", *Separation Science and Technology* 32(1–4), 193–210.

Long, J (1978), *Engineering for Nuclear Fuel Reprocessing*, American Nuclear Society.

Merrill, N, Orr, C, Shaw, R (1990), "Development of the THORP plant – materials and radiometric instruments", *Atom*, 400, 23–29.

Murray, R (2001), *Nuclear Energy: An Introduction to the Concepts, Systems, and Applications of Nuclear Processes*, Butterworth-Heinemann.

Nash, C (2005) "Cesium ion exchange program at the Hanford river protection project waste treatment plant", Waste Management Conference, Tucson, Arizona, USA.

Peterson, R, Geeting, J, Daniel, R (2007), "Estimation of ultrafilter performance based on characterization data", *Chemical Engineering and Technology*, 30(8), 1050–1054.

Phillips, C (1993a), "Commissioning of the solvent extraction processes in the thermal oxide reprocessing plant", *Solvent Extraction in the Process Industries*, Elsevier Applied Science, 1463–1470.

Phillips, C (1993b), "Development and design of the thermal oxide reprocessing plant at Sellafield", *Transactions of the Institute of Chemical Engineers*, 71, Part A, 134–142.

Phillips, C, Richardson, J, Fallows, P (2006), "Maintenance free fluidic transfer and mixing devices for highly radioactive applications – design, development, deployment and operational experience", Waste Management 2006 Conference Proceedings, Tucson, AZ, USA.

Phillips, C, Cavanah, P, Richardson, J (2007), "The use of passive, secure cells for processing highly active nuclear wastes", Waste Management 2007 Conference Proceedings, Tucson, AZ, USA.

Phillips, C, Houghton, D, Crawford, G (2008), "The use of transportable processing systems for the treatment of radioactive nuclear wastes", Waste Management 2008 Conference Proceedings, Phoenix, AZ, USA.

Poirer, M, Fink, S (2007), "Filtration of modified monosodium titanate slurries", American Institute of Chemical Engineers Annual Meeting, Salt Lake City, Utah, USA.

Poirier, M, Peters, T, Brass, E, Brown, S, Geeting, M, Johnson, L, Coleman, C, Crump, S, Barnes, M, Fink, S (2008), "Full-scale testing of a caustic side solvent extraction system to remove cesium from Savannah River Site radioactive waste", *Separation Science and Technology*, 43, 2797–2813.

Washiya, T, Ogino, H, Aoshima, A (2004), "Development of a centrifugal contactor for fast reactor spent fuel reprocessing", Atalante 2004, Nimes, France.

Wilson, P (1996), *The Nuclear Fuel Cycle: From Ore to Wastes*, Oxford University Press.

4

Spectroscopic on-line monitoring for process control and safeguarding of radiochemical streams in nuclear fuel reprocessing facilities

S. A. BRYAN, T. G. LEVITSKAIA, A. J. CASELLA,
J. M. PETERSON, A. M. JOHNSEN, A. M. LINES, and
E. M. THOMAS, Pacific Northwest National Laboratory, USA

Abstract: Separation processes for highly radioactive and chemically complex spent nuclear fuel require advanced safe technologies and process models based on large databases. Availability of advanced methodologies for on-line control and safeguarding of aqueous reprocessing flowsheets will accelerate implementation of the closed nuclear fuel cycle. This report reviews application of the absorption and vibrational spectroscopic techniques supplemented by physicochemical measurements for radiochemical process monitoring. In this context, our team experimentally assessed potential of Raman and spectrophotometric techniques for on-line real-time monitoring of the U(VI)/nitrate ion/nitric acid and Pu(IV)/Np(V)/Nd(III), respectively, in the solutions relevant to spent fuel reprocessing. Both techniques demonstrated robust performance in the repetitive batch measurements of each analyte in the wide concentration range using simulant and commercial dissolved spent fuel solutions. Static spectroscopic measurements served as training sets for the multivariate data analysis to obtain partial least squares predictive models, which were validated during on-line centrifugal contactor extraction tests. Achieved satisfactory prediction of the analytes concentrations in these preliminary experimentation warrants further development of the spectroscopy-based methods for radiochemical process control and safeguarding.

Key words: spectroscopic process monitoring, Raman, vis-NIR, uranium, plutonium, neptunium, nitric acid, nitrate, nuclear fuel reprocessing.

4.1   Introduction

There is a renewed interest worldwide to promote the use of nuclear power and close the nuclear fuel cycle under the Global Nuclear Energy Partnership (GNEP) Program, the Advanced Fuel Cycle Initiative (AFCI), and more recently under the Fuel Cycle Research and Development Program (FCRD). The long-term successful use of nuclear power is critically dependent upon adequate and safe disposal of the spent nuclear fuel, and implementation of the closed nuclear fuel cycle recently regained attention in the

95

US community. Liquid-liquid solvent extraction is a separation technique commonly employed for the processing of the dissolved spent nuclear fuel. Availability of the closed nuclear fuel cycle requires precise solution control during processing. For example, extraction and recovery of minor actinides within an aqueous separation scheme necessitates precise control of aqueous redox conditions and acid concentrations at various places within the processing loop. Traditionally, the process performance of a given solvent extraction run is determined through sampling of the various process steams and subsequent laboratory analysis of those samples. Due to the highly radioactive nature of the process streams, this is a risky and time-consuming process. Remotely controlled on-line monitoring capabilities can help guide choice and adjustment of conditions to be used in processing of irradiated fuel and allow immediate feedback on changes made to the processing conditions. As a result, there is a renewed and urgent need for methods to provide on-line monitoring and control of the radiochemical processes currently being developed and demonstrated. The instrumentation used to monitor these processes must be robust, require little or no maintenance, and be able to withstand harsh environments (e.g., high radiation fields and aggressive chemical matrices). The ability for continuous online monitoring allows the following benefits:

- accountability of the fissile materials
- control of the process flowsheet
- information on flow parameters, solution composition, and chemical speciation
- enhanced performance by eliminating the need for traditional analytical "grab samples"
- improvement of operational and criticality safety
- elimination of human error.

Sophisticated on-line monitor capabilities significantly enhance not only control over a process flowsheet but also accountancy of the inventory of a nuclear material. The increasing effectiveness of safeguards in spent fuel reprocessing plants is a great challenge to national and international communities. The International Atomic Energy Agency (IAEA) has established international safeguards standards for fissionable materials at reprocessing plants to ensure that significant quantities of weapons-grade nuclear material are not diverted over a specified time frame. Because proliferant diversions are possible via deliberate modification of flowsheet chemistry, it is necessary to confirm proper operational performance to verify that facilities function under adequate safeguard-declared conditions. In any reprocessing facility, variability in process is expected under normal operations, and currently, large-scale deviations can readily be detected and measured with certainty. Small-scale deviations in large facilities, however,

are currently not well detected. Many of the methods useful for detecting deviations involve sending individual samples to a laboratory for processing, which can be time-consuming, thus delaying accurate appraisals of process conditions.

The application of multiple online monitoring capabilities provides a unique ability to rapidly identify unwanted/suspect deviations from normal operating conditions. The feasibility of this kind of on-line control of nuclear fuel reprocessing streams via analytical techniques was investigated as early as the 1970s (Parus 1977), and researchers have examined both the direct measurement of actinides, via spectrophotometry, and the use of physico-chemical measurements, such as temperature, density, and dielectric properties, to indirectly measure actinide concentrations. These analytical methods can also be used to measure other solution components, such as NO_3^- or organic solvents that control actinide behavior, providing another method for actinide quantification.

Raman spectroscopy (Madic 1983, 1984; Guillaume 1982) and ultraviolet-visible (UV-vis) spectroscopy (Schmieder 1972; Ertel 1976, 1985; Baumgartner 1980; Yamamoto 1988; Bürck 1991; Colston 2001) are analytical techniques that have been used extensively to measure concentrations of various organic and inorganic compounds, including actinides (Bryan 2007). Additionally, measurement of dielectric properties has also been proposed for on-line monitoring of fuel reprocessing systems (Yamamoto 1988).

The spectroscopic signatures of U, Pu, and Np analytes in different oxidation states have been extensively measured in solution and widely known (Madic 1983; Guillaume 1982; Maya 1981; Nguyentrung 1992). Even though Pu(VI) (Madic 1983) and Np(VI) (Guillaume 1982) species are Raman active, they are expected to be present in the dissolved fuel at low enough concentrations to prohibit their quantification by the Raman method. In our work, we employ Raman spectroscopy for the determination of U(VI), HNO_3, and NO_3^- in various aqueous and organic streams. Plutonium species can be measured by visible absorption spectroscopy using multiple wavelengths for its quantification (Ryan 1960; Cleveland 1979) and neptunium species can be monitored by vis-NIR spectroscopy (Burney 1974; and Stout 1993).

Armenta *et al.* reviewed the most recent literature (2000–2006) concerning the general (non-actinide applications) combination of flow-injection techniques and vibrational spectroscopy analysis and noted that both techniques have significant advantages. Flow-injection analysis is the technique in which a sample aliquot is injected into a reagent stream, where it disperses and the mixture flows past a detector. Flow-injection analysis offers "automated sample processing, high repeatability, adaptability to micro-miniaturization, containment of chemicals, [and] waste reduction," while

vibrational spectroscopy allows for "(i) fast monitoring of the whole spectrum; (ii) high resolution and wide wavenumber range; (iii) many bands that can be employed for determination of each single compound; [and] (iv) simultaneous control of several compounds in the same sample." These characteristics have allowed several commercial instruments to be applied successfully to quality and process control in the dairy, wine, gasoline, diesel, and lubricating oils industries. The authors also note that new flow-injection techniques in development have the potential to lower sample sizes and increase sensitivity (Armenta 2007).

Multiple laboratories have successfully constructed systems for remote in-line photometric measurements of actinides using spectrometers capable of scanning the entire visible and NIR range quickly enough for process measurements (Bürck 1991). On a larger scale, Lascola *et al.* (2002) successfully constructed a system for the on-line measurement of uranium from process tanks. Tank samples were routed through an initial vial to ensure proper mixing and were then sent through a flow-through optical cell connected via fiber optics to a diode-array spectrophotometer measuring in the 350–600 nm range. Partial least squares (PLS) models allowed for concentration measurements up to 11 g/L uranium, as well as uncertainties (2σ; concentration dependent) no greater than 0.30 g/L.

Several authors have conducted density studies of typical actinide reprocessing solutions for use in criticality and process monitoring. Sakurai and Tachimori (1996) analyzed published density data for solutions containing plutonium(IV), uranium(VI), and nitric acid. Using regression analysis, they correlated solution density with analyte concentration that expanded the range of actinide concentrations to Pu < 173 g/L and U < 380 g/L and provided standard error (0.00294 g/cm^3) that improved upon the error associated with previously established relationships. Kumar and Koganti (1998) extended this work to include mixed organic solutions, reporting density for $UO_2(NO_3)_2$ and HNO_3 in TBP/*n*-dodecane solutions ranging from 0 to 100% tri-butyl phosphate (TBP).

While Sakurai and Kumar have reported the most recent empirical density relations that are considered to be the most accurate empirical equations thus far, several authors have pursued theoretical calculations of actinide/nitrate solution densities in order to clarify the density functions at higher concentrations where the empirical equations begin to deviate from experimental data. Thermodynamic modeling for binary (or isopiestic) solutions have been applied to make small but important corrections for solutions with high concentrations of the following components: $UO_2(NO_3)_2$, $U(NO_3)_4$, $Pu(NO_3)_4$, $Pu(NO_3)_3$, $Th(NO_3)_4$, $Am(NO_3)_3$, and HNO_3 (Charrin 2000a, 2000b; LeClaire 2003).

Enokida and Suzuki (1992a, 1992b) used a set of computer models to theoretically test the feasibility of using temperature profiles to determine

the uranium(VI) concentrations during solvent extraction processes from nitric acid into 30% TBP/*n*-dodecane organic phase. Using literature values for the heat of the TBP complexation, along with mass and heat balance equations, the authors created a model that calculated both steady- and transient-state uranium(VI) concentrations when given a temperature profile and a set of flow rates and feed concentrations for a typical set of counter-current mixer-settler extractors. Their model compared favorably with other models that calculated uranium(VI) concentrations using distribution coefficients, which showed that using temperature profiles at various process stages is a feasible means of uranium(VI) concentration measurement.

Yamamoto (1988) used a flow-through cell system to measure the dielectric properties of the 30% TBP/*n*-dodecane-HNO_3-H_2O and 30% TBP/*n*-dodecane-HNO_3-H_2O-$UO_2(NO_3)_2$ systems commonly used in spent nuclear fuel reprocessing. The estimated dielectric constants were found to vary much more significantly with HNO_3 than with equivalent molar additions of H_2O or $UO_2(NO_3)_2$. The measurements were found to be sufficient to accurately measure the HNO_3 concentration in the (30% TBP/*n*-dodecane)-HNO_3-H_2O system and could be used to measure the HNO_3 concentration in the (30% TBP, *n*-dodecane)-HNO_3-H_2O-$UO_2(NO_3)_2$ system if the $UO_2(NO_3)_2$ concentration is known.

On-line monitoring of nuclear waste streams was successfully demonstrated by combining spectroscopic measurements with physicochemical measurements (conductivity, density, and temperature) in real-time quantitative determination of chemical components in the waste (Bryan *et al.* 2005; Bryan 2008). This new on-line monitoring system, which features Raman spectroscopy combined with a Coriolis meter and a conductivity probe, was developed by our research team to provide immediate chemical data and flow parameters of high-level radioactive waste streams. This process monitoring system was used to measure the concentration of components of high brine/high alkalinity waste solutions, such as nitrite, chromate, aluminate, phosphate, sulfate, carbonate, and hydroxide, during retrieval from Hanford waste storage tanks. The Raman bands of interest for these species are well resolved and have been easily incorporated into a chemometric model for quantitative analysis of the solution components.

By inclusion of visible/near-infrared (vis-NIR) spectrocopy, this system was modified to monitor spent fuel reprocessing streams. A fiber-optic Raman probe allows monitoring of various species encountered in both aqueous and organic phases. Raman active species include: 1) metal oxide ions, such as uranyl, neptunyl, and pertechnetate ions, 2) organics, 3) inorganic oxo-anions, and 4) water. The trivalent and tetravalent actinides and lanthanides in both the aqueous and organic phases are monitored by vis-NIR spectroscopy, as are pentavalent or hexavalent Np and Pu

complexes that are expected to be at concentrations too low to be determined by Raman spectroscopy. Process monitoring and control is feasible at various points within the fuel reprocessing streams. Notably, process monitoring/control is not specific to any single flowsheet because alternate flowsheets also contain Raman and/or UV-vis-NIR active species that can be measured spectroscopically. In addition, Coriolis (for density and flow) and conductivity instruments can be used on most process streams.

The Raman and vis-NIR spectrometers used under laboratory conditions are easily convertible to process-friendly configurations to allow remote measurements under flow conditions using different sampling capabilities, such as fiber-optic probes, dip probes, and flow-through cell geometries as have been demonstrated by our research team in the centrifugal contactor flow tests. Spectroscopic data collected during the flow test served for the validation of the chemometric predictive models developed under static batch conditions as described in Sections 4.2 and 4.3.

4.2   Static spectroscopic measurements

The uranium extraction (UREX) solvent system was selected as a model flowsheet for testing Raman and absorbance spectroscopic techniques for process monitoring and safeguarding purposes and served as a guide for selecting the various feed concentrations and solvent system bounding the choice of spectroscopic measurements. The initial effort was directed toward evaluation of current UREX flowsheet specifications received from Argonne National Laboratory (ANL) (Vandegrift 2004). Based on this report evaluation, specifications were developed for preparing solutions that simulate the UREX process flowsheet streams. These solutions were used to evaluate capabilities for testing in-house instrumentation applicable for on-line process monitoring. To demonstrate the feasibility of using spectroscopic techniques for the process monitoring and control of the UREX flowsheet, a 0.8 M HNO_3 solution matrix was selected. The simple baseline feed solution contained 1.33 M $UO_2(NO_3)_2$ in 0.8 M HNO_3 (labeled Simple Feed). The Simple Feed simulant served as a matrix for the Pu(IV, VI) and Np(V) measurements at variable concentrations in the 0–10 mM range. The organic solvent extraction solution containing 30 vol% TBP in *n*-dodecane was prepared and loaded with actinide nitrates by the batch contact equilibration with the UREX feed simulant solutions.

Raman spectra were collected on an InPhotonics, Inc. RS2000 echelle spectrograph. The system was equipped with a stabilized 670 nm, 150 mW visible diode laser as the excitation source. Data were collected at 1 cm^{-1} spectral resolution over a range of 200–4000 cm^{-1} stokes shift (Raman shift from 670 nm). Samples were measured with an InPhotonics focused fiber-optic probe (RamanProbe™) with a thermoelectrically cooled CCD

detector, normal operating temperature −55°C. The laser beam was coupled to the sample through a 10m fiber-optic cable and probe assembly which focused the excitation beam directly into the sample; this also precluded any air gap between the laser source and the sample. The focal point of the laser beam was 5 mm beyond the end of the laser probe tip, the measured laser intensity at the sample was typically 50 mW, and the excitation laser beam diameter at the sample was measured as 3 mm. Molecue® acquisition software with GRAMS 32® data manipulation software was used to process the Raman data. Typically, an integration time of 2 to 20 seconds was used for each acquisition. Vis-NIR measurements were performed using a 400 series dual source reflectance fiber-optic probe (SI Photonics) coupled with an LS-1 Tungsten Halogen Light Source (Ocean Optics) and a USB2000-vis-NIR spectrophotometer (Ocean Optics). SpectraSuite (Ocean Optics) software was used for collection and processing of the spectrophotometric data.

4.2.1 Raman measurements

The UREX Simple Feed simulant was subjected to Raman spectroscopic measurements. The Raman spectrum in Fig. 4.1 (blue spectrum) shows two strong bands due to UO_2^{2+} (870 cm^{-1}) and NO_3^- (1047 cm^{-1}). The UREX simple feed stimulant was contacted with 30% TBP/n-dodecane, resulting in an organic phase loaded with $UO_2(NO_3)_2$. The Raman spectrum of the loaded solvent shown in Fig. 4.1 (red spectrum) contains bands due to dodecane, TBP, uranyl, and nitrate were observed. The UO_2^{2+} (859 cm^{-1}) and NO_3^- (1029 cm^{-1}) bands were both shifted to lower energy in the
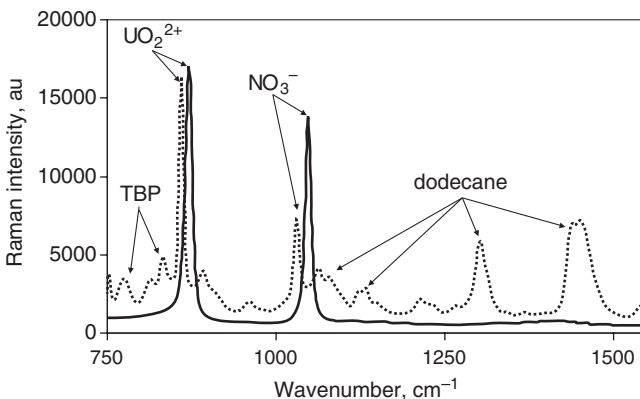
4.1 Raman spectra of aqueous Simple Feed solution (1.3 M $UO_2(NO_3)_2$ in 0.8 M HNO_3) (blue spectrum) and its extract into 30 vol% TBP in dodecane (red spectrum).
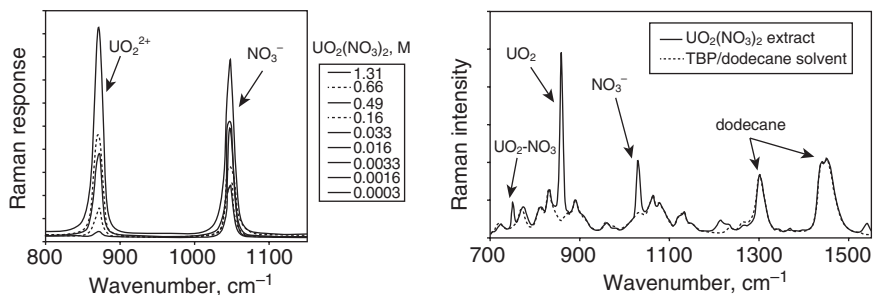
4.2 Raman spectra of variable aqueous $UO_2(NO_3)_2$ solutions in 0.8 M HNO_3 (left) and their extracts (right) into TBP/docecane solvent.

organic phase spectrum compared to the aqueous phase spectrum due to the $UO_2(TBP)_2(NO_3)_2$ complex formation. The spectrum of the loaded solvent was compared to the spectrum of water-washed TBP/*n*-dodecane, and it was found that the bands due to the solvent do not interfere with the uranyl or nitrate Raman bands. It was demonstrated that the depletion of uranyl ions from the aqueous phase upon extraction can be easily followed using Raman spectroscopy. The intensity of the uranyl band (870 cm^{-1}) decreased from the initial spectrum to the final spectrum, indicating a reduced concentration of UO_2^{2+} in the aqueous phase after extraction.

In order to evaluate the detection limit for U(VI) and nitrate in the UREX Simple Feed system, a series of feed simulant solutions containing 0.0003–1.31 M $UO_2(NO_3)_2$ in 0.8 M HNO_3 were prepared and subjected to Raman spectroscopic measurements. The spectral overlay obtained is shown in Fig. 4.2 (left). A linear relationship was established between the Raman response of the respective UO_2^{2+} (870 cm^{-1}) and NO_3^- (1047 cm^{-1}) bands and the concentration of $UO_2(NO_3)_2$ and nitrate in the 0.8 M HNO_3 solution. A treatment recommended by the International Union of Pure and Applied Chemistry (IUPAC) was used for the evaluation of the detection limit (Long 1983). In this treatment, the detection limit is calculated using equation 4.1,

$$DL = \frac{kS_b}{m + tS_m} \qquad\qquad 4.1$$

where DL is the detection limit, k is a numerical coefficient, m is the slope, S_b and S_m are the standard errors for the intercept and slope of a calibration plot, respectively, and t is Student's value for $(n - 2)$ degrees of freedom at the chosen confidence level. In accord with IUPAC recommendations, a k value of 3 was applied, which in turn calls for a 99.87% confidence level. This confidence level was used in the linear regression analysis, and the denominator in equation 4.1 was taken as the upper 99.87% value of the

slope. This treatment yielded the detection limit of 3.1 mM for UO_2^{2+} and 2.6 mM for NO_3^- under the applied measurement conditions. The analogous Raman calibration measurements using extraction solvent containing 30 vol% TBP/n-dodecane loaded with $UO_2(NO_3)_2$ afforded detection limits of 1.9 and 21 mM for UO_2^{2+} and nitrate, respectively. The Raman spectra of variable $UO_2(NO_3)_2$ extracted into TBP/n-dodecane solvent is shown in Fig. 4.2 (right). To account for variable baseline shifts in the organic solvent system, the intensity of the UO_2^{2+} and nitrate bands (858.9 cm^{-1} and 1029 cm^{-1}, respectively) were normalized to the intensity of the dodecane solvent band at 1300.9 cm^{-1}. The 1300.9 cm^{-1} Raman band in dodecane is a strong vibrational band ascribed to the $-(CH_2)_n-$ in-phase twist characteristic of n-alkanes (Lin-Vien 1991). Due to its constant concentration as the diluent, this dodecane band is used as an internal standard.

Initial chemometric analysis of the Raman spectral data was undertaken using PLS analysis of the di-component uranyl nitrate – nitric acid solutions. Predictive models based on PLS analysis of Raman spectral data (containing variable UO_2^{2+}/total nitrate/proton concentrations) showed linear response over the 0–1.3 M and 0–3.5 M range for uranyl and nitrate species, respectively. Results of the PLS modeling based on Raman UO_2^{2+}, NO_3^-, and H^+ measurements are depicted in Fig. 4.3.

4.2.2   Visible-near infrared measurements

A series of solutions containing 0.1–10 mM Pu(IV) in the Simple Feed matrix was subjected to vis-NIR measurements. The spectral overlay obtained is shown in Fig. 4.4 (left). It was observed that Pu(IV) spectral features at 500–1000 nm were not obstructed by spectroscopic features of
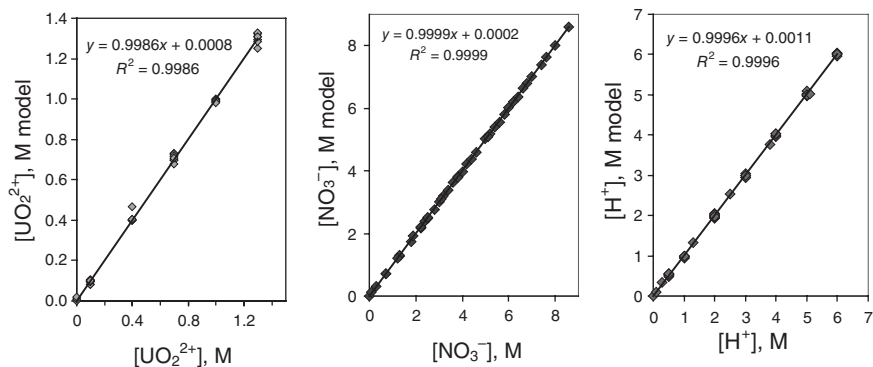
4.3 Chemometric PLS modeling of uranyl (left), total nitrate (middle), and nitric acid (right) concentrations based on Raman spectral data.
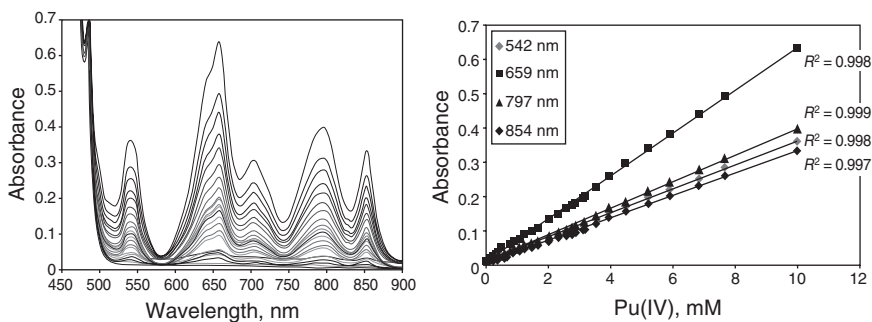
4.4 Absorption spectra of 0.1–10 mM Pu(IV) (left) in Simple Feed (1.33 M $UO_2(NO_3)_2$ and 0.8 M HNO_3) and corresponding calibration plots for Pu(IV) (right).
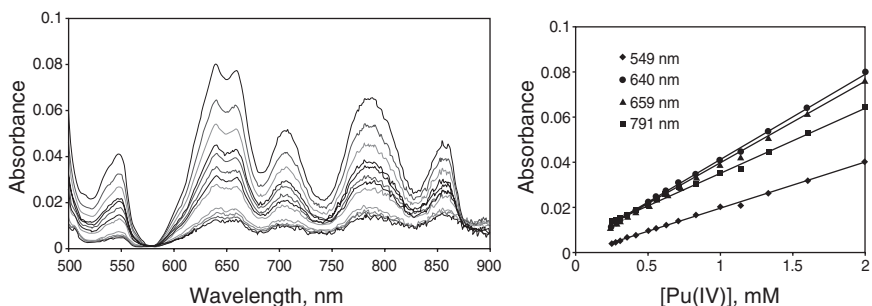
4.5 Vis-NIR spectra of variable Pu(IV) in TBP/dodecane extraction phase (left) and corresponding calibration plots for Pu(IV) (right). Detection limit is 0.014 mM for Pu(IV) using the 640 nm band.

$UO_2(NO_3)_2$ or HNO_3, and linear calibration plots were obtained using four characteristic Pu(IV) bands in this region (Fig. 4.4 right). The detection limit for Pu(IV) was determined to be 0.08 mM using the 659 nm band.

The distribution of Pu(IV) from the aqueous phase into the organic phase can be followed using vis-NIR spectroscopy of both the aqueous and organic phases. The characteristic Pu(IV) bands in the TBP/*n*-dodecane solution were slightly different than those in the aqueous nitrate solution, which reflects expected changes in the inner coordination environment of the Pu(IV) ion upon transport into the organic solvent.

To quantitatively determine Pu(IV) in the extraction phase, a series of solutions containing 0.2–2 mM Pu(IV) in 30% TBP/*n*-dodecane was measured by vis-NIR spectroscopy. The resulting spectral overlay is shown in Fig. 4.5 (left). The linear standard curves of the resulting Pu(IV) data are displayed in Fig. 4.5 (right). The detection limit for Pu(IV) in 30% TBP/*n*-dodecane was determined to be 0.014 mM using the 640 nm band.

Neptunium is present in the dissolved spent fuel predominantly as Np(V, VI) in the NpO_2^+ and NpO_2^{2+} chemical forms (Madic 1984). However, its redox equilibrium $Np(IV) \Leftrightarrow Np(V) \Leftrightarrow Np(VI)$ highly depends on the multiple factors including solution composition, temperature, etc. (Guillaume 1981). This redox chemistry determines Np distribution into 30% TBP/*n*-dodecane phase, and therefore, its spectroscopic monitoring is desirable. The aqueous speciation of Np(V) is complex because of its coordination with nitrate anion and formation of cation-cation complexes in accord with reactions 4.2 and 4.3 (Colston 2001):

$$NpO_2^+ + n\ NO_3^- \Leftrightarrow [NpO_2^+ \cdot n\ NO_3^-] \qquad 4.2$$

$$NpO_2^+ + M^{n+} \Leftrightarrow [NpO_2^+ \cdot M^{n+}] \qquad 4.3$$

where M^{n+} is transition or f-metal cation. In the dissolved spent fuel, the complex species $NpO_2^+ \cdot UO_2^{2+}$ formed as described by reaction 4.3 are the most prominent.

The single NpO_2^+ band observed in 1 M HNO_3 solution splits into two bands in the presence of U(VI). A second neptunium band nm emerges in the presence of U(VI) at the concentration ranges typical to the dissolved spent fuel streams (Steele 2007). As a result, Np(V) spectroscopic properties are highly mobile and dependent on solution composition. To this end, understanding and quantification of Np(V) chemistry is needed to correctly interpret its vis-NIR spectra.

To investigate the spectral nature of Np in the UREX process, a series of solutions of variable Np(V) concentration in 1.33 M $UO_2(NO_3)_2$ and 0.8 M HNO_3 were prepared; the vis-NIR spectra are shown in Fig. 4.6 (left).
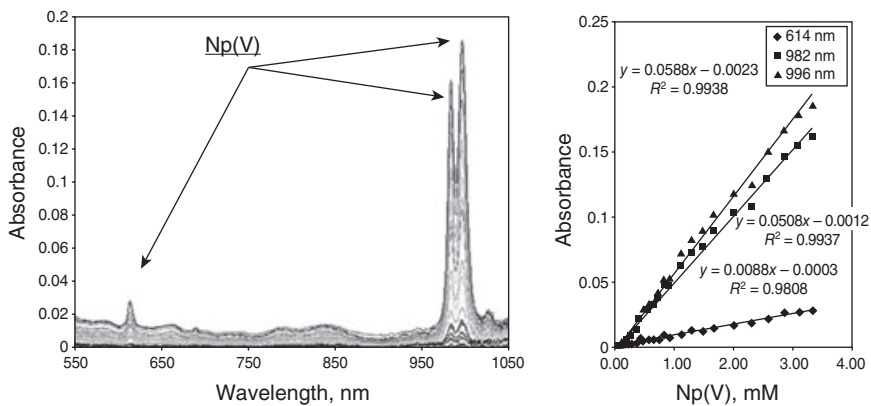
4.6 Absorption spectra of Np(V) (left) in the Simple Feed (1.3 M $UO_2(NO_3)_2$ in 0.8 M HNO_3) and corresponding calibration plots for Np(V) (right).
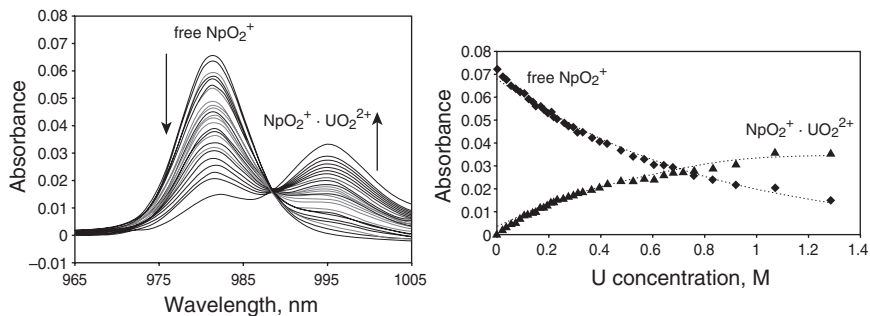
4.7 Spectral layout of 0.3 mM NpO_2^+ titrated with variable $UO_2(NO_3)_2$ solution, in 2.75 M HNO_3 (left), and corresponding relative concentrations of the "free" and "uranyl-bound" NpO_2^+ species in solution (right).

Two bands observed for the Np(V) in the UREX feed solution located at 981 and 992 nm in agreement with previous reports (Steele 2007). Figure 4.6 (right) shows the standard curves for the Np(V) vis-NIR data in the Simple Feed solution (Fig. 4.6, left). To illustrate the interaction of the $[NpO_2^+ \cdot UO_2^{2+}]$ cation-cation complex, a spectrophotometric titration was carried out in which uranyl nitrate was titrated into a constant concentration of Np(V). Figure 4.7 (left) shows the spectral overlay of the resulting vis-NIR spectra, revealing the gradual depletion of the "free" NpO_2^+ ion and the gradual increase of the "uranyl-bound" $[NpO_2^+ \cdot UO_2^{2+}]$ complex. The speciation diagram for the relative concentrations of the "free" and "bound" Np species are shown in Fig. 4.7 (right).

To evaluate the feasibility of Np(V) quantification in solutions containing significant concentrations of Pu(IV), a series of feed simulant solutions containing 0.1 mM Np(V) and a variable concentration of Pu(IV) (0.1–10 mM) in 1.33 M $UO_2(NO_3)_2$ and 0.8 M HNO_3 matrix was measured using vis-NIR (Fig. 4.8). The spectral overlay shown in this figure illustrates that the Np(V) is detected in the presence of large excesses of Pu(IV) and U(VI); Np was 100 times less concentrated than Pu, and 13 000 times less concentrated than U in solution (Levitskaia 2008). A conservative measure of the detection limit of Np(V) can be established at < 0.1 mM under UREX flowsheet conditions. An initial distribution experiment using a UREX feed containing Np(V), 10 mM Pu(IV) and 1.3 M $UO_2(NO_3)_2$ in 0.8 M HNO_3 showed no detectible Np(V) in the loaded 30% TBP/*n*-dodecane solvent by UV-vis-NIR as would be expected for the known low extractability of Np(V).

Initial chemometric analysis of vis-NIR spectral data was undertaken using separate Simple Feed solutions containing variable Np(V), U(VI),
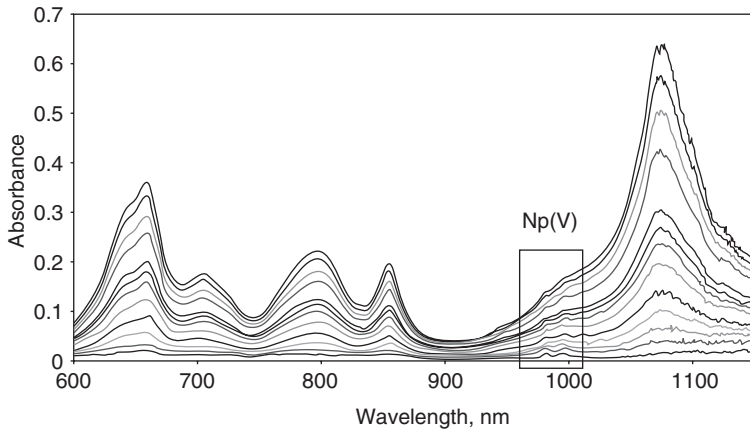
4.8 Absorption spectra of 0.1 mM Np(V) at variable 0.1–10 mM Pu(IV) in Simple Feed (1.3 M UO$_2$(NO$_3$)$_2$ in 0.8 M HNO$_3$).
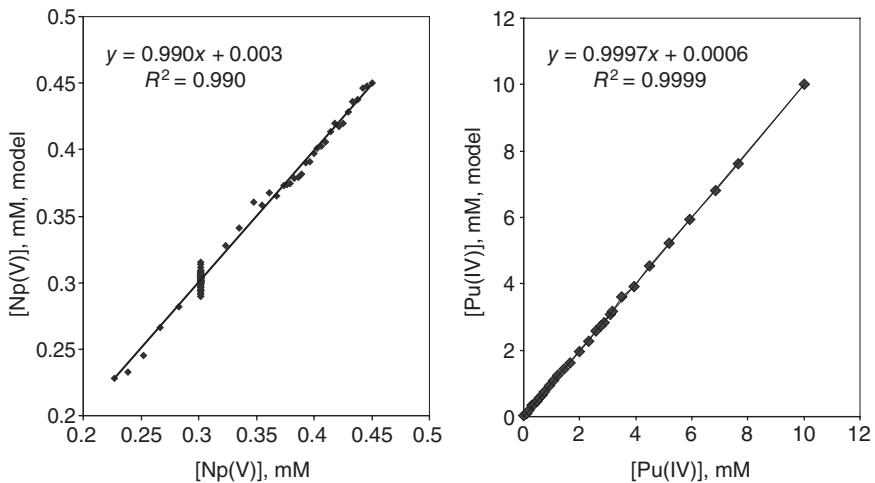
4.9 Chemometric PLS analysis results of vis-NIR spectral data for Np(V) (left) and Pu(IV) (right).

and Pu(IV). PLS analysis of vis-NIR spectral data (containing variable UO$_2$$^{2+}$/Np(V)/nitric acid concentrations) yielded linear response over 0–0.5 mM range for Np(V). A PLS model of the vis-NIR spectral region for Pu(IV) in UREX feed solution (Pu(IV) in 1.3 M UO$_2$(NO$_3$)$_2$ in variable HNO$_3$) showed a linear response over the 0–10 mM range for Pu. Figure 4.9 contains the results of the PLS analysis for Np(V) (left) and Pu(IV) (right).

4.3   Demonstration of spectroscopic methods

The spectroscopic methods discussed above are amenable for measuring components in commercial fuel and fuel simulant feeds. Section 4.3.1 discusses work performed using actual spent commercial fuel, including the preparation and dissolution of the fuel and the spectroscopic measurements of these fuel samples. The spectroscopic measurements were compared with ICP-MS analyses and ORIGEN code calculations. Section 4.3.2 describes real-time spectroscopic monitoring tests using a centrifugal contactor system deployed at PNNL. This section contains measurements resulting from "cold" testing of the contactor system containing HNO_3, $Nd(NO_3)_3$, and $NaNO_3$ and a "hot" demonstration using solutions containing $UO_2(NO_3)_2$ and Np(V) in nitric acid.

4.3.1   Spectroscopic demonstration using commercial fuel

Samples of commercial fuel were taken from a high-burnup ATM-109 fuel (Vaidyanathan 1997). The ATM-109 fuel consists of 6 rods that were also produced by General Electric (GE). The rods were initially irradiated in the Quad Cities I reactor beginning in February 1979 until September 1987 in a normal assembly amassing an average exposure of 43 MWd/kgU. The rods were then moved to a carrier assembly and irradiated from November 1989 until September 1992. When removed from the reactor, the average exposure reached 79 MWd/kgU. The rods spent a total of 3508 on-power days in the reactor. Post-irradiation examinations were performed at GE's Vallecitos Nuclear Center. The fuel sample dissolved for the spectroscopic demonstration had a burnup of 70 MWd/kgU and an initial enrichment of approximately 3%.

Fuel dissolution and sample preparation

A portion of ATM-109 fuel was removed from its cladding, dissolved in concentrated nitric acid, filtered, and partially evaporated. The equal aliquots of the dissolved fuel solution were diluted to the same volume by the variable nitric acid solutions to adjust uranium concentration to approximately 0.7 M and the acid strength to 0.3, 1.3, 2.5, 3.8, and 5.1 M to mimic the feed stream for a PUREX or UREX process in uranium concentration and provide a range of acid variations that might occur in the feed stream. The uranium and other fuel component concentrations remained the same in each sample, regardless of the acid strength.

Using a batch technique for the first stage of the PUREX process, the acid-adjusted aqueous solutions were contacted with equal volume of a 30 vol% TBP/*n*-dodecane solvent. The mixtures were allowed to reach an
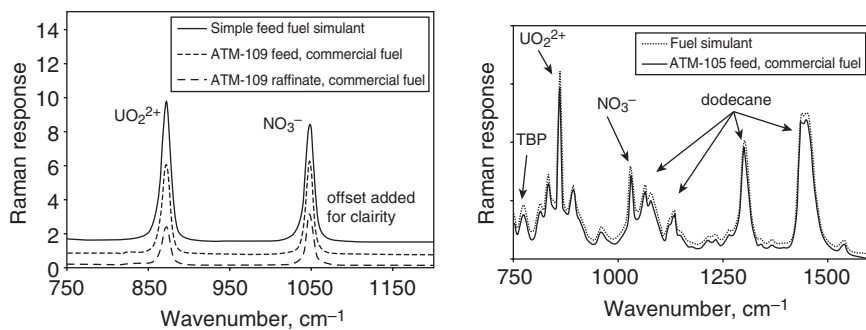
4.10 Raman spectra of (A) ATM-109 BWR commercial fuel 0.3 M HNO$_3$ feed, raffinate, and simple feed simulant solution (1.33 M uranyl nitrate in 0.8 M HNO$_3$); and (B) TBP-dodecane extraction solutions of ATM-109 feed and simple feed simulant solutions.

equilibrium distribution; then, the phases were separated. The feed, raffinate, and extract samples were subjected to spectroscopic analysis as described in the next section.
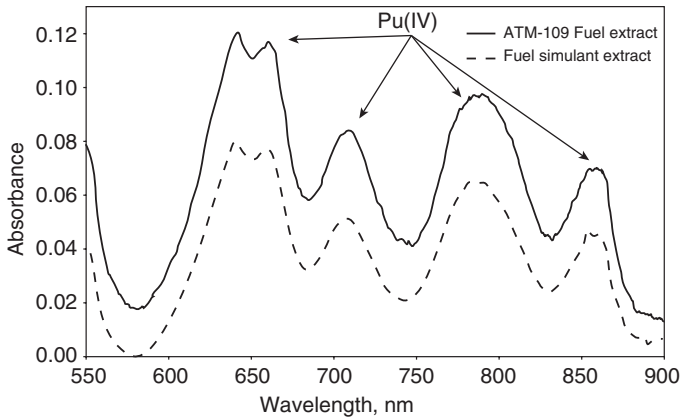
Spectroscopic measurements of commercial fuel

The goal of Raman and vis-NIR spectroscopic measurements of the dissolved ATM-109 fuel solutions was to assess the utility of optical process monitoring methods employing Raman and vis-NIR for the direct measurement of dissolved fuel feed, 30% TBP/*n*-dodecane extraction, and raffinate phases under the conditions of complex composition of the dissolved commercial fuel containing multiple light-absorbing species potentially interfering with detection and quantification of the target analytes.

Direct Raman measurements of the aqueous nitric acid feed and raffinate solutions performed on commercial fuel ATM-109 are shown in Fig. 4.10 (left). This figure also contains a spectrum of the Simple Feed fuel simulant (containing 1.3 M UO$_2$(NO$_3$)$_2$/0.8 M HNO$_3$) for comparison of the Raman response between simulants and actual fuel samples. The spectral features responsible for the UO$_2^{2+}$ and NO$_3^-$ bands (870 and 1047 cm^{-1}, respectively) in the fuel feed and raffinate samples are in excellent agreement with those contained within the Simple Feed simulant. The TBP/*n*-dodecane extract phase of ATM-109 fuel was also measured by Raman spectroscopy. Figure 4.10 (right) compares the Raman spectra of TBP/*n*-dodecane extracts of ATM-109 feed and Simple Feed simulant. No shift of the UO$_2^{2+}$ and NO$_3^-$ bands Raman bands (858 and 1029 cm^{-1}, respectively) between the extraction phases loaded using actual commercial fuel and simulant solutions was observed. Other bands observed in the extraction phase Raman spectra were assigned to the solvent (TBP and *n*-dodecane).
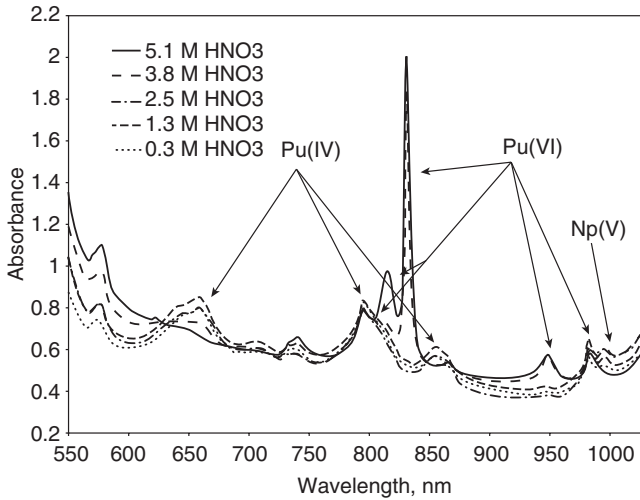
4.11 Absorption spectra of aqueous ATM-109 commercial fuel solution in 0.3–5.1 M HNO₃.

4.12 Absorption spectra of TBP/dodecane extraction phase of ATM-109 commercial fuel 3.8 M HNO₃ solution and of simple feed simulant solution containing 10 mM Pu(IV).

Spectrophotometric measurements of the aqueous feed solutions of the ATM-109 commercial fuel samples were performed using the vis-NIR spectral region. Plutonium in both Pu(IV) and Pu(VI) oxidation states was observed in the commercial fuel feed, with varying concentrations depending on the HNO₃ concentration, as is apparent in Fig. 4.11. Neptunium as Np(V) was evident in the ATM-109 fuel (Fig. 4.11).

Figure 4.12 (top) shows the vis-NIR spectra of the organic extraction phase from ATM-109 in 5.1 M HNO₃. The spectral bands observed in

Table 4.1 Analytical results for ATM-109 commercial fuel sample

ATM-109	Nd, M	Np, M	U, M	Pu, M
ORIGEN	1.1E-02	4.6E-04	7.2E-01	7.5E-03
ICP-MS	8.4E-03	4.7E-04	7.2E-01	9.0E-03
Spectroscopic[a]	5.4E-03	3.0E-04	7.3E-01	9.6E-03
ORIGEN / ICP ratio	*1.3*	*1.0*	*1.0*	*0.8*
Spectroscopic / ICP ratio	*0.6*	*0.6*	*1.0*	*1.1*

a) Spectroscopic values are preliminary estimate based on combination of chemometric analysis and traditional Beers Law analysis.

Fig. 4.12 are those diagnostic for Pu(IV). For comparison, a fuel simulant containing a feed composition of 1.33 M $UO_2(NO_3)_2$ in 0.8 M HNO_3 with a Pu(IV) concentration of 2 mM was contacted with the 30% TBP/*n*-dodecane PUREX solvent followed by spectroscopic measurement by vis-NIR spectroscopy, with the resulting spectra shown in Fig. 4.12 (bottom). There is excellent agreement in comparing the Pu(IV) bands between the actual commercial fuel extract (Fig. 4.12, top) and fuel simulant extract (Fig. 4.12, bottom).

The Raman and vis-NIR spectra of the ATM-109 feeds were subjected to chemometric analysis and standard Beers Law spectral analysis to determine the concentrations of U, Pu, and Np present in solution. The resulting concentrations are contained in Table 4.1. For comparison, the ICP-MS results are also displayed, along with both the ORIGEN code calculations for these fuel samples and the computed ratios of analytical results for ORIGEN/ICP and Spectroscopic/ICP data. From this table, it is evident that the spectroscopic method is in excellent agreement with the standard ICP-MS analysis.

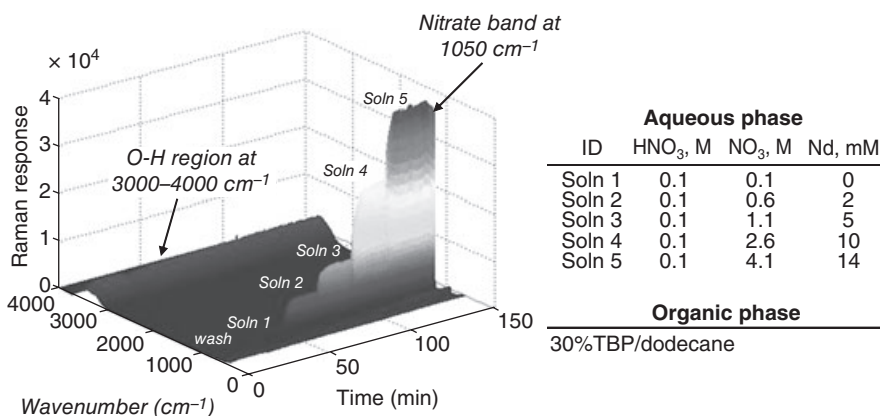## 4.3.2 Demonstration of real-time spectroscopic monitoring using centrifugal contactors

Two banks of multiple counter-current 2-cm centrifugal contactors were instrumented with vis-NIR and Raman spectroscopy probes in order to demonstrate the ability to measure solution components in real-time within a solvent extraction system. Typically the centrifugal contactors operated at 3600 rpm, with an aqueous phase feed rate of 12 ml/min, and an organic phase (30% TBP/*n*-docecane) feed rate of 18 ml/min. The effluent containing the raffinate stream from the extraction bank was passed through a commercial vis-NIR flow cell (2.5 cm path length, Custom Sensors Inc), followed by a custom fabricated flow-through Raman cell containing a commercial 180° backscatter Raman probe (Inphotonics Inc). A bank

consisting of four contactors was located in a non-radiological fume hood for "cold" testing, while a similar bank consisting of 16 contactors was located within a radiologically shielded glovebox allowing for demonstration with feed solutions containing uranium and neptunium.

Process monitoring demonstration using centrifugal contactor: cold testing

Initial non-radioactive tests to evaluate performance of the spectroscopic equipment under the flow conditions employed 30% TBP/*n*-docecane and five aqueous solutions containing variable nitric acid and neodymium nitrate concentrations were introduced into the extractor bank in a counter-current manner. The spectroscopic probes were positioned to measure the effluent from the extractor banks of the raffinate (aqueous) stream. Starting with a water wash and then proceeding with solutions 1–5 (compositions are given in Fig. 4.13) in sequential order, approximately 200 mL of each aqueous phase solution was delivered through the contactors, while the organic phase delivery was constant during the experiment. The Raman spectra collected during the experiment are shown in Fig. 4.13.

The nitrate and neodymium concentrations of the solutions were determined using PLS analysis of the spectroscopic data. Figure 4.14 shows the plots of both the nitrate and neodymium concentrations as a function of experimental time from the Raman and vis-NIR data, respectively. The initial feed concentration is outlined in light grey, and the measured concentration in the raffinate is indicated as dark grey symbols. As expected, the nitrate concentration in the raffinate (Fig. 4.14 a) nearly mirrors the

Aqueous phase			
ID	HNO_3, M	NO_3, M	Nd, mM
Soln 1	0.1	0.1	0
Soln 2	0.1	0.6	2
Soln 3	0.1	1.1	5
Soln 4	0.1	2.6	10
Soln 5	0.1	4.1	14

Organic phase
30%TBP/dodecane

4.13 Raman spectra of aqueous raffinate solutions collected on-line during counter current flow extraction experiment showing variable nitrate response at 1050 cm^{-1}.
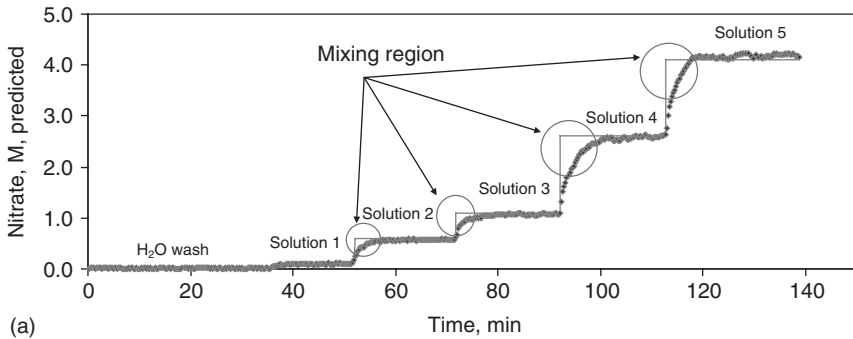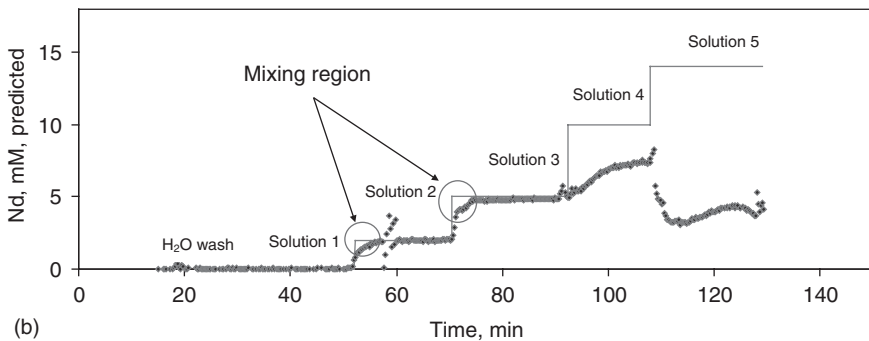
4.14 PLS predictions of (a) nitrate and (b) neodymium concentrations based on on-line Raman and vis-NIR measurements, respectively, as a function of experimental time. The light gray line denotes the concentration of analyte species in the feed solution; the dark gray symbols denote the PLS predicted concentration in raffinate stream; the analyte concentrations for solutions 1–5 are shown in Fig. 4.13.

concentration in the feed, attributed to the insignificant extraction of total nitrate into the organic phase. In contrast, the neodymium shows appreciable extraction when the total nitrate concentration exceeds approximately 1 M (Fig. 4.14 b). This figure also depicts the noticeable mixing regions reflecting the consequent switching of the feed solutions; the measured concentration of the analyte lags in time because of the time needed for the new solution to be integrated into the counter-current contactor bank.

The results of a batch contact distribution experiment for $Nd(NO_3)_3$ in variable nitrate with 30% TBP/*n*-dodecane is shown in Fig. 4.15. The measured concentrations for Nd^{3+} in the feed and raffinate are plotted in the figure at left, and the resulting distribution values for Nd (D_{Nd}) as a function of total nitrate concentration are shown in the figure on the right. Distribution values for Nd^{3+} depend linearly on the nitrate concentration
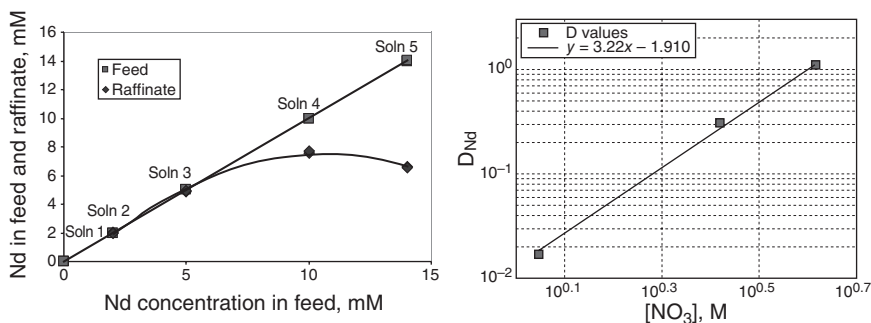
4.15 Batch contact distribution experiment for Nd(NO$_3$)$_3$ in variable nitrate (composition of solutions 1–5 are shown in Fig. 4.13) with TBP/dodecane.

in the aqueous phase with the corresponding slope of nearly 3 (3.22) confirming the extraction of Nd(NO$_3$)$_3$ by TBP. This verifies that the decrease of Nd optical signal observed in the raffinate stream (for solutions 4 and 5) is due to the enhanced Nd extraction leading to the depletion of the Np in aqueous phase and not due to the instrumental failure.

Process monitoring demonstration using centrifugal contactors: hot testing

A series of feed solutions sequentially increasing in nitric acid and then increasing in UO$_2$(NO$_3$)$_2$ concentration were introduced into the "hot" centrifugal contactor system to test the online performance of the spectroscopic equipment as part of the centrifugal contactor system. At this stage, no contact with TBP/*n*-dodecane was done. Raman spectra were collected concurrent with the additions of HNO$_3$ and UO$_2$(NO$_3$)$_2$ into the feed. Figure 4.16 shows the accumulated Raman spectra taken over the time frame of the nitric acid and uranyl nitrate additions. Several spectral features are apparent: the water region at 3000–4000 cm^{-1}; the nitrate band at 1050 cm^{-1}; and the UO$_2^{2+}$ at 871 cm^{-1}. Collected spectra were subjected to a previously developed chemometric model, and a successful translation of the model based on static UO$_2$(NO$_3$)$_2$/HNO$_3$ measurements to the flow on-line monitoring was achieved. Figure 4.17 contains the expected and predicted concentrations of the Raman on-line measurements and shows excellent agreement between values. It is worth noting that the model is capable of not only predicting the UO$_2^{2+}$ and nitrate concentrations but is also capable of differentiating between total nitrate and nitric acid. The distinction between nitrate and nitric acid is possible due to the inclusion of all the spectral data within the Raman spectrum, including the water region (3000–4000 cm^{-1}) and multiple nitrate bands (of which 1050 cm^{-1} is the largest),

	Fuel Feed Simulant, M		
ID	HNO$_3$	UO$_2$(NO$_3$)$_2$	NO$_3$ total
HNO$_3$-1	0.5	0	0.5
HNO$_3$-2	1	0	1.0
HNO$_3$-3	2	0	2.0
HNO$_3$-4	4	0	4.0
HNO$_3$-5	5	0	5.0
HNO$_3$-6	6	0	6.0
UO$_2$-1	6	0.1	6.2
UO$_2$-2	6	0.2	6.4
UO$_2$-3	6	0.3	6.6
UO$_2$-4	6	0.4	6.8
UO$_2$-5	6	0.5	7.0
UO$_2$-6	6	0.6	7.2
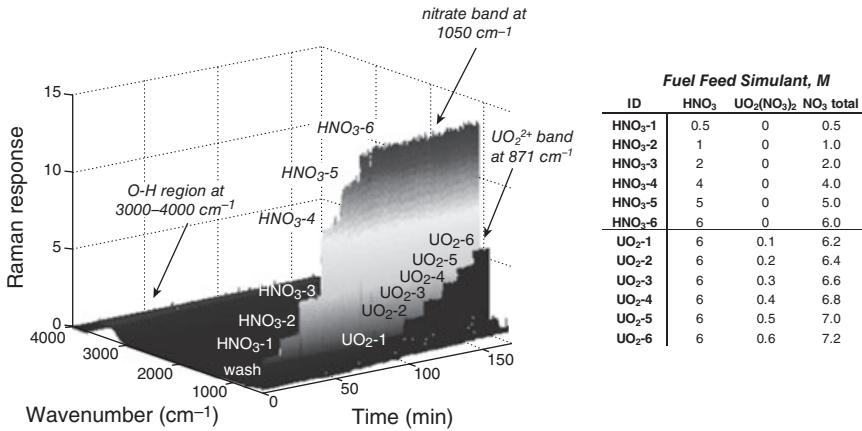
4.16 On-line Raman monitoring of the composition of the raffinate solution in the centrifugal contactor extraction experiment. Fuel feed simulant solutions: 0–6 M HNO$_3$ and 0–0.6 M UO$_2$(NO$_3$)$_2$. Organic phase: 30% TBP-dodecane solution.
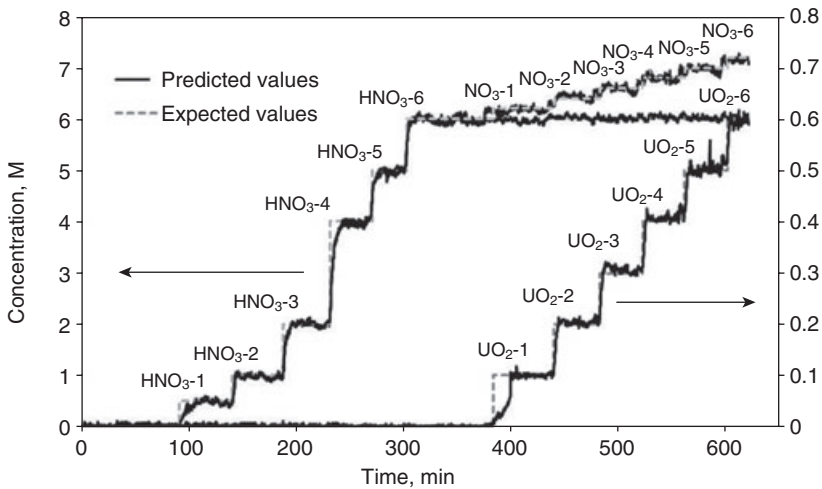
4.17 On-line PLS predictions of nitric acid, total nitrate, and uranyl concentrations based on on-line Raman measurements as a function of experimental time. Measured and predicted Raman on-line measurements showing excellent agreement between values. The light gray lines are the instantaneous concentrations of added analyte in solution (assuming zero mixing time); the dark gray lines are the predicted concentration of HNO$_3$, total nitrate, and UO$_2$(NO$_3$)$_2$ respectively.

which show subtle but reproducible changes based on acid content and the ionic strength of the solution.

4.4   Conclusions

Raman- and vis/NIR-based methods show promise for real-time on-line monitoring of spent fuel reprocessing via aqueous schemes. This chapter summarizes proof-of-principle preliminary spectroscopic measurements and chemometric predictive modeling of aqueous and organic 30% TPB/*n*-dodecane-based solutions. In-house Raman and optical spectroscopic instrumentation exhibited adequate performance (sensitivity, detection limit, and resolution) for measurements of uranium, plutonium, neptunium, and nitrate species in simulant and actual commercial fuel solutions. The real-time analysis of a variable feed nitric acid/UO_2^{2+}/nitrate system was demonstrated using a counter-current extraction system instrumented with on-line spectroscopic process monitoring probes. It was concluded that spectroscopic training data sets for the chemometric model development can be acquired under static conditions and translated to the on-line flow monitoring with minor modifications. Future experimentation is needed to incorporate temperature/density/conductivity into the predictive modeling. Further studies on possible modifications of the spectroscopic instrumentation targeting improved and stable on-line performance over long periods of time and enhanced mathematical processing are warranted.

4.5   Acknowledgments

4.6   References

Armenta, S., Garrigues, S. & De La Guardia, M., 2007. Recent developments in flow-analysis vibrational spectroscopy. *Trends in Analytical Chemistry*, 26(8), pp. 775–787.

Baumgartner, F. & Ertel, D., 1980. The modern PUREX process and its analytical requirements. *The Journal of Radioanalytical and Nuclear Chemistry*, 58(1–2), pp. 11–28.

Bryan, S.A., Levitskaia, T.G. & Sinkov, S.I., 2005. *Process Monitor Development Project: Acceptance Test Report*, PNNL-15360, Pacific Northwest National Laboratory, Richland, Washington.

Bryan, S.A. & Levitskaia, T.G., 2007. *Monitoring and Control of UREX Radiochemical Processes*. GLOBAL 2007, Boise, Idaho.

Bryan, S.A., Levitskaia, T.G., Sinkov, S.I. & Schlahta, S., 2008. *Raman Based Process Monitor For Continuous Real-Time Analysis Of High Level Radioactive Waste Components*. Waste Management WM2008 Conference, Phoenix, Arizona.

Bürck, J., 1991. Spectrophotometric determination of uranium and nitric acid by applying partial least squares regression to uranium(VI) absorption spectra. *Analytica Chimica Acta*, 254(1–2), pp. 159–165.

Burney, G.A. & Harbour, P.J., 1974. *Radiochemistry of Neptunium, in United States Atomic Energy Commission*. National Technical Information Service; Springfield, Virginia.

Charrin, N., Moisy, P. & Blanc, P., 2000a. Determination of fictive binary data for plutonium(IV) nitrate. *Radiochimica Acta*, 88(1), pp. 25–31.

Charrin, N., Moisy, P. & Blanc, P., 2000b. Contribution of the concept of simple solutions to calculation of the density of ternary and quaternary solutions of thorium(IV) or plutonium(IV) nitrate: $An(NO_3)_4/UO^2(NO_3)_2/HNO_3/H_2O$. *Radiochimica Acta*, 88(8), pp. 445–451.

Cleveland, J.M., 1979. *The Chemistry of Plutonium*. American Nuclear Society, La Grange Park, Illinois.

Colston, B.J. & Choppin, G.R., 2001. Evaluating the performance of a stopped-flow near-infrared spectrophotometer for studying fast kinetics of actinide reactions. *The Journal of Radioanalytical and Nuclear Chemistry*, 251(1), pp. 21–26.

Enokida, Y., Shiga, M. & Suzuki, A., 1992a. Determination of uranium(VI) over wide concentration ranges in aqueous nitric-acid and 30-percent tri-n-butyl phosphate by laser-induced thermal lensing spectroscopy. *Radiochimica Acta*, 57(2–3), pp. 101–104.

Enokida, Y. & Suzuki, A., 1992b. Estimation of uranium(VI) concentrations by temperature profile in solvent-extraction processes using 30-percent tri-normal-butyl phosphate diluted with normal-dodecane. *The Journal of Nuclear Science and Technology*, 29(5), pp. 461–471.

Ertel, D., 1985. Analytical methods in the PUREX process. *Atomkernenergie-Kerntechnik*, 46(2), pp. 89–94.

Ertel, D., Groll, P., Knittel, G. & Thessis, W., 1976. Process analysis in PUREX method. *Journal of Radioanalytical Chemistry*, 32(2), 297–314.

Guillaume, B., Hobart, D.E. & Bourges, J.Y., 1981. Cation-cation complexes of pentavalent actinides 2. Spectrophotometric study of complexes of Am(V) with UO_2^{2+} and NpO_2^{2+} in aqueous perchlorate solution. *Journal of Inorganic & Nuclear Chemistry*, 43(12), pp. 3295–3299.

Guillaume, B., Begun, G.M. & Hahn, R.L., 1982. Raman spectrometric studies of cation cation complexes of pentavalent actinides in aqueous perchlorate solutions. *Inorganic Chemistry*, 21(3), pp. 1159–1166.

Kumar, S. & Koganti, S.B., 1998. Prediction of densities of mixed organic solutions containing $UO_2(NO_3)_2$ and nitric acid. *Journal of Nuclear Science and Technology*, 35(4), pp. 309–312.

Lascola, R.J. & Cooper, G.A., 2002. *Feasibility of Uranium Concentration Measurements For H Canyon Tank 16.7*, WSRC-TR-2002-00568, Westinghouse Savannah River Company, Savannah River Site, Aiken, SC 29808.

LeClaire, N.P., Anno, J.A., Courtois, G., Dannus, P., Poullot, G. & Rouyer, V., 2003. Criticality calculations using the isopiestic density law of actinide nitrates. *Nuclear Technology*, 144(3), pp. 303–323.

Levitskaia, T.G. & Bryan, S.A., 2008. On-line monitoring and control of radiochemical streams at spent fuel reprocessing plant. In CEA, (Commissariat à l'énergie atomique, the French Atomic Energy Commission) *3rd International ATALANTE Conference*. Montpellier, France 19–23 May 2008.

Lin-Vien D., Colthup, N.B., Fateley, W.G. & Grasselli, J.G., 1991. *The Handbook of Infrared and Raman Characteristic Frequencies of Organic Molecules*. San Diego, Academic Press, Inc.

Long, G. L. & Winefordner, J. D., 1983. Limit of detection: a closer look at the IUPAC definition. *Analytical Chemistry*, 55, pp. 712A–724A.

Madic, C., Hobart, D.E. & Begun, G.M., 1983. Raman spectrometric studies of actinide(v) and actinide(VI) complexes in aqueous sodium-carbonate solution and of solid sodium actinide(V) carbonate compounds. *Inorganic Chemistry*, 22(10), pp. 1494–1503.

Madic C., Begun, G.M., Hobart, D.E. & Hahn, R.L., 1984. Raman spectroscopy of neptunyl and plutonyl ions in aqueous solution: hydrolysis of Np(VI) and Pu(VI) and disproportionation of Pu(V). *Inorganic Chemistry*, 23, pp. 1914–1921.

Maya, L. & Begun, G.M., 1981. A Raman-spectroscopy study of hydroxo and carbonato species of the uranyl(VI) ion. *Journal of Inorganic & Nuclear Chemistry*, 43(11), pp. 2827–2832.

Nguyentrung, C., Begun, G.M. & Palmer, D.A., 1992. Aqueous uranium complexes 2. Raman-spectroscopic study of the complex-formation of the dioxouranium(VI) ion with a variety of inorganic and organic-ligands. *Inorganic Chemistry*, 31(25), pp. 5280–5287.

Parus I., Kierzek, J. & Zoltowski, T., 1977. Online control of nuclear fuel reprocessing. *Nukleonika*, 22(9), pp. 759–776.

Ryan, J.L., 1960. Species involved in the anion-exchange absorption of quadrivalent actinide nitrates. *Journal of Physical Chemistry*, 64(10), pp. 1375–1385.

Sakurai, S. & Tachimori, S., 1996. Density equation of aqueous solution containing plutonium(IV), uranium(VI) and nitric acid. *Journal of Nuclear Science and Technology*, 33(2), pp. 187–189.

Schmieder, H. & Kuhn, E., 1972. Automatic measurement and control of nuclear fuel reprocessing by spectrophotometry and conductivity measurements. *Chemie Ingenieur Technik*, 44(3), p. 104.

Steele, H. & Taylor, R.J., 2007. A theoretical study of the inner-sphere disproportionation reaction mechanism of the pentavalent actinyl ions. *Inorganic Chemistry*, 46(16), pp. 6311–6318.

Stout, B.E., Choppin, G.R., Nectoux, F. & Pages, M., 1993. Cation cation complexes of NpO2+. *Radiochimica Acta*, 61(2), pp. 65–67.

Vaidyanathan, S., Reager, R.D. & Warner, R.W., 1997. High burnup BWR fuel pellet performance. In American Nuclear Society, *Proceedings of the International Topical Meeting on Light Water Reactor Fuel Performance*, pp. 471, March 2–6, 1997, Portland, Oregon.

Vandegrift, G.F., Regalbuto, M.C., Pereira, C., Aase, S., Bakel, A., Bowers, D., Byrnes, J.P., Clark, M.A., Emery, J.W., Falkenberg, J.R., Gelis, A.V., Hafenrichter, L., Tsai, Y., Quigley, K.J. & Vander Pol, M.H., 2004. *Results of the UREX+ spent fuel demonstration.* Letter Report, Argonne National Laboratory, Argonne, Illinois.

Yamamoto, M., 1988. Determination of nitric acid concentration in 30 vol percent TBP-n-dodecane by measuring dielectric properties. *Journal of Nuclear Science and Technology*, 25(6), pp. 540–547.

4.7   Appendix: acronyms

ANL   Argonne National Laboratory
IAEA   International Atomic Energy Agency
IUPAC   International Union of Pure and Applied Chemistry
PLS   partial least squares
PNNL   Pacific Northwest National Laboratory
RPL   Radiochemical Processing Laboratory
TBP   tri-butyl phosphate
UREX   uranium extraction
vis-NIR visible-near-infrared spectroscopy
UV-vis   ultraviolet-visible spectroscopy

5

Safeguards technology for radioactive materials processing and nuclear fuel reprocessing facilities

K. M. GOFF, G. L. FREDRICKSON and D. E. VADEN,
Idaho National Laboratory, USA

Abstract: The safeguarding of nuclear materials is a critical technical and political aspect of nuclear fuel reprocessing. Simply defined, nuclear safeguards are measures used to verify that civil nuclear materials are properly accounted for and are not diverted to undeclared uses. The goals of international nuclear safeguards are to detect proliferation and diversion of nuclear material from the civilian nuclear fuel cycle and to provide notification of potential diversion to the international community in a timely fashion so that the consequences of the diversion can be reduced. Although safeguards technologies and processes have advanced considerably over the last 60 years, they remain a significant focal point for concerns and discussions with respect to deployment of recycle technologies for used fuel.

Key words: safeguards, proliferation, International Atomic Energy Agency (IAEA), nuclear materials, material accountancy, nuclear material containment and surveillance extrinsic measures, intrinsic measures, nuclear fuel cycle, diversion, spent fuel treatment.

5.1   Introduction

The safeguarding of nuclear materials is a critical technical and political aspect of nuclear fuel reprocessing. Simply defined, nuclear safeguards are measures used to verify that civil nuclear materials are properly accounted for and are not diverted to undeclared uses (IAEA 1998, IAEA 2001). From an international perspective, the objectives of safeguards are to assure the international community that nations are not involved with the proliferation of non-peaceful applications of nuclear technology and to deter diversion of nuclear materials to the production of nuclear weapons or the misuse of safeguarded facilities to produce unsafeguarded materials (IAEA 1981). Although safeguards technologies and processes have advanced considerably over the last 60 years, they remain a significant focal point for concerns and discussions with respect to deployment of recycle technologies for spent fuel.

120

In January 1946, the United Nations (UN) Atomic Energy Commission was created through the first resolution passed by the UN General Assembly (IAEA 1981, OTA 1995). The justification was the "establishment of a commission to deal with the problems raised by the discovery of atomic energy" (OTA 1995, UN 1946, Wu 1972). The aspect of nuclear safeguards was one of the key issues to be addressed by this newly formed commission.

Prior to this international action, the United States established a commission to address safeguards. It was chaired by Under Secretary of State Dean Acheson (OTA 1995). The Acheson-Lilienthal Report (Lilienthal *et al.* 1946) was issued in March 1946, and it foresaw the need for international organizations to control fissionable materials.

The plan set forth by the United States government at the first session of the UN Atomic Energy Commission (UNAEC) became known as the Baruch Plan (Baruch 1946). It was named after Bernard Baruch who represented the United States on the UNAEC. This proposal, issued in June 1946, also called for an international control mechanism. However, the plan was not approved due to conflicts concerning the role of the UN Security Council (OTA 1995). The UNAEC was eventually dissolved in 1952 (IAEA 1981).

In the 1950s, work again progressed on establishing an international organization to support nuclear materials safeguards. In December 1953, President Eisenhower made his "Atoms for Peace" speech to the UN in which he proposed an international atomic energy agency and his vision was that "the most important responsibility of the new agency would be to devise methods whereby fissionable material would be allocated to serve the peaceful pursuits of mankind" (Eisenhower 1953). From this start, the International Atomic Energy Agency (IAEA) became operational in 1957.

The powers of the IAEA were limited. The IAEA did not control nuclear materials or have highly intrusive powers of inspection or enforcement (OTA 1995). The IAEA was given the power to establish safeguards agreements with nations to ensure materials and equipment were not used for the production of nuclear weapons. In 1959, the IAEA concluded the first such agreement with Japan. A more comprehensive IAEA safeguards regime was not established until 1965.

In May 1970, the UN General Assembly endorsed the Treaty on the Non-Proliferation of Nuclear Weapons (NPT), which expanded the scope of IAEA safeguards activities. Those nations that joined the NPT could receive technology on the peaceful uses of nuclear energy, provided they also agreed to not acquire nuclear weapons. These NPT nations also became subject to IAEA safeguards requirements.

5.2   Requirements

Requirements for safeguarding nuclear materials exist both internationally and domestically. Nations involved with nuclear activities, either at a governmental or industrial level, must establish a regulatory framework to oversee aspects of the work including worker safety, environmental protection, and nuclear safeguards. In the United States, domestic requirements are established through the Nuclear Regulatory Commission and the Department of Energy. Internationally, the IAEA is responsible for nuclear materials safeguards. According to the IAEA, "The IAEA is the world's nuclear inspectorate, with more than four decades of verification experience. Inspectors work to verify that safeguarded nuclear material and activities are not used for military purposes" (IAEA 2005a).

In general, the goals of international nuclear safeguards are to detect proliferation and diversion of nuclear material from the civilian nuclear fuel cycle and to provide notification of potential diversion to the international community in a timely fashion so that the consequences of the diversion can be reduced. Nuclear material is specifically defined as either special fissionable material or source material. Special fissionable material is plutonium-239 or uranium enriched in either uranium-235 or uranium-233. Source material is material that can be used to produce special fissionable material, which includes natural uranium, depleted uranium, and thorium.

A goal of the IAEA is to detect diversion of significant quantities of nuclear material. In general terms, a significant quantity of material is considered a "threshold" amount needed to make a weapon (IAEA 1975). For example, spent light water reactor fuel contains both uranium and plutonium. For the reprocessing of spent nuclear fuel, plutonium is the main special fissionable material of concern. A significant quantity of plutonium is considered 8 kg total plutonium (Thomas and Longmire 2002). If dealing with highly-enriched uranium, a significant quantity is considered 25 kg of contained uranium-235 (IAEA 1981).

Safeguards goals focus on both detection and timeliness. Timeliness goals are applied to the input spent fuel and separated products, and specific timeliness goals are established based on the attractiveness level of the material of concern. For example, a timeliness goal may be based on the estimated minimum time required to convert a specific material into a form that can be used in a weapon. Conversion times can range from weeks to months and in some cases may extend to over a year (OTA 1995). A general goal is to be able to detect the diversion or loss of one significant quantity of plutonium (i.e., 8 kg) within one month. Goals for the detection of material in spent fuel are lower because the attractiveness level of that material

is much lower. Therefore, the timeliness goal for detection of a significant quantity of material from spent fuel is three months.

Low-enriched uranium is also recovered from the reprocessing of spent fuel. Low-enriched uranium contains less than 20% of the uranium-235 isotope. The timeliness goal for low-enriched uranium recovered from reprocessing is that no more than 75 kg of uranium-235 is unaccounted for within a one-year period (Thomas and Longmire 2002).

The two major components of nuclear safeguards are nuclear material accountancy and nuclear material containment and surveillance. Nuclear material accountancy is the system used to determine the amount of nuclear material present in a facility and to track the changes in the quantity of material as process activities are performed in the facility. It is basically an accounting system for keeping track of amount, type, form, and location of nuclear material in a facility. Measurement systems to establish these quantities are a major part of nuclear material accountancy.

Containment and surveillance complement nuclear material accountancy. Containment and surveillance are the methods used to ensure that movements of nuclear material are tracked. Containment specifically deals with ensuring that once nuclear material is placed into a physical container (whether a room, vault, enclosure, or container) that its location is known or tracked. Devices to support containment and surveillance include physical barriers, cameras, detectors, high radiation environments, and tamper indicating devices.

Nuclear material accountancy and nuclear material containment and surveillance are the backbone of nuclear materials safeguards for both the national and international communities. Operators of nuclear facilities, like a spent fuel reprocessing facility, establish systems for accountancy, containment, and surveillance. The data generated from these systems are provided to State agencies and the IAEA.

One function of the IAEA with respect to safeguards is to examine and evaluate the data provided by nations hosting nuclear facilities. The IAEA also has a significant role in data verification. They independently collect data and information from the facilities as well as perform inspections. IAEA inspections often include independent data collection and analysis using equipment that is independently designed, operated, and maintained by the IAEA. Inspections also provide verification of facility and process designs by ensuring that the facility is performing only the declared functions.

Since the nuclear material accountancy system relies on various measurements, the uncertainties associated with quantitative analytical measurements and mass, volume, and density measurements impact the interpretation

of the data. The nuclear accountancy system should be able to determine the quantity of material at the facility that is not accounted for, which is termed Material Unaccounted For (MUF). The MUF is sometimes referred to as the Inventory Difference (ID). In an ideal situation where there is perfect accountancy, when the nuclear accountancy books for a facility are closed, the MUF will assume a value of zero. However, because measurement uncertainties always exist, the value of MUF must be compared against the value of the measurement uncertainty. The accountancy system needs to be able to distinguish, to a reasonable degree, if the MUF values are "not significant", in which case they are indicative of the expected measurement uncertainties, or are "significant", in which case they are indicative of possible diversion. Obviously, high uncertainties would make it impossible to detect diversion, regardless of the MUF value.

Facilities will have detection goals to determine if the MUF values are significant. In establishing these goals, detection systems can result in two types of error. The first type of error is a false positive, where an alarm is signaled, but in fact no loss of material has occurred. False positive alarms obviously have significant operational issues in a production facility, not the least of which is loss of credibility for the system's integrity. The second type of error is a false negative, where an alarm is not signaled, but in fact a loss of material has occurred. This situation is much more serious because it results in a case where material loss or diversion is not detected. Typical IAEA thresholds are established at a 90% detection probability for detecting diversion of a significant quantity of nuclear material and 5% as the maximum accepted value for a false alarm rate (OTA 1995).

In the event that the IAEA receives evidence that diversion of nuclear material may have occurred, the protocol is for the IAEA Director General to deliver a report to the IAEA Board of Governors, which must then make an evaluation. If they are unable to verify that no diversion has occurred, the Board of Governors may take actions, which can include reporting to the UN General Assembly or the UN Security Council. The Security Council, the only UN body with executive powers, has authority to take action including the implementation of international sanctions.

There are presently 146 IAEA member states and 237 safeguards agreements in force in 163 countries. In 2007, 2122 safeguards inspections were performed. The IAEA's detection and verification system is not perfect. To note from IAEA documentation, "safeguards can neither predict diversions ahead of time, nor physically predict them, nor be guaranteed to detect them 100 percent of the time, and they should not be expected to do so" (Thomas and Longmire 2002). Still the IAEA, working with individual nations, serves an extremely important function with respect to safeguards.

Transparency is also a critical component of safeguards and non-proliferation. Transparency consists of actions taken by a facility or nation to enhance the openness of activities to ensure other nations or organizations like the IAEA that they are not performing clandestine operations. Transparency would include allowing inspectors greater access to facilities, more openness in the timing of inspections, and wider environmental sampling to potentially detect undeclared activities.

5.3   Safeguards technology

Although many safeguards discussions focus on reprocessing facilities, the scope of facilities under IAEA safeguards is much broader. Uranium enrichment plants are also a major focus. Other types of facilities subject to some degree of IAEA safeguards include conversion plants, reconversion plants, fuel fabrication plants, nuclear power reactors, interim fuel storage facilities, and waste repositories. Based on 2002 data, there were 239 reactors, 80 fuel storage facilities, 41 fuel fabrication facilities, and 10 enrichment plants under IAEA safeguards. In contrast, there are only 6 reprocessing plants under some level of IAEA safeguards (IAEA 2003).

With the anticipated growth of nuclear power, there is a potential that reprocessing may expand. This has justifiably resulted in increased concerns about sustainability and environmental issues associated with spent fuel management. Nuclear reactors are unloading more than 10 500 MTHM of spent fuel per year, and there are estimated to be 340 000 MTHM in storage in 2010. With the capacity for commercial reprocessing at only 5 550 MTHM per year (IAEA 2008), more plants may need to be deployed to manage the existing inventories.

Reprocessing plants do have challenges with respect to nuclear materials safeguards. Verification requirements for reprocessing facilities impose what are probably the most complex design aspects of nuclear facilities. Verification activities for a reprocessing plant require more than 750 man-years compared to 6 to 12 man-years for a light water reactor (IAEA 2005b). Many of the challenges are associated with the nature and scale of large chemical plants that have potential high-throughputs of nuclear materials. As noted earlier, a goal of safeguards is the detection of a significant quantity of nuclear material in a timely manner. This goal is independent of the amount of material processed through the facility.

A typical commercial reprocessing facility may process on the order of 800 MTHM of light water reactor fuel per year. This spent fuel contains approximately one percent plutonium. Therefore, the annual plutonium throughout is 8 000 kg. This equates to more than 660 kg of plutonium processed on a

monthly basis, or 83 significant quantities. At these high throughput rates, detection of the loss of a significant quantity of plutonium (i.e., 8 kg) can be extremely challenging based solely on the uncertainties associated with verification measurements. Continual improvements are being made in reprocessing technologies, facility designs, and measurement techniques in order to further enhance the ability to safeguard reprocessing facilities.

In addition to the safeguard issues associated with large quantities of special nuclear material, reprocessing facilities also have a couple of other unique challenges. Reprocessing facilities subject to IAEA safeguards presently deploy aqueous separations technologies. For example, variations on the PUREX technology are routinely used. From the PUREX process, relatively pure separated plutonium is recovered. In the process portion of the plant, the fissile material is sometimes hard to assay accurately because the material is in the form of a solution as it is being processed.

IAEA safeguarded facilities have ranged from the first commercial reprocessing plant, EUROCHEMIC, built in Belgium during the 1960s to the Rokkasho Reprocessing Plant expected to come on line in Japan in 2009. As reprocessing technologies have advanced with respect to efficiencies and reduction of environmental impacts, steps have also been taken to further improve nuclear materials safeguards. Advancements in the separations technologies have also focused on non-proliferation aspects of reprocessing.

Safeguards remain a key factor to reduce the risk of proliferation from reprocessing facilities, as well as other nuclear facilities. With respect to reprocessing, technology development has also focused on areas outside of safeguards to potentially reduce the risk of proliferation. Proliferation barriers are divided into two groups, intrinsic and extrinsic. Intrinsic barriers are those that are inherently part of the system, while extrinsic barriers are more institutional or administrative in nature.

Much of the technology development associated with reprocessing has focused recently on increasing intrinsic barriers. Examples include development of new process flowsheets that do not result in the separation and recovery of purified plutonium. This work includes development of flowsheets that result in the recovery of a plutonium-uranium product instead of a purified plutonium product. A flowsheet of this type is deployed in Rokkasho. Another type of intrinsic feature is complete group recovery of all actinides (i.e., uranium, plutonium, neptunium, americium, and curium). Recent developments in both aqueous and dry separation technologies are focused on these efforts. Other intrinsic features include co-location of facilities to minimize transportation of special nuclear material. Co-location of fuel fabrication facilities has long been integrated with deployment of

some dry process technologies, but it is also now being considered for aqueous systems (Vinoche *et al.* 2005). Development of fuel types that are harder to process would also be considered an intrinsic feature. Extrinsic measures include activities such as the application of robust nuclear safeguards. Both extrinsic and intrinsic barriers are critical measures for non-proliferation.

As noted, a key component of safeguards is nuclear material accountancy, which is the system for tracking the quantity and movement of nuclear material in a facility. Because of the challenges associated with reprocessing plants, the specific physical areas over which measurements are performed are critical. These areas are called the material balance areas (MBAs) and they are incorporated into the physical design of the facility. An MBA is defined as an area inside or outside a facility over which the quantity of nuclear material transferred into or out of the facility can be determined. Additionally, the inventory within the MBA must be able to be determined (IAEA 2001). It is the movements of nuclear materials across the boundary surrounding the MBA that are reported to oversight groups like the IAEA.

An example of MBAs for a reprocessing plant consists of three distinct MBAs (OTA 1995, Thomas and Longmire 2002). The first MBA is associated with the receipt and storage of spent nuclear fuel to be processed. Fuel chopping and dissolution would be included in this MBA. The second MBA is associated with the reprocessing operations. The final MBA is associated with storage for the final products. Within MBAs, there are key measurement points or the locations where nuclear materials are in a form that is amenable to quantitative measurement. In general, these points need to occur near the inputs and outputs to the MBAs, but they are not limited to those locations.

Measurements to establish the inventory within a given MBA or process unit operation can involve a number of different techniques and physical data are needed. Depending on the form of the material measured, critical measurements may include mass, volume, flow rate, density, temperature, and chemical composition.

Analytical samples for safeguards measurements have some unique requirements. First, the sampled material must be homogeneous and, most importantly, the sample must be representative of the bulk material being considered. Next, the sample integrity must be maintained by chain-of-custody tracking to ensure that potential diversion is not masked by sample tampering or sample switching. Samples for safeguards purposes may be taken by the facility operator, but samples are also taken independently by the IAEA for verification. Those samples must be independently analyzed

by the IAEA and may require shipment to off-site IAEA laboratories. For a large reprocessing facility like Rokkasho, the IAEA established an on-site laboratory (Duhamel *et al.* 2005).

Concentration measurement techniques are generally divided into destructive and non-destructive analysis. Destructive analysis employs techniques that result in the destruction of the sample. Non-destructive analysis employs techniques that do not produce a significant physical or chemical change in the sample. Destructive analyses are used to quantify inventories fairly precisely. Non-destructive analyses are used predominately for verification (DeMuth *et al.* 2007).

Samples in a reprocessing plant consist of in-process solutions, final products, and waste streams. Examples of waste streams include cladding hulls after dissolution of spent fuel and undissolved solids.

The analytical technique employed for a sample depends on the sample form, characteristics to be measured, and the required uncertainty. For safeguards purposes, there are requirements to know both elemental composition (uranium and plutonium) and isotopic composition (uranium-235, uranium-238, plutonium-239, etc.).

Mass spectrometry is one key class of analytical techniques for these types of measurements. It is a destructive analysis. Mass spectrometry works by first ionizing the elements or compounds and then measuring their mass to charge ratios. Thermal ionization mass spectrometry (TIMS) is a critical technique for measurement of plutonium and uranium isotopics. The instrument is capable of high precision and accuracy. It can be used for many materials containing plutonium and uranium, and is the primary analytical method used for solutions of dissolved spent fuel. Isotopic dilution mass spectrometry (IDMS) is also employed as a technique for increased precision and accuracy. This technique involves dissolution of a known amount of a given isotope from the elements of concern in the sample. When analyses of spiked and unspiked samples are compared, significant improvement can be achieved in the precision and accuracy. Other destructive analysis techniques include X-ray fluorescence, potentiometric titration, controlled potential coulometry, ignition gravimetry, K-edge absorption densitometry, alpha spectrometry, and gamma ray spectrometry (OTA 1995, IAEA 2003).

Gamma ray spectrometry can also be used as a non-destructive technique. This technique takes advantage of the fact that most nuclear materials emit gamma rays of specific energies. Neutron detection can also be employed. Neutrons are emitted from spontaneous fission, induced fission, and reactions from the emission of alpha particles (alpha-neutron reactions).

Technology development and deployment activities are continuing to occur to further improve measurement techniques to enhance further

nuclear materials safeguards. For large reprocessing plants this work is beneficial to meeting detection goals in a timely manner. Much of this work has focused on a concept known as near-real-time accountancy. Inventories at the facilities are performed monthly and annually. The annual inventories are extensive and typically require the facility to stop process operations. The monthly inventories may be less precise because the facility is not necessarily shutdown, implying that the measurements are less precise for in process inventories. To improve detection of diversion, unattended instruments may be positioned in the facility at key points to provide measurements of nuclear materials. These instruments typically deploy non-destructive techniques like neutron coincidence counting (OTA 1995). Rokkasho is making extensive use of unattended sampling and measurement devices. Approximately three quarters of the data collection is performed unattended (IAEA 2005b). Data from process monitoring can also be used to support safeguards to verify that the facility is being used in the manner for which it was designed.

As mentioned earlier, a key aspect of safeguards is containment and surveillance, which complements nuclear material accountancy. This technology is also used extensively for safeguards by IAEA. Containment and surveillance technologies are divided into two categories: optical surveillance and sealing systems. Optical surveillance works very effectively for storage areas to observe movement and transfers of materials. Fuel storage pools are good candidates for deployment of cameras. Seals in general are applied to containers to help indicate if nuclear material has been removed or added to a container.

5.4   Safeguards applications for aqueous separations

Among the best examples of the implementation of IAEA safeguards to commercial nuclear facilities are those found in the Japanese industrial complexes located in the coastal villages of Tokai-mura in the Naka-gun District, Ibaraki-ken Prefecture, and Rokkasho-mura in the Kamikita-gun District, Aomori-ken Prefecture.

The Tokai and Rokkasho industrial complexes each include several of the manufacturing facilities required to support the Japanese nuclear energy industry, which is based primarily on light water reactor (LWR) technologies. The trend is that Japan is to moving toward a nuclear fuel cycle program similar to that practiced by France. These industrial complexes include uranium conversion, uranium enrichment, uranium re-conversion, uranium oxide fuel fabrication, nuclear power generation, spent fuel reprocessing, mixed oxide (MOX) fuel fabrication, interim spent fuel storage, and radioactive waste storage facilities (IAEA 2009). Our focus here is on the

spent fuel reprocessing and MOX fuel fabrication facilities, which standout as closely integrated facilities in an already highly integrated industry.

The basic function of a spent fuel reprocessing plant is to effect separations between uranium, plutonium, and fission products. Fission products and fuel assembly hardware ultimately report to waste, while uranium and plutonium report to separate purified process streams as nitrates. A portion of the uranium stream is converted into oxide that is returned to the process path for uranium oxide fuel production. The remaining portion of the uranium stream is mixed with the plutonium stream and the two metals are co-converted into a mixed oxide that becomes the feedstock for MOX fuel production. There are many technical variants of aqueous reprocessing and only the high-level common goals are described here. From this simple description it is easy to understand why such technologies attract international attention and require the application of IAEA safeguard principles, practices, and technologies.

In terms of Japan's national reprocessing capability, the "pilot scale" Tokai Reprocessing Plant (TRP) is the predecessor of the "commercial scale" Rokkasho Reprocessing Plant (RRP). Construction of the TRP began in 1971 and commercial reprocessing operations continued intermittently from September 1977 to March 2006, at which time commercial reprocessing operations were ceased. The TRP was operated from its inception until 1988 by the Power Reactor and Nuclear Fuel Development Corporation (PNC), from 1988 to 2005 by the Japan Nuclear Cycle Development Institute (JNC), and from 2005 to present by the Japan Atomic Energy Agency (JAEA). During its nearly 30 years of commercial operation, the TRP processed over 1130 MT spent fuel and achieved a maximum realized annual capacity in 1995 of approximately 95.7 MT spent fuel (Yamamura *et al.* 2008). The MOX product from the TRP was used to make fuels in the co-located Plutonium Fuel Fabrication Facility (PFFF) and the Plutonium Fuel Production Facility (PFPF). The TRP presently fulfills the role of a research and development facility for the JAEA. Operations include reprocessing MOX fuel from the Advanced Test Reactor Fugen.

As a result of a history of exceptional cooperation between Japan and the IAEA, the TRP served, *per se*, as a research and development laboratory for many of the IAEA inspection and verification techniques used at TRP, RRP, and other international sites.

Construction of the RRP began in 1993 and commercial reprocessing operations are scheduled to begin in 2009. The RRP is operated by Japanese Nuclear Fuel Limited (JNFL). The purpose of the RRP is to continue and expand the commercial reprocessing operations formerly conducted at the TRP. The design annual capacity is 800 MT spent fuel containing approxi-

mately 8 MT plutonium. The MOX product from the RRP will report to the JNFL MOX Fuel Fabrication Plant (J-MOX), which is scheduled to begin commercial operation in 2012 or later.

The latest safeguards technologies are being incorporated into the design and construction of the RRP (Johnson *et al.* 2001, Iwamoto *et al.* 2006, Durst *et al.* 2007). The continuous measurement and analytical technologies include accurate tank level and volume measurement (Hosoma *et al.* 1993) and plutonium and uranium concentration measurement via X-ray fluorescence (XRF) and hybrid k-edge densitometry (Bean 2007). The engineered safeguards systems used to monitor, track, and verify the flow of nuclear materials through the RRP are numerous, complex, and highly integrated. Included are such systems as the Integrated Head-End Verification System (IHVS), Near Real Time Accountancy (NRTA) System, Interim Inventory Verification (IIV) System, Automatic Sampling Authenticated System (ASAS), Spent Fuel Transfer Pool Video (FTPV) System, Solution Measurement and Monitoring System (SMMS), Hull Measurement and Monitoring System (HMMS), and Vitrification Wastes Coincidence Counter (VWCC) (Johnson *et al.* 2001, Iwamoto *et al.* 2006, Durst *et al.* 2007, Yamamura *et al.* 2008).

5.5   Safeguards applications for pyrochemical separations

An example of a safeguards application to a pyrochemical separation plant is found at the Fuel Conditioning Facility (FCF) located at Idaho National Laboratory (INL). INL, owned by the Department of Energy (DOE) and operated by the Battelle Energy Alliance (BEA), must comply with specific DOE orders regarding nuclear material control and accountability (DOE 2007). This order establishes a program for the control and accountability of nuclear materials at DOE-owned and DOE-leased facilities and DOE-owned nuclear materials at other facilities that are exempt from licensing by the Nuclear Regulatory Commission (NRC). Nuclear material control and accountability must be integrated with the Safeguards and Security Program for two reasons. First, it provides a mechanism for detecting a potential loss of nuclear material for safeguards and security. Second, it provides a periodic check of inventories to ensure that processes and materials are within control limits (Vaden *et al.* 1996).

The basic FCF mission is to support the Fuel Cycle Research and Development Program (the successor to the Advanced Fuel Cycle Initiative (AFCI)) by treating sodium-bonded metal fuel and producing interim storage products and final waste forms. FCF has two adjacent hot cells known as the "air cell" (that contains a purified air atmosphere) and the
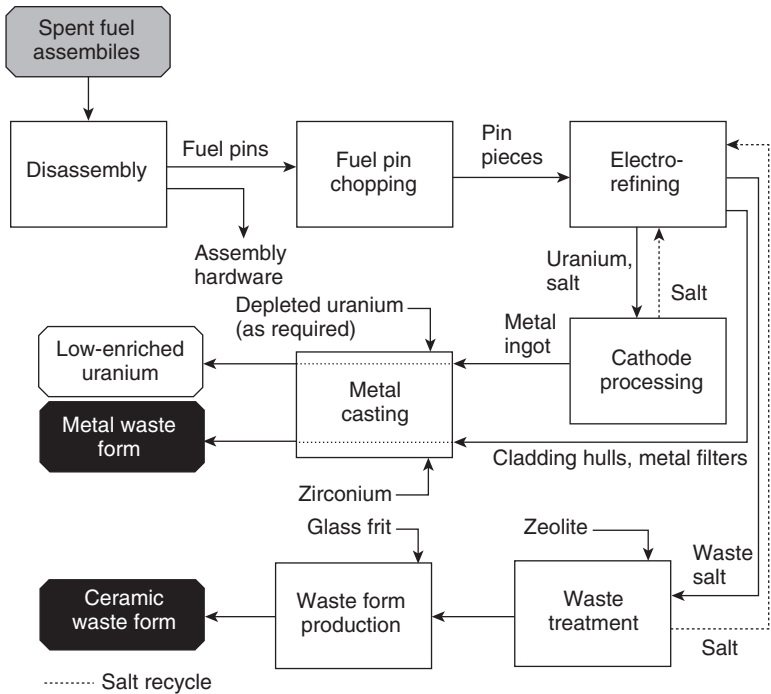
5.1 Block flow diagram of the process in FCF.

"argon cell" (that contains a purified argon atmosphere). Both hot cells house the remotely operated equipment used to electrochemically treat spent metallic nuclear fuel and are considered one Material Balance Area (MBA). Figure 5.1 shows a block diagram of the basic process steps. Simply stated, the operations performed in FCF consist of: 1) receipt of nuclear material and preparation into a form suitable for electrochemical processing; 2) electrochemical processing to remove nuclear material from fission products, bond sodium, etc.; 3) production of a low-enriched product for storage; and 4) preparation of waste forms. The process has been described in greater detail by Ackerman (1991) and Mariani (1993).

Because nuclear materials processed in FCF are contained in many material types and forms, material accountability requires measuring the nuclear material content of all flow streams entering and exiting the MBA and the physical inventory of nuclear material within the MBA. The inventory difference (ID) is defined as the difference between the measured inventory and what is expected to be in the inventory based on the previous

inventory and measured flows into and out of the process. The ID is calculated via the following equation (DOE 1995).

$$ID = (BI + TI) - (EI + TO)$$

In this equation the summation of the ending inventory (EI) and transfers of nuclear material out of the MBA (TO) are subtracted from the summation of the beginning inventory (BI) and transfers of nuclear material into the MBA (TI). Because measurement errors will occur, the actual amount of material measured will differ somewhat from the expected quantity, most likely resulting in a non-zero ID. The probability of detecting the loss of a given quantity of material (the loss detection capability) depends upon the uncertainty associated with the determination of the ID. In the FCF, material control and accountability uses twice the standard deviation of the inventory difference for the limit of error, which is propagated from all measurement and sampling uncertainties in an operation. The limit of error means the true ID has a 95% probability of being within two sigma of the measured ID. The true ID is zero if all materials have been measured and accounted for.

Near-real-time accountancy (NRTA) in FCF is accomplished by a combination of neutronics calculations, process models, physical measurements, and a computer-based mass tracking (MTG) system. The MTG system tracks the location and masses, by element and isotope, of nuclear material-containing items in near real time. Items may be storage containers, processing equipment, and fuel elements and assemblies. The masses are determined using in-cell balances with isotopic and elemental compositions determined by neutronics calculations, by previous measurements, or by computations based on process models. The neutronics calculations and process models are established by measurements applied to a particular process step. Mass values derived from process models are updated when measurement results are available. The MTG system provides a model of discrete accountable items distributed in space and time and constitutes a complete historical record (Adams *et al.* 1996). Figure 5.2 is a photograph of some of the tracking stations in FCF that assist in the NRTA.

With this database, material accountancy over the whole facility can be calculated for any specified time interval and space. Material accountancy uses the item weights and compositions and associated uncertainties. The system uses the best available information, which may either include measured or model weights. The *Materials Accounting with Sequential Testing* (MAWST) computer code is typically used for propagating the errors and establishing the inventory difference and limit of error (Picard and Hafer 1991).
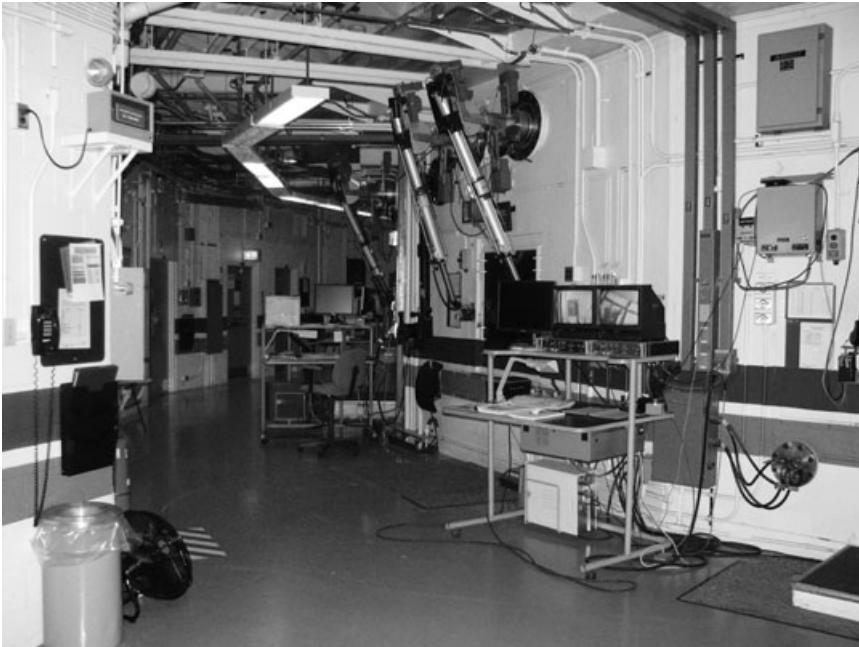
5.2 FCF mass tracking monitoring stations.

Moving beyond the Fuel Conditioning Facility, safeguarding any processing facility requires periodic material balances (Li *et al.* 2002). This necessitates measuring the input streams and output streams. In addition, an accounting of all materials in the physical inventory is also necessary to close the material balance. Two approaches are proposed, a clean out of the physical inventory or measuring the physical inventory. A complete cleanout of the physical inventory is very disruptive to the process and may not be possible in some cases. Measuring the physical inventory is difficult and may result in large uncertainties in the measurement and material balance. As stated in the FCF example, measuring the physical inventory allows for NRTA. Research has just barely begun on non-destructive assay (NDA) of the input stream. In-situ measurements of the physical inventory have not been fully developed. FCF relies heavily on process modeling for its NRTA. In conclusion, a major research and development effort is necessary to measure the input and output streams and the physical inventory to establish NRTA for safeguarding a dry processing facility.

5.6   Acknowledgement

5.7   References

Ackerman J P (1991), Chemical Basis for Pyrochemical Reprocessing of Nuclear Fuel, *Industrial and Engineering Chemistry Research*, Vol. 30, No. 1, pg. 141–145

Adams C H, Beitel J C, Birgersson G, Bucher R G, Derstine K L, Goin R W, Keyes R W, Toppel B J, Vollmer M A (1996), *The Mass Tracking System – Computerized Support for MC&A and Operations at FCF*, Proceedings of the Embedded Topical Meeting on DOE Spent Nuclear Fuel & Fissile Material Management, Reno, Nevada, June 16–20

Baruch B (1946), *The Baruch Plan*, United States Government Proposal Presented in a Speech by Bernard Baruch before the First Session of the United Nations Atomic Energy Commission, Hunter College, New York, June 14

Bean R (2007), *Aqueous Processing Material Accountability Instrumentation*, INL/EXT-07-13431, Idaho National Laboratory, Nuclear Nonproliferation, Idaho Falls, ID

DeMuth S, Thomas K, Tobin S (2007), *Proliferation Resistance and the Advanced Fuel Cycle Facility (AFCF)*, Proceedings of Global 2007 International Conference, Boise, Idaho, September 9–13

DOE (1995), *Guide for Implementation of DOE 5633.3B: Control and Accountability of Nuclear Materials*, US Department of Energy, Office of Security Affairs, Office of Safeguards and Security, Washington, DC

DOE (2007), *Nuclear Material Control and Accountability*, Manual DOE M 470.4-6, US Department of Energy, Office of Security and Safety Performance Assurance, Washington, DC

Duhamel G, Kuhn E, Zahradnik-Gueizelar P, Kuno Y, Radecki Z, Ariyoshi M, Tomikawa H, Iwanaga M, Tsutaki Y, Midorikawa M, Iwamoto T, Nakashima S, Tokai Y (2005), *Establishing the Joint IAEA/JSGO/NMCC Safeguards On Site Laboratory for the Rokkasho Reprocessing Plant*, Proceedings of Global 2005 International Conference, Tsukuba, Japan, October 9–13

Durst P C, Therios I, Bean R, Dougan A, Boyer B, Wallace R, Ehinger M H, Kovacic D N, Tolk K (2007), *Advanced Safeguards Approaches for New Reprocessing Facilities*, PNNL-16674, Pacific Northwest National Laboratory

Eisenhower D W (1953), *Atoms of Peace*, Address Before the General Assembly of the United Nations on Peaceful Uses of Atomic Energy, New York City, December 8

Google Earth (2009), A 3D Interface to the Planet, http://earth.google.com, Accessed May 25 2009

Hosoma T, Maruishi Y, Aritomi, M, Kawa T (1993), Accurate Volume Measurement System for Plutonium Nitrate Solution, *Journal of Nuclear Science and Technology*, Vol. 30, No. 5, pg. 425–435

IAEA (1975), The Technical Objective of Safeguards, *IAEA Bulletin*, Vol. 17, Issue 2, pg. 13–17

IAEA (1981), *IAEA Safeguards: An Introduction*, IAEA/SG/INF/3, International Atomic Energy Agency, Vienna, Austria

IAEA (1998), *The Evolution of IAEA Safeguards, International Nuclear Verification Series No. 2*, International Atomic Energy Agency, Vienna, Austria

IAEA (2001), *IAEA Safeguards Glossary 2001 Edition, International Nuclear Verification Series No. 3*, International Atomic Energy Agency, Vienna, Austria

IAEA (2003), *Safeguards Techniques and Equipment, 2003 Edition, International Nuclear Verification Series No. 1 (Revised)*, International Atomic Energy Agency, Vienna, Austria

IAEA (2005a), *In the Service of Peace, 2005 Nobel Peace Prize*, International Atomic Energy Agency, Vienna, Austria

IAEA (2005b), *Status and Trends in Spent Fuel Reprocessing*, IAEA-TECDOC-1467, International Atomic Energy Agency, Vienna, Austria

IAEA (2008), *Spent Fuel Reprocessing Options*, IAEA-TECDOC-1587, International Atomic Energy Agency, Vienna, Austria

IAEA (2009), *Nuclear Fuel Cycle Information System, A Directory of Nuclear Fuel Cycle Facilities, 2009 Edition*, International Atomic Energy Agency, Vienna, Austria

Iwamoto T, Ebata T, Fujimaki K, Ai H (2006), *Establishment of the Safeguards at Rokkasho Reprocessing Plant*, Proceedings of the 15th Pacific Basin Nuclear Council Conference, Sydney, Australia

Johnson S J, Abedin-Zadeh R, Pearsall C, Hiruta K, Creusot C, Ehinger M, Chesnay B, Robson N, Higuchi H, Takeda S, Fujimaki K, Ai H, Uehara S, Amano H, Hoshi K (2001), *Development of the Safeguards Approach for the Rokkasho Reprocessing Plant*, Proceedings of the Symposium on International Safeguards Verification and Nuclear Material Security, Vienna, Austria, October 29–November 2

Li T K, Burr T L, Thomas K E, Menlove H O, Furushima M, Hori M (2002), *A Study of Safeguards System on Reprocessing for Fast Breeder Reactor*, Proceedings of the Pacific Basin Nuclear Conference, Shenzhen, China, October 21–25

Lilienthal D E, Barnard C I, Oppenheimer J R, Thomas C A, Winne H A (1946), *A Report on the International Control of Atomic Energy*, Prepared for The Secretary of State's Committee on Atomic Energy, Department of State Publication 2498, Washington, DC

Mariani R D (1993), *Basics of Electrorefining in the Fuel Cycle Facility*, Argonne National Laboratory Report, ANL-IFR-212

OTA (1995), *Nuclear Safeguards and the International Atomic Energy Agency*, OTA-ISS-615, U.S. Congress, Office of Technology Assessment, Washington, DC

Picard R P, Hafer J F (1991), *MAWST: Materials Accounting With Sequential Testing*, Los Alamos National Laboratory, Report N-4/91-633

Thomas K and Longmire V (2002), *IAEA Safeguards Approach for Reprocessing Facilities*, Los Alamos National Laboratory, Report LA-UR-02-5276

UN (1946), *United Nations General Assembly Resolution I, Resolutions Adopted by the General Assembly During the First Part of Its First Session from 10 January to 14 February 1946*, United Nations Document A/64, London, England, Church House, 1946

Vaden D, Benedict R W, Goff K M, Keyes R W, Mariani R D, Bucher R G, Yacout A M (1996), *Material Accountancy in an Electrometallurgical Fuel Conditioning Facility*, Proceedings of the Embedded Topical Meeting on DOE Spent Nuclear Fuel & Fissile Material Management, Reno, Nevada, June 16–20

Vinoche R, Drain F, Foare G (2005), *The Treatment Plant of the Future: An AREVA Point of View*, Proceedings of Global 2005 International Conference, Tsukuba, Japan, October 9–13

Wu L N (1972), *The Baruch Plan: U.S. Diplomacy Enters the Nuclear Age*, Foreign Affairs Division, Congressional Research Service, prepared for the Subcommittee on National Security Policy and Scientific Developments, House Committee on Foreign Affairs

Yamamura O, Yamamoto R, Nomura S, Fujii Y (2008), Development of Safeguards and Maintenance Technology in Tokai Reprocessing Plant, *Progress in Nuclear Energy*, Vol. 50, pg. 666–673

6

Standard and advanced separation: PUREX processes for nuclear fuel reprocessing

R. S. HERBST, Idaho National Laboratory, USA,
P. BARON, CEA, France and
M. NILSSON, University of California Irvine, USA

Abstract: The PUREX process for separating uranium and plutonium from irradiated nuclear fuels has been extensively studied and successfully operated industrially over the preceding five plus decades. It is anticipated that PUREX will play an important role in upcoming and advanced future nuclear fuel cycles. The first objective of this chapter is to provide the background information required to status the present state of the art as currently practiced at the industrial scale. The second objective is to examine the modifications ready, or nearly so, for implementation into the next generation of PUREX reprocessing facilities, thereby further expanding the utility and operation of the process for use in nuclear fuel cycles of the future.

Key words: PUREX, tributyl phosphate, uranium separation, plutonium separation, solvent extraction, nuclear separations, nuclear fuel cycle.

6.1   Introduction

The PUREX (<u>P</u>lutonium, <u>U</u>ranium, <u>R</u>eduction, <u>EX</u>traction) process was first reported in 1949 and subsequently operated with irradiated nuclear fuel at the large scale in 1954 (Lanham 1949). In the ensuring 50+ years, it has been widely described, publicized, and reviewed in the open literature, and remains the only technology internationally practiced on an industrial scale to reprocess (recover U and Pu) from used nuclear fuels. A major objective of this chapter is then, not to provide an in depth review of PUREX technology (that has already been eloquently accomplished in a plethora of previous reports, articles, and treatises), but rather to provide the necessary background information to logically status the current state of the art, as practiced today, at the industrial scale. The second, and perhaps more timely objective is to provide insight into the modifications ready or near-ready to be implemented into the next generation of PUREX reprocessing facilities, thereby further expanding the utility and operation of the process in the ever-changing climate of technical, political, and environmental considerations.

141

It should be noted that initially, PUREX was developed and applied primarily to produce a pure Pu stream for military (weapons) applications and was consequently cloaked in great secrecy under the auspices of "national security." Those countries that have produced substantial amounts of Pu for military purposes have done so by means of the PUREX process. Today, the Pu and U products are commercially recovered from used fuels from civilian nuclear power plants (NPP) and fabricated into fresh fuel for recycle back to NPPs for electricity production. Interestingly, many of the intricate details associated with present-day commercial reprocessing facilities are considered "propriety information" and are therefore often protected as well as (or better than) what were formerly considered to be national secrets.

6.2   Process chemistry

PUREX is based, by definition, on liquid-liquid solvent extraction chemistry of the well-known extractant, tri-n-butyl phosphate (TBP), diluted to nominal 20–30% (by volume) with a normal paraffinic hydrocarbon (NPH) organic diluent. Note that the diluent is required only to maintain the physical characteristics of the organic phase (primarily viscosity and density) in a workable range for use in the salient solvent extraction equipment. In its simplest representation, the process is indicated in Fig. 6.1. The primary inputs are irradiated nuclear fuel and numerous process chemicals, predominately nitric acid (HNO_3). Three major output streams result: 1) a relatively pure Pu nitrate solution, 2) a relatively pure U nitrate solution, and 3) process wastes. The U and Pu nitrate products can be further purified in additional cycles of PUREX processing and are subsequently converted to solids, typically the metal oxides. The waste is further classified into three categories; high, intermediate, and low level, as specified by the relative radioactivity content. The overarching objectives of PUREX are to produce
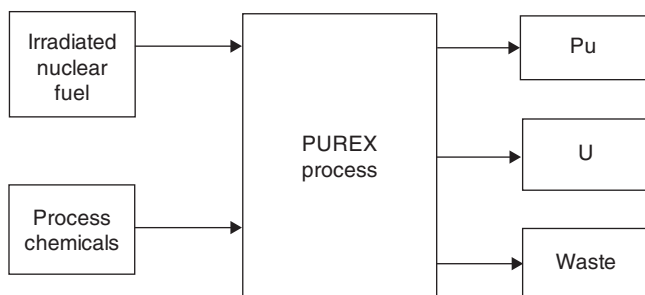
6.1 Generic PUREX Process.

Table 6.1 Distribution ratios of actinides at trace concentration levels, 2 M HNO_3, 30% TBP, and 22 °C

	Uranium	Neptunium	Plutonium
Oxidation state IV	1.2	2.1	8
Oxidation state VI	15	11	2.1

pure U and Pu products in very high yield and purity, while minimizing the losses to and volumes of the resulting waste streams.

Actinide chemistry in the PUREX process is relatively straightforward. TBP is a very selective extractant for the actinides in the +6 and +4 oxidation states; therefore the uranyl (U(VI), as UO_2^{2+}) and Pu^{+4} (Pu(IV)) cations are readily transferred to the organic phase due to the formation of neutral nitrate-TBP complexes in 2–4 M nitric acid. The distribution ratio of the actinides are exemplified in Table 6.1. The extraction mechanisms are indicated by the following chemical equilibria for nitric acid/nitrate media:

$$UO_2^{2+} + 2NO_3^- + 2TBP \rightleftarrows [UO_2(NO_3)_2 \cdot 2TBP] \qquad 6.1$$

$$Pu^{+4} + 4NO_3^- + 2TBP \rightleftarrows [Pu(NO_3)_4 \cdot 2TBP] \qquad 6.2$$

The affinity of TBP is substantially lower for the +5 oxidation state, notably Np(V) as NpO_2^+, and virtually nil for the +3 and lower oxidation states (i.e., Pu(III), Am(III), Cm(III), Cs(I), Sr(II), etc.). The pivotal point of the process chemistry is the high thermodynamic stability of UO_2^{2+} (predominate species under all process conditions) and relative ease with which the oxidation state of Pu can be controlled or adjusted, either chemically or electrochemically. Thus, by controlling the plutonium as Pu(IV) during the extraction step, both U and Pu are transferred (almost quantitatively) to the organic phase. The U-Pu partitioning is accomplished by using conditions conducive to the reduction of Pu(IV) to the virtually inextractable Pu(III) oxidation state, effectively back-extracting plutonium from the loaded organic. The U(VI) is subsequently recovered or stripped from the organic using dilute nitric acid. Several important nuances of PUREX process chemistry as related to TBP and the associated extraction chemistry (Eq. 6.1, 6.2) should also be noted:

- simple stoichiometric ratio of TBP to U or Pu
- excess NO_3^- drives the equilibrium to the right, a salting-in effect
- TBP measurably extracts nitric acid into the organic phase
- TBP is slightly (but measurably) soluble in the aqueous phase.

Used nuclear fuels, even after dissolution, can be likened to "the cat's breakfast" in that a large proportion of the entire periodic table resides in

solution, due primarily to the complicated spectrum of elements formed by the fission process, i.e. the fission products. Due to very high selectivity of TBP, the desired decontamination of U and Pu from most of these elements is easily attained. However, there are a few fission products considered to be problematic or troublesome because their decontamination to the desired levels has proven difficult. A notable source of residual radioactive contamination of the products is from the short-lived isotopes ^{95}Zr with a half life of $t_{1/2}$ ~64 days and its radioactive decay daughter ^{95}Nb with $t_{1/2}$ ~ 35 days. Consequently, residual contamination with ^{95}Nb is always concomitant with ^{95}Zr contamination. In modern reprocessing plants, ^{95}Zr/^{95}Nb contamination is controlled or alleviated by cooling the used nuclear fuel for >3 years prior to reprocessing. Another obstinate source of residual radioactive contamination of the U and Pu products is from ^{106}Ru and its ^{106}Rh daughter, both with a $t_{1/2}$ ~ 1 year. Impractical cooling times of >10 years would be required to obtain the same benefit from cooling as observed for Zr. Consequently, provisions for the acceptable decontamination of the U and Pu products from ^{106}Ru/^{106}Rh must occur in the flowsheet. Iodine and Tc are problematic for environmental reasons; furthermore, Zr interferes with Tc decontamination and Pu partitioning. Iodine, on the hand, is largely reduced to unimportant levels with the typical >3 year cooling period and controlling the fuel dissolution chemistry, and will subsequently not be further discussed. Last, but not least, larger quantities of Np are formed in higher burn up LWR fuels associated with modern reactor core management techniques. Coupled with environmental concerns, Np chemistry in PUREX has been extensively studied in recent years. The chemistries of these elements are comprehensively reviewed in the literature (Shultz 1984, Benedict 1981, Sood 1996).

The inner working of a PUREX "black box" as represented in Fig. 6.1 is obviously a rather complicated series of interrelated process steps that function to achieve the overall objectives of the process. The process steps can be characterized in general terms to include:

1. Dissolution of the solid used nuclear fuels to produce liquid feed to the separation (solvent extraction) operations. This portion of the process, typically termed headend operations, is an important consideration in determining and controlling the underlying chemistry of the subsequent separations processes. Obviously, the characteristics of irradiated fuel vary widely with a variety of interrelated factors, e.g. fuel type (metallic, UO_2, MOx, etc.); reactor type (PWR, LWR, BWR, Fast, etc.); burnup; and enrichment.
2. Solvent extraction cycles are dedicated to virtually complete recovery of the uranium and plutonium products with a high degree of purification from the other constituents of used nuclear fuels, particularly with

regard to fission products. Recovery and purification is achieved by going through a succession of liquid–liquid extraction, scrub, back-extraction, and solvent cleanup cycles. Note that the concomitant high performance requirements of purity and recovery in nuclear reprocessing are uncommon to typical hydrometallurgical applications; in conventional metal recovery industries, the aim is to promote recovery efficiency, at the expense of purity, or vice versa.

3. The organic phase is recycled in the process and solvent cleaning and regeneration are important aspects of the process flowsheets.

4. Due to the solubility of TBP in the aqueous phase, all flowsheets include a "diluent wash" step to back extract or recover TBP from the aqueous effluents. This is a particularly important aspect if a stream is to be concentrated via evaporation (e.g., with nitric acid recovery) to mitigate potential safety concerns and precipitate formation.

5. Treatment of the radioactive waste effluents ultimately results in the solidification or vitrification of the process wastes for final storage and, ultimately, disposal. Additional steps in the waste treatment cycle may include evaporation, process chemical recovery (notably HNO_3) for recycle into the process, and compositional adjustments.

6. The final uranium and plutonium products are typically oxides. A conversion process is included to recover U and Pu from aqueous nitrate media as the solid metal oxides. Typical steps included in the conversion process are precipitation, usually as U peroxides and Pu oxalates (which often facilitates further decontamination), with subsequent roasting or calcination to the solid metal oxides.

6.3   Current industrial application of PUREX

Referring to Table 6.2, current commercial reprocessing of LWR reactor fuels occurs in four countries: France (La Hague), the UK (Thorp), Japan (Tokai-mura, Rokkasho-mura), and Russia (Mayak). Additionally, India (Kalpakkam, Tarapu; PHWR fuels) and the UK (Sellafield B205; Magnox fuels) operate plants to reprocess other types of used nuclear fuels. It is apparent that the lion's share of international reprocessing capacity is associated with LWR fuels from thermal NPPs and, as such, will be the focus of the ensuing description of the typical PUREX flowsheet. One of the most exciting developments of current times is the fact that the Rokkasho plant in Japan is in the midst of hot startup at the time of this writing. This additional capacity of 800 tHM/year marks the first new PUREX plant that has been brought on line in well over a decade. Additional planned capacity throughout the world speaks well for the renewed interest and commitment to nuclear power and the prominence of the nuclear fuel cycle to the global economy.

Table 6.2 World commercial reprocessing data

	Plant	Capacity, tHM[a]/yr	Additional planned capacity, tHM/yr	Cumulative fuel reprocessed, tHM[b]
LWR fuel:	France, La Hague (UP2/UP3)	1,700		22,450[c]
	UK, Sellafield (THORP)	900		5,800
	Russia, Ozersk (Mayak)	400	1500 (2025)	3,550
	Japan (Rokkasho-mura)		800 (2009)	
	(Tokai-mura)	90		1,000[d]
	China (Jiuquan, Lanzhou)	–	825 (2020)	
	Total approx	3,000	3,125	32,800
Other nuclear fuels:	UK, Sellafield	1,500		42,000
	India	275	300 (2010)	
	Total approx	1,750		
Totals		4,750	3,425	75,068[e]

[a] tHM = metric tonnes heavy metal.
[b] As of the end of 2006.
[c] An additional 100 tHM FBR and 150 tHM MOX fuels have also been reprocessed.
[d] An additional 18 tHM MOX fuel have also been reprocessed.
[e] Includes the MOX and FBR quantities processed at La Hague & MOX at Tokai (see above).
Sources: OECD/NEA 2006 Nuclear Energy Data, Nuclear Eng. International Handbook 2007.
Spent Fuel Reprocessing Options, IAEA-TECDOC-1587, 2008.

Equally important is the fact that the "next generation" of used fuel reprocessing will likely be based on technologies that tweak standard PUREX process chemistry to achieve very similar results. Consequently, these advanced flowsheets will appear very similar to the traditional PUREX flowsheets in operation today. It is therefore of practical utility to review the PUREX process with greater scrutiny. The typical PUREX solvent extraction flowsheet used in the modern commercial plants of La Hague and Rokkasho-mura is set forth schematically in Figs 6.2 and 6.3. The primary difference between this flowsheet and that used at the other commercial plants indicated in Table 6.2 is inclusion of the Tc scrub (scrub 2) and complementary extraction, which is specific to the La Hague and Rokkasho-mura facilities (Baron 1993, 2003). The individual units operations and process chemistries are reviewed with greater detail in the ensuing description.

Partitioning step

Solvent cleanup and recycle

HNO_3

U strip

TBP scrub

U purification

Diluent

Pu scrub

HNO_3

U(IV) HNO_3

Pu reduction

U(IV) HNO_3

U scrub

HNO_3

TBP scrub

Pu purification

Codecontamination step

HNO_3
HNO_3

Scrub 2

Complementary extraction

TBP scrub

Waste

Solvent

Diluent

Scrub 1

HNO_3

Fuel dissolution & feed adjustment

Main extraction

TBP scrub

Waste

Solvent
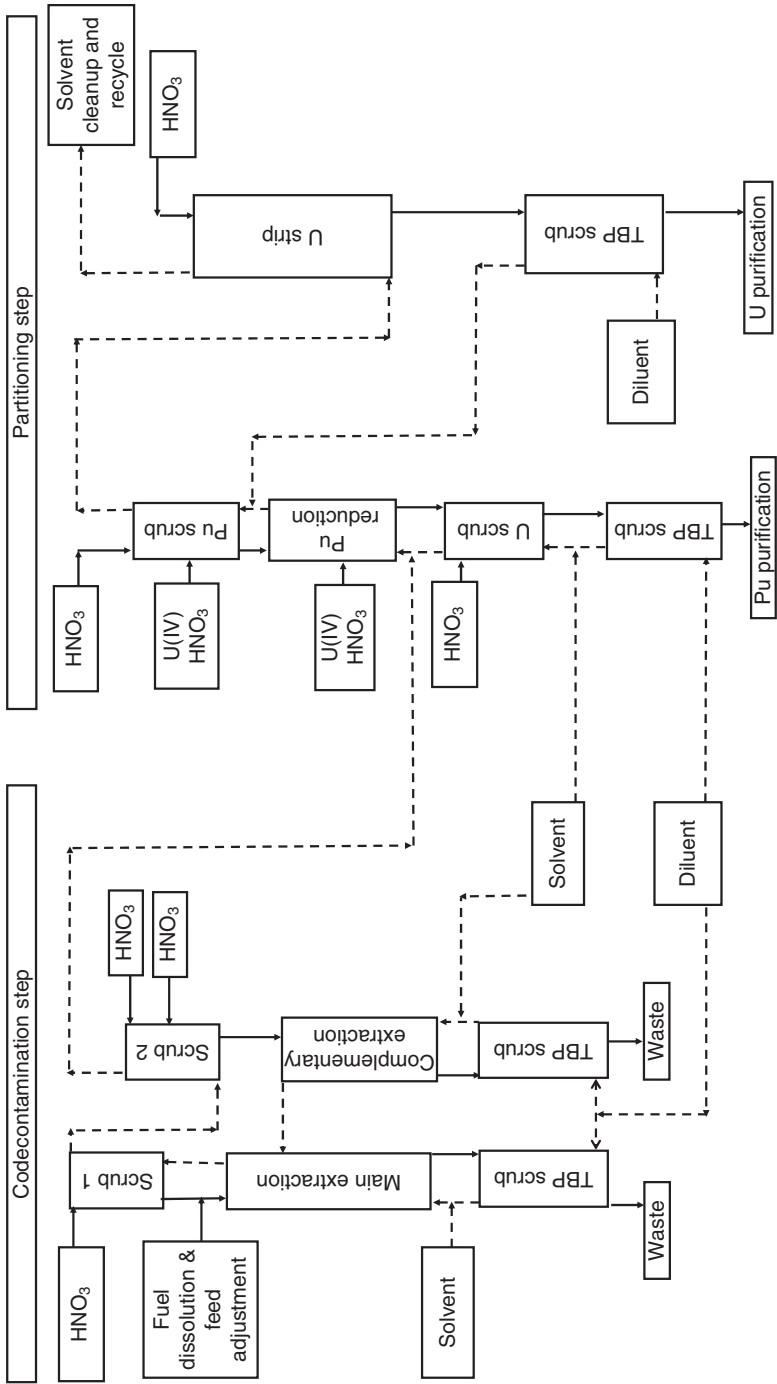
6.2 First cycle (codecontamination and partitioning) of the PUREX flowsheet.

Plutonium purification cycle

Uranium purification cycle

From Pu partitioning

Scrub

Intercycle adjustment

Organic TBP in NPH

PP1 — Pu extraction / scrub

Waste

Pu strip reductant

PP2 — Pu stripping

Solvent cleanup and recycle

Pu product

From U partitioning

Scrub

Intercycle adjustment

Organic TBP in NPH

UP1 — U extraction / scrub

Waste

U Strip Dilute HNO3

UP2 — U stripping

Solvent cleanup and recycle

U product

6.3 U and Pu purification cycles.

6.3.1 First cycle

The aqueous solution resulting from the fuel dissolution/clarification/chemical adjustment operation provides the liquid feed to the first extraction cycle in which codecontamination and U/Pu partitioning steps are lumped together. Regardless of the semantics, there is some value in describing the codecontamination and partitioning steps separately. The objective of the codecontamination cycle is to extract U and Pu together and provide the major decontamination from (or scrubbing of) the fission products. Since codecontamination includes several strongly coupled unit operations; the initial "extraction" ensures adequate extraction efficiency, while the subsequent "scrubbing" operations are aimed at removing those problematic fission products mentioned previously. To satisfactorily explain and appreciate the careful balances associated with the initial extraction/scrub portion of the flowsheet mandates a brief review of the conflicting chemistries prevalent in the process.

Zirconium

In nitric acid solutions, zirconium exists only as Zr(IV), albeit in many chemical forms depending primarily on acidity, Zr concentration, and temperature. Hydrolysis and polymerization both increase with increasing temperature and decreasing acidity and change the Zr(IV) speciation in solution. Increasing nitric acid concentration and/or temperature increase the extraction of Zr. The ever-present radiolytic and hydrolytic degradation products of TBP and diluent in the solvent are yet another principal reason for the extraction of Zr. Though these degradation products cannot be eliminated, their concentration can be minimized by reducing the radiation exposure to the solvent and consequently the radiolytic degradation products.

Ruthenium

The chemistry of Ru is complicated due to the variety of ruthenium species that may be present in the solution and the relatively slow rate of their interconversion. In the dissolved fuel solution Ru is present as complexes of the ruthenium nitrosyl cation, $RuNO^{3+}$, where the anions may be NO_3^-, NO_2^-, OH^- and H_2O. Fast extraction and slow scrubbing improve decontamination for both Ru and Zr. However, scrubbing of Ru from the organic phase is facilitated by higher acid concentration, conditions which exacerbate Zr extraction. Often, a split scrub is used, one with high acidity (and perhaps temperature) which favors Ru decontamination and the other with low acidity for Zr decontamination.

Technetium

During fuel dissolution, the bulk of the Tc is dissolved and present in its highest oxidation state, Tc(VII), as the pertechnetate anion, TcO_4^-. Pertechnetate extracts into the organic phase by displacement of a nitrate ion in the extracted complexes, represented by the following chemical equilibria:

$$H^+ + TcO_4^- + 3TBP \rightleftarrows HTcO_4 \cdot 3TBP \qquad 6.3$$

$$UO_2(NO_3)_2 \cdot 2TBP + TcO_4^- \rightleftarrows UO_2(NO_3)(TcO_4) \cdot 2TBP + NO_3^- \qquad 6.4$$

$$M(NO_3)_4 \cdot 2TBP + TcO_4^- \rightleftarrows M(NO_3)_3 (TcO_4) \cdot 2TBP + NO_3^- \qquad 6.5$$
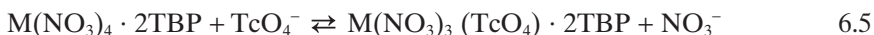
where M in Eq. 6.5 can be Zr or Pu. The extraction equilibrium given by Eq. 6.3 is least important with regard to the dissolved fuel solution, since it increases with increasing HNO_3 concentrations up to ~0.7 M, then decreases with further increases in HNO_3 concentrations. Technetium extraction also decreases with increasing temperature. In accord with equilibria (6.4) and (6.5), the ever-present U(VI), Pu(IV), and Zr(IV) in the dissolver solution enhances the extraction of Tc. The coextraction of Tc with Zr(IV) is the most predominant. It has been reported that for the conditions to be used in the THORP plant, the Zr(IV) present in the fuel solution causes 100% extraction of Tc from the fuel solution (Phillips 1989). Application of the law of mass action to the equilibria described by Eq. (6.4) and (6.5) implies that increased nitrate concentration would drive the equilibria to the left and remove Tc from the organic phase. In practice, a high HNO_3 concentration in a scrub stream is therefore used to facilitate the back extraction of Tc; such conditions are also conducive to the Ru decontamination while keeping U and Pu salted into the organic phase.

Codecontamination step

With the above brief explanation of the underlying chemistry, the explanation of the codecontamination cycle is more fruitful. The reader's attention is re-directed to the decontamination cycle in Fig. 6.2 for the ensuing discussion.

The dissolved fuel solution enters the main extraction contactor at moderate nitric acid concentration of ~3 M HNO_3. As the aqueous flows counter-currently to the organic stream, U and Pu are extracted virtually quantitatively into the organic phase. Under these conditions, Zr, Ru, and Tc are also extracted to varying degrees in accord with the above descriptions of their chemistries. Also noteworthy is that the conditions of the dissolved solution favor the formation of neptunium in the higher, i.e., Np(V) and Np(VI), oxidation states; the former is inextractable while the

latter is very extractable by TBP into the organic phase. The proportion-ation between these Np oxidation states is a complex function of the exact NO_3^-/NO_2^- concentrations and redox kinetics, which can even be influenced by the type and design of the process equipment. It has been reported that ~25% of the Np is rejected, as Np(V), to the raffinate (waste) in the La Hague plant (Dinh 2008); however, the point is that some fraction of the Np in the dissolved feed is extracted into the organic phase and subse-quently carries through into the downstream processes.

First scrub

The loaded organic stream exiting the first extraction contactor is next subjected to the first scrubbing operation with a dilute HNO_3 solution (dilute relative to the feed or ~2 M HNO_3) to facilitate Zr and Ru removal from the organic phase. Other fission products that can be considered "entrained" versus "extracted", such as Cs or Sr, are also removed from the organic phase in this step. The concentration of HNO_3 must be judiciously chosen to prevent back extraction of U and Pu from the loaded solvent; however, the aqueous phase from the initial scrub potentially contains some uranium and plutonium, in addition to the scrubbed impurities, and is recombined with the incoming aqueous feed and returned to the extraction operation to minimize U and Pu losses.

Second scrub

The organic solvent emanating from the first scrub operation still contains the bulk of the Tc and Np that coextracted with the U and Pu. The organic is next subjected to a "technetium scrub," where it is contacted with two scrub solutions containing different concentrations of HNO_3. The first scrub with higher concentration nitric acid solution (10 M HNO_3) effectively scrubs Tc from the organic phase (Baron 1993). The second scrub with a lower 1.5 M HNO_3 solution essentially back extracts acid from the organic phase and limits the acidity of the organic exiting the system (Baron 1993).

Complementary extraction

The outgoing aqueous scrub phase, containing a significant fraction (but not necessarily all) of the TcO_4^-, then undergoes a "complementary" extraction with fresh organic phase to recover plutonium and uranium inadvertently back-extracted with the Tc. The solvent from this complementary extraction operation is recycled to the main extraction section to maintain a high concentration of U and Pu in the outgoing solvent of the codecontamina-tion step and to avoid undesired losses of uranium and plutonium to process

wastes. Obviously, the aqueous product from the Tc scrubbing operation cannot be re-combined directly with the previous scrub or feed streams since the higher concentrations of HNO_3 would exacerbate the extraction of Zr in the main extraction section and negate the benefits afforded by the dual scrub approach. Consequently, the aqueous raffinate from the complementary scrub operation is sent directly to the waste in combination with the raffinate from the main extraction (Baron 1993, 2003).

In passing, it should be noted that the aqueous streams from the main extraction and Tc scrubbing and complementary extraction operations are subjected to a diluent scrub. The purpose being to wash traces of TBP, lost from the organic via solubility, to the aqueous phase. Such diluent washing has become a standard feature of the PUREX process for aqueous streams that are concentrated in evaporators, and is a standard safety feature in modern reprocessing facilities. The diluent used in these washing steps is recycled to the process to minimize TBP losses. Diluent washing is noted at multiple points in Fig. 6.2 and will not be further discussed.

The diversity of the impurities targeted in the scrub sections of codecontamination often involves a compromise, that, when reduced to practice, leads to the use of several different scrub solutions. Other important design requirements of the first cycle include minimization of U and Pu losses to the liquid waste emanating from the cycle, thereby restricting these losses to very low levels (typically <0.1%). Finally, the rather high concentrations of U, typically approaching 300 g/L in the incoming aqueous feed, allows favorable flow ratios of organic and aqueous to be achieved, as the organic can be heavily loaded with uranium. The flowrate of the organic solvent is slightly in excess of that required for the quantity of U and Pu to be extracted; however, a large excess of organic must be avoided in order to restrict excessive extraction of impurities.

In general, there is a high degree of separation of actinides and fission products after the codecontamination step. Typical decontamination factors reported from UP-3 at La Hague are Ru DF $\sim 10^4$, Cs DF $> 10^7$, and a Tc DF > 3 was initially targeted (Baron 1993), but is now typically $DF_{Tc} \sim 10$ or higher (Baron 2003).

6.3.2 Partitioning step

The organic phase exiting the codecontamination cycle contains most of the actinides (U, Pu, and Np) initially present in the dissolved fuel. Some residual fission products, notably Tc and Zr, are also present in the organic phase. The next step of the process (referring to Fig. 6.2) is partitioning, which involves the selective stripping of Pu and U from the loaded organic in two complementary steps. The first is Pu partitioning and the later is U stripping.

Plutonium partitioning

The first operation in the partitioning cycle involves selective plutonium back-extraction or stripping from the loaded organic phase. This is accomplished by the reduction of extractable Pu(IV) to the inextractable Pu(III) oxidation state. A variety of reducing agents have historically been used for the reduction and concomitant partitioning of plutonium, the most prominent being: (a) uranous cation, U(IV), (b) hydroxylamine nitrate (HAN), or (c) ferrous sulphamate, $Fe(NH_2SO_3)_2$. Of these reducing agents, the later, ferrous sulphamate, is no longer used in modern PUREX plants and will not be further discussed. Hydroxlyamine nitrate is used in some instances in the downstream Pu purification cycle and will be further described subsequently. The reductant universally used in modern facilities for Pu partitioning is U(IV). However, to explain the logic behind the process diagram, it is once again convenient to regress to a brief review of the pertinent process chemistry.

Partitioning with U(IV) and hydrazine

Thermodynamically, U(IV) is a stronger reducing agent for Pu(IV) than either HAN or Fe(II) and has the additional advantage that it does not introduce any additional metal into the system. However, it is imperative to understand that Pu(III) is an unstable species at the conditions of Pu partitioning, and rapidly reoxidizes to Pu(IV) in the presence of nitrous acid. The oxidation reaction is autocatalytic in that there is no net consumption of HNO_2 in accord with the proposed reactions (Schultz 1984):

$$HNO_3 + HNO_2 \rightarrow N_2O_4 + H_2O \qquad 6.6$$

$$N_2O_4 + Pu^{3+} + H^+ \rightarrow Pu^{4+} \, HNO_2 + NO_2 \qquad 6.7$$
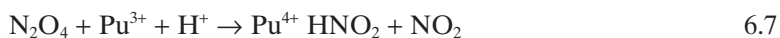
This is also the case for U(IV), which is oxidized by a similar mechanism. The point is that *either* of the aforementioned reducing agents, U(IV) and Fe(II), must be supported by a nitrite scavenger to prevent this autocatalytic reoxidation of Pu(III) to Pu(IV) and thereby inhibit Pu partitioning.

Hydrazine nitrate ($N_2H_5NO_3$) is commonly added as a nitrite scavenger, preventing Pu(III) oxidation and helps stabilize U(IV). Hydrazine destroys NO_2^- in accordance with the following reactions:

$$N_2H_5^+ + NO_2^- \rightarrow HN_3 + 2H_2O \qquad 6.8$$

$$HN_3 + H^+ + NO_2^- \rightarrow N_2O + N_2 + H_2O \qquad 6.9$$
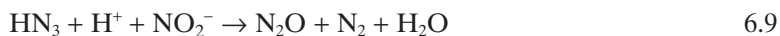
Since excess hydrazine is always added in the process, reaction (6.9) can be neglected. Note that HAN is also a nitrite scavenger, albeit less effective than hydrazine, (*vide infra*, equation 6.11). Consequently, HAN is always

used in conjunction with hydrazine in industrial flowsheets. At this point, it is also relevant to mention another nuance of Tc chemistry that becomes prominent in connection with the Pu partitioning operation under discussion. Coextracted Tc remaining in the loaded organic and entering the Pu partitioning process complicates the Pu partitioning of U and Pu when N_2H_4 is used as a nitrite scavenger. Technetium is a catalyst for both hydrazine destruction and the U(IV) oxidation, which results in the concomitant increase in the consumption of N_2H_4. In modern PUREX operations, it is now well recognized that to avoid the excessive consumption of N_2H_4 it is necessary to remove coextracted Tc in the solvent prior to U-Pu partitioning. This is the predominant consideration for including the Tc scrub operation in the aforementioned codecontamination step of the first extraction cycle.

Since U(IV) is extractable by TBP, albeit to a lesser extent than U(VI) (refer to Table 6.1), at least two hydrazine stabilized U(IV) aqueous streams are used in the Pu partitioning contactor. Referring again to Fig. 6.2, a stream containing U(IV) at a moderate ~1 to 2 M HNO_3 concentration is fed to the Pu partitioning contactor at a location near the organic feed entry (Sood 1996). The acidity in this stream is useful in salting the U(IV) into the organic phase, thereby facilitating the reduction of Pu(IV). A second U(IV) containing aqueous stream with a lower 0.2 M HNO_3 concentration is fed near the organic effluent (Fig. 6.2, Pu scrub contactor), effectively scrubbing Pu from the U laden organic product; the lower acidity also facilitates reduction of Pu (IV) to Pu(III) by U(IV). A fresh organic scrub stream of 20–30% TBP is fed at the opposite end (Fig. 6.2, bottom of the U scrub contactor) to remove residual uranium from the aqueous plutonium product stream. This organic phase, containing some uranium and plutonium, is recombined with the organic feed in the stripping operation. Normally, the amount of U(IV) used in the partitioning process is four to six times the stoichiometric requirement (Sood 1996).

Other design criteria built into the Pu partitioning step are worth mentioning. In addition to purity of the Pu stream, another important consideration in the plutonium partitioning cycle is that it be operated in a manner conducive to concentration of Pu in the final aqueous product from this operation. This is one of the benefits of the reductive stripping operation, since Pu concentration in the partitioning step makes it possible to eliminate intercycle evaporative concentration operations between the codecontamination and the second Pu purification cycles. The partitioning of uranium and plutonium early in the overall process flowsheet has been universally adapted to segregate issues related to treatment capacity from those relating to criticality risk management. For example, the equipment used for the codecontamination and uranium purification cycles requires a

large throughput of several tonnes/day, with very high liquid flowrates. For the plutonium purification cycles, the equipment design is more complex to preclude the associated criticality risks; conversely, the fact that smaller quantities of material streams are being handled calls for equipment of greatly reduced size.

Uranium stripping

The final step in the partitioning cycle is the uranium stripping operation (Fig. 6.2, U strip contactor) to recover the U from the organic phase prior to solvent cleanup and recycle. At this point in the process, uranium is the predominant metal present in the organic phase. Because of the strong affinity of TBP for the uranyl ion, U back extraction is somewhat more difficult than for many of the other extracted metals. The uranium stripping operation is universal and relatively straightforward in PUREX processing: the metal laden organic is contacted with a low-acidity (0.01 M HNO_3) aqueous phase, at elevated temperature (50 °C). The aqueous-to-organic phase ratio (O/A) is slightly higher than unity to help maintain a large concentration profile between phases.

6.3.3   Uranium and plutonium purification cycles

The separated U and Pu streams emanating from the partitioning cycle still contain some fission product impurities. In order to complete decontamination of products, complementary purification cycles are required based on the same principles of the extraction chemistry described above. These two independent purification cycles are represented in Fig. 6.3. The primary contaminants in the Pu stream are typically Ru, Rh, and in some cases Np (depending on the operation and design of the early partitioning step), and the Pu purification cycle allows additional decontamination factors to be achieved with respect to these fission products. The uranium purification cycle is used primarily to enhance the decontamination from Np; it has been reported that 75% of the Np initially in the dissolved feed ends up in the uranium product from partitioning that goes to uranium purification. Of that, 99.8% of this Np is recovered in the raffinate of the uranium purification cycle. A Np decontamination factor of DF > 150 has been reported for the uranium purification cycle (Baron 1993).

Plutonium purification cycle

The purpose of the plutonium purification cycle is to complete Pu decontamination and to concentrate the plutonium stream prior to the conversion

step to the solid oxide. The plutonium entering this step is in the Pu(III) oxidation state, and as a prerequisite to extraction, the plutonium must undergo reoxidation to Pu(IV). This oxidation is typically accomplished by sparging the solution with nitrous vapors (in essence, the chemical reaction in Eq. 6.7), and subsequently with air to remove excess nitrous acid. Subsequent to this reoxidation step, the plutonium extraction and back-extraction operations both result in increased concentration. It should be noted that such concentration of the plutonium stream may be enhanced by providing recycle of part of the production stream to the head end of the cycle.

Flowsheets have been developed using uranous cation, U(IV), as the reductant for Pu partitioning in the purification cycle. However, reductive stripping in the Pu purification cycle is sometimes performed using hydroxylamine nitrate (HAN) as the reductant. Hydroxylamine nitrate, although not as effective as U(IV) for Pu reduction, is considered better suited than U(IV) for plutonium cycles involving higher plutonium concentrations. Furthermore, the re-addition of uranium back into the Pu purification cycle seems counter-intuitive since that negates the desired separation obtained in the initial partitioning cycle. Hydroxylamine nitrate (HAN) can readily reduce Pu(IV) to Pu(III) as follows:

$$4Pu^{4+} + 2NH_3OH^+ \rightarrow 4Pu^{3+} + N_2O + H_2O + 6H^+ \qquad 6.10$$

Furthermore, HAN will also scavenge HNO_2 at low acidities, up to ~1 to 1.5 M HNO_3:

$$NH_3OHNO_3 + HNO_2 \rightarrow N_2O + HNO_3 + 2H_2O \qquad 6.11$$

The additional nitrate available from HAN also provides a salting effect at low acidity which partly compensates to help keep uranium in the organic phase. HAN is not required in large excess and it can be readily destroyed by heating the solution to >60 °C before the subsequent plutonium finishing steps.

Even with the use of HAN as the primary Pu reductant, purification flowsheets can include a "plutonium barrier", using hydrazine stabilized U(IV) to complete plutonium stripping from the solvent, prior to the solvent regeneration operation. In the La Hague plants, HAN is used as the reductant in the Pu purification cycles: UP-3 uses the HAN flowsheet in pulsed columns; UP-2 uses HAN in centrifugal contactors. In the UP-2 plant, the Pu product from the first (codecontamination) cycle requires no additional decontamination from U; additionally, the introduction of a single reductant (HAN) is much simpler than adding several as would be the case for uranous nitrate. The Pu product from UP-2 is reportedly quite pure with <5000 ppm total impurities, <0.1 μCi β-γ activity, and <100 ppm U (Baron 2008).

Uranium purification cycle

A fraction of the neptunium coextracted with uranium, and plutonium follows the uranium stream through the process. The uranium stripping operation in the partitioning step is operated such that the uranium product stream is at a relatively low concentration in dilute nitric acid. This stream is concentrated in evaporators prior to treatment in the uranium purification cycle. This concentration increase is necessary if the extraction operation is to be carried out with favorable organic to aqueous flow ratios. During the concentration step, neptunium is oxidized to Np(V) and Np(VI) and the acid concentration is increased in the aqueous solution fed to the U purification cycle. In order to complete uranium purification from Np, hydrazine nitrate is introduced into the extraction step to reduce extractable Np(VI) to the inextractable Np(V) species. The uranium stripping operation is then similar to that carried out in the first cycle.

Solvent regeneration

It is a well-known fact that the organic solvent (both TBP and albeit, to a lesser extent, the diluent) degrades due to the effects of radiolysis, and hydrolysis. These degradation products must be removed prior to solvent recycle, lest they build-up in the organic phase with a concomitant decrease in process performance. Solvent cleanup and treatment, both physical and chemical are an important aspect of PUREX processing. These treatments can include scrubbing or washing the solvent with basic (carbonate and/or hydroxide) solutions to remove acidic degradation products. Carbonate solutions have the ability to form soluble carbonate complexes with residual metal cations in the organic phase, thus precluding any risk of metal cation precipitation during solvent wash. The organic is typically subjected to a subsequent acid rinse operation with dilute HNO_3 to remove traces of the basic solution from the organic and slightly re-acidify the organic prior to recycle to the extraction operations. Finally, complementary solvent treatment operations involving evaporation and subsequent rectification operations allows recovery of purified TBP solution and diluent. Evaporation makes it possible to remove the heavier, stubborn degradation products such as polymers, while the rectification operation serves to remove the lighter degradation products. These operations are performed on a continuous basis with a slip stream on a fraction of the total solvent inventory at the La Hague and Rokkasho plants. The evaporation and rectification cycles are not always performed in continuous mode, but can also be batch type operations preformed on a small fraction of the total solvent inventory. The solvent cleanup operations are carried out as separate unit operations from the various extraction, scrub, and strip cycles.

Liquid-liquid extraction equipment

Liquid-liquid extraction (solvent extraction) is intimately coupled to the PUREX process and has been the workhorse of the nuclear industry for 50+ years. Liquid-liquid extraction plays on the unequal distribution of the components between two immiscible liquid phases, and is therefore highly dependent on the chemistry of those species as well as the extractant molecule(s). Much of this information has been described in the previous discussions for the PUREX process. However, it is important to realize the extension of chemical phenomena is promulgated in the equipment design and operational logistics of a large plant at the industrial scale. While limited mass transfer can be completed in a single, batch equilibrium contact of the two phases, one of the primary advantages of liquid-liquid extraction processes is the ability to operate in a continuous, multistage, countercurrent flow mode. This allows for very high degree of separation while operating at high processing rates. The aqueous and organic steams flow countercurrently from stage to stage, and the final products are the solvent loaded with the solute(s), and the aqueous raffinate, depleted in solute(s). In this manner, the concentration gradient between the phases remains quite high across all of the stages in the system. This concentration gradient is the motive force for mass transfer and provides the basic phenomena upon which countercurrent solvent extraction is based.

  While countercurrent processes could be performed in laboratory glassware, their primary advantage is to enable continuous processing at high throughputs. In order to achieve continuous processing, specific equipment is needed that can efficiently mix and separate the two phases in a continuous operating mode. In the nuclear industry, specific constraints, such as remote operation and maintenance must be considered, since the solutions processed are highly radioactive. There are three basic types of equipment used in industrial-scale nuclear solvent extraction processes: mixer-settlers, columns, and centrifugal contactors. The basic design and operation of this equipment is well described in the literature (Benedict 1981, Long 1967). It is only noted here that the selection of the type of equipment to be used in large-scale reprocessing hinges on a number of different process parameters and design considerations, including (but not limited to):

• process foot print and building size/height
• operational flexibility (long-term continuous operation or frequent start/stop operation)
• solvent inventory and in-process volume holdup
• degradation of solvents due to radiolysis/hydrolysis (residence time)
• time required to reach steady-state operation
• potential to operate linked, complex multi-cycle processes
• tolerance to cross-phase entrainment

- tolerance to solids in process solutions
- tolerance to process upsets
- mass transfer kinetics
- process chemistry (e.g. kinetics of valance adjustment)
- remote maintenance capabilities
- criticality constraints.

The equipment type chosen for a particular process application should be based on several factors as indicated in the list above. In-depth reviews and comparisons of pulse columns, mixer-settlers, and centrifugal contactors have culminated with a recent rating of the different equipment designs relative to the criteria aforementioned. Results of a recent review performed as part of the United States Department of Energy's Plutonium Technical Exchange Committee is indicated in Table 6.3 (Todd 1998).

For comparison, the equipment currently used in the world's major reprocessing facilities is summarized in Table 6.4. Note that the use of pulsed columns and mixer-settlers is far more common than for centrifugal contactors. That trend may change in future applications as additional capacity is brought on-line and the next generation reprocessing plants are designed and built.

6.4   Future industrial uses of PUREX

The long and successful history of PUREX begs the question of its utility in the future of nuclear energy. In the current climate of developing a truly "closed," "next generation," or "advanced" nuclear fuel cycle, it is highly probable the first incremental improvements would be initially based on the capabilities of the current industrial standard, i.e. PUREX. Hot topics regarding the concepts of future fuel cycles are multi-faceted, but could be broadly categorized as containing two objectives: proliferation resistance (i.e., "no pure Pu" separation) and environmental concerns relating to radiotoxicity and disposal of the nuclear waste. The important capabilities of PUREX are the separation of major actinides prevalent in used nuclear fuel, primarily U, Pu, and Np (as well as the long lived and environmentally mobile fission product Tc). The next generations of PUREX processing will likely involve modification in the process chemistry to recover Np for recycle with the U and Pu into future mixed oxide (MOX) fuels and preclude the separation of a pure Pu stream by keeping some fraction of the U and/or Np with the Pu product. Another potential use of PUREX would be the separation of the minor actinides (MA), notably Am, by making use of the accessibility of higher oxidation states, albeit this use of PUREX is conceptual and much further down the road and consequently will not be further discussed here.

Table 6.3 Comparison of mixer-settler, pulse column and centrifugal contactors

Criteria	Ratings[a]			Comments
	Mixer-settler	Pulse column	Centrifugal contactor	
Building headroom	5	1	5	
Floor space required	1	5	3	May be small percentage of total floor area.
Low hold up volume	2	3	5	
Reach steady state quickly	2	3	5	
Process flexibility[b]	4	3	5	
Ability to tolerate solids	2	5	2	
Equipment reliability	4	5	3	
Rapid restart	5	2	5	After temporary shutdown.
Long residence time[c]	5	4	1	
Short residence time[d]	1	2	5	
Instrumentation/control	5	4	5	
Ease of scale up	3	3	5	
Equipment capital cost	4	5	4	May be insignificant in relation to building cost.
High throughput	2	5	5	Based on criticality safe by geometry equipment.

[a] 5 = superior; 4 = good; 3 = average; 2 = below average; 1 = poor.
[b] Process flexibility includes such factors as the range of O/A flow ratio, the turndown in flowrate, and the ease with which the location of feed and product streams can be changed.
[c] Considered an advantage when process chemistry and kinetics requires long residence time.
[d] Considered an advantage when solvent degradation is a concern.

The process details discussed above indicate that there are several reasons to improve the current PUREX process. The distribution of neptunium between product streams that require additional decontamination, especially the uranium product, is one of the major concerns. Currently, Pu is separated in high purity, converted to an oxide and subsequently back blended with U to prepare MOX. Intuitively, separating a combined U and Pu product (preferably in the appropriate and controllable ratios for MOX fuels) would substantially simplify the overall process, decrease the number of unit operations, and alleviate proliferation concerns. Also, there is inter-

Table 6.4 Equipment currently used in reprocessing plants

Country	Plant	Equipment	Processing section
United Kingdom	THORP, UK	Pulse columns	1st cycle, 2nd Pu cycle
		Mixer-settlers	1st cycle solvent cleanup, 2nd U cycle
Japan	Tokai	Mixer-settlers	All processes
	Rokkasho	Annular pulse columns	1st cycle
		Mixer-settlers	2nd Pu and 2nd U cycles, all solvent cleanup
France	UP-2, La Hague	Annular pulse columns	1st cycle extraction, Pu/U partitioning
		Mixer-settlers	1st cycle U stripping, 2nd U cycle, solvent cleanup
		Centrifugal contactors	2nd Pu cycle
	UP-3, La Hague	Annular pulse columns	1st cycle extraction, Pu/U partitioning
		Pulse columns	2nd Pu cycle
		Mixer-settlers	1st cycle U stripping, 2nd U cycle, solvent cleanup

est in introducing centrifugal contactors in advanced separation cycles due to the benefits of short residence time, small footprint, lower holdup volumes, and decreasing the risks from criticality issues. This technology obviously limits the chemical reactions to those with fast kinetics putting further constraints on the future use of PUREX processes.

Much work has been carried out in the United Kingdom and in France to improve PUREX into an "Advanced PUREX" or COEX™ process, respectively. This work has aimed at bleeding U (and possibly Np) into the Pu product to eliminate the pure Pu stream and to reduce the number of solvent extraction cycles. Furthermore, by controlling the neptunium oxidation state and providing a single route for the neptunium, the uranium purification cycle could conceivably be eliminated, simplifying the process and effectively decreasing the amount of waste (Taylor 1997). Using similar means to achieve an improved PUREX process, the path considered in the US is slightly different due to other political goals (Laidler 2001). The possibility to dispose of uranium as low-level waste (Vandegrift 2004) without the need for uranium purification cycle(s) would require thorough decontamination of the uranium from plutonium and neptunium. This route has been dubbed the "UREX" process since the goal is URanium EXtraction and the process is very similar to the PUREX process but eliminates plutonium extraction such that the Pu would follow the remaining transuranic actinides.

6.4.1 Neptunium control

The adaptations of the PUREX process, whether it is Advanced PUREX, COEX™ or UREX, all use the TBP/kerosene solvent and extract actinides from nitric acid media. As previously discussed, neptunium will be present in several oxidation states where only the pentavalent is completely unextractable into the TBP containing organic solvent. Depending on the ultimate fate of the neptunium (and plutonium) in the process, several adaptations to the PUREX process are possible (Taylor 1997, Fox 2006).

One option is to route the neptunium to the high active raffinate in the codecontamination cycle of Fig. 6.2 and dispose of it as waste. This requires that neptunium is held at the pentavalent state as NpO_2^+ while not interfering with the extraction of plutonium, i.e. any reducing agent to reduce Np(VI) to Np(V) cannot reduce Pu(IV) to Pu(III). This criterion makes the single decontamination step of neptunium in PUREX very difficult. Furthermore, this option is also not advantageous from the standpoint of advanced fuel cycles in that the Np and the minor actinides (Am and Cm) would still need to be separated in subsequent steps.

A second option would be to let neptunium extract together with U and Pu in the first cycle and selectively strip neptunium in a separate contactor before the partitioning cycle of Fig. 6.2. This has the same inherent problems as the first option in that the reduction of neptunium to Np(IV) may affect the Pu oxidation state, and therefore Pu behavior.

The final options are all based on the simultaneous extraction and separation of neptunium and plutonium together, creating a relatively pure uranium product and a Np/Pu product. This could be accomplished in the Pu reduction and scrub sections of the partitioning cycle (Fig. 6.2), which is the preferred route in the UK (Fox 2006) and one option of the French COEX™ process. Alternatively, this could be accomplished in the codecontamination cycle, routing both neptunium and plutonium together with the fission products and minor actinides to the raffinate; which is a preferred route in the US and provides the reasoning behind the UREX process. In either case, the technique and redox reactions chosen must also take into consideration the possibility to use centrifugal contactors, i.e. the requirements of fast kinetics, and the aggressive environment, i.e. stable chemical compounds or degradation products that will not interfere with the process.

Several methods for controlling the Pu and Np oxidation states have been investigated. The French have largely focused on established redox techniques such as HAN and HNO_3 concentration. In the UK and US, the emphasis has been on the use of simple hydroxamic acids for the combination of reduction together with aqueous phase complexation of neptunium and plutonium, effectively decontaminating the uranium product. The current hydroxamic acid candidates are either acetohydroxamic acid
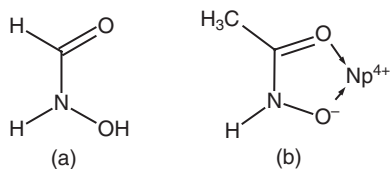
6.4 Chemical structures of (a) formohydroxamic acid and (b) acetohydroxamate coordinating to neptunium(IV).

(AHA) or formohydroxamic acid (FHA), both having been proven to reduce and strip Np(VI) from the organic solution and to complex Np(IV) and Pu(IV) in the aqueous phase (Taylor 1998, May 1999).

6.4.2 Role of AHA in the PUREX process

Hydroxamic acids are organic ligands which have the ability to form stable five membered chelate rings with metal ions as indicated Fig. 6.4. An example of the complexation reaction between Pu(IV) and acetohydroxamic acid, denoted HL, is shown below with the coordinated nitrates omitted for clarity:

$$Pu^{4+} + nHL \rightleftarrows PuL_n^{4-n} + nH^+ \qquad 6.12$$

where n = 1, 2 or 3 AHA molecules coordinated to each tetravalent metal ion (Carrott 2007). Both AHA and FHA are hydrophilic molecules that are not extracted by themselves into the TBP solvent (Taylor 1998). Larger or longer chain hydroxamic acids may be susceptible to distribution between the two phases; consequently, only the smaller molecules (FHA and AHA) have been considered for advanced PUREX applications.

Since the introduction of hydroxamic acid as a potential reduction/complexation agent in the PUREX process, several research groups have made complementary investigations on different aspects of AHA chemistry. Both formo- and acetohydroxamic acid are prone to hydrolysis in nitric acid media, FHA more so than AHA. Both hydroxamic acids break down to hydroxylamine and carboxylic acid according to the reaction below (Taylor 1999, Carrott 2008).

$$CH_3CONHOH + H_2O + H^+ \rightarrow CH_3COOH + NH_3OH^+ \qquad 6.13$$

This degradation potentially creates a problem in the process due to a decrease in the hydroxamic acid available for Np and Pu complexation/reduction. However, the hydroxylamine produced will reduce Pu(IV) to Pu(III) in accord with the earlier discussion (see Eq. 6.10), and would have a beneficial effect on the process. The rate of degradation of AHA in acidic media translates to a destruction half-life of around 300, 100 and 60 minutes

at 1, 3 and 5 M HNO_3, respectively (Nunez 2001). This degradation rate is only of concern for relatively long process times. If future processes use centrifugal contactors with short residence times, this will be a minor or negligible problem. Furthermore, the aqueous strip/scrub solution containing the hydroxamic acid will likely not be recycled after leaving the process; instead the remaining free hydroxamic acid and AHA-Np/Pu complexes will be deliberately destroyed downstream to facilitate the extraction of neptunium and plutonium away from the other fission and activation products, e.g., NPEX (*vide infra*).

The complexation and reduction of pertechnetate by AHA was investigated to see if AHA addition interferes with the extraction of technetium (Gong 2008). The study showed that it is possible for AHA to reduce and complex technetium; however, the rate of reduction at moderate AHA concentrations is low and, although an important observation, it is not an issue for short contact times in centrifugal contactors. Studies have also shown that pertechnetate does not react with hydroxylamine to any large extent (Koltunov 2000).

The reduction of Np(VI) to Np(V) by AHA is a rapid reaction and has been suggested to proceed by the following route (Chung 2005):

$$2NpO_2^{2+} + 2CH_3CONHOH \rightarrow 2NpO_2^+ + 2CH_3COOH + N_2 + 2H^+ \qquad 6.14$$
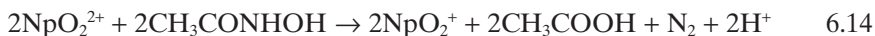
This reaction was shown to be kinetically rapid enough for successful use of centrifugal contactors (Taylor 1998, 1999).

Even though the addition of AHA will not affect the extraction of U(VI) (Taylor 1998) the presence of a uranyl-hydroxamate complex in the TBP solvent has been identified (Tkac 2008). This will most likely not cause any problems downstream in the uranium purification stage, see UREX below.

The incorporation of AHA into the PUREX flow sheet for Np/Pu separation has potential benefits, and the results thus far from several research groups indicate no major disturbances to process performance. The small-scale process tests carried out to date have been mostly successful (Vandegrift 2004, Birkett 2004), see below, and this chemistry may be considered to be very close to ready for full-scale testing. Of course, a major byproduct from AHA is acetic acid (refer to equations 6.13 and 6.14 above), the behavior and impact of which (e.g., effluent treatment and acid recycle) must yet be evaluated. Finally, the political climate and possible use of plutonium and neptunium as reactor fuel will still determine how the final process will be shaped.

6.4.3   UREX flowsheet

The UREX process was tested in miniature centrifugal contactors during 2003 as part of a series of five different solvent extraction processes called

UREX+ (Vandegrift 2004). A fuel pin with an estimated burn-up of 29,600 MWd/MT, 4.6% initial ^{235}U enrichment, and a cooling time of 21 years was dissolved and used as feed in this process test. After dissolution, the first solvent extraction step was the UREX process where U and Tc were separated from the other actinides and fission products. The process used AHA in the scrub section of the flowsheet to remove neptunium and plutonium from the organic phase (Fig. 6.5), and route these actinides to
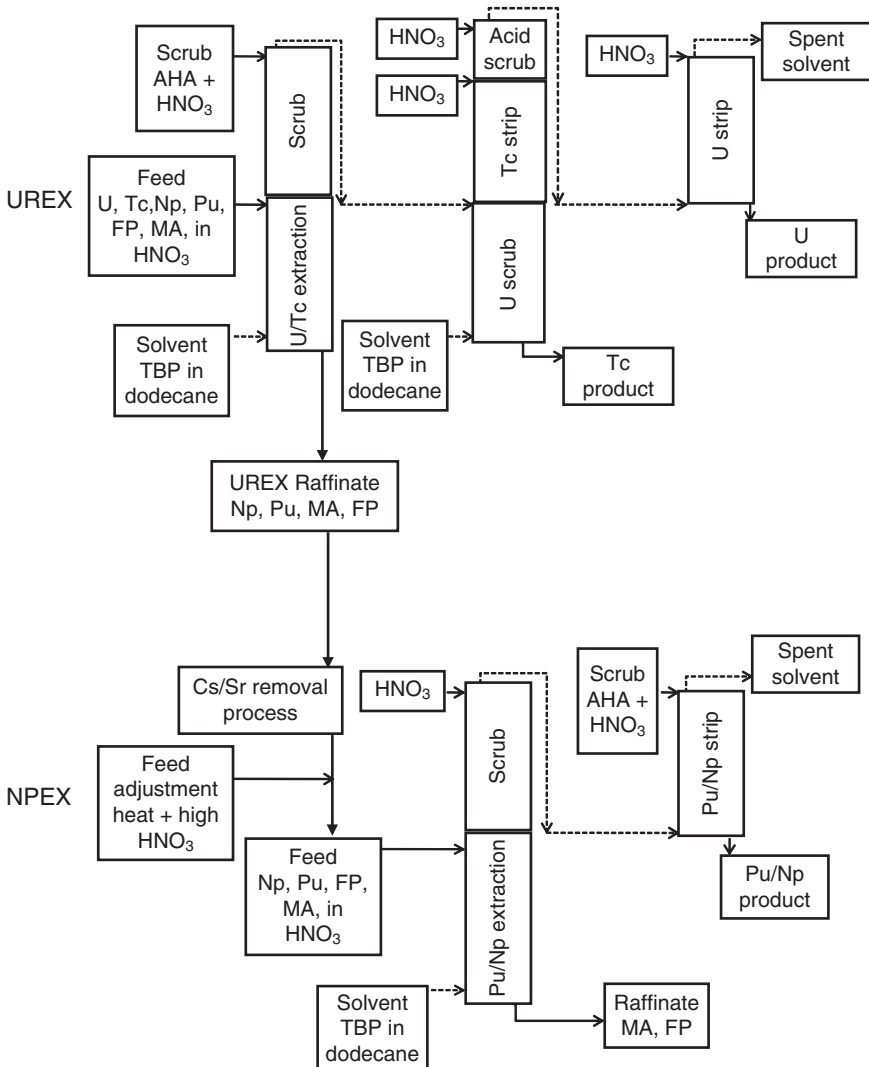
6.5 UREX and NPEX process flowsheet as part of the UREX+ process test at ANL 2003.

the raffinate end of the cascade. In order for the AHA to complex the tetravalent actinides, the acidity of the feed solution was adjusted to a fairly low acidity of ~1 M HNO_3, which also resulted in increased technetium extraction. A separate technetium strip contactor using higher acid concentration was included in the UREX process (Fig. 6.5). To remove excess nitric acid, an acid scrub contactor was included after the Tc strip, but before the final uranium strip. The uranium product obtained from this process test reached the limits for FP decontamination. But due to a mechanical failure during processing, the desired TRU decontamination was unsuccessful. The indications were positive and a second test was carried out one year later. Tc recovery was 95% which was in line with the requirements set on the process. Recycling of the spent solvent was not carried out during the test, but solvent degradation is fairly well established as discussed above, and would likely not be affected by the addition of AHA to the process. As previously mentioned, hydroxamic acid has low solubility in the organic solvent and a solvent clean up stage would remove any residual AHA along with any dissolved HNO_3.

6.4.4   Neptunium-plutonium extraction (NPEX)

In UREX, the Np and Pu are rejected into the aqueous waste stream by the use of AHA. It is then of interest to extract Np and Pu away from the other fission products and minor actinides, especially if the Pu or Pu + Np will be converted to fresh MOX fuel. To accomplish this, the aqueous raffinate from UREX is thermally treated (evaporated) to destroy AHA and increase the nitric acid concentration. The objective is to retain plutonium and neptunium in the extractable (IV) and (VI) oxidation states, respectively, and thereby extract them into the organic solvent of TBP in dodecane. In this process, called NPEX, the Np and Pu will behave much like in the PUREX process described earlier. After extraction, the plutonium and neptunium are removed from the solvent using AHA in a stripping stage to obtain a Np/Pu product stream. This was tested at the same time as the UREX test described above (Vandegrift 2004), see Fig. 6.5, and it was observed that the neptunium was not completely extracted due to difficulties maintaining the Np(VI) oxidation state. However, the goal of not creating a pure plutonium product was still fulfilled and the residual Np remaining in the NPEX raffinate was recovered in the subsequent TRUEX (TRansUranic Extraction) segment of the UREX+ flowsheet (Vandegrift 2004).

6.4.5   UREX+2 process test

Another version of the UREX+ process was tested in miniature centrifugal contactors at Argonne National lab in 2004 using the same spent fuel feed

as previously described (Pereira 2005). Changes to the process included the coextraction of U, Tc, Np and Pu from the rest of the waste, see Fig. 6.6, routing the high active waste to further Cs/Sr removal. The benefit of this methodology, compared to the previous UREX+ flowsheet, is that the low specific activity of U, Tc, Np and Pu would be separated from the rest of the high active waste early in the process. This would make handling of the U/Tc + Np/Pu product streams much easier considering dose rates and shielding required. Another improvement is that less organic solvent is needed since only one extraction section is required followed by re-extraction of uranium and technetium and reductive stripping of Np and Pu. Furthermore, no feed adjustment is needed for the second extraction of neptunium and plutonium where AHA is destroyed. The flowsheet for creating both U/Tc + Np/Pu product streams (Fig. 6.6) can be compared to only the upper part of the flowsheet of Fig. 6.5, for the UREX process. As in the first UREX+ test, the organic phase was not recycled. The recovery of neptunium and plutonium in the Np/Pu product was 87.2 and 99.8%, respectively. As before, some neptunium was lost to the raffinate but was recovered downstream. The largest impurity in the Np/Pu product was
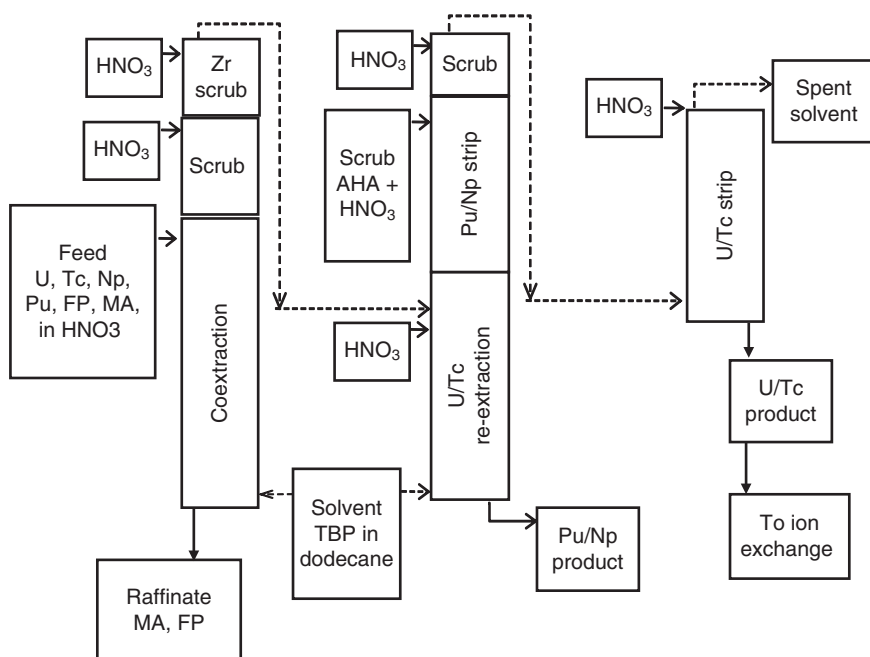
6.6 Co-extraction and selective separation of U/Tc and Np/Pu process flowsheet as part of the UREX+2 process test at ANL 2004.

zirconium, although this was claimed to relate to hydraulic problems in the Zr scrub section rather than chemical behavior.

The U/Tc separation was accomplished by anion exchange where the pertechnetate was retained by the resin and the uranium was effectively purified to a high degree, reaching all goals set for disposal as low level waste. The use of ion exchange as part of the PUREX process for Tc separation has been investigated separately (Dileep 2008) where anion exchange was used as a purification step for obtaining a pure plutonium product after the U/Pu split.

A number of flowsheets of the same general setup as those shown in Figs 6.5 and 6.6 have been tested in the UK since 2003 and are summarized in a publication by Birkett *et al*. (Birkett 2007). The U+Pu or U+Np product streams were first coextracted from the high active waste and transported by the loaded solvent to a separate stage for U/Np or U/Pu separation with the aid of AHA. Different tests were carried out to investigate the feasibility of this process for different concentrations of Pu in the feed, and simulated 1) thermal MOX-fuel (7 wt.% Pu); 2) fuel from fast reactors (20 wt.% Pu); and 3) treatment of exotic Pu legacy waste (40 wt.% Pu). In all tests pure uranium product could be obtained. The purity of the plutonium product could potentially be controlled to accommodate proliferation resistance.

6.4.6   COEX™ flowsheet

The COEX™ or <u>COEX</u>traction process has been developed by French workers, and is designed to bleed some of the U (and possibly Np) into the Pu product to eliminate the pure Pu stream (Baron 2007). The development of this new reprocessing and recycling COEX™ process was aimed at:

- further enhancing proliferation resistance
- maintaining a high level of process performance
- minimizing both investment (capital) and operational costs
- taking full advantage of present industrial experience
- keeping open possible evolutions to take into account new types of reactors or future changes in management strategies of the transuranic elements.

The separation flowsheets used in the COEX™ process (Drain 2008) are based on the expertise accruing from the design, and deployment of the PUREX process, but equally from operational feedback with that process. The design for the extraction cycles has extensively relied on a simulation tool, validated by experimental investigations carried out in the workshops at the La Hague plants, and equally by comparisons with findings from industrial operations. Consequently, the COEX™ process is basically an
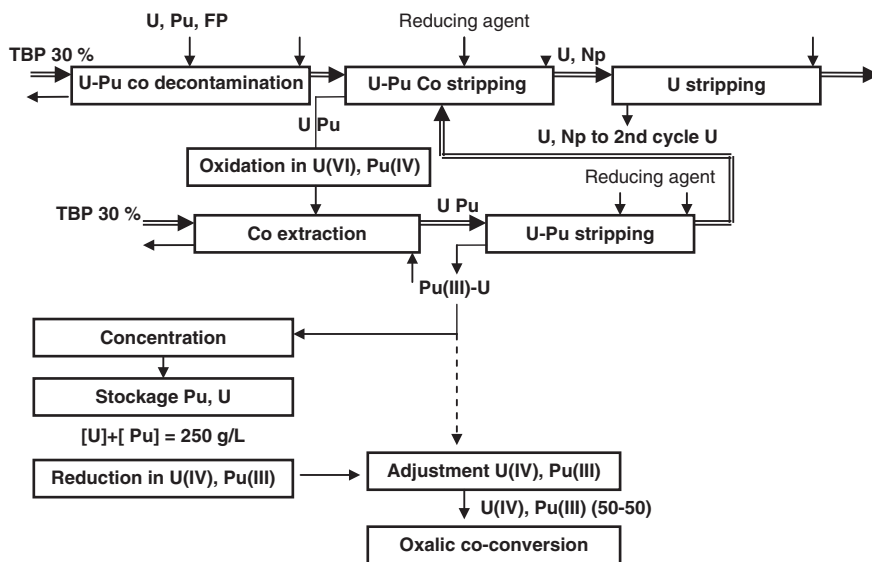
6.7 COEX™ process.

evolution of the PUREX process, by modifying it to produce a U + Pu mixture (U/Pu >20%), rather than pure plutonium: no pure plutonium is separated at any point of the process (see Fig. 6.7). The advantage of so doing is to curb proliferation risks and to produce a perfectly homogeneous mixed oxide, for the purposes of MOX fuel fabrication, affording enhanced performance.

The proposed COEX™ flowsheet is indicated in Fig. 6.7, and involves an initial U/Pu codecontamination step that is fairly similar to the first purification cycle, as implemented in the La Hague and Rokkashomura plants (see Fig. 6.2). The codecontamination step is unchanged: this covers the extraction flowsheet, including measures to allow removal of technetium. The plutonium stripping part is modified by including conditions that results in uranium scrubbing into the Pu strip product. This function is slightly tweaked from uranium scrub to neptunium scrub, to allow some uranium to remain in the plutonium stream. The function further allows neptunium to be extracted from the plutonium stream, directing the neptunium thus extracted to the cycle's uranium product stream, thanks to higher distribution coefficient of Np(IV) compared to U(IV) (see Table 6.1).

To ensure the plutonium becomes extractable by the solvent phase again, an adjustment is made to the solution yielded by the first cycle, by raising the nitric acid concentration, concomitant with reoxidation of plutonium to oxidation state IV, uranium being adjusted to oxidation state VI. The stream then undergoes treatment in the form of a U–Pu cycle, only involving

plutonium extraction, and back-extraction (stripping) functions. Reductive plutonium stripping is effected using hydroxylamine nitrate.

Topping up with uranium is provided for, at the head end of this operation, to adjust the Pu/U ratio in the production stream. Finally, the stripped solvent is recycled in the plutonium stripping operation carried out upstream, in the first cycle. This measure makes it possible to tolerate some loss of plutonium to the stripped solvent, and thus limit the number of stages used for the plutonium stripping operation (hence the term "mini-cycle," for this complementary purification cycle).

A uranium purification cycle, identical to the cycles implemented at the La Hague plant, is further provided for – on the one hand, to complete decontamination of the uranium stream, with respect to β and γ emitters, and, on the other hand, to ensure removal of neptunium.

Technetium control

The behavior of Tc in the COEX™ process is basically the same as in PUREX flowsheet presented in Fig. 6.2. More than 95% of Tc from the dissolution solution is recovered in raffinate of the complementary extraction, so in an effluent presenting a relative low activity (the bulk of the other fission products is eliminated during the first extraction-scrubbing steps). The other 5% of Tc is recovered in the raffinate of the second U/Pu purification cycle ("mini-cycle").

Neptunium control

In the version of the COEX™ process indicated in Fig. 6.7, the bulk of the Np is recovered in the raffinate of the uranium purification cycle. Variants for the flowsheet have, at the same time, already been suggested that allow for evolutions in the near future, that would cater to neptunium recycling. A very simple modification of Pu stripping flowsheet in first extraction cycle (suppression of the Np scrub and use of HAN as reducing agent) allows neptunium to follow the plutonium-uranium stream. Then in Pu-U purification cycle, with a minor flowsheet modification, neptunium will follow U-Pu stream up to concentration stage.

For subsequent advances to a fully closed nuclear fuel cycle, it could also be envisaged to separate other minor actinides (MA), mainly americium and curium, for specific management. In this case, the COEX™ flowsheet would be operated to route the Np into the U/Pu product. The additional MA/fission product separations could then be achieved by implementing DIAMEX (DIAMide Extraction) and SANEX (Selective ActiNide Extraction) processes on the raffinates of first extraction cycle as shown on Fig. 6.8.

Feeding
U + Pu + Np + FP + MA

FP   MA
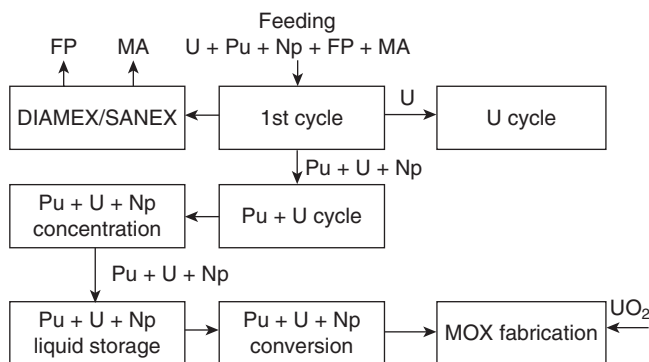
6.8 COEX™ process with separation of minor actinides.

6.4.7 Co-conversion of uranium and plutonium with the COEX™ process

The joint conversion of uranium and plutonium to the oxide form makes it possible to do away with the complicated step of blending and grinding the two distinct oxide powders, as currently employed for the purposes of MOX fuel fabrication. Over the past few years, a number of co-conversion routes have thus been revisited or devised on the basis of original chemical principles, in order to innovate in the area of uranium and plutonium management. Drawing on 50 years industrial experience and feedback, CEA/DEN, in partnership with Areva NC, are proposing to extend oxalic conversion of Pu(IV) to Pu oxide to the oxalic co-conversion of uranium and plutonium.

Of the various possible variants, the current reference route is the U(IV)–Pu(III) variant, owing to the following advantages (Grandjean 2005):

- Unexpectedly, U(IV) and Pu(III) co-crystallize into a single oxalate structure, thus ensuring homogeneous distribution of the two actinides, at the molecular scale (Arab-Chapelt 2007). This structure is an oxalate solid solution, over a broad range of Pu/(U + Pu) ratios: 0–50% (mol/mol).
- The mixed oxalate exhibits very low solubility in a nitric acid solution carrying excess oxalic acid: solubility is about the same as that of the plutonium(IV) oxalate precipitate.
- Calcination of this mixed oxalate in an inert atmosphere yields a solid solution of $(U,Pu)O_2$ oxide; the homogeneity of uranium and plutonium distribution, at the molecular level, is thus conserved, from the solution to the oxide.
- Technology similar to that operated in the current plutonium conversion workshops at La Hague may be used.

A major advantage of oxalic co-conversion is to produce mixed oxides exhibiting physicochemical characteristics directly tailored to fuel fabrication, affording, in particular, the *ability to use this raw material directly, with no further specific chemical, or mechanical treatment.* More broadly speaking, from PUREX to COEX™, the evolution to an oxalic U–Pu co-conversion process, combined with a process adapted from a MIMAS-type process, affords the following advantages:

- A process yielding a uranium–plutonium mixture, without at any point involving the handling of separated plutonium, thus reducing proliferation risks.
- The $(U,Pu)O_2$ oxide solid solution obtained from co-conversion, as the endproduct of spent fuel treatment by the COEX™ process, and raw material for the fabrication of advanced MOX fuel, results in an enhanced homogeneity of plutonium distribution within the fuel (compared with the current upstream grinding operations with mixtures of UO_2 and PuO_2 powders). This translates to the anticipation of improved in-reactor behavior for MOX fuel fabricated from such raw material, bringing benefits with regard to increased burnups.
- Reduced contamination potential and limited exposure to radiation, during fuel fabrication using COEX™-produced powder.
- A further outcome would be simplified management of fabrication scrap, and a likely improvement in MOX fuel solubility, subsequent to irradiation (no PuO_2 islands).

6.5   Conclusions

PUREX was developed in the US in the late 1940s originally as a separation system for production of pure plutonium for military applications. In a way, PUREX was an industrial revolution and the success of this process led to the development of modern liquid-liquid extraction processes. More than half a decade after its development, PUREX is still the foundation of all modern separation processes for spent nuclear fuel used on industrial scale. The system utilizes tributyl phosphate (TBP) to extract uranium and plutonium away from most other elements in the spent nuclear material. The preference of tetravalent and hexavalent (as MO_2^{2+}) ions is the key to the selective extraction. The stability of UO_2^{2+} combined with the relative ease of changes to the oxidation state of plutonium, predominantly between the +3 and +4 state, is the other critical aspect of this process. The current state of the art PUREX processes for commercial reprocessing are used in four countries in the world (France, Japan, the UK, and Russia) and have an annual capacity of more than 5500 tonne heavy metal (including the new

Rokkasho-Mura plant). The reprocessing plants combine extraction (TBP) and redox reagents (e.g. U(IV), hydroxylamine, hydrazine) in several counter current liquid-liquid extraction batteries under different conditions to extract, scrub and strip selected elements to obtain a pure product. PUREX is not entirely without problems and elements such as Np, Tc, Zr, Nb and Ru put high demands on the process such as increased number of stages and the need for parallel decontamination batteries. Improvements and changes made to the PUREX process over the years include more advanced equipment to facilitate easier handling and increase throughput. Although PUREX has been used successfully for a long time, research has been continuous and a number of recent discoveries and ideas are close to being implemented to a future PUREX process, e.g. Advanced PUREX, SuperPUREX, COEX, UREX, etc. These new processes are being developed to meet new or future policies regarding waste and product stream composition. One major issue has been to avoid a pure Pu product by routing either neptunium (UREX and NPEX) or uranium (COEX) into the Pu-product stream, thereby increasing proliferation resistance. The complicated issue of neptunium control have been addressed using simple hydroxamic acids and successful pilot scale processes has been administered in both U.S. (UREX+), the UK (Adv. PUREX) and France (COEX). All these processes look promising for the future successful use of PUREX-like chemistry in advanced nuclear fuel reprocessing and the adaptability of this process is all but proven to accommodate for future restrictions on waste and product stream composition.

6.6   References

Arab-Chapelet, B., Grandjean, S., Nowogrocki, G., Abraham, F. (2007), *Journal of Alloys and Compounds*, 444–445, pp. 387–390.

Baron, P., Boullis, B., Germain, M., Gue, J.P., Miquel, P., Poncelet, F.J., Dormant, J.M., Dutertre, F. (1993), "Extraction Cycles Design for La Hague Plants", Proc. Global '93, Seattle, WA (USA) 12–17 Sept. 1993 pp. 63–70.

Baron, P., Lecomte, M., Boullis, B., Simon, N., Warin, D. (2003), "Separation of the Long Lived Radionuclides: Currnt Status and Future R&D in France", Proc. Global 2003, New Orleans, LA (USA) 16–20 Nov. 2003 pp. 508–511.

Baron, P., Dinh, B., Masson, M., Drain, F., Emin, J-L. (2007), "Process for Reprocessing A Spent Nuclear Fuel and of Preparing a Mixed Uranium–Plutonium Oxide", United States Patent Application No. US 2007/0290178 A1, Dec. 20, 2007.

Baron, P., Dinh, B., Duhamet, J., Drain, F., Meze, F., Lavenu, A. (2008), Proc. ISEC 2008, Tucson, AZ, Vol. I, 587.

Benedict, M., Pigford, T.H., Levi, H.W. (1981), *Nuclear Chemical Engineering*, McGraw Hill Book Co., N.Y.

Birkett, J.E., Carrott, M.J., Fox, O.D., Maher, C.J., Roube, C.V., Taylor, R.J. (2004), Proc. ATALANTE 2004, Nimes (France), June 21–25, 2004.

Birkett, J.E., Carrott, M.J., Fox, O.D., Jones, C.J., Maher, C.J., Roube, C.V., Taylor, R.J., Woodhead, D.A. (2007), *J. Nucl. Sci. Technol.*, 44(3), 337–343.

Carrott, M.J., Fox, O.D., Maher, C.J., Mason, C., Taylor, R.J., Sinkov, S.I., Choppin, G.R. (2007), *Solvent Extr. Ion Exch.*, 25(6), 723–745.

Carrott, M.J., Fox, O.D., LeGurun, G., Jones, C.J., Mason, C., Taylor, R.J., Andrieux, F.P.L., Boxall, C. (2008), *Radiochim. Acta*, 96, 333–343.

Chung, D.Y., Lee, E.H. (2005), *Bull. Korean Chem. Soc.*, 26(11), 1692–1694.

Dileep, C.S., Jagasia, P., Dhami, P.S., Achuthan, P.V., Dakshinamoorthy, A., Tomar, B.S., Munshi, S.K., Dey, P.K. (2008), *Desalination*, 232, 157–165.

Dinh, B., Moisy, P., Baron, P., Calor, J., Espinoux, D., Lorrain, B., Brnchikouhne-Ranchoux, M. (2008), Proc. ISEC 2008, Tucson, AZ, Vol. I, 581.

Drain, F., Emin, J.L., Vinoche, R., Baron, P. (2008), Proc. WM'08, Granada, Spain.

Fox, O.D, Jones, C.J., Birkett, J.E., Carrott, M.J., Crooks, G., Maher, C.J., Roube, C.V., Taylor, R.J. (2006), "Advanced PUREX Flowsheets for Future Np and Pu Fuel Cycle Demands", *Separations for the Nuclear Fuel Cycle in the 21st Century*, Lumetta et al (eds) American Chemical Society Symposium Series, pp 89–102.

Gong, C-M.S., Lukens, W.W., Poineau, F., Czerwinski, K.R. (2008), *Inorg Chem.*, 47, 6674–6680.

Grandjean, S., Bérès, A., Rousselle, J., Maillard, C. (2005), "Method for co-precipitation of actinides in different oxidation states and method for preparation of mixed actinide compounds", patent No. WO/2005/119699.

Koltunov, V.S., Taylor, R.J., Gomonova, T.V., Savilova, O.A., Zhuravleva, G.I., Denniss, I.S. (2000), *Radiochim. Acta*, 88, 425–430.

Laidler, J.J., Burris, L., Collins, E.D., Duguid, J., Henry, R.N., Hill, J., Karell, E.J., McDeavitt, S.M., Thompson, M., Williamson, M.A., Willit, J.L. (2001), *Prog. Nucl. Energy*, 38(1–2), 65–79.

Lanham, W.B., Runion, T.C. (1949), USAEC, "PUREX Process for Plutonium and Uranium Recovery", Report ORNL-479.

Long, J.T. (1967), *Engineering for Nuclear Fuel Reprocessing*, Gordon Breach Sci. Publ., N.Y. 173.

May, I., Taylor, R.J., Denniss, I.S., Wallwork, A.L. (1999), *Czech. J. Phys.*, 49 (Suppl. S1), 597–601.

Nunez, L., Vandegrift, G.F. (2001), Argonne National Laboratory technical report, ANL-00/35.

Pereira, C., Vandegrift, G.F., Regalbuto, M.C., Aase, S., Bakel, A., Bowers, D., Byrnes, J.P., Clark, M.A., Emery, J.W., Falkenberg, J.R., Gelis, A.V., Hafenrichter, L., Leonard, R., Quigley, K.J., Tsai, Y., Vander Pol, M.H., Laidler, J.J. (2005), Proc. WM'05, Tucson, AZ (USA), Feb 27–March 3, 2005.

Phillips, C. (1989), *Atom*, 394, 13.

Schulz, W.W., Burger, L.L., Navratil, J.D., Bender, K.P. (Eds) (1984), *Science and Technology of Tributyl Phosphate*, CRC Press Inc., Boca Raton.

Sood, D.D., Patil, S.K. (1996), *J. Radioanal. Nucl. Chem. Articles*, 203, 2, 547.

Taylor, R.J., Denniss, I.S., Wallwork, A.L. (1997), *Nuclear Energy*, 36(1), 39–46.

Taylor, R.J., May, I., Wallwork, A.L., Denniss, I.S., Hill, N.J., Galkin, B.Ya., Zilberman, B.Ya., Fedorov, Yu.S. (1998), *J. Alloys Comp.*, 271–273, 534–537.

Taylor, R.J., May, I. (1999), *Czech. J. Phys.*, 49 (Suppl. S1), 617–621.

Tkac, P., Matteson, B., Bruso, J., Paulenova, A. (2008), *J. Radioanal. Nucl. Chem.*, 277(1), 31–36.

Todd, T.A. *et al.,* (1998), Waste, Nuclear, Reprocessing and Treatment Technologies, *Encyclopedia of Chemical Processing and Design*, John J. McKetta editor, Marcell Dekker Inc., NY, Vol. 65.

Vandegrift, G.F., Regalbuto, M.C., Aase, S., Bakel, A., Battisti, T.J., Bowers, D., Byrnes, J.P., Clark, M.A., Cummings, D.G., Emery, J.W., Falkenberg, J.R., Gelis, A.V., Pereira, C., Hafenrichter, L., Tsai, Y., Quigley, K.J., Vander Pol, M.H. (2004), Proc. ATALANTE 2004, Nimes (France), June 21–25, 2004.

7

Alternative separation and extraction: UREX+ processes for actinide and targeted fission product recovery

M. C. REGALBUTO, Argonne National Laboratory, USA

Abstract: The separations strategy for the UREX+ type processes is based on an optimization approach for which key objectives for a closed or partially closed fuel cycle are pre-determined. The overall process is composed of a sequence of separation steps or modules linked to generate a desired set of outputs, whether products or intermediates. Processing options are shown for the case of LWR recycle, where incentives exist to separate and recycle the actinides, and separate and manage fission products. The UREX+ approach was successfully tested for the recycle of LWR SNF for a number of different product and waste forms configurations and the results from these tests are given.

Key words: LWR recycle, UREX+, GNEP, AMUSE, FPEX, NPEX, TALSPEAK, TRUEX, CCD-PEG.

7.1   Introduction

The original goal of actinide separations research in the US, which dates back to the 1940s, was the recovery of plutonium for defense purposes. The ultimate result was the development of large-scale chemical processes for the separation of plutonium from irradiated uranium. A number of chemical processes were tested (US Nuclear Regulatory Commission, 2008, p. 13) at the Hanford and Savannah River sites. By far the most successful was the PUREX process, which has now been developed commercially to treat spent power reactor fuel. By the mid 1950s, advancements in nuclear power technology, the then-perceived scarcity of uranium-bearing ore, and the high energy requirements of gaseous diffusion for uranium enrichment, resulted in the belief that there would be a shortage of uranium fuel supplies if nuclear power expanded significantly. In response, efforts were begun to develop reactors that could breed plutonium to serve as the fissile component in fuel, along with reprocessing facilities to recover the bred plutonium.

Although the plutonium was intended for use in commercial power reactors (rather than defense applications), the goal remained the isolation of plutonium from the other components of spent fuel, as it was the product

176

of interest. Uranium was also collected as a product in PUREX but required re-enrichment to serve as a fuel for light water reactors. Because of this early development work, PUREX is the only current industrial process for recovery of plutonium (and uranium) from commercial spent fuel. In the early 2000s, the reprocessing of spent fuel re-emerged as an area of interest driven by the forecasted growth in nuclear power (MIT, 2003) and the need to develop sustainable, environmentally acceptable and economic closed fuel cycles (Williamson *et al.*, 2004). The separations goal this time had changed from recovery of plutonium to management of all minor actinides and fission products not only for reuse of material as fuel but also to help address the waste management challenges still facing nuclear power generation (Wigeland *et al.*, 2006).

7.2   Separation strategy

The separation strategy for the UREX+ type processes is based on an optimization approach for which key objectives of the fuel cycle are pre-determined. Currently the US operates an "open fuel cycle," in which all of the spent fuel is scheduled for disposal. Recycling of all of the fissile components, as is currently done in several countries, yields a partially "closed fuel cycle." Recycling of both the fissionable and fissile components is referred to as a completely closed fuel cycle, although not all components are fully transmuted. Because a fast reactor is required to transmute the fissionable components, the completely closed cycle is often called a "fast reactor fuel cycle." All fuel cycles generate high-level waste, but the volume and radiotoxicity is a function of the extent to which the spent fuel is separated and critical components transmuted. Isolation of specific fission products, in addition to the actinides, can have a significant bearing on the performance of the wastes and repositories.

For a closed fuel cycle, the first step is to define the specific target products that need to be recovered to meet the requirements of the selected recycle and waste options. The second step is to determine the feedstock to the separations process. The feedstock is a selection of SNF from the current inventory that is to be processed to yield the desired products. The third step is to determine the process flowsheet. Given the large variation within the SNF inventory, the process flowsheets are designed to accommodate the wide variation in composition. The flowsheet selection methodology identifies what combination of solvent extraction systems accomplishes the segregation of the specified target products. Processing options need not be limited to solvent extraction; ion exchange, crystallization, electrochemical and other processes can be used in combination. However, the integration requires that the processes be compatible chemically. In summary the UREX+ approach requires:

1. Definition of the specific target products that need to be separated.
2. Determination of the feedstock for the separations process; historically it is SNF, but targets and other forms of nuclear waste may be used.
3. Selection or development of technologies that can accomplish the desired separations so that the final products and waste forms meet either the product specifications or waste acceptance criteria.

7.2.1 Defining products/wastes streams

The first step in the development of a UREX+ separation strategy is to establish what the desired separation products are. This is done by evaluating the benefit derived from the recovery of specific components from the feed. To illustrate, one can consider the case of a closed fuel cycle strategy based on transmutation of actinides in a fast reactor. The strategy may include the following benefits:

1. Recycle fissile materials to the power generator reactor (resource conservation).
2. Avoid sending fissile materials to a geologic repository or a long-term storage facility (non-proliferation, safety).
3. Transmute long-lived material (environment, safety).
4. Sequester fission products in superior (relative to SNF) storage and/or disposal forms to reduce their environmental impact (environment).

In this case there is an incentive to separate a fissile fraction as a product, a fraction that contains long-lived non-fissile materials as a second product, and another fraction that retains all of the residual components as a waste.

Although specifically developed for commercial spent fuel, a UREX+ approach can be tailored to treatment of high- or low-level wastes, such as legacy defense waste. Similar approaches can be taken for wastes resulting from R&D, medical or other industrial applications, though the volumes involved are likely more suited to small-scale operations.

7.2.2 Determining process feedstock

The feedstock to the process is expected to have a great deal of variation whether its origin is SNF, or other high- or low-level wastes (legacy defense, medical, industrial, etc.). The feedstock is usually characterized by a range of potential expected compositions, from different SNF assemblies, waste tanks, or medical processes. This is critical as the process needs to be designed to accommodate variations in the feed. Similarly, bracketing the acceptable feed compositions also sets the optimal combination of feed candidates.

7.2.3 Selecting the separations modules

Once the product and waste streams, and feedstocks are defined, the next step is to determine the separations modules needed to accomplish this goal. Options are not limited to solvent extraction; hybrid processes may include ion exchange, precipitation, electrochemistry and others. The overall process is composed of a sequence of separation steps or modules linked to generate a desired set of outputs, whether products or intermediates. Although minimizing the number of steps is always desirable, process reliability must take precedence. Caution is needed in assessing the compatibility of different steps. Often the adjustments to intermediate process streams are as critical to the success of the overall process as are the actual separations themselves.

   The selection of separations steps requires understanding the fundamental chemistry and engineering involved. A process that looks attractive chemically may prove untenable industrially because of unforeseen chemical interactions, poor process behavior, or instability under process conditions (temperature, pH, radiation, etc.). The selection is first done by choosing a candidate chemical system that is known to accomplish the desired separation. Design of a detailed process flowsheet that will yield the desired goal then follows. Optimization of the process flowsheet requires a sound understanding of the interactions between different process variables. Such an understanding can best be gained through high fidelity models of both the chemistry and the unit operations.

   Laboratory data are used to develop or refine computer models to simulate the process. Bench-scale process flowsheets are then designed from these simulations and tested, first with simulants then, if practical, with actual spent fuel or radioactive waste. Quite often the genuine feed performs differently than simulants, even when the feed is relatively simple in composition. It is critical that a flowsheet be developed from small-scale tests, preferably on prototypical equipment and under prototypical conditions to provide data on process kinetics, hydraulics, parameter selection, and any other effects arising from process variability. The use of prototypical equipment is critical as it reduces the number of variables that must be accounted for during scale-up, thus reducing process uncertainty.

   Although the heart of a separations facility is the chemical processing (solvent extraction, ion exchange, etc.), precisely recovering the targeted components and stabilizing the separated constituents is not a trivial operation. In fact, the footprint of the post-separations processing is often larger than that required for the separations themselves. In nuclear systems, the footprint is a major driver of the process economics because of the shielding requirements. As a result, great effort must be made to select additives

and complexants that minimize the potential to adversely affect final stabilization.

7.3   UREX+ LWR SNF GNEP application: separation strategy

For the case of LWR recycling, a number of incentives exist to separate and recycle the actinides, and to separate and manage fission products. The main incentive for LWR spent fuel separations under the Global Nuclear Energy Partnership (GNEP) program was to extend the US geologic repository capacity by: 1) recycling of transuranic elements for ultimate destruction and recovery of energy content, and 2) reducing the volume of waste, long-term radiotoxicity and heat load in a geologic repository (GNEP, 2007). To achieve this goal, a number of separations product and waste streams were identified. Table 7.1 lists these product and waste streams along with the separation incentive.

Table 7.1 GNEP LWR SNF recycle product/waste streams

Product/waste stream	Specification	Driver
Uranium	Sufficient purity that it can be stored inexpensively for future use	To achieve substantial reduction of waste volume in the repository[1] compared to SNF disposal. The recovered uranium could be stored for future use or disposed as a Class C low level waste.
Technetium and Iodine	Greater than 95% recovery	To reduce long-term dose at the repository boundaries by recovering and immobilizing in waste forms suitable for geologic disposal.
Cesium and Strontium	Sufficient purity that waste can be classified as non-TRU[3]	To reduce repository heat load for the first centuries after discharge by separate management and disposal in an optimized facility.
Transuranic[2] elements, individual or as a group	Greater than 99% recovery and 99.9% purity	Recovering then fissioning transuranic elements in fast spectrum reactors substantially benefits the repository capacity by reducing long-term radiotoxicity.

Notes: (1) The repository addressed by the GNEP program was Yucca Mountain. (2) Transuranic elements (of concern): Pu – plutonium, Np – neptunium, Am – americium and Cm – curium. (3) Non-TRU: Waste containing no more than 3700 becquerels (100 nanocuries) of alpha-emitting transuranic isotopes per gram of waste and half-lives greater than 20 years.

Table 7.2 UREX+ process options for LWR spent nuclear fuel treatment

Process	Product #1	Product #2	Product #3	Product #4	Product #5	Product #6	Product #7
UREX+1	U	Tc	Cs/Sr	TRU/Ln	FP		
UREX+1a	U	Tc	Cs/Sr	TRU	FP/Ln		
UREX+1b	U	Tc	Cs/Sr	U/TRU	FP/Ln		
UREX+2	U	Tc	Cs/Sr	Pu/Np	Am/Cm/Ln	FP	
UREX+2a	U	Tc	Cs/Sr	U/Pu/Np	Am/Cm/Ln	FP	
UREX+3	U	Tc	Cs/Sr	Pu/Np	Am/Cm	FP/Ln	
UREX+3a	U	Tc	Cs/Sr	U/Pu/Np	Am/Cm	FP/Ln	
UREX+4	U	Tc	Cs/Sr	Pu/Np	Am	Cm	FP/Ln
UREX+4a	U	Tc	Cs/Sr	U/Pu/Np	Am	Cm	FP/Ln

(1) In all cases, iodine is removed as an off-gas from the dissolution process.
(2) Processes are designed for the generation of no liquid high-level wastes.
U: Uranium (contributor to dose rate, and the mass and volume of high-level waste).
Tc: Technetium (long-lived fission product, minor contributor to long-term dose).
Cs/Sr: Cesium and strontium (primary short-term heat generators, affect waste form loading and repository drift loading).
TRU: Transuranic elements: Pu – plutonium, Np – neptunium, Am – americium, Cm – curium (primary long-term dose rate contributors).
Ln: Lanthanide fission products.
FP: Fission products other than cesium, strontium, technetium, iodine, and the lanthanides.

Table 7.2 shows the processing options for LWR SNF based on the targeted distribution of the various product streams given in Table 7.1. Each of the process outputs will require further processing to a solid form. This form will have an associated set of requirements that must be met for acceptability. In the case of the product, such as a mixed plutonium-uranium stream, the material must be suitable for use as a reactor fuel. Though some further chemical modification may be possible as part of the solidification processing, it is unlikely that significant chemical rework will be a component of fuel fabrication. Waste forms will likely have looser tolerances than recycled fuel, but the solidified waste precursor must eventually yield a waste form that is acceptable to the ultimate disposal site.

7.3.1   UREX+ LWR SNF GNEP application: process flowsheets

From 2003 to 2007 a number of potential flowsheets for the processing of commercial LWR spent fuel were developed and tested with actual spent fuel at laboratory-scale. These processes are outlined in Fig. 7.1. The UREX+1 series was intended for extraction of the TRU elements as a
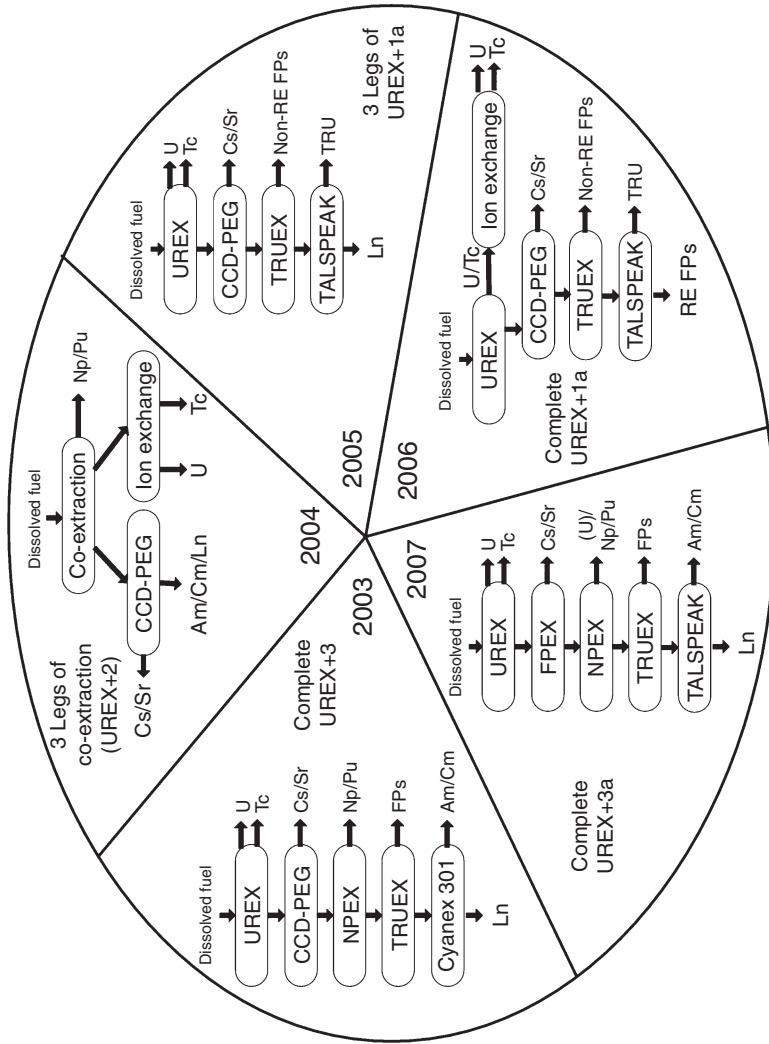
7.1 UREX+ flowsheets for the treatment of LWR SNF based on the GNEP identified repository benefits given in Table 7.1.

group; there is no separation among the TRUs which are to be burned as fuel in fast spectrum reactors (FR). The UREX+2 and UREX+3 process series were intended for LWR or FR reactor recycle of plutonium and neptunium. The combined product is a recycle fuel feedstock that could be manipulated and fabricated into fuel in a glovebox facility rather than a shielded cell. Because of the large relevant database on fuel performance from prior testing programs, such a fuel may be easier to qualify than the TRU fuel. The UREX+4 process series was selected as it provides the added option of burning americium in specially designed target assemblies. Separation of Cm from the Am reduces shielding requirements for target fabrication. With the isolation of Cs and Sr, the other fission products remaining after any of the UREX+ process strategies have relatively low radiation levels and heat generation rates, and can therefore be immobilized at high concentrations in durable ceramic or glass waste forms. The approximately 30-year half-lives of ^{137}Cs and ^{90}Sr isotopes imply that storage is required for 500 years or less.

Many of the head-end operations necessary for an advanced reprocessing plant using the UREX+ strategy are similar to those currently used at the commercial spent fuel reprocessing facilities at LaHague (France), Sellafield (United Kingdom), and Rokkasho (Japan). While there may be qualities unique to the fuel to be processed that require some head-end conditioning differing from that used at these facilities, the major operations and process streams will be similar. As these facilities are designed for PUREX, the major change would be adjusting the dissolver product conditions to meet the requirements of the UREX process.

Off-gases emanating from the fuel-chopper and the dissolver will contain radioactive ^{129}I, tritium, ^{14}C, and ^{85}Kr. In the current reprocessing plants in Europe and Asia, these are not fully captured. If capture and sequestration of volatile radionuclides is mandated, the effectiveness of capture by various adsorbents or scrubbers must be evaluated, and methods to recover the radionuclides and sequester them in waste or storage forms must be developed.

Post-process treatment and solidification of effluents is an area where data are limited for many of the UREX+ separations. There is extensive plant-scale experience in converting uranium and plutonium to solid oxides but not for mixed actinide streams. Conversion of high-level liquid wastes to solid forms by either calcination or vitrification has been demonstrated at industrial scales but not for high activity Cs/Sr and Am/Cm solutions. Extensive data exist for acid-water evaporation, acid recycling, and waste-water treatment. However, information on reagent cleanup and recycle is less extensive. Data on recovery and calcination of trace organics in aqueous streams is likely available, though not for all of the organic species used in a UREX+ processes.

Design of the UREX+ flowsheets developed for the treatment of LWR SNF to achieve the repository benefits listed in Table 7.1 was done by combining solvent extraction systems in series. Figure 7.1 shows how several different solvent extraction modules were combined for several of the options. The solvent extraction process modules were tuned to meet the disposition goals of the program, also given in Table 7.1. It should be noted that isolation of any of the products listed in Table 7.2 could be omitted by recombination or exclusion of specific separation modules. In achieving these product goals, the developer is free to select any extraction process that will yield the desired products and can be made compatible with other process modules through intermediate processing.

The PUREX process is fully developed and will yield separate Pu and U streams. Recent modifications to the basic PUREX process are intended to result in incomplete separations, so that Pu is recovered with neptunium and/or uranium. These mixed PUREX separations, have been developed by both DOE and commercial companies, and are referred to generically as co-decontamination processes. Specific examples include, COEX® developed by Areva, and the first separation in Energy Solutions' NUEX process. The concept has been demonstrated at both Argonne and Oak Ridge National Laboratories with actual spent fuel.

The UREX process was uniquely developed to recover technetium, in addition to uranium. The solvent for the UREX process is the typical PUREX solvent, tributyl phosphate (TBP) dissolved in n-dodecane. Uranium and technetium are extracted from the bulk of the dissolved fuel, but co-extraction of Pu and Np is prevented by introduction of a complexant/reductant. Once stripped from the solvent, uranium is separated from Tc by anion exchange. Technetium was targeted because its mobility in the environment, as pertechnetate, contributed to the potential long-term dose to the public from the Yucca Mountain Repository. With UREX, it can be recovered in high yield, >95%. This level of recovery of technetium with a co-decontamination-type separation is difficult.

After the lead UREX separation, there is flexibility in the follow-on separations modules. Using the UREX+3a process, as an example, we can follow a typical separations scheme based solely on aqueous solvent extraction to achieve the desired separations. UREX+3a is a cascade of five solvent separate extraction processes, referred to here as "process modules" and one ion exchange process. Following UREX and ion exchange, the process steps include: (1) recovery of Cs and Sr (CCD-PEG or FPEX), (2) separation and recovery of a mixed U, Pu and Np product (NPEX), (3) separation of transition metal fission products from lanthanide fission products and Am and Cm (TRUEX), and (4) separation and recovery of Am and Cm from lanthanides (TALSPEAK). Similar separations can be done for a co-decontamination front end, but in this case, the NPEX

segment is omitted as the Pu and Np are recovered in the initial separation segment as shown in Fig. 7.1 (2004).

There is some flexibility in both the sequencing and selecting the process for Cs and Sr recovery. Cs and Sr can be recovered immediately after UREX using either the FPEX or the CCD-PEG process with appropriate feed adjustment. The CCD-PEG solvent is a mixture of chlorinated cobalt dicarbollide (CCD) and polyethylene glycol (PEG); the diluent is phenyltrifluoromethyl sulfone (FS-13). An alternative process is FPEX, which uses a solvent containing a calixarene, a crown ether, and a modifier, all in Isopar-L® (a refined kerosene) diluent. The FPEX diluent is more compatible with the other processes, which are based on n-dodecane, but the CCD-PEG process is more mature. In all of the schemes shown in Fig. 7.1, the raffinate from the UREX segment is the feed to the CCD-PEG or FPEX process segment. However, these processes can be run to recover Cs and Sr from the TRUEX raffinate rather than the UREX raffinate. Reducing the amount of processing prior to TRU recovery should result in a purer product, though shielding requirements are higher. This would remove one process from the main sequence, which may be beneficial for actinide product purity for recycle in reactor fuel.

The NPEX process separates plutonium and neptunium from the other components in the FPEX or CCD-PEG raffinate. Like UREX, the solvent for NPEX is the typical PUREX solvent. Although the process was designed to extract Pu and Np, uranium is added to the extracted Pu and Np in the strip section to yield a U-Pu-Np product with a controllable elemental ratio.

The TRUEX process separates the lanthanide and transuranic actinides from the other components in the NPEX raffinate. The solvent is a mixture of CMPO (octyl(phenyl)-N,N –diisobutylcarbamoylmethyl phosphine oxide) and TBP in n-dodecane. If TRUEX follows NPEX, Am and Cm are recovered with the lanthanides. If NPEX is omitted, Pu and Np are also contained in the "grouped TRU" product.

The actinide:lanthanide separation is achieved using TALSPEAK. TALSPEAK solvent is HDEHP (bis(2-ethylhexyl)phosphoric acid dissolved in n-dodecane while the aqueous phase is a buffered lactate solution containing DTPA. Extraction of the lanthanides over actinides is regulated by control of pH and operating conditions. The product contains Am and Cm for UREX+2, 3 and 4 series, and all of the transuranics in the case of the UREX+1 series. If a suitable separation is devised, Am can be further separated from Cm, yielding UREX+4 in Table 7.1. At the moment there are no proven candidates for the separation of Am from Cm at an industrial scale.

These separation module sequences (except for Am from Cm separation) are based on proven or at least lab-tested processes that can be run on

prototypical equipment. Other aqueous processing concepts have been proposed, but are not currently suitable for bench-scale process tests. As it is attractive to reduce the number of processing steps required to achieve the separations, much current focus is on finding extractants that are highly elective for actinides. One approach under development which has shown promise is a TRUEX-TALSPEAK hybrid, christened TRUSPEAK, which separates actinides from all fission products in a single process module rather than two sequential modules.

7.4   Benefits of using models to design flowsheets

Unlike other components of a closed fuel cycle, the feedstock to the recycling facility has a great deal of variation whether its origin is SNF, or other high- or low-level wastes (legacy defense, medical, industrial, etc.). In addition, the final product and/or waste form needs to meet very tight product specifications or waste acceptance criteria. Failure to do so results at best in materials that need to be reprocessed, or at worst in an orphan waste form with no disposition path. The need to design a robust process that can accommodate variations in the feed and tight product and waste specifications requires bracketing the acceptable feed compositions and testing the process at a wide range of conditions. It is unfeasible to do so experimentally, as not all possible feed combinations can be reproduced and it is prohibitively costly. The use of models to design flowsheets allows the design of a facility for a wide range of feed compositions and an optimized process that ensures product and waste specifications are meet.

7.4.1   The Argonne model for universal solvent extraction (AMUSE) for flowsheet design

The development of accurate predictive models is critical to the development of novel separations and to the design and refinement of existing processes. The flowsheets for each UREX+ process module were developed using the AMUSE code (Regalbuto *et al.*, 2004). AMUSE is an updated version of the Generic TRUEX Model (GTM). The GTM was developed during the 1980s to design multistage countercurrent flowsheets for the TRUEX solvent extraction process (Vandegrift *et al.*, 1993, 1995).

   AMUSE predicts how components distribute among the aqueous and organic phases based on the compositions and characteristics of the aqueous and organic phases at given process conditions. It accomplishes this by calculating the distribution ratios, or D values, of the stream components. The predicted distribution ratios are highly accurate over a wide range of aqueous phase compositions due to the use of chemically correct models that are based on the thermodynamic activities. A countercurrent mass

balance algorithm yields the final predicted elemental composition in the extraction system for both organic and aqueous phases.

The AMUSE code is composed of two major sections, SASSE and SASPE. The material balance calculations are performed in the SASSE section, which calculates multistage countercurrent flowsheets using calculated distribution ratios. The SASPE section performs the distribution ratio calculations, for all of the components, based on elemental compositions and characteristics of the aqueous and organic phases. When AMUSE is used to calculate flowsheets based on the user defined input such as (1) equipment type, (2) feed compositions and locations, and (3) general flowsheet specifications (e.g., number of stages, temperature, flow rates) an iterative process among the SASSE and SASPE sections is performed as follows:

1. The SASPE section of the model will calculate distribution ratio (D) values from stage compositions generated by SASSE.
2. The SASSE section will then refine the calculated D-values based on the compositions calculated with SASPE.
3. The iterative process continues until convergence among the two modules is achieved.
4. The output report is generated that includes the compositions of all of the components in the organic and aqueous phases for each stage of the process.

AMUSE readily calculates flowsheets for PUREX, UREX, SREX, CCD-PEG and TRUEX as it can estimate the distribution coefficients for these processes internally. Flowsheets for other solvent extraction processes, including CSSX, FPEX, and TALSPEAK can be generated using appropriate user specified D-values. AMUSE is then used to perform sensitivity analysis on the designed process flowsheets in order to determine the effects of flow rate variation, compositional variability, other-phase carryover, temperature excursions, etc. The results of the sensitivity analysis establish the process operating envelope.

7.4.2   Flowsheets for UREX+ LWR SNF GNEP applications designed using AMUSE

All of the flowsheets developed for the UREX+ demonstrations, conducted at Argonne National Laboratory, were designed to be operated using 2 cm countercurrent centrifugal contactors as the separation equipment. The flow rates were adjusted to the equipment design maximum. To ease the demonstration the solvent was not recycled, with the exception of the CCD-PEG and FPEX process tests where the supply of solvent was limited. In an actual plant application, a solvent wash section would be added to
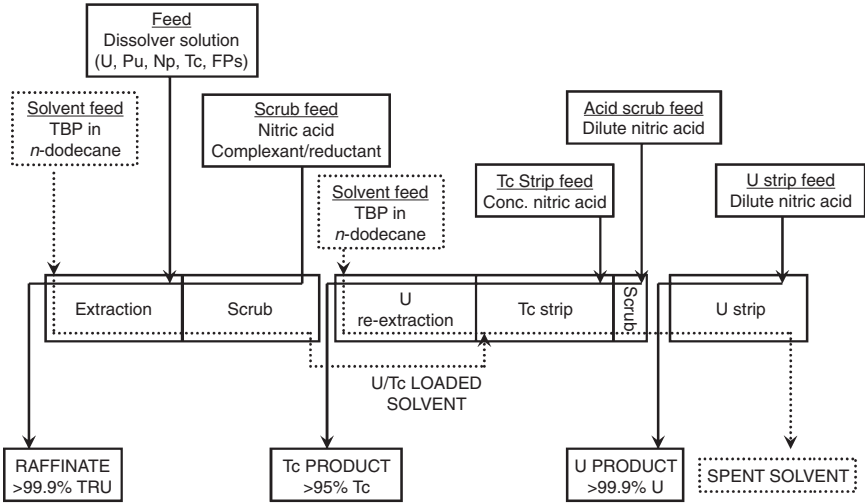
7.2 UREX flowsheet with Tc recovery by solvent extraction.

each process module, before recycling the solvent to the front end of the process module.

UREX and co-extraction flowsheets

Two variations of the UREX process flowsheets were developed as part of the UREX+ demonstrations (Pereira *et al.*, 2005). The original flowsheet was developed to allow recovery of technetium by solvent extraction as shown in Fig. 7.2. Solid lines are aqueous phase streams and the dashed lines are organic phase streams. In the first process segment, uranium and technetium are extracted from the bulk of the dissolved fuel. Co-extraction of Pu and Np is prevented by introduction of a complexant/reductant in the scrub section. Technetium is stripped into concentrated acid, and uranium is subsequently recovered via a low acid strip. Technetium recovery was lower than desired, and so in subsequent tests, the loaded solvent is stripped of U and Tc by dilute nitric acid, as shown in Fig. 7.3. Technetium is removed, as pertechnetate, from the U/Tc-strip product by an anion exchange process.

The co-extraction process designed has three parts and is shown in Fig. 7.4 (Pereira, 2005). In the first process segment plutonium, neptunium, uranium and technetium are extracted from the bulk of the dissolved fuel. Plutonium and neptunium are then stripped by a complexant/reductant in dilute acid in the Np/Pu-strip segment. The Np/Pu product stream is then scrubbed of uranium in the U/Tc-Re-extraction section. The combined solvent is scrubbed of excess nitric acid with a feed of dilute nitric acid
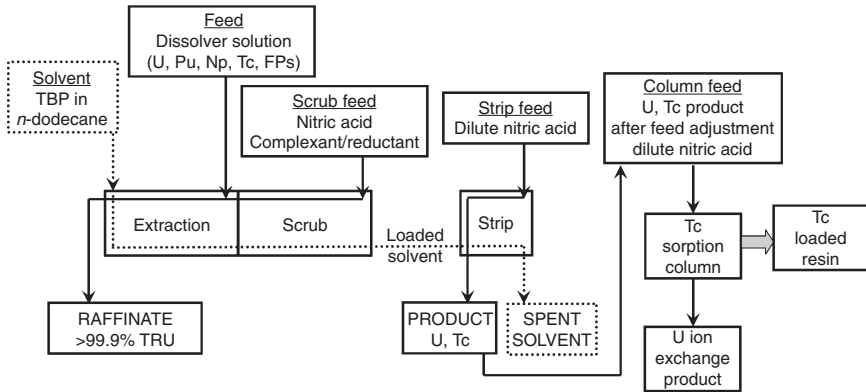
7.3 UREX flowsheet with Tc recovery by ion exchange.
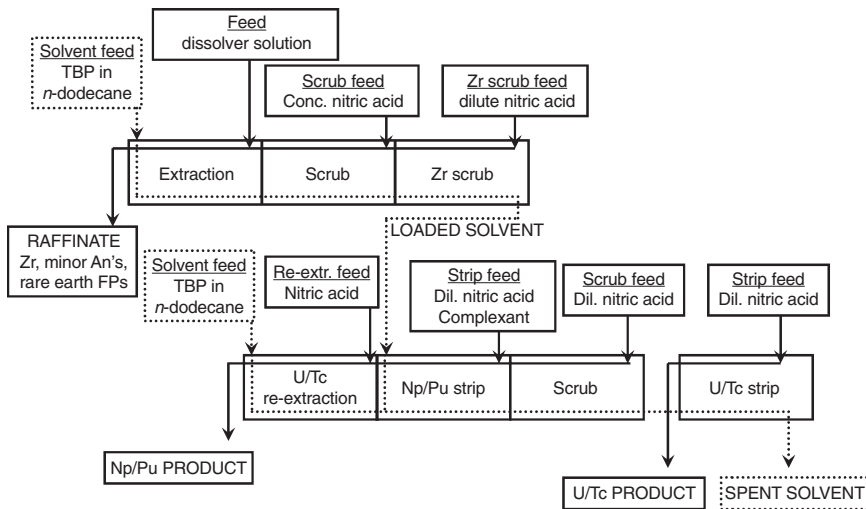
7.4 Co-extraction flowsheet for a UREX+2 strategy.

before entering the U/Tc-strip section, where a dilute nitric acid feed removes uranium and technetium from the solvent.

CCD-PEG and FPEX flowsheets

The raffinate from the UREX separations module becomes the feed to the CCD-PEG process segment, shown in Fig. 7.5 (Pereira, 2007a), or the alternative FPEX process shown in Fig. 7.6. Because the supply of CCD-PEG solvent was limited, a wash was incorporated into the flowsheet to enable its recycle. In the extraction section, Cs and Sr (with Rb and Ba) are

```
                          ┌──────────────┐
                          │    Feed      │
                          │ UREX raffinate│
                          │ All TRU and FPs│
                          └──────────────┘
```

Feed
UREX raffinate
All TRU and FPs

Recycle solvent
CCD-PEG
in FS-13

Scrub feed
Nitric acid

Strip feed
Guanidinium
carbonate/DTPA

Wash feed
PEG-nitric acid

| Extraction | Scrub | Strip | Wash |

RAFFINATE
ALL TRU and FPs

PRODUCT
Cs, Sr, Rb, Ba

SPENT
WASH

7.5 CCD-PEG process.

Feed
UREX raffinate
All TRU and FPs

Recycle solvent
FPEX solvent

Scrub feed
Nitric acid

Strip feed
Dilute nitric acid

Wash feed
Nitric acid

| Extraction | Scrub | Strip | Wash |

RAFFINATE
ALL TRU and FPs

PRODUCT
Cs, Sr, Rb, Ba

SPENT
WASH

7.6 FPEX process.

extracted into the solvent. In the scrub section, a solution of nitric acid at moderate concentration, scrubs other species, primarily transuranic and lanthanide elements (TRU), from the solvent. In the strip section, the alkali and alkaline-earth cations are stripped by a combination of an organic ammonium carbonate salt and a complexing agent.

Because of uncertainty in the supply of both CCD and FS-13, an alternative to the CCD-PEG process was developed at Oak Ridge and Idaho National Laboratories. The FPEX process, fig. 7.6 (Pereira, 2007b), was

based on the CSSX process developed to treat the alkaline tank wastes at the Savannah River Site and at Oak Ridge National Lab. The FPEX solvent was designed to be stable at low acid concentrations. The solvent uses a solution containing a calixarene to extract Cs, a crown ether to extract Sr, a modifier, and trioctylamine in a kerosene diluent, Isopar L. The use of a kerosene diluent is significant as it is highly compatible with the hydrocarbon diluents used in the other separations modules.

NPEX flowsheet

In UREX+3 process series, the NPEX process follows either CCD-PEG or FPEX. However, prior to NPEX (for recovery of a pure Pu/Np product) there is a significant feed adjustment step. Feed adjust is required to: (1) thermally destroy the reductant/complexant added in the UREX process to suppress extraction of plutonium and neptunium, (2) increase the concentration of nitric acid, and (3) convert and maintain plutonium and neptunium in the extractable (IV) oxidation state.

The CCD-PEG or FPEX raffinate is fed to the NPEX process following feed adjustment as shown in Fig. 7.7 (Pereira, 2007b). The NPEX solvent composition is the same as for UREX, typical PUREX solvent. Impurities are removed from the solvent in the scrub section, and plutonium and neptunium are stripped using the same reductant/complexant that was fed to the scrub section of the UREX process. Uranyl nitrate may be added to
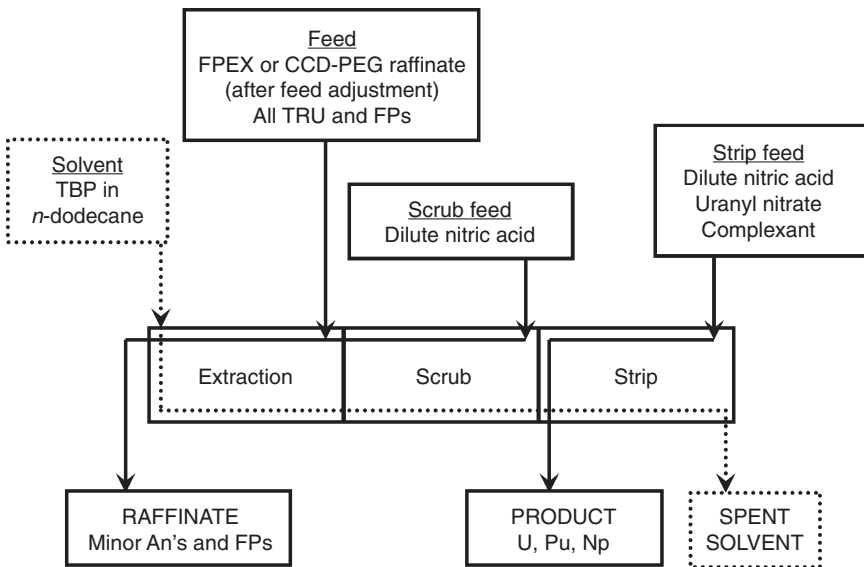
7.7 NPEX flowsheet.
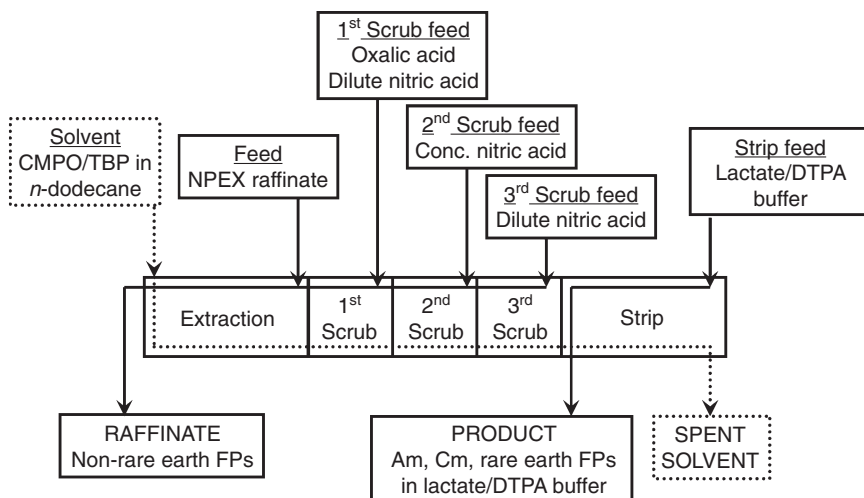
7.8 Three-scrub TRUEX flowsheet.

the strip solution to yield a product with a controllable U:Pu ratio, suitable for mixed oxide or metallic fuel fabrication.

TRUEX flowsheet

The TRUEX process separates the lanthanides and transuranic actinides from the other components in the CCD-PEG, FPEX or NPEX raffinates, notably zirconium and noble metals. Two TRUEX flowsheets have been tested in the demonstrations. The first TRUEX flowsheet is shown in Fig. 7.8 (Pereira, 2007a). Americium, curium and the lanthanide elements are extracted by the TRUEX solvent, which consists of CMPO and TBP diluted by n-dodecane. When the NPEX step is omitted, plutonium and neptunium are also extracted. Lesser amounts of other fission products are also extracted and must be scrubbed from the solvent. The first TRUEX flowsheet is unique to the UREX+ process by having three scrub sections. In the first scrub section the impurities are removed from the solvent using oxalic acid. Moderately concentrated nitric acid scrubs oxalic acid from the solvent in the second scrub section. In the third scrub section, addition of dilute nitric acid lowers the acid concentration in the solvent to allow effective stripping. The transuranic actinides and lanthanide elements are stripped from the solvent using a lactate buffer containing a complexant which becomes the feed to TALSPEAK. An acetate solution was used when the Cyanex 301 based process followed. In the simplified TRUEX flowsheet shown in Fig. 7.9 (Pereira, 2007b), the three scrub sections were reduced to a single scrub section by adding oxalic acid to the feed directly. The single
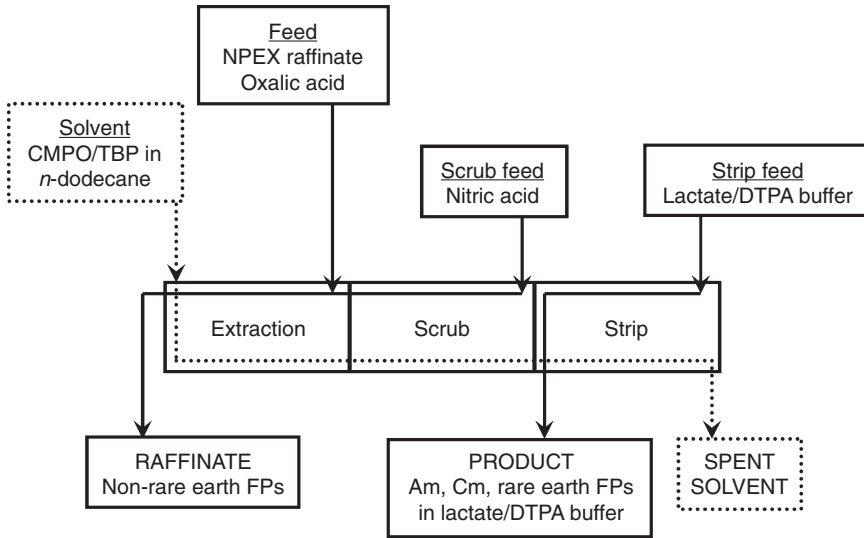
7.9 One-scrub TRUEX flowsheet.

scrub section is used to adjust the acidity of the organic phase prior to entering the strip section.

The raffinate of the NPEX process can be fed directly to the extraction section of the TRUEX segment with no feed adjustment. To serve as the TRUEX feed, the CCD-PEG or FPEX raffinate compositions were adjusted by addition of concentrated nitric acid. Just prior to introduction of the feed, a reductant was added to reduce Np(V) to extractable Np(IV).

TALSPEAK and Cyanex 301 flowsheets

Cyanex 301 was investigated for separating trivalent actinides from the TRUEX product. (Fig. 7.10) (Vandegrift, 2004). Cyanex 301 is a commercial product supplied in an impure form by Cytec Industries, Canada. The predominant ingredient is bis(2,4,4-trimethylpentyl)dithiophosphinic acid, which must be extensively purified before it can be used for actinide/lanthanide separations. The purified Cyanex 301 was dissolved in a mixture of TBP and n-dodecane. The scrub feed is the acid form of the weak complexant in the feed and the strip feed is an ammonium salt of a powerful complexant. Because of the tendency of the Cyanex 301 to decompose both as a solid and in solution, it was not deemed a suitable material for industrial-scale actinide/lanthanide separations. Subsequent investigations focused on using the TALSPEAK process to separate the trivalent lanthanides from the actinides.
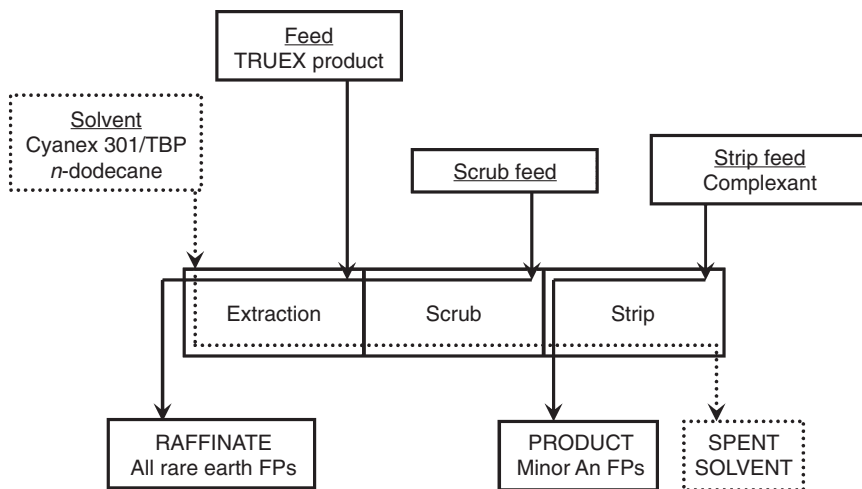
7.10 Actinide/lanthanide separation using Cyanex 301® extractant.
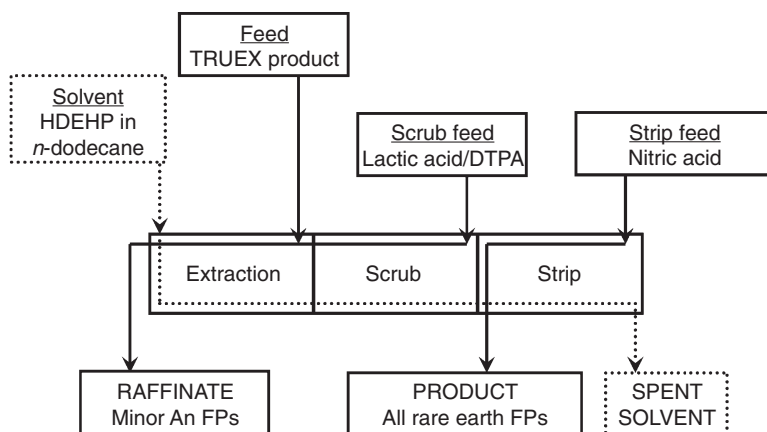
7.11 TALSPEAK flowsheet.

Since the TRUEX strip is a buffered lactic acid feed similar to the TALSPEAK feed, only a minor pH adjustment is required to prepare the TRUEX strip solution for feed to TALSPEAK. The TALSPEAK process segment has three sections: extraction, scrub, and strip, as shown in Fig. 7.11 (Pereira, 2007b). The actinide:lanthanide separation achieved by TALSPEAK is based on the preferential complexation of actinides by aminopolyacetic acids and effective extraction of trivalent lanthanides by bis(2-ethylhexyl)phosphoric acid (HDEHP). In the extraction section, the more weakly complexed lanthanides are extracted, while the stronger

actinide/DTPA complexes remain in the aqueous phase. The scrub removes the small fraction of Am and Cm that are co-extracted by HDEHP. The lanthanides are stripped from the solvent with moderately concentrated nitric acid.

7.4.3 UREX+ LWR SNF GNEP demonstrations results

Several of the UREX+ process alternatives for the treatment of LWR SNF based on the GNEP identified repository benefits were demonstrated at Argonne National Laboratory from 2003 to 2007 (Fig. 7.1). Under the GNEP program the objective was to demonstrate that all desired spent-fuel constituents could be separated by aqueous processing and that product specifications for recycle or disposal were achievable: All of the flowsheets demonstrated proved the viability of achieving the target separations goals.

The R&D conducted in support of UREX+ process development included:

1. collection and modeling of chemical data for the Argonne Model for Universal Solvent Extraction (AMUSE)
2. process design and optimization using AMUSE
3. equipment design.

All test runs were conducted using an ANL-designed 2-cm countercurrent centrifugal contactors and were run until steady state was achieved. The fuel-derived feed to the demonstrations was LWR SNF dissolved in nitric acid using 0.5 to 1 kg fuel batches.

The UREX+ processes were operated to produce separate U and Tc product streams, a mixed fission product stream, and a lanthanide stream. The UREX+1a process, conducted in 2005 and 2006, yielded two additional streams: a Cs/Sr stream and a TRU product containing Pu, Np, Am and Cm. The UREX+3 process was conducted in 2003 and 2007, yielding Pu/Np and Am/Cm products, as well as a Cs/Sr stream. A UREX+2 process based on co-extraction of U, Pu, and Np as a first step was conducted in 2004; this process also yielded separate Pu/Np, Am/Cm/Ln and Cs/Sr products. All five demonstrations proved the feasibility of the various UREX+ alternative processes to achieve the GNEP separations goals and can be summarized as follows:

1. The UREX separation module was repeatedly demonstrated to be viable for the selective extraction of U and Tc. The U-Tc separations was demonstrated by selective stripping and ion exchange with the latter being a more amendable industrial application.
2. The Co-extraction of U, Pu, Np, and Tc with subsequent selective stripping of Pu/Np and U/Tc proved viable.

3. Both CCD-PEG and FPEX separation modules prove viable for recovery of Cs/Sr.
4. The NPEX separation module proves viable for recovery of Pu with Np to produce a U/Pu/Np product.
5. The TRUEX separation module was repeatedly demonstrated to be viable for the separation of actinides from lanthanides at high purities as required for fuel fabrication.
6. The TALSPEAK separation module successfully separated actinides from lanthanides at high purities as required for fuel fabrication.

Specific results for several of the UREX+ alternative process are given below.

UREX+1a

The process was demonstrated in 2005 and 2006 and yielded high recovery of all products. Excellent TRU/Ln recovery was obtained with TRUEX, and a refined TALSPEAK process for the 2006 test met target specifications. The CCD-PEG separations module was not run as part of the 2005 demonstration. Results are given in Table 7.3.

UREX+2

The process was demonstrated in 2004 and yielded high recovery of all products. All primary components reported to their desired product streams.

Table 7.3 UREX+1a demonstration results. Percent distribution of process effluents

Year	2005		2006	
Component	Product	Other effluents	Product	Other effluents
UREX				
U	>99.98	<0.02	99.997	0.003
Tc	97.1	2.9	95.5	4.5
CCD-PEG				
Cs	NA	NA	>99.85	<0.15
Sr	NA	NA	99.1	0.1
TALSPEAK				
Pu	99.8	0.2	>99.995	<0.005
Am	99.999	0.001	>99.97	<0.03
Ln	12	88	<0.03	>99.97

NA: Not applicable.

Table 7.4 UREX+2 demonstration results. Percent distribution of process effluents

Component	Product	Raffinate
2004 Co-extraction		
U	>99.9994	0.003
Tc	80.1	18.6
Pu	99.8	0.2
Np	87.2	12.8
2004 CCD-PEG		
Cs	99.7	0.3
Sr	>98.6	<1.4

The Tc and Np fractions found in the streams in which they were targeted were lower than the target values. Zirconium reported to the Np/Pu product, rather than the raffinate, due to other-phase carryover that was ascribed to a mismatch between the contactor design and loaded-solvent density. Results are given in Table 7.4.

UREX+3

The process was demonstrated in 2003 and 2007. Different separations modules were tested for the recovery of Cs/Sr and Am/Cm products. In 2003, CCD-PEG and Cyanex 301 were tested. In 2007, FPEX and TALSPEAK were tested. In addition, in 2003, Tc was separated from uranium by selective stripping while in 2007 an ion exchange resin was used to make the process more amendable to an industrial application.

In 2003, the Np fraction was lower than the target value and a high lanthanide content was observed in the Am/Cm product which deemed the Cyanex 301 separation module unacceptable. Process adjustments in NPEX resulted in an excellent recovery of Np in 2007. In addition, the replacement of the Cyanex 301 separation module with TALSPEAK resulted in excellent recovery of Am/Cm from the Ln fission products. Both CCD-PEG and the FPEX separations modules demonstrated high Cs/Sr recoveries. Results are given in Table 7.5.

7.5   Advantages and disadvantages of techniques

The UREX+ separations strategy provides the advantage of a focused optimization approach for the recovery of products that meet predetermined key objectives for a fuel cycle or a waste disposal strategy. The concept has been successfully tested for the recycle of LWR SNF for a number of different product and waste form configurations. The complexity

Table 7.5 UREX+3 demonstration results. Percent distribution of process effluents

Year	2003		2007	
Component	Product	Raffinate	Product	Raffinate
		UREX		
U	99.96	0.02	99.999	0.001
Tc	94.40	4.60	NA	NA
	CCD-PEG		FPEX	
Cs	NA	NA	(100)	BD
Sr	NA	NA	>99.9	<0.1
		NPEX		
Pu	99.6	0.4	99.93	0.07
Np	70.3	29.69	100	Bkgd
	Cyanex 301		TRUEX*	
Am	99.98	0.02	100	BD
RE	27.2	82.8	NA	NA

* TALSPEAK was omitted from 2007 UREX+3a demonstration.
BD: Below detection limit.
Bkgd: Background.
NA: Not applicable.

of this separations approach increases as the desired number of products or waste forms increases. As this complexity increases so does the cost of the separations facility. The use of various separations modules requires that the integrated process be tested in order to determine any incompatibilities between process modules.

7.6   Future trends

The separation of minor actinides (Am and Cm) from SNF enables transmutation of the minor actinides to short-lived radionuclides. The similar chemical behavior of the trivalent actinides and lanthanides makes separation difficult at the industrial scale. Sequential processing (TRUEX-TALSPEAK or DIAMEX-SANEX) has been demonstrated but increases the process complexity. Approaches that can simplify this separation are a very desirable goal. The use of solvent combinations such as TRUEX and TALSPEAK extractants to design a robust industrially-feasible process will continue. This concept is illustrated in Fig. 7.12.

The least studied separation in the UREX+ suite of processes is the separation of americium from curium. Separation of Am from Cm would allow the recycling of Am as a fast reactor fuel or target while simplifying
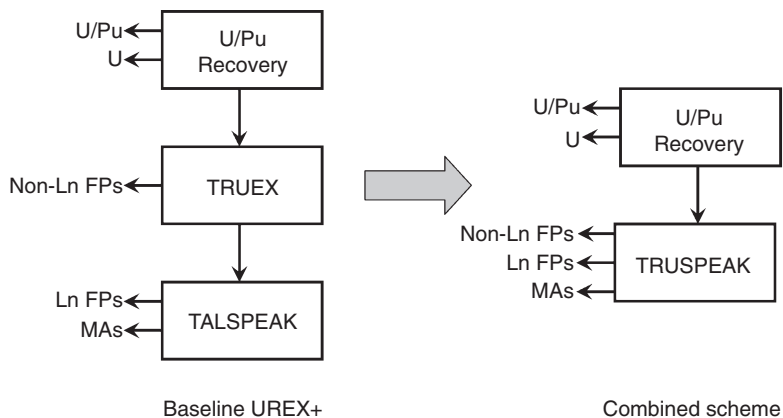
7.12 Reducing complexity of actinide:fission product separations.

fabrication and handling by removing Cm, a neutron emitter. Using molecular modeling techniques to design better extractants, resins, or separation media is one path toward accomplishing Am/Cm separation. Other separation techniques such as column chromatography or electrochemical techniques are potential alternatives. There are no viable options for achieving this separation at the plant scale in the near term. Additional research is required to develop a truly feasible process.

7.7   References

GNEP (2007), *Global Nuclear Energy Partnership Technology Development Plan*, Global Nuclear Energy Partnership Technical Integration Office, Idaho Falls, ID, July 25.

MIT (2003), *The Future of Nuclear Power: An Interdisciplinary MIT Study*, Massachusetts Institute of Technology, Cambridge, MA.

Pereira, C, Vandegrift, GF, Regalbuto, MC, Aase, S, Bakel, A, Bowers, D, Byrnes, JP, Clark, MA, Emery, JW, Falkenberg, JR, Guelis, AV, Hafenrichter, L, Leonard, R, Quigley, KJ, Tsai, Y, Vander Pol, MR, and Laidler, JJ (2005), Waste Management '05 Symposium, *Lab-scale Demonstration of the UREX+2 Process Using Spent Fuel*, February 27–March 3, Tucson, AZ.

Pereira, C, Vandegrift, GF, Regalbuto, MC, Bakel, A, Bowers, D, Guelis, AV, Hebden, AS, Maggos, LE, Stepinski, D, Tsai, Y, and Laidler, JJ (2007a), Waste Management '07 Symposium, *Lab-scale Demonstration of the UREX+1a Process Using Spent Fuel*, February 25–March 4, Tucson, AZ.

Pereira, C, Vandegrift, GF, Regalbuto, MC, Bakel, AJ, and Laidler, JJ (2007b), Global 2007: Advanced Nuclear Fuel Cycles and Systems, *A Summary of the Lab-Scale Demonstration of UREX+ Processes at Argonne National Laboratory*, September 12, Boise, ID.

Regalbuto, MC, Copple, JM, Leonard, R, Pereira, C, and Vandegrift, GF (2004), Eighth Information Exchange Meeting, *Solvent Extraction Process Development for Partitioning and Transmutation of Spent Fuel*, November 9–11, Las Vegas, NV.

U.S. Nuclear Regulatory Commission (2008), *Background, Status, and Issues Related to the Regulation of Advanced Spent Nuclear Fuel Recycle Facilities: ACNW&M White Paper (NUREG-1909)*, report prepared by A.G. Croff, R.G. Wymer, L.L. Tavlarides, J.H. Flack, H.G. Larson, Advisory Committee on Nuclear Waste and Materials, U.S. Nuclear Regulatory Commission, Washington DC.

Vandegrift, GF, Chamberlain DB, Conner C, Copple JM, Dow JA, Everson L, Hutter JC, Leonard RA, Nuñez L, Regalbuto MC, Sedlet J, Srinivasan B, Weber S, and Wygmans DG (1993), "Development and Demonstration of the TRUEX Solvent Extraction Process," *Proceedings of WM-93*, Vol. 2, pp. 1045–1050.

Vandegrift GF and Regalbuto MC (1995), "Validation of the Generic TRUEX Model Using Data from TRUEX Demonstrations with Actual High-Level Waste," Proceedings of the Fifth International Conference on Radioactive Waste Management and Environmental Remediation (ICEM'95) Vol. 1, Cross-Cutting Issues and Management of High-Level Waste and Spent Fuel, September 3–7, pp. 457–462, Berlin, Germany.

Vandegrift GF, Regalbuto MC, Aase, S, Bakel, A, Battisti, TJ, Bowers, D, Byrnes, JP, Clark, MA, Emery, JW, Falkenberg, JR, Guelis, AV, Pereira, C, Hafenrichter, L, Tsai, Y, Quigley, KJ and Vander Pol, MH (2004), ATATLANTE 2004, Advances for Future Nuclear Fuel Cycles International Conference, *Designing and Demonstration of the UREX+ Process Using Spent Nuclear Fuel*, Jun 21–24, Nimes, France.

Wigeland, RA, Bauer, TH, Fanning, TH, Morris, EE (2006), *Separations and Transmutation Criteria to Improve Utilization of a Geological Repository*, *Nuclear Technology*, Vol. 154, pp. 95–106.

Williamson, MA, Regalbuto, MC, Ebert, WL, and Lewis, D, ATALANTE 2004 – Advances for Future Nuclear Fuels, *Nuclear Fuel Cycle Programs of Argonne's Chemical Engineering Division*, June 21–24, Nimes, France.

Advanced reprocessing for fission product separation and extraction

E. D. COLLINS, G. D. DEL CUL and B. A. MOYER,
Oak Ridge National Laboratory, USA

Abstract: The United States inventory of used nuclear fuels contains approximately 2 to 5 wt % fission products, depending on the extent of fuel burnup during irradiation, with the greater amounts produced in higher burnup fuels. For reprocessing of used nuclear fuels, fission products are more often divided into categories according to their chemical and radiological properties. Advanced reprocessing includes further separations processes to enable capture and disposal of the volatile fission product elements in improved solid waste forms, as well as additional separations processes being developed (1) to enable recovery and recycle of the remaining minor transuranium element actinides, neptunium, americium, and curium, and (2) to segregate the lanthanide fission products and the intermediate-lived heat-generating radionuclides, $^{137}Cs/^{137m}Ba$ and $^{90}Sr/^{90}Y$.

Key words: separation/extraction techniques, voloxidation, transition metal behavior, lanthanide recovery, cesium-strontium isolation.

8.1 Introduction

The United States inventory of used nuclear fuels contains approximately 2 to 5 wt % fission products, depending on the extent of fuel burnup during irradiation, with the greater amounts produced in the higher burnup fuels. The fission products are produced predominantly in two mass fractions, typically centered around a peak of mass 90–100 in the light fraction and 135–145 in the heavy fraction. For reprocessing of used nuclear fuels, the fission products are more often divided into categories according to their chemical and radiological properties, as illustrated in Table 8.1.[1,2]

The properties shown in Table 8.1 represent used fuels from light water reactors (predominantly thermal-neutron-driven fission of ^{235}U). The fission product elements – tin, antimony, and tellurium – are included here but would become more important when produced in higher concentration from fast neutron-driven fissions. The radioisotopes of significance shown in Table 8.1 were confined to long-lived and intermediate-lived isotopes that are most significant in reprocessing used fuels that have been stored for five years or more after reactor discharge. The significant

Table 8.1 Fission products of interest in light water reactor used fuel reprocessing

FP Category (mass % in used fuel)	Valence[1]		Stable isotopes[2]	Significant radioisotopes (half life)[2]		
	Normal	Others		Long-lived	Intermediate-lived	Secular equilibrium
Volatiles (20%)						
Xe	0	2,4,6	131,132,134,136			
Kr	0		84		85 (10.7y)	
I	−1	5,2	127	129 (1.57E7y)		
H	1		1		3 (12.3y)	
C	4,−4		12	14 (5730y)		
Alkali metals/Alkaline earths (15%)						
Cs	1		133	135 (2.3E6y)	124 (2.06y), 137 (30.17y)	
Rb	1		85	87 (5E10y)		
Ba	2		138,137			137m (with Cs-137)
Sr	2		88,86		90 (29.1y)	
Lanthanides (30%)						
Y	3		89			90 (with Sr-90)
La	3		139			
Ce	3	4	140,142		144 (0.78y)	
Pr	3	4	141			144m (with Ce-144)

Element	Oxidation states		Stable isotopes	Long-lived isotope (half-life)	Radioactive isotope (half-life)	Notes
Nd	3	4,2	143,144,145,146,148,150		147 (2.62y)	
Pm	3					
Sm	3	2	149,152,154			
Eu	3	2	151,153		154 (8.8y), 155 (4.71y)	
Gd	3	2	155,156,157,158,160			
Transition metals (35%)						
Zr	4		90,91,92,94,96	93 (1.5E6y)		
Nb	5					
Mo	6	5,–2	95,97,98,100	93 (3.5E3y)		
Tc	7	5,4		99 (2.1E5y)		
Ru	4,3	8,6,2	101,102,104		106 (1.02y)	
Rh	3	5,4,1	103			106 (with Ru-106)
Pd	2	4	105,106,108,110	107 (6.5E7y)		
Ag	1	2	109		110m (0.68y)	
Cd	2		111,112,114,116	113 (9E15y)		
In	3			115 (5E14y)		
Sn	4,2		117,118,119,120,122,124		119m (0.8y)	
Sb	3	5,–3	121,123		125 (2.76y)	
Te	4	6,–2	125,126,128,130			125m (with Sb-125)
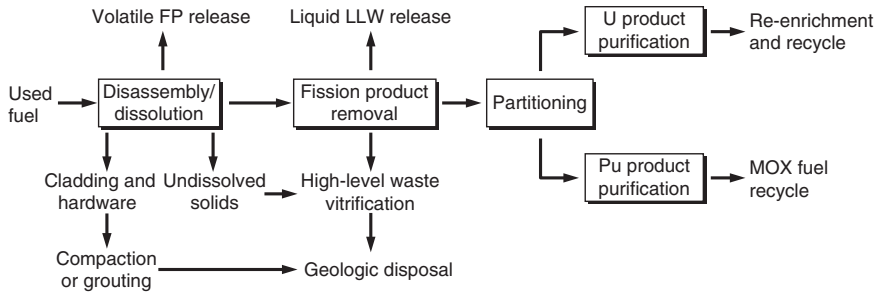
8.1 Used fuel component separations in current plants.

radionuclide-decay isotope pairs that are in secular equilibrium are shown in Table 8.1 because, in effect, they double the radioactivity emitted by the parent radioisotope.

In established reprocessing plants (Fig. 8.1), the volatile fission products, xenon and krypton, are vented to the environment, while the iodine is trapped from the off-gas and then released to the sea as liquid waste. Carbon-14 is scrubbed from the off-gas and released to the sea as low-level liquid waste or converted to insoluble barium carbonate and encapsulated in a solid waste form, such as cement. After dissolution of the fuel components, the cladding hulls and hardware are removed by screening and put into a solid waste form (compacted metal or grout) for subsequent geologic disposal. The dissolved fuel solution still contains finely divided undissolved solids (UDS), composed of variable portions of the transition metal elements. The UDS are removed by centrifugation and disposed in vitrified high-level waste, along with the soluble fission products that are separated from the uranium and plutonium products by means of solvent extraction processes.

Advanced reprocessing will include further separations processes to enable capture and disposal of the volatile fission product elements in improved solid waste forms. Also, additional separations processes are being developed (1) to enable recovery and recycle of the remaining minor transuranium element actinides, neptunium, americium, and curium, and (2) to segregate the lanthanide fission products and the intermediate-lived heat-generating radionuclides, primarily ^{137}Cs/^{137m}Ba and ^{90}Sr/^{90}Y. Details of the advanced fission-product recovery processes are described below. The actinide recovery processes are described in other chapters.

8.2   Separation methods, advantages/disadvantages, and future trends

8.2.1   Removal and separation of volatile and semi-volatile components

Voloxidation process

A dry head-end process for oxidation of used fuel has been developed and is being considered for application in advanced reprocessing to remove volatile components and allow selective trapping from the off-gas, prior to performing other separations processes for removal of non-volatile fission products. Among several benefits, the dry head-end treatment removes volatile tritium prior to any aqueous separations that may be subsequently used and, thus, prevents accumulation of tritiated water in the aqueous systems. In addition, there are significant potential benefits for removal and capture of radioiodine.

In the voloxidation process, the oxidation reaction is carried out at temperatures above 400°C in an oxygen-containing atmosphere. The UO_2 in the fuel reacts with oxygen to form U_3O_8, and the reaction is accompanied by a volumetric expansion of about 30%. The expansion breaks the ceramic oxide fuel structure and generates a fine powder form of U_3O_8, which is a significantly less dense material than the ceramic UO_2. Powder size distribution depends on the temperature of the oxidation process[3,4] and other factors related to the used fuel characteristics, but nearly all oxidized particles are produced in sizes less than 20 μm in diameter, with a good fraction less than 10 μm.[5] Higher temperatures increase the rate of oxidation but increase the grain size of the U_3O_8 powder produced, with a wider distribution of particle sizes.

Tritium removal

As originally developed, the voloxidation process is carried out in an air atmosphere at 480°C to 600°C, primarily to remove tritium from the fuel. During oxidation of the UO_2-based fuel, tritium, which may be present in the fuel in elemental form, diffuses to the surface of the particles where it reacts with oxygen to form water, which enters the gas stream.[6,7] The rate of reaction at 480°C is such that >99.9% of the tritium is released from the fuel in about 4 h.

A significant portion of the tritium in the used fuel assemblies is associated with the cladding as zirconium hydride (ZrT_x).[5] The fraction of tritium in the cladding has been reported at 40%[8] and higher.[6] The hydride should readily oxidize, releasing the tritium, if it were accessible by the oxygen. However, experimental data indicate that oxidation has little effect on

the tritium held in the cladding when processed for 6 h at a temperature of 480°C.[9]

Removal of Kr, Xe, and C

In the standard process using air (about 480°C and 4 h processing time), about half of the ^{14}C is volatilized, and minor fractions of fission products are volatilized, including about 5% of krypton and xenon; 1% of iodine and bromine; and ~0.2% of the ruthenium, antimony, and cesium. With higher temperatures and longer reaction times, larger fractions of the noble gases are released – up to 60% of the krypton at 750°C in 8–10 h.[10] Using an oxygen-enriched atmosphere enhances the release of ^{14}C to nearly 100%. Higher temperatures, oxidation to UO_3, repeated cycles of oxidation-reduction, and mechanical agitation will enhance the release.

Removal of semi-volatiles (I/Br, Ru, Rh, Tc, Cs, Rb, Mo, Se/Te, etc.)

Semi-volatile species, which include the elements I/Br, Ru, Rh, Tc, Cs, Rb, Mo, and Se/Te, can be released under certain processing conditions. Early removal of the semi-volatiles simplifies the off-gas treatment compared with recovery from wet NO_x-laden off-gas generated from the downstream dissolution process. Iodine is difficult to fully remove from liquid dissolver solutions and can be problematic as a corrosive. Also, the early removal of specific semi-volatiles can simplify the downstream separations processes; for example, the recovery of technetium by means of dry volatilization will eliminate the need to co-extract it with uranium and separate the technetium under conditions that may complicate the uranium recovery. Moreover, the recovery of molybdenum by means of dry volatilization will eliminate the major source of precipitates (e.g., zirconium molybdates) that can foul the evaporation and solvent-extraction equipment.[11]

In the basic voloxidation process (oxidation in air at 480°C), less than about 0.2% of each of the semi-volatiles, ^{106}Ru, ^{125}Sb, and $^{134–137}$Cs, is evolved. Higher temperatures and vacuum operation increase the fraction evolved.

Collaborative tests by Idaho National Laboratory (INL), the Korean Atomic Energy Research Institute, and Oak Ridge National Laboratory (ORNL) showed that nearly 100% of the semi-volatiles can be separated under a variety of conditions using air or oxygen as the oxidant atmosphere, temperatures up to 1250°C, and vacuum operation. The removal effectiveness was highly dependent on the processing conditions. In general, initial oxidation at relatively low temperature (around 500°C) to generate the fine fuel powder with increased surface area is beneficial. Increasing temperatures enhanced the amounts of the semi-volatiles released in the following approximate order: Ru + Rh, Tc, Cs, Te, and Mo.[12,13]

Enhanced oxidation, at selected temperatures and with alternative reagents such as ozone, NO_2, and steam has been tested at ORNL to complete the removal of volatiles (all xenon, krypton, carbon, and iodine) and to remove semi-volatiles (molybdenum, technetium, and others). At low temperature (200–300°C), the U_3O_8 powder obtained by conventional voloxidation may be further oxidized with ozone (O_3) to produce a finer UO_3 powder. Also, NO_2 can be used and will oxidize UO_2 or U_3O_8 to UO_3. The fine UO_3 powder may be heated to higher temperatures, in a secondary step if necessary, to remove those species released by diffusion-controlled processes. Although higher temperatures cause UO_3 to revert to U_3O_8, the benefit of the finer particles will remain. Additionally, the process can be cycled between UO_3 and U_3O_8. Further fracture of the particles will enhance the release of volatile species and can be accomplished by cycling between higher and lower oxide species.

For example, in the AIROX[14,15] and DUPIC[16,17,18] processes, the fuel is first subjected to oxidation in air to obtain U_3O_8 powder. The resulting powder is then subjected to repeated cycles of hydrogen reduction to UO_2 (usually at temperatures between 600°C and 800°C) and then re-oxidization of the UO_2 to U_3O_8. Alternatively, a cycle between U_3O_8 and UO_3 can be carried out using O_3 or NO_2 to generate UO_3, then heated above 450°C to decompose the UO_3 to U_3O_8. This is a lower temperature cycle that avoids any potential complication due to alternating hydrogen and oxygen atmospheres.

8.2.2 Effects of fuel oxidation on separation of non-volatile components

Fuel-cladding separation

The generation of the finely divided fuel powder by means of the voloxidation process enables separation of the oxide fuel from the segmented or punctured cladding by means of screening. Under adequate agitation provided by a rotary or vibrated oxidation reactor, over 99% of the fuel can be cleanly separated. A small amount (0.1 to 1 wt %) of the finely powdered fuel clings to the surface of the cladding and can be recovered by acid washing. Tests with a variety of sources of commercial used fuel, ranging from low-burnup, long-decayed fuel to very high burnup, short-time-decayed fuel have demonstrated that an efficient separation (>99%) of fuel from cladding is possible.

Fuel dissolution

The reduction in particle size greatly accelerates the rate of dissolution. The higher oxidation state of the uranium reduces the nitric acid requirement

Table 8.2 Effect of uranium oxidation state on dissolution nitric acid requirements

Dissolution reaction(s)	HNO$_3$ (M)	Reference
$3UO_2 + 8HNO_3 \rightarrow 3UO_2 (NO_3)_2 + 2NO + 4H_2O$	<10	9
$UO_2 + 4HNO_3 \rightarrow UO_2 (NO_3)_2 + 2NO_2 + 2H_2O$	>10	9
$U_3O_8 + 7.35HNO_3 \rightarrow 3UO_2 (NO_3)_2 + NO_2 + 0.35NO + 3.65H_2O$	~8	19
$UO_3 + 2HNO_3 \rightarrow UO_2 (NO_3)_2 + H_2O$	all	a

[a] Theoretical; in actual practice a very small amount of NO$_x$ is produced.

Table 8.3 Transition metal (TM) fission products in undissolved solids (UDS)

Fuel burnup, GWd/MT	18	23	31
Total UDS, wt%	0.026	0.18	0.20
Total UDS after voloxidation, wt%	0.28	0.37	0.59
% of TM elements in UDS			
Zr		5[a]	
Mo		20	
Tc		50	
Ru		44[b]	
Rh		38[b]	
Pd		99	

[a] Zr is apparently from residual cladding fines.
[b] Prior to dissolution, 50% of Ru and Rh apparently was removed by volatilization during the voloxidation or dissolution process. Of the non-volatilized portion, 80–90% was in the UDS.

and reduces the amount of NO$_x$ evolved (see Table 8.2).[9,19] When produced, UO$_3$ powder dissolves readily in >0.3 M HNO$_3$ acid with only trace levels of NO$_x$ generated.

8.2.3   Transition metal fission-product behavior

Undissolved solids (UDS) and secondary oxide precipitations

Following dissolution of fuel components in nitric acid solutions, a variable fraction of the transition elements remain as insoluble metal precipitates. The amounts of each element vary according to the prior fuel burnup and dry heat pretreatments, such as the voloxidation process. Data obtained from typical experimental measurements are illustrated in Table 8.3.

The chemical nature and behavior of the fission products from oxide fuels have been studied extensively and described thoroughly by Kleycamp and others.[20] The insoluble transition metals were described as metallic inclusions or precipitates. Other studies have shown that the Mo, Tc, and portions of the Ru and Rh in the UDS can be dissolved in 4 M KOH solution and the remaining Ru, Rh, and all Pd can be dissolved in aqua regia. These special dissolutions may be necessary if recovery of the valuable noble metals is pursued in advanced reprocessing.

After clarification of the dissolved nitric acid fuel solution by centrifugation to remove the UDS, secondary oxide precipitations of some fuel components occur during the subsequent feed adjustment, solvent extraction, and waste treatment processes. The amount of precipitation can be affected by the heat treatments applied during these operations, or simply upon storage of the solutions for extended periods. The finely divided oxide precipitates have been shown to cause the development of interfacial cruds during solvent-extraction operations, but operational problems have apparently been avoided or minimized by the use of pulsed extraction columns, which apparently are not affected seriously by the presence of the finely divided oxide particulates.

Table 8.4[21] shows precipitated and crystallized solid fission products that have been observed during laboratory studies of evaporation and acid reduction processes used to treat the solvent-extraction high-level waste solutions. These studies have shown that the solids contain primarily Zr, Mo, Ba, Sr, and Sn. The solids are a combination of hydrous precipitates and crystallites that are insoluble in concentrated nitric acid. Although cesium would be expected to be highly soluble, the presence of 24% in the precipitate may have been by occlusion with other hydrated precipitates.

Table 8.4 Secondary oxide precipitation

FP element	% of original solution in precipitate
Ba	87
Zr	85
Mo	70
Sr	70
Sn	47
Cs	24
Lanthanides	<0.05
Actinides	<0.001

*Soluble technetium: solvent extraction using tri-butyl phosphate (TBP)
as the extractant*

Established reprocessing plants utilize the PUREX process (Chapter 6) to
separate and remove the non-volatile and nitric-acid-soluble fission prod-
ucts from the uranium and plutonium products. Advanced reprocessing may
use derivatives of the process for co-processing operations to produce a
plutonium or plutonium-neptunium product containing part of the uranium,
thereby reducing the proliferation risk by making access to the fissile
material less attractive. In those TBP-based solvent-extraction processes,
where the feed stream contains both zirconium and soluble technetium
fission products, the technetium will form a complex with uranium and be
co-extracted.

The technetium distribution coefficient is reduced at high solvent load-
ings with uranium and with higher nitric acid concentrations in the aqueous
phase, as shown in Fig. 8.2.[22] These data indicate that separation of the
technetium from the loaded solvent can be accomplished by scrubbing with
>5 M nitric acid. Alternatively, the technetium can be allowed to remain
with the uranium and be co-stripped into a low-acidity aqueous product,
from which the technetium can be preferentially adsorbed onto an anion-
exchange resin.
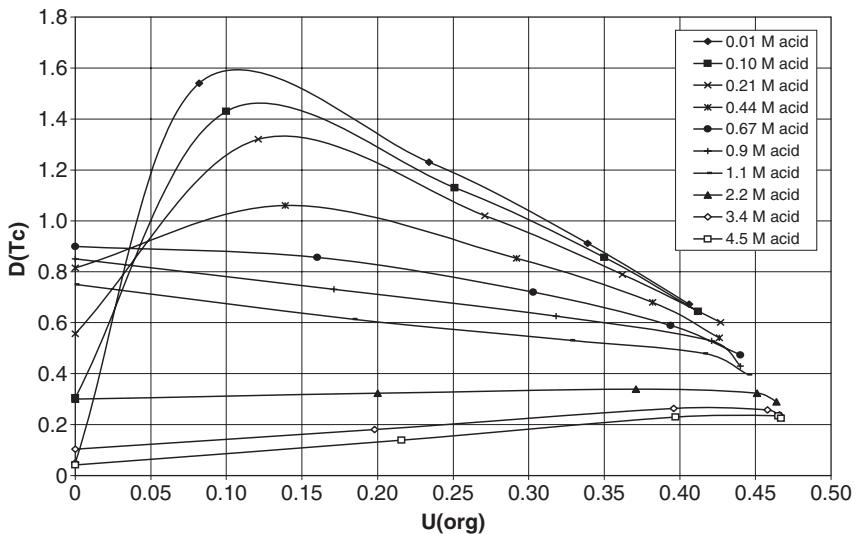
Calculated from Equation 32 in D. J. Pruett, *The Solvent Extraction of Heptavalent Technetium and
Rhenium by Tributyl Phosphate*, ORNL/TM-8668, Oak Ridge National Laboratory, December 1984.

8.2 Technetium distribution coefficient.

8.2.4 Lanthanide recovery and separation

The lanthanide fission products are not separated from the high-level waste in established plants and are planned to be disposed to a geologic repository in a vitrified waste form (Chapters 6 and 7). Advanced reprocessing studies are emphasizing development of processes for recovery of the trivalent actinides (Chapter 11). Most of the actinide recovery processes being considered include an initial separation of the combined trivalent actinides and lanthanide fission products, followed by a process to partition the lanthanides from the actinides. Examples include the combination of TRUEX-TALSPEAK processes (Fig. 8.3) developed in the United States and the DIAMEX-SANEX processes developed in France. Both combinations are dependent on the use of poly-amino-poly-carboxylate complex agents, together with buffering agents that permit precise control of pH in the process solutions. Following the actinide-lanthanide separation, another process is required to remove the complex agents from the product solutions. A group separation is obtained but with varying separation factors for the different lanthanide elements, as indicated in Table 8.5.[23]

If a separation of the individual lanthanide elements is needed, a multi-stage chromatographic separation process using pressurized ion exchange, strong complex agents, and precise pH control would need to be employed.[24] These could be operated using either elution chromatography from an ammonium-form cationic resin or displacement cationic-exchange methods

Feed = Raffinate Stream from TBP Extraction
Am-Cm-Ln Fission Products (FPs) – Other FPs

TRUEX solvent extraction
Solvent: 1.4 M TBP – 0.2 M CMPO
in n-paraffin diluent   → Other FPs

Am-Cm + Ln FPs

TALSPEAK solvent extraction
Solvent: 1 M HDEHP in n-paraffin diluent
Complexant: 0.05 M DTPA in 1.5 M lactic acid
pH ~3   → Ln FPs

Am-Cm product
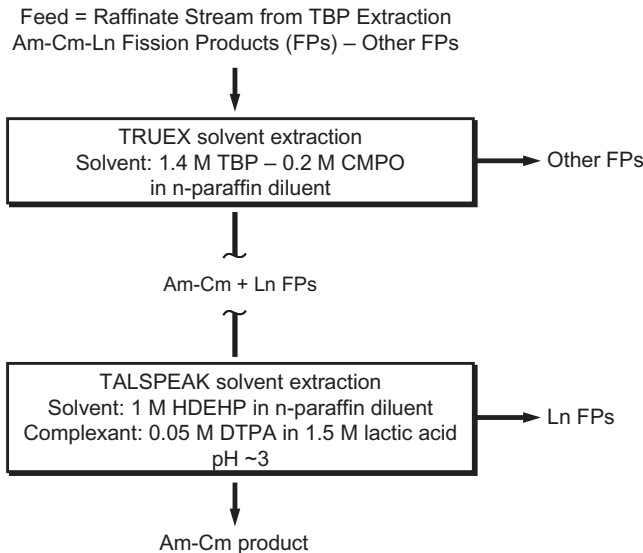
8.3 Am-Cm recovery using the TRUEX-TALSPEAK processes.

Table 8.5 TALSPEAK separation factors

Element	Calculated SF	Measured SF
La	644	70
Ce	177	126
Pr	101	57
Nd	41	39
Sm	49	48
Eu	83	107
Gd	102	Not measured

that utilize a "barrier" metal, such as zinc or nickel. The barrier ion blocks elution of elements that form weaker complexes than the ion being eluted. Large systems of this type have been operated for rare earth recovery.

8.2.5   Separation of the intermediate-lived heat-generating fission products $^{137}Cs/^{137m}Ba$ and $^{90}Sr/^{90}Y$

Historical perspective and current trends

Interest in the separation of fission-product cesium and strontium dates back to the early days of reprocessing over half a century ago. This interest has been reflected in a large body of scientific research and process development that is growing unabated to this day. Motivation has been threefold: advanced reprocessing, waste management, and industrial applications.[25,26] Separations of ^{137}Cs and ^{90}Sr being considered for advanced reprocessing today are driven by the expected increase in repository capacity upon reducing the heat load that would otherwise result from inclusion of these two fission products.[27–29] Given the large cost of adding unit operations to a reprocessing plant, however, separation may not be preferable to decay-storage,[30] at least using currently available separation technologies. Nevertheless, research has continued to the point of demonstration and even multimegacurie separations have been done,[31] thereby establishing a baseline of mature technology options for future consideration. Major use of ^{137}Cs and ^{90}Sr separations technology occurs in the area of waste management.[32–37] Wastes include a great variety of stored radioactive materials but are dominated in volume by >10^8 gal of legacy defense reprocessing wastes stored in the United States and Russia. Strategies generally aim to concentrate radionuclides into a compact volume for disposal with concomitant high decontamination of the bulk volume of the waste stream. Environmental risk is thereby reduced, and cost savings accrue by reducing the volume of high-activity waste destined for expensive storage facilities. Radiation

sources containing ^{137}Cs or ^{90}Sr have been in demand for multiple industrial uses dating back to the 1950s, motivating considerable research and mega-curie recovery operations.[25,26,37,38] Historically, legacy wastes, such as the separated radiocesium and radiostrontium currently stored at Hanford, have been viewed as a resource in this regard.

The status of technology development to separate cesium and strontium from both acidic and alkaline solutions was reviewed comprehensively approximately two decades ago,[25,26] describing the considerable progress that had been made in previous decades and laying out the needs and challenges for future processing. A need was singled out therein for new solvent-extraction technologies for cesium and strontium removal from acidic streams. The potential of crown ethers, recognized in the radiochemical community since the 1970s,[39–42] had not yet led to a practical system, and promising dicarbollide chemistry. Although promising dicarbollide chemistry had gained the attention of Czech researchers as early as 1974,[43] it had not yet emerged from dependence on toxic diluents like nitrobenzene. Several ion-exchange and precipitation systems had been in use on the acid side, but all were seen as having drawbacks,[25] such as difficult recovery of the radionuclide from the reagent, low capacity, or instability. A number of separations on the alkaline side, pertaining mainly to cesium, were available or being implemented, such as the In-Tank Precipitation (ITP) process using tetraphenylborate for cesium removal from tank waste at the Savannah River Site (SRS),[44] phenol-formaldehyde resin functionalized with sulfonic acid groups (Duolite ARC-359), zeolites, and several solvent-extraction systems.[25,26,33] Strontium, largely insoluble as hydroxide or carbonate salts or as co-precipitated with other metals, is not as important as cesium for separation on the alkaline side, but monosodium titanate had been demonstrated to be effective in sorbing traces from tank waste.[44] Megacurie recovery of strontium from acidified tank sludge had been carried out previously.[25]

Ion exchange

In the last two decades, ion-exchange, precipitation, and solvent-extraction techniques for cesium and strontium separation have seen the most development, with some notable implementation in the waste-management arena. Ion-exchange materials selective for cesium and strontium have become more practical, making possible demonstrations and use of column-based technologies, on both the acid and alkaline sides, and some new materials have been introduced. Although the solid sorbents being demonstrated on the acid side tend to be the same chemical compositions that were previously known to be effective, especially copper and cobalt ferrocyanides[45] and ammonium molybdophosphate, the development of engineered forms has

allowed the technologies to advance.[37,46–48] Elution of the loaded inorganic ion exchange sorbents is relatively difficult, and more often, the loaded exchangers have been dried and used directly as waste forms; for example, loaded ferrocyanide exchangers have been used in this manner.[36] On the alkaline side, recent developments in ion exchange continue to be driven by needs for pretreatment technologies for tank waste in the United States.[33] Monosodium titanate (MST) has been implemented since 2008 in the Actinide Removal Process at SRS for simultaneous removal of trace Sr^{2+} and Pu from tank waste.[49–51] The MST is added to the waste as a slurry in batches at 0.4 g/L, and accumulated loaded MST is then vitrified in borosilicate glass at the Defense Waste Processing Facility (DWPF). MST can now be produced in spherical bead form for use in column technology.[52] In the early 1990s, a material related to MST, referred to as crystalline silicotitanate (CST) and commercially available as IONSIV® IE-911, was discovered to be an effective ion-exchange material for cesium.[53] Following rapid development, column ion exchange using CST was demonstrated at the ORNL in the removal of 1142 Ci of ^{137}Cs from 31 000 gal of waste.[33,53] CST is currently being considered for an in-tank column technology called Small Column Ion Exchange at the SRS.[33] A practical elution of cesium from CST has not been reported, and as in the case of MST, loaded CST is directly vitrified. Remarkably, CST can function over the entire pH range and has even been considered for treatment of acidic waste at the INL.[48] Elutable resin technology will be implemented for cesium removal from alkaline tank waste at the Hanford Waste Treatment Plant (WTP).[33,54] Originally, plans called for using the proprietary material SuperLig® 644 to separate Cs at the WTP; however, plant designers recently have favored using a spherical form of resorcinol-formaldehyde (RF) resin. Granular RF materials have been known since their development at the SRS in the early 1980s and are now gaining attention in India.[38] Although RF materials in general exhibit good uptake of cesium under alkaline conditions and good elution behavior, a perennial problem has been chemical instability, even on storage; satisfactory storage under nitrogen has been demonstrated.[55] The instability represents a nuisance in terms of added handling precautions, limited resin cycling lifetime, and inconsistent characterization, but its effectiveness in other respects keeps the RF materials under consideration for alkaline waste treatment.

Crystallization and precipitation

A de facto separation and concentration of fission products can be achieved by crystallization of bulk fission-product components, such as occurs during nitric acid recovery evaporations. In advanced reprocessing schemes, such as the Japanese NEXT process,[56] this approach takes the form of an initial crystallization of uranyl nitrate. For cleanup of Hanford alkaline tank waste,

proposed fractional crystallization of sodium nitrate achieves an equivalent result.[57,58] Given that low concentrations of strontium are present in alkaline wastes, especially those with complexants, a useful decontamination can be achieved by isotopic dilution upon addition of strontium nitrate and resulting precipitation of strontium carbonate.[33] In the mid 1990s, the ITP process for cesium removal by precipitation with sodium tetraphenylborate was implemented at SRS.[59] Owing to the insolubility of cesium tetraphenylborate, an impressive decontamination of 1 Ci/L alkaline waste can be reduced to <10 µCi/L. However, due to the action of trace catalysts to accelerate tetraphenylborate decomposition, unexpectedly large benzene levels occurred in the tank headspace and led to shutdown of this process. A modification of the process, called the Small Tank Precipitation Process, was developed to overcome the benzene evolution by exploiting the induction period of the catalyst. The modified process was successfully demonstrated[60] but has not been adopted for use.

Solvent extraction

Solvent-extraction technologies for cesium and strontium have matured on the acid side,[25] mainly because of further developments in crown-ether and dicarbollide chemistry.[61–63] In the meantime, calixarenes have emerged as a family of powerful extractants for many different metals, including Cs^+ and Sr^{2+}, and were quickly put to use for both acid and alkaline media.[61,64] These developments are described below in more detail. A significant trend toward combining extractants[65] has been realized in the past two decades and, in fact now predominates, so that cesium and strontium are typically recovered simultaneously and in some case with actinides from acid solution.[63,65,66] In reprocessing and waste-management applications, combined processes potentially yield large cost savings, because there is overall process simplification and a net footprint reduction. However, there can be tradeoffs, attenuating the benefits:[63] namely, the chemical complexity of the combined process necessarily increases and selectivity decreases, making it more difficult to find and maintain optimal process conditions. Nevertheless, the potential advantages are compelling, and as testing of more complex solvent systems continues, the price of greater process control is gaining acceptance. Because of the flexibility of solvent extraction in accommodating the development of combined processes, solvent extraction has gained an important advantage over other separation techniques in recent years, at least for separation of fission products from aqueous solution, if not also for separation of actinides.

Dicarbollide-based solvent extraction has opened the door to new technologies for extraction of cesium alone or usually with other targeted metals, including strontium and actinides.[61,62] Cesium enjoys a privileged

position in the periodic table, in which its univalent cation has the largest ionic radius of any metal cation (except for short-lived Fr^+) and therefore has the least charge density and the weakest hydration.[67] These properties make cesium the easiest metal to extract, and as long as the solvent contains no components that can electrostatically interact with competing metal ions (e.g., H^+, Na^+, K^+, Hg^{2+}, Ba^{2+}) by coordination or ion pairing, the extraction is extraordinarily cesium selective simply by solvation principles.[68] In the mid-1970s, this potentially was actualized by the introduction of the large, hydrophobic, dumbbell-shaped bis(dicarbollyl)cobaltate sandwich anion $[3\text{-Co-}(1,2\text{-}C_2B_9H_{11})_2]^-$ as a cation-exchange extractant in its acid form.[43,69] The parent cobalt dicarbollide anion can be chemically substituted in a variety of ways, giving rise to a large family of anions generally known simply as dicarbollides.[62] However, applications have mainly made use of the hexachlorinated cobalt dicarbollide derivative (abbreviated as HCCD) because of its robustness to attack by strong nitric acid. Early process development employed nitrobenzene and its mixtures with other solvents, but less objectionable polar fluorinated solvents are now preferred. One such diluent is phenyltrifluoromethylsulfone (FS-13) for which the cesium extraction equilibria have been characterized.[70] Flowsheets designed for removal of cesium alone have performed well in demonstrations at Gatchina in the early 1980s (0.06 M HCCD in 60 vol % nitrobenzene/40 vol % CCl_4) and more recently at INL (0.15 HCCD in a Fluoropol diluent, a 40:60 vol/vol mixture of di(tetrafluoropropyl) ethers of diethylene glycol and ethylene glycol).[62] The latter flowsheet achieved a removal efficiency of >99.998% from acidic tank waste with co-extraction of 50% and 34% of the K^+ and Hg(II) in the feed, respectively.

Combined extraction of Cs^+ together with Sr^{2+} and actinides using dicarbollide-based technology has proven extremely successful.[61,62] Unlike, Cs^+ ion, the much more hydrated Sr^{2+} and actinide ions do not partition significantly to polar solvents using dicarbollide or other inert large anions by themselves. Therefore, synergistic additives are needed to preferentially coordinate with the other desired cations, though these additives invariably compromise cesium extraction. Crown ethers[43] and polyethylene glycols (PEGs), sometimes called pseudo crown ethers, were found effective for Sr^{2+}, and the cheaper PEGs are now preferred in practice. Megacurie-scale removal of ^{137}Cs and ^{90}Sr from high-level waste dates back to the 1980s at the Russian Mayak facility.[31,61,62] The most recent solvent system in use at Mayak has been 0.1 M HCCD in m-trifluoromethylnitrobenzene with 2% p-octylphenyldecaethylene glycol (OP-10). The solvent is stripped with 9 M HNO_3 with 25 g/L hydrazine nitrate. Flowsheet development and countercurrent testing of an HCCD solvent on simulated acidic legacy waste has been carried out jointly at INL and the Khlopin Radium Institute (KRI).[71] At KRI, 0.13 M HCCD in FS-13 with 3 vol % p-nonylphenylnonaethylene

glycol (Slovafol-909) was employed, while at INL the solvent consisted of 0.08 M HCCD in FS-13 with 0.6 vol % PEG-400 (nonaethylene glycol). At KRI, 3 M methylamine nitrate in 3 M HNO_3 was the stripping reagent, while INL employed 100 g/L guanidinium carbonate with 20 g/L diethyl-enetriamine pentaacedic acid (DTPA). Excellent recoveries of Cs and Sr were achieved in both cases. Removal of Pb and Ba was nearly quantitative along with significant carryover of Na, K, and Ca. The INL flowsheet has been adopted for development of a process applicable to Cs and Sr removal in future US reprocessing.[72] With further addition of a carbamoylmethylphosphine oxide to the CCD-PEG solvent system, it is possible to effect the simultaneous extraction of Cs, Sr, and actinides, which has been demonstrated for treatment of acidic INL and Russian wastes.[31,66] This is a complicated solvent system that has been undergoing development jointly by INL and KRI since 1995, primarily motivated by the potential for processing INL acidic waste. Engineering tests were carried out in both Russia and the United States with simulants and actual waste, converging on a solvent system containing a 5:1:1 molar ratio of CCD, PEG-400, and diphenyl-*N*,*N*-di-*n*-butylcarbamoylmethylphosphine oxide (CMPO). Removal efficiencies were excellent in the latest test in 2001 with dissolved INL calcine: 99.99% ^{137}Cs, 99.73% ^{90}Sr, and 99.9% alpha emitters. However, owing to the complexity of the solvent, other metals such as Ba and Pb get co-extracted, and hold-back reagents like HF or citrate are required to suppress extraction of metals like Zr, Fe, and Mo in the feed.

Molecular recognition

One of the most important developments for nuclear separations in the past two decades has been the emergence and rapid implementation of technologies for fission-product separation from aqueous streams based on molecular recognition. Simple neutral crown ethers provided an initial starting point for developing extractants selective for cesium and strontium,[25,26,39–43,61,63,73,74] but calixarenes have now supplanted crown ethers for cesium extraction.[61,64] As its name implies, molecular recognition is associated with high selectivity, making the job of extraction simpler and more efficient, but just as important is the ability to strip with water or very dilute aqueous solutions. Downstream operations for production of waste forms or perhaps a radiation source stand to be greatly simplified with less secondary waste if the radionuclide is concentrated into a pure solution in water. A major challenge with using simple crown ethers for process development has been weak extraction strength, leading researchers at first to use large counteranions like phosphomolybdate or hexachloroantimonate, which was demonstrated for cesium extraction from medium-activity waste.[74,75] Alternatively, by mixing crown ethers with cation exchangers like

HCCD[43,61,62] or lipophilic sulfonic, carboxylic, or phosphoric acids,[41,73,76] synergistic extraction of Cs and Sr can be effected. However, these systems have the same disadvantage of stripping with strong acid. Furthermore, their use would make sense only for Sr, since no synergist for dicarbollide is needed for good Cs selectivity. The problem of extraction strength was adequately solved by judicious selections of crown ether, diluent, and sometimes modifier; in addition, rather high concentrations of crown ether are needed, on the order of 100-fold more capacity than required for stoichiometric loading. A careful study of the effect of diluent showed that $Sr(NO_3)_2$ could be adequately extracted from nitric acid by *cis*-dicyclohexano-18-crown-6 (*cis*-DCH18C6),[77] giving rise to the successful SREX process, which employs the more lipophilic crown ether bis(*tert*-butylcyclohexano)-18-crown-6 (DtBuCH18C6) in either 1-octanol[78] or TBP-modified Isopar L.[79] Stripping is effected with dilute nitric acid. Among a number of countercurrent demonstrations of SREX, for example, workers at INL achieved 99.997% removal of the ^{90}Sr in acidic waste.[80] In the same time period, Russian researchers employed fluorinated alcohols as diluents, making possible an effective process with DCH18C6.[81–83] More recently, Chinese researchers, who call the process CESE, have also employed DCH18C6, achieving a >99.96% removal of the ^{90}Sr in high-level liquid waste effluent from a TRPO process raffinate.[84] DtBuC18C6 may be added to the TRUEX solvent to achieve a combined extraction of ^{90}Sr and actinides.[85]

Cesium extraction with crown ethers proved even more difficult, hindered by weak extraction strength for $CsNO_3$ and modest selectivity over Na and K. Benzo-substituted crown ethers of various ring sizes exhibit useful cesium selectivity to varying degrees, the best selectivity being achievable with dibenzo-21-crown-7 (DB21C7) or its more lipophilic analog bis(*tert*-butylbenzo)-21-crown-7.[76,86–88] Russian workers proceeded with process development using DB21C7[81] or a derivative bearing phosphoryl substituents on the benzo groups, used in a polyfluorinated alcohol diluent (Fluoropol-732).[88] The latter crown ether was also mixed with DCH18C6 to achieve a simultaneous recovery of Cs and Sr. Workers in the United States noted that extraction strength was highest with dibenzo-18-crown-6 bearing 1-hydroxy-2-ethylhexyl substituents on each benzo group.[87] This crown ether was mixed with DtBuC18C6 in Isopar L modified with TBP and lauryl nitrile to obtain the CSEX-SREX combined process for simultaneous removal of Cs and Sr, demonstrated in a countercurrent test with INL waste simulant.[63,85,89]

In the mid-1990s, the advent of the family of calix[4]arene-crown-6 compounds[90,91] dramatically changed the technological possibilities for cesium extraction, as recently reviewed.[61,64] These compounds feature cesium binding strength[92] and selectivity[93] both on the order of 100-fold higher than DB21C7, and stripping can again be effected with water or dilute aqueous

solutions. A useful way to understand the structure of the calix[4]arene-crown-6 compounds is to consider them as crown ethers with aromatic rings preorganized to lie above and below the crown cavity. The resulting pocket is extraordinarily complementary for the Cs^+ ion. French investigators showed the feasibility of developing useful processes on the acid- or alkaline-side based on a TBP-modified aliphatic diluent.[94] In the United States, acid-side conditions were worked out with alcohol modifiers in Isopar L, which allowed much lower calixarene concentrations to be employed.[95] It was subsequently shown that a simultaneous extraction of Sr and Cs could be obtained with calix[4]arene-bis(*tert*-octylbenzocrown-6) (BOBCalixC6) mixed with DtBuCH18C6 in Isopar L modified with 1-(2,2,3,3-tetrafluoropropoxy)-3-(4-*sec*-butylphenoxy)-2-propanol (Cs-7SB modifier).[96] Further development on this system, called the FPEX process, is continuing, as BOBCalixC6 suffers from low solubility and mild nitration by nitric acid.[95] While the removal of Cs and Sr in reprocessing may be questionable,[30] alkaline-side process development has proceeded quickly to industrial implementation by more urgent needs for processing alkaline tank waste in the United States.[32,33] The current implementation of the process, known as the Caustic-Side Solvent Extraction process (CSSX), employs a solvent system consisting of 0.007 M BOBCalixC6, 0.75 M Cs-7SB modifier, and 0.003 M tri-*n*-octylamine in Isopar L.[97,98] The loaded solvent is scrubbed and stripped with 0.050 M and 0.001 M HNO_3, respectively, to produce a practically pure stream of $CsNO_3$ in mildly acidic water. Countercurrent demonstrations using centrifugal contactors with simulated[99] and real[100] SRS tank waste showed that decontamination factors of >40 000 and concentration factors of 15 can be readily achieved, and plans call for implementation in the SRS Salt Waste Processing Facility (SWPF) in 2014.[32,33] The Modular CSSX Unit (MCU) at the SRS started operation in 2008 as an interim pilot facility intended for pretreatment of several million gallons of low-curie SRS salt waste.[101] It achieves ^{137}Cs decontamination and concentration factors of >100 and 12, respectively, and the strip product is being vitrified in the DWPF. A proposed next-generation CSSX flowsheet using the more soluble extractant calix[4]arene-bis(2-ethylhexylbenzo-crown-6) (BEHBCalixC6)[102] concentrates ^{137}Cs into a dilute boric acid strip solution, which is itself a glass component for the downstream borosilicate vitrification process.[103]

8.3   Conclusions and future trends

Fission-product separations technology will continue to see progress in the future to meet the needs of advanced reprocessing and waste management in different countries. Addition of dry head-end pyrochemical treatment, such as the voloxidation process, can enable selective separation and capture of the volatile and semi-volatile fission products, while converting ceramic

used fuels into finely divided oxide powder that can be separated relatively easily from the fuel cladding and can simplify the dissolution process. Separation and recovery of selected fission products, such as xenon gas, volatile noble metals, and lanthanide elements for reuse may become economical, thus reducing the waste discharges from used fuel reprocessing. In the advanced aqueous reprocessing arena, a dedicated unit operation for Cs and Sr separation is of uncertain net benefit, which will undoubtedly dampen the pace of applied development in the near term. However, the desirability of reducing the heat load on geologic repositories will likely keep interest alive for improved separations in the long term.

In the long run, there will remain a significant need for improved fission-product separations associated with the nuclear industry. Although declared needs from the industry are often erratic, it will remain true that science-driven advances in technology can always have a transformational impact. This must be true in that existing and developing technologies are not even close to ideal, even as impressive as developments have been in the past two decades. In view of these realities, available technologies will change as well as the way in which technologies are invented and developed. While there can be no substitute for creative inspiration, for example, increasingly the power of computational design of new separation agents that function by molecular recognition can be expected to lead to targeted properties. Already, the first inkling of such capability has occurred, as evidenced by the computer-aided design of self-assembled capsules for selective crystallization of sulfate.[104] Expansion of applicable techniques beyond solvent extraction, ion exchange, and precipitation can be expected. Electrochemical methods, supercritical fluid extraction, and membrane technologies, for example, are likely to play a role. Finally, the need for, and challenge of, combined separations cannot be overestimated. The ability to target specific *combinations* of radionuclides for separation simultaneously without adjustment of feed conditions, use of special hold-back reagents, complicated scrubbing, and concentrated stripping reagents will ultimately prove compelling. In summary, the need for advanced fission-product separation technologies to move toward more ideal characteristics will remain strong in the context of new fuel cycles and continued waste cleanup, and in response, both new technologies and the way new technologies are conceived may be expected.

8.4   References

1. Knolls Atomic Power Laboratory, "Periodic Table of the Elements," General Electric Co., 1996.
2. T. R. England and B. F. Rider, *Fission Product Yields, Thermal Neutron Induced Fission, Uranium-235*, LA-UR-94-3106, ENDF-349, Los Alamos National Laboratory, 1993.

3. M. Iwasaki, T. Sakurai, N. Ishikawa, and Y. Kobayashi, "Oxidation of UO_2 Pellets in Air: Effect of Heat-Treatment of Pellet on Particle Size Distribution of Powders Produced," *J. Nucl. Sci. Technol.* **5**(12), 652–653 (December 1968).

4. K. A. Peakall and J. E. Antill, "Oxidation of Uranium Dioxide in Air at 350–1000°C," *J. Nucl. Mater.* **2**(2), 194–195 (1960).

5. G. Uchiyama *et al.*, "Study on Voloxidation Process for Tritium Control in Reprocessing," *Radioactive Waste Management and the Nuclear Fuel Cycle* **17**(1), 63–79 (1992).

6. J. H. Goode and R. G. Stacy, *Head-End Reprocessing Studies with H. B. Robinson-2 Fuel*, ORNL/TM-6037, Oak Ridge National Laboratory, June 1978.

7. M. Benedict, T. Pigford, and H. Levi, *Nuclear Chemical Engineering*, 2nd ed., McGraw Hill, New York, 1981.

8. J. H. Shaffer, *Head-End Processing of Spent Breeder Reactor Fuels: Status of Laboratory Research and Development Activities*, ORNL/TM-8710, Union Carbide Corporation, Oak Ridge National Laboratory, Oak Ridge, Tennessee, June 1983.

9. J. H. Goode, R. G. Stacy, and V. C. A. Vaughen, *Comparison Studies of Head-End Reprocessing Using Three LWR Fuels*, ORNL/TM-7103, Union Carbide Corporation, Oak Ridge National Laboratory, June 1980.

10. J. H. Goode *et al.*, *Voloxidation – Removal of Volatile Fission Products from Spent LMFBR Fuels*, ORNL-TM-3723, Union Carbide Corporation, Oak Ridge National Laboratory, January 1973.

11. A. Magnaldo, M. H. Noire, E. Esbelin, J. P. Dancausse, and S. Picart, "Zirconium Molybdate Hydrate Precipitates in Spent Nuclear Fuel Reprocessing," *Proc. Atalante 2004*, Nimes, France, 2004, pp. 1–25.

12. B. R. Westphal *et al.*, "Fission Product Removal from Spent Oxide Fuel by Head-End Processing," *Proceedings of GLOBAL 2005*, paper no. 345, Tsukuba, Japan, October 9–13, 2005.

13. *Development of Voloxidation Process for Treatment of LWR Spent Fuel*, INL-KAERI-ORNL, I-NERI Final Report, Project 2004-004-K, December 2007.

14. D. Majumdar, *Recycling of Nuclear Spent Fuel with AIROX Processing*, DOE/ID-10423, 1992.

15. G. E. Barnd and E. W. Murbach, *Pyrochemical Reprocessing of UO_2 by AIROX Summary Report*, NAA-SR-11389, 1965.

16. J. S. Lee, M. S. Yang, H. S. Park, J. D. Sullivan, P. G. Boczar, and R. D. Gadsby, "The DUPIC Fuel Cycle Synergism Between LWR and HWR," *Proc. IAEA Tech. Comm. Mtg. on Fuel Cycle Options for LWRs and HWRs*, Victoria, Canada, 1998.

17. Jang Jin Park *et al.*, "Technology and Implementation of the DUPIC Concept for Spent Nuclear Fuel in the ROK," LLNL Nuclear Cooperation Meeting on Spent Fuel and High-Level Waste Storage and Disposal, Las Vegas, Nevada, March 7–9, 2000.

18. Myung Seung Yang *et al.*, "The Status and Prospect of DUPIC Fuel Technology," *Nucl. Eng. Technol.* **38**(4), 359–373 (June 2006).

19. B. E Lewis, *An Unsteady-State Material Balance Model for a Continuous Rotary Dissolver*, ORNL/TM-9019, Union Carbide Corporation, Oak Ridge National Laboratory, Oak Ridge, Tennessee, September 1984.

20. H. Kleykamp, "The Chemical State of Fission Products in Oxide Fuels at Different Stages of the Nuclear Fuel Cycle," *Nucl. Technol.* **80**, 412–422 (March 1988).

21. D. Serrano-Purrog, B. Christiansen, R. Malnikeck, J. P. Glatz, P. Boron, C. Madis, and G. Modolo, "First DIAMEX Partitioning Using Genuine High Active Concentrate," *Proceedings of Atalante 2004 International Conference, Nimes, France*, 2004.

22. D. O. Campbell, "Considerations of Tc Behavior in TBP Extraction Flowsheet," personal communication, February 17, 2003.

23. J. C. Posey, *Process for the Recovery of Curium-244 from Nuclear Waste*, ORNL-5687, Oak Ridge National Laboratory, Oak Ridge, Tennessee, October 1980.

24. D. O. Campbell, "Separation of Lanthanide and Trivalent Actinides with Pressurized Ion Exchange," *Sep. Purif. Methods* **5**(1), 97–138 (1976).

25. W. W. Schulz and L. A. Bray, "Solvent Extraction Recovery of Byproduct Cs-137 and Sr-90 from HNO_3 Solutions – A Technology Review and Assessment," *Sep. Sci. Technol.* **22**(2&3), 191–214 (1987).

26. *Feasibility of Separation and Utilization of Caesium and Strontium from High Level Liquid Waste*, International Atomic Energy Agency, Vienna, 1993.

27. S. Tachimori, "Overview of Solvent Extraction Chemistry for Reprocessing," in *Ion Exchange and Solvent Extraction*, edited by B. A. Moyer, CRC Press, Boca Raton, Florida, 2010, Vol. 19, pp. 1–63.

28. T. A. Todd and R. A. Wigeland, "Advanced Separation Technologies for Processing Spent Nuclear Fuel and the Potential Benefits to a Geologic Repository," in *Separations for the Nuclear Fuel Cycle in the 21st Century*, edited by G. J. Nash, K. L. Clark, S. B. Friese, and G. J. Lumetta, American Chemical Society, Washington, D.C., 2006, Vol. 933, pp. 41–55.

29. J. J. Laidler, "An Overview of Spent-Fuel Processing in the Global Nuclear-Energy Partnership," in *International Solvent Extraction Conference ISEC 2008*, edited by B. A. Moyer, Canadian Institute of Mining, Metallurgy, and Petroleum, Tucson, Arizona, 2008, Vol. 1, pp. 695–701.

30. S. T. Arm, C. Phillips, and A. Dobson, "Industrial Applications of GNEP Solvent-Extraction Processes," in *Proceedings of the International Solvent Extraction Conference ISEC 2008*, edited by B. A. Moyer, Canadian Institute of Mining, Metallurgy, and Petroleum, Tucson, Arizona, 2008, Vol. 1, pp. 709–714.

31. V. N. Romanovsky, "Management of Accumulated High Level Waste at the Mayak Production Association in the Russian Federation," in *Issues and Trends in Radioactive Waste Management*, Proceedings of an International Conference, Vienna, 9–13 December, 2002, International Atomic Energy Agency, Vienna, 2003, pp. 359–372.

32. *Report to Congress: Status of Environmental Management Initiatives to Accelerate the Reduction of Environmental Risks and Challenges Posed by the Legacy of the Cold War*, DOE/EM-0001, U.S. Department of Energy, Office of Environmental Management, January 2009.

33. W. R. Wilmarth, M. E. Johnson, G. Lumetta, M. R. Poirier, M. C. Thompson, and N. Machara, *The Role of Liquid Waste Pretreatment Technologies in Solving the DOE Clean-up Mission*, Report No. SRNL-STI-2008-00426, Savannah River National Laboratory, October 2008.

34. "Nuclear Wastes: Technologies for Separations and Transmutation," National Research Council, National Academy Press, Washington, D.C., 1996.

35. T. L. Stewart, J. A. Frey, D. W. Geiser, and K. L. Manke, "Overview of U.S. Radioactive Tank Problem," in *Science and Technology for Disposal of*

Radioactive Tank Wastes, edited by W. W. Schultz and N. J. Lombardo, Plenum Press, New York, 1998, pp. 3–13.

36. E. H. Tusa, A. Paavola, R. Harjula, and J. Lehto, "Industrial-Scale Removal of Cesium with Hexacyanoferrate Exchanger – Process Realization and Test Run," *Nucl. Technol.* **107**(3), 279–284 (1994).

37. A. Kumar, L. Varshney, C. P. Kaushik, and K. Raj, "Recovery of Cs from High Level Radioactive Waste," in *Proc. DAE-BRNS Biennial Symposium on Emerging Trends in Separation Science and Technology*, edited by P. N. Pathak, R. M. Sawant, T. G. Srinivasan, V. S. Parmar, and V. K. Manchanda, Department of Atomic Energy, New Dehli, India, 2008, pp. 64–72.

38. S. K. Samanta, "Recovery of ^{137}Cs from Radioactive Liquid Waste," in *DAE-BRNS Symposium on Emerging Trends in Separation Science and Technology*, edited by P. K. Mohapatra, R. M. Sawant, B. Venkataramani, and V. K. Manchanda, Department of Atomic Energy, Mumbai, India, 2006, pp. 32–41.

39. J. Rais and P. Selucky, "New Extraction Agents for Cesium-III. Complex Formed between Some Cesium Salts and 2,3,11,12-Dibenzo-1,4,7,10,13,16-hexaoxocyclooctadeca-2,11-diene (dibenzo-18-crown-6)," *Radiochem. Radioanal. Lett.* **6**(4), 257–264 (1971).

40. V. V. Yakshin, V. M. Abashkin, and B. N. Laskorin, "Effect of Anions on the Extraction of Alkali Metal Salts," *Dokl. Akad. Nauk SSSR* **252**(2), 373–376 (1980).

41. W. J. McDowell and R. R. Shoun, "An Evaluation of Crown Compounds in Solvent Extraction of Metals," in *International Solvent Extraction Conference (ISEC 77)*, edited by B. H. Lucas, G. M. Ritcey, and H. W. Smith, Canadian Institute of Mining and Metallurgy, Montreal, Canada, 1977, Vol. 1, pp. 95–100.

42. P. R. Danesi, H. Meider-Gorican, R. Chiarizia, and G. Scibona, "Extraction Selectivity of Organic Solutions of a Cyclic Polyether with Respect to the Alkali Cations," *J. Inorg. Nucl. Chem.* **37**, 1479–1483 (1975).

43. J. Rais, M. Kyrs, and L. Kadlecova, "Extraction of Some Univalent and Bivalent Metals in the Presence of Macrocyclic Polyether," in *Proceedings of the International Solvent Extraction Conference (ISEC '74)*, Society of Chemical Industry, London, 1974, Vol. 2, pp. 1705–1715.

44. H. D. Martin, M. A. Schmitz, M. A. Ebra, D. D. Walker, L. L. Kilpatrick, and L. M. Lee, "In-Tank Precipitation Process for Decontamination of Water Soluble Radioactive Waste [SodiumTetraphenylborate]," *Waste Management '84*, Tucson, Arizona, March 11, 1984; Report DP-MS-84-11, E. I. DuPont de Nemours & Co., Savannah River Laboratory, Aiken, South Carolina, 1984.

45. P. A. Haas, "A Review of Information on Ferrocyanide Solids for Removal of Cesium from Solutions," *Sep. Sci. Technol.* **28**, 2479–2506 (1993).

46. T. J. Tranter, T. A. Vereshchagina, and V. Utgikar, "An Inorganic Microsphere Composite for the Selective Removal of [137]Cesium from Acidic Nuclear Waste Solutions. 2: Bench-Scale Column Experiments, Modeling, and Preliminary Process Design," *Solvent Extr. Ion Exch.* **27**(2), 219–243 (2009).

47. T. J. Tranter, R. S. Herbst, T. A. Todd, A. L. Olson, and H. B. Eldredge, "Evaluation of Ammonium Molybdophosphate-Polyacrylonitrile (AMP-PAN) as a Cesium Selective Sorbent for the Removal of Cs-137 from Acidic Nuclear Waste Solutions," *Adv. Environ. Res.* **6**(2), 107–121 (2002).

48. T. A. Todd, K. N. Brewer, D. J. Wood, P. A. Tullock, N. R. Mann, and L. G. Olson, "Evaluation and Testing of Inorganic Ion Exchange Sorbents for the Removal

of Cesium-137 from Actual Idaho Nuclear Technology and Engineering Center Acidic Tank Waste," *Sep. Sci. Technol.* **36**(5–6), 999–1016 (2001).

49. T. B. Peters, M. R. Poirier, C. A. Nash, F. F. Fondeur, S. D. Fink, S. J. Brown, and E. A. Brass, "Testing and Startup of the Savannah River Site Integrated Salt Disposition Process," in *Waste Management 2009 (WM2009)*, American Nuclear Society, Phoenix, Arizona, 2009, Paper 9193.

50. T. B. Peters, M. J. Barnes, D. T. Hobbs, D. D. Walker, F. F. Fondeur, M. A. Norato, S. D. Fink, and R. L. Pulmano, "Strontium and Actinide Separations from High Level Nuclear Waste Solutions Using Monosodium Titanate 2. Actual Waste Testing," *Sep. Sci. Technol*. **41**(11), 2409–2427 (2006).

51. D. T. Hobbs, M. J. Barnes, R. L. Pulmano, K. M. Marshall, T. B. Edwards, M. G. Bronikowski, and S. D. Fink, "Strontium and Actinide Separations from High Level Nuclear Waste Solutions Using Monosodium Titanate 1. Simulant Testing," *Sep. Sci. Technol*. **40**(15), 3093–3111 (2005).

52. R. D. Hunt, J. L. Collins, K. Adu-Wusu, M. L. Crowder, D. T. Hobbs, and C. A. Nash, "Monosodium Titanate in Hydrous Titanium Oxide Spheres for the Removal of Strontium and Key Actinides from Salt Solutions at the Savannah River Site," *Sep. Sci. Technol.* **40**(14), 2933–2946 (2005).

53. J. E. Miller, N. E. Brown, J. L. Krumhansl, D. E. Trudell, R. G. Anthony, and C. V. Philip, "Development and Properties of Cesium Selective Crystalline Silicotitanate (CST) Ion Exchangers for Radioactive Waste Applications," in *Science and Technology for Disposal of Radioactive Tank Wastes*, edited by W. W. Schultz and N. J. Lombardo, Plenum Press, New York, 1998, pp. 269–286.

54. C. A. Nash, W. R. Wilmarth, D. D. Walker, C. E. Duffey, B. D. King, M. R. Thorson, J. Meehan, D. J. Sherwood, S. K. Fiskum, K. P. Brooks, I. E. Burgeson, S. T. Arm, and D. L. Blanchard, Jr., "Cesium Exchange Program at the Hanford River Protection Project Waste Treatment Plant," in *Waste Management '05*, Tucson, Arizona, 2005, Paper 5343; Report WSRC-MS-2004-00802, Savannah River National Laboratory, Aiken, South Carolina.

55. S. K. Fiskum, S. T. Arm, M. K. Edwards, M. J. Steele, and K. K. Thomas, *Storage and Aging Effects on Spherical Resorcinol-Formaldehyde Resin Ion Exchange Performance*, Report No. WTP-RPT-148, Rev. 0, Pacific Northwest National Laboratory, Richland, Washington, September 2007.

56. T. Takata, Y. Koma, K. Sato, M. Kamiya, A. Shibata, K. Nomura, H. Ogino, T. Koyama, and S. Aose, "Conceptual Design Study on Advanced Aqueous Reprocessing System for Fast Reactor Fuel Cycle," *J. Nucl. Sci. Technol.* **41**(3), 307–314 (2004).

57. L. Nassif, G. Dumont, H. Alysouri, and R. W. Rousseau, "Pretreatment of Hanford Medium-Curie Wastes by Fractional Crystallization," *Environ. Sci. Technol.* **42**(13), 4940–4945 (2008).

58. D. L. Herting, *Fractional Crystallization Flowsheet Tests with Actual Tank Waste*, Report No. RPP-RPT-31352, CH2M HILL Hanford Group, Inc., Richland, Washington, April 2007.

59. D. D. Walker, M. J. Barnes, C. L. Crawford, R. A. Peterson, R. F. Swingle, and S. D. Fink, "In-tank-preparation with tetraphenylborate: recent progress and research results," in *Science and Technology for Disposal of Radioactive Tank Wastes*, edited by W. W. Schultz and N. J. Lombardo, Plenum Press, New York, 1998, pp. 219–230.

60. T. B. Peters, M. J. Barnes, F. F. Fondeur, S. D. Fink, R. W. Blessing, R. E. Norcia, J. G. Firth, C. W. Kennell, T. R. Tipton, and B. B. Anderson, *Demonstration of Small Tank Tetraphenylborate Precipitation Process Using Savannah River Site High Level Waste*, Report WSRC-TR-2001-00211, Savannah River National Laboratory, Aiken, South Carolina, May 31, 2001.

61. J. F. Dozol, M. Dozol, and R. M. Macias, "Extraction of Strontium and Cesium by Dicarbollides, Crown Ethers and Functionalized Calixarenes," *J. Incl. Phenom. Macrocycl. Chem.* **38**(1–4), 1–22 (2000).

62. J. Rais and B. Grüner, "Extraction with Metal Bis(dicarbollide) Anions: Metal Bis(dicarbollide) Extractants and Their Applications in Separation Chemistry," in *Ion Exchange and Solvent Extraction*, edited by Y. Marcus, A. K. Sengupta, and J. A. Marinsky, Marcel Dekker, New York, 2004, Vol. 17, pp. 243–334.

63. E. P. Horwitz and W. W. Schulz, "Solvent Extraction in the Treatment of Acidic High-Level Liquid Waste: Where Do We Stand?" in *Recent Advances in Metal-Ion Separation and Preconcentration*, edited by A. H. Bond, M. L. Dietz, and R. D. Rogers, American Chemical Society, Washington, D.C., 1999, Vol. 716, pp. 20–50.

64. J.-F. Dozol and R. Ludwig, "Extraction of Radioactive Elements by Calixarenes," in *Ion Exchange and Solvent Extraction*, edited by B. A. Moyer, CRC Press, Boca Raton, Florida, 2010, Vol. 19, pp. 195–318.

65. V. A. Babain, "Simultaneous Removal of Radionuclides by Extractant Mixtures," in *Ion Exchange and Solvent Extraction*, edited by B. A. Moyer, CRC Press, Boca Raton, Florida, 2010, Vol. 19, pp. 359–380.

66. R. S. Herbst, J. D. Law, T. A. Todd, V. N. Romanovskiy, I. V. Smirnov, V. A. Babain, V. N. Esimantovskiy, and B. N. Zaitsev, "Development of the Universal Extraction (UNEX) Process for the Simultaneous Recovery of Cs, Sr, and Actinides from Acidic Radioactive Wastes," *Sep. Sci. Technol.* **38**(12–13), 2685–2708 (2003).

67. Y. Marcus, *Ion Properties*, Marcel Dekker, New York, 1997.

68. B. A. Moyer and Y. Sun, "Principles of Solvent Extraction of Alkali Metal Ions: Understanding Factors Leading to Cesium Selectivity in Extraction by Solvation," in *Ion and Exchange and Solvent Extraction*, edited by Y. Marcus and J. A. Marinsky, Marcel Dekker, New York, 1997, Vol. 13, pp. Chap. 6, pp. 295–391.

69. J. Rais, P. Selucky, and M. Kyrs, "Extraction of Alkali Metals into Nitrobenzene in the Presence of Univalent Polyhedral Borate Anions," *J. Inorg. Nucl. Chem.* **38**, 1376–1378 (1976).

70. R. S. Herbst, D. R. Peterman, and R. D. Tillotson, "Aspects of the Fundamental Chemistry of Cesium Extraction from Acidic Media by HCCD," *Czech. J. Phys.* **56**, D477–D482 (2006).

71. R. S. Herbst, J. D. Law, T. A. Todd, V. N. Romanovskii, V. A. Babain, V. M. Esimantovski, B. N. Zaitsev, and I. V. Smirnov, "Development and Testing of a Cobalt Dicarbollide Based Solvent Extraction Process for the Separation of Cesium and Strontium from Acidic Tank Waste," *Sep. Sci. Technol.* **37**(8), 1807–1831 (2002).

72. J. D. Law, R. S. Herbst, D. R. Peterman, R. D. Tillotson, and T. A. Todd, "Development of a Cobalt Dicarbollide/Polyethylene Glycol Solvent Extraction Process for Separation of Cesium and Strontium to Support Advanced Aqueous Reprocessing," *Nucl. Technol.* **147**(2), 284–290 (2004).

73. W. J. McDowell, "Crown Ethers as Solvent Extraction Reagents: Where Do We Stand?" *Sep. Sci. Technol*. **23**, 1251–1268 (1988).

74. E. Blasius and K.-H. Nilles, "The Removal of Cesium from Medium-Active Waste Solutions. I. Evaluation of Crown Ethers and Special Crown-Ether Adducts in the Solvent Extraction of Cesium," *Radiochim. Acta* **35**, 173–182 (1984).

75. E. Blasius and K.-H. Nilles, "The Removal of Cesium from Medium-Active Waste Solutions. II. Solvent-Extraction Using Adducts of Dibenzo-21-crown-7 with 12-Heteropoly-Compounds and Hexachloroantimonates(V) in an Organic-Solvent – Continuous Extraction – Preparation, Capacities, Bleeding and Regeneration of the Extractants," *Radiochim. Acta* **36**(4), 207–214 (1984).

76. W. J. McDowell, G. N. Case, J. A. McDonough, and R. A. Bartsch, "Selective Extraction of Cesium from Acidic Nitrate Solutions with Didodecylnaphthalene-sulfonic Acid Synergized with Bis(*tert*-butylbenzo)-21-crown-7," *Anal. Chem*. **64**, 3013–3017 (1992).

77. E. P. Horwitz, M. L. Dietz, and D. E. Fisher, "Correlation of the Extraction of Strontium Nitrate by a Crown Ether with the Water-Content of the Organic-Phase," *Solvent Extr. Ion Exch*. **8**(1), 199–208 (1990).

78. E. P. Horwitz, M. L. Dietz, and D. E. Fisher, "SREX – A New Process for the Extraction and Recovery of Strontium from Acidic Nuclear Waste Streams," *Solvent Extr. Ion Exch*. **9**(1), 1–25 (1991).

79. M. L. Dietz, E. P. Horwitz, and R. D. Rogers, "Extraction of Strontium from Acidic Nitrate Media Using a Modified PUREX Solvent," *Solvent Extr. Ion Exch*. **13**(1), 1–17 (1995).

80. J. D. Law, R. S. Herbst, and T. A. Todd, "Integrated AMP-PAN, TRUEX, and SREX Testing. II. Flowsheet Testing for Separation of Radionuclides from Actual Acidic Radioactive Waste," *Sep. Sci. Technol*. **37**(6), 1353–1373 (2002).

81. N. N. Egorov, M. A. Zakharov, L. N. Lazarev, R. I. Lyubtsev, A. S. Nikiforov, M. V. Strakhov, and E. A. Filippov, "New Solutions to the Problem of Handling Long Lived Radionuclides," *Sov. At. Energy* **72**(2), 148–150 (1992).

82. E. A. Filippov, E. G. Dzekun, A. K. Nardova, I. V. Mamakin, V. M. Gelis, and V. V. Milyutin, "Application of Crown Ethers and Ferrocyanide-Based Inorganic Material for Cesium and Strontium Recovery from High-Level Radioactive Wastes," in *Waste Management '92*, Tucson, Arizona, March 1–5, 1992, Vol. 2, pp. 1021–1025.

83. I. V. Mamakin, A. K. Nardova, E. A. Filippov, T. V. Zhavoronkova, L. D. Efimova, E. G. Dzekun, Yu. Z. Prokopchuk, A. I. Bardov, and N. G. Yakovlev, "Recovery of Strontium from Liquid Nitric Acid–Containing Wastes from Nuclear Power Plants by Extraction with Organic Solution of Dicyclohexyl-18-crown-6," *Izobreteniya* **37**(3), (1992).

84. J. C. Wang and C. L. Song, "Hot Test of Partitioning Strontium from High-Level Liquid Waste (HLLW) by Dicyclohexano-18-crown-6 (DCH18C6)," *Radiochim. Acta* **89**(3), 151–154 (2001).

85. M. L. Dietz and E. P. Horwitz, "Combining Solvent Extraction Processes for Actinide and Fission Product Separations," in *Science and Technology for Disposal of Radioactive Tank Wastes*, edited by W. W. Schulz and N. J. Lombardo, Plenum Press, New York, 1998, pp. 231–243.

86. R. A. Sachleben, Y. Deng, and B. A. Moyer, "Ring-Size and Substituent Effects in the Solvent Extraction of Alkali Metal Nitrates by Crown Ethers in

1,2-Dichloroethane and 1-Octanol," *Solvent Extr. Ion Exch.* **14**(6), 995–1015 (1996).

87. M. L. Dietz, E. P. Horwitz, M. P. Jensen, S. Rhoads, R. A. Bartsch, A. Palka, J. Krzykawski, and J. Nam, "Substituent Effects in the Extraction of Cesium from Acidic Nitrate Media with Macrocyclic Polyethers," *Solvent Extr. Ion Exch.* **14**(3), 357–384 (1996).

88. I. V. Smirnov, V. N. Romanovskii, and V. I. Kal'chenko, "New Extraction Systems Based on Crown-Ethers for Selective Recovery of Cesium from High-Level Wastes," in *International Topical Meeting on Nuclear and Hazardous Waste Management, Spectrum '94*, American Nuclear Society, August 14–18, 1994, Atlanta, Georgia, 1994, Vol. 2, pp. 1547–1549.

89. E. P. Horwitz, M. L. Dietz, and M. P. Jensen, "A Combined Cesium-Strontium Extraction/Recovery Process," in *International Solvent Extraction Conference (ISEC '96)*, University of Melbourne, Melbourne, Australia, March 17–21, 1996, Vol. 2, pp. 1285–1290.

90. R. Ungaro, A. Casnati, F. Ugozzoli, A. Pochini, J. F. Dozol, C. Hill, and H. Rouquette, "1,3-Dialkoxycalix[4]arenecrowns-6 in 1,3-Alternate Conformation: Cesium-Selective Ligands that Exploit Cation-Arene Interactions," *Angew. Chem.-Int. Edit. Engl.* **33**, 1506–1509 (1994).

91. Z. Asfari, C. Bressot, J. Vicens, C. Hill, J. F. Dozol, H. Rouquette, S. Eymard, V. Lamare, and B. Tournois, "Doubly Crowned Calix[4]arenes in the 1,3-Alternate Conformation as Cesium-Selective Carriers in Supported Liquid Membranes," *Anal. Chem.* **67**, 3133–3139 (1995).

92. T. J. Haverlock, P. V. Bonnesen, R. A. Sachleben, and B. A. Moyer, "Analysis of Equilibria in the Extraction of Cesium Nitrate by Calix[4]arene-bis(*t*-octylbenzo-crown-6) in 1,2-Dichloroethane," *J. Incl. Phenom. Mol. Recogn. Chem.* **36**, 21–37 (2000).

93. R. A. Sachleben, P. V. Bonnesen, T. Descazeaud, T. J. Haverlock, A. Urvoas, and B. A. Moyer, "Surveying the Extraction of Cesium Nitrate by 1,3-Alternate Calix 4-arene crown-6 Ethers in 1,2-Dichloroethane," *Solvent Extr. Ion Exch.* **17**(6), 1445–1459 (1999).

94. J. F. Dozol, N. Simon, V. Lamare, H. Rouquette, S. Eymard, B. Tournois, D. De Marc, and R. M. Macias, "A Solution for Cesium Removal from High-Salinity Acidic or Alkaline Liquid Waste: The Crown Calix[4]arenes," *Sep. Sci. Technol.* **34**, 877–909 (1999).

95. P. V. Bonnesen, T. J. Haverlock, N. L. Engle, R. A. Sachleben, and B. A. Moyer in *Calixarene Molecules for Separations*, edited by G. J. Lumetta, R. D. Rogers, and A. S. Gopalan, American Chemical Society, Washington, DC, 2000, Vol. 757, pp. 26–44.

96. C. L. Riddle, J. D. Baker, J. D. Law, C. A. McGrath, D. H. Meikrantz, B. J. Mincher, D. R. Peterman, and T. A. Todd, "Fission Product Extraction (FPEX): Development of a Novel Solvent for the Simultaneous Separation of Strontium and Cesium from Acidic Solutions," *Solvent Extr. Ion Exch.* **23**, 449–461 (2005).

97. B. A. Moyer, J. F. Birdwell, Jr., P. V. Bonnesen, and L. H. Delmau, "Use of Macrocycles in Nuclear-Waste Cleanup: A Real-World Application of a Calix-crown in Technology for the Separation of Cesium," in *Macrocyclic Chemistry – Current Trends and Future Perspectives*, edited by K. Gloe, Springer, Dordrecht, 2005, pp. 383–405.

98. P. V. Bonnesen, L. H. Delmau, B. A. Moyer, and G. J. Lumetta, "Development of Effective Solvent Modifiers for the Solvent Extraction of Cesium from Alkaline High-Level Tank Waste," *Solvent Extr. Ion Exch.* **21**(2), 141–170 (2003).

99. R. A. Leonard, S. B. Aase, H. A. Arafat, C. Conner, D. B. Chamberlain, J. R. Falkenberg, M. C. Regalbuto, and G. F. Vandegrift, "Experimental Verification of Caustic-Side Solvent Extraction for Removal of Cesium from Tank Waste," *Solvent Extr. Ion Exch.* **21**, 505–526 (2003).

100. M. A. Norato, M. H. Beasley, S. G. Campbell, A. D. Coleman, M. W. Geeting, J. W. Guthrie, C. W. Kennell, R. A. Pierce, R. C. Ryberg, D. D. Walker, J. D. Law, and T. A. Todd, "Demonstration of the Caustic-Side Solvent Extraction Process for the Removal of ^{137}Cs from Savannah River Site High Level Waste," *Sep. Sci. Technol.* **38**, 2647–2666 (2003).

101. T. B. Peters, M. R. Poirier, C. A. Nash, F. F. Fondeur, S. D. Fink, S. J. Brown, and E. A. Brass, in *Proceedings Waste Management 2009 (WM2009)*, Phoenix, Arizona, March 1–5, 2009, American Nuclear Society, Phoenix, Arizona, 2009, Paper 9193.

102. N. L. Engle, P. V. Bonnesen, B. A. Tomkins, T. J. Haverlock, and B. A. Moyer, "Synthesis and Properties of Calix 4 arene-bis 4-(2-ethylhexyl)benzo-crown-6, a Cesium Extractant with Improved Solubility," *Solvent Extr. Ion Exch.* **22**, 611–636 (2004).

103. L. H. Delmau, J. F. Birdwell, Jr., J. McFarlane, and B. A. Moyer, "Robustness of the CSSX Process to Feed Variation: Efficient Cesium Removal from the High Potassium Wastes at Hanford," *Solvent Extr. Ion Exch.* **28**(1), 19–48 (2010).

104. R. Custelcean, J. Bosano, P. V. Bonnesen, V. Kertesz, and B. P. Hay, "Computer-Aided Design of a Sulfate-Encapsulating Receptor," *Angew. Chem. Int. Ed.* **48**, 4025–4029 (2009).

9

Combined processes for high level radioactive waste separations: UNEX and other extraction processes

V. N. ROMANOVSKIY, I. V. SMIRNOV, V. A. BABAIN, and A. YU SHADRIN, Khlopin Radium Institute, Russia

Abstract: This chapter concerns the development of the universal extraction (UNEX) process and some new variations in its application. Choice of synergistic additives and diluents for chlorinated cobalt dicarbollide (CCD) are discussed. The results of many tests with actual and simulated high-level wastes (HLW) were observed and compared. The use of regenerable stripping solutions containing methylamine carbonate allows simplification of the handling and a volume reduction in the high-level strip product. The replacement of carbamoylphosphine oxides by diamides of dipicolinic acid as constituents of the UNEX extractant makes it possible to use less expensive extractants which can also treat wastes with elevated concentrations of rare-earth elements (REE). Possibilities for radionuclide group separation by the UNEX process were investigated using different stripping solutions. In this way, the following group separations are possible: An + REE + Sr and, separately, Cs; An + REE and, separately, Cs + Sr; finally, Cs, Sr, and An + REE separately. Recovery of radionuclides into individual fractions permits their transformation into more stable storage matrices.

Key words: chlorinated cobalt dicarbollide, UNEX process, treatment of radioactive wastes, waste partitioning, extraction of actinides.

9.1 Introduction to universal extraction process (UNEX) and other processes

Today, in many countries possessing highly developed nuclear power, the concept of a closed nuclear fuel cycle (NFC) with reprocessing of spent nuclear fuel (SNF) prevails. One advantage of the closed NFC is the possibility of a radical solution to the problem concerning long-term safe management of long-lived radionuclides, as SNF reprocessing allows these radionuclides to be recovered and handled individually.

Transmutation is a reliable method for the management of long-lived radionuclides. Another promising method is based on the creation of especially strong matrices to be disposed of in geological formations. In both cases, the long-lived radionuclides contained in SNF must be selectively recovered. The bulk of long-lived radionuclides are contained in liquid high-level wastes (HLW) arising from SNF reprocessing. Therefore, the

229

problem of individual or group separation of long-lived radionuclides from HLW calls for the development of effective partitioning methods. The composition of the fractions depends on the chosen method for further management of ecologically hazardous radionuclides, i.e. on their transmutation or production of stable matrices for their prolonged storage or final disposal.

The most important fractions generated by HLW reprocessing are:

- cesium and strontium (in combination or separately);
- actinides and lanthanides (in combination or separately).

Among the different ways of HLW partitioning (precipitation, sorption, chromatography, etc.), extraction processes are of special interest. The following extraction systems should be considered as most promising:

- neutral organophosphorus compounds (alkylphosphine oxides [1,2,3], carbamoylphosphine oxides [4,5], phosphorilated calixarenes [6]);
- acidic organophosphorus compounds (diisodecylphosphoric acid [7], zirconium salts of dialkylphosphoric acids [8]);
- macrocyclic compounds (crown-ethers [9], calix-crowns [10]);
- diamides (DIAMEX-process [11,12] or ARTIST-process [13]);
- hydrophobic anions in polar diluents (chlorinated cobalt dicarbolide – CCD [14]);
- synergistic mixtures of different extractants [15–18].

So far, the only method which has found commercial application is extraction of cesium and strontium by CCD [19]. CCD was first proposed for Cs and Sr extraction by Czech scientists [20] and the technological bases of this process were then elaborated by Czech and Russian scientists; thereafter, specialists at the Khlopin Radium Institute (KRI) and Production Association Mayak (Mayak PA) developed the process up to its introduction at a radiochemical plant [21].

A problem encountered in the development of technology for HLW management concerned the recovery of actinides (uranium, neptunium, plutonium, americium, curium) and rare-earth elements (REE), along with cesium and strontium. The problem could be solved by using the above-listed extraction systems, for example the UREX (Uranium Extraction) process [22]. However, the extraction of several extractants in several extraction cycles is more expensive when compared to extracting everything in one extraction cycle, so extractants for the simultaneous recovery of different fractions from HLW are of great interest.

9.2   Universal processes for recovery of long-lived radionuclides

Czech scientists proposed the mixture of CCD with bifunctional neutral organophosphorus compounds (BNOPC) for the extraction of actinides,

lanthanides and cesium (strontium was inadequately recovered in this case) [23]. Studies at the Radium Institute have shown [24,25] that the synergistic mixtures of CCD with long-chained (n > 5) phosphorylated polyethylene glycols (PGP – $Ph_2P(O)CH_2O(CH_2CH_2O)_nCH_2P(O)Ph_2$) can simultaneously recover cesium, strontium, actinides and lanthanides from HNO_3 media.

None of the then known extraction systems had such unique extraction properties, and these new developments therefore permitted a universal extraction mixture (UEM) to be patented in 1990. This mixture was successfully proven to work for simulated and real HLW. Tests were conducted on the recovery of radionuclides from a solution simulating the PUREX process raffinate, containing 1 M HNO_3 and the following metals (g/l): REE – 2.1; cesium – 0.3; strontium – 0.25; sodium – 1.5; iron – 1.0 with a total salt content of ~10 g/l. From this solution, the UEM (containing 0.14 M CCD and 0.08 M PGP-300 in metanitrobenzotrifluoride (F-3)) recovered radionuclides with distribution ratios of: U(VI) – 6.0; Pu(IV) – 5.1; Np(V) – 4.0; Np(VI) – 6.4; Am – 1.2; Cs – 2.6; Sr – 16.

Extraction of several radionuclides from HLW was proven in a continuous regime in the centrifugal extraction bench EZ-40–18 at Mayak PA (Fig. 9.1) by using a UEM composition of 0.14 M CCD and 0.08 M PGP-300 in F-3, with density of 1426 g/cm^3 and viscosity 5,4 mPa*s at 20°C.

More than 20 L of simulated HLW were treated within 20 hours, with the organic phase making over 15 recycles. Cesium, strontium and REE were
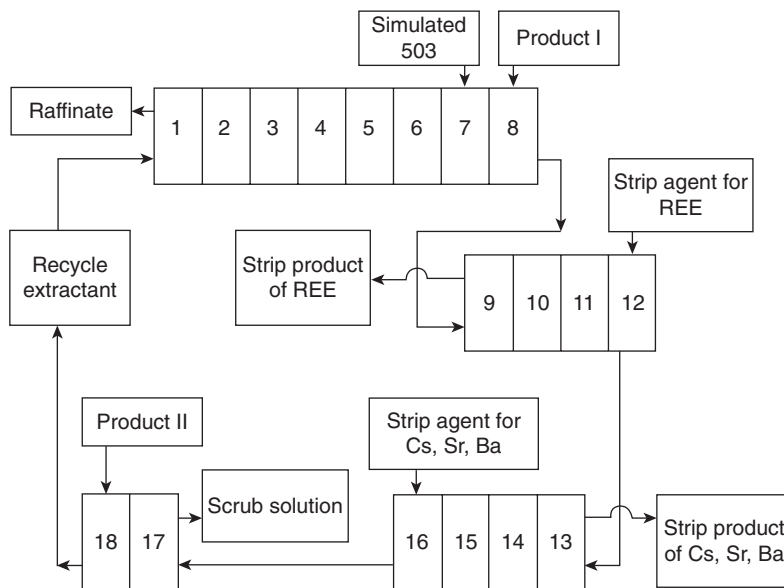
9.1 Flowsheet of HLW treatment.

Table 9.1 Distribution of metals in process solutions (Fig 9.1)

Element	Content, % of initial value		
	Raffinate	Strip agent of REE	Strip agent of Cs, Sr, Ba
Cs, Sr, Ba	<0.5	~1	>98
Y	<0.2	>98	~1
Fe	~5	~90	~5
Al	>90	~6	<1
Ni, Cr	>98	<1	<0.5

completely recovered (by more than 99.5%) at a flow ratio of organic and aqueous phases up to 1.2. In addition to the radionuclides, only barium and iron were markedly co-extracted (Table 9.1). After tests in accordance with data analysis for cobalt and phosphorus, the organic phase contained 0.17 M CCD and 0.09 M PGP-300, these increases being connected to the high solubility of F-3 in 5 M HNO_3. The extraction, hydrodynamic and kinetic characteristics of the system were unchanged during the tests. The UEM was also proven on real HLW under static conditions. Real HLW containing 1.5 M HNO_3, ~20 g/l salts, $1\cdot10^{10}$ Bq/l α-nuclides (13% Pu, 55% Am, 31% Cm) and $7.4\cdot10^{10}$ Bq/l β- and γ-nuclides was used as the feed solution.

In the course of testing, no precipitates, second organic phase or interphase films were formed. In extraction operations, more than 99.97% α-nuclides and ~96% β- and γ-nuclides were recovered from HLW by five successive contacts with fresh extractant. After double treatment of the extract by strip agents, firstly using 5 M HNO_3 + 100 g/l hydrazine nitrate + 100 g/l acetamide, and secondly using 1 M HNO_3 + 20 g/l oxyethylidene biphosphonic acid (OEDPA) + 100 g/l acetamide, less than 0.1% α- and less than 1% β- and γ-nuclides remained in the organic phase.

Hence, the tests performed demonstrated the possibility of using the UEM system for recovery of long-lived radionuclides from HLW in the framework of a single-extractant work flow. However, its practical application was hampered for the following reasons:

- the need to decrease HLW acidity resulting in an increase of volumes of feed solutions;
- the use of complexones and salts of organic acids for stripping of actinides and lanthanides, which makes further handling of the strip product more difficult;
- insufficient mutual purification of Cs-Sr and An-Ln fractions.

Additionally, the use of this system is complicated by the fact that the synthesis and purification of phosphorylated PEGs is a rather sophisticated

and cumbersome process, which is difficult to achieve even on a laboratory scale.

These circumstances have encouraged scientists at the Radium Institute (RI) and the Idaho National Laboratory (INL), USA, to collaborate on the modification of the above extraction system, which has resulted in the elaboration of the so-called UNEX process (UNiversal EXtraction process). In the UNEX process, a mixture of the commercial reagents CCD, PEG-400 and diphenyl-N,N-dibutylcarbamoyl-phosphinoxide is used in the diluent as the extraction system.

9.3 Development and testing of the universal extraction (UNEX) process and its modifications

9.3.1 Composition and properties of extractant for joint recovery of cesium, strontium, actinides and REE from HLW (UNEX process)

On the basis of data already available in the literature, it can be assumed that the three-component mixture of CCD-PEG-BNOPC in the diluent should simultaneously extract Cs, Sr, actinides and REE from acidic media. Preliminary tests have confirmed this assumption, but they have also revealed the complexity of such a system. It has been established that the content of each component of the extraction mixture concurrently affects the extraction of all radionuclides. So, with a constant content of CCD and BNOPC, but increasing PEG concentration, the distribution coefficients of Cs decrease monotonically, whilst those of Sr increase rapidly and then decrease; in the case of Eu these values increase slightly and then decrease.

With increasing BNOPC concentration the distribution coefficients of Cs and Sr decrease, those of Eu increase fast and then decrease slowly. Additionally, it has been found that CCD forms complexes with BNOPC which are soluble in organic solvents to a lesser degree than are individual CCD and BNOPC. The strong dependence of Eu extraction by CCD-BNOPC mixtures on the structure of the latter is also detected. Therefore, to determine the best composition of a UNEX extractant, it is necessary to select the correct BNOPC, PEG and diluent in such a manner that the high extraction ability of the mixture is in good agreement with its stability.

Choice of BNOPC for UNEX extractant

For BNOPCs, a high extraction ability in mixtures with CCD is manifested by diphosphine dioxides and carbamoylphosphineoxides. When selecting a

Table 9.2 Extraction of metals from 3 M HNO₃ 0.06 M CCD solution and 1% vol. Slovafol-909 in F-3 as a function of BNOPC concentration

CMPO	Concentration of BNOPC, M/l	Distribution coefficients					
		Cs	Sr	Eu	Pu	Np	Am
PhOct(Bu)₂	0.01	7.02	15.2	1.97	23	11	–
	0.02	4.78	14.8	4	140	75	–
	0.03	1.98	10.9	250	–	–	–
	0.04	1.10	8.24	>1000	490	370	–
Ph₂Bu₂	0.01	6.1	12.3	17.9	430	770	–
	0.02	4.0	11.5	300	700	>500	–
	0.03	2.3	9.4	>1000	–	–	–
	0.04	0.95	6.0	>1000	430	>2000	–
	0.06	0.26	3.7	>1000	–	–	–
OctO₂Bu₂	0	9.2	–	0.002	–	–	0.01
	0.02	2.8	9.2	0.4	60	13	0.69
	0.03	0.98	5.7	1.8	–	–	3.9
	0.04	0.35	2.5	4.1	200	33	14.3
	0.06	0.17	0.8	7.1	–	–	20
	0.1	0.1	0.2	8.2	90	10	25

BNOPC for UNEX-extractant, preference is given to carbamoyl compounds, because synthesis of diphosphine dioxides is much more complicated and they are poorly soluble even in polar diluents. Furthermore, positive experience has been accumulated on the use of carbamoyl compounds in radiochemical processes (in the TRUEX-process).

The extraction properties of CCD mixtures with the three most used BNOPCs, of carbamoyl type, were investigated:

1. phenyl(octyl)-N,N-diisobutylcarbamoylphosphineoxide (PhOctiBu₂);
2. diphenyl-N,N-dibutylcarbamoylmethylenephosphineoxide (Ph₂Bu₂);
3. dioctyl-N,N-dibutylcarbamoylmethylene phosphonate (Oct₂Bu₂).

The first of these compounds is used in the "classical" TRUEX process, the second in the Russian version of the TRUEX process, and the third – carbamoylphosphonate – is chosen as the most simple to synthesize and most readily soluble in any diluent. The results of investigations of the extraction properties of CCD mixtures with these compounds are presented in Table 9.2.

The data given in Table 9.2 bear witness to the crucial possibility for application of any one of the investigated BNOPCs in the composition of a UNEX extractant. The extraction properties of CCD-BNOPC mixtures have been compared and the stability of these mixtures has been verified in the course of the extraction process (Table 9.3).

Table 9.3 Extraction of metals from 3 M HNO_3 0.06 M CCD solution + 1% vol. Slovafol-909 + 0.02 M CMPO in F-3

CMPO	Distribution coefficients				
	Cs	Sr	Eu	Pu	Np
$Ph_2(Bu)_2$	4	12	300	700	>500
$PhOct(iBu)_2$	5	15	4	140	80
$OctO_2Bu_2$	3	9	0.4	60	10

It follows from Table 9.3 that a mixture of CCD – Ph_2Bu_2 exhibits the best extraction properties, but this mixture can be prepared only with the use of nitroaromatic diluents. The mixtures of CCD with $PhOct(iBu)_2$ and especially with $OctO_2Bu_2$ are also stable in less polar diluents such as fluorinated ethers. However, further studies have shown that such extractants in contact with simulated HLW solutions form a third phase, due to the insufficient solubility of metal solvates with CCD and BNOPC. Thus, irrespective of CMPO type, a diluent with high solvability should be used for preparation of the universal extraction mixture.

Choice of polyethylene glycol (PEG) for the UNEX process

Polyethylene glycol (PEG) is known to be a synergistic additive to CCD, increasing Sr recovery from strongly acidic media. The mechanism of this effect is not uniquely determined, but it may be assumed that PEG molecules form a complex with CCD possessing a similar crown cavity which provides solvation of the strontium cation. It has been established that in the CCD-PEG system the synergistic effect takes place when the PEG molecule contains no less than six oxyethyl links. From a practical point of view it is more reasonable to use the substituted PEGs, since they are scrubbed out of the organic phase to a lesser extent. In previous investigations [20], it was shown that Slovafol-909 – n-nonylphenyl ether of nonaethylene glycol – could be used as a synergistic addition to the CCD-PEG system. Slovafol-909 as a component of a UNEX extractant also allows good recovery of strontium (Table 9.4).

It is evident from the data presented in Table 9.4 that, by increasing the Slovafol content in the UNEX extractant, the degree of recovery increases for strontium and decreases for cesium, i.e. the same regularities as those of double mixtures of CCD – PEG are observed. Slovafol does not practically affect the extraction of actinides and REE. To choose a PEG for practical purposes, extraction of radionuclides by mixtures of CCD-PEG-CMPO containing different PEGs was investigated. The results obtained

Table 9.4 Extraction of metals from 3 M HNO_3 0.06 M CCD, 0.02 M CMPO and Slovafol-909 in F-3

CMPO	Concentration of Slovafol-909, %	Distribution coefficients				
		Cs	Sr	Eu	Pu	Np
PhOct(iBu)$_2$	0.4	10.0	7.7	4.1	340	90
	0.6	7.8	10.4	3.5	–	–
	1.0	5.3	15.1	3.6	170	75
	1.5	2.6	17.2	5.8	–	–
Ph$_2$Bu$_2$	0.4	7.2	6.1	270	850	>1000
	0.6	5.8	8.9	260	–	–
	1.0	3.65	11.5	310	650	>1000
	1.5	1.7	12.2	93	–	–

Table 9.5 Extraction of radionuclides from simulated solution of Idaho HLW (see Table 9.4) by mixture of 0.15 M CCD + 0.025 M Ph$_2$Bu$_2$ + 1 % PEG in F-3

Polyethylene glycol	Distribution coefficients		
	Cs	Sr	Eu
Slovafol-909	8.9	0.46	37
OP-10*	9.1	0.3	7.2
PEG-1500	6.3	0.6	41
PEG-400	4.5	4.1	43
PEG-300	6.7	4.0	60

*OP-10 (GOST 8433–81) – product of oxyethylation of mono- and dialkylphenols mixture by ethylene oxide (10-CH$_2$CH$_2$O- groups).

are presented in Table 9.5. It follows from Table 9.5 that a triple mixture extracts strontium better when non-substituted PEGs with a short (8–10) oxyethyl chain are used.

As an increased content of PEG in the mixture suppresses the extraction of cesium, it is necessary to use only a minimal amount of PEG. Table 9.6 gives the data concerning the effect of PEG content in the triple mixture on the extraction of cesium and strontium.

It follows from Table 9.6 that the optimal content of PEG-600 should be ~1%, corresponding to 0.016 M/l. As for PEG-400, its best content is equal to 0.6%, i.e. 0.015 M. So, the molar ratio of components in the triple mixture should be close to CCD:CMPO:PEG = 5:1:1. In this case, the recovery of all long-lived radionuclides is ensured.

Table 9.6 Extraction of radionuclides from Idaho simulated HLW by mixtures of 0.08 M CCD + 0.013 M Ph_2Bu_2 + (0.6–1.5) % PEG-600 in MNBTF

Content of PEG-600, %	Distribution coefficients	
	Cs	Sr
0.6	3.7	0.6
0.7	2.8	0.8
0.8	2.5	1.0
1.0	1.9	1.2
1.5	0.4	1.0

Choice of diluent for UNEX extractant
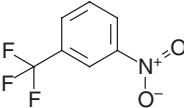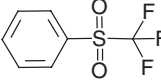
Metanitrobenzotrifluoride (F-3) is known to be used as the diluent for CCD at the operational industrial facility UE-35 (PA "Mayak", Ozersk, Russia), meeting all the requirements imposed in Russia on diluents being applied in radiochemistry. In the USA, there are severe restrictions placed on the use of nitroaromatic compounds; therefore, during the joint development (by RI and INL) of a double-extractant workflow (CCD + POR) for treatment of acidic wastes in Idaho, a search was conducted for some new diluents of CCD containing no nitrogroups. In this connection, preference was given to those organofluoric compounds having high chemical and radiation resistance, explosion-fire safety and acceptable hydrodynamic characteristics.

Amongst the investigated organofluoric compounds (ethers, esters, ketones, sulfones) particular attention was paid to the class of fluorinated sulfones. Sulfones are compounds of formula RSO_2R_F, where R – aryl or alkyl, R_F – polyfluoroalkyl C_nF_{2n+1}; they have many common properties with nitroaromatic compounds, because the sulfonic group is an acceptor, especially in polyfluoroalkylsulfones, and also forms a conjugate system with an aromatic ring.

A series of polyfluoroalkylsulfones with different substituents was synthesized and their main characteristics were determined with respect to the possibility of using them as a diluent for CCD. With an allowance for the total complex of properties, phenyltrifluoromethylsulfone (FS-13) proved to be the most promising. In Table 9.7 the main properties of FS-13 are shown and compared to those of metanitrobenzotrifluoride (F-3) which is used at UE-35 PA "Mayak".

Table 9.8 presents the extraction properties of CCD in FS-13 as compared to CCD diluted with F-3. It follows from the data in Tables 9.7 and 9.8 that phenyltrifluoromethylsulfone (FS-13) possesses high density, moderate viscosity and low solubility in nitric acid, while the solubility of CCD in FS-13 is rather high. The extraction ability of CCD in FS-13 is somewhat lower than in F-3, but quite sufficient for successful extraction

Table 9.7 Main properties of FS-13 as compared to F-3

Formula	Technical name	ρ, g/cm^3	η, mPa·s	Solubility in 3 M HNO$_3$, g/l	D_{Cs}*	ε
(structure)	F-3	1.436	3.02	1.23	16	22.3
(structure)	FS-13	1.41	3.6	0.65	3.8	29.0

* D_{Cs} for 0.06 M CCD solution in diluent – 3 M HNO$_3$.

Table 9.8 Extraction properties of 0.06 M CCD solutions in F-3 and in FS-13

Diluent		D at extraction from 3 M HNO$_3$ into organic phase containing:		
Formula	Technical name	0.06 M CCD	0.06 M CCD + 1% Slovafol	
		D_{Cs}	D_{Cs}	D_{Sr}
m-NO$_2$PhCF$_3$	F-3	16.7	9.3	14
PhSO$_2$CF$_3$	FS-13	3.8	2.2	7.2

Table 9.9 Extraction of radionuclides from simulated Idaho HLW by mixture of 0.08 M CCD + 0.013 M Ph$_2$Bu$_2$ + 0.6% PEG-400 in F-3 and in FS-13

Diluent		Distribution coefficients		
Formula	Technical name	Cs	Sr	Eu
m-NO$_2$PhCF$_3$	F-3	4.0	3.2	4.1
PhSO$_2$CF$_3$	FS-13	1.0	1.7	2.7

of radionuclides from HNO$_3$ solutions. These results provide reason to investigate the possibility of using FS-13 as a diluent of the universal extractant containing CCD, CMPO and PEG. The extraction properties of mixtures based on FS-13 and F-3 are shown in Table 9.9.

Taking all of the above data, it can be concluded that phenyltrifluoromethylsulfone (FS-13) as well as metanitrobenzotrifluoride (F-3) could be
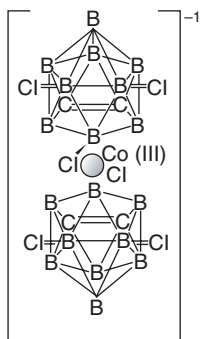
Structure of hexachlorodi-(orthocarboranyl)-cobaltate-anion

$HO(CH_2CH_2O)_{8-10}H$

Polyethyleneglycol-400
(PEG-400)
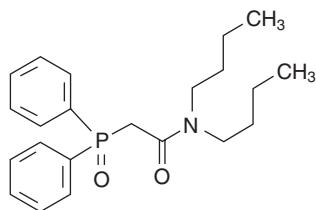
Diphenyl-N,N-dibutylcarbamoylphosphineoxide (CMPO)
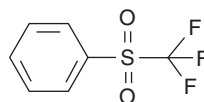
Phenyltrifluoromethylsulfone
(FS-13)

9.2 Components of universal extraction mixture (UNEX-extractant).

feasible for dilution of the universal mixture. Hence, the universal extraction mixture should contain the following components (Fig. 9.2): chlorinated cobalt dicarbolide, diphenyl-N,N-dibutylcarbamoylphosphineoxide, polyethylene glycol and phenyltrifluoromethylsulfone.

Properties of UNEX extractant

Composition of the universal extraction mixture may be varied depending on the characteristics of HLW being treated, in the range of 0.06–0.12 M CCD, 0.005–0.03 M CMPO, 0.075–0.25 M PEG-400 in diluent FS-13. Such composition provides the balance needed for effective recovery of Cs, Sr, An and REE with acceptable physico-chemical and hydrodynamic properties of the extractant.

Figure 9.3 shows typical dependence of the distribution coefficients for metals on the acidity of the aqueous phase.

In addition to radionuclides, the UNEX extractant recovers some stable elements: analogs of strontium, barium and lead are completely recovered; potassium and molybdenum are partly extracted; co-extraction
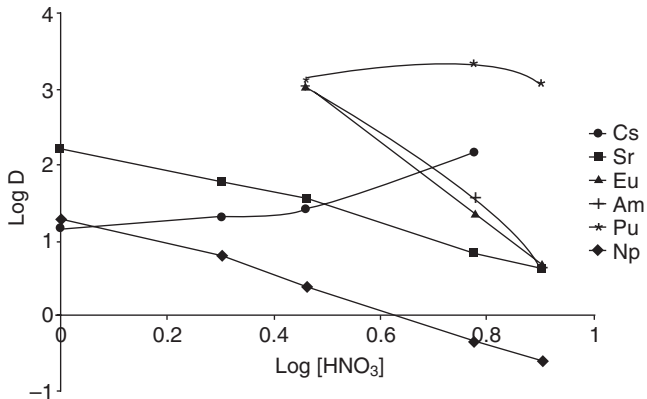
9.3 Extraction of metals (Cs, Sr, Eu (III), Pu(IV), Np(V)) from nitric acid by UNEX-extractant: 0.08 M CCD + 0.02 M Ph_2Bu_2 + 0.5% PEG-400 in FS-13.

of zirconium and iron considerably decreases in the presence of fluoride-ions; other metals (HLW components) are practically not extracted at all.

The high extraction ability of the UNEX extractant makes the subsequent stripping of radionuclides more difficult. Cesium and strontium can be stripped by HNO_3 containing additions such as amines, amides, alcohols. These additions facilitate the transfer of a proton into the organic phase and the displacement of Cs and Sr cations from it.

To strip REE and An, it is necessary to use solutions of rather efficient complexones like oxyetylidenediphosphonic acid. Uranium is stripped by carbonate solutions only. In the presence of complexones, ammonium carbonate also strips Sr, REE and An. Essential differences in the behavior of radionuclides at the stripping stage (stripping from the UNEX-extractant) allow partitioning of radionuclides to be made. If required, sufficiently pure fractions of Cs, Sr, U, REE and An can be obtained.

To produce concentrates of all radionuclides in the HLW treatment process, a common strip agent should be applied. Since uranium is stripped by carbonate solutions, the possibility of using complexone solutions with carbonate was investigated. It was found that a solution containing 1.0 M guanidine carbonate and 0.05 M DTPA effectively stripped Cs, Sr, An and REE.

Stability of UNEX-extractant

A UNEX-extractant (0.08 M CCD, 0.02 M Ph_2Bu_2 and 0.5% PEG-400 in FS-13) has a density of 1.4 g/cm^3 and viscosity of 4 mPa*s at 20°C. Stability of all components of the extraction system is rather high for treatment of

HNO_3 solutions of radioactive waste. So, CCD in FS-13 on contact with concentrated HNO_3 is stable even at elevated temperatures (>100°C). Diphenyldibutyl-carbamoylphosphineoxide and PEG-400 are also stable in contact with HNO_3. The UNEX-extractant and diluent FS -13 do not enter into exothermal reactions with HNO_3 even at temperatures above 100°C.

Fire safety of the UNEX-extractant depends primarily on the properties of the diluent FS-13, which is the main component of the mixture. The high flash temperature of FS-13 (93°C) is responsible for the fire-proof nature of the UNEX-extractant; for comparison, it should be noted that the flash temperature of dodecane (the diluent used in the PUREX-process) is 70°C. Other components of the UNEX-system (CCD, CMPO, PEG) have a high boiling point and are low fire-hazard compounds. As in the two-phase aqueous-organic extraction process, a temperature higher than 100°C is practically never reached, and the UNEX-process should be considered fire proof.

Specialist studies have revealed the high radiation resistance of FS-13. The total yield of radiation decomposition for pure sulfone and for sulfone in contact with HNO_3 was 4.5–5.0 molecules/100 eV. The low yield of fluorine-ions in this (0.15 ions/100 eV) makes the UNEX-extractant relatively corrosion-proof when compared to stainless steel. Radiolysis products do not exert any marked effect on the extraction and hydrodynamic properties of the UNEX-extractant. No interphase films, precipitates and emulsions were detected on exposure.

Since the extractant is used over multiple cycles in the process, an important characteristic is the prolonged stability of its properties, which may depend on differences in the solubility of individual components in the aqueous phase. Polyethylene glycol is the most soluble component during the stripping operation (up to 250 mg/l). Since PEG concentration in the extractant is critical for Sr extraction, this component should be replenished during the course of the process. With the exception of compensation for PEG losses (for example, by its introduction into the stripping solution), the properties of the UNEX-extractant do not practically change over time. This was confirmed by prolonged testing of the UNEX-process at RI and Idaho National Laboratory.

9.3.2 Development of UNEX-process flowsheets for the recovery of cesium, strontium, actinides and REE from HLW

Investigation of conditions for extraction of radionuclides from salt-rich solutions

Laboratory studies of the possibility of simultaneous recovery of long-lived radionuclides from HLW in the framework of a single process have resulted

Table 9.10 Effect of zirconium on distribution coefficients of europium. Aqueous phase – 1 M HNO_3; Organic phase – 0.08 M CCD + 0.024 M CMPO + 1.4% PEG-400 in FS-13

Zr, g/l	0	1	2.5	10	15
D $_{Eu}$	1500	550	0.17	0.039	0.03

Table 9.11 Effect of iron on distribution coefficients of europium. Aqueous phase – 1 M HNO_3; Organic phase – 0.08 M CCD + 0.024 M CMPO + 1.4% PEG-400 in FS-13

Fe, M	0	0.005	0.01	0.02	0.025	0.03	0.05
D_{Eu}	10^3	$7 \cdot 10^2$	$6 \cdot 10^2$	$3 \cdot 10^2$	90	13	0.2

in the development of a flowsheet for waste treatment on the basis of the CCD, CMPO and PEG in diluent FS-13 extraction system. Since HLW, as a rule, has a complicated chemical composition, the influence of different HLW components on the extraction of long-lived radionuclides needs to be investigated to create an effective technology.

In particular, owing to the rather low concentration of CMPO in the extraction mixture, its extraction properties with regard to trivalent TPE and REE depend strongly on the concentration and state of such extractable impurities such as zirconium and iron, which may compete with TPE and REE. Tables 9.10 and 9.11 show the effect of zirconium and iron on the distribution coefficients of europium from 1 M HNO_3, using an extractant of 0.08 M CCD + 0.024 M CMPO + 1.4% PEG-400 in FS-13.

Tables 9.10 and 9.11 show that zirconium and iron exert a suppressing effect on europium extraction. Increasing the aqueous solution acidity to 1.5 M reduces the iron effect drastically, and thus special precautions should be taken to suppress zirconium extraction.

The extraction of hindering impurities and thus their effect can be suppressed with the use of different complexones, such as fluorine-ion or citric acid. As citric acid deteriorates the properties of cement (in the case of cementing LLW-raffinate) after the extraction of radionuclides, preference was given to fluorine-ion. Table 9.12 shows the effect of fluorine-ion on europium extraction at various concentrations of zirconium.

The data given in Table 9.12 illustrate the possibility of establishing conditions for the application of fluorine-ion to suppress zirconium extraction. As to the iron effect, the table shows that, even at the molar ratio 1:1 between iron and fluorine-ion, iron extraction is effectively suppressed.

Table 9.12 Distribution coefficients of europium at extraction by UNEX-extractant from 1 M HNO_3 at various concentrations of zirconium and fluorine-ion. Organic phase – 0.08 M CCD + 0.024 M CMPO + 1.4% PEG-400 in FS-13

NH_4F, M	Zr, g/l				
	0.25	0.5	2.5	5.0	10
0	2400	380	0.22	0.06	$\leq 10^{-3}$
0.01	1500	480	0.86	0.05	$\leq 10^{-3}$
0.05	3300	3100	7.4	1.3	0.32
0.1	1700	2800	800	2.8	0.33

Investigation of stripping conditions from the universal mixture

The high extraction rates possible with the CCD-CMPO-PEG system pose problems for subsequent stripping stages of the process. In principle, cesium and strontium can be stripped by HNO_3 solutions with additions facilitating proton transfer into the organic phase (alcohols, amides of acids, amines). TPE and REE can be extracted by complexone solutions in the presence of buffer additions providing pH > 3. The same solution at pH = 6 strips plutonium and neptunium. To strip uranium it is necessary to use sodium or ammonium carbonates.

As for the partitioning of radionuclide fractions, different variants for stripping of Cs, Sr, An and REE from combined extract were considered and tested, and the following variants for production of radionuclide fractions by using the UNEX-process have been elaborated.

Variant 1
- stripping of strontium, actinides and REE by a solution of 0.5 M guanidine carbonate and 0.05 M DTPA;
- stripping of cesium by a solution of 4 M HNO_3 containing 200 g/l acetamide.

Variant 2
- stripping of cesium and strontium by a solution containing 1 M guanidine nitrate, 0.1 M HNO_3 and 0.03 M citric acid;
- stripping of actinides and REE by a solution containing 1 M guanidine carbonate, 0.2 M acethydroxamic acid and 0.03 M DTPA.

In the case of treatment of HLW with the aim of producing a concentrate of all long-lived radionuclides and its subsequent solidification, a variant combining the stripping of cesium, strontium, actinides and REE has been developed.

Variant 3

- stripping of Cs, Sr, An and REE by a solution containing 1 M guanidine carbonate and 20 g/l DTPA.

On the basis of experimental results concerning the processes of extraction and stripping, the flowsheets using the UNEX-extractant have been developed which involve the fraction or combined separation of long-lived radionuclides from HLW.

Flowsheet based on the UNEX process with selective recovery of the cesium fraction

If the selective recovery of the cesium fraction from HLW is required, the work flow involves the following operations:

- Combined extraction of Cs, Sr, An and REE by the UNEX-extractant (8 stages).
- Scrubbing of the extract with a solution of 0.5 M citric acid (1 stage).
- Stripping of Sr, An and REE by a solution of 0.5 M guanidine carbonate and 20 g/l DTPA (5 stages).
- Stripping of cesium by a solution containing 5 M HNO_3 and 100 g/l acetamide (6 stages).
- Regeneration of the extractant by a 10 M HNO_3 solution (3 stages).
- Regeneration of the extractant by a 0.1 M HNO_3 solution (1 stage).

Figure 9.4 represents a work flow with selective withdrawal of cesium which has been proven under dynamic conditions at RI and Idaho National Laboratory.

Flowsheet based on the UNEX process with production of two fractions (Cs + Sr and An + REE)

A flowsheet with selective stripping of Cs and Sr has been developed for partitioning HLW with long-lived (Cs-137 and Sr-90) and ultralong-lived (An) radionuclides into fractions. The flowsheet involves the following operations:

- Combined extraction of Cs, Sr, An and REE by a UNEX-extractant (11 stages).
- Scrubbing of the extract with a solution of 1 M HNO_3 containing 0.03 M citric acid (1 stage).
- Combined stripping of Cs and Sr by a solution containing 1 M guanidine nitrate, 0.1 M HNO_3 and 0.03 M citric acid (6 stages).
- Stripping of An and REE by a solution containing 1 M guanidine carbonate, 0.2 M acetohydroxamic acid and 0.03 M DTPA (3 stages).
- Regeneration of the extractant by a 3 M HNO_3 solution (5 stages).
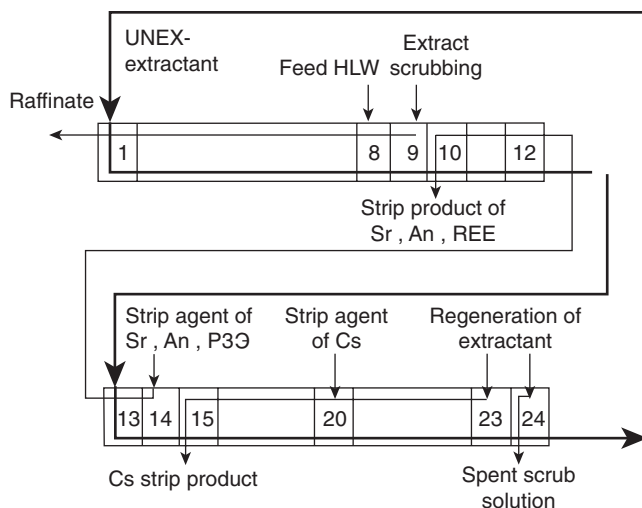
9.4 Flowsheet of UNEX-process with selective recovery of cesium fraction.
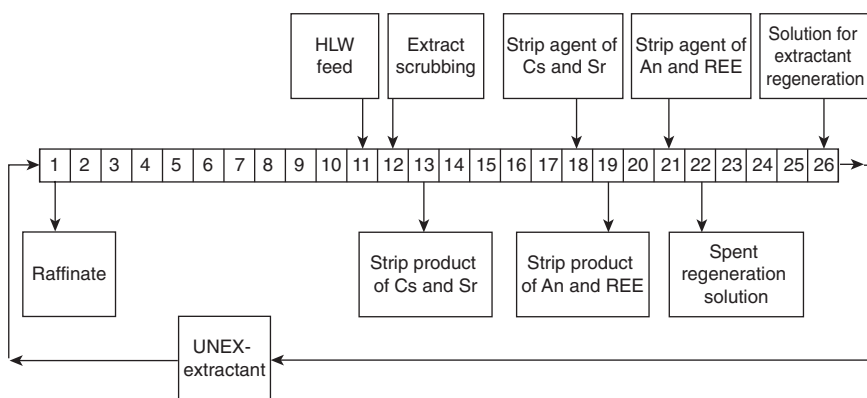
9.5 UNEX-process flowsheet with recovery of fractions Cs + Sr and An + REE.

This flowsheet (Fig. 9.5) was also tested at pilot plants with centrifugal contactors at RI and the Idaho National Laboratory.

Flowsheet based on the UNEX process obtaining a combined strip product of Cs, Sr, An and REE

In connection with the treatment of salted HLW to produce a radionuclide concentrate to be solidified, the task was set to combine extraction and
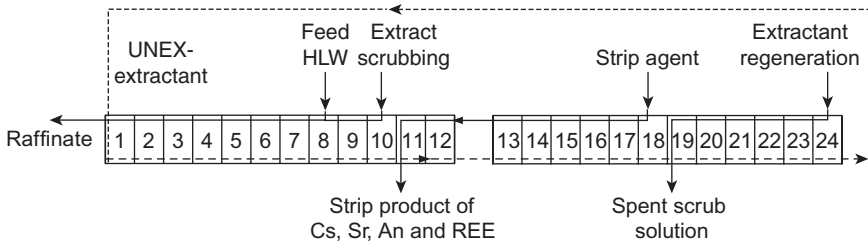
9.6 UNEX-process flowsheet with extract scrubbing combined stripping of Cs, Sr, An and REE.

stripping of Cs, Sr, An and REE. The developed flowsheet involved the following operations:

- combined extraction of Cs, Sr, An and REE by the UNEX-extractant (8 stages);
- scrubbing of the extract with a solution of 0.3 M citric acid in 0.05 M HNO_3 (2 stages);
- combined stripping of Cs, Sr, An and REE by a solution containing 1 M guanidine carbonate and 10 g/l DTPA (8 stages);
- regeneration of the extractant by a 1 M HNO_3 solution (6 stages).

This variant of the UNEX-process (see Fig. 9.6) was also tested on actual acidic HLW at RI and Idaho National Laboratory facilities.

Improved UNEX process flowsheet with combined stripping of Cs, Sr, An and REE

The objective of optimizing the UNEX-process flowsheet with a combined stripping of Cs, Sr, An and REE was to achieve the largest possible decrease in the number of operations, and to achieve a reduction in the volume and number of categories of secondary wastes. As a result of investigations conducted at pilot plants operated by RI and Idaho National Laboratory, the flowsheet presented in Fig. 9.7 was developed and tested.

9.3.3   Test results for workflows based on the UNEX process at KRI, NIKIMT and Idaho National Laboratory plants

The flowsheets developed based on the UNEX process were proven in the course of a series of tests at RI and Idaho National Laboratory plants. At RI, the tests were performed using simulated HLW solutions with actual,
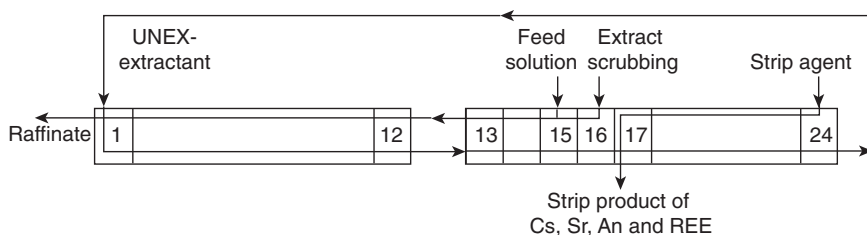
9.7 Improved UNEX-process flowsheet for combined recovery of Cs, Sr, An and REE.

Table 9.13 Composition of sodium-containing HLW of Idaho National Laboratory

Component	Concentration, M	Component	Concentration, M
HNO_3	1.55	Na	1.14
Al	0.68	NO_3	4.38
B	0.016	Zr	0.0054
Ba	3.4E-05	$\Sigma\alpha$	473 (nCi/g)
Ca	0.049	^{241}Am	54 (nCi/g)
Cr	0.011	^{134}Cs	0.16 (Ci/m³)
F	0.13	^{137}Cs	185 (Ci/m³)
Fe	0.038	^{238}Pu	343 (nCi/g)
Pb	0.0016	^{239}Pu	71 (nCi/g)
Hg	0.0041	^{99}Tc	0.034 (Ci/m³)
Mo	0.012	^{90}Sr	181 (Ci/m³)
K	0.15	U	0.087 (g/L)

long-lived radionuclides, whilst in Idaho actual HLW from this nuclear center were used.

Three types of centrifugal contactors served as the extraction equipment:

- 12-staged miniature centrifugal contactor (MC 12–30) with a stage working volume of 30 cm³, manufactured by NIIAR (Dimitrovgrad);
- centrifugal contactors with rotors of 3.3 cm in diameter and with stirring and settling chamber capacities of 22 cm³ and 32 cm³, respectively; the contactors were designed and manufactured at NIKIMT (Moscow);
- centrifugal contactors with rotors of 2 cm in diameter, designed and manufactured at the Argonne National Laboratory (USA).

The typical composition of the HLW solutions used in the experiments performed is shown in Table 9.13.

Results of the UNEX process tests with selective recovery of cesium (flowsheet in Fig. 9.4)

In tests with selective recovery of cesium, the following indices for recovery of long-lived radionuclides (%) were obtained: Cs^{137} – 99.94, Sr^{90} – 99.81, Eu^{154} – 99.76, U^{238} – 99.98, Np^{237} – 99.95, $Pu^{239,240}$ – 99.98, Am^{241} – 99.18.

The degree of concentration of Sr, An and REE in the strip product of these radionuclides was 2.5. During the experiments, no precipitates and suspensions in the process products were detected.

Results of the UNEX process tests with recovery of Cs + Sr and An+REE fractions (flowsheet in Fig. 9.5)

When testing the UNEX process for recovery of the Cs+Sr and An+REE fractions, the following results for recovery of radionuclides were attained: Cs – 99.7%, Sr > 99.98%, Eu > 99.92%. These data permit the bulk HLW being treated to be transferred into the low-level waste (LLW) category, suitable for cementing and subsequent near-surface storage. Barium and lead were almost completely co-extracted with long-lived radionuclides in this process; zirconium and molybdenum were also partly co-extracted. Sodium, potassium iron and mercury remained in the low-level raffinate. In this UNEX process variant, the recovery of HLW components is shown in Table 9.14.

Results of UNEX process tests with the combined recovery of Cs, Sr, An and REE (flowsheet in Fig. 9.6)

When testing the UNEX process, prime attention was given to the work flow which included the combined recovery of Cs, Sr, An and REE into one high-level product to be solidified. It was necessary to reach a degree of

Table 9.14 Content of HLW components in raffinates produced on testing of UNEX process with recovery of fractions Cs+Sr and An+REE

No Test	Cs	Sr	Eu	Hg	Zr	Ba
1	0.33%	<0.012%	<0.079%	86.3%	18.6%	<0.43%
2	1.0%	0.023%	<0.074%	89.4%	20.0%	<0.40%

No Test	Na	K	Fe	Pb	Mo	
1	81.4%	60.8%	80.1%	<0.22%	37.4%	
2	88.3%	74.8%	84.3%	<0.21%	38.6%	

Table 9.15 Distribution of radionuclides in UNEX process flowsheet with combined withdrawal of Cs, Sr, An and REE

Product	^{137}Cs	^{90}Sr	Alpha	^{241}Am
Raffinate	0.57%	0.0052%	0.040%	0.0002%
Strip agent	100.6%	108.1%	100.4%	105.6%
Scrub solution	0.006%	0.0003%	0.001%	–
Extractant	0.005%	0.005%	0.02%	0.2%
Material balance	101.1%	108.1%	100.4%	105.8%

Product	^{238}Pu	^{239}Pu	^{154}Eu	^{99}Tc
Raffinate	0.006%	0.002%	0.42%	81.2%
Strip agent	96.9%	103%	78.6%	<0.14
Scrub solution	–	–	0.015%	–
Extractant	0.005%	0.0006%	0.075%	0.013%
Material balance	97.0%	103.9%	79.1%	81.3%

Table 9.16 Distribution of HLW macrocomponents in UNEX process flowsheet with combined withdrawal of Cs, Sr, An and REE

Product	Al	Ba	Ca	Fe	Hg
Raffinate	108.2%	<1.05%	97.8%	74.7%	110.9%
Strip product	0.14%	105.7%	9.9%	8.3%	<1.2%
Wash	–	–	–	–	–
Solvent	0.022%	3.9%	<1.2	0.44%	0.04%
Material balance	108.4%	106.8%	107.7%	83.0%	110.9%

Product	K	Mo	Na	Nd	Pb	Zr
Raffinate	74.6%	79.1%	108.0%	<2.4%	1.2%	13%
Strip product	27.9%	31.7%	0.13%	112%	83.2%	68.6%
Wash	0.008%	–	0.01%	–	–	–
Solvent	0.15%	<15,6%	0.02%	<5.5%	<0.62%	0.09%
Material balance	102.4%	110.8%	109.0%	112–114.4%	84.4%	81.6%

radionuclide recovery such that the UNEX-process raffinate conforms to standards established for LLW. The distribution of radionuclides obtained from tests on real HLW in the Idaho National Laboratory is presented in Table 9.15. The distribution of HLW macrocomponents over the workflow products is shown in Table 9.16.

The results of testing show that the recovery rates for Cs, Sr and An are equal to 99.4%, 99.995% and 99.96%, respectively. These recovery rates are sufficient to move the raffinate (the bulk of the wastes being treated) into the LLW category.

The combined stripping of radionuclides was carried out effectively by a solution containing 1 M guanidine carbonate and 20 g/l DTPA. The HLW macrocomponents Ba and Pb were extracted almost completely, whilst Zr, Mo, K, Ca and Fe were only partly extracted (by 87%, 32%, 28%, 10% and 8%, respectively).

Results of prolonged tests of the UNEX process in an improved flowsheet (flowsheet in Fig. 9.7)

To confirm the effectiveness of the UNEX-extractant under operating conditions, special tests of a prolonged continuous process duration (66 hours) were performed at RI and the Idaho National Laboratory. Over this period of time, the extractant made 89 recycles. The tests demonstrated that:

- extractable components are not accumulated in the recycled extractant;
- concentration of the most water-soluble component (PEG-400) can be maintained by its addition to the fed strip agent;
- increase in the degree of radionuclide concentration in the strip product is attained due to a temperature rise to 60°C at the stripping operation stage;
- rates of recovery of radionuclides (Cs – 99.78%, Sr – 99.984%, Eu – 99.997%) allow the transfer of the raffinate into the LLW category;
- elimination of the extractant regeneration operation from the improved flowsheet did not result in accumulation of extractable components in the recyclable organic phase;
- as far as metal macroimpurities were concerned, Ba and Pb were almost completely extracted during the tests, whilst Ca, Fe, K, Mo were partially extracted.

The results presented have already been partly published [26–29]. All the UNEX tests up to 2001 year were reviewed in [30] (see Table 9.17). The UNEX process was patented in Russia and in the US. [31]

In order to verify the UNEX process within the framework of DOE Project EM-50/JCCEM under contract with Sandia National Laboratories' "Testing and demonstration of UNEX-process technology", an extraction setup was created in hot cells at the Central Plant Laboratory of the Radiochemical Plant (RChP) at Mining Chemical Combine (MCC), Zheleznogorsk, Russia. The EZ-33 centrifugal contactors developed and manufactured by NIKIMT were the main extraction process equipment used. The UNEX-process was tested in two stages – on simulated and actual waste feeds [32]. The experimental objective was to: determine the technological parameters of the UNEX process when treating simulated and actual liquid HLW; to investigate the distribution of stable and radioactive

Table 9.17 Summary of the flowsheet tests completed during UNEX development. [30]

	Flowsheet test					
	Test 1	Test 2	Test 3	Test 4	Test 5	Test 6
Test year	1997	1998	1999	2000	2000	2001
Waste	Surrogate tank	Actual tank	Actual tank	Surrogate tank	Surrogate calcine	Actual calcine
UNEX solvent composition	0.08M CCD 0.5% PEG 0.02M CMPO	0.08M CCD 0.6% PEG 0.02M CMPO	0.08M CCD 0.5% PEG 0.02M CMPO	0.08M CCD 0.35% PEG 0.008M CMPO	0.08M CCD 0.35% PEG 0.01M CMPO	0.08M CCD 0.4% PEG 0.01M CMPO
UNEX diluents	Mixture of Octyldifluoromethyl sulfone & p-xylene	Phenyltetrafluoroethyl sulfone (FS-24)	Phenyltrifluoromethyl sulfone (FS-13)	Phenyltrifluoromethyl sulfone (FS-13)	Phenyltrifluoromethyl sulfone (FS-13)	Phenyltrifluoromethyl sulfone (FS-13)
Feed adjustments	Addition of solid citric acid for 0.03 M citrate in the feed	1.1 vol % dilution w/ 10 M HF	10 vol % dilution w/ 5.2 M HF	10 vol % dilution w/ 3.3 M HF	20 vol % dilution w/ 0.1 M HF	30 vol. % dilution w/ 0.5 HF
Scrub solutions	0.03 M citric acid in 1 M HNO_3	0.1 M HF in 0.4 M HNO_3	0.3 M citric acid in 0.1 M HNO_3	0.3 M HF 0.05 M ANN^e 0.1 M HNO_3	M HF 0.017 M ANN 0.033 M HNO_3	0.2 M NH_4NO_3
Strip solutions	2 Strip sections: Cs/Sr: 1 M GN^a 0.1 M HNO_3, 0.03 M citrate Act.: 1 M GC^b, 0.2 M AHA^c, 0.03 M $DTPA^d$	2 Strip sections: Cs/Sr: 100 g/L GN 0.1 M AHA Act.: 1 M GC 0.03 M DTPA	1 Strip section: 1 M GC 0.06 M DTPA	1 Strip section w/ 2 strip solutions: Strip #1: 1.1 M GC Strip #2: 0.11 M GC 0.06 M DTPA	1 Strip section w/ 2 strip solutions: Strip #1: 1.1 M GC Strip #2: 0.11 M GC 0.06 M DTPA	1 Strip section: 0.56 M GC 0.03 M DTPA

Table 9.17 Continued

	Flowsheet test					
	Test 1	Test 2	Test 3	Test 4	Test 5	Test 6
Solvent wash	3 M HNO$_3$	5 M HNO$_3$	2 M HNO$_3$	None	None	None
Radionuclide removal efficiencies	Cs 99.4% Sr 99.97% Eu 4.3% to >99.92%	^{137}Cs 99.95% ^{90}Sr 99.985% Alpha 95.2%	^{137}Cs 99.4% ^{90}Sr 99.995% Alpha 99.96%	Cs > 97.5% Sr > 99.993% Eu 17.2% to 34.1%	Cs 99.95% Sr > 99.999% Nd > 98.3% Ce > 99.6%	^{137}Cs 99.99% ^{90}Sr 99.73% Alpha > 99.9%
Matrix metal Removal efficiencies	Zr 52% Mo <3.1% Fe 10% Ba 99.5% Pb 99.8% K 20%	Zr >97.7% Mo 19% Fe 6.9% Ba >87% Pb >98.5% K 17%	Zr 87% Mo 32% Fe 8% Ba > 99% Pb > 98.8% Ca 10% K 28%	Zr < 6.4% Mo < 19.2% Fe < 13.2% Ba > 99.6% Pb > 99.94%	Zr 3% Mo > 2% Fe 9% Ba 99.7% K 50%	Zr 0.7% Mo 12% Fe 2% Ba, Pb 100% Mn 23%
Notes	Two tests with light phase solvent; flooding and precipitation observed in strip section of initial test.	4 hour test with solvent recycle. Flooding was observed in the actinide strip section.	3 hour test with solvent recycle. No precipitation or flooding was observed.	66 hr run time w/ solvent recycle. No precipitation or flooding was observed.	4 hour test with solvent recycle. No precipitation or flooding was observed.	3 hour test with solvent recycle. No precipitation or flooding was observed.

elements over the various stages of the extraction units; to check the operational reliability of the EZ-33 centrifugal contactors with high radiation loadings under prolonged operational conditions.

Initially a simulated solution, corresponding to real process waste but composed of stable macrocomponents, was treated. The duration of the experiments was 48 hours and the volume of treated solution was 29 l. The process flowsheet of the setup involved the following operations: extraction of target elements (18 stages); extract scrubbing (2 stages); combined stripping of target elements (16 stages).

In the second part of the experiment, actual high-level waste from a radiochemical plant (Pr. 501) was used, with the following composition: Pu – 152 mg/l; U – 102 mg/l; Np – 0.38 mg/l; Am – 68 mg/l; Th – < 0.5 mg/l; Fe – 645 mg/l; Cr – 340 mg/l; Mn – 1,2 g/l; Ni – 510 mg/l; Pb – 6 mg/l; Al – 220 mg/l; Ba – 12 mg/l; Ca – 230 mg/l; F-ion – 2,7 g/l; Si – 100 mg/l; HNO_3 – 69 g/l; $NaNO_3$ – 47 g/l; ^{90}Sr – 0.3 Ci/l; gross α-activity – 1,4 Ci/l.

The specific volumetric activities of the radionuclides in Bq/l were:-^{125}Sb – 4.89*10^7; ^{134}Cs – 1.02*10^7; ^{137}Cs – 5.3*10^8; ^{155}Eu – 5.82*10^8; ^{154}Eu – 3.37*10^7; ^{144}Ce – 9.31*10^9; ^{60}Co – 2.67*10^7; ^{106}Ru – 2.07*10^9. In the second test 77 l of actual waste were treated. The time operating on the actual solution was 128 hours, and the solvent made 51 recycles. Results of checks on the extraction properties of the recycled solvent and its chemical analysis during the test did not reveal any considerable deviations from initial characteristics. Some decrease of Sr and Cs distribution coefficients were noted – by 10 and 18.5% of their initial values, respectively; however, this fact did not affect the process parameters as a whole.

On treatment of actual waste, the recovery rates of target radionuclides, as calculated from their content in the raffinate, was: Pu – 99.76%; Am – >99.02%; Sr-90 – 99.99%; U – >99.0%; Eu-155 – >99.91%; Eu-154 – >98.75%; Cs-137 – 99.95%; Ce-144 – >99.98%. Al, Cr, Ru and Sb are not recovered totally (their content in the strip product is below detection levels), while Pb and Ba are extracted and are removed with the strip product. Up to 20% Ca, 25% Fe, 23% Mn, 5% Co and 3% Ni (measured as a percentage of their content in the feed solution) are also withdrawn with the strip product.

Testing of the UNEX process on commercial centrifugal contactors

The potential for using the UNEX-extractant for the treatment of Idaho acidic HLW required substantiating all process characteristics, primarily all its hydrodynamic properties, as applied to extraction equipment on an industrial scale.

For this purpose, the main operations of the UNEX process work flow were checked by using Idaho simulated HLW on the EZR125 commercial
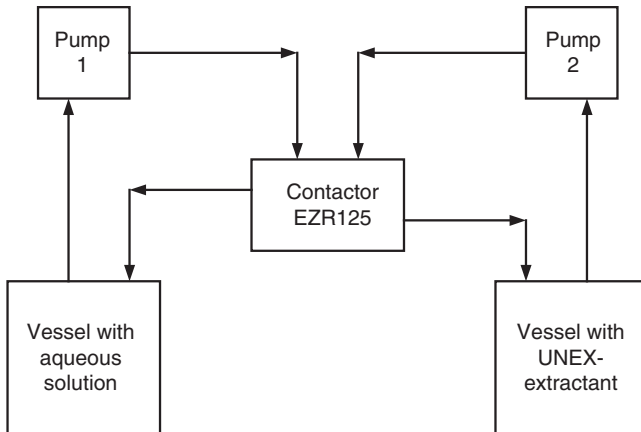
9.8 Basic diagram of bench for UNEX process on commercial contactor EZR125.

centrifugal contactor at the Research and Construction Institute of Assembling Technology (NIKIMT, Moscow). The operating conditions for the experiments corresponded to those of the previously performed tests for the improved work flow using real HLW. A basic diagram of the test rig for the UNEX process using a commercial centrifugal contactor is presented in Fig. 9.8.

The tests of the UNEX process using industrial equipment provided the following evidence:

- the centrifugal contactor EZR125, working under UNEX process conditions, has a flowrate of 800 L/hour in total for all phases of the process (this corresponds to with the PUREX process system, with 30% TBP in kerosene and 2 M HNO_3);
- entrainment of the aqueous phase into the organic was no more than 0.1%, while the aqueous phase did not practically contain any of the organic phase;
- adjusting the best interphase position in the contactor rotor for each of the specific process operations allows entrainment of the aqueous phase into the organic phase to be eliminated.

9.3.4 Development and testing of methods for management of UNEX process end products

As shown in the previous section, in the course of the UNEX process the only end products formed are a high-level strip product (a concentrate of

all the recovered radionuclides) and a low-level raffinate; the spent UNEX-extractant withdrawn after its use from the process could be considered as a third product of the process.

The most important condition for evaluating the suitability of a HLW treatment technology is the effective and safe management of end (secondary) products of such a treatment. Therefore, methods for management of the strip product, raffinate and spent extractant were tested to assess the suitability of the UNEX process.

Vitrification of the high-level strip product of the UNEX process

Test results on the development and elaboration of the UNEX process have shown that the treatment of 1 volume of feed HLW generates 0.5 volume of strip product containing recovered radionuclides, guanidine carbonate, DTPA and 4–5 g/L of non-radioactive metals. The well-known borosilicate-glass production technique was tested on this product. The main non-volatile components of the strip product are sodium (20%), potassium (40%) and iron (10%). Taking these into account, the composition of the flux for glass was determined: it contained silicon dioxide, boric acid, sodium nitrite and zinc oxide.

The glass production process included the following operations:

- drying of the strip product;
- calcination of residue at 700°C;
- preparation of the flux and its drying at 450°C;
- mixing of the calcinated residue with the flux at 1100–1200°C.

The borosilicate glass samples produced were homogeneous, did not contain any non-molten inclusions and did not crack in storage. 1 m³ of strip product produces 15–20 kg (~10 L) of borosilicate glass.

Solidification of low-level raffinate of UNEX process

To assess the possibility of solidification of the low-level raffinate, with the aim of its near-surface storage, the traditional LLW cementing technique was tested.

Test results indicated that, during cementing, the solidification process proceeded uniformly, and the cement blocks produced did not crack on discharge from the mold or in subsequent storage. Although the cement bulk per volume of raffinate being solidified was rather high (1.5 m³ per 1 m³ raffinate), the cost of the cementing process should not be very high, because the low content of radionuclides in the raffinate (LLW) allows the solidification process to be undertaken with the use of routine non-radiochemical equipment.

Handling of spent UNEX-extractant

To regenerate the spent UNEX-extractant, a technique for the distillation of the diluent (phenyltrifluoromethylsulfone – FS-13) water steam in the presence of sodium carbonate was elaborated. In this way it is possible to distill more than 90% of practically pure diluent (with purification coefficients from the radionuclides – above 1000). During this process, over 40% CCD transfers into the sodium carbonate aqueous solution, from where it can be precipitated in the form of cesium salt suitable for re-use.

Specific experiments have shown that the properties of UNEX-extractant prepared from regenerated FS-13 and CCD do not differ from those of a fresh extractant. By using this regeneration technique, the radionuclides contained in the spent extractant remain almost completely in the still residue along with CMPO, PEG and a portion of CCD. This residue is a viscous liquid which can be removed and then treated with other high-level waste.

General flowsheet for treatment of the UNEX process end products

Following on from the above discussions, Figure 9.9 presents a basic flowsheet proposed for the management of HLW treatment end products by UNEX-extractant, as applied to sodium-bearing waste of INL. Hence, the
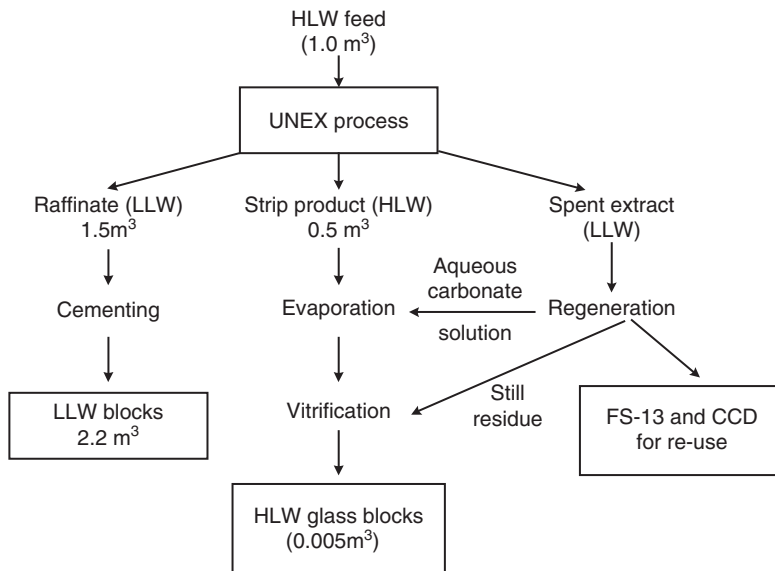
9.9 General basic diagram for management of end products of HLW treatment by UNEX process.

implementation of the UNEX-process together with subsequent treatment of its end products enables HLW volumes to be reduced by a factor of 200.

The effectiveness of the UNEX process was confirmed by a feasibility study conducted in 2000 by a US engineering company, with participation of RPA KRI. It was shown that, in the case of vitrification of Idaho acidic HLW without radionuclide recovery, 1 m^3 HLW would produce 324 kg of glass. Further, with the vitrification of the UNEX-strip product, the amount of glass produced would decrease to 14 kg, i.e. by a factor of 23.

9.3.5 Optimization of the process for combined stripping of radionuclides from UNEX process extract

A drawback of the traditional UNEX process was the use of guanidine carbonate solution + DTPA bearing a large quantity of guanidine carbonate (0.5–1 mole/L) for stripping. Clearly, all of the guanidine carbonate remained in the strip product. Its destruction prior to vitrification is possible, but this is a cumbersome process, especially taking into account the high radioactivity of the strip product.

Alkylamine nitrates have also been proposed for stripping of metals from CCD-based extractants [33]. The effect of methylamine, dimethylamine and trimethylamine nitrates on the stripping of cesium and barium from CCD + PEG solutions was considered. Solutions of these amine nitrates stripped metals from the organic phase efficiently but, they should also be destructed in the resultant strip product before vitrification. All the earlier proposed complexones were found to be inadequate for stripping metals from a UNEX-extractant, with the main difficulties concerning the stripping of cesium.

However, when a solution of methylamine carbonate + DTPA or methylamine carbonate + nitrilotriacetic acid (NTA) was proposed instead of guanidine carbonate + DTPA for stripping in the UNEX process [34, 35], all the metals extracted proved to be efficiently stripped. The essential difference in the proposed solution is that it is a regenerable strip agent. Methylamine carbonate is easily regenerated and the strip product prepared from regenerated methylamine carbonate exhibits features identical to those of the initial compound. It has therefore been possible to sharply reduce the number of organic compounds in the strip product, easing the problem of its subsequent solidification. The possibility of using methylamine carbonate was confirmed in the course of two dynamic experiments on simulated solutions performed concurrently at Idaho National Laboratory and RI. The basic flowsheet for HLW treatment by a regenerable strip agent is presented in Fig. 9.10.

Emphasis should now be placed on reducing HLW volume during the process (~20 times). Radiolysis of methylamine carbonate solutions with
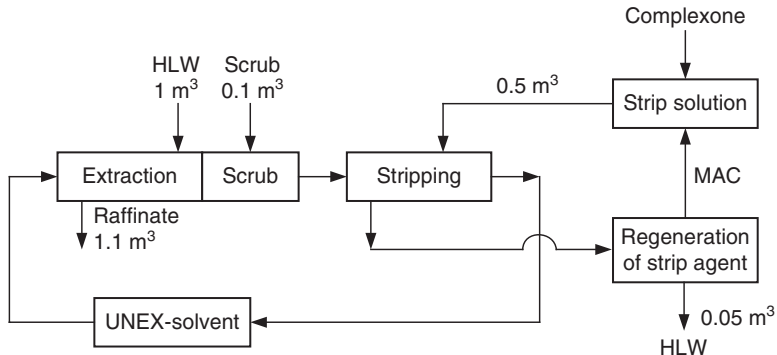
9.10 Basic flowsheet for HLW treatment with regeneration and re-use of strip.
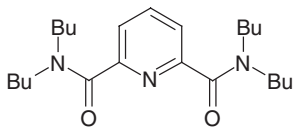
9.11 Tetrabutyldiamide of dipicolinic acid (TBDPA).

complexones was investigated. The results obtained bear witness to the high radiation stability of the complexones and methylamine carbonate by itself, which allows these solutions to be used for the treatment of high-level waste [36]. The radiolysis products at an absorbed dose to 3 MGy do not affect the extraction and stripping processes.

9.3.6 UNEX process with use of diamides of dipicolinic acid instead of carbamoylphosphineoxide

Of special interest from a practical point of view is the modification of the extraction mixture, i.e. the use of dipicolinic acid diamides (DPA) instead of carbamoylphosphineoxide. The mixture of CCD with DPDA shows the synergistic effect for Am extraction [37]. The proposed mixture of CCD + DPDA + polyethylene glycols manifests the extraction of Cs, Sr, REE and TPE, similar to the classical UNEX-extractant [38]. The formulae of some investigated DPDAs are presented in Figs 9.11 and 9.12.

The data on extraction of radionuclides are given in Table 9.18 and Fig. 9.13, from where it can be seen that diamides effectively extract radionuclides even from 3 M HNO_3.

The advantages of DPAs compared to carbamoylphosphineoxides are their rather simple synthesis and the possibility for a wide variation in their
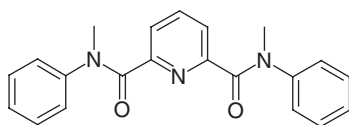
9.12 N,N′-diphenyl-N,N′-dimethyldiamide of dipicolinic acid (PhMDPA).
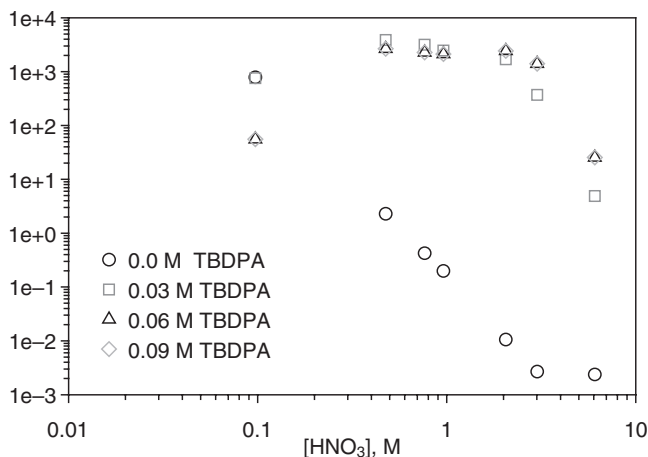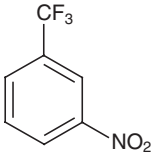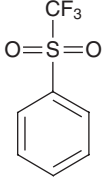
9.13 Extraction of europium by mixture of 0.13 M CCD + 0.027 M PEG-400 + TBDPA in FS-13 as function of HNO_3 concentration and content of diamide in organic phase.

Table 9.18 Extraction of Cs, Sr and Eu by 0.02 M CCD + 0.01 M diamide + 0.002M PEG-400 in F-3 as function of HNO_3 concentration

	HNO_3	Cs^{137}	Sr^{85}	Eu^{152}
TBDPA	1 M	13	64	>100
	3 M	2.8	6	60
	6 M	0.6	1.3	1.1
PhMDPA	1 M	14	84	54
	3 M	1.7	2.5	1.3
	6 M	0.5	1.1	0.2

structure. Further, metal solvates with DPDA are more easily soluble when compared to those with CMPO, and thus one can use higher concentrations of DPDA in the extraction mixture which leads to an increase in the extraction mixture capacity for trivalent metals. This is of importance for the treatment of solutions with a high content of REE. Furthermore, DPAs extract TPE to a greater extent than REE.

	CF_3	
CF_3 (nitrobenzotrifluoride structure with NO_2)	$O{=}S{=}O$ (phenyltrifluoromethylsulfone structure)	$(HCF_2CF_2CH_2OCH_2CH_2)_2O$
F-3	FS-13	F-8

9.14 Formulas of nitrobenzotrifluoride (F-3), phenyltrifluoromethylsulfone (FS-13) and bis-tetrafluoropropyl ether of diethylene glycol (F-8).

As in other systems based on CCD, the extraction ability of CCD – DPDA and CCD – DPDA – PEG systems varies depending on the diluent in the row of F-3 ≥ FS-13 > F-8 (see Fig. 9.14).

The above data indicate that diamides of dipicolinic acid are of interest as synergistic additions to CCD. The CCD – DPDA mixtures effectively extract REE and An from acidic solutions of HNO_3. Diamides are easier to synthesize and thus they are significantly cheaper than carbamoylphosphineoxides. At the same time, the extraction properties of CCD – DPDA and CCD – CMPO mixtures are practically the same. It should be also emphasized that, by applying DPDA instead of CMPO one can use higher concentrations of DPDA and thus increase the limiting concentration of REE and An in the extractant. This property is of prime importance for treatment of waste with a high REE content. The modified UNEX-extractant CCD-TBDPA – Slovafol-909 in F-3 was tested on simulated waste with high REE content. Cesium, strontium and minor actinides were recovered rather efficiently. At extraction from the simulated solution bearing more than 4 g/L REE, the high separation factors of americium remained even after three successive contacts with fresh portions of aqueous solutions. Dynamic testing of this extractant was performed at Mayak PA in collaboration with RI. The extraction process was stable and americium was extracted more effectively than europium. Hydrodynamic and extraction properties were unaffected during the tests.

Selective stripping is one possible direction for UNEX process development. The data on selective stripping of metals from both organic solvents are presented in Tables 9.19 and 9.20. It can be seen that, in the case of a saturated UNEX solvent (0.08 M CCD + 0.015 M PEG-400 + 0.013 M CMPO in FS-13), actinides and lanthanides can first be stripped with a solution (A) of ammonium carbonate and acetohydroxamic acid (AHA), and then Sr can be stripped separately from Cs with a solution of $(NH_4)_2CO_3$ with AHA and DTPA (B). Cesium is stripped in the last stage using 2 M methylamine carbonate solution [39].

Table 9.19 Selective stripping of metals from UNEX solvent (0.08 M CCD + 0.015 M PEG-400 + 0.013 M CMPO in FS-13)

Stripping solution	D					
	Cs	Sr	Eu	Pu	Np	U
A 1 M $(NH_4)_2CO_3$ + 0.1 M AHA	4.4	2.3	0.005	0.02	0.005	0.02
B 1 M $(NH_4)_2CO_3$ + 0.1 M AHA + 0.05 M DTPA	4.1	0.002	0.002	0.01	0.001	0.06

Table 9.20 Stripping of metals from *modified* UNEX solvent (0.1 M CCD + 0.025 M PEG-400 + 0.05 M TBDPA in FS-13)

Aqueous phase	D			
	Cs	Sr	Am	Eu
A 1 M $(NH_4)_2CO_3$ + 0.13 M AHA	1.9	2.7	21	561
C 1 M $(NH_4)_2CO_3$ + 0.078 M Citric acid	1.7	0.45	11	–
D 1 M $(NH_4)_2CO_3$ + 0.052 M NTA	2.0	0.46	1.2	–
E 1 M $(NH_4)_2CO_3$ + 0.024 M HEDPA	2.1	1.1	2.9	–
F 1 M $(NH_4)_2CO_3$ + 0.013 M DTPA	1.8	0.009	0.04	0.02
G 1 M $(NH_4)_2CO_3$ + 0.039 M DTPA	2.0	0.008	0.04	0.0001
H 1 M $(NH_4)_2CO_3$ + 0.2 M Glycine + 0.013 M DTPA	1.8	0.031	1.6	–
I 1 M $(NH_4)_2CO_3$ + 0.2 M Glycine + 0.026 M DTPA	2.1	0.030	1.4	–

The same stripping solutions were examined for the recovery of metals of interest from the modified UNEX-solvent (0.1 M CCD + 0.05 M TBDPA + 0.025 M PEG in FS-13). Unlike in the previous case, the use of 1 M $(NH_4)_2CO_3$ + 0.013 M AHA does not provide stripping of Ln and An elements; therefore, different complexants were examined, such as citric acid, nitrilotriacetic acid (NTA), hydroxyethylene-diphosphonic acid (HEDPA), diethylene triamine pentaacetic acid (DTPA), mixed with ammonium carbonate. The most promising data were obtained with aminoacetic acid (glycine) used as a buffer compound (solutions H and I). The principal scheme for selective stripping is indicated in Fig. 9.15. As a first stage, the selective stripping of Sr with a solution H (1 M $(NH_4)_2CO_3$ + 0.02 M glycine + 0.013 M DTPA) is applied. At the second stage, a solution G (1 M $(NH_4)_2CO_3$ + 0.039 M DTPA) provides the selective separation of An and Ln. Cesium can be stripped in the last stage using 2 M methylamine carbonate solution.

The data presented confirm that it is possible to achieve the separation of nuclide groups by selective stripping.

1 M $(NH_4)_2$ CO_3 +
0.02 M Glycine +
0.013 M DTPA

1 M $(NH_4)_2CO_3$ +
0.039 M DTPA

2 M MAC

| Extraction | Stripping 1 | Stripping 2 | Stripping 3 |

Sr

An + Ln

Cs
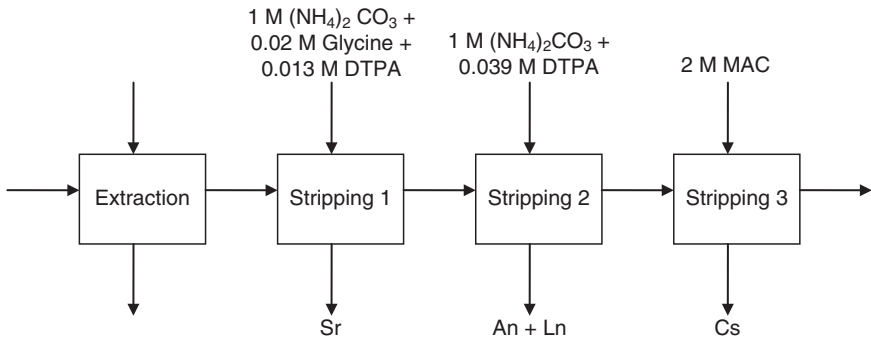
9.15 Scheme of selective metal stripping from the modified UNEX-solvent.

9.4   Conclusions

As a result of collaboration between RI and INL, the universal extraction system based on CMPO or DPDA, CCD and PEG in polar diluents have been developed, which permit the recovery of Cs, Sr, An and Ln.

The optimal composition of the UNEX-solvent was determined and the conditions for extraction (combined and fraction) of long-lived radionuclides were established. The high chemical and radiation resistance of the UNEX system, as well as its corrosion, explosion and fire safety, were demonstrated under operating conditions.

Variants of work flows based on the UNEX process were developed and tested at pilot plants belonging to KRI, NIKIMT and MCC in Russia, and at INL in the USA, with the use of real and simulated HLW of different compositions. Optimization of the UNEX process resulted in creation of a simple-to-realize work flow involving the three following operations: combined extraction of Cs, Sr, An and REE, scrubbing of the extract and combined stripping of all radionuclides under study; the recovery rates of radionuclides attained in the course of tests allowed the main HLW bulk to be transferred into the category of low-level waste.

The possibility for realizing the UNEX process on a commercial scale was verified by its testing with the use of the commercial EZR125 centrifugal contactors and with simulated HLW. As to the secondary (end) products of the UNEX process (raffinate and strip product), techniques for their solidification were proven; the traditional technique of cementing was checked for low-level raffinate; the vitrification process for high-level strip products demonstrated the possibility of producing glass blocks with a volume of 5 L for every 1 m^3 of HLW being treated. The method for regeneration of spent extractant of the UNEX process was elaborated and tested, which made it possible to return more than 90% FS-13 diluent and 40% CCD for re-use.

Thus, the technologies developed and tested for HLW treatment have shown the possibility of deep recovery of radionuclides which allows to transfer the main bulk of wastes into the category of low-level wastes (LLW) suitable for inexpensive near-surface storage. The results of feasibility study, conducted by Idaho National Laboratory have confirmed that the use of UNEX process should reduce the amount of solidified HLW by a factor of 23.

9.5　References

1. Liu, X., Liang, J., Xu, J. *Solv. Extr. Ion Exch.*, 2004, V.22(2), pp. 163–173
2. Duan, W., Wang, J., Chen, J., *et al. J. Radioanal. Nucl. Chem.*, 2007, V.273(1), pp. 103–107
3. Law, J.D., Herbst, R.S., Todd, T.A., *et al. Proc. Topic. Meet. Spectrum'96*, Seattle, WA, USA, Aug. 18–23, 1996, V.3, pp. 2308–2313
4. Horwitz, E.P., Kalina, D.G., Diamond, H., *et al.* The TRUEX process – a process for the extraction of the transuranic elements from nitric acid wastes utilizing modified Purex solvent *Solv. Extr. Ion Exch.*, 1985, V.3(1&2), pp. 75–109
5. Ozawa, M., Koma, Y., Nomura, K., Tanaka, Y. Separation of actinides and fission products in high-level liquid wastes by the improved TRUEX process *J. Alloys Compd.*, 1998, V.271–273, pp. 538–543
6. Arnaud-Neu, F., Schwing-Weill, M.-J., Dozol, J.-F. Calixarenes for nuclear waste treatment in *Calixarenes 2001*, 2002, V. Böhmer, Ed., pp. 642–662
7. Mukaiyama, T., Kubota, M., Takizuka, T., *et al. Proc. Int. Conf. Global 1995*, Versailles, France, Sept. 11–14, 1995, V.1, pp. 110–117
8. Ya., B., Zilberman, Yu., Fedorov, S., Shmidt, O.V., Esimantovskiy, V.M., Shishkin, D.N., Puzikov, E.A., Egorova, O.N., Rodionov, S.A., Goletskiy, N.D., Choppin, G.R. Dibutyl phosphoric acid and its acid zirconium salt as an extractant for the separation of transplutonium elements and rare earths and for their partitioning *J. of Radioanal. Nucl.Chem.*, 2009, V.279(1), pp. 193–208
9. Dozol, J.F., Dozol, M., Macias, R.M. Extraction of strontium and cesium by dicarbollides, crown ethers and functionalized calixarenes *J. Incl. Phenom. Macrocyclic Chem.*, 2000, V.38(1–4), pp. 1–22
10. Bonnesen, P.V., Delmau, L.H., Moyer, B.A., Leonard, R.A. A Robust Alkaline-Side CSEX Solvent Suitable for Removing Cesium from Savannah River High Level Waste *Solv. Extr. Ion Exch.*, 2000, V.18(6), pp. 1079–1108
11. Madic, C., Boullis, B., Baron, P., Testard, F., Hudson, M.J., Liljenzin, J.-O., Christiansen, B., Ferrando, M., Facchini, A., Geist, A., Modolo, G., Espartero, A.G., De Mendoza, J. Futuristic back-end of the nuclear fuel cycle with the partitioning of minor actinides *J. Alloys Compd.*, 2007, V.444–445, pp. 23–27
12. Malmbeck, R., Courson, O., Pagliosa, G., *et al. Radiochim. Acta*, 2000, V.88(12), 865–871
13. Sasaki, Y., Sugo, Y., Suzuki, H., *et al. Proc. Int. Conf. Atalante 2004*, France, June 21–24, paper #P1–53
14. Rais, J., Grüner, B. Extraction with metal Bis(dicarbollide) anions in: *Ion Exchange and Solvent Extraction*, V.17, Y. Marcus and A. K. SenGupta, Eds., Marcel Dekker, Inc, New York, NY, 2004, pp. 243–334

15. Glagolenko, J.V., Logunov, M.V., Mamakin, I.V., *et al.* Extraction of radio-nuclides by crown ether-containing extractants Pat WO2006036083 (Publ. 06 Apr 2006)

16. Riddle, C.L., Baker, J.D., Law, J.D., McGrath, C.A., Meikrantz, D.H., Mincher, B.J., Peterman, D.R., Todd, T.A. Fission Product Extraction (FPEX): Development of a novel solvent for the simultaneous separation of strontium and cesium from acidic solutions *Solv. Extr. Ion Exch.*, 2005, V.23(3), pp. 449–461

17. Dhami, P.S., Chitnis, R.R., Gopalakrishnan, V., Wattal, P.K., Ramanujam, A., Bauri, A.K. Studies on the partitioning of actinides from high level waste using a mixture of HDEHP and CMPO as extractant *Sep. Sci. Technol.*, 2001, V.36(2), pp. 325–335

18. Gannaz, B., Chiarizia, R., Antonio, M.R., Hill, C., Cote, G. Extraction of lanthanides(III) and Am(III) by mixtures of malonamide and dialkylphosphoric acid *Solv. Extr. Ion Exch.*, 2007, V.25(3), pp. 313–337

19. Romanovskiy, V.N. Review of historical development and application of separation technologies in Russia, in *Chemical Separation Technologies and Related Methods of Nuclear Waste Management*, 1999 Kluwer Academic Publishers, pp. 17–18

20. Rais, J., Selucky, P., Kyrs, M. Extraction of caesium into nitrobenzene in the presence of univalent polyhedral borate anions *J. Inorg. Nucl. Chem.*, 1976, V.38(7), pp. 1376–1378

21. Zilberman, B. Ya., Romanovskii, V.N., Extraction Studies at the Khlopin Radium Institute *Radiochemistry*, 2003, V.45(3), 211–218

22. Vandegrift, G.F., Regalbuto, M.C., Aase, S., Bakel, A., Battisti, T.J., Bowers, D., Byrnes, J.P., Clark, M.A., Emery, J.W., Falkenberg, J.R., Gelis, A.V., Pereira, C., Hafenrichter, L., Tsai, Y., Quigley, K.J., Vander Pol, M.H. Designing and Demonstration of the UREX+ Process Using Spent Nuclear Fuel ATATLANTE 2004, International Conference, Nimes, France, June 21–24, 2004, paper 012–01

23. Rais, J., Tachimori, S. Extraction separation of tervalent americium and lanthanides in the presence of some soft and hard donors and dicarbollide *Sep. Sci. Technol.*, 1994, V.29(10), pp. 1347–1365

24. Smirnov, I.V. Recovery of long-lived radionuclides from HLW by extraction mixtures on the base of cobalt dicarbollide and phosphorylated polyethylene glycols Spectrum-96, Seattle, USA, Proceedings, ANS Inc, 1996, pp. 2115–2118

25. Smirnov, I.V., Babain, V.A., Shadrin, A.Y. Combined reprocessing of HLW by Universal Solvent on the Base of Cobalt Dicarbollyde and Phosphorylated Polyethylehe Glycol Spectrum-98, Denver, Colorado, USA, September 13–18, 1998, Proceedings, American Nuclear Society Inc, USA, 1998, pp. 606–609

26. Romanovskiy, V.N., Smirnov, I.V., Todd, T.A., Herbst, R.S., Law, J.D., Brewer, K.N. The Universal Solvent Extraction (UNEX) Process. I. Development of the UNEX Process Solvent for the Separation of Cesium, Strontium, and the Actinides from Acidic Radioactive Waste *Solv. Extr. Ion Exch.*, 2001, V.19(1), pp. 1–21

27. Law, J.D., Herbst, R.S., Todd, T.A., Romanovskiy, V.N., Esimantovskiy, V.M., Smirnov, I.V., Zaitsev, B.N. The Universal Solvent Extraction (UNEX) Process. II. Flowsheet Development and Demonstration of the UNEX Process Solvent for the Separation of Cesium, Strontium, and the Actinides from Actual Acidic Radioactive Waste *Solv. Extr. Ion Exch.*, 2001, V.19(1), pp. 23–36

28. Herbst, R.S., Law, J.D., Todd, T.A., Romanovskiy, V.N., Babain, V.A., Esimantovskiy, V.M., Smirnov, I.V., Zaitsev, B.N. Universal Solvent Extraction (UNEX) Flowsheet Testing For The Removal Of Cesium, Strontium, And Actinide Elements From Radioactive, Acidic Dissolved Calcine Waste *Solv. Extr. Ion Exch.*, 2002, V.20(4&5), pp. 429–445

29. Todd, T.A., Law, J.D., Herbst, R.S., Romanovskiy, V.N., Smirnov, I.V., Babain, V.A., Esimantovskiy, V.M., Zaitsev, B.N., Nazin, E.G., Egorov, G.F. Development and characterization of a universal solvent mixture for the separation of Cs, Sr, actinides and rare-earth elements from acidic radioactive waste ISEC-2002, Proceedings pp. 1220–1228

30. Herbst, R.S., Law, J.D., Todd, T.A., Romanovskiy, V.N., Smirnov, I.V., Babain, V.A., Esimantovskiy, V.M., Zaitsev, B.N. Development of the Universal Extraction (UNEX) Process for the Simultaneous Recovery of Cs, Sr, and Actinides From of Acidic Radioactive Wastes, *Sep. Science & Technology*, 2003, V.38(12&13), pp. 2685–2708

31. Romanovskiy, V.N., Smirnov, I.V., Babain, V.A., Todd, T.A., Brewer, K.N., RF patent 2163403, publ.BI N∘5, 20.02.2001
    Method for the Simultaneous Recovery of Radionuclides from Liquid Radioactive Wastes Using a Solvent. 2001, US Patent 6258333
    Solvent for the simultaneous recovery of radionuclides from liquid radioactive wastes 2002, US Patent N 6,468,445 B2

32. Alekseenko, S., Babain, V., Bondin, V., Viznyi, A., Esimantovskiy, V., Krivitskiy, Y., Kuznetsov, G., Rodionov, S., Romanovskiy, V., Smirnov, I., Todd, T., Shklyar, L. Testing of UNEX-process on Centrifugal Contactor Mocup of Mining and Chemical Combine Proceedings of GLOBAL 2005, Tsukuba, Japan, Oct 9–13, 2005, Paper No. 347

33. Rais, J., Selucky, P., Kyrs, M., Kadlecova, L. Extraction of cesium and barium by dicarbollide and polyethyleneglycol in the presence of alkylammonium cations *J. Radioanalyt & Nucl. Chem.*, 1994, V.178(1), pp. 27–39

34. Romanovskiy, V.N., Babain, V.A., Smirnov, I.V., *et al.* RF Patent N∘ 2235375 Method for stripping of metals. Bull. Inv. N∘ 24, 27.08.2004; US patent 7,494,630 Method of stripping metals from organic solvents (February 24, 2009)

35. Law, J.D., Herbst, R.S., Peterman, D.R., *et al.*, Development of a Regenerable Strip Reagent for Treatment of Acidic Radioactive Waste with Cobalt Dicarbollide-based Solvent Extraction Processes *Solv. Extr Ion Exch.*, 2005, V.23(1), pp. 59–84

36. Egorov, G.F., Tkhorgnitsky, G.P., Romanovskiy, V.N., *et al.*, Radiation stability of regenerated stripping solutions for high-level waste processing *J. Radioanalyt. & Nucl. Chem.*, 2005, V.266(2), pp. 349–353

37. Alyapyshev, M.Y., Babain, V.A., Smirnov, I.V. Extractive properties of Synergistic mixtures of Dipicolinic Acid Diamides and Chlorinated Cobalt Dicarbollide *Radiochemistry*, 2004, V.46(3), pp. 270–271

38. Romanovskiy, V.N., Babain, V.A., Alyapyshev, M.Y., Smirnov, I.V., Herbst, R.S., Law, J.D., Todd, T.A. Radionuclide extraction by 2,6-pyridinedicarboxylamide derivatives and chlorinated cobalt dicarbollide *Separation Science and Technology*, 2006, V.41(10), pp. 2111–2127

39. Babain, V., Smirnov, I., Alyapyshev, M., Todd, T., Law, J., Herbst, R., Paulenova, A. Radionuclide partitioning in the modified UNEX process. Proc. of ISEC 2008 Int.Conf., Tucson, USA, 2008, pp. 665–670

Nuclear engineering for pyrochemical treatment of spent nuclear fuels

T. KOYAMA, Central Research Institute of
Electric Power Industry, Japan

Abstract: In this chapter, state of the art in nuclear technology development as well as basic principles of pyrochemical treatment, in other words, dry reprocessing, are described. Although this technology has not been commercialized yet, engineering-scale tests with real spent fuels and/or surrogates are underway in many countries, especially in the US, Russia and Asia. As the technology has an intrinsic nuclear proliferation resistance, due to its inherent difficulty in separation of pure plutonium, it is regarded as one of the most promising nuclear fuel cycle technologies of the next generation.

Key words: pyroprocess, dry reprocessing, electrorefining, molten salt, liquid metal, injection casting.

10.1 Introduction

What do we expect for pyrochemical treatment? As indicated by the prefix, '*pyro*' ('fire' in Greek), we need high temperature, and we must use an unfamiliar liquid medium, *a molten salt*, in an inert atmosphere. However, pyrochemistry is expected to be the most promising method to solve the difficulties related to the treatment of spent fuel. For example, radiation damage of the solvent is not a concern at all because the molten salt is a fully dissociated ionic liquid. Hence, the treatment of relatively short-cooled spent fuel as well as a decrease in secondary waste due to radiation damage of the solvent are expected. Because water, which acts as a neutron moderator, is not present in pyrochemistry, a larger quantity of fissile materials can be handled compared with aqueous processing. In addition, simple but incomplete purification techniques such as electrorefining can be applied because the recycled nuclear fuel will later be used in fast neutron reactors. Hence, pyrochemistry is potentially more compact than aqueous technologies, and a reduction of the fuel cycle cost is expected. The incomplete purification implies the group recovery of actinides in any step of pyrochemistry, which results in an inherent difficulty in separating weapon-usable plutonium. Although purification is not complete, the recovery of minor actinides (MA) such as neptunium, americium and curium,

269

separating them from fission products (FP), is sufficient to supply the products required for fast reactors.

For these reasons, various types of pyrochemical processes using different molten salts have been proposed by many nuclear research institutes. Argonne National Laboratory (ANL) and Idaho National Laboratory (INL) have proposed a pyrochemical treatment, referred to as a 'pyroprocess', suitable for metal fuel processing. Because the process uses chloride molten salts with relatively low melting points, for example, 352 °C for LiCl-KCl, without the evolution of a corrosive gas, engineering difficulties related to the materials are reduced. This might be the reason why this pyrochemical process is the most developed technology and has already been used to treat approximately 4 tons of heavy metals (HM) of spent fuels from the Experimental Breeder Reactor (EBR)-II, and has been applied in many institutes such as the Central Research Institute of Electric Power Industry (CRIEPI) in Japan and the Indira Gandhi Centre for Atomic Research (IGCAR) in India for spent fuel reprocessing, and at the Korea Atomic Energy Research Institute (KAERI) in Korea for spent fuel treatment.

Another pyrochemical process is electrorefining of oxide fuels in NaCl-CsCl molten salt bath, proposed by the Research Institute of Atomic Reactors (RIAR) in Russia. The recovery of plutonium and uranium as oxide forms was demonstrated using irradiated fast breeder reactor (FBR) MOX fuels. As the details of experimental results have not been reported, issues related to nuclear engineering at a higher temperature (650 °C) in the presence of chlorine gas are not apparent. The recovery of MA is another matter to be clarified. The fluoride processes being developed at the Commissariat à l'Énergie Atomique (CEA) in France, and other institutes are still at the stage of laboratory-scale experiments and require progress in engineering. The Nuclear Research Institute Řež plc of Czech Republic is developing a fluoride volatility process for the reprocessing of oxide fuels. Fluorination furnaces as well as UF_6 condensers have operated well on an engineering scale; however, experiments with irradiated fuel are required to demonstrate the process. Thus, in this chapter, state-of-the-art nuclear engineering for pyrochemistry will be described, mainly focusing on the *pyroprocess* being developed at ANL, INL, CRIEPI, KAERI and IGCAR.

For newcomers to the study of pyrochemistry, the difficulties lie in the lack of specific technological knowledge on the handling of high temperature molten salts, e.g. purification and control of the atmosphere, the selection of compatible materials, the fabrication of stable reference electrodes, and so on. Although it is not described explicitly, the nuclear engineering discussed in this chapter has been developed on the basis of the technological knowledge accumulated in each laboratory. Unfortunately, know-how

is rarely described in published papers; thus, literature containing technical details are cited in Section 10.8 for further reference.

10.2   Process chemistry and flowsheet of pyrochemical processing

10.2.1 The pyrometallurgical process for metal fuels

There are different versions of the pyroprocess depending on the material to be treated. Figure 10.1 shows a flowchart of the pyroprocess for reprocessing a metal fuel, i.e. U-Pu-10wt%Zr alloy for the core fuel and U-10wt%Zr alloy for the blanket fuel of a fast neutron reactor. In this section, the principles of each step of the pyroprocess will be described.

Disassembly and chopping

In the 'disassemble and chopping' process, hexagonal spent fuel assemblies are disassembled, and fuel elements with stainless steel cladding are chopped into small segments. The technologies developed for oxide fuel assemblies can be applied in this process.

Electrorefining

The next step is the electrorefining process, schematically shown in Fig. 10.2, where the chopped spent metal fuels are dissolved in an anode basket,

AC = U, Pu, MA
NFP = Noble FPs (Ru, Rh, Pd, Mo, Tc, Zr)
LFP = Less noble FPs (Cs, Sr, Ba, Y, Ln, I)
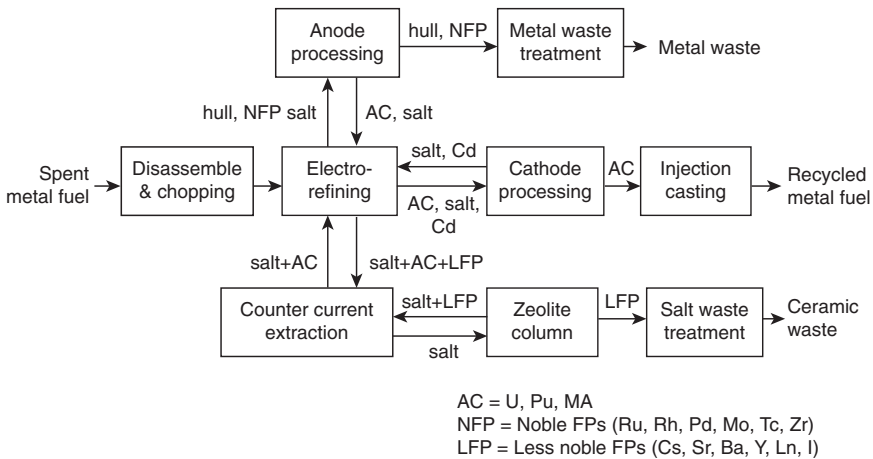
10.1 Process flowsheet of pyroprocess for metal fuel reprocessing. (Revised by the author according to the latest experimental results.)
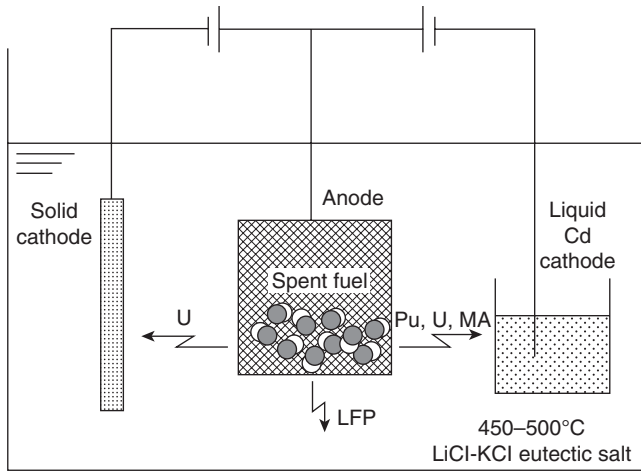
10.2 Schematic view of electrorefining process.

whilst actinide metals are recovered at a solid cathode, or a liquid Cd cathode. The main reaction schemes of electrorefining are described as follows:

Anode:	$U_{\text{in spent fuel}} \rightarrow U^{3+} + 3e^-$	10.1
	$Pu_{\text{in spent fuel}} \rightarrow Pu^{3+} + 3e^-$	10.2
Cathode (solid):	$U^{3+} + 3e^- \rightarrow U$	10.3
Cathode(liquid Cd):	$U^{3+} + 3e^- \rightarrow U_{\text{in Cd}}$	10.4
	$Pu^{3+} + 3e^- + 6Cd \rightarrow PuCd_6$	10.5
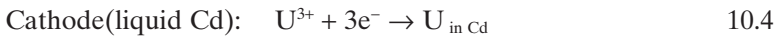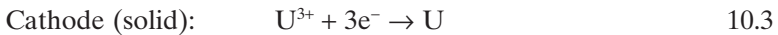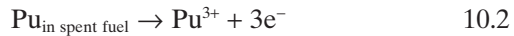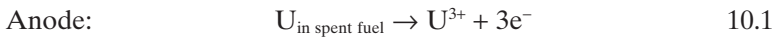
This process utilizes the oxidation-reduction potentials of the relevant elements shown in Table 10.1. The constituents of the spent fuel that have lower standard potentials than zirconium, i.e. actinides and less noble FP (LFP) such as the alkali metal FP, the alkaline-earth metal FP and lanthanide FP, are electrochemically dissolved at the anode. Conversely, elements having higher standard potentials, i.e. zirconium, iron (cladding), cadmium, and noble FP (NFP) such as ruthenium, rhodium, palladium, technetium and molybdenum, remain undissolved in the anode basket. At the solid cathode, uranium is preferentially reduced and collected since it is the most easily reduced element among the dissolved materials. Other actinides, such as plutonium, neptunium, americium and curium are recovered with uranium in the liquid cadmium cathode because the reduction potentials of these elements are very close to that of uranium, as shown in the right-hand column of Table 10.1, due to their strong affinity with cadmium, i.e.

Table 10.1 Oxidation-reduction potentials of elements in LiCl-KCl eutectic melt at 450 °C

Solid electrode	Standard potential		[Cd electrode]	Reduction potential*	
	(V vs. Cl_2/Cl^-)			(V vs. Cl_2/Cl^-)	
Ru(III)/Ru(0)	−0.358	(Plambeck, 1976)			
Rh(III)/Rh(0)	−0.447	(Plambeck, 1976)			
Pd(II)/Pd(0)	−0.430	(Plambeck, 1976)			
Fe(II)/Fe(0)	−1.388	(Plambeck, 1976)			
Cd(II)/Cd(0)	−1.532	(Plambeck, 1976)			
Zr(IV)/Zr(0)	−2.076	(Plambeck, 1976)			
U(III)/U(0)	−2.468	(Sakamura, 1998)	U(III)/U-Cd	−2.557	(Sakamura, 1998)
Np(III)/Np(0)	−2.674	(Sakamura, 2000)	Np(III)/Np-Cd	−2.560	(Johnson, 1965)
Pu(III)/Pu(0)	−2.773	(Sakamura, 2001)	Pu(III)/Pu-Cd	−2.564	(Johnson, 1965)
Am(II)/Am(0)	−2.827	(Sakamura, 1998)	Am(III)/ Am-Cd	−2.576	(Sakamura, 2001)
Gd(III)/Gd(0)	−2.990	(Sakamura, 1995)	Gd(III)/Gd-Cd	−2.665	(Sakamura, 1995)
Pr(III)/Pr(0)	−3.040	(Sakamura, 1995)	Pr(III)/Pr-Cd	−2.631	(Sakamura, 1995)
Nd(III)/Nd(0)	−3.047	(Sakamura, 1995)	Nd(III)/Nd-Cd	−2.633	(Sakamura, 1995)
Ce(III)/Ce(0)	−3.056	(Sakamura, 1995)	Ce(III)/Ce-Cd	−2.636	(Sakamura, 1995)
Y(III)/Y(0)	−3.068	(Sakamura, 1995)	Y(III)/Y-Cd	−2.753	(Sakamura, 1995)
La(III)/La(0)	−3.103	(Sakamura, 1995)	La(III)/La-Cd	−2.661	(Sakamura, 1995)
Li(I)/Li(0)	−3.626	(Plambeck, 1976)	Li(I)/Li-Cd	−2.765	(Lewis, 1990)

*The reduction potentials of elements in LiCl-KCl eutectic salt into liquid cadmium alloy were derived when the concentrations of the elements in the salt and in liquid cadmium were the same (0.001 mole fraction).

(a)   (b)
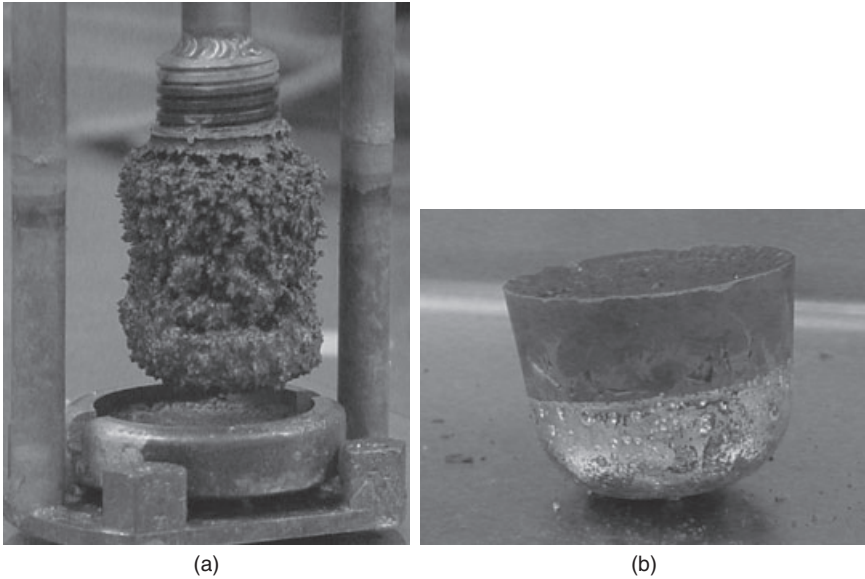
10.3 Typical cathode products obtained in a laboratory-scale electrorefiner. (a) dendritic U deposit on solid cathode (b) Pu-U-MA-Cd alloy covered with frozen salt.

they form intermetallic compounds such as $PuCd_6$. Consequently, this gives a proliferation-resistant nature to the process, since it is almost impossible to separate out pure plutonium. Typical cathode products obtained in a laboratory-scale electrorefiner (Koyama, 2002) are shown in Fig. 10.3, where (a) is a uranium deposit on the solid cathode and (b) is a plutonium-uranium-MA deposit in the cadmium cathode. As shown in this figure, the actual cathode deposits contain adhering salt and/or alloying cadmium in addition to actinide metals, though the actinide cations are reduced into metal form at the cathodes.

Cathode processing

After the deposits are mechanically removed from the solid cathode rod or from the cathode crucible used at the electrorefining process, each deposit is heated in a 'cathode processing' step to separate the actinide metals by distillation of adhering salt and cadmium. As shown in Fig. 10.4, the vapour pressures of cadmium and chlorides are sufficiently higher than those of the actinide elements to be separated from them by distillation.
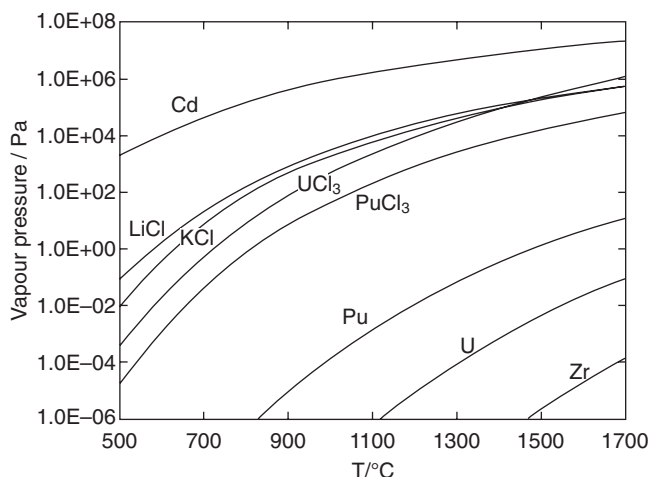
10.4 Equilibrium vapour pressures over relevant substances.

Injection casting

The actinide metals obtained in the cathode processing step are treated in an 'injection casting' process, with additional uranium and zirconium to adjust the composition of the recycled fuels. The uranium-zirconium alloy is vacuum melted at approximately 1560 °C and the plutonium-uranium-MA-zirconium alloy at approximately 1480 °C (Nakamura, 2009), before they are then injection-casted into a bundle of quartz moulds by ambient pressure to form metal fuel rods consisting of core and blanket fuels, respectively. Recycled metal fuel elements are fabricated by inserting these rods into steel cladding with sodium metal as thermal bonding.

Anode processing

After the electrorefining operation, the dissolution residue (which mainly consists of the stainless steel cladding hull, zirconium and NFP) remain in the anode basket. The composition of the residue strongly depends on the electrorefining conditions. As the chopped U-Pu-Zr or U-Zr metal fuel dissolves from outside to inside, it leaves behind a zirconium layer that acts as a dissolution barrier (Koyama, 2002) and it is necessary to charge a higher anode potential to dissolve the zirconium and ensure complete dissolution of the actinides. Experiments with spent U-Zr fuels have shown that an average 99.7 wt% uranium dissolution is achieved with the dissolution of approximately 88 wt% zirconium, while approximately 75% of NFP was retained in the cladding hulls (Li, 2005). About one-third of the

dissolved zirconium was electrochemically deposited on the solid cathode along with uranium to be cathode processed, while the rest of the dissolved zirconium fell down to the bottom of the electrorefiner (Li, 2007). The electrochemical recovery of zirconium from the bottom cadmium layer was carried out, and a zirconium-rich uranium deposit was obtained. Alternatively, a dissolution mode to leave zirconium and NFP in the anode basket is an operation to reduce the effort of recovering these materials from the bottom of the electrorefiner, although part of the actinides remain undissolved. Whichever mode is selected, the dissolution residue in the anode basket is further treated in an 'anode processing' step to recover residual actinide, depending on the recovery ratio required.

Metal waste treatment

In the 'metal waste treatment' step, the dissolution residues obtained in the anode processing step are melted together with zirconium and NFP (recovered from the bottom of the electrorefiner) to synthesize a metal ingot, called a metal waste form (MWF). At the same time, the entrained salt is distilled and separated from the MWF to be recycled in the electrorefiner. Zirconium or stainless steel is added to the metal waste before melting to produce MWF ingots that have a consistent composition, phase assemblage and microstructures. The target composition of the MWF is stainless steel with 15 wt.% zirconium, because the Fe-Zr phase diagram indicates that Fe-15Zr has a relatively low solidus temperature of 1325 °C (Arias, 1993). MWF is a multiphase alloy comprising two Fe rich solid-solution phases and several $FeZr_2$-type intermetallic phases. NFP are distributed in either one or both of the main solid solution and $FeZr_2$-type intermetallic phases, while actinide elements are preferentially incorporated into the intermetallic phase. According to extensive examination and testing undertaken by ANL and INL to gain acceptance for the Yucca Mountain geological repository, MWFs are extremely robust with regard to retention of NFP in repository-like conditions (Ebert, 2005).

Counter current extraction

In the electrorefiner, LFP in the molten salt gradually builds up during processing of the spent fuels. In order to limit the decay heat content and the contamination of the cathode products, the molten salts in the electrorefiner are periodically treated in the 'counter current extraction' process and 'zeolite column' process to decrease LFP content. As shown in Fig. 10.5, feed salt from the electrorefiner comes in contact with liquid cadmium at approximately 450 °C to extract actinides into liquid cadmium (as a
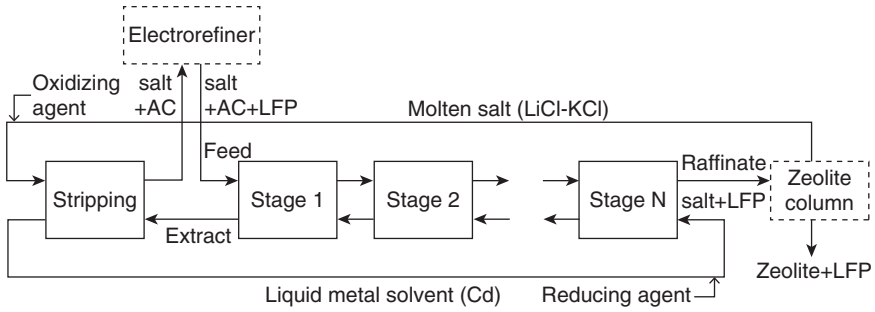
10.5 Flowsheet for counter current extraction.
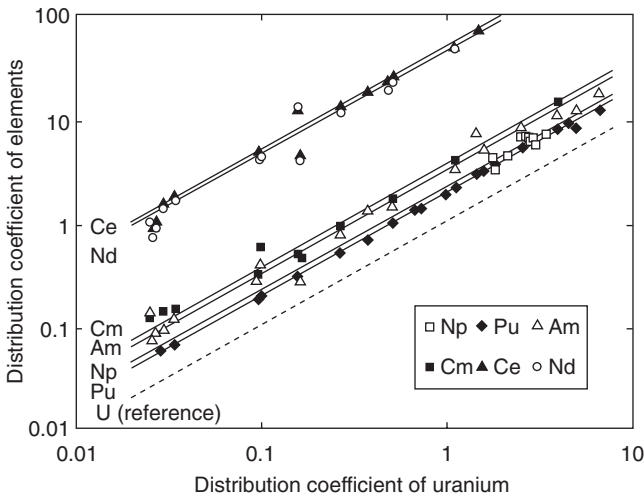
10.6 Distribution of actinides and lanthanide elements between molten salt and liquid cadmium.

liquid metal solvent). The treated salt (raffinate) is additionally decontaminated during the 'zeolite column' process, and the decontaminated salt comes in contact with the cadmium (extract) from the first stage of the counter current extraction, to strip actinides from the molten salt to be recycled in the electrorefiner. The number (N) of stages necessary depends on the separation requirements and distribution characteristics. Figure 10.6 shows the measured distribution data that rules separation efficiency at each stage (Koyama, 1992). In a liquid chloride salt and cadmium metal system, equilibrium among the elements is achieved by redox reaction between cations in the salt and metal atoms in the cadmium. The chlorine anions remain in the salt and are not oxidized. Thus, the equilibrium among

two cations can be represented as an exchange reaction between the pair of elements. Take, for example

$$nUCl_3 + 3M = nU + 3MCl_n \qquad\qquad 10.6$$

The equilibrium constant, Ke, for the reaction is

$$Ke = \left(\frac{[MCl_n]}{[M]}\right)^3 \left(\frac{[U]}{[UCl_3]}\right)^n$$
$$= \exp\left(\frac{-[\Delta G^\circ(MCl_n) - \Delta G^\circ(UCl_3)]}{RT}\right) \qquad\qquad 10.7$$

where [M], [MCl$_n$], ΔG°, R and T denotes activity of M in the cadmium phase, activity of M in the salt phase, standard free energy of formation, gas constant and temperature in Kelvin, respectively.

Here the distribution coefficient of an element, M, in a molten salt and liquid metal system is defined as

$$D_M = \frac{Y_M}{X_M}, \qquad\qquad 10.8$$

where Y_M and X_M denotes mole fraction of M in salt, and atom fraction of M in metal, respectively.

The separation factor of element M relative to uranium is defined as

$$SF_M = \frac{D_M}{D_U} \qquad\qquad 10.9$$

According to the thermodynamic relationship described in equation [10.7], the separation factor is described as

$$SF_M = Ke^{1/3} D_U^{(n-3)/3} \left(\frac{\gamma_M}{\gamma_{MCln}}\right) \left(\frac{\gamma_{UCl_3}}{\gamma_U}\right)^{n/3} \qquad\qquad 10.10$$

where γ denotes the activity coefficient.

As shown in Fig. 10.6, the distribution coefficients of actinides and lanthanides have a linear relationship with that of uranium. Agreement of the slopes suggest that these chlorides are the same, actually in trivalences. Hence, equation [10.10] can be simplified as

$$SF_M = Ke \left(\frac{\gamma_M}{\gamma_{MCln}}\right) \left(\frac{\gamma_{UCl_3}}{\gamma_U}\right). \qquad\qquad 10.11$$

This equation clearly shows the nature of the separation factor in this system. It is not just a chemical technological value but a function of thermodynamic properties that depends only on the temperature. In the counter current extraction process, therefore, each stage has different distribution coefficients but the same separation factor for each pair of elements. As

Table 10.2 Separation factors of elements from uranium in LiCl-KCl eutectic melt and liquid cadmium system at 500°C

Elements	Separation factor relative to uranium	
U	1.00	[basis]
Np	2.12	(Koyama, 1992)
Pu	1.88	(Koyama, 1992)
Am	3.08	(Koyama, 1992)
Cm	3.52	(Koyama, 1992)
La	130	(Ackermann, 1993)
Ce	49	(Ackermann, 1993)
Pr	43	(Ackermann, 1993)
Nd	44	(Ackermann, 1993)
Gd	150	(Ackermann, 1993)
Y	6000	(Ackermann, 1993)
Sm, Eu, Li, Ba, Sr*	$>10^{10}$	(Ackermann, 1993)

*The separation factors of divalent elements (Sm, Eu, Ba, Sr) and the monovalent element (Li) are the values when the distribution factor of uranium is 1.00.

shown in Table 10.2, the measured separation factors of trivalent lanthanides are more than ten times larger than those of trivalent actinides, suggesting that sufficient separation between actinides and lanthanides can be expected for the counter current extraction of several stages.

Zeolite column

Although the raffinate salt contains very low concentrations of actinides, it still needs to be treated at the 'zeolite column' process to remove LFP elements, by ion exchange with structural elements of zeolite or by occlusion of chloride molecules in the 3-dimensional cage structures of zeolite. Figure 10.7 shows the equilibrium absorption characteristics of alkali metal chlorides, alkaline-earth chlorides and lanthanide chlorides in zeolite-4A at temperatures ranging from 400°C to 450°C (Tsukada, 2008). As the figure shows, the amount of absorption depends on the fraction of the element in the salt and on the valence of the element. At the same equivalent fraction of approximately 0.1, the amount of lanthanide elements loaded is about twice that of alkali metal elements, while the amount of alkaline-earth elements loaded is about 1.5 times that of alkali metal elements. Though further study is still needed to gain detailed absorption behaviours, it is clear that zeolite-4A works as a potential absorbent of LFP from LiCl-KCl eutectic salt. To use zeolite as an LFP absorbent, a continuous system with a zeolite column is preferable from the point of view of efficiency; however, a batch-type system with a zeolite bed is also possible. Whichever system is employed, the LFP-loaded zeolite still needs further treatment to form
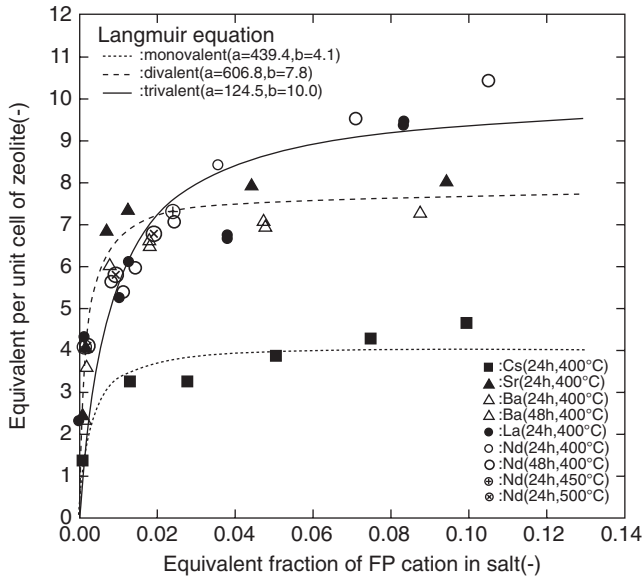
10.7 Absorption characteristics of alkali metal chloride, alkaline-earth chloride and lanthanide chloride in zeolite 4A.

acceptable waste because a certain amount of free salt containing LFP adheres to the surface of the zeolite.

Salt waste treatment

At the 'salt waste treatment' stage, the salt-loaded zeolite is mixed with fresh zeolite at approximately 500 °C to absorb the free salt, and the mixture is then heated up to approximately 925 °C to convert the salt-loaded zeolite into a more stable *sodalite* structure, $Na_8(AlSiO_4)_6Cl_2$, with borosilicate glass powder as a bonding material to microencapsulate the grains of sodalite. The glass-bonded sodalite obtained is referred to as ceramic waste form (CWF). The long-term stability of CWF is expected from the natural analogue of sodalite mineral, which contains chloride salt and iodine in its cage structure, in a stable form. Actually, sufficiently stable characteristics to meet Yucca Mountain requirements were reported for CWF based on the extensive studies carried out by ANL and INL from the early 1990s (Ebert, 2005).

10.2.2 The pyrochemical process for oxide fuel

The pyroprocess can be applied to spent oxide fuels if they can be converted into a metal form. Figure 10.8 shows a flowchart of the *pyrox process* for
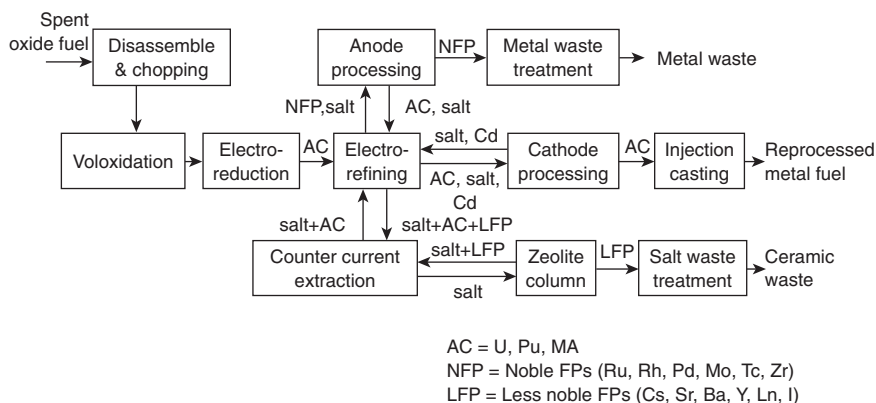
10.8 Pyrochemical process flowsheet for oxide fuel treatment.

oxide fuel treatment which employs voloxidation and electroreduction steps at the front-end. 'Voloxidation' is a process to facilitate the removal of spent uranium oxide fuel from its cladding. Sections of clad spent nuclear oxide fuels are subjected to high temperature and an oxygen-bearing atmosphere to convert UO_2 to U_3O_8 with a 30% volume expansion; the fuel matrix is consequently pulverized and dislodged from its cladding. During the voloxidation, partial removal of volatile fission products such as Cs, Te, Ru, Mo and Tc is expected (Westphal, 2008).

Electroreduction

'Electroreduction' is a relatively new technique to convert oxide fuel into a metal form, generating less radioactive waste than conventional reduction steps using a Ca reductant. In an electroreduction cell, schematically shown in Fig. 10.9, cathode baskets loaded with decladded oxide fuels and inert anode rods are immersed in a $LiCl$-Li_2O electrolyte, and electrolysis is carried out at approximately 650 °C to remove oxygen from the oxide fuel at the cathode and to generate oxygen gas at the anode. The main reactions at both electrodes are described as:

Anode: $yO^{2-}_{\text{in salt}} \rightarrow (y/2)O_2 + 2ye^-$ 10.12

Cathode: $M_xO_y + 2ye^- \rightarrow xM + yO^{2-}_{\text{in salt}}$ 10.13
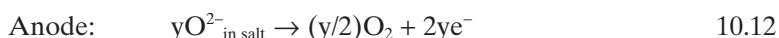
where M denotes actinides such as uranium and plutonium. The oxygen is electrochemically ionized, and the actinide metal remains at the cathode. The ionized O^{2-} is transported through the salt and is discharged at the anode to form O_2 gas. When a graphite anode is used, CO_2 or CO is evolved instead of O_2. During the reaction, some LFP elements such as
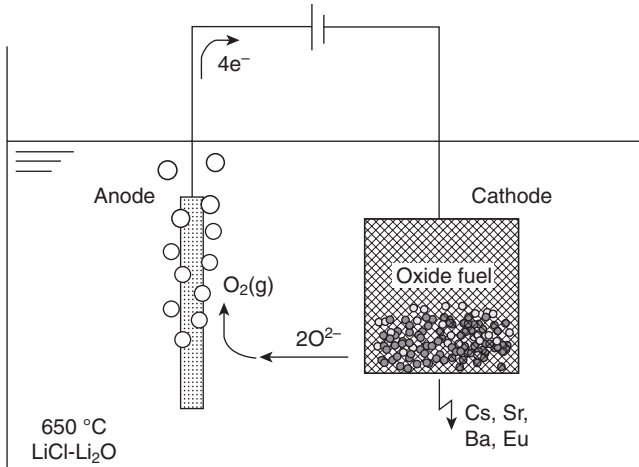
10.9 Schematic figure of electroreduction process.

cesium, strontium, barium and europium are dissolved into the salt phase. As the redox potentials for the reduction reaction have not yet been assessed, the formation energies of the oxides provide useful indexes for determining the reaction. Table 10.3 gives the standard Gibbs free energy of formation of oxide obtained from the thermodynamic database MALT-II (Japan Calorimetry Society, 1992). As this table shows, the possible reductions are of UO_2 and Pu_2O_3 because they are less stable than Li_2O. However, reductions of americium were observed in experiments on unirradiated mixed oxide fuel (Iizuka, 2006) and irradiated UO_2 fuel (Herrmann, 2005), suggesting the decrease of the chemical activity of americium due to the formation of a plutonium-americium solid solution in addition to the stabilization of O^{2-} in LiCl. The metal product obtained in the electroreduction step is then charged in the anode basket of the electrorefiner, and consequently treated in the same way as chopped spent metal fuels.

10.3   Design and installation of process equipment

10.3.1 Design characteristics of pyroprocess equipment

As for aqueous reprocessing, an economically feasible facility should have a throughput as much as several hundred tons HM/y. On the other hand, a pyrochemical reprocessing facility is expected to be economically feasible with a throughput of several tens of tons HM/y, because the processing equipment can handle a larger amount of actinides compared with aqueous reprocessing, owing to the difference in the nuclear criticality issue. Once

Table 10.3 Standard Gibbs free energy of formation at 650 °C*

Oxide	ΔG_f° (kJ/mol-O)
UO_2	−462.6
Pu_2O_3	−471.8
Li_2O	−475.8
Am_2O_3	−487.8
La_2O_3	−509.6
Ce_2O_3	−506.1
Pr_2O_3	−515.5
Nd_2O_3	−515.1
Sm_2O_3	−518.0
Gd_2O_3	−520.7
Y_2O_3	−545.6

*According to the thermodynamic database MALT-II assessed by Japan Calorimetry Society (Japan Calorimetry Society, 1992).

the pyrochemical process equipment has been demonstrated for several tens of tons HM/y, commercial facilities of several hundred tons HM/y can be realized by multiplexing the process equipment. Hence, the first phase of development is focused on demonstrating the feasibility of engineering-scale equipment capable of dealing with several tens of kg HM/batch (several tons HM/y), and the second phase is to increase throughput by design improvements, since an increase in throughput will directly improve the economies of processing. In this section, development of the main process equipment (described in the flowcharts in the previous section) is reported.

10.3.2 Electrorefiners

Since the electrorefining step is a core piece of the pyroprocess, an electrorefiner has been developed from a laboratory-scale model to an engineering-scale model after many experiments with irradiated and non-irradiated materials. The Mark IV electrorefiner shown in Fig. 10.10 is the first commercial-scale model developed by ANL and INL in the early 1990s, and has treated more than 1000 kg HM of EBR-II spent driver fuel in batches of about 24 kg HM since 1995 (Li, 2005). The electrorefiner vessel is made of steel (2.25Cr-1Mo) with an internal diameter of 1.0 m and a height of 1.0 m. The vessel contains a bottom layer of molten cadmium approximately 10 cm thick and a top layer of molten LiCl-KCl eutectic salt approximately 32 cm thick, containing approximately 10 wt.% UCl_3. The molten salt and
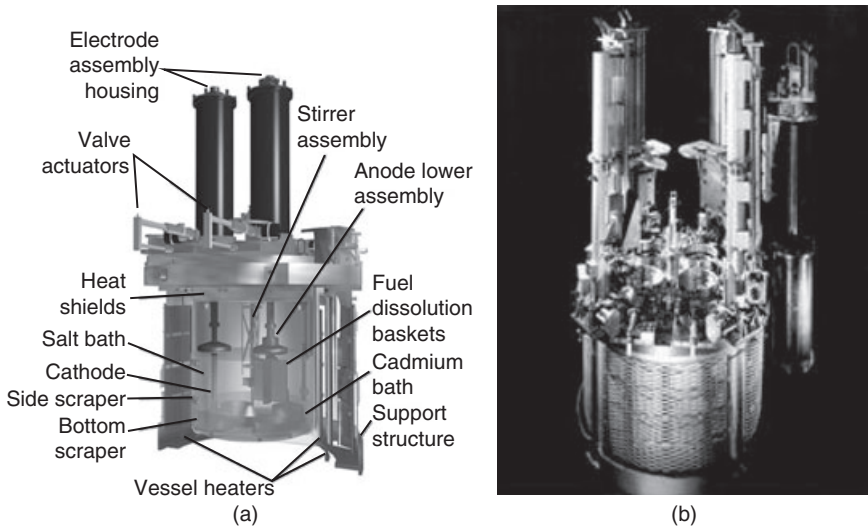
10.10 Schematic view and photograph of Mark-IV electrorefiner.

cadmium are maintained at around 500 °C during the operation. The salt phase and cadmium phase are stirred during electrorefining. The cover flange has four ports (25.4 cm diameter), through which two anode and two cathode assemblies can be inserted into the molten salt bath. Inside the vessel, rotating side scrapers are mounted to reduce the build up of a uranium deposit (Li, 2000).

To use the electrorefiner on an industrial scale, a larger throughput and process scale-up parameters are needed to show its technical feasibility. As shown in Fig. 10.11, ANL and INL have developed a next-generation electrorefiner, Mark V, with four high-throughput 'anode–solid cathode' modules in a vessel of almost the same size as that used in Mark IV. The module consists of concentric rings of anode baskets that rotate inside a concentric cathode tube. It was designed to increase current by decreasing the anode-cathode distance and increasing the cathode area. As shown in Fig. 10.12 (Vaden, 2002), the uranium deposit is continuously scraped off the cathode tube, and collected in a basket at the bottom of the cathode assembly to reduce the dead volume in the electrorefiner due to the growth of a dendritic uranium deposit. About 3.2 tons of spent EBR-II blanket fuels have already been treated in this electrorefiner. After some modification, the throughput of the Mark V was increased to 660 gU/h/electrode (Westphal, 2000), about 20 times greater than that of the Mark IV. To avoid any mechanical difficulty in scraping off the deposit, INL has optimized the operational conditions such as the rotation speed and reverse current mode, while CRIEPI has developed a new module (Fig. 10.13)
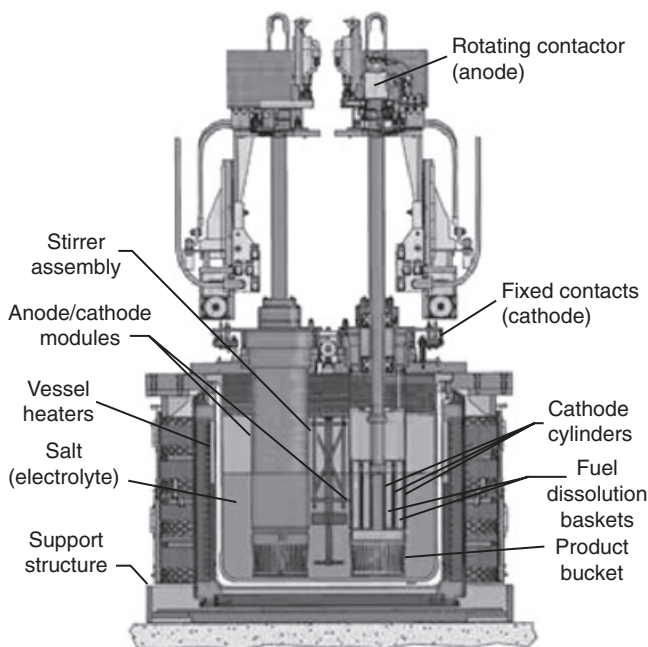
10.11 Schematic view of Mark-V electrorefiner.

with a separate scraper to be operated after electrodeposition (Iizuka, 2009). Whichever anode-cathode module is employed, the throughputs obtained for these two modules are similar and sufficiently high for commercial use.

An engineering-scale liquid Cd cathode was tested in an electrode port of the Mark V electrorefiner for the simultaneous recovery of plutonium and uranium (Vaden, 2008). As shown in Fig. 10.14(a), the cathode module consisted of about 25 kg of liquid Cd charged in a ceramic crucible and with a ceramic paddle, which rotates and oscillates up and down slightly above the salt/cadmium interface, to push materials depositing on the cadmium surface into the bulk of the liquid cadmium. In the electrorefining tests with a current of 20 A, corresponding to 60 gHM/h/electrode and with a high plutonium to uranium ratio in the salt (from 3.32 to 10.8), a kilogram-scale amount of plutonium with uranium were successfully recovered in the liquid Cd cathode with more than 90% current efficiencies (see Fig. 10.14(b)). Although further improvement to increase the electrorefining current is necessary, this is a very important result to demonstrate the simultaneous recovery of plutonium, MA and uranium from actual spent metal fuels. In an electrorefining test with a lower plutonium to uranium ratio in the salt (from 2.87 to 3.32), however,

(a)
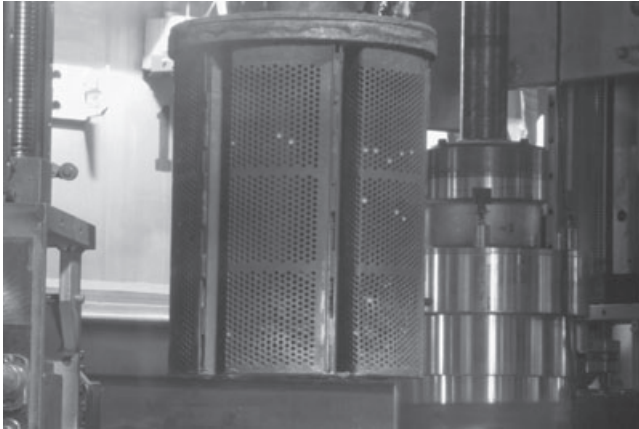
APR 10 2002
(b)

10.12 Anode (top) and recovered uranium (bottom) in product bucket of high-throughput anode-cathode module of Mark-V electrorefiner.

deposition in the liquid cadmium cathode with the same current exhibited an unexpected low current efficiency due to the formation of dendritic material exterior to the liquid cadmium (see Fig. 10.14(c)). Similar behaviour is often observed in liquid cadmium cathode experiments when deposition conditions such as current density, salt composition and stirring are not optimized (Koyama, 1997; Iizuka, 2001b). Under appropriate conditions, the recovery of a plutonium-uranium mixture in a liquid cadmium cathode, with a cathode density of 200 A/cm^2, corresponding

10.13 High-throughput anode-cathode module of CRIEPI.
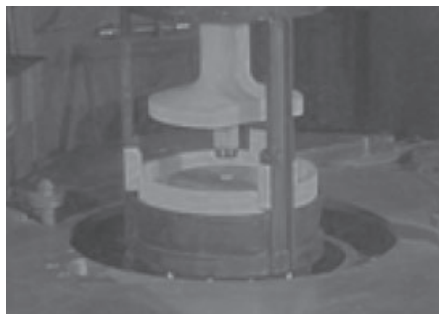
(a)
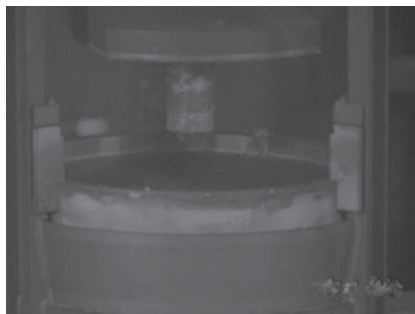
(b)

(c)

10.14 Kilogram-scale transuranium recovered in liquid cadmium cathode.

to 6 gHM/cm^2/h, was attained in laboratory-scale experiments (Kato, 2003).

To increase further the throughput of the liquid cadmium cathode, improvements are necessary to decrease the time required for the operation without passing the electrorefining current because the cathode current density and the cathode area are limited by electrorefining conditions. One of the most time-consuming operations is moving the liquid cadmium cathode assembly before and after electrorefining, because it takes a long time to heat up and cool down the cathode to minimize thermal shock to the ceramic crucible. CRIEPI has developed an electrorefiner equipped with a liquid Cd transport system. The cathode products, Cd-actinide alloys, are directly transported to the cathode processor while pure Cd, obtained as a distillation product, is transported back to the cathode crucible. The feasibility of the concept was demonstrated by experiments on an engineering-scale model (Fig. 10.15), where an liquid cadmium cathode of 25 cm inner diameter was connected to a distillation furnace by ½″ tubing, using gadolinium as a surrogate for actinides (Koyama, 2007, 2009).
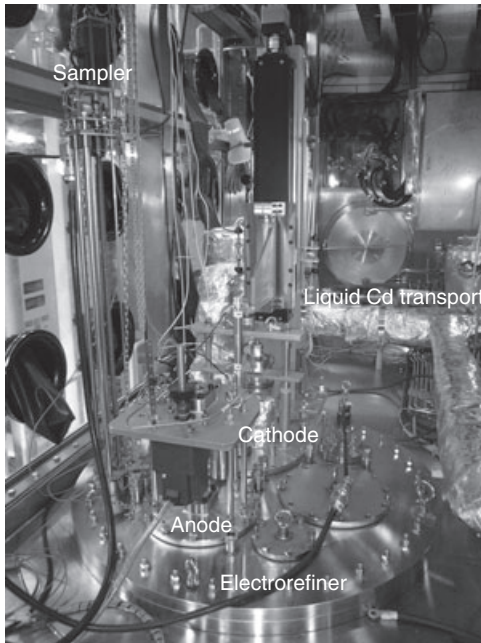
10.15 Engineering-scale electrorefiner equipped with liquid Cd transport system. A sampler is installed on the left edge of the electrorefiner flange.

Temperature
sensors

Splatter
shield

Induction
coil

Graphite
liner
(susceptor)

Process
crucible

Auxiliary
heater

Thermal
radiation
shield

Condenser
assembly

Receiver
crucible
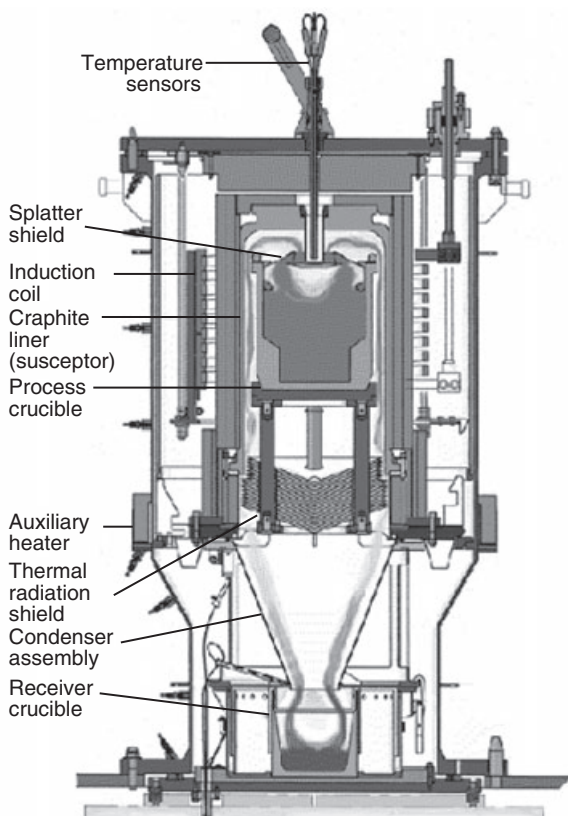
10.16 Schematic view of cathode processor.

10.3.3 Cathode processor

The cathode processor heats up the cathode deposits from the electrorefiner to separate chloride salt and/or cadmium metal from actinide metal by distillation. Figure 10.16 shows the cathode processor developed by ANL and INL. It comprises an induction-heated furnace that can reach temperatures of up to 1400 °C and a vacuum of 0.1 Torr. The furnace region contains a passively cooled induction coil and a graphite furnace liner that acts as a susceptor to heat the process materials (Westphal, 2000). The cathode processor has been operated for over 300 batches of solid cathode deposits (dendritic uranium with adhering salt), and the recovered salts were recycled back to the electrorefiners. No impurities have been detected in the electrorefiners as a result of the salt recycling. However, the cathode processor has undergone fewer experiments with liquid cadmium cathode deposits (Pu-U-MA-Cd alloys). Three experiments were carried out with actual

10.17 Plutonium-uranium-MA ingot obtained in cathode processing.

plutonium-uranium-MA products obtained from liquid cadmium cathode tests in the Mark V electrorefiner (see Fig. 10.14). According to the temperature profile of the condenser, the distillation of cadmium was completed within about two hours at temperatures up to 700 °C. The cadmium distillation rate was 0.41 g/min/cm^2 and more than 99 wt% of the cadmium was collected. Fig. 10.17 shows the recovered plutonium-uranium-MA ingot (Westphal, 2007).

10.3.4 Counter current contactor

The counter current contactor is another important piece of equipment used to recover actinides from the salt in electrorefiners with separating lanthanide FPs. A high-temperature centrifugal contactor, a *pyrocontactor*, was developed by ANL (Laidler, 1998). The design of the pyrocontactor was based on an aqueous contactor (Leonard, 1988) to achieve intensive mixing by chemical reactions between solutes in both the molten salt and liquid metals, and to ensure the clean separation of these streams. The four-stage pyrocontactor was installed in an Ar glove box, and extraction tests were carried out using Ce, La and Y as substitutes for U, Pu(MA) and lanthanides, respectively. Although details of both the design and the experimental conditions were not described in the literature, stage efficiencies approaching 99% of the theoretical value were reported at rotor speeds of nearly 3200 rpm (Laidler, 1998). By contrast, CRIEPI has developed a different type of counter current contactor that requires a rotation speed of only approximately 300 rpm with the aim of increasing long-term integrity. Because radiation damage on molten salt and liquid metal is negligible compared with that of organic solvents used in aqueous reprocessing, the
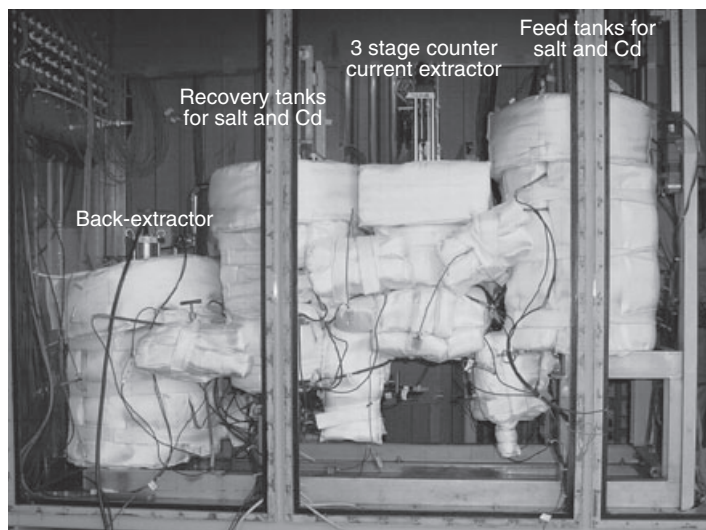
10.18 Three-stage counter current contactor installed in Ar glove box.

flow rate of the counter current contactor can be decreased. Using the material balance calculated for commercial throughput, the required flow rate was sufficiently slow to complete reduction reaction without strong mixing. The large density difference between molten salt (1.7 g/cm^3) and liquid Cd (7.8 g/cm^3) eases the phase separation problem. On the basis of this consideration, a three-stage counter current contactor was developed and installed in an Ar glove box, as shown in Fig. 10.18. The contactor was connected to four separate tanks used for salt supply, Cd supply, salt recovery and Cd recovery, respectively. Each stage of the contactor has a capacity of 300 ml molten salt and 300 ml liquid Cd. Molten salt and liquid Cd were supplied from the tanks at a constant rate of 10 to 50 ml/min. Extraction tests were carried out using molten salt and liquid Cd at 450 °C. Three rare earth elements, Ce, Gd and Y, were used as substitutes for U, transuranic elements and rare earth FPs, respectively. In three-stage counter current extraction test, a high recovery ratio of close to 100% with efficient separation was achieved (Kinoshita, 2007, 2008).

10.3.5 Zeolite column

The development of a zeolite column in a continuous system is in the early stage of engineering. Figure 10.19 shows the zeolite column test equipment installed in an Ar glove box at CRIEPI (Koyama, 2009). According to the results of smaller-scale experiments, it is designed to supply molten salt

10.19 Zeolite column test equipment of CRIEPI.

including LFP surrogates by pressurized Ar gas, and to ensure contact between molten salt and several zeolite columns of 30 cm length.

10.3.6 Salt waste treatment equipment

In the current INL program to treat irradiated EBR-II fuels, electrorefiner salt is directly converted to glass-bonded sodalite without the condensation of LFP by a zeolite column, nor with the separation of actinides by counter-current extraction. According to INL (Priebe, 2008), the major steps for forming ceramic waste from the electrorefiner salt are:

1) to blend zeolite and salt at approximately 500 °C to form salt-loaded zeolite;
2) to mix the salt-loaded zeolite with glass; and
3) to heat the mixture to form glass-bonded zeolite.

Frozen salt blocks are crushed and ground to a particle size of 100–200 μm then mixed with dried zeolite-4A powder (with a particle size of 45–250 μm) in the rotating V-mixer shown in Fig. 10.20 at 525 °C for about 18 h. During the mixing, the electrorefiner salt is absorbed into the zeolite structure to form salt-loaded zeolite. The V-mixer is then allowed to cool to ambient temperature, and samples are taken to confirm that the content of free chloride is in an acceptable range. In the next step, a glass frit with a particle size of 45–250 μm is added to the salt-loaded zeolite and mixed at the ambient temperature to ensure homogeneity. The fraction of glass in the
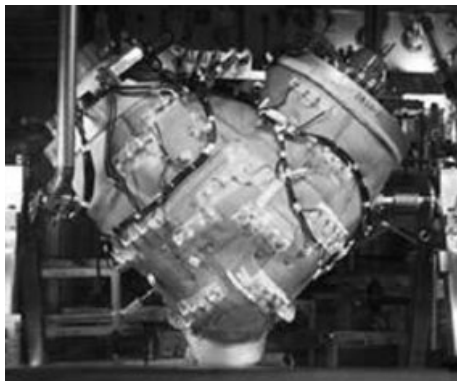
10.20 V-mixer installed in the hot cell of INL.

(a)   (b)

10.21 Ceramic waste furnace (left) and processed ceramic waste (right).

mixture is about 25%. Finally up to 400 kg of the salt-loaded zeolite and glass mixture is loaded into a production furnace with internal dimensions of 68 cm diameter and 3 m height, as shown in Fig. 10.21. The furnace temperature is increased to around 925 °C which is maintained for approximately 72 h to allow complete consolidation. The furnace is then cooled to ambient temperature, to allow the monolithic, glass-like CWF (as shown in Fig. 10.21) to be removed. The furnace is currently being subjected to quali-
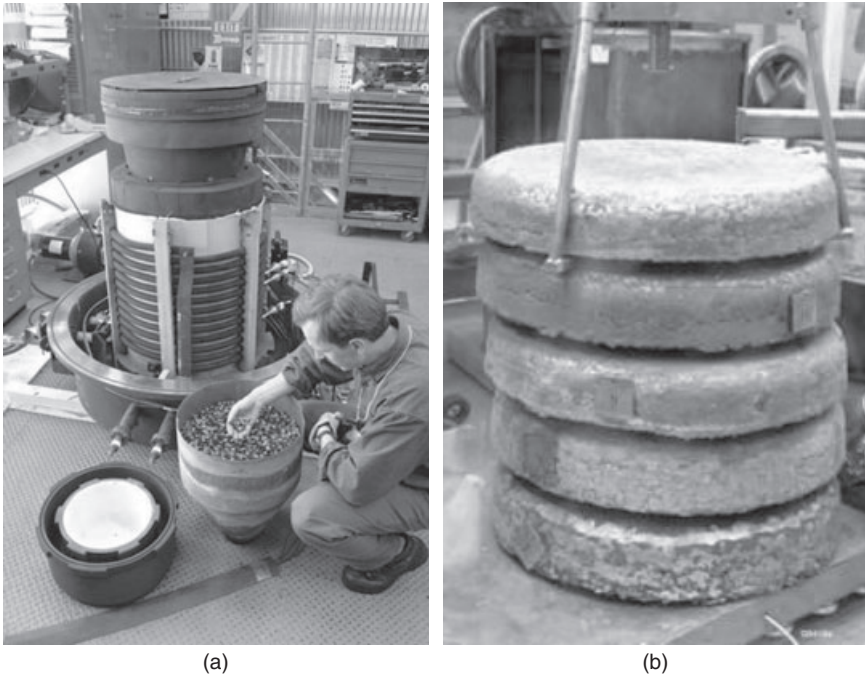
10.22 Metal waste furnace (left) and processed metal waste (right).

fication tests out of the cell in preparation for hot-cell operation (Goff, 2009).

10.3.7 Metal waste treatment equipment

To process the metal waste forms from the pyrochemical treatment of irra-diated EBR-II fuel, an engineering-scale furnace has been designed (see Fig. 10.22) to separate the adhering salt from the metal waste (consisting of steel cladding, zirconium and NFP) by distillation, and then to melt the metal waste in a crucible assembly while recovering the salt vapour in the condenser located above the crucible assembly (Marsden, 2005). The furnace has a vacuum vessel of approximately 1.2 m diameter and 2 m height, together with convective cooling fins to cool the condenser region and a heat shield to limit thermal flux to the hot-cell window. Induction heating can be operated at 1700 °C and 200 mTorr using a 25 mm square copper tube for the induction coil. After demonstrating the successful pro-duction of surrogate metal waste in a glovebox, a furnace of nearly identical design was installed in the INL hot-cell, as shown in Fig. 10.23, and process testing is ongoing (Goff, 2009).

10.23 Furnace for producing metal waste form installed in hot cell of INL.

10.3.8 Voloxidizer

A voloxidizer and electroreduction cell are pieces of equipment specific to spent oxide fuels treatment. Voloxidation is a well-known technique; however, most experiments have been carried out at the laboratory scale. KAERI is developing engineering-scale voloxidizers for decladding and pulverization of oxide fuel. A voloxidizer of 20 kg HM/batch was designed to oxidize fuels on a vibrating mesh where powdered products are separated from unreacted chunks of fuel. The effectiveness of the vibration on the oxidation rate was reported for the tests with 20 kg unirradiated UO_2 (Kim, 2005). Figure 10.24 shows a new model of the voloxidizer, equipped with a rotating mesh basket in the furnace. The chopped spent fuels are crushed by impact from a ceramic ball, and small pieces of pellet are pulverized by oxidation. The fuel powder is collected in the collector located under the mesh basket. In this voloxidizer, simulated fuels (90% W and 10% SiO_2) equivalent to 20 kg spent fuel were tested. Oxidation was completed in 13 hrs, and the obtained recovery ratios for hull and powders were 100% and 97.6%, respectively (Kim, 2009).
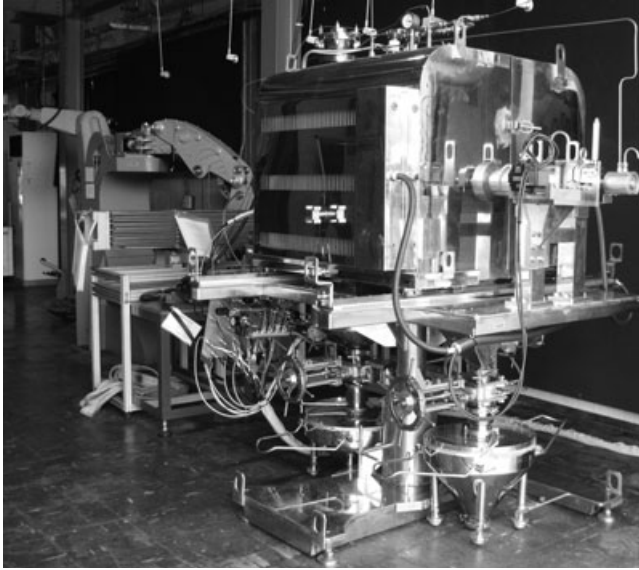
10.24 High throughput voloxidizer of KAERI.

10.3.9 Electroreduction cell

The electroreduction of oxide fuel is carried out by removing oxygen from the oxide fuel at the cathode and generating oxygen gas at the anode. Most studies are mainly focused on obtaining design parameters for the anode and cathode, to achieve high throughput and high reduction yield. In the case of a cathode to charge spent oxide fuel; however, the basket has contradictory design requirements. According to visual examination of incomplete reduction products, the reaction proceeds from the outside to the inside of the oxide particle. This suggests that diffusion in the grain boundary or in cracks in the particle is the rate-determining step. To complete the reaction earlier, a cathode basket with smaller holes is better for charging smaller oxide particles. On the other hand, a cathode basket with larger holes is required to accelerate the circulation of molten salt to diffuse oxygen ions from the inside to the outside of the basket. With regard to the importance of particle size, KAERI has developed an engineering-scale electroreduction cell using a porous MgO crucible (18 cm ID × 42 cm H) as the cathode basket, surrounded by six platinum anode rods (3 cm OD × 30 cm H). Figure 10.25 shows an electroreduction cell of 50 cm ID, which has been used only for on-irradiated materials. When 10 kg of U_3O_8 powder (10–30 μm) was charged in this electroreduction cell, more than 99% of the reduction reaction was completed in about 100 h (Jeong, 2008). As the concentration of Li_2O in the molten salt decreased with time, the permeabil-
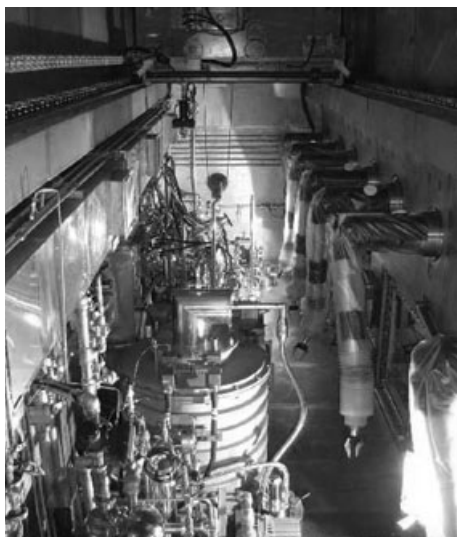
10.25 Engineering-scale electroreduction cell installed in hot cell of KAERI.

ity of oxygen ions through the MgO crucible was found to be very slow, suggesting that the holes in the MgO crucible were too small. However, INL employed a percolated stainless-steel basket to charge crushed spent oxide fuel particles with 0.45–2.8 mm diameter (Herrmann, 2005) but no decrease in Li_2O concentration was observed, and it took 36 h to complete the reduction reaction of 41 to 50 g of spent fuel. INL continued reduction experiments using voloxidized spent oxide fuel powder of less than 45 μm diameter in small baskets made of stainless-steel mesh, with sintered stainless-steel frit (Herrmann, 2007). With either mesh or sintered frit stainless-steel baskets, a higher current can be passed for the powder form than for crushed particles. As an alternative, CRIEPI has proposed processing porous chunks from the voloxidized fuel powder for charging in a stainless-steel basket with a large opening. According to experiments, using roughly sintered UO_2 pellets with a porosity of approximately 30%, the time to complete the reduction reaction was less than 10 h and was unaffected by an increase in the amount of fuel pellets from 10 g to 100 g (Sakamura, 2008). Although the procedure is more complex, it is one possible method for realizing practical throughput.

With regard to anode design for generating oxygen gas, developments have been mainly focussed on the durable anode material, which will be described in the next section. An effective evacuation of the oxygen gas from the vicinity of anode is another key issue for anode design.

10.4   Materials behaviour and interactions

The selection of compatible materials depends strongly on the process environment. As described in the first section of this chapter, most of the materials used for the pyroprocess are in moderate corrosion conditions during normal operation. Carbon steels and stainless steels can be used without corrosion problems. For example, long-term durability of steel materials has been tested with LiCl-KCl salt and liquid Cd with actinides and FP at approximately 500 °C. On the other hand, stainless-steels are not suitable for the crucible containing liquid Cd because nickel dissolves in them. No detectable damage has been reported for a mild steel crucible in a laboratory-scale electrorefiner (Battles, 1993) or for Mo a steel crucible in INL's engineering-scale electrorefiner. The integrity of Mo steel was also confirmed in CRIEPI's experiments with an electrorefiner and with a counter current contactor. The materials suitable for the more severe conditions in the pyroprocess are described in this section.

10.4.1 Materials for the electroreduction cell

The electroreduction cell is exposed to oxygen gas and LiCl-Li$_2$O salt at 650 °C. According to the small-scale electroreduction tests, stainless steel is expected to be a durable material as both cathode and cell crucible. However, the severe corrosion of Fe-Cr-Ni alloys and Ni alloys such as Inconel-600 and Hastelloy C-276 was reported in material tests carried out by KAERI (Cho, 1999). This difference can be ascribed to the extreme experimental conditions of the latter experiments, such as the higher temperature (up to 1000 °C) and higher Li$_2$O concentration (up to 25 wt%). When MgO is used for the cathode material, corrosion of the cell has to be considered because initial Li$_2$O concentration must be high enough to compensate the consumption of Li$_2$O during electrolysis. In cases when meshed or percolated material is used for the cathode, the Li$_2$O concentration can be kept low at approximately 1 wt% during electrolysis, resulting in moderate corrosion of the cell material.

On the other hand, the anode material undergoes severe corrosion because the liberation of oxygen occurs at the interface between the anode surface and the LiCl-Li$_2$O electrolyte. Although the integrity of the Pt anode is expected from many experiments, different materials have been tested to find cheaper alternatives. The requirements for the anode material are that it is nonconsumable and has a high current density. In addition to metals, different types of materials such as ceramics and crystals are currently being tested; however, an alternative material to meet the requirements has not yet been reported.

10.26 Zirconia-lined graphite crucible after cathode processing.

10.4.2 Crucible materials for distillation and melting

An important requirement of pyrochemical processing is being able to limit the interaction between pure metals and the processing equipment. Graphite crucibles with a zirconia coating have been utilized as heating crucible for the cathode processor. After each run, the coating has to be removed and a new coating applied. This action is labour-intensive and limits the throughput of the equipment. The coating also reacts with uranium to form dross, which is primarily uranium oxide. This uranium oxide must be reduced to a metal form and recycled. To minimize the formation of dross and to increase actinide metal throughput, alternative materials for the crucible of the cathode processor are under study. INL has developed a niobium crucible with a hafnium nitride coating and a zirconia-lined graphite crucible (Benedict, 2007). They have reported that very little dross was formed in the former and that five runs could be carried out before the coating had to be reapplied, while in the latter, 0 to 1% dross was formed, as shown in Fig. 10.26.

10.5 Developments in monitoring and control for pyrochemical processing

The accounting methods currently applied for pyrochemical experiments are conventional destructive analyses such as ICP-AES, ICP-MS and γ spectroscopy for concentration analyses, and weight measurements for bulk analyses. Because destructive analyses usually require a long time to prepare the liquid solution from salt or metal samples, it is important to develop a

method for on-line monitoring of the concentrations of elements in molten salt. It might be difficult to measure the weights of materials in a large vessel; thus, a method of measuring bulk amounts using level probes and density equations to calculate weights from volumes must be developed. It is also important to develop sampling technology to decrease sampling errors in pyrochemistry. In this section, the development of monitoring techniques specific to pyrochemistry is summarized.

10.5.1 Concentration probes for molten salt

The potential applicability of electrochemical methods such as normal pulse voltammetry to the on-line monitoring of actinide concentration in molten chlorides was reported by CRIEPI (Iizuka, 2001a). The device used consists of wire electrodes (W, Ta) and a reference electrode connected to a potentiostat. As shown by the linear relationship between the reduction current and concentration in Fig. 10.27, the applicability of electrochemical methods was demonstrated for concentrations of U or Pu in LiCl-KCl-UCl$_3$-PuCl$_3$ molten salt of up to 1.7 wt%.

10.5.2 Level probes for molten salt and liquid metals

Probes for detecting the height of the salt/gas interface or salt/cadmium interface by resistivity measurement have been used in electrorefiner
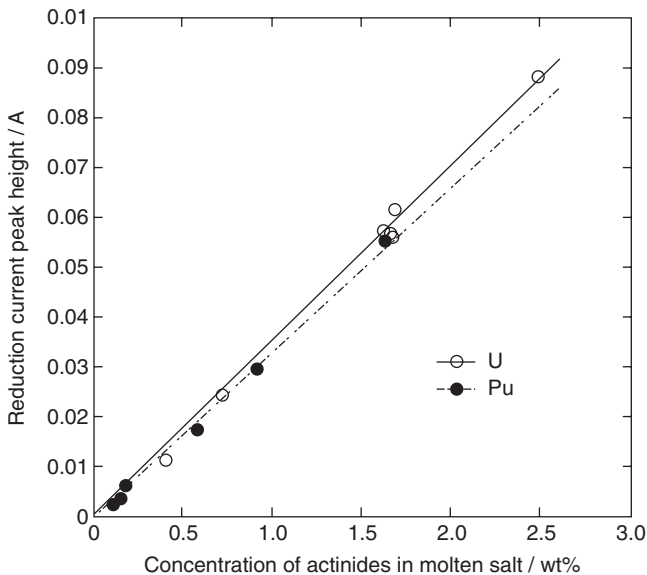
10.27 Linearity obtained for electrochemical on-line analyses.
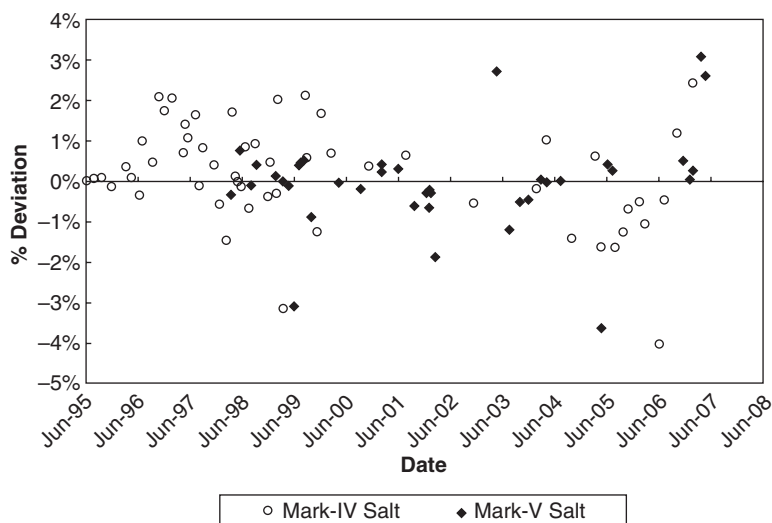
10.28 Percentage deviation of predicted salt volume relative to measured salt volume.

experiments. The mass of the salt inventory in the electrorefiner was obtained from the product of the fluid volume measured by level probes and the density, assuming additive volumes. Figure 10.28 shows a time plot comparing the predicted salt volume with the measured salt volume of an electrorefiner in INL. For the Mark IV electrorefiner, the average percentage deviation of the predicted salt volume relative to the measured salt volume was reported to be 0.18% with a standard deviation of 1.26%, while it was 0.04% with a standard deviation of 1.25% for the Mark V electrorefiner (Vaden, 2007). This indicates that calculating the salt density via additive volumes is a satisfactory method.

10.5.3 Sampling device

To sample molten salt and liquid metals, remote semi-automatic devices have been developed for engineering-scale experiments carried out in several laboratories. A sampling device for molten salt and liquid cadmium was installed in the engineering-scale electrorefiner at CRIEPI, as shown in Fig. 10.14. It sucks small amounts of liquids into stainless-steel tubes submerged at a predetermined depth. To separate the liquids from solid precipitates (such as oxides and intermetallic compounds), a metal frit is attached to the head of the stainless-steel tubes. By contrast, a sampling device for actinide metal ingots has been demonstrated during metal fuel fabrication for EBR-II, which uses a high-temperature vacuum injection-

casting furnace equipped with quartz moulds to produce actinide metal rods. Because of the stirring effect of induction heating, the sample has sufficient homogeneity to be accepted as a reactor fuel.

10.6 Techniques for safe and effective interoperation of equipment

Because operations of pyroprocess are carried out in a batch mode, solid ingots are the main products needed to be transported between different process equipment. To attain higher efficiency, techniques for transporting other forms, such as powders and high-temperature liquids, are being developed for appropriate interoperations.

Transport technologies for high-temperature liquids (molten salt and liquid cadmium) enhance the interoperation of the processes between the electroreduction cell, electrorefiner, counter current contactor and/or cathode processor by decreasing the time required for freezing and remelting. Although the success of large-capacity centrifugal pumps for molten salt reactor systems has been reported (Rosenthal, 1972), the development of small transport systems applicable to pyrochemical processing has not been reported in detail. A molten salt transport test rig (Fig. 10.29) and liquid metal transport test rig (Fig. 10.30) have been installed at CRIEPI to develop transport technologies suitable for pyrochemical treatment (Hijikata 2009a, 2009b). The applicability of a high-temperature centrifugal pump, suction pump and valves has been tested at 500 °C, and the controllability of the flow rate in a practical range of several L/min demonstrated, as shown in Fig. 10.31. The durability of the high-temperature centrifugal pump was demonstrated by repeating its operation about 500 times during a total of 700 h operation.

Similar to the pellet fabrication system of oxide fuels, handling of the fine fuel powder produced during the voloxidation process needs special care. The voloxidizer installed in KAERI is designed to recover the uniform powder in the bottom vessel after percolation using a vibrating mesh, and the vessel is transported to the electroreducer by a master-slave manipulator (Kim, 2005).

10.7 Future trends

As described in Section 10.3, design improvements in process equipment for higher throughput is the key to achieving economic competitiveness for pyrochemical processing of irradiated nuclear fuel. ANL is developing a design for a new planar electrode electrorefiner (PEER), as shown in Fig. 10.32 (Lewis, 2004). Electrodeposited uranium is scraped off the planar
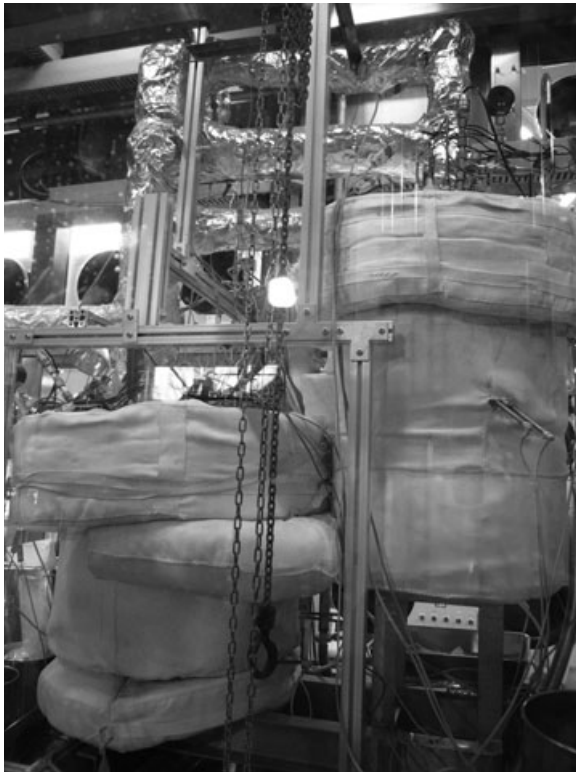
10.29 Molten salt transport test rig installed in Ar glove box.
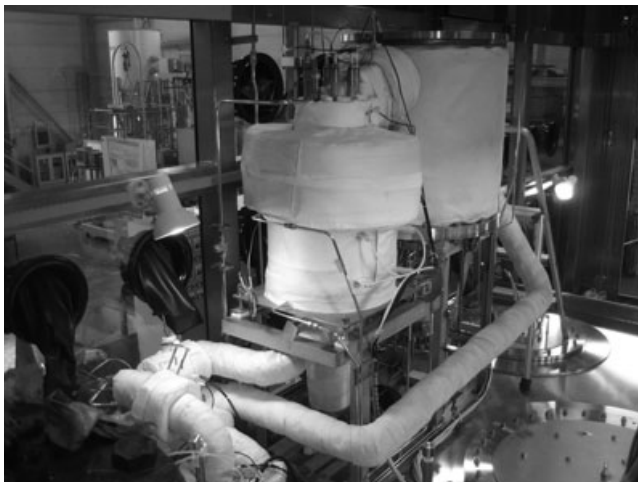
10.30 Liquid metal transport test rig installed in Ar glove box.
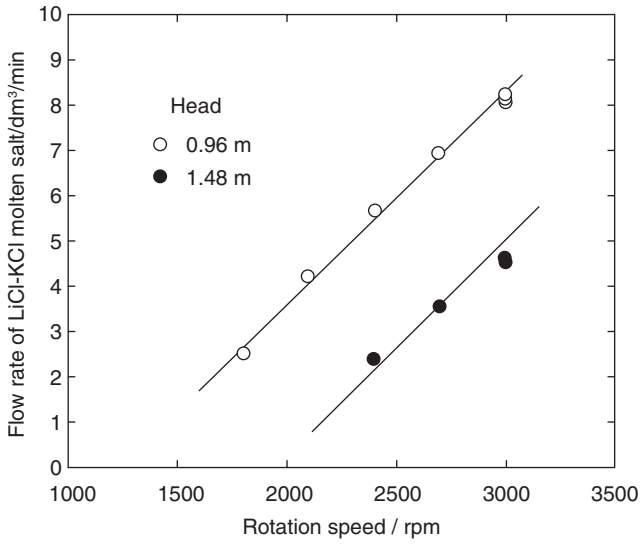
10.31 Flow rate controllability of high-temperature centrifugal pump.

10.32 Design of PEER prototype test module.

10.33 Conceptual design of continuous high-throughput electrorefiner of KAERI. 1) cathode module, 2) anode basket, 3) reactor wall, 4) deposit withdrawer, 5) noble metal withdrawer, 6) heat shield.

cathodes by vertical-motion scrapers. The dislodged uranium slides down the sloping bottom of the vessel into a collection basket that is periodically raised and inverted, dumping the product down the product funnel into the receiver crucible. KAERI is also developing the design of a higher-through-put electrorefiner with graphite electrodes where the uranium deposited is dispatched without scraping. As shown in Fig. 10.33, uranium dispatched from the cathode and the noble metal fines that fall from the anode basket are expected to be separately recovered through different withdrawers.

Another challenge in improving the electrorefiner is to find alternatives to a liquid cadmium cathode. Because the separation efficiency of the liquid cadmium cathode is not very high, an additional separation process such as a counter current extraction step is necessary to satisfy the required recovery ratio and decontamination factors. As shown in the left side column of Table 10.1, a solid cathode is a possible method for realizing better separation between actinides and lanthanides. The electrolysis of uranium and plutonium chlorides has been demonstrated at a laboratory-scale at ANL (Willit, 2005). Further studies to confirm the recovery of actinides along with elements having parasitic reactions, i.e. americium, are necessary, in addition to the optimization of the anode and cathode design.

Elsewhere, the Institute for Transuranic Elements (JRC-ITU) is investigating an aluminum cathode for the group recovery of actinides. The deposition of uranium, plutonium and americium on an aluminum cathode was demonstrated in a laboratory-scale test using a metal alloy anode with a composition of U_{61}-Pu_{22}-Am_2-$Nd_{3.5}$-$Gd_{0.5}$-$Y_{0.5}$-$Ce_{0.5}$-Zr_{10} (Souček, 2009). A
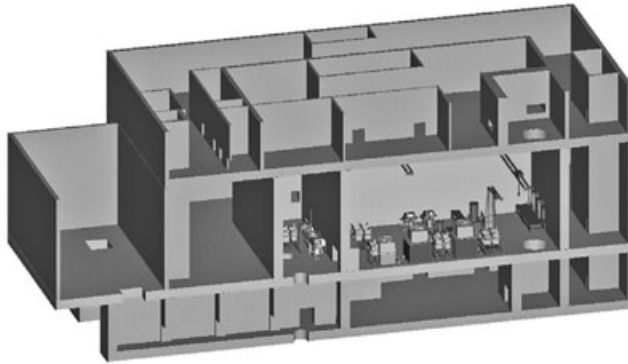
10.34 Conceptual design of main operation floor of treatment facility.

potential advantage of an aluminum cathode is that it has an inherent dif-
ficulty in separating pure plutonium Because the actinides are recovered as
solid actinide-aluminum alloys, a simple method to back-extract the actinides
from the alloys would need to be developed.

Conceptual design studies of pyrochemical fuel cycle facilities are being
made in several institutes to evaluate costs and feasibility. A conceptual
design study for the processing of 100 ton/year of heavy metals was carried
out by ANL employing the PEER. Figure 10.34 shows a three-dimensional
view of the treatment facility (Lewis, 2004).

In addition to improving throughput, efforts should be continued to
increase the reliability and stability of process equipment as well as the
operational system for realization of the actual deployment of the pyro-
chemical facility.

10.8   Sources of further information and advice

To study details on techniques of utilizing molten salts, the '*Molten Salt
Techniques*' series, volume 1 (Lovering, 1983), volume 2 (Gale, 1984),
volume 3 (Lovering, 1987) and volume 4 (Gale, 1991), provides the most
important and comprehensive information. It describes experimental tech-
niques specific to molten salt study and, in particular, techniques and instru-
mentation such as purification methods for molten salts and stable reference
electrodes, etc.

Further, to study techniques specific to the pyrochemical treatment of
nuclear fuels, '*The Fuel Cycle Stories*' (Stevenson, 1987) is an old but still
valuable textbook. It describes developments in the remote adaptation of
installations and the design of pyrochemical equipment and Ar hot-cells.
The details of key progress in the pyroprocess using EBR-II spent fuels are

described in the report from the National Academy of Science (2000) and from Argonne National Laboratory (Ebert, 2005).

Thanks to the Argonne National Laboratory, Idaho National Laboratory, Korea Atomic Energy Research Institute and Central Research Institute of Electric Power Industry, many valuable photos and figures are able to be cited in this chapter. Parts of this chapter are the results of 'Development and improvement of electrorefining process', 'Development of engineering technology basis for electrometallurgical pyroprocess equipment' and 'Application of electrochemical reduction to pyrochemical reprocessing for oxide nuclear fuel', entrusted to CRIEPI by the Ministry of Education, Culture, Sports, Science and Technology of Japan (MEXT).

10.9   References

Ackerman J P and Settle J L (1993), 'Distribution of Pu, Am, and several rare earth fission product elements between liquid cadmium and LiCl-KCl eutectic', *J Alloy Compd*, 199, 77.

Arias A, Granovski M S, Abriata J P and Okamoto H (1993), 'Phase diagram of binary iron alloys', ASM International Material Park, OH, 467.

Battles J E, Myles K M, Laidler J J and Green D W (1993), *Chemical Technology Division Annual Technical Report 1992*, ANL-93/17.

Benedict R W, Solbrig C, Westphal B, Johnson T A, Li S X, Marsden K and Goff K M (2007), 'Pyroprocessing progress at Idaho National Laboratory', *Proceedings of GLOBAL 2007*, Boise, Idaho, 741–747.

Cho S H, Park S C, Zhang J S, Shin Y J and Park H S (1999), *Korean J Mater Res*, 9, 556.

Ebert W L (2005), *Testing to Evaluate the Suitability of Waste forms Developed for Electrometallurgically Treated Spent Sodium-bonded Nuclear Fuel for Disposal in the Yucca Mountain Repository*, ANL-05/43.

Gale R J and Lovering D G eds (1984), *Molten Salt Techniques*, 2, Plenum Publishing Corp, ISBN: 0306415496.

Gale R J and Lovering D G eds (1991), *Molten Salt Techniques*, 4, Plenum Publishing Corp, ISBN: 0306435543.

Goff K M and Simpson M (2009), 'Dry processing of used nuclear fuel', *Proceedings of GLOBAL 2009*, Paris, France, Paper No. 9516, 979–984.

Goff K M, Benedict R W, Howden K L, Teske G M and Johnson T A (2005), 'Pyrochemical treatment of spent nuclear fuel', *Proceedings of GLOBAL 2005*, Tsukuba, Japan, Paper No. 364.

Herrmann S D, Li S X and Simpson M F (2005), 'Electrolytic reduction of spent oxide fuel – bench test results', *Proceedings of GLOBAL 2005*, Tsukuba, Japan, Paper No. 488.

Herrmann S D, Li S X, Sell D A and Westphal B R (2007), 'Electrolytic reduction of spent nuclear oxide fuel – Effects of fuel form and cathode containment materials on bench-scale operations', *Proceedings of GLOBAL 2007*, Boise, Idaho, USA, 758–762.

Hijikata T and Koyama T (2009a), 'Development of high-temperature transport technologies for liquid cadmium in pyrometallurgical', *J Eng Gas Turb Power*, 131.

Hijikata T and Koyama T (2009b), 'Development of high-temperature molten salt transport technology for pyrometallurgical reprocessing', *J Power Energy Sys*, 3(1), 170–181.

Iizuka M, Inoue T, Shirai O, Iwai T and Arai Y (2001a), 'Application of normal pulse voltammetry to on-line monitoring of actinide concentrations in molten salt electrolyte', *J Nucl Mater*, 297, 43–51.

Iizuka M, Uozumi K, Inoue T, Iwai T, Shirai O and Arai Y (2001b), 'Behavior of plutonium and americium at liquid cadmium cathode in molten LiCl-KCl electrolyte', *J Nucl Mater*, 299, 32–42.

Iizuka M, Sakamura Y and Inoue T (2006), 'Electrochemical reduction of (U-40Pu-5Np)$_2$ in molten LiCl electrolyte', *J Nucl Mater*, 359, 102–113.

Iizuka M, Omori M, Ogata T and Tsukada T (2009), 'Development of an innovative electrorefiner for high uranium recovery rate from metal fast reactor', *J Nucl Sci and Technol*, 46(7), 699–716.

Japan Calorimetry Society (1992), *Thermodynamic Data Base MALT-II*, Kagaku-gijutsusya.

Jeong S M, Hur J-M, Hong S S, Kang D S, Choung M S, Seo C-S, Yoon J-S and Park S-W (2008), 'An electrochemical reduction of uranium oxide in the advanced spent-fuel conditioning process', *Nucl Technol*, 162, 184–191.

Johnson I, Chasanov M G and Yonco R M (1965), 'Pu-Cd system: thermodynamics and partial phase diagram', *Trans Metallurg Soc AIME*, 233, 1408.

Kato T, Uozumi K, Inoue T, Shirai O, Iwai T and Arai Y (2003), 'Recovery of plutonium and uranium into liquid cadmium cathodes at high current densities', *Proceedings of Global 2003*, New Orleans, LA, 1591–1595.

Kim Y-M, Yoon J-S, Jung J-H, Hong D-H and UHM J-B (2005), 'Development of vol-oxidizer for oxidation of UO$_2$ pellets, 20 kg HM/batch', *Proceedings of Global 2005*, Tsukuba, Japan, Paper No. 260.

Kim Y-H, Park B-S, Jung J-H, Kim G-H, Yoon J-S and Kim H-D (2009), 'A study on high throughput vol-oxidizer for a decladding and vol-oxidaition of a spent fuel', *Proceedings of Global 2009*, Paris, France, Paper 9103.

Kinoshita K and Tsukada T (2008), 'Counter-current test in LiCl-KCl and liquid Cd system for pyropartitioning and pyro-reprocessing', *Proceedings of 10th P&T Meeting of OECD/NEA*, Mito, Japan.

Kinoshita K, Tsukada T and Ogata T (2007), 'Signal-stage extraction test with continuous flow of Molten LiCl-KCl salt and liquid Cd for pyro-reprocessing of metal FBR fuel', *J Nucl Sci Technol*, 44, 12, 1557–1564.

Koyama T, Johnson T R and Fischer D F (1992), 'Distribution of actinides in molten chloride salt/cadmium metal systems', *J Alloy Comp*, 189, 37.

Koyama T, Iizuka M, Shoji Y, Fujita R, Tanaka H, Kobayashi T and Tokiwai M (1997), 'An experimental study of molten salt electrorefining of uranium using solid iron cathode and liquid cadmium cathode for development of pyrometallurgical reprocessing', *J Nucl Sci Technol*, 34(4), 384–393.

Koyama T, Kinoshita K, Inoue T, Malmbeck R, Glatz J-P and Koch L (2002), 'Study of electrorefining of U-Pu-Zr alloy fuel', *J Nucl Sci Technol*, Supplement 3, 765–768.

Koyama T, Hijikata T, Yokoo T and Inoue T (2007), 'Development of engineering technology basis for industrialization of pyrometallurgical reprocessing', *Proceedings of Global 2007*, Boise, Idaho, 1038–1043.

Koyama T, Sakamura Y, Hijikata T, Iizuka M, Kinoshita K, Murakami T and Tsukada T (2009), 'Pyroprocess and metal fuel development for closing actinide fuel cycle with reduced waste burden', *Proceedings of Global 2009*, Paris, France.

Laidler J J, Myles K M, Einziger R E, Mcpheeters C C and Green D W (1998), *Chemical Technology Division Annual Technical Report 1997*, ANL-98/13.

Leonard R A (1988), 'Recent advances in centrifugal contactor design', *Sep Sci and Technol*, 23(12&13), 1473–1487.

Lewis D, Graziano D, Miller J F and Vandegrift G (2004), *Chemical Technology Division Annual Technical Report 2003*, ANL-04/06.

Lewis M A and Johnson T R (1990), 'A study of the thermodynamic and reducing properties of lithium in cadmium at 773 K', *J Electrochem Soc*, 137, 1414.

Li S X, Vaden D, Mariani R D and Johnson T A (2000), 'Experimental observations on the roles of the cadmium pool in Mark-IV ER', *Proceedings of the Embedded Topical Meeting on DOE Spent Nuclear Fuel and Fissile Material Management*, San Diego, California, 167–176.

Li S X, Johnson T A, Westphal B R, Goff K M and Benedict R W (2005), 'Electro-refining experience for pyrochemical processing of spent EBR-II driver fuel', *Proceedings of GLOBAL 2005*, Tsukuba, Japan, Paper No. 487.

Li S X, Vaden D, Westphal B R, Fredrickson G L, Benedict R W and Johnson T A (2007), 'Integrated efficiency test for pyrochemical fuel cycle', *Proceedings of GLOBAL 2007*, Boise, USA, 766–771.

Lovering D G and Gale R J eds (1983), *Molten Salt Techniques*, 1, Plenum Publishing Corp, ISBN: 0306413078.

Lovering D G and Gale R J eds (1987), *Molten Salt Techniques*, 3, Plenum Publishing Corp, ISBN: 0306425041.

Marsden K, Knight C, Bateman K, Westphal B and Lind P (2005), 'Process and equipment qualification of the ceramic and metal waste forms for spent fuel treatment', *Proceedings of GLOBAL 2005*, Tsukuba, Japan, Paper No. 585.

Nakamura K, Ogata T, Kato T, Nakajima K and Arai Y (2009), 'Fabrication of metal fuel slug for an irradiation test in JOYO', *Proceedings of GLOBAL 2009*, Paris, France, Paper No. 9163.

National Academy of Science (2000), *Electrometallurgical Techniques for DOE Spent Fuel Treatment Final Report*, Washington, National Academy Press.

Plambeck J A (1976), 'Fused salt systems', *Encyclopedia of Electrochemistry of the Elements*, Vol X, N.Y. and Basel, A.J. Bard, Editor, Marcel Dekker, Inc.

Priebe S and Bateman K (2008), 'The ceramic waste form process at Idaho National Laboratory', *Nucl Technol*, 162, 199–207.

Rosenthal M W (1972), 'The development status of molten salt breeder reactors', ORNL-4812.

Sakamura Y, Inoue T, Storvick T S and Grantham L F (1995), 'Development of pyropartitioning process – Separation of transuranium elements from rare earth elements in molten chlorides solution: electrorefining experiments and estimation by using the thermodynamic properties', *Proceedings of GLOBAL '95*, Verseilles, France, 2, 1185.

Sakamura Y, Hijikata T, Kinoshita K, Inoue T, Storvick T S, Krueger C L, Roy J J, Grimmett D L, Fusselman S P and Gay R L (1998), 'Measurement of standard potential of actinides (U, Np, Pu, Am) in LiCl-KCl eutectic salt and separation of actinides from rare earths by electrorefining', *J Alloys Comp*, 271–273, 592.

Sakamura Y, Shirai O, Iwai T and Suzuki Y (2000), 'Thermodynamics of neptunium in LiCl-KCl eutectic/liquid bismuth systems', *J Electrochem Soc*, 147(2), 642.

Sakamura Y, Shirai O, Iwai T and Suzuki Y (2001), 'Distribution behavior of plutonium and americium in LiCl-KCl eutectic/liquid cadmium systems', *J Alloy Comd*, 321, 76–83.

Sakamura Y, Omori T and Inoue T (2008), 'Application of electrochemical reduction to produce metal fuel material from actinide oxides', *Nucl Technol*, 162, 169–178.

Souček P, Malmbeck R, Mendes E, Nourry C and Glatz J-P (2009), 'Recovery of actinides from spent nuclear fuel by pyrochemical reprocessing', *Proceedings of GLOBAL 2009*, Paris, France, Paper No. 9217, 1156–1165.

Stevenson C E (1987), *The EBR-II Fuel Cycle Story*, American Nuclear Society, ISBN: 0894480316.

Tsukada T and Takahashi K (2008), 'Absorption characteristics of fission product elements on zeolite', *J Nucl Technol*, 162, 229–243.

Vaden D and Fredrickson G L (2007), 'Material control and accountability experience at the fuel conditioning facility', *Proceedings of GLOBAL 2007*, 170–175.

Vaden D, Li S X and Johnson T A (2002), 'Electrometallurgical processing of Experimental Breeder Reactor-II spent fuel', *Proceedings of Fifth Topical Meeting on DOE Spent Nuclear Fuel and Fissile Materials Management*, Charlestone, South Carolina, USA, ISBN: 0894486683.

Vaden D, Li S X, Westphal B R, Davies K B, Johnson T A and Pace D M (2008), 'Engineering-scale liquid cadmium cathode experiments', *J Nucl Technol*, 162, 124–128.

Westphal B R, Mariani R D, Vaden D, Sherman S R, Li S X and Keiser D D (2000), 'Recent advances during the treatment of spent EBR-II fuel', *Proceedings of the Embedded Topical Meeting on DOE Spent Nuclear Fuel and Fissile Material Management*, San Diego, California, 153–158.

Westphal B R, Price J C, Vaden D and Benedict R W (2007), 'Engineering-scale distillation of cadmium for actinide recovery', *J Alloy Compd*, 444–445, 561–564.

Westphal B R, Bateman K J, Morgan C D, Berg J F, Crane P J, Cummings D G, Giglio J J, Huntley M W, Lind R P and Sell D A (2008), 'Effect of process variables during the head-end treatment of spent oxide fuel', *J Nucl Technol*, 162, 153–157.

Willit J L, Laplace A F, Fletcher G A, Williamson M A and Laquement J (2005), 'Electrodeposition of uranium and transuranics metals on solid cathode', *Proceedings of MS7*, Tourouse, France, 1, 607–610.

Development of highly selective compounds for solvent extraction processes: partitioning and transmutation of long-lived radionuclides from spent nuclear fuels

C. HILL, CEA, France

Abstract: This chapter discusses the methodology deployed in the European partitioning strategy to design highly selective extractants for long-lived radionuclide separation: calix[4]arenes for caesium, malonamides for the co-extraction of trivalent minor actinides (Am, Cm) and lanthanides (Ln(III)), and nitrogen-donor ligands, such as bis-triazinyl-pyridines, for the separation of trivalent minor actinides from Ln(III).

Key words: selectivity, calixarene-crowns, diamides, bis-triazinyl-pyridines.

11.1   Introduction

In the quest to develop mature technologies capable of partitioning long-lived radionuclides (LLRN) from spent nuclear fuels, hydrometallurgy has consensually become a reference route, probably because of the successes of PUREX[1] process industrial implementations in Europe and elsewhere since the 1970s (Benedict *et al.*, 1981, Schulz *et al.*, 1990, Birkett *et al.*, 2005). Furthermore, solvent extraction allows high selectivity and recovery yields to be reached without generating excessive volumes of secondary waste; its flexibility in adapting to various spent nuclear fuel characteristics and fuel cycle options, as envisaged in the GenIV initiative, appears industrially attractive. Solvent extraction has been a subject of intensive nuclear research activities in Europe, Russia, China, Japan, India, and the United States since the early 1960s (Marcus and Kertes, 1969, Sekine and Hasegawa, 1977, Musikas, 1986, Rydberg *et al.*, 1992, Danesi, 2004, Rydberg *et al.*, 2004).

After a brief introduction on the advantages of the Partitioning and Transmutation (P&T) strategy, this chapter identifies the LLRN targeted in the European P&T policy. The methodology deployed to design highly

[1] PUREX process, for Plutonium URanium EXtraction

selective lipophilic compounds is then illustrated by three examples: (i) calix[4]arenes for caesium separation, (ii) diamides for the co-extraction of trivalent minor actinides and lanthanides from PUREX raffinates, and (iii) nitrogen-donor ligands for the discrimination between trivalent minor actinides and lanthanides. Finally, the main progress achieved in these respective processes is described.

11.2   Which long-lived radionuclides to partition and why?

The transformation of uranium or mixed uranium/plutonium (U/Pu) oxides through fission and/or neutron capture reactions in pressurized (PWR) or boiling (BWR) water nuclear reactors generates more than 400 radionuclides (representing 40 elements of the periodic table) with differing physical and chemical properties and making spent nuclear fuels extremely radioactive. The fissile and/or fertile properties of the major actinides, U and Pu, heighten the interest of recycling them (they are moreover the major contributors to the long-term radiotoxicity of spent nuclear fuel). The PUREX process not only separates valuable U and Pu from the waste by taking advantage of the extracting properties of tributyl-phosphate (TBP), it also allows nuclear waste to be conditioned in a safe, inert glass matrix while generating a minimum of secondary technological waste. Spent nuclear fuel reprocessing thus significantly reduces the mass, volume, toxicity, and thermal activity of the ultimate nuclear waste to be disposed of in deep geological repositories (Schulz *et al.*, 1990). Furthermore, recycling purified Pu in MOX fuel, which in turn can be reprocessed after fission, makes the option of closing the fuel cycle ever more possible.

Further possible innovative routes have been identified beyond this first but nevertheless essential step towards developing sustainable nuclear energy, preserving natural fossil resources and minimizing the impact on the human environment. Future nuclear fuel cycles will undeniably require recycling of not only U and Pu but of all the valuable and hazardous radionuclides, such as long-lived fission products and minor actinides (MA: neptunium, Np, americium, Am, and curium, Cm). Although they account for only a thousandth of the mass of the major actinides, the MA remain, after several centuries, the major contributors to the radiotoxicity of spent nuclear fuel (provided Pu has been eliminated). The current P&T research policy is not driven strictly by the problem of waste repository safety since it has been demonstrated that, under certain reductive geological conditions, the glass matrix alteration would be very slow and the release of LLRN from the ultimate waste negligible (although variable according to the geological repository conditions). The issue is rather that of limiting the potential radiotoxicity of nuclear waste.

Nevertheless, the potential noxiousness of Am is different from those of Cm and Np, since Am is the major long-term radiotoxic contributor before Cm and Np. After a century of decay of the thermal fission products and Cm isotopes, Am-241 is the largest contributor to the heat release of nuclear waste. On the other hand, the problems encountered when recycling LLRN are not equivalent: recycling Am appears less detrimental than for Cm because of the presence of Cm-244, a radioactive, thermal, and neutron-emitting isotope that worsens the difficulties of fabricating Cm-based fuels or targets.

A few hundred years after nuclear waste disposal, the fission products would contribute to only a negligible fraction of its radiotoxicity. Although computational studies carried out on the chemical behaviour of deep geological repositories revealed that some fission products, such as iodine-129, caesium-135, and technetium-99, could be released to the biosphere after several hundred thousand years, because of their high solubility in water (OECD/NEA, 1999), recent studies of nuclear waste storage scenarios have confirmed the mobility of iodine, but invalidated those of caesium and technetium, especially in clay repositories. Nonetheless, the strategy adopted in France – where two waste management acts were enacted in 1991 and 2006 to organize French research programs on P&T and help prepare the construction of both an industrial workshop for manufacturing MA-based fuels and an actinide burner reactor by 2020 (Warin, 2007) – has focused on the development of separation processes for iodine, caesium, technetium, neptunium, americium, and curium. This policy was further followed in Europe, where EURATOM has funded many collaborative projects since the 1990s (Dozol *et al.*, 1997, Madic and Hudson, 1998, Dozol *et al.*, 2000a, Madic *et al.*, 2000, Dozol *et al.*, 2004, Madic *et al.*, 2004). It still consists in:

- Taking advantage of the potentialities of the PUREX process to separate most of the iodine and technetium and at least 99% of the neptunium by optimizing the operating conditions: increasing the feed acidity actually forces the oxidation of Np(V) into its +VI valence state, which is better extracted by TBP. The remaining Np is expected to be quantitatively recovered in the following Am and Cm recovery step.
- Devising and developing complementary separation steps, making use of highly selective molecules (since TBP is only suitable for extracting elements at valence states above +III) to recover caesium and more than 99.9% of americium and curium downstream from the PUREX process.

Calculations actually proved that the time required for the radiotoxicity of a spent nuclear fuel to decrease below that of natural U (extracted from

the mine to manufacture the fuel) is estimated to exceed 100 000 years. This period shortens to 10 000 years if Pu is recycled, and shrinks to only three centuries if MA are also recycled (leaving less than 0.1% of the latter radionuclides in the nuclear glass waste). However, for physical reasons of transmutation efficiency in reactors, the decontamination factors of Am and Cm with regard to the lanthanides (Ln, known as neutron-absorbing elements unfavourable to MA transmutation) were set so as to limit to 5 wt.% the fraction of Ln in the final 'Am + Cm' product.

11.3   How to develop selective ligands and extractants?

The methodology currently applied in France and Europe to develop new highly selective hydrophilic or lipophilic compounds for partitioning LLRN is more or less the same as elsewhere in the world:

(i)   It starts with the design of a new structure of complexing molecule that could suit the chemical properties of the target LLRN. Radiochemists can search, through comprehensive literature reviews, for existing natural or tailored molecules known for their ability to complex or extract mimicking nonradioactive elements. However, although significant progress has been made in recent years on the use of computational tools to develop macrocyclic ligands for selective metal binding (Hay *et al.*, 2004, 2005), radiochemists can hardly rely on computational modelling approaches, such as those adopted by pharmacologists to design effective drugs, to develop potentially interesting ligands to selectively extract minor actinides from PUREX raffinates, probably because the intrinsic complexity of the chemical systems implemented in their partitioning processes deters chemists from identifying and understanding the physicochemical phenomena underlying solvent extraction, both qualitatively and quantitatively.

Whatever the objectives when describing a chemical system (its energy, the behaviour of its molecular orbital electrons, the main source of its chemical reactivity, its mechanics, or the geometry of its studied complexes), this system can be conceptualized and modelled in different referentials. Nevertheless, these referentials consist of parameters and basic data only achievable after establishing chemical models, which in turn have to be confronted with experimental physical data. Unfortunately, these experimental data are not easy to obtain, since preparing and analyzing radioactive samples in glove boxes is often difficult and limited to specific chemical environments.

Furthermore, the conditions used are usually far from those encountered when reprocessing spent nuclear fuel at industrial scale, where concentrated solutions are implemented. In concentrated solutions, the chemical reactivity of the radionuclides is actually considerably modified as compared to that in diluted solutions. This difficulty, which is currently overcome by using approximate interpolated and/or extrapolated functions, makes the quantitative prediction of the behaviour of a solute in a complex medium almost impossible without experimental data. However, recent coupling of two mathematical approaches proved to be successful in predicting the thermodynamic properties of concentrated solutions: Molecular Dynamics on the one hand, which allows microscopic parameters to be calculated (such as the diameter of the hydrated cations in infinitely dilute solutions or the parameters describing the changes in the size of the hydrated cations with the concentration), and the Binding Mean Spherical Approximation theory on the other hand, which allows osmotic coefficients and thus activity coefficients (γ_I, which accounts for the solute chemical reactivity in concentrated solutions) to be estimated via a microscopic representation of the solutions (Ruas *et al.,* 2006).

Statistical approaches aiming at establishing empirical mathematical relationships between sets of ligand structures and their chemical properties (such as complexation or extraction of target LLRN) are sometimes used to help design optimized ligand structures (Ionova *et al.*, 2001). For instance, a quantitative structure-activity relationship can correlate chemical structures with well defined chemical reactivity parameters (Drew *et al.*, 2004a, Varnek *et al.*, 2007). On a more fundamental level, quantum chemistry and molecular dynamics calculations, such as density functional theory, have been used concomitantly with structural and spectroscopic characterization to enrich basic knowledge of actinide complex formation and/or extraction (Boehme and Wipff, 1999a,b, Karmazin *et al.*, 2002, Baaden *et al.*, 2003, Coupez *et al.*, 2003). Beyond the difficulties of characterizing the radioactive systems investigated, this modelling approach seeks to define independent physical criteria that can be experimentally observed at different scales (molecular, microscopic as well as macroscopic) and correlated with modelling calculations (Guillaumont *et al.*, 2006, Foreman *et al.*, 2006, Petit *et al.*, 2007, Gaunt *et al.*, 2008).

(ii) Small quantities (sometimes a few hundred milligrams) of the desired compound are synthesized and chemically characterized to validate its structure and determine its purity utilizing suitable analytical tools such as nuclear magnetic resonance (NMR), mass spectrometry or elementary analysis.

(iii) The complexing and/or extracting properties of the synthesized compound are then assessed by general screening tests in micro-tubes, first on surrogate solutions, then on solutions spiked with the target LLRN and containing some of (or all) the competing elements present in the genuine nuclear waste.

(iv) If the ligand presents promising complexing and/or extracting properties toward the target LLRN, the chemical reactions involved may be studied more deeply from a thermodynamic and kinetic standpoint, but this requires the synthesis of larger quantities of compounds. These investigations are carried out both at molecular and supra-molecular scales implementing analytical methods adapted to the nuclear environment to probe radioactive complexes. Analytical techniques used to investigate complexes at molecular scale include NMR (Wietzke *et al.*, 1998, Lefrançois *et al.*, 1999, Dozol and Berthon, 2007), UV-Visible spectrophotometry (Miguirditchian *et al.,* 2006), X-ray crystallography (Wietzke *et al.*, 1998, Berthet *et al.*, 2005, Baaden *et al.*, 2003, Coupez *et al.*, 2003, Foreman *et al.*, 2006, Gaunt *et al.*, 2008), X-ray absorption spectroscopy (Hudson *et al.*, 1995, Denning *et al.*, 2002, Den Auwer *et al.*, 2004, Gannaz *et al.*, 2006), time-resolved laser-induced fluorescence spectroscopy (Colette *et al.*, 2004, Pathak *et al.*, 2009), microcalorimetry (Miguirditchian *et al.,* 2005), gas chromatography and electrospray ionization mass spectrometry (Lamouroux *et al.*, 2006, Leclerc *et al.*, 2008, Antonio *et al.*, 2008). Examples of analytical techniques used to investigate complexes at supra-molecular scale are vapour pressure osmometry, small-angle neutron scattering, and small-angle X-ray scattering (Hudson *et al.*, 1995, Erlinger *et al.*, 1999, Berthon *et al.*, 2007).

(v) As the compound will sooner or later be degraded whilst being implemented to partition the target LLRN, through acidic hydrolysis and α/γ radiolyses of the spent nuclear fuel dissolution solution, understanding the ligand degradation pathways will help improve its chemical resistance (by modifying its structure or changing the formulations of the separation system) and minimize the effect of its degradation products on the process efficiency (by developing specific solvent washing methods).

(vi) In parallel, systematic parametric tests to acquire partitioning data in test tubes (such as the solvent loading capacity or the variation of the distribution ratios of the target LLRN with a given parameter, as for instance the extractant concentration, acidity, pH, or ionic strength) will allow the formulations of the different aqueous and organic solutions to be optimized and the mass action laws to be determined. Thermodynamic models will consequently be developed to interpolate the extraction isotherms.

(vii) In some cases a counter-current separation flowsheet is calculated utilizing process simulation codes, taking into account both the phase transfer kinetics and the hydraulic characteristics of the contactors (e.g., mixing efficiency, droplet size). The implementation (after scaling up the synthesis of the compound) of this counter-current flowsheet in laboratory scale contactors (mixer-settlers, centrifuges, small-scale pulsed or rotating columns), first on surrogate feeds to test the hydrodynamic behaviour of the partitioning system, and then on genuine nuclear waste feeds (arising from the dissolution of spent nuclear fuel in concentrated nitric acid) validates or invalidates the process separation performance. Analysis of the counter-current pilot test and comparison of the observed experimental results with modelling calculations improve the accuracy of the process simulation codes, which can subsequently be employed to extrapolate the design of the workshops in the industrial reprocessing plant.

This methodology is rather long and complicated: it requires a range of skills and involves many researchers as the work progresses. The design of a highly selective hydrophilic or lipophilic compound is therefore intrinsically combined with the development of the partitioning process in which the compound is used alone or in a synergistic mixture. The optimizations of both the selective compound itself and of the related partitioning process are therefore almost inseparable.

In fact, only a very few molecules are developed up to the counter-current demonstration test and most often the compounds investigated do not reach the third step, thus implying continuous iteration between steps (i) and (iii). It is commonly accepted, although difficult to satisfy, that highly efficient and selective compounds must fulfil many criteria, among which are:

- simplicity of preparation: excessive synthesis costs to scale up the production of a highly selective complexant or extractant might be a disincentive for an industrial application;
- high complexation or extraction efficiency and a high selectivity toward the target element(s) to ensure high decontamination factors;
- reversibility of the target element complexation or extraction to ensure a high recovery yield;
- high resistance to chemical and radiochemical attack, generating only manageable degradation compounds;
- no formation of precipitate, the occurrence of which could trap some radionuclides and thus decrease their recovery yields, not to mention a criticality event;
- minimum secondary waste generation (burnable compounds consisting of carbon, hydrogen, oxygen, and nitrogen atoms are expected to release only gases);

- fast mass transfer kinetics to ease the implementation of the partitioning process in short time contactors;
- no occurrence of stable emulsions, which block counter-current process implementation.

With regard to the extractant loading capacity (that is to say the amount of metallic cation it can take up from the aqueous feed without inducing third phase formation or organic phase splitting), the major factor to consider is the balance between its hydrophilic character and its lipophilicity. The hydrophilic character of a ligand is enhanced by the polar nature of its chemical functions bearing the electron-donor atom(s), whereas the lipophilicity of a ligand is favoured by the length of the hydrophobic carbon chains grafted onto its skeleton. However, due to the presence of these two differing parts in its structure (the polar head interacting with the metallic cation(s) at the water/oil interface and the long hydrocarbon tail(s) facilitating its dissolution and that of its metallic complex(es) in organic diluents), the compound usually presents surface active properties which may cause aggregation in the organic phase. Although aggregation could improve the extraction efficiency through the formation of reverse micelles (Chiarizia *et al.*, 1999, Yaita *et al.*, 2004, Jensen *et al.*, 2002, 2007, Testard *et al.*, 2008), it may also lead to the formation of a stable emulsion in certain experimental conditions (Nave *et al.*, 2004) and consequently to hydrodynamic problems when running the process.

With regard to the selectivity and the complexation/extraction efficiency of a given ligand, considered as a base in Pearson's 'Hard and soft acids and bases' theory (Pearson, 1963), the main factors governing the thermodynamics of its chemical reactivity are (i) the nature ('soft' or 'hard') and (ii) the number of its electron-donor atom(s), which interact with the electron deficient metallic cation (considered as an acid in Pearson's theory), as well as (iii) its structure (i.e., the three-dimensional geometric orientation of its chemical function(s) bearing the electron-donor atom(s)). The better the fit between the ligand donating function(s) and the metallic cation free orbitals, the stronger the coordination interactions. Multiple denticity, chelation, cyclization, and pre-organization of the chemical functions are complementary but nevertheless significant parameters that induce energy-stabilizing effects on the thermodynamics of the chemical reactivity and selectivity of a given ligand. For instance, the higher the degree of coordination of a neutral extractant to the targeted metallic cation, the stronger the metal-ligand bonding interactions, because of the increased entropy variation term ($\Delta S > 0$) due to amplification of the system disorder, mainly resulting from dehydration of the metallic cation (Musikas, 1986, Nash, 1993).

11.4   Examples of development of highly selective compounds in European partitioning and transmutation (P&T) strategy

From the early 1990s to the beginning of the 2000s, various extracting systems have been investigated in the framework of European collaborative projects (Dozol *et al.*, 1997, Madic and Hudson, 1998, Dozol *et al.*, 2000a, Madic *et al.*, 2000, Dozol *et al.*, 2004, Madic *et al.*, 2004). This thriving exploratory period ended in France with a demonstration phase, between 2000 and 2005, during which the research activities focused on the most mature separation processes, tested on genuine PUREX raffinates to assess their scientific feasibility (validation of the partitioning concept) and technical feasibility (global validation of all the separation processes). These tests aimed at consolidating the process flowsheets in order to ensure their robustness by assessing their long-term implementation in laboratory equipment simulating industrial contactors, and by developing efficient spent solvent cleaning treatments to cope with the degradation of the solvents through acidic hydrolysis and radiolysis, as if they were recycled in industrial processes. The remainder of this chapter will describe some of the research programmes deployed in Europe during the past two decades to develop and optimize the design of highly selective ligands for partitioning schemes, in order to limit the long-term noxiousness of nuclear waste and/or to close future nuclear fuel cycles. Note that this chapter will not review thoroughly the various ligands studied, but focus on three chosen examples: (i) calix[4]arenes for caesium separation, (ii) diamides for the co-extraction of trivalent minor actinides (An(III)) and lanthanides (Ln(III)), and (iii) nitrogen-donor ligands for An(III)/Ln(III) separation.

11.4.1 Caesium separation by calix[4]arenes-crown-n

Challenges of the selective extraction of caesium

After five years of cooling, one tonne of a spent PWR uranium oxide fuel (with a burnup of 60 GWd/t) still contains 4.6 kg of caesium (1.89 kg of stable isotope Cs-133, 50 g of two-year half-life Cs-134, 769 g of 2.3 million-year half-life Cs-135, and 1.93 kg of 30-year half-life Cs-137), which together with strontium is the main short-term heat source in the vitrified waste. In addition to the need for selective caesium extraction from dissolver liquors to decrease this thermal source, selective extraction of caesium from acidic effluents containing large quantities of sodium nitrate arising from the neutralization of nuclear plant technological waste streams by concentrated

soda, as well as from basic sludge contaminated with alpha emitters inherited from decades of military research programs, is of primary importance in nuclear waste management.

In aqueous nitric acid solutions, the caesium metallic cation is monovalent and considered as a 'hard acid' in Pearson's theory. It therefore interacts preferentially with 'hard bases', such as anions or molecules containing fluoride or oxygen donor atoms and inducing electrostatic interactions. Studies reported in the literature point out the difficulties of extracting caesium selectively from acidic solutions, especially in the presence of other alkali elements (Moyer and Su, 1997, Herbst *et al.*, 2002a).

The first extracting agents envisaged in the 1980s were the crown ethers: macrocyclic polyethers discovered by Pedersen (1967). Parametric studies carried out on the extraction of alkali cations by crown ethers (Danesi *et al.*, 1975, Sadakane *et al.*, 1975, Gerow *et al.*, 1981, Schulz and Bray, 1987, Wood *et al.*, 1995, Dozol *et al.*, 1995, Dietz *et al.*, 1996, Kumar *et al.*, 1998, Kikuchi and Sakamoto, 2000) have shown that the quantity of metallic cation extracted in the organic phase depends on the following factors: the polarity of the organic diluent used to dissolve the crown ether, the nature of the co-extracted anion, the size of the crown ether cavity relative to the alkali cation diameter, the chemical composition of the aqueous solution (acidity, ionic strength), and the type of the chemical functions grafted onto the crown ether. The most evolved design of a crown ether for caesium extraction is that of di-(tert-butyl-benzo)-21-crown-7 (Fig. 11.1) because the cavity size of its crown, containing seven oxygen atoms, matches the coordination shell of the caesium cation, and because the tert-butyl-benzo groups grafted onto its skeleton enhance its hydrophobicity.

Although di-(tert-butyl-benzo)-21-crown-7 can extract caesium from nitrate feeds of low acidity, it definitely requires the addition of a synergistic cation exchanger, such as dinonyl-naphthalene sulfonic acid (Kozlowski *et al.*, 2002, 2007), or even better hexabrominated bis(dicarbollide) anion (Grüner *et al.*, 2002), a very strong cation exchanger used in the UNEX process (Herbst *et al.*, 2002a,b, 2003), to extract caesium from PUREX acidic raffinates. Nevertheless, the drawback of synergistic mixtures composed of solvating agents (such as crown ethers, which extract metallic cations with increasing efficiency as the ionic strength increases) and cation exchangers (such as cobalt dicarbollides, which extract metallic cations more efficiently at low acidity) is the difficulty encountered when stripping the metallic cations, because of competition between the two extractants. The same problem occurs for crown ethers that have been functionalized with a cobalta bis(dicarbollide) cage (Fig. 11.1) to extract caesium from acidic feeds (Grüner *et al.*, 2002). Their caesium extraction efficiency is comparable with that of the corresponding synergistic mixtures composed of hexabrominated bis(dicarbollide) anion and crown ethers. Their selectiv-

Di-(tert-butyl-benzo)-21-crown-7 (^{t}Bu-Bz-21C7)	Functionalized 21-crown-7 with cobalta bis(dicarbollide) cage
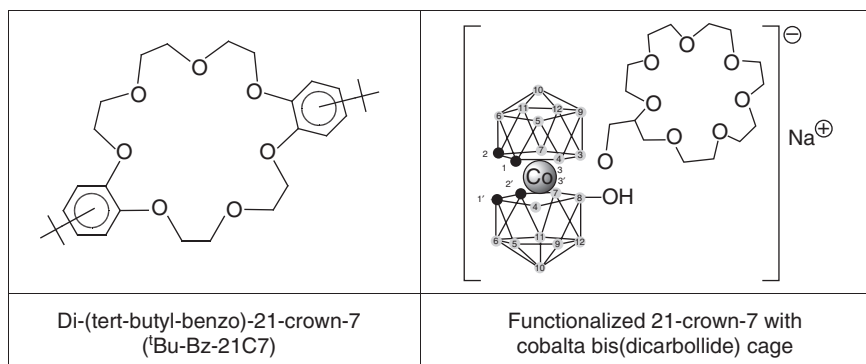
11.1 Examples of crown-ethers developed for caesium extraction.

ity with respect to Na$^+$ cation is sometimes even higher (separation factor: SF$_{Cs/Na}$^{2} > 100 for trace elements) than that of the corresponding synergistic mixtures, yet too low in the presence of high contents of sodium ions to develop a process for decontaminating technological nuclear waste streams.

When dissolved in organofluorine diluents such as 1,1,7-trihydrodo-decafluoroheptanol, di-(tert-butyl-benzo)-21-crown-7 and other crown ethers appear to extract caesium from acidic feeds ([HNO$_3$] > 3 mol.L^{-1}, Yakshin *et al.*, 2008), but the complexity of their preparation and consequently their high cost, as well as their poor Cs$^+$/Na$^+$ selectivity, still hinder their use on an industrial scale.

Calixarenes: chemical platforms suitable for the design of selective extractants

It sometimes happens in organic chemistry that already known compounds are re-examined by researchers to meet challenging new demands, or as interest rises in potential applications. This is the case for the calixarenes: cyclic oligomers obtained at the end of the 19th century by condensing formaldehyde on *para*-substituted (*p*-tert-butyl, *p*-octyl, ...) phenolic acids to produce Bakelite.

Non functionalized ('parent') calix[n]arenes are macrocyclic platforms consisting of *p*-tert-butyl-phenol units bridged through their *ortho* positions by methylene spacers (the degree of condensation, [*n*], usually ranges from 4 to 8). In the solid state, the basket form of the calix[4]arene molecules, resembling a chalice (hence their name: calixarene, in which the *arene* suffix stems from the aryl rings they are made of), presents two cavities (Fig. 11.2):

^{2} SF$_{Cs/Na}$ = D_{Cs}/D_{Na}, where D_M is the distribution ratio of the extracted alkali cation M.
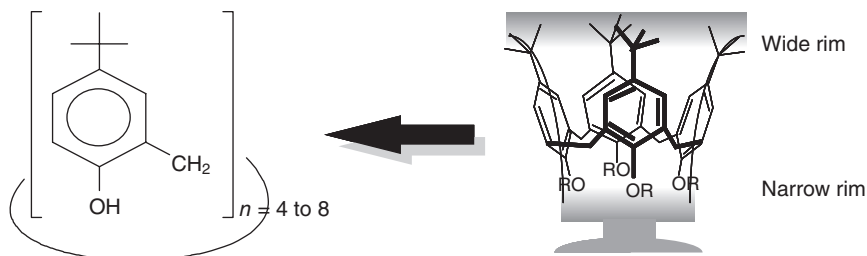
11.2 Parent calix[n]arenes of chalice shape.

1. A hydrophilic cavity, delimited by the phenol functions: the 'narrow rim';
2. A lipophilic cavity, delimited by the *p*-tert-butyl groups: the 'wide rim'.

    In the late 1980s, Gutsche's team investigated the condensation reactions of calixarenes and pointed out the importance of the experimental conditions (heat, reaction time, nature and concentration of the basic catalyst) on the product yield and composition (Gutsche, 1989, 1998). At the same time, Izatt *et al.* (1983, 1985) were the first to test 'parent' calix[n]arenes for carrying alkali cations through supported liquid membranes. However, since phenolate base is very strong, caesium transportation only occurred from very basic feeds (pH ≥ 12) and not from nitrate feeds. Furthermore, although the caesium flow increases with [n], the selectivity toward caesium surprisingly increases as [n] decreases. Inclusion of a caesium cation in the lipophilic 'wide rim' cavity of the 'parent' calix[4]arene (probably because of the small cavity size of its 'narrow rim') was later demonstrated by X-ray diffraction studies assuming the existence of specific electrostatic interactions between the caesium cation and the negative charge delocalized on the aryl rings of the deprotonated 'parent' calix[4]arene (Harrowfield *et al.*, 1991).

    Unfortunately, 'parent' calix[n]arenes appeared totally inappropriate for developing a process for caesium separation from acidic PUREX raffinates or other acidic nuclear waste streams. Nevertheless, this family of macrocyclic compounds appeared doubly interesting in the European P&T strategy, because:

- the scalable synthesis of 'parent' calix[n]arenes was demonstrated (high production yields could be expected);
- the functionalization of calix[n]arenes (either through the hydroxyl groups at the 'narrow rim' or through the *p*-tert-butyl groups at the 'wide rim') could lead to a wide range of chemically substituted molecules (Vicens and Böhmer, 1991, Ungaro and Pochini, 1991, Creaven *et al.,* 2008).

Cone

Partial cone

1,2 -alternate

1,3 -alternate
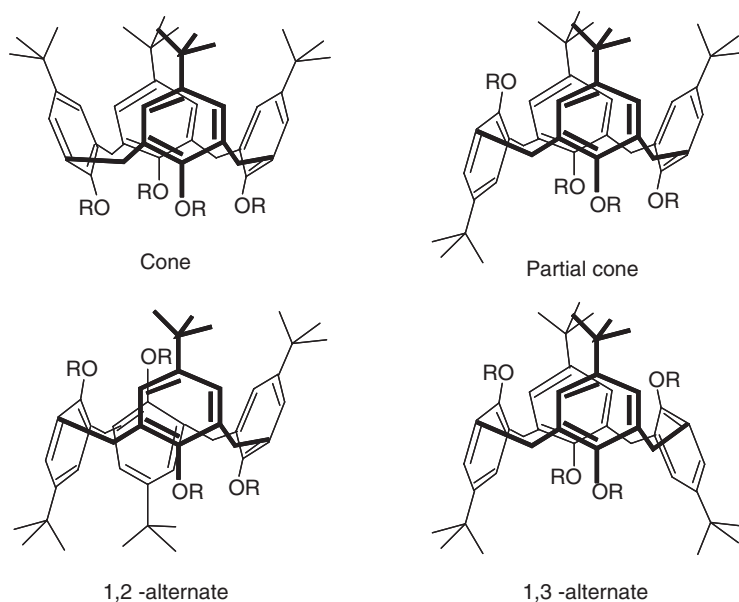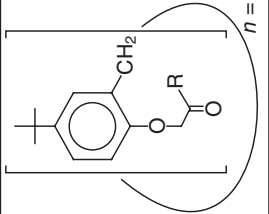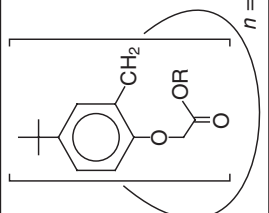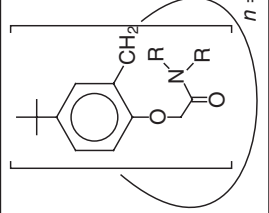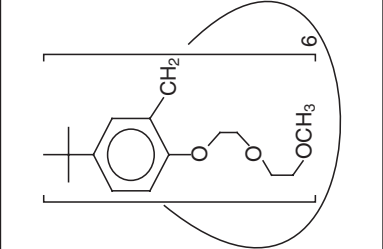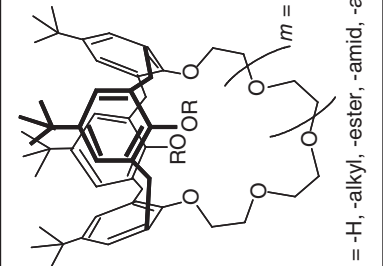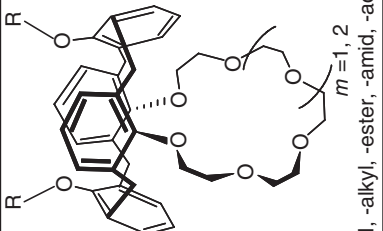
11.3 The four main conformations of calix[4]arenes.

If the shape of the 'parent' calix[4]arene is actually fixed in the solid state, the rotation freedom in solution of its phenol units around its methylene bridges lets the calix[4]arene molecule adopt various conformations (Cornforth *et al.*, 1955). The four main ones were named by Gutsche as: *cone*, *partial cone*, *1,2-alternate*, and *1,3-alternate*, depending on the number of phenol units that have flipped through the mid-plane of the molecule (Fig. 11.3).

This pre-organization feature of calix[4]arenes has definitely been the driving force for the design of caesium selective ligands, because caesium complexes of functionalized calix[4]arenes were expected to be increasingly stable as the changes (induced by the complexation reaction) in the organization of the substrate (calix[4]arene), receptor (caesium), and solvent, were small (Lein and Cram, 1985). It appeared particularly interesting to block specific conformations of the calix[4]arene platforms in order to orientate suitable chemical functions (that is to say functions able to bind to caesium cations) in desired directions to fit the alkali cation inner coordination shell.

Ester, ketone, and amide based calix[n]arenes

Ester, ketone, and amide functions have been introduced on the 'narrow rim' of calix[n]arenes (Fig. 11.4) in order to mimic natural substrates (Chang

11.4 Examples of functionalized calix[n]arenes at the narrow rim.

Ketone functionalized calix[n]arenes — $n = 4$ to 8

Ester functionalized calix[n]arenes — $n = 4$ to 8

Amide functionalized calix[n]arenes — $n = 4$ to 8

p-tert-butyl[Calix[6]arene-hexa(ethoxy-ethoxy-methoxyether)

p-tert-butyl[Calix[4]arenes-crown-n in the *cone* conformation — $m = 1, 2, ...$ R = -H, -alkyl, -ester, -amid, -acid, ...

Calix[4]arenes-crown-n in the *1,3-alternate* conformation — $m = 1, 2$ R = -H, -alkyl, -ester, -amid, -acid, ...

and Cho, 1986, 1987, Arnaud-Neu *et al.*, 1989). The trends observed while investigating the complexing properties of these ligands can be summed up as follows, although the experimental conditions often differ:

- The blocked *cone* conformation and the four 'hard' donor functions (bearing oxygen atoms) pointing in the same direction confer the substituted calix[4]arenes interesting complexation and extraction properties toward sodium cation, in the following order: esters < ketones < amides (Arduini *et al.*, 1988, Schwing *et al.*, 1989, Arnaud-Neu *et al.*, 1991, 1995, Gradny *et al.*, 1996). The stability constants of the 1:1 (metal:ligand) complexes measured in solution are greater than those observed with crown ethers, almost challenging those of cryptands, thus enabling the use of these substituted calix[4]arenes as active agents for chemical sensors (Forster *et al.*, 1991, Brunink *et al.*, 1991, Ganjali *et al.*, 2006).
- The ester derivatives of calix[6]arene extract potassium better than sodium and show a selectivity plateau for voluminous alkali cations. The amide derivatives of calix[6]arene extract the alkaline-earth elements better than the alkali elements, with a preference for calcium and strontium.
- Calix[8]arene derivatives are the least efficient extractants of the series.

Podant calix[n]arenes

Polyethylene chains have been introduced on the 'narrow rim' of calix[n]arenes (Fig. 11.4) by Ungaro's team as early as 1982 (Bocchi *et al.*, 1982). If the tetramer derivative adopts a *partial cone* conformation, the hexamers and octamers are mobile in solution and their complexing properties are therefore weaker than those of classical crown ethers. However, caesium extraction can be improved by enhancing the ligand lipophilicity, for example by increasing the length of the polyethylene chains.

Crown-ether based calix[n]arenes
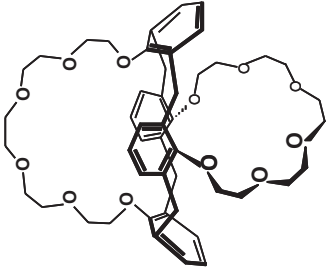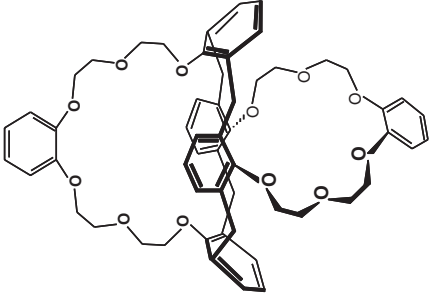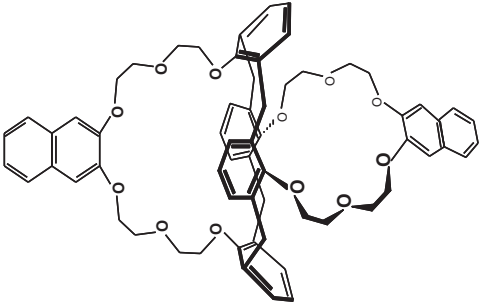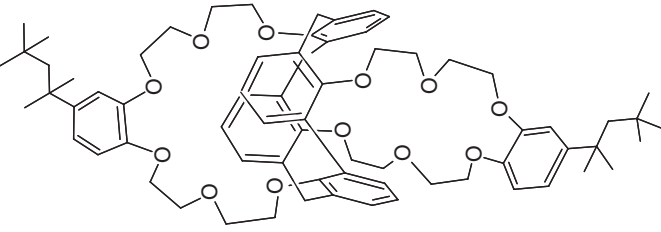
The thermodynamic and crystallographic studies carried out on crown-ether based calix[4]arenes, in which one polyethylene chain ($-CH_2-CH_2-O)_n$ bridges two oxygen atoms of two opposite phenol units at the 'narrow-rim' (as shown in Fig. 11.4), have led to the following observations:

- *p*-tert-Butylcalix[4]arenes-dimethoxy-monocrown-*n* ($n = 5$ or 6) better complex large alkali cations, such as potassium and rubidium, because they can adopt a flattened *partial cone* conformation (Ghidini *et al.*, 1990), which is impossible for larger alkoxy functions.

- As soon as the two remaining functions grafted onto the 'narrow-rim' of a calix[4]arene contain more than two carbon atoms, any of the four conformations encountered (Fig. 11.3) can be blocked in solution.
- Unlike a podant-based calix[4]arene, the selectivity of which favours sodium complexation only if it adopts the *cone* conformation, the presence of a polyether bridge on the 'narrow rim' of a calix[4]arene, that has been blocked in the *cone* conformation, enhances its complexing and extracting properties toward alkali cations and offers additional control of the selectivity through the adjustment of the size of its coordinating cavity to the targeted metallic cation radius. As a result, a bridge presenting five oxygen atoms appears suitable for potassium complexation, whereas a bridge containing six O-atoms better fits the caesium cation radius (Ungaro and Pochini, 1991).
- The presence of a polyether bridge on the 'narrow rim' of a calix[4] arene, blocked in the *1,3-alternate* conformation, strongly increases both its extraction efficiency toward caesium from acidic feeds and its selectivity versus other alkali cations, which is assumed to be due to a favourable enthalpy contribution (Ungaro *et al.*, 1994, Casnati *et al.*, 1995, 1996, 2001, Sachleben *et al.*, 1999, Talanov *et al.*, 2000, 2002).

In reality, the benefit of the *1,3-alternate* conformation for caesium selective extraction was first observed with the symmetrical doubly crowned calix[4]arenes (Fig. 11.5), synthesized by Vicens' team who looked for easier manufactured bridged calix[4]arenes, obtainable in single-step syntheses avoiding the alkyl substitution of the two remaining phenol units of the calix[4]arenes-monocrown-*n* (Asfari *et al.*, 1992, 1995). Like crown ethers and calix[4]arenes-monocrown-*n*, the calix[4]arenes-biscrown-*n* perfectly illustrate the benefit of matching the size of the coordinating cavity of the ligand with the ionic radius of the target cation. For instance, calix[4]arenes-biscrown-*n*, bearing five ($n = 5$) or seven ($n = 7$) oxygen atoms in their ether-crowns, show neither high extraction yields toward caesium, nor higher selectivity toward Cs^+ (over other alkali cations) than di-(tert-butyl-benzo)-21-crown-7. As the caesium aqua complex possesses six water molecules, the six O-atoms of the ether-bridges of calix[4]arenes-biscrown-6 are consequently well pre-organized to displace the six water molecules of caesium inner co-ordination sphere.

Furthermore, outstanding Cs^+/Na^+ selectivity ($SF_{Cs/Na}$, exceeding 30 000) was obtained with calix[4]arenes-crown-6, the polyether bridges of which contain aryl rings such as benzyl or naphthyl (Fig. 11.5, Hill *et al.*, 1994, Dozol *et al.*, 1999). The selectivity of these ligands toward caesium is so high that they are better Cs^+ sensors than any other functionalized calix[4]arenes

Calix[4]arene-bis(*ter*-octylbenzo-crown-6) :BOBCalixC6

Examples of biscrown-calix[4]arenes

11.5 Examples of doubly bridged calix[4]arenes with functionalized crown ethers.

(Pérez-Jiménez *et al.*, 1998). Molecular Dynamics calculations as well as X-ray crystallographic data suggest that, provided no steric hindrance is introduced in the polyether bridge(s), hydrophobic interactions exist between the extracted alkali cations and the π electrons of the aryl rings, hence favouring the binding of the less hydrated caesium cation as compared to harder alkali cations, such as sodium (Wipff and Lauterbach, 1995, Lauterbach and Wipff, 1996, Thuery *et al.*, 1996, Lamare *et al.*, 1997, 1998, 1999, 2001, Asfari *et al.*, 1999, Jankowski *et al.*, 2003).

As expected, although unusual in metallic complexation, the symmetrical arrangement of calix[4]arenes-biscrown-6 with two complexing cavities, is well adapted to the formation of both 1:1 (ligand:metal) and 1:2 complexes, as indicated by NMR, electro-spray ionization mass spectrometry (ESI-MS), and X-ray crystallographic studies (Arnaud-Neu *et al.*, 1996, Allain *et al.*, 2000).

The design of calix[4]arenes-crown-6, presenting one (or two) polyether chain(s) bridging two opposite phenol units of calix[4]arenes, blocked in the *1,3-alternate* conformation, has therefore allowed both concepts (ligand pre-organization and host-guest complementarity through size fitting between substrate and receptor) to be tested in the search for caesium selective lipophilic extractants.

Development of caesium partitioning processes using calix[4]arenes-crown-6

Most of the batch experiments relevant to caesium selective extraction studies, involving calix[4]arenes-(mono/bis)crown-6, have been carried out in polar aromatic organic diluents, such as *o*-nitro-phenyl-alkylethers. Although they greatly enhance the extraction properties of calix[4]arenes-(mono/bis)crown-6 compared with alkanes conventionally used in the nuclear industry, these organic diluents are nonetheless incompatible with the implementation of counter-current process flowsheets: their viscosity and density are too high, and the kinetics of mass transfer too slow. This is why, in order to demonstrate the scientific feasibility of caesium partitioning from acidic nuclear waste streams, efforts at the CEA Cadarache (France) have focused on the substitution of *o*-nitro-phenyl-alkylethers by mixtures of hydrogenated tetrapropene (HTP), the diluent used in the French PUREX process, and modifiers allowing the use of calix[4]arenes-monocrown-6 without third-phase occurrence. Two reference systems presenting sufficiently high and selective caesium extraction from acidic nuclear waste have been optimized (Fig. 11.6):

1. The first is based on 1,3-(di-*n*-octyloxy)-2,4-calix[4]arene-crown-6 (0.065 mol.L^{-1}) and tributyl phosphate (1.5 mol.L^{-1}) as phase modifier.

System 1

Calix[4]arene-Crown-6
«Octyl»

1,3-[di-n-octyloxy]-2,4-calix[4]arene-cr-6

Modifier: TBP

TributylPhosphate

System 2

Calix[4]arene-Crown-6
«R14»

1,3-[(2,4-diethyl-heptylethoxy)oxy]-2,4-calix[4]arene-cr-6

A8

Methyloctyl-2-dimethylbutanamide

Aliphatic organic diluent: HTP
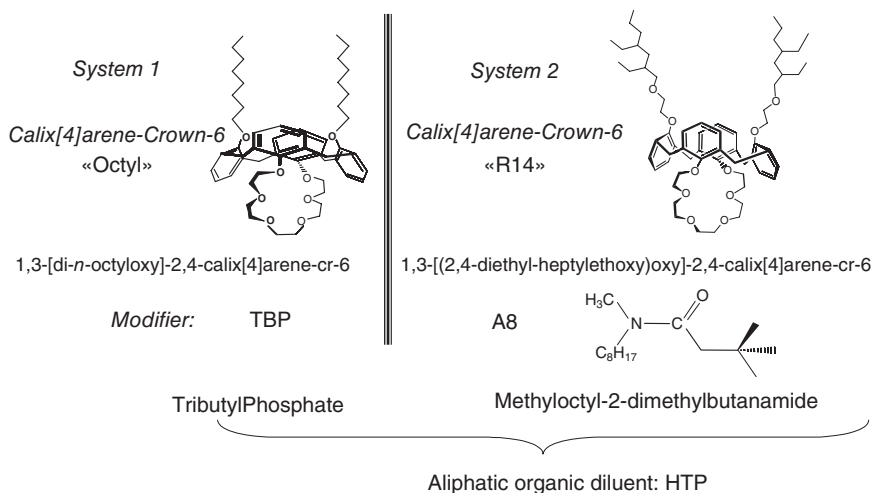
11.6 The two reference systems chosen at the CEA to selectively
extract caesium from acidic nuclear waste streams.

2. The second is based on 1,3-(2,4-diethyl-heptylethoxy)-2,4-calix[4]arene-crown-6 (0.1 mol.L^{-1}), more difficult to synthesize, and methyloctyl-1,2-dimethylbutanamide (1 mol.L^{-1}) as phase modifier.

   Process flowsheets have been developed for both systems and counter-current tests have been performed implementing laboratory-scale contactors (e.g., centrifuges, Taylor-Couette effect columns, and 15 mm diameter pulsed columns) and surrogate feeds. More than 99.9% of caesium was extracted and back-extracted in the centrifuge test, in agreement with flowsheet modelling. Although satisfactory, the hydrodynamic behaviour of the second system (calixarene + monoamide) appeared more emulsifying in the pulsed and Taylor columns than the first system.

   In the light of these promising results, two hot tests were performed in the hot cells of the Atalante facility on a genuine DIAMEX raffinate[3] (see Fig. 11.7 for the flowsheet implemented). By adding oxalic acid to the genuine feed, the extraction of molybdenum and zirconium was prevented and very high caesium recovery yields (>99.9%) were observed, thus confirming the ability of calix[4]arenes-monocrown-6 based solvents to partition caesium efficiently and selectively from acidic nuclear waste streams (Madic *et al.*, 2002).

[3] A DIAMEX raffinate is the genuine highly active solution issued from the implementation of a DIAMEX process, co-extracting trivalent actinides and lanthanides from a PUREX raffinate (issued from the reprocessing of a dissolver liquor by TBP solvent to recover uranium and plutonium).
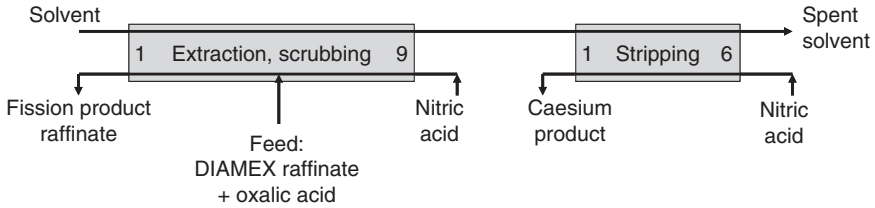
11.7 Flowsheet for caesium partitioning from genuine DIAMEX raffinate implemented in the Atalante facility of the CEA Marcoule (Madic *et al.*, 2002).

The radiolytic degradation of 1,3-(di-*n*-octyloxy)-2,4-calix[4]arene-crown-6 was studied in the presence of nitric acid. High-performance liquid chromatography, directly coupled with ESI-MS, allowed more than 50 distinct degradation products to be observed, and about 30 of them to be identified (as products issued from radical cleavage or addition, oxidation, and aromatic substitution) in aliphatic and aromatic diluents (Lamouroux *et al.*, 2004). Despite the severe degradation conditions tested ($[HNO_3] = 3$ mol.L^{-1} for the acidic hydrolysis and a gamma delivered dose of 10^6 Gy for radiolysis), 1,3-(di-*n*-octyloxy)-2,4-calix[4]arene-crown-6 appeared remarkably stable as illustrated by the limited losses of compound observed: 33.5%.

11.4.2 Trivalent actinide separation from PUREX raffinates

After five years of cooling, one ton of a PWR uranium oxide spent fuel (burn-up of 60 GWd/t) contains 785 g of americium (62.4% of Am-241, 37.4% of Am-243, and 0.2% of Am-242m, all three LLRN), 135 g of curium (8% of Cm-245, 1% of Cm-243, 1% of Cm-246, all three LLRN, and 90% of Cm-244, a short-lived radionuclide), but around 60 kg of fission products, one third of which are the lanthanides.

Properties of trivalent actinides and lanthanides

In nitric acid solutions, such as PUREX raffinates (where $[HNO_3] > 3$ mol. L^{-1}), the 4*f* lanthanide metallic cations (Ln) and the 5*f* americium and curium metallic cations (An) predominantly show the same oxidation state, +III, and many similar physical and chemical properties (Nash, 1993, 1994, Beitz, 1994, Morss, 1994, Marcus, 1997):

- They are considered as 'hard acids' in Pearson's theory (Pearson, 1963).
- The 4*f* and 5*f* orbitals have a rather small radial extension and are more or less protected by the saturated lower electron orbitals, respectively

the $5s^2$-$5p^6$ for the lanthanides and the $6s^2$-$6p^6$ for the actinides. Thus, the nf electrons scarcely interact with electrons of neighbouring ligands and their electronic properties are only slightly affected by their environments.

- The ionic radius shortens along the $4f$ and $5f$ series as the atomic number increases. Thus, it is easy to predict the higher electrostatic reactivity (formalized by the ionic potential closely linked to the charge density) of an element of higher atomic number, Z, compared to that of an element of lower atomic number in the periodic table.

- Since Ln(III) and An(III) have the same positive charge (+3), their discrimination through solvent extraction involving 'hard bases' (e.g., ligands bearing oxygen donor atoms in their structures) will mainly be due to geometric and/or steric hindrance reasons: the better the fitting of a metallic cation radius with the cavity size of the complexing/extracting agent or its coordinating site, the better the discrimination. However, the separation of the two series of trivalent elements will not be complete because of the similarities in the ionic radii among $4f$ and $5f$ elements.

- Ln(III) and An(III) are highly hydrated in aqueous media: 8 to 9 water molecules can be numbered in their inner-coordination spheres, as compared to 4 to 5 only in the case of penta- and hexavalent actinides. It is, however, admitted, although difficult to demonstrate by a structural proof, that an outer-coordination sphere of water molecules exists and interacts with the water molecules present in the inner-coordination spheres of the metallic cations through hydrogen bonds.

- As for other metallic cations, hydration of the $4f$ and $5f$ trivalent elements is of capital importance in their extraction mechanisms, since they can be partly or completely dehydrated while being extracted in organic solvents.

- The coordination numbers in complexes of trivalent lanthanides and actinides vary from 6 to 12, depending on the bonding chemical system involved.

However, a slight chemical behaviour difference does exist between the two series of trivalent elements: the $4f$ orbitals of the lanthanides are slightly more localized around their nuclei than the $5f$ orbitals of the actinides, which can consequently interact more easily with their electronic environments than the corresponding lanthanides (Beitz, 1994, Morss, 1994). Unlike trivalent lanthanides, trivalent actinides create stronger chemical bonds with ligands bearing 'softer' donor atoms than oxygen, such as for instance sulphur or nitrogen (Musikas *et al.*, 1983, Musikas, 1984). The drawback of hydrophilic and/or lipophilic compounds containing sulphur and/or nitrogen atoms is their usually strong affinity for protons in acidic media.
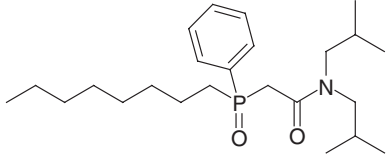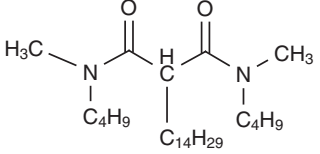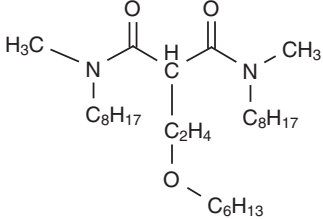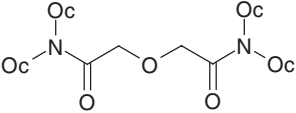
Although more rational (considering the inventory of elements present), the direct and selective extraction of An(III) from PUREX raffinates has been the most challenging of the unresolved research topics radiochemists have addressed for the past 50 years throughout the world. This is why, except for specific single-step processes, such as SETFICS (Nakahara *et al.*, 2007) or DIAMEX-SANEX (Madic *et al.*, 2002) processes which will not be covered by this chapter, most of the strategies adopted to selectively recover trivalent minor actinides from PUREX raffinates show the same two-step process approach:

1. The co-extraction of the An(III) together with the Ln(III) in a front-head process, such as the TRUEX, DIAMEX, or TODGA processes, which make use of oxygen donor extractants ('hard' bases), such as carbamoyl phosphonate/phosphine oxide or diamide compounds, and specific scrubbings with hydrophilic masking agents to achieve the separation of An(III) and Ln(III) from the rest of the fission products (FP).
2. The partition of An(III) from Ln(III) in a second cycle process, either through the selective stripping of the An(III) thanks to a hydrophilic highly selective ligand, or through the selective extraction of the An(III) thanks to a lipophilic highly selective extractant (both types of compounds bearing 'soft base' electron-donor atoms, the use of which is made possible by the lower acidity of the feeds coming from the front-head processes than that of the PUREX raffinates).

Co-extraction of Ln(III) and An(III) from PUREX raffinates by diamides

In France and in Europe, the bidentate oxygen-donor solvation extractants that were investigated in the 1990s to co-extract An(III) and Ln(III) were the *N,N,N′,N′*-tetraalkyl-malonamides (Gasparini and Grossi, 1980, 1986, Musikas, 1987, 1988, Thiollet and Musikas, 1989, Cuillerdier *et al.*, 1991, 1993, Nigond *et al.*, 1994a,b, 1995, Madic and Hudson, 1998): *RR′N(C=O)–CHR″–(C=O)NRR′*, a subgroup of the diamide family bearing a methylene bridge linking the two amide functions (*R*, *R′*, and *R″* representing linear or branched alkyl or phenyl substituents). Malonamides enable the formation of energetically stabilized 6-membered ring complexes when they extract trivalent metallic cations.

Malonamides were designed to compete with carbamoyl-phosphine oxide compounds, such as CMPO (Fig. 11.8), developed in the 1980s at the *Argonne National Laboratory* (ANL, USA) to decontaminate transuranic waste (Navratil and Thomson, 1979, Horwitz *et al.*, 1981, 1982) arising from the production of military grade plutonium. Although of lower efficiency than CMPO when extracting An(III) from nitric acid solutions, lipophilic

n-Octyl-phenyl-N,N'-di(iso)butyl-Carbamoyl-Methyl Phosphine Oxide (CMPO) used in the TRUEX process	N,N'-DiMethyl-N,N'-DiButyl-TetraDecyl-MalonAmide (DMDBTDMA) used in the DIAMEX process
N,N'-DiMethyl-N,N'-DiOctyl-HexylEthoxy-MalonAmide (DMDOHEMA) used in the DIAMEX process	N,N,N',N'-TetraOctyl-3-oxapentaneDiAmide (TODGA)

11.8 Examples of oxygen donor compounds that could be used to co-extract An(III) and Ln(III) from PUREX raffinates.

malonamides (containing a suitable number of carbon atoms) present several advantages over CMPO:

- Malonamides are soluble in hydrogenated tetrapropene: concentrations exceeding 1 mol.L^{-1} can be dissolved in HTP. Therefore, malonamides do not require any phase modifier to cope with the relatively high solvent loading capacities required by PUREX raffinates.
- As malonamides present steeper nitric acid dependence than CMPO, the stripping of extracted elements is facilitated.
- Malonamides are less stable than equivalent neutral organophosphorus compounds, especially versus acidic hydrolysis, but their carboxylic degradation products are less detrimental to the back-extraction of the minor actinides in diluted nitric acid.
- As they are made of carbon, hydrogen, oxygen, and nitrogen atoms, malonamides generate only mineral ashes after incineration.

The affinity of malonamides toward An(III) and Ln(III) decreases as the atomic number of the extracted element increases. The stoichiometry of the extracted complexed M(III) cation is assumed to be ML$_2$(NO$_3$)$_3$ (where L = malonamide) at saturation, although higher stoichiometries have been observed owing to malonamide aggregation. The use of small angle neutron/X-ray scattering techniques and the application of colloidal concepts to malonamide solvents actually proved that these compounds self-organize in small aggregates (Fig. 11.9), consisting of spherical polar cores, mainly
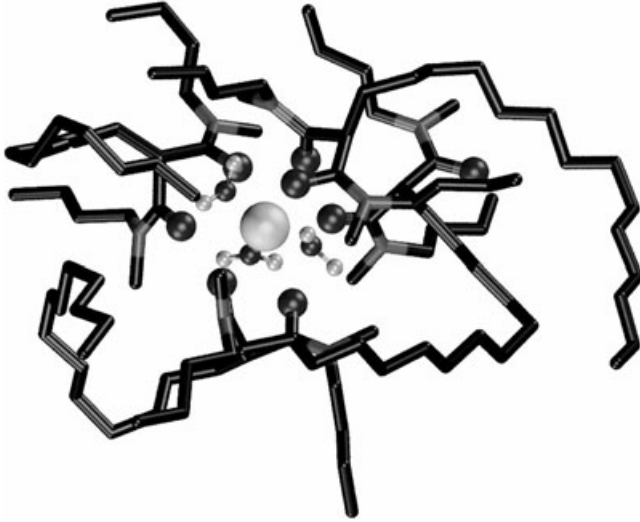
11.9 Schematic representation of malonamide aggregates.

composed of the polar heads of 4 to 10 malonamide molecules and of the extracted solutes ($0.5 \leq \phi_{core} \leq 1.2$ nm), surrounded by non polar crowns, mainly composed of the alkyl chains of the malonamides and of the diluent (Abecassis *et al.*, 2003, Bauduin *et al.*, 2007, Dozol and Berthon, 2007).

It must be remembered, though, that aggregation can easily become detrimental to process implementation, because the polar core attractions can induce the splitting of the loaded solvent into two phases: an enriched one in metallic complexes and another, lighter (called 'third phase'), usually composed of almost pure diluent. The stability of an organic phase containing aggregates depends on the equilibrium between the different interactions: (i) the attractive van der Waals forces taking place between the aggregate polar cores, (ii) the repulsive forces between the polar cores (assimilated as hard, sticky balls in the Baxter model), and (iii) the repulsive forces between the aggregates, due to the stabilizing repulsive steric interactions between the hydrophobic alkyl chains of the extractant and those of the diluent.

Due to the amphiphilic nature of the malonamides, the corresponding solvents behave like reverse micro-emulsions stabilized by surface active compounds. The attractive forces depend on the composition of the polar cores: they increase with the concentration of the extracted solute and depend on its nature. The aggregate repulsive forces depend on the length of the alkyl chains of both the malonamide extractant and the diluent molecules, which act in opposite manner: long alkyl chains for the malonamide and short alkyl chains for the diluent prevent third phase formation, which

will occur as soon as the attractive forces between the aggregates exceed their repulsive forces (Berthon *et al.*, 2007).

Development of the DIAMEX process

The structure of the DIAMEX process reference extractant has evolved between 1991 and 2001, from N,N′-DiMethyl-N,N′-DiButyl-TetraDecyl-MalonAmide (DMDBTDMA, Fig. 11.8, Musikas *et al.*, 1991) to N,N′-DiMethyl-N,N′-Octyl-HexylEthoxy-MalonAmide (DMDOHEMA, Fig. 11.8, Madic *et al.*, 2002), in order to:

- increase the total number of carbon atoms, to enhance both the hydrophobicity of the extractant and the solubility of the extracted metallic complexes in HTP, and hence prevent third phase formation;
- improve the extractant affinity toward trivalent metallic cations, by introducing an ethoxy moiety in the alkyl chain grafted onto the methylene bridge (Spjuth *et al.*, 2000);
- uniformly display the carbon atoms among the alkyl chains grafted onto the malonamide to simplify the elimination of its degradation compounds coming from acidic hydrolysis and radiolysis (Berthon *et al.*, 2001): basic washings of the degraded solvent have proved to be efficient in getting rid of the hydrophilic acidic degradation compounds.

The DMDOHEMA flowsheet was directly adapted from that of DMDBTDMA thanks to the PAREX process simulator code, developed at the CEA. Several counter-current tests have been carried out from 1999 to 2005, both at the CEA Marcoule (France), at Forschungszentrum Jülich (FZJ, Germany), and at the Institute for Transuranium Elements (ITU, Karlsruhe, Germany) during successive collaborative projects funded by EURATOM (Courson *et al.*, 2000, Madic *et al.*, 2000, 2002, 2004, Christiansen *et al.*, 2004, Warin, 2007). These tests put into operation:

- surrogate, spiked, or genuine PUREX raffinates, as well as well as PUREX concentrates (Serrano-Purroy *et al.*, 2005a,b, Modolo *et al.*, 2007a), as the feeds;
- DMDOHEMA dissolved at 0.65 M in HTP, as the solvent;
- mixer-settlers, centrifugal extractors, rotating 'Couette-Taylor' effect columns, and pulsed columns, as the laboratory scale contactors.

Oxalic acid and *N*-(2-hydroxyethyl)ethylenediamine-*N,N′,N′*-triacetic acid (HEDTA) were added to the feeds and the scrubbing solutions to limit the extraction of Mo and Zr on the one hand, and Pd on the other. The DIAMEX flowsheet tested in 2005 at the CEA Marcoule (France) on a genuine PUREX raffinate (31 litres, from the reprocessing of 15 kg of a 52 GWd/t UOX type spent nuclear fuel: 6.5 years of cooling), in three
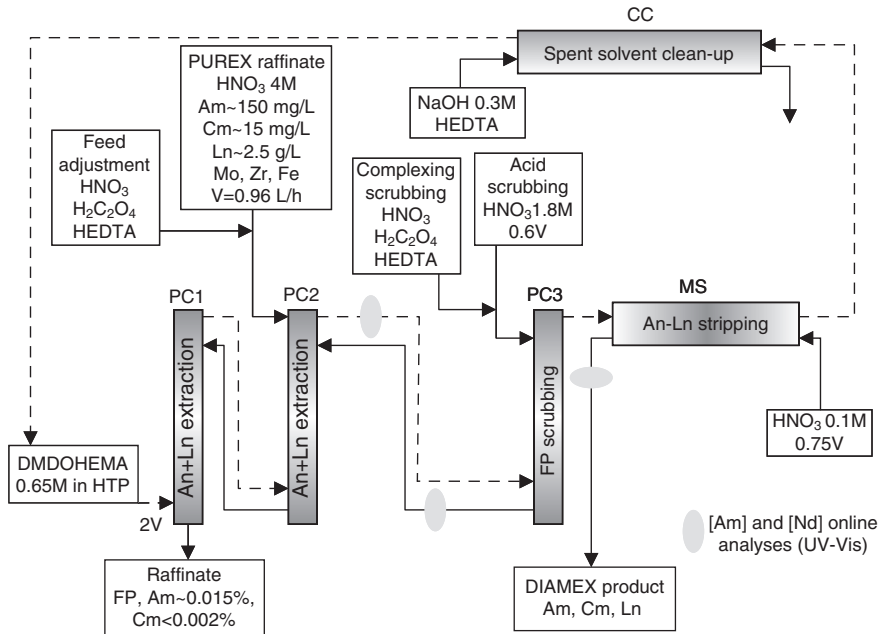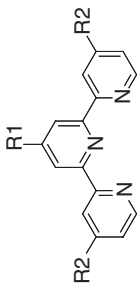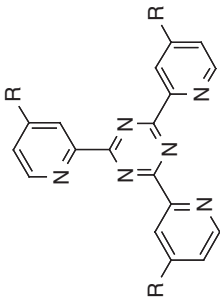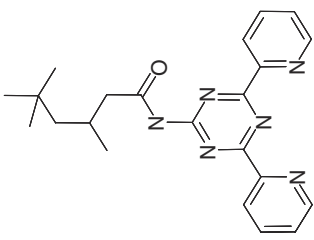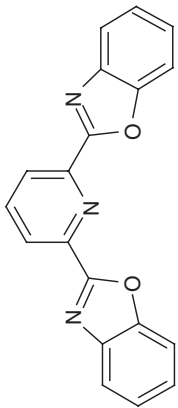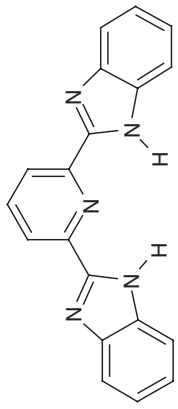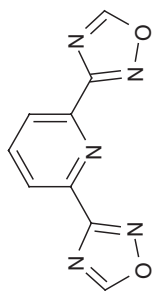
11.10 DIAMEX process flowsheet tested at the CEA Marcoule (France) in 2005 with DMDOHEMA (Warin, 2007).

pulsed columns (two for the extraction of An(III) and Ln(III), and one for FP scrubbing), eight mixer-settlers (for the stripping of An(III) and Ln(III)), and four centrifuges (for the spent solvent clean-up) is shown in Fig. 11.10 (Warin, 2007). This test, as well as a long-term hydrolysis/radiolysis endurance test, in which the DMDOHEMA solvent was recycled after specific caustic washings to eliminate its acidic degradation compounds (such as carboxylic acids and acid-amide), validated the industrial applicability of the DIAMEX process by demonstrating the possible recovery of more than 99.9% of An(III) and Ln(III) from a genuine highly active PUREX raffinate, with high decontamination factors, DF, toward fission products (e.g., $DF_{Zr} \sim 800$).

Separation of trivalent 5f elements from 4f elements by nitrogen ligands

The first nitrogen based systems investigated in France and in Europe to selectively extract An(III) from nitric acid solutions consisted of synergistic binary mixtures of tridentate polyazine ligands and organophilic acids. They played the role of cation exchangers by extracting the cationic complexes formed between the An(III) and the tridentate polyazine ligands, through proton exchange. As illustrated in Fig. 11.11 and more deeply detailed in

Terpyridines (terpy)	TriPyridyl-TriaZines(TPTZ)	2-amino-4,6-di-(pyridine-2-yl)-1,3,5-triazines (ADPTZ)

R_1= -H, -C_nH_{2n+1}, -φ-C_nH_{2n+1} , R_2= -H, -C_nH_{2n+1}
R-Terpyridines (R-Tpy)

R = -H, -Me, -^tBu
R-Tripyridyltriazines (R-TPTZ)

(TMHADPTZ)
R-AminoDiPyridylTriazines

2,6-bis-(benzoxazolyl)-4-pyridine	2,6-bis-(benzimidazolyl)-4-pyridine	2,6-dioxadiazolypyridine

11.11 Examples of nitrogen-donor ligands used in synergistic mixtures with cation exchangers.

the comprehensive reviews of Kolarik (2008) and Ekberg *et al.* (2008), the tridentate polyazine ligands studied belonged to the families of the:

- terpyridines (Drew *et al.*, 2000a);
- monopyridyl-1,2,4-triazines (Hudson *et al.*, 2003a) and dipyridyl-1,2,4-triazines (Boubals *et al.*, 2002, Hudson *et al.*, 2003a,b, Drew *et al.*, 2006);
- dipyridyl-1,3,5-triazines (Drew *et al.*, 2000b) and tripyridyl-1,3,5-triazines (Chan *et al.*, 1996, Cordier *et al.*, 1998, Hagström *et al.*, 1999);
- dioxa-/benzoxa-/binzimida-/zol-pyridines (Kolarik and Müllich, 1997, Andersson *et al.*, 2003, Weigl *et al.*, 2003, Drew *et al.*, 2004b);
- amino-dipyridyl-1,3,5-triazines (ADPTZ).

These tridentate nitrogen-donor ligands all provided moderate selectivity of complexation toward An(III), with selectivity factors versus Ln(III), $SF_{An/Ln}$, ranging from 5 to 20 at most, as demonstrated by Miguirditchian *et al.* (2005, 2006), who investigated the thermodynamics of M(III):ADPTZ complex formation (M = An or Ln) and pointed out the more exothermic complexation reactions of An(III) than Ln(III), thus highlighting the assumed greater covalent character of the N-An(III) bonds, which is supported by quantum chemistry calculations. The X-ray crystal structures of metal:terpyridine solvates resolved by Berthet *et al.* (2002a) also revealed that the U-N(central pyridine) distances are shorter than the U-N(distal pyridines) distances, while the reverse is true for lanthanide compounds. It has been suggested that these differences reflect the presence of a π back-bonding interaction between U and terpyridine.

Unfortunately, the use of carboxylic acids (e.g., octanoic or alpha-bromo-capric acids) and even dinonylnaphthalene-sulphonic acid (HDDNS), as sources of lipophilic anions in synergistic mixtures, was of little help in discriminating between An(III) and Ln(III) from aqueous feeds whose acidity exceeded 0.1 mol.L^{-1}, as is the case for DIAMEX An(III)-product solutions. Therefore, the only two reported counter-current tests implemented in laboratory-scale mixer-settlers used surrogate spiked feeds of low acidity. The first one was carried out by Vitart *et al.* in 1986 and made use of the synergistic mixture composed of TPTZ (Fig. 11.11, R = –H) and HDNNS, dissolved in carbon tetrachloride. The second one was carried out in 2000 with the binary mixture composed of 2-(3,5,5-trimethylhexanoyl-amino)-4,6-di(pyridin-2-yl)-1,3,5-triazine (TMHADPTZ, Fig. 11.11) and octanoic acid (Madic *et al.*, 2002). Although the experimental profiles were in good agreement with the calculated flowsheet, the latter system has not been further developed because of its high sensitivity to pH variations and the necessity to buffer the feed acidity (pH > 3).
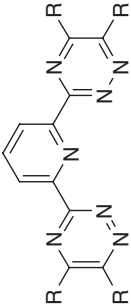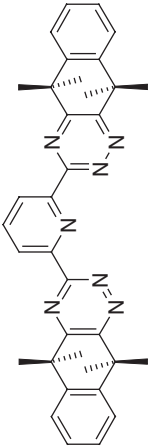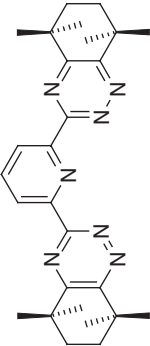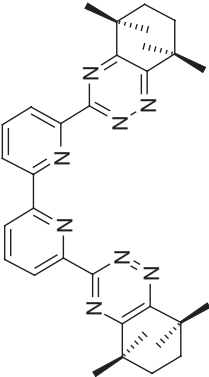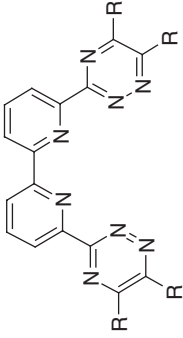
Within the NEWPART collaborative project (Madic *et al.*, 2000), the discovery of the bis-(1,2,4-triazinyl)-pyridines (BTP) synthesized by Zdenek Kolarik appeared as a real breakthrough in the design of nitrogen-donor

extractants selective toward An(III). Surprisingly, BTP ligands firstly precipitated when combined with organophilic carboxylic acids (Kolarik *et al.*, 1999a). Even more unexpectedly, these tridentate compounds, consisting of two dialkylated 1,2,4-triazines attached sideways to a central pyridine (Fig. 11.12), proved to extract Am(III) from acidic aqueous solutions ([HNO_3] > 1 mol.L^{-1}) when dissolved in polar diluents, such as mixtures of HTP and alcohols. Furthermore, their selectivity was shown to be amazingly high as compared to any of the aforementioned nitrogen-donor ligands: $SF_{Am/Eu}$ > 100 (Kolarik *et al.*, 1999b).

Various BTP ligands have been further synthesized in the framework of NEWPART and PARTNEW collaborative projects (Madic *et al.*, 2000, 2004). The parametric and thermodynamic studies carried out on these molecules revealed that the nature (e.g., normal or branched alkyl chains, aromatic rings) and the length, as well as the position of the substituting groups, not only influence the complexing and extracting properties of BTP compounds (An(III)/Ln(III) selectivity and kinetics of extraction), but also their chemical stability (Iveson *et al.*, 2001, Colette *et al.,* 2002, Hill *et al.,* 2002, Hudson *et al.,* 2003a, Weigl *et al.*, 2006).

Several reasons could explain the peculiarity of BTP's extracting behaviour:

- The unsymmetrical positions of the nitrogen atoms within the lateral triazine rings, which give these compounds low and great affinities respectively for protons and An(III) (Petit *et al.,* 2006). As opposed to bis-(1,2,4-triazinyl)-pyridines, symmetrical bis(1,3,5-triazinyl)-pyridines present bad extraction properties (Drew *et al.,* 2004c).
- The M:L$_3$ (metal:ligand) stoichiometry of the extracted complexes pointed out by different structural studies (Fig. 11.13, Drew *et al.*, 2001a,b, Berthet *et al*. 2002b, Colette *et al.,* 2003), which results in the fully saturated inner coordination spheres of the extracted trivalent *f* cations, wrapped by three triply bonded BTP ligands, hence leaving no spare space for extra water or nitrate coordinating molecules (Colette *et al.,* 2004, Deneke *et al.,* 2005, 2007).
- The chemical reactivity of the carbon atoms located on the α-positions of the alkyl groups grafted onto the lateral triazines. Nitrous acid and oxygen tend to oxidize non fully substituted carbon atoms, leading to hydrophilic alcohol and ketone derivates, which degenerate the intrinsic extraction properties of BTP ligands, as experienced during the demonstration hot tests carried out with 2,6-bis-(5,6-di-*n*-propyl-1,2,4-triazine-3-yl)-pyridine (*n*Pr-BTP, dissolved at 0.04 mol.L^{-1} in a mixture of HTP and *n*-octanol (70/30 vol.%)) on genuine DIAMEX An(III)-product solutions, both at the CEA Marcoule (France) and the ITU (Karlsruhe, Germany) in 1999.

2,6-Bis-(5,6-dialkyl-1,2,4-Triazin-3-yl)-Pyridines (BTP)

Bis-Annulated-Triazine-Pyridine (BATP): CyMe₄-BTP

Bis-Annulated-Triazine-Pyridine (BATP): φCyMe₄-BTP

6,6'-bis(5,6-dialkyl-[1,2,4]-triazin-3-yl)-[2.2']-bipyridines (BTBP)

Bis-Annulated-Triazine-Bis-Pyridine (BATBP): CyMe₄-BTBP

11.12 Polypyridine-triazine extractants developed for An(III)/Ln(III) separation.
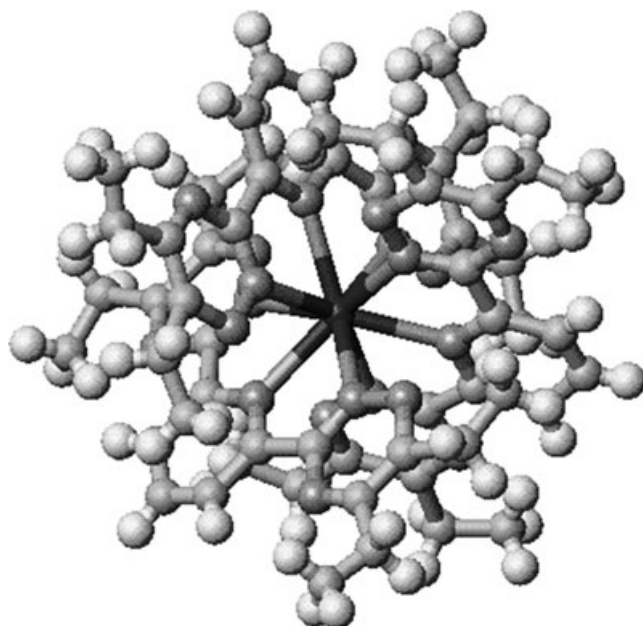
11.13 X-Ray diffraction pattern of a Gd(III) tris-complex with Et-BTP.

• The longer and bulkier are the alkyl chains grafted onto the lateral triazines of the BTP compounds, the slower are their kinetics of mass transfer, probably due to adsorption difficulties at the interface (BTP molecules are not assumed to aggregate). Therefore, the formulation of BTP based solvents most often requires the addition of a mass transfer catalyst (such as a diamide) to aid phase transfer and thus enhance kinetics of extraction and stripping (Hill *et al.*, 2002). However, this additive tends to decrease the selectivity of the BTP toward An(III).

Development of the SANEX[4]-BTP process

The chemical stability of the BTP ligands was improved by branching the alkyl groups grafted onto the lateral triazines. 2,6-bis-(5,6-di-*iso*-propyl-1,2,4-triazine-3-yl)-pyridine (*i*Pr-BTP) successfully passed a once-through hot test performed at the CEA Marcoule (France) in 2001 (Fig. 11.14, Madic *et al.*, 2002). Here, more than 99.9% of Am(III) and more than 99.8% of Cm(III) were recovered from a genuine DIAMEX An(III)-product solu-

[4] SANEX, for Separation of ActiNides by EXtraction. The objectives of the SANEX process are to recover more than 99.9% of the An(III) in a purified product stream containing less than 5 wt.% of Ln(III).
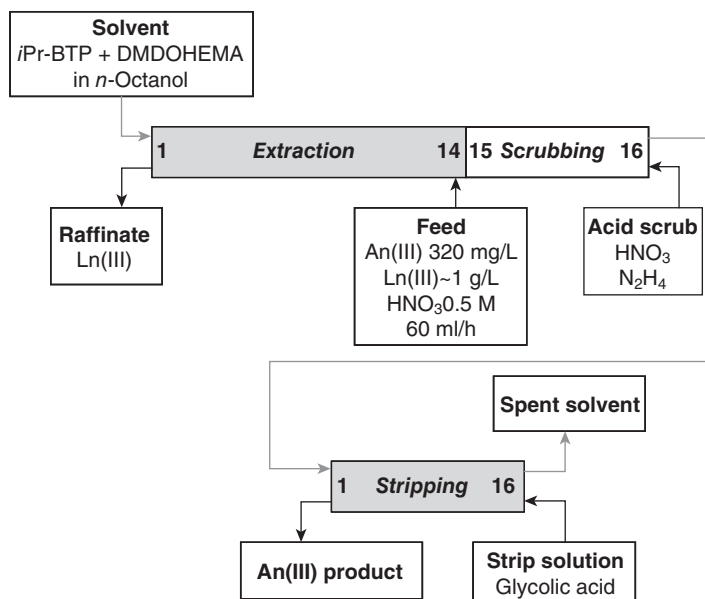
11.14 SANEX-*i*Pr-BTP process flowsheet tested at the CEA Marcoule (France) on a genuine 'An(III)+Ln(III)' DIAMEX product (Madic *et al.*, 2002).

tion, with less than 2.5 wt.% contamination of Ln(III), by implementing in laboratory scale centrifugal contactors a solvent consisting of *i*Pr-BTP dissolved at 0.01 mol.L^{-1} in *n*-octanol, with 0.5 mol.L^{-1} of DMDOHEMA added to increase the mass transfer kinetics. However, the solvent failed when recycled without treatment: *i*Pr-BTP degraded because of alpha/gamma radiolysis and its extraction performances decreased by 40% after two recycles (Hill *et al.*, 2002). This detrimental observation definitively dumped the BTP ligands as potential extractants for the SANEX process development in France.

Attempts to fully substitute the labile α-benzylic hydrogens of the BTP lateral triazines, by synthesizing, for instance, the *tertio*-butyl derivate, have all failed so far. However, Hudson *et al.* (2006) managed to synthesize bis-annulated-triazine-pyridines (BATP, Fig. 11.12), with methyl groups in place of α-benzylic hydrogens. As a result, these compounds present much higher chemical stabilities than alkyl-BTP molecules. Because they possess more carbon atoms in their structures than alkyl-BTP molecules, BATP ligands are also assumed to be more lipophilic than alkyl-BTP compounds, and hence to show higher extraction properties, which is actually the case for 2,6-bis(5,5,8,8-tetramethyl-5,6,7,8-tetrahydrobenzo[1,2,4]triazin-3-yl) pyridine (CyMe$_4$-BTP). Amazingly, the selectivity observed for CyMe$_4$-BTP is

also ten times higher than that of *i*Pr-BTP in the same experimental conditions ($SF_{Am/Eu} > 1500$ at $[HNO_3] = 1$ mol.L^{-1}), and the highest ever reported for a nitrogen-donor ligand. This is probably due to the tris-complex formation, in which the extracted metallic cation is completely dehydrated and the three bulky $CyMe_4$-BTP molecules become so rigid that the complex formed is energetically extremely stable.

In fact, the example of $CyMe_4$-BTP demonstrates that radiochemists' search for ever more efficient and selective extractants could well become detrimental to process development: the drawback of $CyMe_4$-BTP is the almost irreversible extraction of An(III) that makes this compound inapplicable to counter-current test implementation.

11.5   Future trends

11.5.1 Caesium separation

Caesium process development studies stopped in France and Europe after the demonstration tests performed at the CEA Marcoule (France) on a genuine acidic DIAMEX raffinate (see pages 329–330). However, research continued at Oak-Ridge National Laboratory in the USA in order to develop a process (known as the Caustic Side Solvent Extraction process: CSSX) for removing caesium from the Savannah River tanks containing alkaline high level defence waste. The optimized solvent is composed of calix[4]arene-bis-(*tert*-octylbenzo-crown-6) (Fig. 11.5: BOBCalixC6), 1-(2,2,3,3-tetrafluoropropoxy)-3-(4-*sec*-butylphenoxy)-2-propanol used as a phase modifier, tri-*n*-octylamine added to ease caesium stripping, and Isopar L as the diluent (Bonnesen *et al.*, 2000, 2003, Leonard *et al.*, 2001, 2003, White *et al.*, 2003, Delmau *et al.*, 2006). The implementation of the CSSX process in a 33-stage apparatus (2-cm contactors) at the Savannah River National Laboratory was successful: caesium was recovered from both simulated and genuine composite waste of Savannah River Tank n°37H/44F with decontamination factors exceeding 2×10^6 (Norato *et al.*, 2003). The CSSX process is therefore intended to be implemented in the Modular Caustic-Side Solvent Extraction Unit built at the Savannah River Site (Delmau *et al.*, 2009).

11.5.2 Co-extraction of An(III) and Ln(III)

New tridentate diamide extractants – diglycolamides, whose amidic functions are linked by an oxypentyl bridge (Fig. 11.8) – were designed by Tachimori *et al.* at the end of the 1990s to compete with the bidentate malonamides studied in Europe (Tachimori *et al.*, 2002, Sasaki and Tachimori, 2002, Sasaki *et al.*, 2001, 2007a,b, Sugo *et al.*, 2002). As the

N,N,N′,N′-tetraoctyl-3-oxapentanediamide (TODGA) presented a high extraction efficiency toward An(III), it was thoroughly investigated in the frame of the successive collaborative projects PARTNEW (Madic *et al.*, 2004) and EUROPART, as a potential substitute for DMDOHEMA in the DIAMEX process. The solvent formulation (i.e., TODGA and TBP, respectively dissolved at 0.2 and 0.5 mol.L^{-1} in HTP) was optimized to compensate for the low loading capacity of TODGA (Modolo *et al.*, 2007b). Several countercurrent spiked and hot tests were carried out in centrifugal contactors at the FZJ (Jülich, Germany, Modolo *et al.*, 2008) and the ITU (Karlsruhe, Germany, Magnusson *et al.*, 2009a). They confirmed the potentiality of the TODGA solvent to reprocess genuine PUREX raffinates by enabling the recovery of more than 99.99% of the An(III) and the Ln(III), with very high feed decontamination factors (DF ~ 40 000 for Am and Cm), provided strontium extraction is hindered by oxalic acid scrubbings (Magnusson *et al.*, 2009b). Unfortunately, these scrubbing streams increase the volume of liquid waste generated (Fig. 11.15).
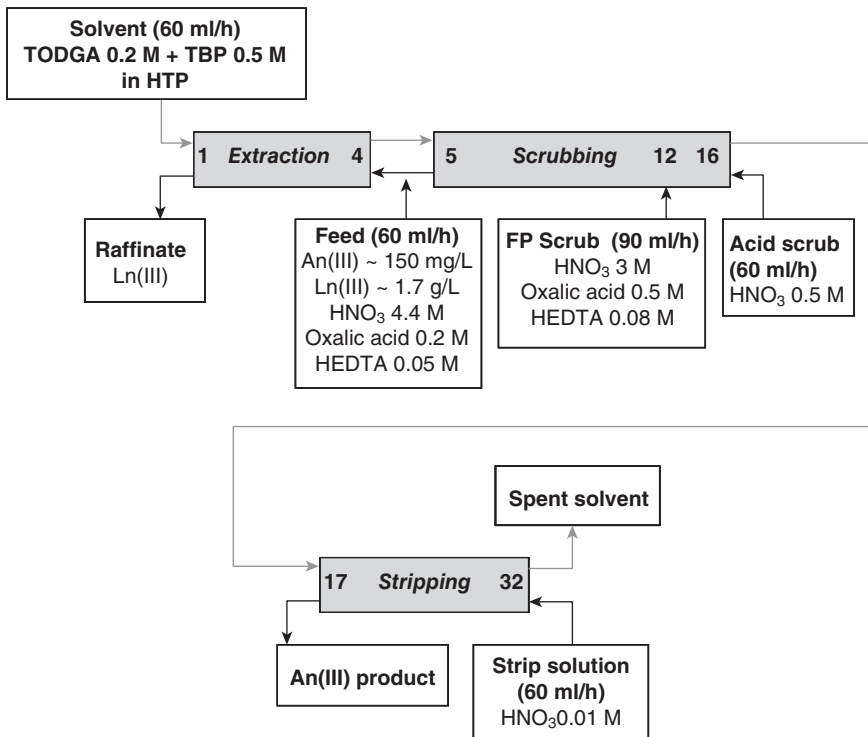
11.15 TODGA process flowsheet tested at the ITU (FZK, Germany) on a genuine PUREX raffinate (Magnusson *et al.*, 2009b).

11.5.3 Separation of An(III) from Ln(III)

Within the EUROPART collaborative project, a new class of N-donor polyazines was designed and synthesized to better conform to the requirements of the SANEX process development: the bis-triazinyl-bipyridines (BTBPs, Fig. 11.12, Foreman *et al.*, 2005, 2006). The extraction properties of these tetradentate ligands were investigated and they appeared to differ from those of BTP ligands, in that $M:L_2$ complexes were identified instead of $M:L_3$ complexes (Drew *et al.*, 2005, Nilsson *et al.*, 2006a,b, Retegan *et al.*, 2007a,b). The selectivity of alkyl-BTBP ligands toward An(III) and their kinetics of extraction are similar to those of alkyl-BTP ligands: the bulkier the alkyl groups are, the slower the mass transfer is, thus requiring a phase transfer catalyst, such as a diamide (Geist *et al.*, 2006).

In the particular case of the bis-annulated-triazine-bipyridines, CyMe$_4$-BTBP appeared less selective toward An(III) (SF$_{Am/Eu}$ > 100) than CyMe$_4$-BTP (SF$_{Am/Eu}$ > 1000), certainly due to the formation of $M:L_2$ complexes as opposed to the rigidified $M:L_3$ complexes observed with CyMe$_4$-BTP. In the $M:L_2$ complexes, two tetradentate CyMe$_4$-BTBP molecules coordinate with the extracted trivalent *f* cations, hence leaving an additional free access to their inner coordination spheres for an extra ligand (water molecule?). This difference in the mass action law of complex formation is somehow beneficial for the development of partitioning processes based on CyMe$_4$-BTBP, in that the impact of the solvent hydrolytic/radiolytic degradation on the extraction performances is reduced: the apparent decrease of extraction efficiency, resulting from the destruction of the extractant, will be smaller for CyMe$_4$-BTBP than for CyMe$_4$-BTP (because $D_M \propto$ [CyMe$_4$-BTBP]^2).

The formulation of the CyMe$_4$-BTBP solvent was optimized, based on the *i*Pr-BTP solvent formulation (i.e., CyMe$_4$-BTBP and DMDOHEMA, respectively dissolved at 0.015 and 0.25 mol.L^{-1} in *n*-octanol), in order to elaborate a SANEX partitioning flowsheet (Geist *et al.*, 2006). Although slow, the kinetics of extraction and stripping allowed a counter-current hot test to be performed in laboratory centrifuges at the ITU (Karlsruhe, Germany), implementing the highly active 'An(III)+Ln(III)' product coming from the TODGA hot test (see Fig. 11.15). Excellent feed decontamination factors for Am (7000) and Cm (1000) were obtained and the recoveries of these elements were higher than 99.9%. More than 99.9% of the lanthanides were directed to the raffinate except Gd for which 0.32% was recovered in the product (Fig. 11.16, Magnusson *et al.*, 2009c). Nevertheless, the radiolytic stability of CyMe$_4$-BTBP is still weaker than those of TBP, CMPO or diamides, and the possibility of recycling CyMe$_4$-BTBP solvents has not been demonstrated yet.
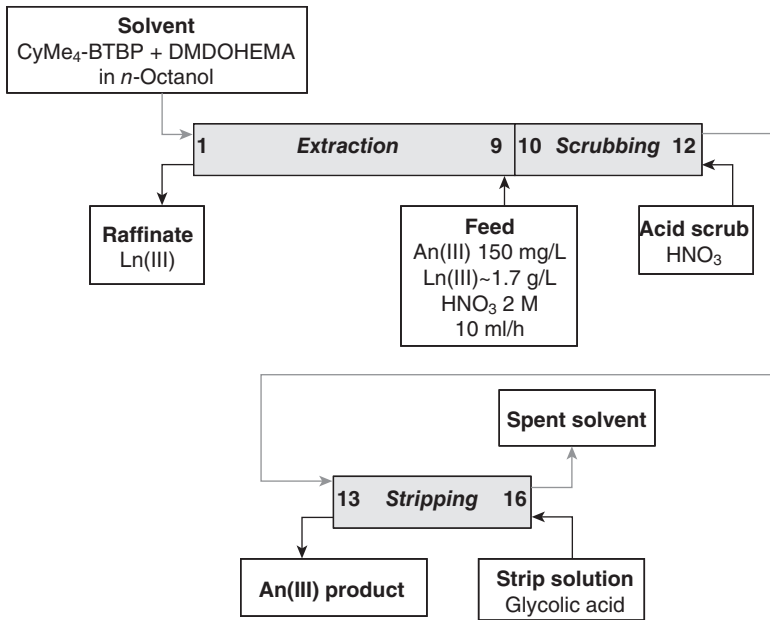
11.16 SANEX-BTBP process flowsheet tested at the ITU (FZK, Germany) on a genuine 'An(III)+Ln(III)' TODGA product (Magnusson *et al.*, 2009c).

11.6   Conclusions

In order to ensure the closure of future nuclear fuel cycles and minimize the long-term radiotoxicity of discarded nuclear waste, the separation of all the valuable and/or hazardous radionuclides, such as long-lived fission products and minor actinides contained in the spent nuclear fuels will undeniably be necessary. The recycling of the minor actinides will probably be managed by applying a partitioning and transmutation policy. Furthermore, separating out the hazardous unrecyclable radionuclides will simplify their future route. The attractiveness of hydrometallurgical partitioning processes to treat spent nuclear fuels or nuclear waste continuously, with high recovery and purification yields but only low energy inputs, largely benefits from the successes of industrial implementations such as the PUREX process.

However, the development of an efficient partitioning process is based on the design of a highly selective hydrophilic ligand or lipophilic extractant, that must fulfil specific requirements of solvent extraction chemistry, such as: a high affinity and selectivity toward the target element(s) to be separated, fast mass transfer kinetics, high chemical resistance, etc.

Thousands of creative ideas have emerged from radiochemists' imaginations, but very few compounds have been developed up to optimized solvent formulations and tested on genuine spent fuel dissolver solutions.

Calix[4]arenes-crown-6 are pleasing examples of macrocyclic extractants, designed by functionalizing a calix[4]arene platform with a crown ether: they are perfectly suited for the selective extraction of caesium from acidic as well as basic nuclear waste. Bis-triazinyl-(bi)pyridines, although not very stable chemically, are another good example of linear nitrogen-donor ligands that are highly selective toward An(III), thanks to their particular mode of polydentate complexation. There are, however, single-step processes currently in developement throughout the world that allow the separation of trivalent minor actinides directly from PUREX raffinates. They are based on the selective stripping of An(III) by hydrophilic ligands, such polyaminocarboxylic acids, in buffered solutions.

11.7   Sources of further information and advice

The readers will find more information in the following books and reviews:

- For solvent extraction: Marcus and Kertes (1969), Sekine and Hasegawa (1977), Rydberg *et al*. (2004), and Danesi (2004);
- For caesium separation: Vicens and Böhmer (1991), Gutsche (1989, 1998), Ungaro and Pochini (1991), Dozol *et al*. (2000b), Creaven *et al*. (2008), and Dozol and Ludvig (2009).
- For An(III) separation: Weaver (1974), Nash (1993, 1994, 1999), Morss (1994), Choppin and Nash (1995), Nash and Choppin (1997), Mathur *et al*. (2001), Nash *et al*. (2006), and Edelmann (2006).

11.8   Acknowledgment

11.9   References

Abecassis B, Testard F, Zemb T, Berthon L, Madic C (2003), 'Effect of n-octanol on the structure at the supramolecular scale of concentrated dimethyl dioctyl ethoxy malonamide extractant solutions', *Langmuir*, 19, 6638–6644.
Allain F, Virelizier H, Moulin C, Jankowski C K, Dozol J F, Tabet J C (2000), 'Electrospray-mass spectrometric studies of selectivity of alkali metal cations extraction by calix[4]arene crowns', *Spectroscopy*, 14, 127–139.
Andersson S, Ekberg C, Foreman M R S, Hudson M J, Liljenzin J O, Nilsson M, Skarnemark G, Saphiu K (2003), 'Extraction behavior of the synergistic system

2,6-bis-(benzoxazolyl)-4-dodecyloxylpyridine and 2-bromodecanoic acid using Am and Eu as radioactive tracers', *Solv Extr Ion Exch*, 21(5), 621–636.

Antonio M R, Chiarizia R, Gannaz B, Berthon L, Zorz N, Hill C, Cote G (2008), 'Aggregation in solvent extraction systems containing a malonamide, a dialkyl-phosphoric acid, and their mixtures', *Sep Sc Technol*, 43(9–10), 2572–2605.

Arduini A, Ghidini E, Pochini A, Ungaro R, Andreetti G D, Calestani G, Ugozzoli F (1988), 'p-t-Butylcalix[4]arene tetra-acetamide: a new strong receptor for alkali cations [1]', *J Inc Phenom*, 6(2), 119–134.

Arnaud-Neu F, Collins E M, Deasy M, Ferguson G, Harris S J, Kaitner B, Lough A J, Mc Kervey M A, Marques E, Ruhl B L, Schwing-Weill M J, Seward E M (1989), 'Synthesis, X-ray crystal structures, and cation-binding properties of alkyl calix-aryl esters and ketones, a new family of macrocyclic molecular receptors', *J Am Chem Soc*, 111(23), 8681–8691.

Arnaud-Neu F, Schwing-Weil M J, Ziat K, Cremin S, Harris S J, Mc Kervey M A (1991), 'Selective alkali and alkaline earth cation complexation by calixarene amides', *New J Chem*, 15, 33–37.

Arnaud-Neu F, Barrett G, Fanni S, Marrs D, Mc Gregor W, Mc Kervey M A, Schwing-Weill M J, Vetrogon V, Wechsler S (1995), 'Extraction and solution ther-modynamics of complexation of alkali and alkaline earth cations by calix[4]arene amides', *J Chem Soc Perkin Trans*, II, 453–461.

Arnaud-Neu F, Asfari Z, Soley B, Vicens J (1996), 'Binding properties of calix[4]-bis-crowns towards alkali cations', *New J Chem*, 20, 453–463.

Asfari Z, Pappalardo S, Vicens J (1992) 'New preorganized calix[4]arenes. Part I. A doubly crowned calix and a double-calix crown derived from 4,6,10,12,16,18, 22,24,25,26,27,28-dodecamethyl-5,11,17,23-tetrahydroxycalix[4]arene', *J Inclus Phenom Mol Recog Chem*, 14, 189–192.

Asfari Z, Bressot C, Vicens J, Hill C, Dozol J F, Rouquette H, Eymard S, Lamare V, Tournois B (1995), 'Doubly crowned calix[4]arenes in the 1,3-alternate conforma-tion as cesium-selective carriers in supported liquid membranes', *Anal Chem*, 67(18), 3133–3139.

Asfari Z, Thuery P, Nierlich M, Vicens J (1999), 'Unsymmetrical calix[4]-bis-crowns-6 with unequivalent crown loops', *Tetrahedron Lett*, 40, 499–502.

Baaden M, Berny F, Madic C, Schurhammer R, Wipff G (2003), 'Theoretical studies on Lanthanide cation extraction by picolinamides: ligand-cation interactions and interfacial behaviour', *Solv Extr Ion Exch*, 21(2), 199–219.

Bauduin P, Testard F, Berthon L, Zemb T (2007), 'Relation between the hydrophile/hydrophobe ratio of malonamide extractants and the stability of the organic phase: investigation at high extractant concentrations', *Royal Soc of Chem*, *Phys Chem Chem Phys*, 9(28), 3776–3785.

Beitz J (1994), 'Similarities and differences in trivalent lanthanide- and actinide-ion solution absorption spectra and luminescence studies', *Handbook on the Physics and Chemistry of Rare Earths*, Vol. 18, lanthanides/actinides chemistry, pp. 159–193, Gschneider, Eyring, Choppin, Lander, Elsevier Science B V.

Benedict M, Pigford T H and Levi H W (1981), *Nuclear Chemical Engineering*, pp. 501–514, Mc Graw-Hill, New York.

Berthet J C, Rivière C, Miquel Y, Nierlich M, Madic C, Ephritikhine M (2002a), 'Selective complexation of uranium(III) over cerium(III) and neodymium(III) by 2,2′:6′,2″-terpyridine – X-ray crystallographic evidence for uranium-to-ligand π back-bonding', *European J Inorg Chem*, 1434–1446.

Berthet J C, Miquel Y, Iveson P B, Nierlich M, Thuéry P, Madic C, Ephritikhine M (2002b), 'The affinity and selectivity of terdentate nitrogen ligands toward trivalent lanthanide and uranium ions viewed from the crystal structures of the 1:3 complexes', *J Chem Soc, Dalton Trans*, 16, 3265–3272.

Berthet J C, Nierlich M, Miquel Y, Madic C, Ephritikhine M (2005), 'Selective complexation of uranium(III) over lanthanide(III) triflates by 2,2′:6′,2″-terpyridine. X-Ray crystal structures of [M(OTf)₃(terpy)₂] and [M(OTf)₂(terpy)₂(py)][OTf] (M = Nd, Ce, U) and of polynuclear μ-oxo uranium(IV) complexes resulting from hydrolysis', *J Chem Soc, Dalton Trans*, 2, 369–379.

Berthon L, Morel J M, Zorz N, Nicol C, Virelizier H, Madic C (2001), 'Diamex process for actinide partitioning: hydrolytic and radiolytic degradations of malonamide extractants', *Sep Sci Technol*, 36(5–6), 709–727.

Berthon L, Martinet L, Testard F, Madic C, Zemb T (2007), 'Solvent penetration and sterical stabilization of reverse aggregates based on the DIAMEX process extracting molecules: consequences for the third phase formation', *Solv Extr Ion Exch*, 25(5), 545–576.

Birkett J E, Carrott M J, Fox O D, Jones C J, Maher C J, Roube C V, Taylor R J, Woodhead D A (2005), 'Recent developments in the PUREX process for nuclear fuel reprocessing: complexant based stripping for Uranium/Plutonium separation', *Int J Chem*, 59(12), 898–904.

Bocchi V, Foina D, Pochini A, Ungaro R, Andreetti G D (1982), 'Molecular inclusion in functionalized macrocycles. Part 3. Synthesis, proton and Carbon-13 NMR spectra, and conformational preference of open chain ligands on lipophilic macrocycles', *Tetrahedron*, 38, 373–378.

Boehme C and Wipff G (1999a), 'Dithiophosphinate complexes of trivalent lanthanide cations: consequences of counterions and coordination number for binding energies and selectivity. A theoretical study', *Inorg Chem*, 38(25), 5734–5741.

Boehme C and Wipff G (1999b), 'Thiophosphoryl complexes of trivalent lanthanide cations: importance of counterions and stoichiometry for binding energies. A theoretical study', *J Phys Chem A*, 103(30), 6023–6029.

Bonnesen P V, Delmau L H, Moyer B A, Leonard R A (2000), 'A robust alkaline-side CSEX solvent suitable for removing cesium from Savannah River high level waste' *Solv Extr Ion Exch*, 18(6), 1079–1107.

Bonnesen P V, Delmau L H, Moyer B A, Lumetta G J (2003), 'Development of effective solvent modifiers for the solvent extraction of cesium from alkaline high-level tank waste', *Solv Extr Ion Exch*, 21(2), 141–170.

Boubals N, Drew M G B, Hill C, Hudson M J, Iveson P B, Madic C, Russel M L, Youngs T G A (2002), 'Americium(III) and europium(III) solvent extraction studies of amide-substituted triazine ligands and complexes formed with ytterbium(III)', *J Chem Soc, Dalton Trans*, 1, 55–62.

Brunink J, Haak J, Bomer J, Reinhoudt D, Harris S, Mac Kervey M A (1991), 'Chemically modified field-effect transistors; a sodium ion selective sensor based on calix[4]arene receptor molecules', *Anal Chim Acta*, 254(1–2), 75–80.

Casnati A, Pochini A, Ungaro R, Ugozzoli F, Arnaud F, Fanni S, Schwing M J, Egberink R J M, de Jong F, Reinhoudt D N (1995), 'Synthesis, complexation, and membrane transport studies of 1,3-alternate calix[4]arene-crown-6 conformers: a new class of cesium selective ionophores', *J Am Chem Soc*, 117, 2767–2777.

Casnati A, Pochini A, Ungaro R, Bocchi C, Ugozzoli F, Egberink R J M, Struijk H, Lugtenberg R, de Jong F, Reinhoudt D N (1996), '1,3-Alternate calix[4]

arenecrown-5 conformers: new synthetic ionophores with better K$^+$/Na$^+$ selectivity than valinomycin', *Chem Eur J*, 2, 436–445.

Casnati A, Sansone F, Dozol J F, Rouquette H, Arnaud-Neu F, Byrne D, Fuang-swasdi S, Schwing-Weill M J, Ungaro R (2001), 'New calix[4]arene-monobenzo- and dibenzo-crown-6 as cesium selective ionophores in the radioactive waste treatment: synthesis, complexation and extraction properties' *J Inclusion Phenom, Macrocyclic Chem*, 41, 193–200.

Chan G Y S, Drew M G B, Hudson M J, Isaacs N S, Byers P, Madic C (1996), 'Complexation of 2,4,6-tri-tert-butylpyridine-1,3,5-triazine ligand(L) with the cerium(IV) nitrate anion', *Polyhedron*, 15, 3385–3398.

Chang S K, Cho I (1986), 'New metal cation-selective ionophores derived from calixarenes: their syntheses and ion-binding properties', *J Chem Soc, Perkin Trans I*, 211–214.

Chang S K and Cho I (1987), 'Calixarene-based amide ionophores for group IIA metal cations', *Chem Letters*, 16(5), 947–948.

Chiarizia R, Urban V, Thiyagarajan P, Herlinger A W (1999), 'Aggregation of complexes formed in the extraction of selected metal cations by P,P′-di(2-ethylhexyl)-methanediphosphonic acid', *Solv Extr Ion Exch*, 17(1), 113–132.

Choppin G, Nash K (1995), 'Actinide separation science', *Radiochim Acta*, 70/71, 225–236.

Christiansen B, Apostolidis C, Carlos R, Courson O, Glatz J P, Malmbeck R, Pagliosa G, Römer K, Serrano-Purroy D (2004), 'Advanced aqueous reprocessing in P&T strategies: Process demonstration on genuine fuels and targets', *Radiochim Acta*, 92(8), 475–480.

Colette S, Amekraz B, Madic C, Berthon L, Cote G, Moulin C (2002), 'Use of electrospray mass spectrometry (ESI-MS) for the study of europium(III) complexation with bis(dialkyltriazinyl)pyridines and its implications in the design of new extracting agents', *Inorg Chem*, 41(26), 7031–7041.

Colette S, Amekraz B, Madic C, Berthon L, Cote G, Moulin C (2003), 'Trivalent lanthanide interactions with a terdentate bis(dialkyltriazinyl)pyridine ligand studied by electrospray ionisation mass spectrometry', *Inorg Chem*, 42(7), 2215–2226.

Colette S, Amekraz B, Madic C, Berthon L, Cote G, Moulin C (2004), 'Eu interaction with a polyazaaromatic extractant studied by TRLIF: a thermodynamical approach', *Inorg Chem*, 43(21), 6745–6751.

Cordier P Y, Hill C, Baron P, Madic C, Hudson M J, Liljenzin J O (1998), 'Am (III)/ Eu (III) separation at low pH using synergistic mixtures composed of carboxylic acids and neutral nitrogen polydendate ligands', *J Alloys Comp*, 271–273, 738–741.

Cornforth J, D'arcy Hart P, Nicholls G, Rees R, Stock J (1955), 'Antituberculous effects of certain surface-active polyoxyethylene ethers', *Brit J Pharmacology*, 10, 73–86.

Coupez B, Boehme C, Wipff G (2003), 'Importance of interfacial phenomena and synergistic effects in cation extraction by dithiophosphinic ligands: a molecular dynamics study', *J Phys Chem,* 107(35), 9484–9490.

Courson O, Lebrun M, Malmbeck R, Pagliosa G, Römer K, Sätmark B, Glatz J P (2000), 'Partitioning of minor actinides from HLLW using the DIAMEX process. Part 1 – Demonstration of extraction performances and hydraulic behaviour of the solvent in a continuous process', *Radiochim Acta*, 88(12), 857–863.

Creaven B S, Donlon D F, Mc Ginley J (2008), 'Coordination chemistry of calix[4]
arene derivatives with lower rim functionalisation and their applications', *Coor-
dination Chem Rev*, 253(7–8), 893–962.

Cuillerdier C, Musikas C, Hoel P, Nigond L, Vitart X (1991), 'Malonamides as new
extractants for nuclear waste solutions', *Sep Sci Technol*, 26(9), 1229–1244.

Cuillerdier C, Musikas C, Hoel P, Nigond L (1993), 'Diamides as actinide extractants
for various waste treatments', *Sep Sci Technol*, 28(1–3), 155–175.

Danesi P R (2004), Solvent extraction kinetics, Chapter 5, *Solvent Extraction Prin-
ciples and Practice*, Marcel Dekker, New York.

Danesi P R, Meider-Gorican H, Chiarizia R, Scibona G (1975), 'Extraction selectiv-
ity of organic solutions of a cyclic polyether with respect to the alkali cations', *J
Inorg Nucl Chem* 37, 1479–1483.

Delmau L H, Bonnesen P V, Engle N L, Haverlock T J, Sloop F V, Moyer B A (2006),
'Combined extraction of cesium and strontium from alkaline nitrate solutions',
Solv Extr Ion Exch, 24(2), 197–217.

Delmau L H, Haverlock T J, Bazelaire E, Bonnesen P V, Ditto M E, Moyer B A
(2009), 'Alternatives to nitric acid stripping in the caustic-side solvent extraction
(CSSX) process for cesium removal from alkaline high-level waste', *Solv Extr Ion
Exch*, 27(2), 172–198.

Den Auwer C, Guillaumont D, Guilbaud P, Conradson S D, Rehr J J, Ankudinov A,
Simoni E (2004), 'Theoretical chemical contribution to the simulation of the L_{III}
X-ray absorption edges of uranyl, neptunyl and osmyl hydrates and hydroxides',
New J Chem, 28(8), 929–939.

Deneke M A, Rossberg A, Panak P J, Weigl M, Schimmelpfennig B, Geist A (2005),
'Characterization and comparison of Cm(III) and Eu(III) complexed with i-C_3H_7-
2,6-di(1,2,4-triazin-3-yl)pyridine using EXAFS, TRFLS, and quantum-chemical
methods', *Inorg Chem*, 44(23), 8418–8425.

Denecke M A, Panak P J, Burdet F, Weigl M, Geist A, Klenze R, Mazzanti M,
Gompper K (2007), 'A comparative spectroscopic study of U(III)/Am(III) and
Ln(III) complexed with N-donor ligands' *C R Chemie*, 10(10–11), 872–882.

Denning R, Green J, Hutchings T, Dallera C, Tagliaferri A, Giarda K, Brookes N,
Braicovich L (2002), 'Covalency in the uranyl ion: a polarized x-ray spectroscopic
study', *J Chem Phys*, 117(17), 8008–8020.

Dietz M L, Philip H E, Jensen M P, Rhoads S, Bartsch RA, Palka A, Krzykawski J,
Nam J (1996), 'Substituent effects in the extraction of cesium from acidic nitrate
media with macrocyclic polyethers', *Solv Extr Ion Exch*, 14(3), 357–384.

Dozol H and Berthon C (2007), 'Characterization of the supramolecular structure
of malonamides by application of pulsed field gradients in NMR spectroscopy',
Royal Soc Chem, Phys Chem Chem Phys, 9, 5162–5170.

Dozol J F, Ludvid R (2009), 'Extraction of radioactive elements by calixarenes', *Ion
exchange and solvent extrachin, A series of advances*, Vol. 19, Chap. 4, B. A. Moyer,
CRC Taylor and Francis.

Dozol J F, Casas J, Sastre A M (1995), 'Transport of cesium from reprocessing con-
centrate solutions through flat-sheet-supported liquid membranes: influence of
the extractant', *Sep Sci Technol*, 30(3), 435–448.

Dozol J F, Böhmer V, McKervey M A, Lopez-Calahorra F, Reinhoudt D N, Schwing
M J, Ungaro R and Wipff G (1997), 'New macrocyclic extractants for radioactive
waste treatment: Ionizable crown ethers and functionalized calixarenes', *EUR-
17615 EN*, European Commission, Luxembourg.

Dozol J F, Simon N, Lamare V, Rouquette H, Eymard S, Tournois B, De Marc D, Macias RM (1999), 'A solution for cesium removal from high-salinity acidic or alkaline liquid waste: the crown calix[4]arenes', *Sep Sci Technol*, 34(6–7), 877–909.

Dozol J F, Schwing-Weill M J, Arnaud-Neu F, Böhmer V, Ungaro R, van Veggel F C J M, Wipff G, Costero A, Desreux J F, De Mendoza J (2000a), 'Extraction and selective separation of long lived nuclides by functionalized macrocycles', *EUR 19605 EN*, European Commission, Luxembourg.

Dozol J F, Dozol M, Macias R M (2000b), 'Extraction of strontium and cesium by dicarbollides, crown ethers and functionalized calixarenes', *J Incl Phenom Macro Chem*, 38(1–4), 1–22.

Dozol J F, Liger K, Arnaud-Neu F, Böhmer V, Casensky B, Casnati A, Desreux J F, Grüner B, Grüttner C, De Mendoza J, Pina G, Selucky P, Verboom W, Wipff G (2004), 'Selective extraction of minor actinides from high activity liquid waste by organised matrices: CALIXPART', *Final Report FIKW-CT-2000-00088*, European Commission, Luxembourg.

Drew M G B, Iveson P B, Hudson M J, Liljenzin J O, Spjuth L, Cordier P Y, Enarsson A, Hill C, Madic C (2000a), 'Separation of americium(III) from europium(III) with tridentate heterocyclic nitrogen ligands and crystallographic studies of complexes formed by 2,2′:6′,2″-terpyridine with lanthanides', *J Chem Soc, Dalton Trans*, 5, 821–830.

Drew M G B, Hudson M J, Iveson P B, Madic C, Russel M L (2000b), 'A study of lanthanide complexes formed with the terdentate nitrogen ligand 4-amino-bis(2,6-(2-pyridyl))-1,3,5-triazine. Relevance to the separation of actinides and lanthanides by solvent *extraction', J Chem Soc, Dalton Trans*, 16, 2711–2720.

Drew M G B, Guillaneux D, Hudson M J, Iveson P B, Russell M L, Madic C (2001a), 'Lanthanide(III) complexes of a highly effective actinide(III) extracting agent – 2,6-bis(5,6-dipropyl-1,2,4-triazin-3-yl)pyridine', *Inorg Chem Comm*, 4, 12–15.

Drew M G B, Guillaneux D, Hudson M J, Iveson P B, Madic C (2001b), 'Unusual complexes formed by the early lanthanides with 2,6-bis(5,6-dialkyl-1,2,4-triazin-3-yl)-pyridines', *Inorg Chem Comm*, 4, 462–466.

Drew M G B, Hudson M J, Youngs T G A (2004a), 'QSAR studies of multidentate nitrogen ligands used in lanthanide and actinide extraction processes', *J Alloys Comp*, 374(1–2), 408–415.

Drew M G B, Hill C, Hudson M J, Iveson P B, Madic C, Vaillant L, Youngs T G A (2004b), 'Separation of lanthanides(III) and actinides (III) using tridentate benzimidazole, benzoxazole and benzothiazole ligands'*, New J Chem*, 28(4), 462–470.

Drew M G B, Hill C, Hudson M, Iveson P B, Madic C, Youngs T G A (2004c) 'Solvent extraction and lanthanide complexation studies with new terdentate ligands containing 1,3,5-triazine moieties', *J Chem Soc, Dalton Trans*, 2, 244–251.

Drew M G B, Foreman M R St J, Hill C, Hudson M, Madic C (2005), '6,6′-*bis*-(5,6-diethyl-[1,2,4]triazin-3-yl)-2,2′-bipyridyl the first example of a new class of quadridentate heterocyclic extraction reagents for the separation of americium(III) and europium(III)'. *Inorg Chem Comm*, 8(3), 239–241.

Drew M G B, Foreman M R St J, Geist A, Hudson M J, Marken F, Norman V, Weigl M (2006), 'Synthesis, structure, and redox states of homoleptic d-block metal complexes with bis-1,2,4-triazin-3-yl-pyridine and 1,2,4-triazin-3-yl-bipyridine extractants', *Polyhedron*, 25(4), 888–900.

Edelmann F T (2006), 'Lanthanides and actinides: Annual survey of their organo-metallic chemistry covering the year 2006', *Coord Chem Rev*, 253, 343–409.

Ekberg C, Fermvik A, Retegan T, Skarnemark G, Froeman M R S, Hudson M J, Englund S, Nilsson M (2008), 'An overview and historical look back at the solvent extraction using nitrogen donor ligands to extract and separate An(III) from Ln(III)', *Radiochim Acta*, 96(4–5), 225–233.

Erlinger C, Belloni L, Zemb T, Madic C (1999), 'Attractive interactions between reverse aggregates and phase separation in concentrated malonamide extractant solutions', *Langmuir*, 15(7), 2290–2300.

Foreman M R St J, Hudson M J, Geist A, Madic C, Weigl M (2005), 'An investigation into the extraction of americium(III), lanthanides and D-block metals by 6,6′-bis-(5,6-dipentyl-[1,2,4]triazin-3-yl)-[2,2′]bipyridinyl(C5-BTBP)', *Solv Extr Ion Exch*, 23(5), 645–662.

Foreman M R St J, Hudson M J, Drew M G B, Hill C, Madic C (2006) 'Complexes formed between the quadridentate, heterocyclic molecules 6,6′-bis-(5,6-dialkyl-1,2,4-triazin-3-yl)-2,2′-bipyridine (BTBP) and lanthanides(III): implications for the partitioning of actinides(III) and lanthanides(III)', *J Chem Soc, Dalton Trans*, 13, 1645–1653.

Forster R J, Cadogan A, Telting Diaz M, Diamond D, Harris S, Mc Kervey M A (1991), 'Calixarenes as active agents for chemical sensors', *Sensors and Actuators*, B(4), 325–331.

Ganjali M R, Norouzi P, Rezapour M, Faridbod F, Pourjavid M R (2006), 'Supramolecular based membrane sensors', *Sensors*, 6, 1018–1086.

Gannaz B, Antonio M A, Chiarizia R, Hill C, Cote G (2006), 'Structural study of trivalent lanthanide and actinide complexes formed upon solvent extraction', *J Chem Soc, Dalton Trans*, 38, 4553–4562.

Gasparini G M, Grossi G (1980), 'Application of N,N-dialkyl aliphatic amides in the separation of some actinides', *Sep Sci Technol*, 15(4), 825–844.

Gasparini G M, Grossi G (1986), 'Long chain disubstituted aliphatic amides as extracting agents in industrial applications of solvent extraction', *Solv Extr Ion Exch,* 4(6)*,* 1233–1271.

Gaunt A J, Reilly S D, Enriquez A E, Scott B L, Ibers J A, Sekar P, Ingram K I M, Kaltsoyannis N, Neu M P (2008), 'Experimental and theoretical comparison of actinide and lanthanide bonding in $M[N(EPR_2)_2]_3$ complexes (M = U, Pu, La, Ce; E = S, Se, Te; R = Ph, iPr, H)', *Inor Chem,* 47(1), 29–41.

Geist A, Hill C, Modolo G, Foreman M R S J, Weigl M, Gompper K, Hudson M J (2006), '6,6′-bis (5,5,8,8-tetramethyl-5,6,7,8-tetrahydro-benzo[1,2,4]triazin-3-yl) [2,2′]bipyridine, an effective extracting agent for the separation of americium(III) and curium(III) from the lanthanides', *Solv Extr Ion Exch*, 2006, 24(4), 463–483.

Gerow I H, Smith Jr J E, Davis Jr M W (1981), 'Extraction of Cs^+ and Sr^{2+} from HNO_3 solution using macrocyclic polyethers', *Sep Sc Technol*, 16(5), 519–548.

Ghidini E, Ugozzoli F, Ungaro R, Harkema S, El-Fadl A, Reinhoudt D N (1990), 'Complexation of alkali metal cations by conformationally rigid, stereoisomeric calix[4]arene crown ethers: a quantitative evaluation of preorganization', *J Am Chem Soc*, 112, 6979–6985.

Gradny T, Cadogan A, Mc Kittrick T, Harris S J, Diamond D, Mc Kervey M A (1996), 'Sodium-selective electrodes based on triester monoacid derivatives of p-tert-butylcalix[4]arene. Comparison with tetraester calix[4]arene ionophores' *Anal Chim Acta*, 336(1–3), 1–12.

Grüner B, Plesek J, Baca J, Dozol J F, Lamare V, Cisarova I, Belohradsky M, Caslavsky J (2002), 'Crown ether substituted cobalta bis(dicarbollide) ions as selective extraction agents for removal of Cs^+ and Sr^{2+} from nuclear waste', *New J Chem*, 26(7), 867–875.

Guillaumont D, Guilbaud P, Sorel C, Gutierrez F, Chalmet S, Defranceschi M (2006), 'Modelling selectivity in liquid/liquid extraction', *Nucl Sc Eng*, 153, 207–222.

Gutsche, C D (1989), *Calixarenes*, Royal Society of Chemistry, Cambridge, UK.

Gutsche C D (1998), *Calixarenes Revisited*, The Royal Society of Chemistry, Cambridge, UK.

Hagström I, Spjuth L, Enarsson Å, Liljenzin J O, Skålberg M, Hudson M J, Iveson P B, Madic C, Cordier P Y, Hill C, Francois N (1999), 'Synergistic solvent extraction of trivalent americium and europium by 2-bromodecanoïc acid and neutral nitrogen-containing reagents', *Solv Extr Ion Exch*, 17(2), 221–242.

Harrowfield J M, Ogden M I, Richmond W R, White A H (1991), 'Calixarene-cupped caesium: a coordination conundrum?', *J Am Chem Soc*, 113(4), 1159–1161.

Hay B P, Firman T K, Lumetta G J, Rapko B M, Garza P A, Sinkov S I, Hutchison J E, Parks B W, Gilbertson R D, Weakley T J R (2004), 'Toward the computer-aided design of metal ion sequestering agents', *J Alloys Comp*, 374(1&2), 416–419.

Hay B P, Oliferenko A A, Uddin J, Zhang C, Firman T K (2005), 'Search for improved host architectures: application of de novo structure-based design and high throughput screening methods to identify optimal building blocks for multidentate ethers', *J Am Chem Soc*, 127(48), 17043–17053.

Herbst R S, Law J D, Todd T A, Romanovskii V N, Babain V A, Esimantovski V M, Zaitsev B N, Smirnov I V (2002a), 'Development and testing of a cobalt dicarbollide based solvent extraction process for the separation of cesium and strontium from acidic tank waste,' *Sep Sci Technol*, 37(8), 1807–1831.

Herbst R S, Law J D, Todd T A, Romanovskiy V N, Babain V A, Esimantovskiy V M, Smirnov I V, Zaitsev B N (2002b), 'Universal solvent extraction (UNEX) flowsheet testing for the removal of cesium, strontium, and actinide elements from radioactive, acidic dissolved calcine waste', *Solv Extr Ion Exch*, 20(4–5), 429–445.

Herbst R S, Law J D, Todd T A, Romanovskiy V N, Smirnov I V, Babain V A, Esimantovskiy V N, Zaïtsev B (2003), 'Development of the universal extraction (UNEX) process for the simultaneous recovery of Cs, Sr, and actinides from acidic radioactive wastes', *Sep Sci Technol*, 38(12–13), 2685–2708.

Hill C, Dozol J F, Lamare V, Rouquette H, Eymard S, Tournois B, Vicens J, Asfari Z, Bressot C, Ungaro R, Casnati A (1994), 'Nuclear waste treatment by means of supported liquid membranes containing calixcrown compounds', *J Incl Phenom Mol Recog Chem*, 19, 399–408.

Hill C, Guillaneux D, Berthon L, Madic C (2002), 'SANEX-Btp process development studies', *J Nucl Sci Technol*, 3, 309–312.

Horwitz E P, Muscatello A C, Kalina D G, Kaplan L (1981), 'The extraction of selected transplutonium(III) and lanthanide(III) ions by dihexyl-*N, N*-diethylcarbamoylmethylphosphonate from aqueous nitrate media', *Sep Sci Technol*, 16(4), 417–437.

Horwitz E P, Kalina D G, Kaplan L, Mason G W, Diamond H (1982), 'Selected alkyl(phenyl)-*N,N*-dialkylcarbamoylmethylphosphine oxides as extractants for Am(III) from nitric acid media', *Sep Sci Technol*, 17(10), 1261–1279.

Hudson E A, Rehr J J, Bucher J J (1995), 'Multiple-scattering calculations of the uranium L3-edge x-ray-absorption near-edge structure', *Phys Rev B*, 52, 13815–13826.

Hudson M J, Foreman M R St J, Hill C, Huet N, Madic C (2003a), 'Studies on the parallel synthesis and evaluation of new heterocyclic extractants for the partitioning of minor actinides', *Solv Extr Ion Exch*, 21(5), 637–652.

Hudson M J, Drew M G B, Foreman M R St J, Hill C, Huet N, Madic C, Youngs T G A (2003b), 'The coordination chemistry of 1,2,4-triazinyl bipyridines with lanthanides(III) elements – implications for the partitioning of americium(III)', *J Chem Soc, Dalton Trans,* 9, 1675–1685.

Hudson M J, Boucher C, Braekers D, Desreux J F, Drew M G B, Foreman M R St J, Harwood L M, Hill C, Madic C, Marken F, Youngs T G A (2006), 'New bis(triazinyl) pyridines for selective extraction of americium(III)', *New J Chem*, 30, 1171–1183.

Ionova G, Ionov S, Rabbe C, Hill C, Madic C, Guillaumont R, Modolo G, Krupa J C (2001), 'Mechanism of trivalent actinide/lanthanide separation using synergistic mixtures of di(chlorophenyl)dithiophosphinic acid and neutral O-bearing co-extractants', *New J Chem*, 25(3), 491–501.

Iveson P B, Rivière C, Guillaneux D, Nierlich M, Thuery P, Ephritikhine M, Madic C (2001), 'Selective complexation of uranium(III) over cerium(III) by 2,6-bis(5,6-dialkyl-1,2,4-triazin-3-yl)pyridines: ^{1}H NMR and X-ray crystallography studies', *Chem Commun*, 12, 1512–1513.

Izatt R M, Lamb J D, Hawkins R T, Brown P R, Izatt S R, Christensen J J (1983), 'Selective M[+]-H^{+} coupled transport of cations through a liquid membrane by macrocyclic calixarene ligands', *J Am Chem Soc*, 105(7), 1782–1785.

Izatt S R, Hawkins R T, Christensen J J, Izatt R M (1985), 'Cation transport from multiple cation mixtures using a liquid membrane system containing a series of calixarene carriers', *J Am Chem Soc*, 107(1), 63–66.

Jankowski C K, Allain F, Lamouroux C, Virelizier H, Moulin C, Tabet J C, Lamare V, Dozol J F (2003), 'Comparison of the stability of calix[4]arene-crown-6-cation binary complexes under electrospray mass spectrometry', *Spectroscopy Lett*, 36, 327–340.

Jensen M P, Bond A H (2002), 'Influence of aggregation on the extraction of trivalent lanthanide and actinide cations by purified Cyanex 272, Cyanex 301, and Cyanex 302', *Radiochim Acta*, 90(4), 205–209.

Jensen M P, Yaita T, Chiarizia R (2007), 'Reverse-micelle formation in the partitioning of trivalent f-element cations by biphasic systems containing a tetraalkyldiglycolamide', *Langmuir*, 23, 4765–4774.

Karmazin L, Mazzanti M, Gateau C, Hill C, Pécaut J (2002), 'The important effect of ligand architecture on the selectivity of metal ion recognition in An(III)/Ln(III) separation with N-donor extractants', *Chem Com*, 23, 2892–2893.

Kikuchi Y and Sakamoto Y (2000), 'Complex formation of alkali metal ions with 18 crown 6 and its derivatives in 1,2-dichloroethane', *Anal Chim Acta*, 403(1–2**)**, 325–332.

Kolarik Z (2008), 'Complexation and separation of lanthanides(III) and actinides(III) by heterocyclic N-donors in solutions', *Chem Reviews*, 108(10), 4208–4252.

Kolarik Z, Müllich U (1997), 'Extraction of Am(III) and Eu(III) by 2-substituted benzimidazoles', *Solv Extr Ion Exch*, 15(3), 361–379.

Kolarik Z, Müllich U, Gassner F (1999a), 'Selective extraction of Am(III) over Eu(III) by 2,6-ditriazolyl- and 2,6-ditriazinylpyridines', *Solv Extr Ion Exch*, 17(1), 23–32.

Kolarik Z, Müllich U, Gassner F (1999b), 'Extraction of Am(III) and Eu(III) nitrates by 2,6-di-(5,6-dipropyl-1,2,4-triazin-3-yl)pyridines', 17(5), 1155–1170.

Kozlowski C A, Walkowiak W, Pellowski W, Koziol J (2002), 'Competitive transport of toxic metal ions by polymer inclusion membranes', *J Radioanal Nucl Chem*, 253(3), 389–394.

Kozlowski C A and Walkowiak W (2007), 'Competitive transport of cobalt-60, strontium-90, and cesium-137 radioisotopes across polymer inclusion membranes with DNNS', *J Memb Sci*, 297(1–2), 181–189.

Kumar A, Mohapatra P K, Manchanda V K (1998), 'Extraction of cesium-137 from nitric acid medium in the presence of macrocyclic polyethers', *J Radioanal Nucl Chem*, 229(1–2), 169–172.

Lamare V, Bressot C, Dozol J F, Vicens J, Asfari Z, Ungaro R, Casnati A (1997), 'Selective extraction of cesium at tracer level concentration from a sodium nitrate solution with calix-crowns. molecular modeling study of the Cs /Na selectivity', *Sep Sci Techno*, 32(1–4), 175–191.

Lamare V, Dozol J F, Ugozzoli F, Casnati A, Ungaro R (1998), 'X-ray crystal structures and molecular modeling studies of calix[4]dibenzocrowns-6 and their alkali metal cation complexes', *Eur J Org Chem*, 1559–1568.

Lamare V, Dozol J F, Fuangswasdi S, Arnaud-Neu F, Thuery P, Nierlich M, Asfari Z, Vicens J (1999), 'A new calix[4]arene-bis(crown ether) derivative displaying an improved cesium over sodium selectivity: molecular dynamics and experimental investigation of alkali-metal ion complexation', *J Chem Soc, Perkin Trans*, 2, 271–284.

Lamare V, Haubertin D, Golebiowski J, Dozol J F (2001), 'Molecular dynamics study of 21C7 crown ether derivatives and their alkali cation complexes. Comparison with 1,3-*alt*-calix-[4]arene-crown-6 compounds', *J Chem Soc, Perkin Trans*, 2, 121–127.

Lamouroux C, Aychet N, Lelièvre A, Jankowski C K, Moulin C (2004), 'High performance liquid chromatography ionization mass spectrometry and diode array detection in the identification and quantification of the degradation of calix[4] arene-crown-6 under radiolysis', *Rapid Commun Mass Spectrom*, 18, 1493–1503.

Lamouroux C, Rateau S, Moulin C (2006), 'Use of electrospray ionization mass spectrometry for the study of Ln(III) complexation and extraction speciation with calixarene-CMPO in the fuel partitioning concept', *Rapid Commun Mass Sp*, 20(13), 2041–2052.

Lauterbach M and Wipff G (1996), *Physical Studies in Supramolecular Chemistry*, pp 65–102, Echegoyen and Kaifer, Kluwer, Dordrecht.

Leclerc E, Guillaumont D, Guilbaud P, Berthon L (2008), 'Mass spectrometry and theoretical investigation of di-alkylphosphoric acid–lanthanide complexes', *Radiochim Acta*, 96(2), 85–92.

Lefrançois L, Hébrant M, Tondre C, Delpuech J J, Berthon C, Madic C (1999), 'Z,E Isomerism and hindered rotations in malonamides: an NMR study of N,N′-dimethyl-N,N′-dibutyl-2-tetradecylpropane-1,3-diamide', *J Chem Soc, Perkin Trans*, 2, 1149–1158.

Lein G M and Cram D J (1985), 'Host-guest complexation. 34. bridged hemispherands', *J Am Chem Soc*, 107(2), 448–455.

Leonard R A, Conner C, Liberatore M W, Sedlet J, Aase S B, Vandegrift G F, Delmau L H, Bonnesen P V, Moyer B A (2001), 'Development of a solvent extraction process for cesium removal from SRS tank waste', *Sep Sci Technol*, 36(5–6), 743–766.

Leonard R A, Aase S B, Arafat H A, Conner C, Chamberlain D B, Falkenberg J R, Regalbuto M C, Vandegrift G F (2003), 'Experimental verification of caustic-side solvent extraction for removal of cesium from tank waste', *Solv Extr Ion Exch*, 21(4), 505–526.

Madic C and Hudson M J (1998), 'High-level liquid waste partitioning by means of completely incinerable extractants', *EUR 18083 EN*, European Commission, Luxembourg.

Madic C, Hudson M J, Liljenzin J O, Glatz J P, Nannicini R, Facchini A, Kolarik Z, Odoj R (2000), 'New partitioning techniques for minor actinides: NEWPART', *EUR 19149 EN*, European Commission, Luxembourg.

Madic C, Lecomte M, Baron P, Boullis B (2002), 'Separation of long-lived radionuclides from high active nuclear waste', *Compte-Rendu de Physique 3. Applied Physics*, 797–811.

Madic C, Testard F, Hudson M J, Liljenzin J O, Christiansen B, Ferrando M, Facchini A, Geist A, Modolo G, Gonzales-Espartero A, De Mendoza J (2004), 'New solvent extraction processes for minor actinides: PARTNEW', CEA-R-6066, France.

Magnusson D, Christiansen B, Glatz J P, Malmbeck R, Modolo G, Serrano-Purroy D, Sorel C (2009a), 'Towards an optimized flow-sheet for a SANEX demonstration process using centrifugal contactors', *Radiochim Acta*, 97(3), 155–159.

Magnusson D, Christiansen B, Glatz J P, Malmbeck R, Modolo G, Serrano-Purroy D, Sorel C (2009b), 'Demonstration of a TODGA based extraction process for the partitioning of minor actinides from a PUREX raffinate. Part III: centrifugal contactor run using genuine fuel solution', *Solv Extr Ion Exch*, 27(1), 26–35.

Magnusson D, Christiansen B, Foreman M R S, Geist A, Glatz J P, Malmbeck R, Modolo G, Serrano-Purroy D, Sorel C (2009c), 'Demonstration of a SANEX process in centrifugal contactors using the CyMe$_4$-BTBP molecule on a genuine fuel solution' *Solv Extr Ion Exch*, 27(2), 97–106.

Marcus Y (1997), *Ion Properties*, Marcel Dekker Inc., New York.

Marcus Y and Kertes A S (1969), *Ion Exchange and Solvent Extraction of Metal Complexes*, Wiley-Interscience, London.

Mathur J N, Murali M S, Nash K L (2001), 'Actinide partitioning – A review', *Solv Ext Ion Exch*, 19(3), 357–390.

Miguirditchian M, Guillaneux D, Guillaumont D, Moisy P, Madic C, Jensen M P, Nash K L (2005), 'Thermodynamic study of the complexation of trivalent actinide and lanthanide cations by ADPTZ, a tridentate N-donor ligand', *Inorg Chem*, 44(5), 1404–1412.

Miguirditchian M, Guillaneux D, François N, Airvault S, Ducros S, Thauvin D, Madic C, Illemassene C, Lagarde G, Krupa J C (2006), 'Complexation of lanthanide(III) and actinide(III) cations with tridentate nitrogen-donor ligands: a luminescence and spectrophotometric study', *Nucl Sc Eng*, 153(3), 223–232.

Modolo G, Vijgen H, Serrano-Purroy D, Christiansen B, Malmbeck R, Sorel C, Baron P (2007a), 'DIAMEX countercurrent extraction process for recovery of

trivial actinides from simulated high active concentrate', *Sep Sci Technol*, 42(3), 439–452.

Modolo G, Asp H, Schreinemachers C, Vijgen H (2007b), 'Development of a TODGA based process for partitioning of actinides from PUREX raffinate Part I: batch extraction optimization studies and stability tests', *Solv Extr Ion Exch*, 25(7), 703–721.

Modolo G, Asp H, Vijgen H, Malmbeck R, Magnusson D, Sorel C (2008), 'Demonstration of a TODGA-based continuous counter-current extraction process for the partitioning of actinides from a simulated PUREX raffinate, Part II: centrifugal contactor runs', *Solv Extr Ion Exch*, 26(1), 62–76.

Morss, L R (1994), 'Comparative thermochemical and oxidation-reduction properties of lanthanides and actinides', *Handbook on the Physics and Chemistry of Rare Earths*, Vol. 18, lanthanides/actinides chemistry, pp. 239–257, Gschneider, Eyring, Choppin, Lander, Elsevier Science B.V.

Moyer B A and Sun Y (1997), *Ion Exchange and Solvent Extraction*, vol 13(6), 295–391, Marcel Dekker, New York.

Musikas C (1984), 'Actinide-lanthanide group separation using sulfur and nitrogen donor extractant', *Actinide/lanthanide separations*, Choppin, Navratil and Schulz. Singapore, World Scientific.

Musikas C (1986), 'Complexes des ions actinides en solutions aqueuses', *J Less Common Metals*, 122, 107–123.

Musikas C (1987), 'Solvent extraction for the chemical separation of the 5f elements', *Inorg Chim Acta*, 140, 197–206.

Musikas C (1988), 'Potentiality of nonorganophosphorus extractant in chemical separations of actinides', *Sep Sci Technol*, 23(12–13), 1211–1226.

Musikas C, Cuillerdier C, Livet J, Forchioni A, Chachaty C (1983), 'Azide interaction with 4*f* and 5*f* ions in aqueous solutions. 1. Trivalent ions', *Inorg Chem*, 22(18), 2513–2518.

Musikas C, Condamines N, Cuillerdier C (1991), 'Separation chemistry for the nuclear industry', *Anal Sci*, 7, Suppl, 11–16.

Nakahara M, Sano Y, Koma Y, Kamiya M, Shibata A, Koizumi T, Koyama T (2007), 'Separation of actinide elements by solvent extraction using centrifugal contactors in the NEXT process', *J Nucl Sci Technol*, 44(3), 373–381.

Nash K (1993), 'A review of the basic chemistry and recent developments in trivalent f-elements separations', *Solv Extr Ion Exch*, 11(4), 729–768.

Nash K (1994), 'Separation chemistry for lanthanides and trivalent actinides', *Handbook on the Physics and Chemistry of Rare Earths*, Vol. 18, lanthanides/actinides chemistry, pp. 198–238, Gschneider, Eyring, Choppin, Lander, Elsevier Science B. V.

Nash K (1999) 'Aqueous complexes in separation of f-elements: options and strategies for future development', *Sep Sci Technol*, 34(6–7), 911–929.

Nash K and Choppin G (1997), 'Separation chemistry for actinide elements: recent developments and historical perspective', *Sep Sci Technol*, 32(1–4), 255–274.

Nash L K, Madic C, Mathur J N, Lacquement J (2006), 'Actinide separation science and technology', *The Chemistry of the Actinide and the Transactinide Elements*, Vol 4, 3rd ed, pp. 2622–2798, Morss, Edelstein, Fuger, Katz, Springer, Dordrecht.

Nave S, Modolo G, Madic C, Testard F (2004), 'Aggregation properties of *N,N,N′,N′*-tetraoctyl-3-oxapentanediamide (TODGA) in *n*-dodecane', *Solv Extr Ion Exch*, 22(4), 527–551.

Navratil J D, Thomson G H (1979), 'Removal of actinides from selected nuclear fuel reprocessing wastes', *Nucl Technol*, 43, 136–145.

Nigond L, Musikas C, Cuillerdier C (1994a), 'Extraction by N,N,N′,N-tetraalkyl-2 alkyl propane-1,3 diamides. I. H_2O, HNO_3 and $HClO_4$', *Solv Extr Ion Exch*, 12(2), 261–296.

Nigond L, Musikas C, Cuillerdier C (1994b), 'Extraction by N,N,N′,N-tetraalkyl-2 alkyl propane-1,3 diamides. H. U(VI) and Pu(IV)', *Solv Extr Ion Exch*, 12(2), 297–323.

Nigond L, Condamines N, Cordier P Y, Livet J, Madic C, Cuillerdier C, Musikas C, Hudson M J (1995), 'Recent advances in the treatment of nuclear wastes by the use of diamide and picolinamide extractants', *Sep Sci Technol*, 30(7–9), 2075–2099.

Nilsson M, Andersson S, Drouet F, Ekberg C, Foreman M, Hudson M, Liljenzin J O, Magnusson D, Skarnemark G (2006a), 'Extraction properties of 6,6′-bis-(5,6-dipentyl-[1,2,4]triazin-3-yl)-[2,2′]bipyridinyl (C5-BTBP)', *Solv Extr Ion Exch*, 24(3), 299–318.

Nilsson M, Ekberg C, Foreman M R S, Hudson M J, Liljenzin J O, Modolo G, Skarnemark G (2006b), 'Separation of actinides (III) from lanthanides (III) in simulated nuclear waste streams using 6,6′-bis-(5,6-dipentyl-[1,2,4]triazin-3-yl)-[2,2′]bipiridinyl (C5-BTBP) in cyclohexanone', *Solv Extr Ion Exch*, 24 (6), 823–843.

Norato M A, Baesley M S, Campbell S G, Coleman A D, Geeting M W, Guthrie J W, Kennell C W, Pierce R A, Ryberg R C, Walker D D, Law J D (2003), 'Demonstration of the caustic-side solvent extraction process for the removal of ^{137}Cs from Savannah River site high level waste', *Sep Sci Technol*, 38(12–13), 2647–2666.

OECD/NEA (1999), 'Actinide and fission product partitioning and transmutation', *Status and Assessment Report*, OECD Publications, Paris.

Pathak P N, Ansari S A, Godbole S V, Dhobale A R, Manchanda V K (2009), 'Interaction of Eu^{3+} with N,N,N′,N′-tetraoctyl diglycolamide: a time resolved luminescence spectroscopy study', *Spectrochimica Acta Part A: Molecular and Biomolecular Spectroscopy*, 73(2), 348–352.

Pearson R G (1963), 'Hard and soft acids and bases', *J Am Chem Soc*, 85, 3533–3539.

Pedersen C J (1967), 'Cyclic polyethers and their complexes with metal salts', *J Am Chem Soc*, 89(26), 7017–7036.

Pérez-Jiménez C, Escriche L, Casabó J (1998), 'Poly(vinyl) chloride membrane caesium-selective electrodes based on doubly crowned 1,3-calix[4]arenes', *Anal Chim Acta*, 371 (2–3), 155–162.

Petit L, Adamo C, Maldivi P (2006), 'Toward a clear-cut vision on the origin of 2,6-di(1,2,4-triazin-3-yl)pyridine selectivity for trivalent actinides: insights from theory', *Inorg Chem*, 45(21), 8517–8522.

Petit L, Daul C, Adamo C, Maldivi P (2007), 'DFT modelling of the relative affinity of nitrogen ligands for trivalent f elements: an energetic point of view', *New J Chem*, 31(10), 1738–1745.

Retegan T, Ekberg C, Dubois I, Fermvik A, Skarnemark G, Wass T J (2007a), 'Extraction of actinides with different 6,6′-bis(5,6-dialkyl-[1,2,4]-triazin-3-yl)-bipyridines (BTBPs)', *Solv Extr Ion Exch*, 25(4), 417–431.

Retegan T, Ekberg C, Englund S, Fermvik A, Foreman M R S, Skarnemark G (2007b), 'The behaviour of organic solvents containing C5-BTBP and CyMe₄-BTBP at low irradiation doses', *Radiochim Acta*, 95(11), 637–642.

Ruas A, Guilbaud P, Den Auwer C, Moulin C, Simonin J P, Turq P, Moisy P (2006), 'Experimental and molecular dynamics studies of dysprosium(III) salt solutions for a better representation of the microscopic features used within the binding mean spherical approximation theory', *J Phys Chem* A, 110(41), 11770–11779.

Rydberg J, Musikas C, Choppin G R (1992), *Principles and Practices of Solvent Extraction*, Marcel Dekker, New York.

Rydberg J, Cox M, Musikas C, Choppin G R (2004), *Solvent Extraction Principles and Practice (2*nd *Edn.)*, Lavoisier, Paris.

Sachleben R A, Bonnesen P V, Descazeaud T, Haverlock T J, Urvoas A, Moyer B A (1999), 'Surveying the extraction of cesium nitrate by 1,3-alternate calix[4]arene crown-6 ethers in 1,2-dichloroethane', *Solv Extr Ion Exch*, 17(6), 1445–1459.

Sadakane A, Iwachido T, Toei K, (1975) 'The extraction of alkali metal picrates with dibenzo-18-crown-6', *Bull Chem Soc Jpn*, 48, 60–63.

Sasaki Y, Tachimori S (2002), 'Extraction of actinides(III), (IV), (V), (VI), and lanthanides(III) by structurally tailored diamides', *Solv Extr Ion Exch*, 20(1), 21–34.

Sasaki Y, Sugo Y, Suzuki S, Tachimori S (2001), 'The novel extractants, diglycolamides, for the extraction of lanthanides and actinides in HNO₃-*n*-dodecane system', *Solv Extr Ion Exch*, 19(1), 91–103.

Sasaki Y, Zhu Z X, Sugo Y, Kimura T (2007a), 'Extraction of various metal ions from nitric acid to n-dodecane by diglycolamide (DGA) compounds', *J Nucl Sci Technol*, 44(3), 405–409.

Sasaki Y, Rapold P, Arisaka M, Hirata M, Kimura T, Hill C, Cote G (2007b), 'An additional insight into the correlation between the distribution ratios and the aqueous acidity of the TODGA system', *Solv Extr Ion Exch*, 25(2), 187–204.

Schulz W W and Bray L A (1987), 'Solvent extraction recovery of byproduct ¹³⁷Cs and ⁹⁰Sr from HNO₃ solutions – a technology review and assessment', *Sep Sci Technol,* 22(2–3), 191–214.

Schulz W W, Burger L L, Navratil J D (1990), 'Applications of tributyl phosphate in nuclear fuel reprocessing', *Science and Technology of Tributyl Phosphate*, vol III, CRC Press, Boca Raton, Florida.

Schwing M J, Arnaud F, Marques E (1989), 'Cation binding properties of alkyl calixaryl derivatives. A new family of molecular receptors', *Pure & Applied Chem*, 61(9), 1597–1603.

Sekine T and Hasegawa Y (1977), *Solvent Extraction Chemistry*, Marcel Dekker, New York.

Serrano-Purroy D, Baron P, Christiansen B, Malmbeck R, Sorel C, Glatz J P, (2005a), 'Recovery of minor actinides from HLLW using DIAMEX process', *Radiochim Acta* 93(6), 351–355.

Serrano-Purroy D, Baron P, Christiansen B, Glatz J P, Madic C, Malmbeck R, Modolo G (2005b), 'First demonstration of a centrifugal solvent extraction process for minor actinides from a concentrated spent fuel solution', *Sep Purif Technol*, 45(2), 157–162.

Spjuth L, Liljenzin J O, Hudson M J, Drew M G B, Iveson P B, Madic C (2000), 'Comparison of extraction behaviour and basicity of some substituted malonamides', *Solv Extr Ion Exch*, 18(1), 1–23.

Sugo Y, Sasaki Y, Tachimori S (2002), 'Studies on hydrolysis and radiolysis of N,N,N′,N′-tetraoctyl-3-oxapentane-1,5-diamide', *Radiochim Acta*, 90(3), 161–166.

Tachimori S, Sasaki S, Suzuki S (2002), 'Modification of TODGA-*n*-dodecane solvent with a monoamide for high loading of lanthanides(III) and actinides(III)', *Solv Extr Ion Exch*, 20(6), 687–699.

Talanov V S, Talanova G G, Bartsch R A (2000), 'New proton-ionizable, cesium-selective calix[4]arene-bis(crown-6-ethers) with markedly enhanced extraction efficiency', *Tetrahedron Letters*, 41, 8221–8224.

Talanov V S, Talanova G G, Gorbunova M G, Bartsch R A (2002), 'Novel cesium-selective, 1,3-alternate calix[4]arene-bis(crown-6-ethers) with proton-ionizable groups for enhanced extraction efficiency', *J Chem Soc, Perkin Trans*, 2, 209–215.

Testard F, Bauduin P, Martinet L, Abécassis B, Berthon L, Madic C, Zemb Th (2008), 'Self-assembling properties of malonamide extractants used in separation processes', *Radiochim Acta*, 96(4–5), 265–272.

Thiollet G and Musikas C (1989), 'Synthesis and uses of the amides extractants', *Solv Extr Ion Exch*, 7(5), 813–827.

Thuery P, Nierlich M, Bressot C, Lamare V, Dozol J F, Asfari Z, Vicens J (1996), 'Crystal and molecular structures of binuclear caesium complexes with 1,3-calix[4]-*bis*-crown-6 and 1,3-calix[4]-*bis*-benzo-crown-6', *J Inclusion Phenom and Molec Recognition in Chem*, 23, 305–312.

Ungaro R and Pochini A (1991), 'Flexible and preorganized molecular receptors based on calixarenes', *Frontiers in Supramolecular Organic Chemistry and Photochemistry*, Schneider and Durr, VCH, Weinheim.

Ungaro R, Casnati A, Ugozzoli F, Pochini A, Dozol J F, Hill C, Rouquette H (1994), '1,3-Dialkoxycalix[4]arenecrowns-6 in 1,3-alternate conformation: cesium-selective ligands that exploit cation-arene interactions', *Angewante Chemie*, 33(14), 1506–1509.

Varnek A, Fourches D, Sieffert N, Solov'ev V, Hill C, Lecomte M (2007), 'QSPR modelling of the Am(III)/Eu(III) separation factor: how far can we predict?', *Solv Extr Ion Exch*, 25(1), 1–26.

Vicens J and Böhmer V (1991), '*Calixarenes: a versatile class of macrocyclic compounds*', Kluwer Academic Publishers, Dordrecht, The Netherlands.

Vitart X, Musikas C, Pasquiou J Y, Hoel P (1986) 'Séparation actinides-lanthanides à contre-courant en batterie de mélangeurs décanteurs', *J Less Common Metals*, 122, 275–286.

Warin D (2007), 'Status of the French research program on P&T', *J Nuc Sc Technol*, 44(3), 410–414.

Weaver B (1974), 'Solvent extraction in the separation of rare earths and trivalent actinides', *Ion Exchange and Solvent Extraction*, vol. 6, Marinsky and Marcus, Marcel Dekker, New York.

Weigl M, Müllich U, Geist A, Gompper K, Zevaco T, Stephan H (2003), 'Alkyl-substituted 2,6-dioxazolylpyridines as selective extractants for trivalent actinides', *J Radioanal Nucl Chem*, 256(3), 403–412.

Weigl M, Geist A, Müllich U, Gompper K (2006), 'Kinetics of americium(III) extraction and back-extraction with BTP', *Solv Extr Ion Exch*, 24(6), 845–860.

White T L, Peterson R A, Wilmarth W R, Norato M A, Crump S L, Delmau L H (2003), 'Stability study of Cs extraction solvent', *Sep Sci Technol*, 38(12–13), 2667–2683.

Wietzke R, Mazzanti M, Latour J M, Pécaut J, Cordier P Y, Madic C (1998), 'Lanthanide(III) complexes of tripodal N-donor ligands: structural models for the species involved in solvent extraction of actinides(III)', *Inorg Chem*, 37(26), 6690–6697.

Wipff G and Lauterbach M (1995), 'Complexation of alkali cations by calix[4]crown ionophores: conformation and solvent dependent Na /Cs binding selectivity and extraction: MD simulations in the gas phase, in water and at the chloroform-water interface', *Supramol Chem*, 6, 187–207.

Wood D J, Tranter T J, Todd T A (1995), 'Effect of the interference of alkali and alkaline earth metal ions on the extraction of ^{90}Sr from acidic nuclear waste solutions by 18-crown-6 derivatives', *Solv Extr Ion Exch*, 13(5), 829–844.

Yaita T, Herlinger A W, Thiyagarajan P, Jensen M P (2004), 'Influence of extractant aggregation on the extraction of trivalent *f*-element cations by tetraalkyldiglycolamide', *Solv Extr Ion Exch*, 22(4), 553–571.

Yakshin V V, Vilkova O M, Tananaev I G, Smirnov I V, Tsivadze A Yu, Myasoedov B F (2008), 'Selective extraction of alkali metals with solutions of dibenzocrown ethers in organofluorine diluents from nitric acid media', *Doklady Phys Chem*, 422(2), 271–274.

Developments in the partitioning and transmutation of radioactive waste

D. M. WARIN, CEA/Marcoule, France

Abstract: The generic objective of partitioning and transmutation strategies is to improve nuclear waste management by minimizing nuclear waste mass, reducing the heat load and the quantity of potential radiotoxic isotopes to be disposed finally in a geological repository. The transmutation performances of the different systems (thermal reactors, fast critical reactors, accelerator driven systems), having the capability of transmuting most of the radiotoxic long-lived elements present in the waste, such as minor actinides (americium, curium and neptunium) and some long-lived fission products (technetium 99, iodine 129 or cesium 135), are compared on the basis of the characteristics of transmutation physics.

It is clearly concluded that minor actinides can be more effectively transmuted in fast spectrum than in thermal spectrum.

Key words: radioactive waste, transmutation, minor actinides, neutron energy, cross section, fuel, irradiation test.

12.1 Introduction to transmutation

As described in the preceding chapters of this book, the generic objective of partitioning and transmutation strategies is to reduce the burden on the geological storage system by minimizing the nuclear waste mass, reducing the heat load and ultimately the quantity of potential radiotoxic isotopes. Studies on transmutation aim at changing the most radiotoxic long-lived elements present in the waste (minor actinides (MAs) americium, curium and neptunium and some long-lived fission products (LLFPs) such as technetium 99, iodine 129 or cesium 135) through recycling in nuclear reactors into non-radioactive or shorter-lived elements. The transmutation of partitioned minor actinides would reduce to a few hundred years the time necessary for the radiotoxicity of the vitrified waste to become similar to that contained in the natural uranium ore originally used.

More specific objectives can be defined as a result of the specific policy that is adopted towards nuclear energy and the specific strategies of reactor development. The following three categories of objectives, based on transmutation of transuranium elements (TRU), can be specified:

363

- Multi-recycling in fast reactors (FR) of TRUs as unloaded from light water reactors (LWR) and, successively, from FRs. This approach is consistent with a waste minimization objective compatible with a sustainable development of nuclear energy and increased proliferation resistance of the fuel cycle. A transition from a LWR fleet to a FR fleet is foreseen.
- Reduction of TRU inventory as unloaded from LWRs. This objective is related to the management of spent fuel inventories, as a legacy of previous operation of nuclear power plants.
- Reduction of the minor actinide inventory. This objective is compatible with a use of Pu as a resource in LWRs, in the hypothesis of a delayed deployment of fast reactors.

An analysis of the transmutation performances of different systems allows streamlining possible options depending on the objective.

12.2 Modelling transmutation processes and effects

The transmutation performances of different systems can be compared on the basis of the characteristics of transmutation physics [1, 2]. The variation of transmutation behaviour with energy spectrum is illustrated in Fig. 12.1; the fission/capture ratio is compared for dominant actinides in the pressurized water reactor (PWR) and SFR (sodium fast reactor) spectra. The fission/capture ratios are consistently higher for the fast spectrum SFR. For fissile isotopes (^{235}U, ^{239}Pu, and ^{241}Pu) over 80% of fast neutron absorptions result in fission, as compared to 60–80% in the PWR spectrum. In addition, the fast spectrum fission fraction can rise to 50% for fertile isotopes as
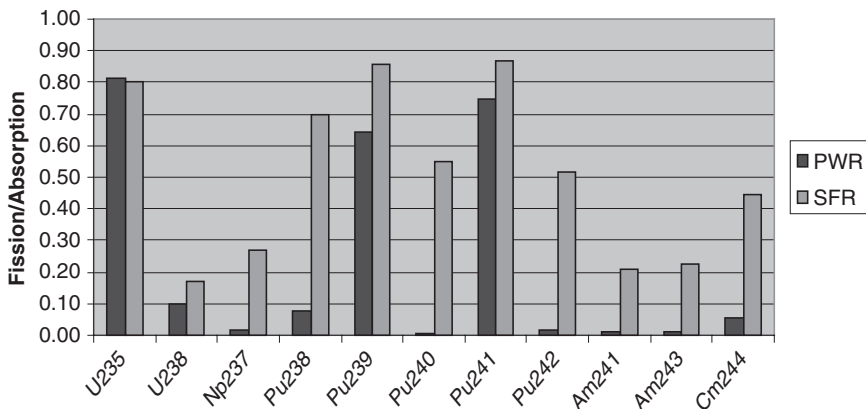
12.1 Comparison of fission/absorption ratios for PWR and SFR.

observed for ^{240}Pu in Fig. 12.1, while remaining low (<5%) in a thermal spectrum. Thus, in a fast spectrum, actinides are preferentially fissioned rather than being transmuted into higher actinides. This implies that fast systems are more "efficient" in destroying actinides because fewer neutrons are lost to capture reactions before eventual fission. Furthermore, higher actinides (americium, curium, etc.) continue to build-up with PWR recycle. These higher actinides tend to be more radioactive and can be problematic for fuel handling and fabrication in a closed fuel cycle (see below).

For resource utilization and sustainability goals, it is useful to compare the overall neutron "balance" of the transmutation process; a physics approach for quantification was developed in Ref. 1. The basic idea is to track the neutron balance for transmutation from the source isotope to extinction; fission and (n,2n) reactions produce neutrons while capture reactions consume neutrons. Six reactor concepts are under consideration for the next Generation-IV systems: pressurized water reactor (PWR), very high temperature reactor (VHTR), super critical water reactor (SCWR), sodium fast reactor (SFR), lead fast reactor (LFR) and gas fast reactor (GFR). For each reactor concept, the results allow comparison of the feasibility of transmutation of the different isotopes. The D-factors are given in Table 12.1 for the dominant actinides; note that a positive D-factor indicates net neutron consumption, while a negative D-factor indicates a neutron excess for transmutation of that isotope. As an example, in the case of the Am isotopes, the Am-241 transmutation is a neutron-consuming process in all the thermal concepts, while Am-243 is a slight producer. The fissile isotopes (^{235}U, ^{239}Pu, and ^{241}Pu) are net producers whatever the spectrum, with more excess neutrons in the fast concepts (e.g., average of about −1.6 for ^{239}Pu).

Table 12.1 Comparison of D-Factors for the Gen-IV concepts

Isotope	Thermal concepts			Fast concepts		
	PWR	VHTR	SCWR	SFR	LFR	GFR
U-235	−0.65	−0.53	−0.70	−1.04	−0.92	−0.84
U-238	−0.02	0.26	0.01	−0.89	−0.71	−0.62
Np-237	0.96	1.11	1.03	−0.88	−0.65	−0.51
Pu-238	0.01	0.12	0.07	−1.50	−1.36	−1.25
Pu-239	−0.83	−0.72	−0.80	−1.71	−1.59	−1.45
Pu-240	0.04	0.12	0.09	−1.28	−1.04	−0.94
Pu-241	−0.95	−0.88	−0.90	−1.42	−1.29	−1.27
Pu-242	0.72	0.79	0.86	−1.12	−0.72	−0.64
Am-241	0.80	0.90	0.88	−0.93	−0.67	−0.58
Am-243	−0.24	−0.20	−0.09	−1.14	−0.85	−0.83
Cm-244	−1.22	−1.19	−1.07	−1.70	−1.53	−1.53

Significant variations in the D-factor are observed between the concepts. In general, all of the fast reactor systems (harder neutron spectrum) exhibit a significantly more favourable neutron balance compared to the thermal systems. Of particular interest is the neutron balance of ^{238}U, which comprises the bulk of natural uranium resources. The VHTR exhibits a significant neutron defect for ^{238}U (0.26 net consumption); this is because the fission peak is much less pronounced in the graphite-moderated systems effectively suppressing the direct threshold fission of ^{238}U. There is a slight neutron excess in the PWR, although the −0.02 will not overcome parasitic losses which will require roughly 0.38 neutrons. This implies that the use of TRU fuel in LWRs requires the addition on fissile isotopes (an economic penalty) and that the amount of MA should be kept low, reducing the transmutation performance.

Conversely, the fast reactors have a neutron excess ranging from 0.62 to 0.89. Thus, the fast systems have the potential to efficiently transmute the base ^{238}U resources, while the thermal systems will require, as indicated above, an additional source of neutrons (fissile feed) to drive the transmutation of the ^{238}U. Finally, the amount of MA that can be loaded in a FR is not limited in principle. However, we will see that there can be limitations in a critical fast reactor, due to safety considerations.

The neutron–nucleus interaction leads mainly to two types of reactions, the reaction of neutron capture by the target nucleus and the reaction of fission. For the fission products, the capture in general makes it possible to generate, after successive transformations, a stable element. The typical example is the technetium 99 ($t_{1/2} = 210\,000$ years) which by neutron capture is transformed into technetium 100 of very short radioactive half-life 15.8 seconds) ending up by beta disintegration at stable ruthenium 100 (Fig. 12.2).
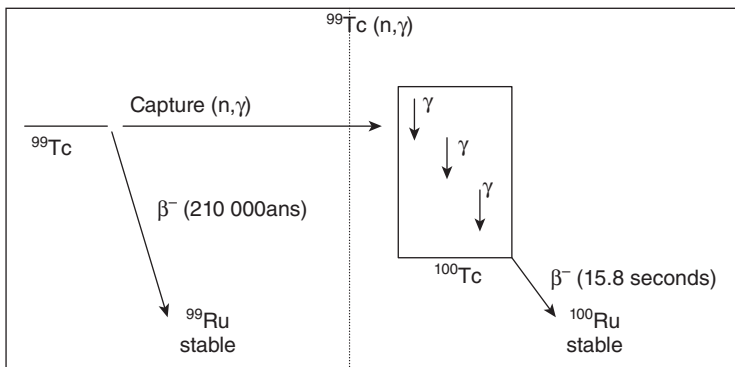
12.2 Technetium 99 decay vs (n,γ) reaction.

For minor actinides, the capture reaction is preferably avoided because it results mainly in generating of other radioactive actinides, which generally does not achieve a decrease of radiotoxicity. For example, in case of ^{241}Am, the reaction of capture gives ^{242}Am and mainly ^{242}Cm (by beta decay). The half-life of this isotope is only of 163 days, but in fact the ^{242}Cm decays to ^{238}Pu and so on up to stable lead. The comparison of the radiotoxicity induced from ^{241}Am and ^{242}Cm (and their daughters) gives less benefit in terms of reduction of radiotoxicity than could be gained if they were fissioned.

It is obviously fission that is necessary to support the destruction of minor actinides, because, on the one hand, fission leads to residues (fission products) with short life then stable, less radiotoxic in the long term than destroyed actinide, and, on the other hand, fission produces additional neutrons usable to destroy other waste or to take part in a feeding reaction chain while producing energy. So the capacity to obtain a process of effective minor actinides transmutation depends on the competition between the two reactions of fission and neutron capture. The probability of occurrence of each reaction is characterized by the cross section of the isotope considered. These cross sections are quantified in Table 12.2 where the values of capture to fission ratio of average cross sections integrated on the spectra of definite neutrons are indicated, representative as the distribution in energy of the neutron population present in the nuclear reactor: a "thermal" PWR spectrum with a UOX fuel, an "epithermal" PWR spectrum with a MOX fuel and a Na-cooled fast reactor spectrum. Clearly, there is a great advantage for fast spectrum by comparison to thermal/epithermal neutron spectra.

The evaluation of the cross sections alone, although a good indicator, is not sufficient. It is also necessary to consider what happens under irradiation, taking into account the other isotopes produced. For a standard irradiation time in PWR type and RNR reactors, the disappearance rates of the considered elements, expressed in percent of the mass presents initially,

Table 12.2 Capture to fission ratio of MA average cross sections

Isotope	PWR UOX	PWR MOX	FR
	$\alpha = \sigma c / \sigma f$	$\alpha = \sigma c / \sigma f$	$\alpha = \sigma c / \sigma f$
^{237}Np	63	30	5.3
^{241}Am	100	45	7.4
^{243}Am	111	63	8.6
^{244}Cm	16	13	1.4
^{245}Cm	0.15	0.2	0.18

Table 12.3 MA transmutation (T) and fission (F) rates for PWR and FR

Reactor	PWR		FR	
Burn up	60 GWd/t		140 GWd/t	
Flux level	2.5×10^{14} n/cm^2/s		3.4×10^{15} n/cm^2/s	
Irradiation time	1500 EFPD		1700 EFPD	
Fission (F) and Transmutation (T) rates	T (%)	F (%)	T (%)	F (%)
Np-237	46	4	63	24
Am-241	70	10	69	24
Am-243	65	6	63	15
Cm-244	44	16	50	27

are indicated in Table 12.3. The rates of fission, integrated over the irradiation time, are also indicated. These fission rates integrate the contributions to fission, not only of the parent isotope present initially, but also those of the daughter isotopes produced during the irradiation.

From the analysis of these results, the following principal points arise:

- Under the standard conditions of reactor's irradiation, it is not possible to reach a complete destruction of the elements considered with only once through irradiation thus multi-recycling is necessary.
- The fission rates obtained in a FR are higher, in a ratio 2 to 6 with those obtained in PWR.
- In a PWR, the transmutation of the considered elements is accomplished primarily by successive captures, the production of higher elements will be very clearly enhanced.

This last point is of great importance. In fast spectrum, production of higher isotopes is quite limited by comparison with thermal spectrum for which production of isotopes higher than curium is much larger. Even if mass production is quite small, due to very high spontaneous fission yield mainly for ^{246}Cm and ^{248}Cm but also upper elements produced like californium, this is quite a large drawback for the fuel cycle operations.

Concerning transmutation of LLFP, the isotopes whose possibilities of transmutation have been assessed are mainly ^{99}Tc, ^{135}Cs and ^{129}I. These isotopes are pure neutron capturers. In PWRs, their transmutation proves very difficult and would require the fuel's overbreeding. The FRs can be used with specific assemblies in which the neutron spectrum is changed locally to benefit from large thermal neutron cross sections. Cesium transmutation is not realistic because the ^{135}Cs capture cross section is very low, about 1 barn in thermal spectrum, and because a prior isotopic partitioning to isolate ^{135}Cs from others Cs isotopes would be necessary before trans-

mutation. The destruction of technetium and iodine is possible in FRs by using targets placed in a moderated neutron spectrum. Nevertheless, calculations show a low transmutation performance, even in optimal neutronic conditions. For example, for technetium's most favourable case, 20 to 30 years of irradiation are needed to reduce the quantity of technetium by half. Technetium and iodine transmutation is therefore hardly realistic when the goal is to reduce their radiotoxicity.

12.3   Systems for transmutation: design and safety

12.3.1 Critical PWR and FR

The main restriction to introducing minor actinides into critical reactors is linked to their impact on the core's reactivity and kinetic parameters [3–5]. This would produce:

- a drop in the fuel temperature coefficients (Doppler effect),
- an increase in reactivity effect linked to the coolant voiding,
- a reduction in delayed neutron yield.

For instance, the impacts of these factors as a function of minor actinides content loading are given for the case of a large fast reactor in Fig. 12.3. The minor actinides content limit is around 3% of total heavy nuclides for large sodium cooled reactors. The gas cooled fast reactor allows a higher
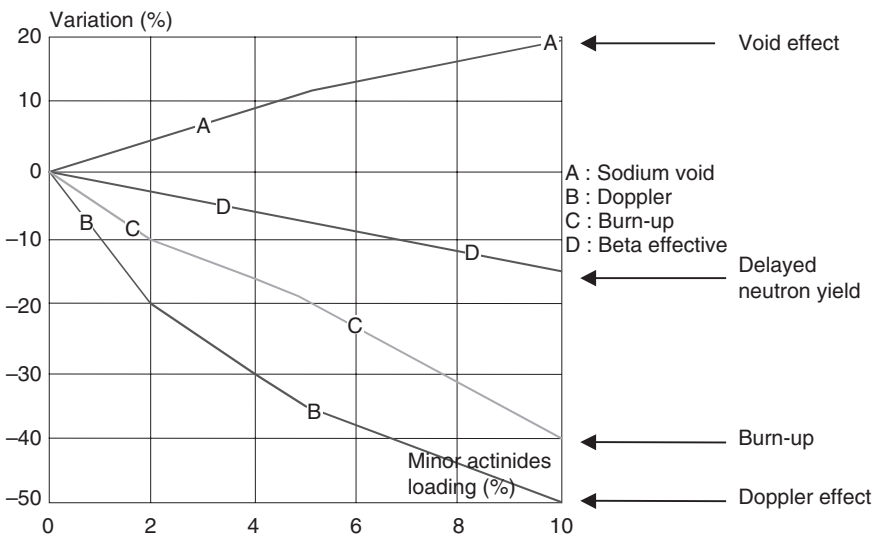
12.3 Impact of the MAs loading on the safety parameters for LMFR.

loading in MA than liquid metal fast reactor due to the disappearance void effect constraint: 5% of MA seems acceptable even for a large core.

The void effect is also actually the most restricting criterion for MA loading in PWR from the point of view of its impact on physics and safety. Without the coolant, the neutron spectrum moves to higher energy and the minor actinides contributions of the thermal and epithermal resonances vanish. The minor actinide content must then be limited to about 1% of total heavy nuclides.

For critical reactors, some conclusions can be proposed:

- The admissible quantities of minor actinides in the core have to be kept low (about 1% for PWR type and 3% to 5% for FR type).
- The maximum MA fission rates are about 5 to 10% in PWRs and from 15 to 30% in FRs. In both cases, a multi recycling is necessary in order to reach satisfactory overall performance.
- In PWRs, curium recycling is to be avoided as it produces by itself and by producing californium, an intense source of neutrons. In FRs, curium recycling also produces upper elements, but they stabilize at a far lower level than in the PWRs and therefore do not pose any specific new problem.

Fast spectrum reactors can operate as breeders or burners, or in a self-sufficient breakeven mode. Breeders incorporate external blankets, both axial and radial. When reflectors replace blankets, FRs become net burners of fissile material. If an appropriate amount of blanket is incorporated, then a self-sufficient mode can be maintained. In whichever mode they operate, FR discharged fuel contains a large fraction of fissile inventory, and hence recycling is mandatory. As a matter of fact, resource utilization improvement is the primary rationale for fast reactors and recycling is required to achieve that goal.

Historically, only uranium and plutonium have been recovered from LWR spent fuels, and only plutonium recycling has taken place or been envisioned for the fast reactor fuel cycle. However, we have seen that minor actinides can be also recycled along with plutonium in fast reactors. Minor actinides and even-mass isotopes of plutonium may not be attractive as fuel for thermal reactors because they have unfavourable ratios of fission to capture, as demonstrated in the previous chapter. These same materials, as well as odd-mass isotopes of plutonium, are fissionable in fast spectrum, where we have seen that the fission to capture ratio is much more favourable. Furthermore, the high content of recycled plutonium may require remote fabrication and hence minor actinides can be more easily incorporated into continuous recycling.

For economic and political reasons and because of proliferation concerns in some countries, fast reactors and their fuel cycle development pro-

grammes have been curtailed since the 1990s, except in China, France, India, Japan and the Russian Federation. Fast reactor concepts for actinide transmutation have been of interest in recent international initiatives such as the International Project on Innovative Nuclear Reactors and Fuel Cycles (INPRO) or Generation IV International Forum (GIF). Apart from these developments, the value of preserving the large technology base developed in Japan, France, Germany, the Russian Federation, the United Kingdom and the USA, as well as information developed in other countries, has been a subject of essential scientific interest.

12.3.2 Accelerator driven systems

Systems specifically dedicated to MA transmutation have been proposed and largely studied in some countries [6]: they comprise a subcritical reactor coupled to an external neutron source supplied by a proton accelerator. Such dedicated ADS (accelerator driven system), operating in a sub critical mode, offers:

- a safety guard against accidental reactivity increase which allows considering large MA loads whose reactivity feedback (Doppler effect) and proportion of delayed neutrons would make them prohibitive with critical cores,
- an acceptance of a greater variation in the fuel's isotopic composition, resulting from transmutation during the cycle, as the system is no longer constrained by self-criticality during the entire time the fuel is in the reactor.

The complexity of these systems means that they cannot be considered as electricity-generating reactors. Their development involves the design of highly technical elements, such as a reliable power accelerator which has to supply an intense high energy proton beam for long periods of time without beam interruption, a spallation target which has to produce high energy neutrons under the effect of the accelerator's proton using the lead bismuth eutectic (LBE) and a window separating the accelerator void from the LBE, and a reactor core operating in sub critical and fast spectrum mode. For the first time ever in 2002–2006, the main components were successfully assembled for studies at zero power in the French CEA Cadarache Masurca reactor. The results of this programme have allowed development of validated sub-criticality level measurement techniques. Nevertheless, several technological constraints still remain and must be overcome before judging the viability of a powerful ADS; studies are ongoing on these subjects as part of the Belgian MYRRHA Demo ADS project and the European EUROTRANS project dealing with ADS designs (both experimental and industrial), neutronics, fuels, LBE technology and specific nuclear data.

12.4   Transmutation fuel development

Because minor actinide bearing fuel is still a new field, a tremendous amount of excellent research has been accomplished to date [7]. It appears that the greatest emphasis has been placed on heterogeneous target fuel concepts with a high content of minor actinides only (i.e., no plutonium). This trend may have been driven by the desire to set the performance envelope, namely to understand and prove performance characteristics in extreme cases. However, this approach may overlook some practical approaches amenable to commercial-scale deployment in practice.

The physicochemical properties of materials involved in the fuel design and fabrication of minor actinide fuels are needed to understand and improve performance of fuel elements exposed to high temperatures, corrosive coolants and a radioactive environment. The objectives for development of a physicochemical properties database are to assemble a database on fuel properties and performance sufficient to support a safety/licensing case, and to develop a fabrication and quality assurance process that will enable effective and economic fuel fabrication. The required physicochemical properties include a range of thermodynamic (enthalpy and heat capacity, melting temperature, enthalpy of fusion, vapour pressure, vaporization, thermal expansion, density and surface tension), transport (thermal conductivity and diffusivity, emissivity and optical constants) and mechanical (hardness creep, thermal shock and swelling) properties.

These properties (Table 12.4) are needed to understand fuel performance and are also required for the modelling of fuel behaviour. Relevant experimental data for all minor actinide elements are not available for all properties, and may include datasets for a mixture of actinides. The database is also sparse for metal, oxide, nitride and other potential fuel forms of the minor actinides. A database is available for a few Np compounds, while data for Am and Cm are sparse. The collection of property data for minor actinides is an ongoing effort.

Table 12.4 Database of properties needed for minor actinide fuels

Thermodynamic	Transport	Mechanical
Enthalpy and heat capacity	Thermal conductivity	Hardness
Melting temperature	Thermal diffusivity	Creep
Enthalpy of fusion	Emissivity and optical constants	Thermal shock
Vapour pressure		Swelling
Vaporization		
Thermal expansion		
Density		
Surface tension		
Surface energy		

The irradiation behaviour of minor actinide fuels may vary from that of conventional fuels in several ways. Most prominent is the increased fuel pin helium gas inventory due to capture and decay sequences associated with ^{241}Am and a significant amount of ^{242}Cm, which decays by α emission (half-life of 169 days) to ^{238}Pu. The additional helium gas inventory can lead to higher fuel swelling rates and is an additional source term for fuel pin over-pressurization. An additional interesting phenomenon relates to the evolution of isotopic mixtures in fuel with high ^{241}Am and ^{237}Np loadings, and the effect this evolution has on pin power. As plutonium isotopes are bred in fuel from neutron capture during irradiation, particularly in the thermal spectrum, fuel rod power increases as a function of irradiation time.

Other issues to be studied include fission product behaviour, and optimization of the oxygen to metal ratio in oxide fuels. Due to the shift in isotopic composition of the starting fuel, the isotopic and chemical distribution of fission products also shifts relative to that of standard MOX fuel.

Many fuel types, encompassing different matrices and chemical forms, have been considered for minor actinide bearing fuels. Several unconventional fabrication techniques have been explored as well. The in-reactor irradiation tests conducted to date are all very promising. As post-irradiation examination results become available, they will provide valuable information to guide additional future irradiation tests. Obviously, more R&D and in-reactor irradiation tests are required to qualify minor actinide bearing fuels. The incorporation of MA has some impact on the physicochemical properties of fuel material. Some results are available for the incorporation of MA in MOX fuel (for example, lower melting temperature, influence of stoichiometry on thermal conductivity, redistribution of Am). But additional data are needed to guarantee the safe operation of reactor and fuel cycle facilities (fuel fabrication and reprocessing).

In the US, AFC fuel test hardware was designed to simulate fast reactor test conditions in Idaho National Laboratory's advanced test reactor ATR: the AFC-1 irradiation test series was designed to evaluate the feasibility of actinide-bearing fuel forms in sodium cooled fast reactors for the transmutation of actinides from spent nuclear fuel [8]. The fuel rods had the same diameter as EBR-II fuel, but were reduced in length. All fuels, both nitride and metal, were sodium bonded inside stainless steel Type 421 (HT-9) cladding with an inert plenum gas. AFC-1B, AFC-1F, and AFC-1Æ irradiation test capsules provided irradiation performance data at intermediate burn ups of 4 to 8 at.% on non fertile and fertile actinide transmutation fuel forms containing plutonium, neptunium and americium isotopes. AFC-1D, AFC-1G, and AFC-1H capsules extended fuel performance with satisfactory results, in terms of gas release and microstructural data compared to U-xPu-10Zr fuel when correlated with fission density.

In Japan, the "Am-1" programme has been conducted in order to investigate the irradiation behaviour of Americium containing MOX fuel in the experimental fast reactor Joyo [9, 10]. Two irradiation experiments were conducted in the Joyo MK-III 3rd operational cycle to research early thermal behaviour of MA–MOX fuel. Six prepared fuel pins included MOX fuel containing 3% or 5% americium (Am–MOX), MOX fuel containing 2% americium and 2% neptunium (Np/Am-MOX), and reference MOX fuel. Ceramography results showed that structural changes such as lenticular pores and a central void occurred early, within the brief 10 min of irradiation. The results of electron probe microanalysis revealed that the concentration of Am increased in the vicinity of the central void. Post irradiation examination of these pins did confirm fuel melting and local concentration evolutions under irradiation of NpO_{2-x} or AmO_{2-x} in the (U,Pu) O_{2-x} fuel. These test results are expected to reduce uncertainties in the design margin for the design of MA-MOX fuels.

The SUPERFACT irradiation in Phenix (1986–1988) represents the main body of existing knowledge on in pile behaviour of MOX fuel loaded with MA [11]. This project demonstrated the feasibility of Am or Np incorporation of up to 2% in MOX fuels. The main constraint in introducing minor actinides into the core (homogeneous recycling mode) is linked to their impact via core reactivity and kinetic factors.

For heterogeneous recycling and in particular in the case of blankets loaded with MAs, high MA content raises the question of managing the large quantity of He produced. Hence, a specific transmutation fuel microstructure must be developed, which requires envisioning several innovative steps in irradiation systems.

Most fast reactor irradiation tests, like the SUPERFACT experiment, were done in the French Phenix SFR, which was finally shut down in 2009 [12]. Since there are only a handful of fast reactors still in operation that can provide prototypic irradiation test environments in fast spectrum, an international collaboration to expand test capabilities and optimize the limited availability of irradiation test facilities is desirable. For example, under the framework of the GEN-IV SFR programme [13], an international collaboration project called GACID (Global Actinide Cycle International Demonstration) is being conducted (2007–2016) with participation of French CEA, US DOE and Japanese JAEA. The objective of the project is to demonstrate the transmutation of minor actinides in a 20% Pu MOX fuel with the Monju SFR located in Tsuruga, Japan. The fuel pins will be manufactured at the French CEA Atalante hot cells in Marcoule, using USA MA feedstocks. Data obtained from the GACID irradiation project will provide a feasibility assessment of MOX fuel matrix for transmutation.

12.5   Future trends

In recent years, partitioning and transmutation of minor actinides have received much attention. This is motivated by the fact that long term radiological toxicity of spent fuel is dominated by minor actinides, in particular americium and curium. Although it is desirable to eliminate long-lived minor actinides from a permanent repository, MA partitioning and transmutation should not be viewed as an end goal for all nuclear programmes. Rather, it should be considered in the context of overall nuclear deployment scenarios, which may dictate different fuel cycle options depending on each country's nuclear policy, cost–benefit considerations, and public acceptance.

In fact, the once through fuel cycle with direct disposal of spent fuel is a reference nuclear deployment scenario in a very large majority of countries using nuclear energy. Technically sound engineered barrier concepts make direct disposal a viable option. Therefore, the question is not whether or not minor actinides have to be partitioned and transmuted, but rather how to best manage minor actinides given a particular envisioned future nuclear deployment scenario. In the same context, the minor actinide transmutation rate has no particular significance depending on the future deployment scenario, and hence should not be adopted as a figure of merit without understanding its implications. In a closed fuel cycle with thermal reactors only, it has been seen that nuclear properties dictate that minor actinides cannot be fully transmuted. Thus, cost–benefit considerations will be a strong factor in deciding the minor actinide management option. If no fast reactors are envisioned, then other dedicated transmutation systems, such as an accelerator driven system, could be considered for minor actinide transmutation. If fast reactors are envisioned, then it would be best to dedicate minor actinide transmutation to fast reactors, although some partial plutonium recycling can be and is being carried out in thermal reactors in the near term. Even in this case, depending on cost–benefit considerations and nuclear energy deployment scenarios, one should not eliminate the possibility of introducing "dedicated transmutation machines" like ADS in double-strata strategies. This is because minor actinides can be more effectively transmuted in fast spectrum strategies and because they become only a small fraction of fast reactor fuel, which typically requires higher fissile contents.

12.6   References

1. M. Salvatores, I. Slessarev, and M. Uematsu, "A Global Physics Approach to Transmutation of Radioactive Nuclei," *Nuclear Science and Engineering*, 116, 1 (1994).

2. M. Salvatores, R. Hill, I. Slessarev, G. Youinou, "The Physics of TRU Transmutation – A Systematic Approach to the Intercomparison of Systems," Proc. PHYSOR 2004 – The Physics of Fuel Cycles and Advanced Nuclear Systems: Global Developments, Chicago, Illinois, on CD-ROM, American Nuclear Society, Lagrange Park, USA, April 25–29, 2004.

3. Physics and Safety of Transmutation Systems, OECD-NEA Report, 2006.

4. D. Warin and C. Courtois, "Overview of French P and T Program and Results for Waste Management", 8th OECD/NEA International Exchange Meeting on P and T, Las Vegas, USA, 2004.

5. The French R&D Programme on the Partitioning and Transmutation of Long-Lived Radionuclides – An International Peer Review, OECD/NEA Nº6210, ISBN 92-64-02296-1, 2006.

6. Accelerator-driven Systems (ADS) and Fast Reactors (FR) in Advanced Fuel Cycles. A comparative study. OECD-NEA Report, 2002.

7. D. Warin and M. Boidron, "Fuels and Targets for Actinide Transmutation", *Proc. of Int. Conf. ATALANTE 2008*: Nuclear Fuel Cycle for Sustainable Future, Montpellier, France, 2008.

8. B. Hilton *et al.*, "The AFC-1Æ and AFC-1F Irradiation Tests of Metallic and Nitride Fuels for Actinide Transmutation", *Proc. of Int. Conf. on Atoms for Prosperity: Updating Eisenhower's Global Vision for Nuclear Energy*, GLOBAL'03, New Orleans, USA, 2003.

9. OECD/Nuclear Energy Agency, "Fuels and Materials for Transmutation: a status report", Nº 5419, NEA/OECD, Paris, France, 2005.

10. K. Maeda *et al.*, "Short-term Irradiation Behaviour of Minor Actinide Doped Uranium Plutonium Mixed Oxide Fuels Irradiated in an Experimental Fast Reactor", *J. Nucl. Mater.*, 385, 413–418, 2009.

11. C. Prunier *et al.*, "Some Specific Aspects of Homogeneous Americium- and Neptunium-based Fuel Transmutation Through the Outcomes of the SUPER-FACT Experiment in PHENIX Fast Reactor", *Nucl. Technol.* 119, 141, 1997.

12. J. Guidez and L. Martin, "Status of Phenix Operation and Sodium Fast Reactors in the World", *Proc. of Int. Congress on Advances in Nuclear Power Plants* (ICAPP 07) SFEN, Nice, France, 2007.

13. GENERATION IV International Forum, OECD/Nuclear Energy Agency, "The Sodium Cooled Fast Reactor (SFR) Features a Fast-Spectrum, Sodium Cooled Reactor and a Closed Fuel Cycle for Efficient Management of Actinides and Conversion of Fertile Uranium, Gen-IV", Paris, France, 2009, http://www.gen-4.org/index.html.

<div align="right">

13

</div>

Solid-phase extraction technology for actinide and lanthanide separations in nuclear fuel reprocessing

T. J. TRANTER, Idaho National Laboratory, USA

Abstract: Solid-phase extraction has become a subject of increased interest for separation applications specific to radioisotopes of the nuclear fuel cycle. The objective of this chapter is to discuss recent advances in the technology with a focus on the separations of minor actinides and lanthanides from streams associated with nuclear fuel reprocessing. The discussion covers various techniques for making solid-phase extraction resins, recent applications, separation flow sheets, column modeling and the potential advantages and disadvantages of the technology.

Key words: solid-phase extraction, extraction chromatography, solvent-impregnated resins, actinide separation, lanthanide separation, nuclear fuel reprocessing, radioactive waste treatment.

13.1 Introduction

The term solid-phase extraction, as used in the context of this chapter, generally refers to macroporous polymers that hold an organic complexing compound or extractant within the pore structure of the polymer. Various literature sources may also refer to this material as extraction chromatography resins, solvent-loaded resins or solvent-impregnated resins. The macroporous polymer supports are roughly spherical beads, appearing much like the resins typical to ion exchange, and may be used in a similar fashion in a column or packed bed configuration. It is often said that solid-phase extraction resins combine the metal selectivity of liquid-liquid solvent extraction with the operational benefits of packed bed ion exchange (Warshawsky, 1981, Cortina *et al.*, 1997). Some of the seminal work in synthesizing the first variants of this material was performed by Small (1961), Fritz *et al.*, (1971) and Spevackova *et al.*, (1970) wherein organic polymers were used as solvent supports for analytical separations. Further pioneering work was done by Warshawsky (1974, 1978) and Grinstead *et al.*, (1974) who investigated solvent-impregnated resins for use in hydrometallurgical and effluent treatment applications.

   Solid-phase extraction has become an accepted separations technology in pharmaceutical and analytical organic chemistry applications. Over the last twenty years it has also gained wide acceptance in radioanalytical

methods for effecting very clean separations of various radionuclides, especially lanthanides and actinides. The technology of solid-phase extraction was, however, in its infancy when much of the industrial-scale separation schemes were developed for reprocessing nuclear fuel. Thus, it has not been implemented at large scales for this purpose to any significant degree. Nonetheless, liquid solvent extraction techniques for partitioning the transactinide (An) and lanthanide (Ln) elements are fairly well understood and it follows that solid supported extractants may offer beneficial improvements for select portions of fuel reprocessing flow sheets. The technology has been steadily improved and has reached a level of maturity for analytical and smaller-scale applications. It is therefore the objective of this chapter to discuss the applications and potential merits of solid-phase extraction technology for separating the common actinide and lanthanide isotopes specific to nuclear fuel reprocessing.

13.2   Basic methodology of solid-phase extraction

First, let us provide a more descriptive definition of solid-phase extraction for the purposes of this discussion. Solid-phase extraction refers to a liquid, semi-liquid or potentially solid complexing agent dispersed more or less homogeneously within an inert, solid medium. A solid-phase extraction material comprises three major components: a solid support or substrate (typically inert polymer), a stationary extractant phase, and a mobile fluid phase (e.g., conditioning, feed, wash, or strip solution). The three phases of a solid-phase extraction resin are depicted in Fig. 13.1.

Various materials have been used for the solid support, e.g. inorganic materials such as silica gel, organic polymers such as polystyrene-divinyl-benzene copolymers and polymethacrylate resins, or resins made of both organic and inorganic materials. The stationary phase is typically an organic extractant, many of which have been well characterized for their use in liquid-liquid extraction. Similar to liquid-liquid extraction, the target metals are converted from the hydrated ionic form to a neutral organophilic metal complex within the stationary phase. The solid-phase extraction material is made in the form of small beads. Although different in terms of functionality, the beads are similar in size and shape to those used in conventional ion exchange practice and can be used in a fixed bed or column arrangement. The solid-phase extraction resin has many of the operational advantages of ion exchange processes and similar methods for modeling and engineering scale-up may also be used as discussed in a later section. The solid-phase extraction resin may, however, provide certain benefits over conventional ion exchange resins that are attractive to the separations scientist or chemical engineer. Potential advantages of solid-phase extraction are summarized as follows:
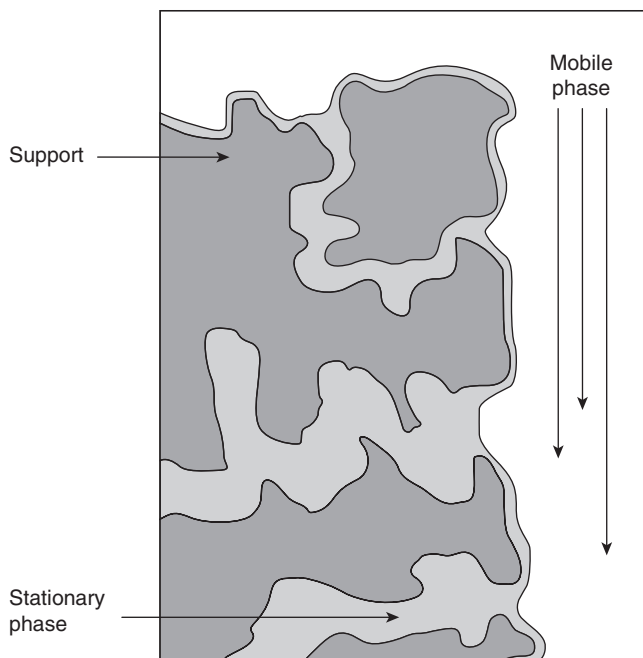
13.1 Three phases of solid-phase extraction resin.

- Selectivity: recent and continuing advances in the synthesis of organic extractants provide numerous options for highly selective An and Ln separations, most especially from dilute streams of high ionic strength.
- Solvent loading: the utilization of macroporous resins can yield higher specific mass loadings of the complexing molecule relative to functionalized ion exchange resins.
- Cost: simple immobilization of complexing agents or extractants within an inert polymer may prove to be a less costly preparation route than the complex synthesis mechanisms of covalently linking a specific functional group to the backbone of the resin.

There are, however, some potential disadvantages of the solid-phase extraction approach which are discussed in a later section.

13.2.1 Methods for the preparation of solid-phase extraction media

There are numerous variants of producing solid-phase extraction material, but the most widely used techniques are based on the physical adsorption of the extractant into the pores of the support material. The preferred

method for incorporating the chosen extractant into the support is often dependent upon the type of extractant-metal complex and is therefore determined by the intended separation process. Preparation routes reported in the literature during the last forty years primarily involve adsorbing the extractant into the lattice of a polymer substrate – known as impregnation methods – or adding the extractant to a mixture of monomers during the bead polymerization process, i.e. the well-known Levextrel resins which incorporate the extractant in polystyrene-divinlybenzene during the copolymerization step (Kauczor *et al.*, 1978, Poinescu *et al.*, 1985, Ionue *et al.*, 1987, Yoshizuka *et al.*, 1990). Other techniques such as adsorbing the extractant in silica gel, silica and organic polymer mixtures or adding the extractant to a dissolved polymer and then precipitating the mixture have also been reported. Excellent reviews of the classical preparation techniques have been presented by Warshawsy (1981) and Cortina *et al.*, (1997) and the reader is directed to these works for detailed descriptions of the synthetic methods. Variants of the classical impregnation methods have received the most recent attention in terms of developing solid-phase materials with extractant systems relevant to An and Ln separations. A brief review of the impregnation methods is therefore germane to this work in order to familiarize the reader with this production scheme.

Recalling the assumption that a solid-phase extraction resin represents a complexing agent dispersed homogeneously within a solid polymeric medium, the impregnated extractant should behave as in liquid-liquid extraction, but maintain a strong affinity for the solid polymer matrix. In order to approximate these criteria, Warshawsky (1981) presents the following requirements for the extractant, polymeric support, and the impregnation process:

- The extractant should be a liquid or retained in the liquid state by the addition of an appropriate diluent.
- The extractant should have a very minimal solubility in the aqueous solution containing the solute to be extracted.
- The polymeric support should be fully expanded and remain so during the impregnation process – macroporous polymers exhibit minimum volume variations during impregnation and are therefore preferred.
- The impregnation process should not have a deleterious effect on the properties of the extractant or polymer.

Previous reviews by Warshawsy (1981) and Cortina *et al.* (1997) have classified the methods for producing extractant impregnated resins as follows:

- Dry impregnation – this is the most often used method wherein the extractant, or extractant diluted with an appropriate organic diluent, is

contacted with the polymer in batch mode for a period of time necessary to obtain maximum saturation of the extractant within the polymer pores. The diluent is then removed via vacuum evaporation resulting in a two-component, polymer-extractant material.

- Wet impregnation – an extractant or extractant and diluent is adsorbed into the polymer as described above, but the water-immiscible organic diluent is not removed by evaporation.

- Modifier addition method – a modifier is added to the extractant-diluent and the mixture is adsorbed into the polymer as described in the above methods. The diluent is then removed by evaporation, leaving a polymer-extractant-modifier resin. The chosen modifier is typically more polar than the extractant and is added to enhance water penetration into the porous network of the polymer.

Of course, slight modifications to these methods may be used depending on the desired application of the solid-phase extraction material. The dry method is preferred for impregnating the more hydrophilic extractants such as amines, ketones, and esters and is the most used technique for making solid-phase extractants applicable to An or Ln separations. The preparation of a small batch of resin using the dry impregnation method is shown in Fig. 13.2.

It should also be noted that the class of inert, macroporous or macroreticular polymers have become the most widely used substrates in the contemporary synthesis of solid-phase extraction media for separating the An

13.2 Resin preparation via dry impregnation – diluent evaporation step.

and Ln elements (Horwitz *et al.*, 2006). These polymeric macroporous resins have a rigid three-dimensional structure that provides minimum solvent swelling during the impregnation process. The inert macroporous resins are also capable of adsorbing large amounts of the extractant due to a high specific surface area (500–900 m^2/g) and typical porosity fraction ranging from 0.4 to 0.6 (Van Hecke *et al.*, 2006). The macroreticular polymers are typified by a continuous gel phase and a continuous pore phase and are manufactured with varying degrees of hydrophobicity. Thus the specific polymer can be matched with the properties of a given extractant to optimize the hydrophobic/hydrophilic balance. This is important in the solid-phase extraction media since the goal is to minimize losses of the extractant to the aqueous phase while maintaining enough hydrophilicity to maximize mass transfer of the solute into the resin pores and between phases. Examples of the macroreticular polymers frequently used are the non-ionic Amberlite XAD and Amberchrom CG series resins.

   Most studies support the assumption that immobilization of the extractant on the internal surface of the macroporous, inert resins is a combination of adsorption via van der Waals forces (Hommel *et al.*, 1983, Bobozka *et al.*, 1985, Cote *et al.*, 1987, Handley *et al.*, 1991, Cortina *et al.*, 1994a, Cortina *et al.*, 1993, Villaescusa *et al.*, 1992) and potentially physical trapping of the ligands within the pores of the resin beads (Handley *et al.*, 1991). Impregnation of the extractant within the stationary phase is considered to be a combination of pore filling and surface adsorption. The extractant first fills the pore space beginning with the smallest pores and moving up to pore sizes of approximately 10 nm. Surface adsorption then becomes the dominant retention mode in the larger pores (Guan *et al.*, 1990). Although it is not yet possible to perform a precise *a priori* prediction of the adsorptive and retention properties of a given ligand-polymer system, the hydrophobic or non-polar sections of a ligand molecule are generally attracted to hydrophobic polymers and the hydrophilic or polar molecules to hydrophilic surfaces. For example, the non-ionic, hydrophilic XAD-2 and XAD-4 resins (Amberlite) are often used with many of the ligands important to An and Ln separations because the non-polar vinyl and styrene groups of the polymeric matrix serve to anchor the extractants through their alkyl chains and/or aromatic rings, while the functional groups in the ligand remain capable of forming the desired metal complex (Fig. 13.3). This has been shown by various studies (Bobozka *et al.*, 1985, Cote *et al.*, 1987, Cortina *et al.*, 1994a, Cortina *et al.*, 1993) wherein the authors concluded that this weak interaction between the extractant molecules and the polymer support is the primary mode of ligand retention, but does not adversely affect the complexing characteristics of the extractant.
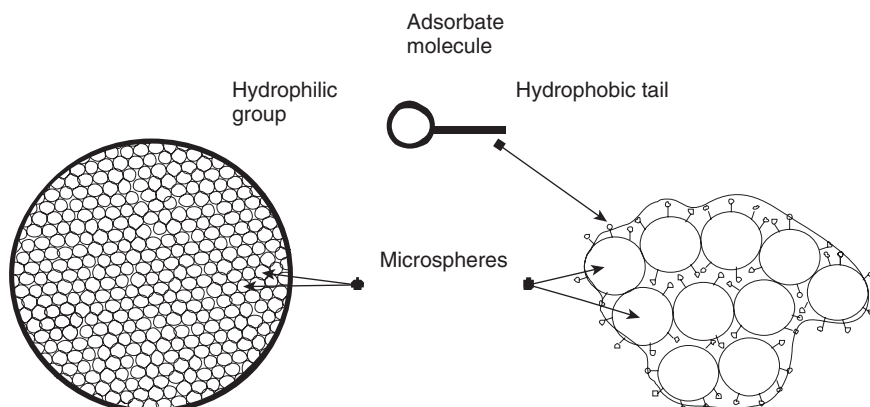
13.3 Depiction of ligand arrangement on polymer substrate.

13.3   Solid-phase extraction sorbents for actinides and lanthnides

A number of extractants for partitioning An and/or Ln elements from dissolved nuclear fuel solutions or accompanying waste streams have been developed or improved upon during the past twenty years. The extractants are generally classified on the basis of structure, extraction and stripping chemistry, and the type of metal complex formed (Sudderth *et al.*, 1986). The four primary groups are: solvating or neutral extractants, chelating extractants, organic acid extractants and ion pairing extractants. They can be further divided into those that co-extract the An(III,IV,VI) and Ln elements and those that are more selective for the trivalent An(III) and Ln(III) species. Examples of the former are the bi-dentate Octyl(phenyl)-N,N-diisobutylcarbamoylmethylphosphine oxide (CMPO, Fig. 13.4) and N,N′-dimethyl-N,N′-dibutyl-2–2-tetradecylmalonamide (DMDBTDMA, Fig. 13.5) extractants, which are the basis of the well-known TRUEX (TRansUranium EXtraction) and DIAMEX (DIAMide EXtraction) processes, respectively.

The development of CMPO was the result of numerous investigations aiming to combine phosphine oxide or neutral phosphonate functional groups with carbamates (Horwitz *et al.*, 1985, Schulz *et al.*, 1988, Schulz *et al.*, 1982, Gatrone *et al.*, 1987a, Gatrone *et al.*, 1987b). The CMPO ligand exhibits excellent extraction properties in nitric acid and diluents that are compatible with a conventional PUREX process. It has been the subject of much study over the last two decades and represents one of the most characterized reagents for total actinide separations from nuclear waste streams (Mathur *et al.*, 2001). A primary disadvantage of the TRUEX process is that
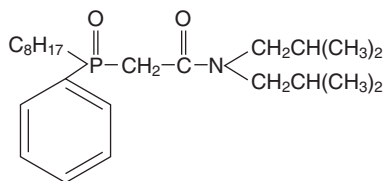
13.4 Chemical structure of CMPO ligand.
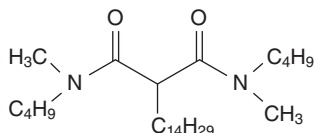
13.5 Chemical structure of DMDBTDMA ligand.

the polar solvent modifier tributyl phosphate (TBP) must be added to reduce hydrolytic and radiolytic degradation of CMPO, improve acid dependences and to prevent third-phase formation. This results in a large phosphorus content which translates into a significant phosphorus residue requiring disposal if incineration is used for solvent destruction. It should be noted that, although the use of reagents that leave no solid residue when incinerated is a reasonable objective, the favorable aspects of organophosphorus extractants may justify a phosphorus ash compatible waste form such as phosphate glass (Van Hecke *et al.*, 2006). In an effort to eliminate the phosphorus ash, French scientists have championed the CHON principle for designing extractants, which means they consist only of C, H, O and N atoms. They may therefore be incinerated to gaseous products and avoid the contaminated solid residue that results from combustion of phosphorus extractants. The malonamide-based extractants (e.g., DMDBTDMA) meet the CHON criteria and are known to be some of the best bidentate diamide ligands (Sasaki *et al.*, 2002).

Variations of extractants with soft donor atoms (N, S) have been proposed for partitioning the group III An elements (Am, Cm) from Ln elements. Examples are the dithiophosphinic acid extractants such as the commercially available Cyanex 301 (Sole *et al.*, 1993, Modolo *et al.*, 1998a, Modolo *et al.*, 1999, Zhu *et al.*, 1996b, Zhu *et al.*, 1996a, Hill *et al.*, 1998). The above mentioned extractants, and numerous others at various stages of maturity, have been documented quite well and the reader is referred to the literature for the applications, advantages and disadvantages of each. Recent reviews are given by Mathur *et al.*, (2001) and by Van Hecke and Goethals (2006).

13.3.1 Established solid-phase extraction resins for actinides and lanthanides

Researchers in the field of solid-phase extraction have sought to exploit the extraction and partitioning characteristics of the extractants often utilized in liquid-liquid extraction by fixing them onto various substrates as discussed in the previous section. Although the field is not new to separation scientists, the use of solid-phase extraction for radiochemical separations is, relatively speaking, a more recent application of the technology. As such, there are very few examples of its use at technical or even pilot scales. The greatest application of solid-phase extraction pertaining to An and Ln partitioning has been in the performance of very pure separations for analytical and radio-analytical chemistry. A very robust suite of these resins has been developed by E.P. Horwitz and co-workers and is sold commercially by EIchrom Technologies Inc., Darien, Illinois. These resins have come to be the primary separation tool in many radiochemistry laboratories over the last two decades and are also gaining substantial acceptance in the field of radio-pharmaceutical chemistry. Many technologists have recognized the potential benefits of employing the technology for treatment of primary and secondary streams in nuclear fuel reprocessing. However, the use of solid-phase extraction technology at the industrial scales necessary for nuclear fuel and/or waste processing involves a number of issues not encountered in very small-scale processes. Potential advantages and disadvantages associated with solid-phase extraction technology for use at nuclear industrial scale are addressed in a later section; however, predominate questions include performance, robustness, and economics of the technology as compared to conventional (e.g., liquid-liquid extraction) or other mature processes. Several investigations have been performed with a small number of established solid-phase extraction sorbents using feed solutions from actual process streams in an effort to obtain data for comparison to conventional process methods. European scientists (Eschrich *et al.*, 1980) evaluated a variant of the PUROCHROMEX (Plutonium Uranium Recovery On CHROMatographic EXtraction columns) process designed primarily for the recovery of uranium and plutonium (Eschrich *et al.*, 1968). The chromatographic column process consists of a silica gel column followed by three TBP solid-phase extraction columns in series. The solid-phase extraction columns used in their investigations were the commercial Levextrel-TBP resins (Lewatit CA 9221, OC1023 – Bayer AG) consisting of 60 wt.% TBP on inert polystyrene-divinylbenzene copolymer beads. A process flow diagram of the PUROCHROMEX process is shown in Fig. 13.6.

A feed solution of dissolved light water reactor (LWR) fuel, adjusted to 5–6 M HNO_3, was introduced via the silica gel columns which retain highly
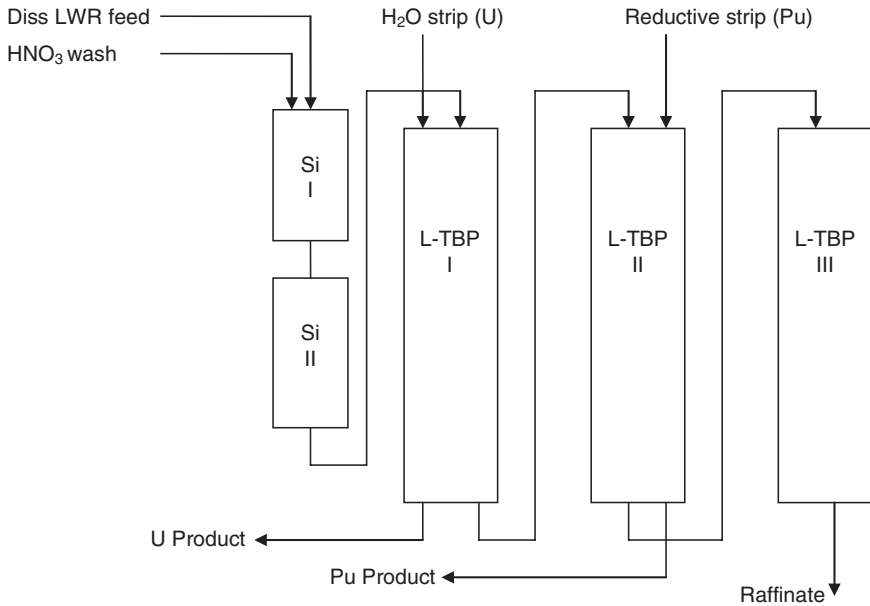
13.6 PUROCHROMEX process flow diagram (Eschrich and Ochsenfeld, 1980).

active undissolved fuel particles, in addition to 50–90% of the zirconium/niobium and more than 60% of the antimony (Van Ooyen *et al.*, 1964, Eschrich *et al.*, 1970). This step was continued until uranium breakthrough was detected by on-line monitors. The train was then washed with 5.7 M HNO_3 to remove unextracted fission and activation products from the system. The authors indicate that, in most cases, uranium is retained by the first TBP column and plutonium by the second, with the third column acting as a polisher. Uranium was eluted from the first column with a few bed volumes of distilled water. Plutonium was removed from the second TBP column via standard reductive stripping, i.e., by eluting with a reducing agent (e.g., dilute solutions of hydrazine or ferrous sulfamate) and converting extractable Pu(IV) to the non-extractable Pu(III) species. Tests were performed with this process and various modifications using solutions of dissolved LWR fuel and different column sizes ranging from 10 to 1000 mL. The authors report single-cycle beta-gamma decontamination factors on the order of 10^7 for the column I uranium product and 10^4–10^5 for the plutonium product stripped from column II. Plutonium contamination of the uranium fraction was insignificant, but uranium carryover in the plutonium product did occur in most cases necessitating further purification of the plutonium fraction. However, some carryover of uranium in the plutonium fraction may actually be beneficial in light of contemporary concerns with

producing pure plutonium and the potential proliferation issues. A mixed plutonium-uranium product may also be compatible with a mixed oxide (MOx) fuel fabrication scheme if the proper ratio can be maintained.

The data from the small-scale PUROCHEOMEX tests are certainly promising although information regarding column performance vs. total throughput was not provided. Problems due to the radiolytic and hydrolytic degradation of the sorbent material were, however, noted and the authors indicate that the availability of a more resistant support would increase the attractiveness of this process.

Lumetta and co-researchers (Lumetta, *et al.*, 1993) investigated the utility of commercially available TRU resin (EIChrom Industries Inc., Darien, Illinois) for use in separating americium and plutonium from actual neutralized cladding removal waste (NCRW) taken from a radioactive waste tank at the US Department of Energy's (DOE) Hanford Site. The TRU chromatographic resin consists of 13% CMPO and 27% TBP adsorbed onto Amberchrom™ CG-71 (Barney *et al.*, 1992) and can be used for the separation of transuranic elements. The NCRW sludge was washed and dissolved in HNO_3-HF to provide a feed solution of composition shown in Table 13.1.

A small aliquot of feed solution (11 mL) was passed through a preconditioned column containing 500 mg of TRU resin. The bed was washed with 2 M HNO_3 and then eluted with 5 mL of 0.01 M HNO_3 followed by 5 mL of 0.01 M 1-hydroxyethane-1,1-diphosphonic acid (HEDPA). The functional ligands in TRU resin are the same extractants used in the TRUEX liquid extraction process, which consists of 0.2 M CMPO and 1.4 M TBP in

Table 13.1 Composition of dissolved NCRW sludge (Lumetta *et al.*, 1993)

Element	Feed I	Feed II	Feed III
	Conc. M	Conc. M	Conc. M
Al	4.1E-3	3.1E-3	1.29E-1
Ba	2.5E-5	2.0E-5	8.9E-5
Ca	1.2E-3	1.0E-3	2.0E-3
K	4.2E-3	3.3E-3	7.7E-3
Na	2.28E-1	1.83E-1	5.87E-2
Si	1.1E-3	6E-4	1.9E-3
Sr	6.3E-6	7.4E-6	9.9E-6
U	6.6E-3	<1E-3	3.4E-3
Zr	1.89E-1	1.53E-1	1.35E-1
F-	3.5E-1	2.9E-1	2.7E-1
H+	1.6	3.5	1.7
Pu	7.8E-2	na[1]	na
Am	4.2E-2	na	na

1. na – not analyzed.

a normal paraffin hydrocarbon diluent (Horwitz *et al.*, 1985). The authors noted that the separation properties of the TRU resin should be similar to those seen with the TRUEX process. The average decontamination factors for Am and Pu were however substantially lower than those achieved with the TRUEX process and dissolved NCRW feed solution (Swanson, 1991). The authors concluded that this was a result of a higher resin affinity for the U as well as some competition from the uncomplexed Zr present in the feed solution. The small mass of solid-phase extraction material used was not sufficient to accommodate loading by U and Zr and did not correlate with the amounts of CMPO available for TRU metal complexation in the TRUEX process. It was noted that the competition from Zr could be reduced by adding a complexing agent to the feed (e.g., fluoride ion). Uranium loading is problematic since increasing the amount of TRU resin to provide enough CMPO capacity to accommodate U loading would be quite expensive at large scale. However, the TRU resin may be a viable option for separating Pu and Am provided the U is first removed from the NCRW solution by some other means (Lumetta *et al.*, 1993).

13.3.2 Novel solid-phase extraction resins for actinides and lanthanides

Separation of An(III) from Ln(III) elements

Separation of Am and Cm, known as the minor actinides (MA), from the fission Ln elements is a key goal of several countries seeking to substantially reduce the mass of radionuclides requiring long-term disposition in a geological repository. The implementation of a partitioning and transmutation technology necessitates the removal of the Ln elements because of relatively large neutron capture cross sections and incompatibility with proposed transmutation targets. The separation of the MA from Ln is, however, a difficult chemical separation to achieve as there are minor differences in the chemical properties of these elements. Studies in recent years have shown that ligands containing soft donor atoms such as N and S offer a higher probability of being more selective for An(III) elements (Kikuchi *et al.*, 2004, Zhu, 1995, Modolo *et al.*, 1998b, Wei *et al.*, 2000a, Iki *et al.*, 1998, Morohashi *et al.*, 2001, Mathur *et al.*, 2001). Although the exact mechanism for this preferential complexing behavior has not been entirely elucidated, many researchers are investigating the merits of using soft donor ligands in solid-phase extraction to perform An(III) separations from Ln(III) elements in high level liquid waste (HLLW) solutions subsequent to upstream removal of U and Pu.

The N-donor ligand, 2,6,-bistriazinylpyridine (BTP) has shown promise for separating An(III) from Ln(III) via differing nitrate dependencies in
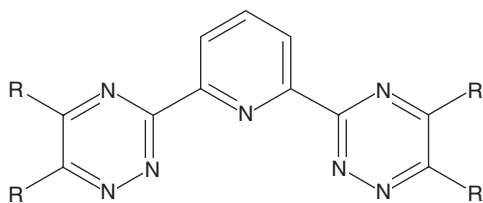
13.7 Chemical structure of BTP ligand; R = *n*-C₃H₉, R = *iso*-C₃H₉.

Table 13.2 Separation factors between Am and Ln(III) in NaNO₃ (Hoshi *et al.*, 2006)

NaNO₃ M	Ce(III)	Nd(III)	Gd(III)
0	>1E3	>1E3	8.82E1
1	>4E3	3.35E2	2.32E1
2	1.04E4	1.64E3	3.92E2
3	2.49E3	5.14E2	9.41E1
4	9.71E2	3.44E2	1.13E2

solutions of moderate acidity (pH ~2). The solubility of the ligand can also be modified via the addition of alky chains. The functionalized forms 2,6-bis-(5,6-dibutyl-1,2,4-triazine-3-yl)-pyridine (*n*-Bu-BTP or *iso*-Bu-BTP) have been synthesized (Fig. 13.7) and a solid-phase extraction material developed by impregnating *n*-Bu-BTP into a silica-co-polymer support (Wei *et al.*, 2004a, Wei *et al.*, 2000b, Hoshi *et al.*, 2006).

The silica co-polymer (SiO₂-P) support is prepared by polymerizing a mixture of formylstyrene and divinylbenzene monomers saturated within the pores of spherical silica particles resulting in 17.6% (w/w) co-polymer embedded in SiO₂. The *iso*-Bu-BTP ligand (2.5g) was incorporated into the SiO₂-P support (5g) via the dry impregnation method and the material tested in batch and small (20 cm³ bed) column tests (Hoshi *et al.*, 2006). Excellent decontamination of Am, Cm, and heavy Ln(III) elements from fission products and light Ln(III) elements was achieved using a simulated HLLW solution (w/o U, Pu) containing 1 M NaNO₃–0.01 M HNO₃. Heavy Ln(III) elements were removed from the column with 0.3 M NaNO₃–0.01 M HNO₃. The strongly sorbed An(III) elements were then eluted from the column by reducing the nitrate concentration with pure water. The resulting separation factors between Am and Ln(III) are listed in Table 13.2.

The observed nitrate dependency of An(III) and Ln(III) extraction by BTP may thus be exploited by the addition of nitrate salts and is quite promising. Batch tests were also performed to examine the stability of BTP against nitric acid. The authors (Hoshi *et al.*, 2006) determined that
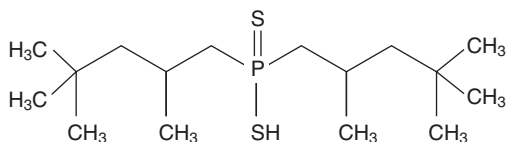
13.8 Chemical structure of Cyanex-301 ligand.

extractant losses increase with increasing nitric acid concentration due to protonation and that branched *iso*-Bu-BTP shows more acid stability than *n*-Bu-BTP. The acid effects may not be an insurmountable issue since the material is used at very low acid concentrations.

A biopolymer microcapsule containing Cyanex 301 (bis(2,4,4-trimethyl-pentyl)dithiophosphinic acid) extractant has been reported by Mimura *et al.*, (2001). The solid phase extraction resin was prepared by mixing the extractant with 1–2.5% (w/w) sodium alginate and then adding drop-wise to 0.5 M nitrate salt solution or 1 M HCl. The beads were allowed to harden in the bath overnight and then filtered and dried. The resin was tested in a small (4.9 cm^3) chromatographic column and the researchers were able to achieve a separation factor of 20 between Am and Eu in a pH range of 1–2 using freshly made resin (<1 day old).

A satisfactory separation of Am from Ln(III) elements with newly pre-pared Cyanex 301-SiO$_2$-P resin has also been reported (Wei *et al.*, 2000b). However, similar testing with 4-week old resin did not produce an accept-able separation between Am and Ln(III). These authors concluded that oxidation impurities formed in the Cyanex 301 are responsible for the poor separation and that methods for stabilizing the extractant are needed. The structure of the Cyanex 301 compound is shown in Fig. 13.8.

A solid-phase extraction resin for separating MA from Ln(III) elements has been prepared by impregnating p-*tert*-butylthiacalix[4]arene com-pounds in a SiO$_2$-P support (Kikuchi *et al.*, 2004) The structure of the ligands (CAPS, CAPS-SO$_2$) is shown in Fig. 13.9.

Batch contacts performed with the CAPS, CAPS-SO2-SiO$_2$-P resin did not show any measureable extraction of Am or Ln elements at pH = 2. However, raising the solution pH to 4 resulted in a separation factor of 10 for Am over Nd and Eu with the CAPS-SiO$_2$-P resin. A separation factor of 500 for Am over Nd and Eu was achieved with CAPS-SO2-SiO$_2$-P resin in tests at the higher pH. A proposed flow sheet for separating the MA is shown in Fig. 13.10.

The effects of gamma radiation on SiO$_2$-P particles loaded with Cyanex 301, CAPS and CAPS-SO2 were evaluated by irradiating the resin particles to a dose of 1 MGy in a weak acid (pH = 4) at ambient temperature (Kikuchi *et al.*, 2004). The irradiation caused a 30% degradation of the Cyanex 301 exchanger and an increased retention of Eu, thus substantially
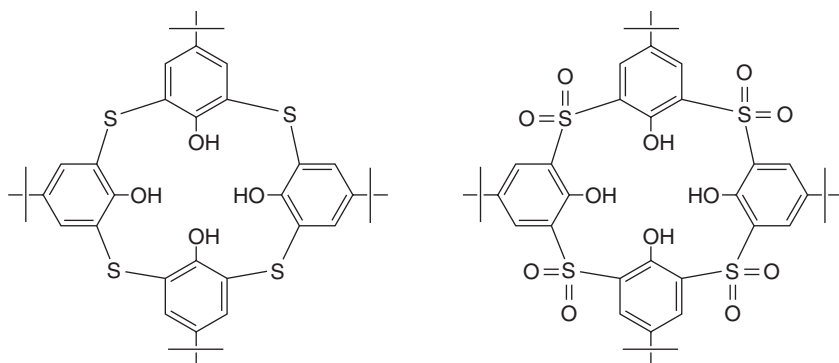
13.9 Chemical structure of CAPS and CAPS-SO2 ligands.
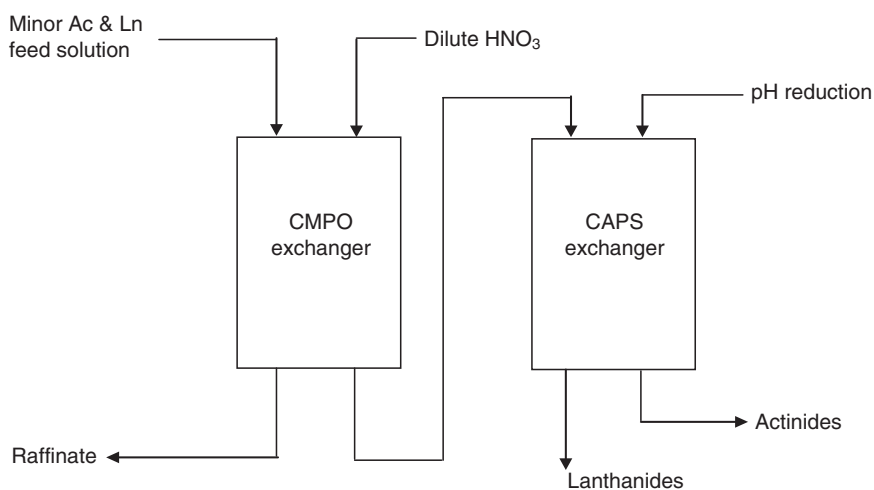
13.10 Potential flow sheet for Ac/Ln separation.

reducing the separation ability between Am and Eu. The irradiation resulted in only 1% degradation of CAPS-SO2-SiO$_2$-P exchanger and the high separation factor of Am relative to Nd and Eu remained constant during and following irradiation. Irradiation of the CAPS-SiO$_2$-P exchanger also produced an increased distribution coefficient for Am. The authors suggest that the sulfur in the CAPS ligand was oxidized during irradiation to become sulfonyl groups, i.e. fully or partially transforming it to CAPS-SO2, which they postulate is the factor contributing to a higher Am selectivity. Although confirmatory analytical data are not given, the hypotheses are certainly credible and merit more detailed investigation.
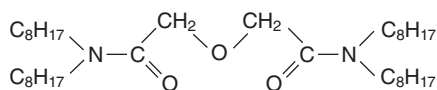
13.11 Chemical structure of TODGA ligand.

Group separation of An(III) and Ln(III) elements

A recently developed tridentate ligand, N,N,N′,N′-tetraoctyl diglycolamide (TODGA) is a promising extractant being considered for the separation of An(III) and Ln(III) from HLLW solutions (Sasaki *et al.*, 2001, Narita *et al.*, 1998, Sugo *et al.*, 2002, Tachimori *et al.*, 2002). The tridentate functionality provided by the additional etheric oxygen has led a number of researchers to consider TODGA over the commonly used neutral diamides with bidentate properties (Ansari *et al.*, 2005). The TODGA ligand structure is shown in Fig. 13.11.

Hoshi *et al.*, (2004) evaluated the use of TODGA impregnated SiO_2-P solid-phase extraction resin for performing group separation of MA and Ln elements from HLLW. This is one step in the proposed ERIX (Electrolytic Reduction and Ion eXchange) process for reprocessing spent fast breeder reactor mixed oxide fuel (FBR-MOX). Column tests using simulated HLLW showed that group separation of Am and some Ln elements relative to other fission products was satisfactory. Zirconium, Ru, Sr, and Y were also extracted; however, all were effectively separated from the An/Ln elements using appropriate elution schemes, i.e. using different concentrations of HNO_3 and oxalic acid for Zr. The authors found the uptake and elution kinetics of Ru to be slow compared to the other elements and were only able to recover 85% of the Ru fed to the column. The loss of TODGA to the aqueous phase was also investigated and the researchers concluded that <0.02% (w/w) of the extractant was lost during one separation cycle.

A solid-phase extraction resin consisting of 30% (w/w) TODGA and 10%(w/w) TBP adsorbed onto Amberchrom CG-71 was evaluated for the separation of An and Ln elements from a simulated PUREX raffinate solution (Modolo *et al.*, 2007). The simulant represented a PUREX raffinate (5000 L/t HM) from fuel having an initial [235]U enrichment of 3.5%, 33 000 MWd/tHM burn-up, and a 3-year cooling period. Small column (22.9 cm^3) studies indicated that the An and Ln elements could be effectively separated from the light fission products using four nitric acid scrubbing steps followed by a strip with 0.01 M HNO_3 and a H_2O wash. Oxalic acid and HEDTA were also included in the first and second scrub steps to effect the complete removal of Zr and Pd from the column. Similar to comparable investigations (Hoshi *et al.*, 2004), a portion of the Ru remained on the resin, as well as a small fraction of Cf and Y. It was noted that this

issue needs further investigation and that a more radiolysis resistant substrate (e.g., silica) may also be needed for large scale applications.

Various flow sheets using CMPO and TODGA sorbed onto SiO2-P have also been proposed and tested for partitioning An(III) and Ln(III) elements as part of the proposed Minor Actinides RECovery (MAREC) process based on solid phase extraction. (Zhang *et al.*, 2004, Wei *et al.*, 2004b, Zhang *et al.*, 2005c, Zhang *et al.*, 2008). The stability of the TOGDA-SiO$_2$-P resin as a function of nitric acid concentration, temperature and γ-radiation was investigated by Zhang *et al.*, (2005a). The authors evaluated the effects of these parameters by comparing the batch adsorption of Nd onto the resin. Nitric acid concentrations up to 3M did not decrease the adsorption properties of the resin at 25ºC. The capacity of the resin was, however, reduced by approximately a factor of three in 3 M HNO$_3$ at 80ºC, presumably due to losses of the extractant to the aqueous phase as evidenced by an increased total carbon concentration in the aqueous fraction. Irradiation of the resin from approximately one to four MGy resulted in a linear decrease in extraction capacity. The highest dose (4.1 MGy) resulted in a 70% reduction of capacity, which was also determined to be from extractant losses. Studies to quantify these losses as intact TODGA molecules or its radiolysis products were inconclusive. Similar investigations were conducted by these researchers (Zhang *et al.*, 2005b) to assess the effects of HNO$_3$, temperature and γ-radiation on CMPO-SiO$_2$-P solid phase extraction resin. Nitric acid (up to 3 M) and increased temperature (80 °C) did not cause a significant decrease in capacity for Nd. The γ-radiation experiments indicated a linear decrease in capacity, with an approximate decrease of 50% at the maximum dose of 4 MGy.

Other solid-phase extraction resins with An and Ln separation capabilities

Efforts to produce a solid-phase extraction media applicable to separations in the Th-U fuel cycle have led to several interesting materials. An amide grafted polymer, p-amino-N,N-dihexylacetamide (ADHA), anchored on high surface area Amberlite XAD-16 resin has been synthesized and characterized by Maheswari and Subramanian (2005). The ADHA ligand was reacted with aminated XAD-16 resin (AXAD-16), in the presence of anhydrous K$_2$CO$_3$ dissolved in dimethyl formamide, to form the AXAD-16-ADHA solid phase extraction resin. The novel material was tested with a synthetic nuclear acidic waste solution to evaluate its efficacy for separating U(VI) and Th(IV). Multiple bench-scale column tests showed the grafted resin matrix to be very effective at partitioning U(VI) from Th(IV) and Ln(III) elements in nitric acid. The Th(IV) and Ln(III) elements were completely washed from the column with 0.1M HNO$_3$ and U(VI) was quantitatively stripped with 0.1 M (NH$_4$)CO$_3$. It is also interesting to note
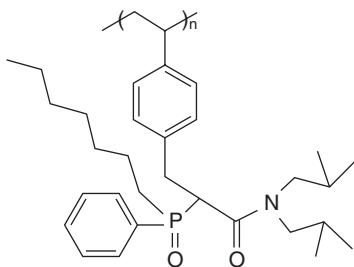
13.12 Chemical structure of MCM-CMPO resin.
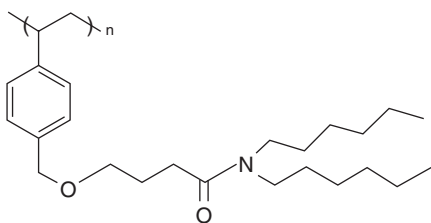
13.13 Chemical structure of AXAD-16-EDHBA resin.

that all metals could be completely removed from the column with de-ionized water. Raju and Subramanian (2005, 2007a, 2007b) and Maheswari and Subramanian (2005) have used similar grafting techniques to attach other ligands, such as CMPO, dimethyl amino-phosphono-methyl phosphinic acid (DAPPA), N,N,-di-hexyl succinamic acid (DHSA) and 4-ethoxy-N,N-dihexylbutanamide (EDHBA) to Merrifield chloromethylated (MCM) or AXAD-16 polymer resins. The authors report the physicochemical properties of these grafted ligand-polymer resins and performed bench-scale tests to evaluate their utility for effecting various U, Th and Ln(III) element separations. Chemical structures of the MCM-CMPO and AXAD-16-EDHBA resins are shown if Figs 13.12 and 13.13, respectively.

In each case, the solid-phase extraction resins derived from grafting the desired ligand to a polystyrene-di-vinyl benzene support showed rapid diffusion kinetics and high capacity for the target metals. Columns of the grafted resins were tested for up to 20 loading-elution cycles without showing significant degradation in performance.

A method for immobilizing CMPO within a polyacrylonitrile (PAN) polymer has been reported (Kamenik *et al.*, 2006, Tranter *et al.*, 2003, Mann *et al.*, 2002). The CMPO and PAN polymer are dissolved in concentrated HNO_3 or dimethyl sulfoxide and subsequently sprayed through a nozzle into a water bath to precipitate solid-phase extraction beads of a desired size range according to methods published by Sebesta (1997). It is posited
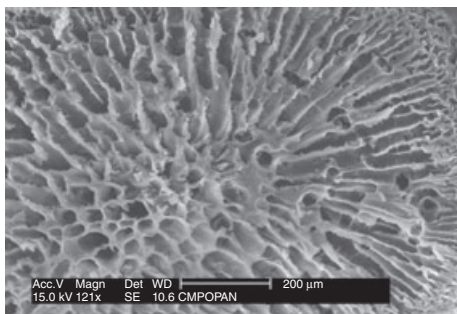
13.14 SEM image: cross section of CMPO-PAN bead (Tranter *et al.*, 2003).
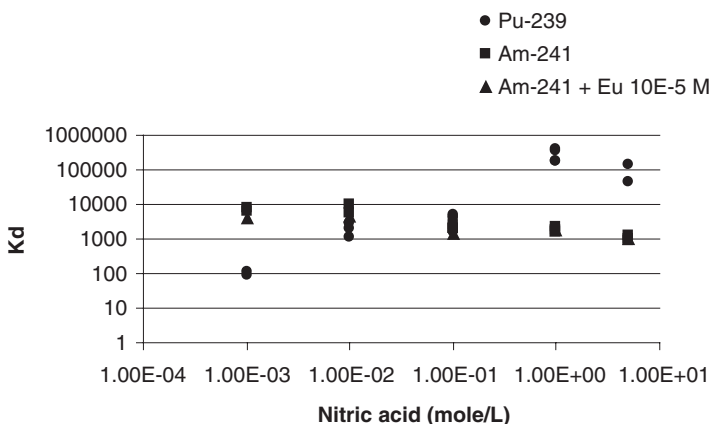
13.15 Isotherm batch contacts with Am and Eu on CMPO-PAN showing high Kd at low [HNO₃] (Mann *et al.*, 2002).

that the CMPO exists as a finely dispersed solid trapped within the PAN matrix. Loadings of approximately 30% (w/w) CMPO in the polymer were obtained and the highly porous structure of the polymer composite facilitates mass transfer. A scanning electron microscopy (SEM) image of the CMPO-PAN composite is shown in Fig. 13.14.

Batch experiments with simulated acidic waste solutions showed good kinetic properties and high distributions for the An and Ln elements tested. Nitric acid dependencies for the An(III) and Ln(III) elements, however, differed from those seen with CMPO in the TRUEX process or CMPO on solid supports, with or without TBP. Distribution coefficients for these elements on the CMPO-PAN material remained higher than 10^3 mL g^{-1} at 10^{-3} M HNO$_3$ as shown in Fig. 13.15. Work to explain this behavior is

ongoing, but it suggests some interesting separation schemes may be possible.

13.4   Modeling of solid-phase extraction systems

The standard approach in the development of a mathematical model for any separations scheme is to begin with the equations of mass continuity and then add additional terms (e.g., equations for equilibrium, mass transfer and reaction kinetics) as needed to accurately describe a specific process. Models developed from first principles are much more flexible than those obtained by regression or simply searching for equations that give the best 'fit' to empirical data. Since they are derived from fundamental principles and ensure energy and/or mass continuity, they can be used to estimate performance when system parameters are changed without the constraint of maintaining dynamic similitude. Nonetheless, the model must be validated or compared to actual performance data in order to assess accuracy and/or modify terms to increase model robustness. Ideally, multiple iterations of this comparison are done for a range of operating parameters. This provides data for refinement and serves to increase confidence in the model and validate its utility for predictive purposes. The extent of this validation process is normally determined by several factors such as model complexity, availability of published material relating to similar models and systems, and the required accuracy of the model in terms of economic, safety and regulatory drivers. From an engineering perspective, modeling solid-phase extraction is quite similar to that of other separation processes wherein solutes are separated from a flowing fluid stream onto particles packed within a column (e.g., adsorption or ion exchange). Contacting the moving fluid with a stationary solid phase is often chosen for separating dilute solutes since the packed bed functions like a very large number of thin contactors in series. Obtaining solutions for models of these systems can, however, be difficult, since the active exchange zone is changing in both spatial and temporal dimensions during the process. Changes in concentration with the radial component can usually be neglected and other simplifying assumptions may also be valid in order to minimize computational effort. The mass balance equation for a multi-component system to account for concentration changes in the axial direction with time is typically written as (Ruthven, 1984, Klein, 1982):

$$\frac{\partial c_i}{\partial t} + v\frac{\partial c_i}{\partial z} - D\frac{\partial^2 c_i}{\partial z^2} + \left(\frac{1-\varepsilon}{\varepsilon}\right)\frac{\partial q_i}{\partial t} = 0 \qquad\qquad 13.1$$

$$\frac{\partial q_i}{\partial t} = kF(c,q) \qquad\qquad 13.2$$

where:

ε = bed void fraction

v = average interstitial fluid velocity

z = the distance from the bed inlet in the axial direction

D = axial dispersion coefficient for the bed

k = effective mass transfer coefficient

c, q = the fluid and solid phase concentrations, respectively

t = time

$F(c,q)$ = a driving force to be specified

With initial and boundary conditions as:

I.C. $(c, q)|_z^{t=0} = 0$; starting with no sorbate on resin

B.C. $c|_{z=0}^t = c_0$

$$\left.\frac{\partial c}{\partial z}\right|_{z=L}^t = 0 \qquad\qquad 13.3$$

Note: specific units are not included in this generic discussion; however, the reader should understand that choices for time, mass, length and volume units must remain consistent throughout.

A few analytical solutions have been obtained for very simple, single-component cases. Approximate solutions can also be attained in some cases by utilizing classical functions of series expansions, but solutions are best achieved by numerical integration. Numerical methods utilizing finite difference, orthogonal collocation, method of characteristics or combinations thereof usually give very accurate solutions; and systems having ≤3 components are efficiently solved with simple finite difference algorithms (Ruthven, 1984, Tranter *et al.*, 2009b, 2005, 2002). Due to the large increase in processing speed over the last two decades, many scientists and engineers now have adequate computational power for performing efficient numerical integrations via desktop computers. Software to perform the necessary matrix operations (e.g., inversion, multiplication) are available commercially or can be written in user friendly languages (e.g., Visual Basic®, C++, or MATLAB®). It is evident from Eqns (13.1) and (13.2) that a driving mechanism or equation for mass transfer and equilibrium must be determined along with the corresponding coefficients for mass transfer, equilibrium and dispersion. It is best to determine the mass transfer and equilibrium parameters by separate batch experiments, since these are very significant to the accuracy of the model. Dispersion effects are often minor in comparison and values obtained from published equations (Ruthven, 1984, Chung *et al.*, 1968) often provide adequate correlation to experimental data. Though, the dispersion coefficient can be derived independently from tracer studies if dispersion effects are determined to be substantial for a given

system. Once the governing parameters and corresponding coefficients are obtained from independent experimentation, the values are used in the dynamic model (Eqn. 13.1 and 13.2) to predict breakthrough curves for a given resin and column configuration. The predicted breakthrough curves are then compared to data obtained from experimental column tests to assess the overall accuracy and rigor of the model.

Numerous expressions for the rate equation (Eqn. 13.2) have been proposed (LeVan *et al.*, 1997, Ruthven, 1984). Although many were originally developed for ion exchange or sorption processes, the mathematics are based on the physical phenomena of diffusion to describe the resulting concentration gradients established within a porous media. They may therefore be applied to describe solid-phase extraction processes with appropriate technical understanding and discretion. An evaluation of the literature shows that the assumption of a linear driving force typically provides sufficient model accuracy and has been used quite successfully by this author and numerous others. A linear driving force in terms of the solid phase concentration is thus used for purposes of this discussion and is written as:

$$\frac{\partial q_i}{\partial t} = k(q_e - q_i) \quad \text{or}$$

$$\frac{\partial q_i}{\partial t} = k(c_i - c_e) \qquad\qquad 13.4$$

where:
c_e, q_e = equilibrium concentration at the fluid-pore interface for the liquid and solid phases, respectively

Solution of Eqn. (13.4) requires additional equations and/or terms for calculating the mass transfer coefficient and fluid-solid pore equilibrium at each time step. The form of the equilibrium equation and corresponding equilibrium constant is specific to a given solid-phase extraction process and is selected to best represent the system and match experimental data. Equilibrium expressions from the extraction stoichiometry are often used. For example, Takeshita (1999) modeled a system for Ln extraction using a styrene-divinylbenzene copolymer impregnated with CMP (dihexyl-N-N-diethylcarbamoylmethylphosphonate) and used the following equilibrium model for calculating phase equilibrium concentrations:

$$K_{Ln} = \frac{[\text{Ln}(\text{NO}_3)_3 \cdot 3\text{CMP}]}{[\text{Ln}^{3+}][\text{NO}_3^-]^3[\text{CMP}]^3} \qquad\qquad 13.5$$

where:
K_{Ln} = equilibrium coefficient for the given Ln element

Other researchers have used the equilibrium isotherm approach wherein solid and liquid phase equilibrium concentrations are obtained over a range

of interest by performing multiple, isothermal batch contacts at varying ratios of sorbent to extractable species. An appropriate isotherm equation is fit to the batch data and this equation is used in the model (Eqn. 13.1) to calculate the fluid-pore phase equilibrium concentrations for each time step in the numerical solution. The Langmuir or Freundlich isotherm models (LeVan *et al.*, 1997) are frequently used to fit the equilibrium data for single component systems and extensions may sometimes be applicable to multicomponent cases. Although the mechanism of extracting the species onto the solid phase differs from the sorption phenomena assumed for the derivation of these models, the isotherm models often provide a good fit to the equilibrium data and can simplify the numerical computation substantially; however, they are limited to the feed conditions under which they were generated and do not provide a straightforward way of accounting for changes of significant parameters in the liquid phase, e.g. nitrate concentration or total ion activity. Ultimately the selection of a model to describe equilibrium, whether more fundamental or empirical, must be based on the complexity of the system, how well it is understood and the appropriate compromise between accuracy and computational difficulty.

The transfer of metal ion into the solid-phase extraction resin consists of several steps: 1) transport of the metal from the bulk fluid to the film interface between fluid and particle, 2) diffusion through the film layer, 3) diffusion through the particle – within the pores or gel phase – and 4) complex formation between the metal and extractant impregnated in the particle. The different regions of mass transfer are depicted in Figure 13.16.

Each of the above steps contributes to the total resistance for metal uptake by the resin; however, one or two of these processes are typically much slower than the rest and become the rate limiting steps for overall mass transfer. Transport through the bulk fluid and the complex formation reaction are usually fast in comparison to film or particle diffusion, thus coefficients for mass transfer of metal in the film and/or particle are most frequently needed for solving the rate expression of Eqn (13.5). Classical methods based on data from batch experiments (Helfferich, 1995) or column interruption tests (Tranter *et al.*, 2009b, Kurath, 1994) may be used to determine whether film or particle resistance dominates, or if both are significant. Equations for each of these cases are written as (Ruthven, 1984):

$$k = k_p a = \frac{15D_e}{R_p^2}; \text{particle controlled diffusion}$$

$$k = k_f a = k_f \frac{3}{R_p}; \text{film controlled diffusion} \qquad 13.6$$

$$\frac{1}{k} = \frac{R_p}{3k_f} + \frac{R_p^2}{15D_e}; \text{both resistances controlling}$$
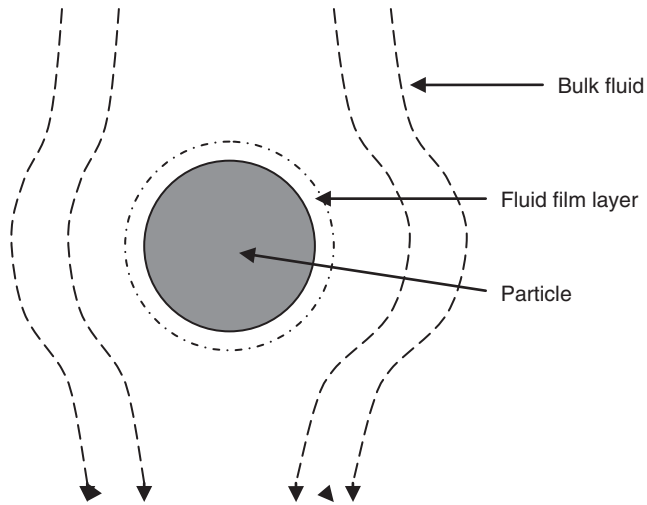
13.16 Regions of mass transport within a solid-fluid system.

where:

k_f = mass transfer coefficient in the film layer

k_p = overall mass transfer coefficient in the particle

R_p = average particle radius

D_e = effective intra-particle diffusivity of the metal

a = area per unit volume of a spherical particle

The above equations (Eqn. 13.6) are simplified in that they represent the overall or effective terms relating to mass transfer for a given component in each phase. It should be recognized that mass transfer in the particle takes place through multiple regions (i.e., macro, micro-pores and extractant), each with potentially different rates of diffusion. The solid portion of the exchanger matrix occupies a substantial portion of the medium and obstructs diffusion of the ions into and out of the matrix. Even if the aqueous phase diffusion coefficients for the ions of interest are known, predicting diffusion rates within the exchanger particle is difficult because of the varied rates within the different phases of the exchanger and the tortuous path the ions must take through the pores to reach the active exchange sites. A simplified approach is often taken by treating the exchanger as a quasi-homogeneous system and assuming an average or 'effective' diffusion coefficient within the particle phase. This approach is frequently used in engineering practice and usually works quite well for modeling purposes. The reader is referred to the comprehensive work by Ruthven (1984) for more detailed discussion and methods of mathematical analysis of mass transfer in sorbents for both liquid and gaseous systems.

Batch kinetic studies to determine mass transfer rates in several solid-phase extraction resins have indicated that film diffusion is the controlling resistance for only a very short time when the solute is first contacted with the sorbent phase – likely corresponding to a monolayer coverage or uptake of the of solute at the pore surface (Juang *et al.*, 1995a, 1995b, Takeshita *et al.*, 2000). The studies indicate that mass transfer resistance in the particle phase is the dominant controlling mechanism throughout most of the period of solute uptake. Since this is likely to be the case with many solid-phase extraction resins of interest, methods for determining the effective mass transfer coefficient in the particle phase will be the focus of this discussion. Kinetic experiments are typically performed in batch mode in order to obtain the necessary data to estimate the diffusion coefficient for a given metal in the solid-phase resin particle. One technique is to simply stir or mix a beaker of solution with known volume and concentration of metal containing a known mass and particle size of resin, and then remove small aliquots of the liquid phase to measure metal uptake as a function of time. This approach has been used successfully by many researchers, but one must to careful to ensure that attrition of the resin particles by the stirring blade does not take place since mass transfer in the particle is dependent upon particle diameter. A preferred method is to use a centrifugal contacting apparatus similar to that described by Helfferich (1995). A device consisting of a stainless steel wire cage housed within the center of a circular Teflon™ housing that is connected to a stirring motor can be easily made for this purpose (Tranter *et al.*, 2009a). Diagrams of top and side views of this type of contactor are shown in Figs 13.17 and 13.18, respectively. The device is fashioned with a threaded top and bottom portion so that the contactor can be opened to allow access to the hollow inner portion holding the wire screen or cage. The solid-phase extraction resin is sieved to obtain a fraction of known particle diameter and a measured amount of the sized exchanger material is placed in the hollow space inside the contactor. The top portion of the apparatus is then threaded tightly back onto the body of the device and it is attached to a stirring motor via the vertical shaft, as shown in Fig. 13.18. The unit is immersed in a solution of known metal ion concentration and stirred at a fixed speed. Centrifugal action produces a rapid circulating flow of solution entering the device at the bottom and exiting the wall through the radial holes in the casing. The contactor allows for very high flow rates around the adsorbent beads, thus shrinking the film layer to a point that the diffusion resistance in the film will be very small compared to that within the particle. Uptake of the solute ion by the exchanger particle is then determined as a function of time by removing and analyzing small aliquots from the bulk solution. It is important that these aliquots are very small relative to the total volume of solution so that the bulk volume remains approximately unchanged, i.e. the total ion
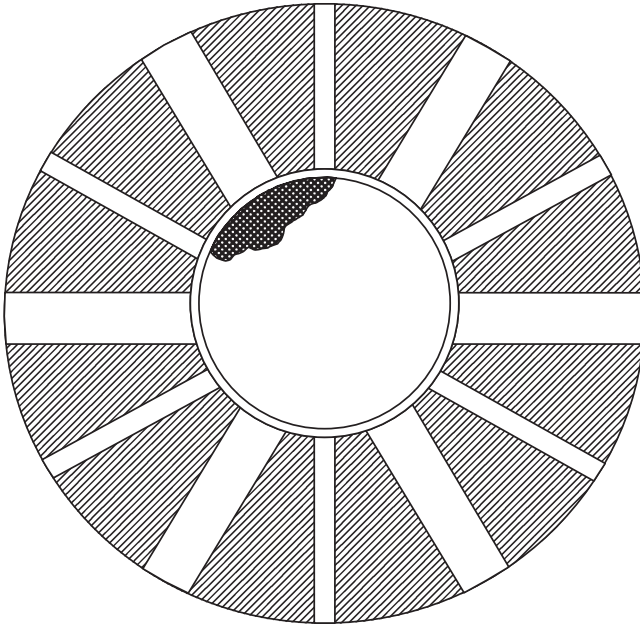
13.17 Diagram (top, inside view) of centrifugal contacting device.
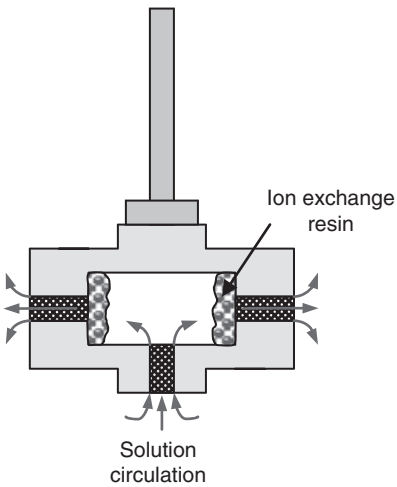
13.18 Diagram (side view) of centrifugal contacting device.

concentration in the fluid phase at any given point in time is not measurably reduced by sampling.

The experimental regime provides a well-stirred finite volume system and the solution method proposed by Crank (1975) for spherical particles may be applied to the kinetic data to solve for the effective intra-particle diffusivity. The following assumptions are made for this analysis:

- The particles are spherical and uniform.
- The particles are initially free of solute.
- The concentration of solute in the bulk phase is always uniform and is initially C_0.
- The fluid velocity is sufficient to reduce the film layer to the point that diffusion in the particle is the rate limiting step for the uptake of solute.

Normalized fractional loading or uptake of the solute (F) by the exchanger during the kinetic test changes with time and is defined as:

$$F = \frac{q_t}{q_\infty} \qquad\qquad 13.7$$

where:
q_t = metal concentration in the solid phase at time t
$q_\circ$ = metal concentration in the solid phase at equilibrium

The fractional attainment of equilibrium is expressed by the following equation (Crank, 1975):

$$F = \frac{q_t}{q_\infty} = 1 - \sum_{n=1}^{\infty} \frac{6\omega(\omega+1)\exp(-D_e\phi_n^2 t / R_p^2)}{9 + 9\omega + \phi_n^2\omega^2} \qquad\qquad 13.8$$

where:
t = elapsed time, min

The parameter ω is calculated from the following relationship:

$$\frac{mq_\infty}{VC_0} = \frac{1}{1+\omega} \qquad\qquad 13.9$$

where:
m = mass of solid-phase extraction resin
V = solution volume
C_0 = initial metal concentration in the solution

The terms for Φ_n are calculated from the non-zero roots of:

$$\tan\phi_n = \frac{3\phi_n}{3 + \omega\phi_n^2} \qquad\qquad 13.10$$

Equation 13.10 is solved for $n = 1$ to 12 and these values are then used to obtain the series solution for F. Beyond $n = 12$, the additional terms usually become insignificant to the solution. Equations 13.8 and 13.9, along with the 12 solutions from Eqn 13.10, are used in to fit the fractional equilibrium data from the kinetic batch experiment. The independent variable in this approach is the elapsed time t, the dependent variable is the fractional attainment of equilibrium F, and the adjustable parameter is the effective intra-particle diffusivity coefficient, D_e, for the metal of interest. The curve fits can be obtained quite easily via the numerous commercial statistical software packages now available for desktop computers. The value for D_e, derived by fitting the data from the kinetic batch tests, is then used in Eqn 13.6 to calculate the mass transfer coefficient for the metal in the particle phase, k_p.

In summary, the general steps for model development are:

1) Perform independent batch experiments to obtain equilibrium data for the metal(s) and solid-phase extraction resin system of interest.
2) Use the equilibrium data to elucidate the best form for the equilibrium equation and derive the corresponding equilibrium coefficients.
3) Perform independent batch experiments to obtain kinetic data for the metal(s) and solid-phase extraction resin system of interest.
4) Use the kinetic data to elucidate the best form for the mass transfer equations and derive the corresponding mass transfer coefficients.
5) Numerically solve the coupled partial differential equations (Eqns 13.1 and 13.2), using the coefficients for equilibrium and mass transfer derived from steps 2 and 4, to generate a predicted breakthrough curve for a specified metal feed concentration and column size of solid-phase extraction resin.
6) Perform column breakthrough experiments with test conditions specified in step 5 and compare the experimental breakthrough data to the modeled results.
7) Perform several iterations of steps 5 and 6 with varying feed concentrations, flow rates and column dimensions to evaluate the efficacy of the model.

13.5   Advantages and disadvantages of solid-phase extraction in treatment processes for nuclear fuel reprocessing streams

The following discussion is not intended to make a case for or against the use of solid-phase extraction technology in nuclear fuel reprocessing. The objective is rather to highlight potential advantages and disadvantages with

the aim of stimulating further discussion and developmental work. The appeal of using solid-phase extraction technology for select treatment processes in the nuclear fuel cycle lies in the potential for achieving the operational advantages inherent to packed bed separations, while maintaining the selectivity provided by ligands historically used in liquid-liquid solvent extraction processes. In theory, the stationary phase functions like a very large number of small, sequential equilibrium contactors, but significantly reduces equipment complexity. A successful implementation of solid-phase extraction for a given separation could potentially eliminate the need for agitated contactors (e.g., mixer-settlers, pulsed columns, centrifugal contactors), which in turn reduces the number of moving parts operating in a hot-cell environment. The shortcomings of the technology are, however, not well known at this point due to the lack of engineering and operating experience with any of the solid-phase extraction resins at process scale. There is some debate regarding how well the ligands mimic their liquid phase behavior after they are fixed onto a solid substrate. Several studies have shown deviations to be negligible (Pierce *et al.*, 1963a, Pierce *et al.*, 1963b, Sebesta, 1970, Akaza *et al.*, 1970, Akaza, 1975). Yet other researchers have found some marked differences between ligand performance in certain liquid-liquid and solid-phase extraction systems and suggest that the choice of support may influence ligand behavior (Cortina *et al.*, 1994b, Strikovsky *et al.*, 1996). Horwitz *et al.* (2006) published a comprehensive study comparing the solid-phase and liquid-liquid extraction performance of three acidic organophosphorus extractants for a number of Ln(III) elements. The authors found essentially the same selectivity sequence among the two techniques, but noted that a prediction of solid-phase extraction capacity factors from liquid-liquid distribution data was difficult. This was attributed to potential unavailability of a portion of the extractant in the micropores and/or inexplicable differences in nitric acid dependency between the two systems; also seen with CMPO-PAN studies mentioned previously (Kamenik *et al.*, 2006, Mann *et al.*, 2002). Minor deviation in extractant performance between the two techniques is likely an insignificant factor as long as the design parameters and performance of the solid-phase extraction resin are well characterized prior to scale-up. Nonetheless, any effects due to substrate morphology (e.g., pore-size distribution) and extractant impregnation must remain consistent among resin batches and will consequently influence the manufacturing tolerances and economics of the material.

Primary concerns with the application of the resins at industrial scale are the stability of the composite material against radiolysis and acid hydrolysis. It is not expected that degradation of the extractant will be significantly worse than in liquid-liquid extraction for an equivalent amount of absorbed dose. But the potential for longer residence times in the columns, as compared to liquid-liquid contactors, could result in higher doses to the

extractant phase. The polymer substrates independently are typically very resistant to acid, and many of the polymers have been shown to remain physically stable up to radiation doses of 10^6 Gy and cross-linking promoters, known as 'prorads' can be added to the polystyrene-based polymers to increase the degree of cross-linking under high radiation doses (Drobny, 2003, Sebesta *et al.*, 1995a, 1995b). There are, however, many unknowns regarding how these processes affect the composite material in terms of extractant retention on the substrate and its performance in sequential cycles of loading, washing, stripping and re-conditioning. For instance, can the degradation products be effectively washed from the column, e.g., with caustic wash similar to liquid-liquid extraction systems? Or will they build up on the column over time and reduce stripping efficiency? It is also important that the width of the exchange zones established during the metal loading and stripping cycles remains relatively constant from cycle to cycle. Otherwise, the volume and/or strength of stripping solutions will need to be increased as a reprocessing campaign progresses. A broadening of the exchange zones produces tailing, reducing the purity of separation between metals, and will eventually lead to incomplete column regeneration between cycles. Significant loss of the extractant to the aqueous phase is another key issue from an engineering design and operations perspective. It is desirable that losses are minimal, but also that they are consistent for a given application. Reproducible performance is essential so that any decrease in performance with process cycles is known and can be accommodated in design and with manageable adjustments to operating parameters.

13.6   Future trends in solid-phase extraction technology for nuclear fuel reprocessing applications

Advances in the field of solid-phase extraction, along with substantial improvements in automated control systems and on-line monitoring, suggest that the technology merits further consideration for nuclear fuel reprocessing applications. The technology is probably more suited to MA and Ln separations subsequent to the removal of U and Pu by other means, or for polishing applications in any number of processing and/or raffinate streams. Issues with high U loading will likely preclude the use of solid-phase extraction materials for primary actinide separations, but this decision is ultimately a function of the stability of the given material and economics of the process under consideration. It is noteworthy that many researchers have recognized the need for more information regarding the robustness of the solid-phase extraction composites. This is evidenced by attempts to increase substrate stability via the addition of inorganic materials as well

as bench-top studies to assess extractant losses and radiation effects. Still, more data is needed to evaluate the issues mentioned in the previous section. Future work should include comprehensive assessments of resin performance under the multiple cycles of loading and stripping corresponding to those typical of an actual process. Some testing at larger scales, and smaller tests using actual reprocessing solutions, will also be needed to accurately assess the viability of the technology. The added complexity of these studies will certainly drive up cost and likely require some type of programmatic support. This is typically the issue when transferring any technology from small scale to large scale applications. The information to be gained is, however, essential for performing adequate engineering and cost-benefit analyses of the technology.

13.7   Sources of further information and advice

The works by Cortina *et al.*, (1994a,b), Braun and Ghersini (1975), and the numerous journal publications by E.P. Horwitz and coworkers are excellent sources for more detailed information on solid-phase extraction.

13.8   Acknowledgment

13.9   References

Akaza, I. (1975), 'Correlation between extraction chromatography and liquid-liquid extraction', in Braun, T. and Ghersini, G, *Extraction Chromatography*, Elsevier, New York, 17–44.

Akaza, I., Kiba, T., Kiba, T. (1970), 'The separation of gold, platinum, and palladium by reversed-phase partition chromatography', *Bulletin of the Chemical Society of Japan*, 43, 2063–2067.

Ansari, S.A., Pathak, P.N., Manchanda, V.K., Hussain, M., Prasa, A.K., Parmar, V.S. (2005), 'Extraction chromatographic studies employing N,N,N′,N,′-tetraoctyl diglycolamide', *BARC Newsletter*, 273, 73–79.

Barney, G.S., Cowan, R.G. (1992), *Separation of Actinide Ions from Radioactive Waste Solutions Using Extraction Chromatography*, WHC-SA-1520-FP, Westinghouse Hanford Company, Richland, Washington.

Bobozka, L., Cote, G. (1985), 'Spectroscopic investigation of adsorbed 7-(4-ethyl-1-methyloctyl)-8-quinolinol (kelex 100) and of its gallium(III) complex: Comparison with the behaviors observed in solvent extraction systems', *Polyhedron*, 4, 1499.

Braun, T., Ghersini, G. Eds. (1975), *Extraction Chromatography*, Journal of Extraction Chromatography Library Vol. 2, Elsevier, New York.

Chung, S.F., Wen, C.Y. (1968), 'Longitudinal dispersion of liquid flowing through fixed and fluidized beds', *American Institute of Chemical Engineers Journal*, 14, 857–866.

Cortina, J..L., Warshawsky, A. (1997), In *Ion Exchange and Solvent*, Vol. 13, Marcus, Y., Ed., New York, Marcel Dekker.

Cortina, J.L., Miralles, N., Sastre, A., Aguilar, M., Profumo, A., Pesavento, M. (1993), 'Solvent-impregnated resins containing di-(2,4,4-trimethylpentyl) phosphonic acid I. Comparative study of di-(2,4,4-trimethylpentyl)phosphinic acid adsorbed into Amberlite XAD-2 and dissolved in toluene', *Reactive Polymers*, 21, 89.

Cortina, J.L., Miralles, N., Aguilar, M., Sastre, A. (1994a), 'Solvent impregnated resins containing Di-(2-ethylhexyl) phosphoric acid. I. Prepration and study of the retention and distribution of the extractant on the resin', *Solvent Extraction and Ion Exchange*, 12, 349.

Cortina, J.L., Miralles, N., Aguilar, M., Sastre, A. (1994b), 'Solvent impregnated resins containing di(2-ethylhexyl)phosphoric acid. II. Study of the distribution equilibria of Zn(ii), Cu(II), and Cd(II)', *Solvent Extraction and Ion Exchange*, 12, 371–391.

Cote, G., Laupretre, F., Chassagnard, C. (1987), 'Magic-angle carbon-13 NMR investigation of solvent-impregnated resins: application to 7-(4-ethyl-1-methyloctyl)-8-quinolinol (Kelex 100) adsorbed on amberlite XAD-7', *Reactive Polymers*, 5, 141–150.

Crank, J. (1975), *The Mathematics of Diffusion*, 2nd Edition, Oxford University Press, New York, 92–96.

Drobny, J.G. (2003), *Radiation Technology for Polymers*, CRC Press, Boca Raton, FL.

Eschrich, H., Hundere, I. (1968), Eurochemic Technical Report, ETR-226.

Eschrich, H., Ochsenfeld, W. (1980), 'Application of extraction chromatography to nuclear fuel reprocessing', *Separation Science and Technology*, 15(4), 697–732.

Eschrich, H., Herrera-Huertas, M., Tallberg, K. (1970), Eurochemic Technical Report, ETR-268.

Fritz, J.S., Beureman, D.R., Richard, J.J. (1971), 'Chromatographic separation of copper with an α-hydroxyoxime', *Talanta*, 18, 1095.

Gatrone, R.C., Kaplan, L., Horwitz, E.P. (1987a), 'The synthesis and purification of carbamoylmethylphosphine oxides', *Solvent Extraction and Ion Exchange*, 5, 1075.

Gatrone, R.C., Rickert, P.G. (1987b), 'The spectral properties of the carbamoylmethylphosphine oxides', *Solvent Extraction and Ion Exchange*, 5, 1117.

Grinstead, R.R., Jones, K.C. (1974), 'Aliphatic amidines: A new solvent extraction system', *Journal of Nuclear Inorganic Chemistry*, 36, 391.

Guan, Y., Wu, X.Y. (1990), 'The theory and application of solvent impregnated resins', *Ion Exchange and Absorption*, 6, 60–67.

Handley, H.W., Jones, P., Ebdon, L., Barnett, N.W. (1991), 'Research and development topics in analytical chemistry', *Analytical Proceedings*, 28, 37.

Helfferich, F. (1995), *Ion Exchange*, 194, Dover Publishing, Mineola, NY, Reprint of Original 1st Edition, Verlag Chemie, Weinheim, Germany, 1959.

Hill, C., Madic, C., Baron, P., Ozawa, M., Tanaka, X. (1998), 'Trivalent minor actinides/lanthanides separiton using organophosphinic acids', *Journal of Alloys and Compounds*, 271–273, 159.

Hommel, H., Legrand, A.P. (1983), 'Study of the properties of a liquid ion exchanger adsorbed on a macroreticular resin', *Reactive Polymers*, 1, 267–271.

Horwitz, E.P., Kalina, D.G., Diamond, H., Vandegrift, G.F., Schuluz, W.W. (1985), 'The TRUEX process – a process for the extraction of the transuranic elements from nitric acid wastes utilizing modified PUREX solvent', *Solvent Extraction and Ion Exchange*, 3, 75–109.

Horwitz, E.P., McAlister, D.E., Dietz, M.L. (2006), 'Extraction chromatography versus solvent extraction: how similar are they?', *Separation Science and Technology*, 41, 2163–2182.

Hoshi, H., Wei, Y., Kumagai, M., Asakura, T., Morita, Y. (2004), 'Group separation of trivalent minor actinides and lanthanides by TODGA extraction chromatography for radioactive waste management', *Journal of Alloys and Compounds*, 374, 451–453.

Hoshi, H., Wei, Y., Kumagai, M., Asakura, T. Morita, Y. (2006), 'Separation of trivalent actinides from lanthanides by using R-BTP resins and stability of R-BTP resin', *Journal of Alloys and Compounds*, 408–412, 1274–1277.

Iki, N. Morohashi, N., Narumi, F., Miyano, S. (1998), 'High complexation ability of thiacalixarene with transition metal ions. The effects of replacing methylene bridges of tetra(*p-t*-butyl)calix[4]arenetetrol by epithio Groups', *Bulletin of the Chemical Society Japan*, 71, 1597–1653.

Ionue, K., Baba, Y. Sakamoto, Y., Egawa, H. (1987), 'Adsorption of nickel(II) and cobalt(II) from aqueous solutions on levextrel resin containing acidic organophosphinic extractant and phosphorus-based chelating resins: Comparative study on the selectivity of the resins', *Separation Science and Technology*, 22, 1349.

Juang, R.S., Lin, H.C. (1995a), 'Metal sorption with extractant-impregnated macroporous resins. 1. Particle diffusion kinetics', *Journal of Chemical Technology and Biotechnology*, 62, 132–140.

Juang, R.S., Lin, H.C. (1995b), 'Metal sorption with extractant-impregnated macroporous resins. 2. Chemical reaction and particle diffusion kinetics', *Journal of Chemical Technology and Biotechnology*, 62, 141–147.

Kamenik, J., Sebesta, F. (2006), 'Study of europium and selected actinides uptake on composite material CMPO-PAN', *Czechoslovak Journal of Physics*, 56, 493–500.

Kauczor, H.W., Meyer, A. (1978), 'Structure and properties of Levextrel resins', *Hydrometallurgy*, 3, 65.

Kikuchi, T., Nogami, M., Suzuki, K. (2004), 'Separtion performance for trivalent actinides from lanthanides by thiacalix[4]arenes compounds impregnated silica ion-exchanger', *Journal of Alloys and Compounds*, 374, 272–276.

Klein, G. (1982), 'Column design for sorption processes', in Liberti L. and Helfferich F.G., *Mass Transfer and Kinetics of Ion Exchange*, Martinus Nijhoff, Boston, 226–227.

Kurath, D.E. (1994), *Experimental Data and Analysis to Support the Design of an Ion Exchange Process for the Treatment of Hanford Tank Waste Supernatant Liquids*, Pacific Northwest Laboratory, PNL-10187, 2.21.

LeVan, M.D., Carta, G., Yon, C.M. (1997), 'Adsorption and ion exchange', in Perry R.H. and Green D.W., *Perry's Chemical Engineers' Handbook*, 7th edition, McGraw-Hill, New York.

Lumetta, G.J., Wester, D.W., Morrey, J.R., Wagner, M.J. (1993), 'Preliminary evaluation of chromatographic techniques for the separation of radionuclides from high-level radioactive waste', *Solvent Extraction and Ion Exchange*, 11(4), 663–682.

Maheswari, M. A., Subramanian, M.S. (2005), 'Extraction chromatographic method for the separation of actinides and lanthanides using EDHBA grafted AXAD-16 polymer', *Talanta*, 65, 735–742.

Mann, N.R., Todd, T.A., Tranter, T.J, Sebesta, F. (2002), 'Development of novel composite sorbents for the removal of actinides from environmental and analytical solutions', *Journal of Radioanalytical and Nuclear Chemistry*, 254, 41–45.

Mathur, J.N., Murali, M.S., Nash, K.L. (2001), 'Actinide partitioning-a review', *Solvent Extraction and Ion Exchange*, 19(3), 357–390.

Mimura, H., Hoshi, H., Akiba, K., Onodera, Y. (2001), 'Separation of americium from europium by biopolymer microcapsules enclosing Cyanex 301 extractant', *Journal of Radioanalytical and Nuclear Chemistry*, 247(2), 375–379.

Modolo, G., Odoj, R. (1998a), 'The separation of trivalent actinides from lanthanides by dithiophosphinic acids from HNO_3 acid medium', *Journal of Alloys and Compounds*, 271, 248–251.

Modolo, G., Odoj, R. (1998b), 'Influence of the purity and irradiation stability of Cyanex 301 on the separation of trivalent actinides from lanthanides by solvent extraction', *Radioanalytical Nuclear Chemistry*, 228, 83–88.

Modolo, G., Odoj, R. (1999), 'Synergistic selective extraction of actinides(III) over lanthanides from nitric acid using new aromatic diorganyldithiophosphinic acids and neutral organophosphorus compounds', *Solvent Extraction and Ion Exchange*, 17, 33–53.

Modolo, G., Asp, H., Schreinemachers, C., Vijgen, H. (2007),'Recovery of actinides and lanthanides from high-level liquid waste by extraction chromatography using TODGA+TBP impregnated resins', *Radiochemical Acta*, 95, 391–397.

Morohashi, N., Iki, N., Sugawara, A., Miyano, S. (2001), 'Selective oxidation of thiacalix[4]arenes to the sulfinyl and sulfonyl counterparts and their complexation abilities toward metal ions as studied by solvent extraction', *Tetrahedron*, 57(26), 5557–5563.

Narita, H., Yaita, T., Tamura, K., Tachimori, S. (1998), 'Solvent extraction of trivalent lanthanides with N,N′-dimethyl-N′,N′-diphenyl-3-oxapentanediamide', *Radiochimica Acta*, 81, 223–226.

Pierce, T.B., Hobbs, R.S. (1963a), 'The separation of the rare earths by partition chromatography with reversed phases. Part I. Behavior of column material', *Journal of Chromatography*, 12, 74–80.

Pierce, T.B., Peck, P.F., Hobbs, R.S. (1963b), 'The separation of the rare earths by partition chromatography with reversed phases. Part II. Behavior of individual elements on HDEHP-corvic columns', *Journal of Chromatography*, 12, 81–88.

Poinescu, I., Popescu, V., Carpov A., Angew. (1985), 'Synthesis of porous styrenedivinylbenzene copolymers', *Makromolekulare Chemic-macromolecular Chemistry and Physic*, 21, 135.

Raju, C.S.K., Subramanian, M.S. (2005), 'DAPPA grafted polymer: an efficient solid phase extractant for U(VI), Th(IV) and La(III) from acidic waste streams and environmental samples', *Talanta*, 67, 81–89.

Raju, C.S.K., Subramanian, M.S. (2007a), 'A novel solid phase extraction method for separation of actinides and lanthanides from high acidic streams', *Separation and Purification Technology*, 55, 16–22.

Raju, C.S.K., Subramanian, M.S. (2007b), 'Sequential separation of lanthanides, thorium and uranium using novel solid phase method from high acidic nuclear wastes', *Journal of Hazardous Materials*, 145, 315–322.

Ruthven, D.M.(1984), *Principles of Adsorption and Adsorption Processes*, John Wiley and Sons, New York.

Sasaki, Y., Tachimori, S. (2002), 'Extraction of actinides(III), (IV), (V), (VI) and lanthanides(III) by structurally tailored diamides', *Solvent Extraction and Ion Exchange*, 20, 21–34.

Sasaki, Y., Sugo, Y. Shinichi, S., Tachimori, S. (2001), 'The novel extractants, diglyco-lamides, for the extraction of lanthanides and actinides in HNO_3-*n*-dodecane system', *Solvent Extraction and Ion Exchange*, 19(1), 91–103.

Schulz, W.W., Horwitz, E.P. (1988), 'The TRUEX process and the management of liquid TRU waste', *Separation Science and Technolgoy*, 23, 1191–1210.

Schulz, W.W., Navratil, J.D. (1982) in *Recent Developments in Separation Science*, Vol 7 Boca Raton, Florida, CRC Press.

Sebesta, F. (1970), 'Extraction chromatography using chelating agents. I. System zinc-dithizone-carbon tetrachloride', *Journal of Radioanalytical Chemistry*, 6, 41–46.

Sebesta, F. (1997), 'Methods of modification of properties of inorganic ion-exchangers for application in column packed beds', *Journal of Radioanalytical Nuclear Chemistry*, 220, 77–88.

Sebesta, F., John, J., Motl, A., Stamber, K. (1995a), Sandia National Laboratory, SAND95-2729.

Sebesta, F., John, J., Motl, A., Watson, J. (1995b), ICEM 95 – Proceedings of the 5th international conference on radioactive waste management and environmental remediation, Vol. 1, Sept. 3–7, Berlin, ASME, New York, 361.

Small, H. (1961), 'Gel liquid extraction – The extraction and separation of some metal salts using tri-n-butyl phosphate gels', *Journal of Inorganic Nuclear Chemistry*, 18, 232.

Sole, K.C., Hiskey, J.B., Ferguson, T.L. (1993), 'An assessment of the long-term stabilities of Cyanex 302 and Cyanex 301 in sulfuric and nitric acids', *Solvent Extraction and Ion Exchange*, 11, 783–796.

Spevackova, V., Krivanek, M. (1970), 'Separation of cobalt from mixtures of iron radioisotopes by means of extraction chromatography', *Radiochemical and Radioanalytical Letters*, 3, 63.

Strikovsky, A.G., Jerabek, K., Cortina, J.L., Sastre, A.M., Warshawsky, A. (1996), 'Solvent impregnated resin (SIR) containing dialkyldithiophosphoric acid on Amberlite XAD-2: Extraction of copper and comparison to liquid-liquid extraction', *Reactive and Functional Polymers*, 28, 149–158.

Sudderth, R.B., Kordosky, G.A. (1986), 'Some practical considerations in the evaluation and selection of solvent extraction reagents', *Chemical Reagents in the Mineral Processing Industry*. Eds Malhotra, D. and Riggs, W.F., S.M.E., Littleton Colorado. 181–196.

Sugo, Y., Sasaki, Y., Tachimori, S. (2002), 'Sudies on hydrolysis and radiolysis of N,N,N′,N′-tetraoctyl-pentane-1,5-diamide', *Radiochimica Acta*, 90, 161–165.

Swanson, J.L. (1991), 'Use of the TRUEX process for the pretreatment of neutralized cladding removal waste (NCRW) sludge – results of a design basis experiment', Pacific Northwest Laboratory report, PNL-7734.

Tachimori, S., Sasaki, Y., Morita, Y., Suzuki, S. (2002), Recent progress of partitioning processes at JAERI: development of amide-based ARTIST process. *Proceedings of the Seventh Information Exchange Meeting on Actinide and Fission Product*

Partitioning and Transmutation, 14–16 October 2002, Jeju, Republic of Korea, pp. 441–444.

Takeshita, K. (1999), 'A mathematical model to predict extraction behavior of metal ions between a polymer gel and an aqueous phase', *Solvent Extraction and Ion Exchange*, 17(2), 301–316.

Takeshita, K., Nakano, Y. (2000), 'Prediction of breakthrough curve of metal ion on extraction chromatographic column', *Solvent Extraction and Ion Exchange*, 18(5), 953–963.

Tranter, T.J., Herbst, R.S., Todd, T.A. (2002), 'Determination of a solid phase mass transfer coefficient for modeling and adsorption bed system using ammonium molybdophosphate-polyacrylonitrile as a sorbent for the removal of ^{137}Cs from acidic nuclear waste solutions', *Adsorption*, 8(4), 291–299.

Tranter, T.J., Mann, N.R., Todd, T.A. (2003), 'Evaluation of a novel solid phase extraction composite for the removal of actinides from nuclear waste solutions', *Czechoslovak Journal of Physics*, 53, 589–594.

Tranter, T.J., Tillotson, R.D., Todd, T.A., Argyle, M.D. (2005), 'Laboratory-scale column testing using crystalline silicotitanate for removing cesium from acidic tank waste stimulant. 2: Determination of cesium exchange capacity and effective mass transfer coefficient from a 500-cm^3 column experiment', *Solvent Extraction and Ion Exchange*, 23(4), 595–609.

Tranter, T.J. Vereshchagina, T.A., Utgikar, V. (2009a), 'An inorganic microsphere composite for the selective removal of [137]cesium from acidic nuclear waste solutions. 1: Equilibrium capacity and kinetic properties of the sorbent', *Solvent Extraction and Ion Exchange*, 27, 199–218.

Tranter, T.J. Vereshchagina, T.A., Utgikar, V. (2009b), 'An inorganic microsphere composite for the selective removal of [137]cesium from acidic nuclear waste solutions. 2: Bench-scale column experiments, modeling, and preliminary process design', *Solvent Extraction and Ion Exchange*, 27, 219–243.

Van Hecke, K., Goethals, P. (2006), *Research on Advanced Aqueous Reprocessing of Spent Nuclear Fuel: Literature Study*, Open report of the Belgian Nuclear Research Centre, SCK•CEN-BLG-1030.

Van Ooyen, J., Bac, R., Bonnevie-Svendsen, M., Eschrich, H. (1964), *Proceedings of the Third International Conference on the Peaceful Uses of Atomic Energy*, Geneva, Vol. 10, 402.

Villaescusa, I., Salvado, V., de Pablo, J., Valiente, M., Aguilar, M. (1992), 'Liquid-solid extraction of gold(III) from aqueous chloride solutions by macroporous resins impregnated with triisobutyl phosphine sulfide (Cyanex 471)', *Reactive Polymers*, 17, 69.

Warshawsky, A. (1974), 'Solvent-impregnated resins in hydrometallurgical applications', *Institute of Mining and Metallurgy Transactions*, 83, C101.

Warshawsky, A. (1978), 'Impregnated resins: Metal-ion complexing agents incorporated physically in polymeric matrices', *Israel Journal of Chemistry*, 17, 307–315.

Warshawsky, A. (1981), 'Extraction with solvent impregnated resins', *Ion Exchange and Solvent Extraction*, Vol. 8, Marinsky, J.A., Marcus, Y., Eds., New York, Marcel Dekker, 229–310.

Wei, Y. Sabharwal, K., Kumagai, M., Asakura, T., Uchiyama, G., Fujine, S. (2000a), 'Preparation of novel silica-based nitrogen donor extraction resins and their adsorption performance for trivalent americium and lanthanides', *Journal of Nuclear Science and Technology*, 37(12), 1108–1110.

Wei, Y., Kumagai, M., Takashima, Y. (2000b), 'Studies on the separation of minor actinides from high-level wastes by extraction chromatography using novel silica-based extraction resins', *Nuclear Technology*, 132, 413–423.

Wei, Y., Hoshi, H., Humagai, M., Asakura, T., Morita, Y. (2004a), 'Separation of Am(III) and Cm(III) from trivalent lanthanides by 2,6-bistriazinylpyridine extraction chromatography for radioactive waste management', *Journal of Alloys and Compounds*, 374, 447–450.

Wei, Y., Zhang, A., Kumagai, M., Watanabe, M., Hayashi, N. (2004b) 'Development of the MAREC process for HLLW partitioning using a novel silica-based CMPO extraction resin', *Journal of Nuclear Science and Technology*, 41, 315–322

Yoshizuka, K., Sakamoto, Y., Baba, Y., Ionue, K. (1990), 'Distribution equilibria in the adsorption of cobalt(II) and nickel(II) on levextrel resin containing Cyanex 272', *Hydromettallurgy*, 23, 309.

Zhang, A., Kuraoka, E., Hoshi, H., Kumagai, M. (2004) 'Synthesis of two novel macroporous silica-based impregnated polymeric composites and their application in highly active liquid waste partitioning by extraction chromatography' *Journal of Chromatography A*, 1061, 175–182.

Zhang, A., Wei, Y., Hoshi, H., Kumagai, M., Kamiya, M., Koyama, T. (2005a), 'Resistance properties of macroporous silica-based N,N,N′,N′,-tetraoctyl-3-oxapentane-1-5-diamide-impregnated polymeric adsorption material against nitric acid, temperature and γ-radiation', *Radiation Physics and Chemistry*, 72, 669–678.

Zhang, A., Wei, Y., M., H., Kumagai, Koma, Y., Koyama, T. (2005b), 'Resistance behavior of a novel silica-based octy(phenyl)-N-N-diisobutyl carbamoylmethylphoshine oxide neutral extraction resin against nitric acid, temperature and γ-radiation', *Radiation Physics and Chemistry*, 72, 455–463.

Zhang, A., Wei, Y., Kumagai, M., Koma, Y. (2005c) 'A new partitioning process for high-level liquid waste by extraction chromatography using silica-substrate chelating agent impregnated adsorbents', *Journal of Alloys and Compounds*, 390, 275–281.

Zhang, A., Hu, Q., Wang, W., Kuraoka, E. (2008) 'Application of a macroporous silica-based CMPO-impregnated polymeric composite in group partitioning of long-lived minor actinides from highly active liquid by extraction chromatography', *Industrial and Engineering Chemistry Research*, 47, 6158–6165.

Zhu, Y. (1995), 'The separation of americium from light lanthanides by Cyanex 301 extraction', *Radiochimica Acta*, 68(2), 95–98.

Zhu, Y. Chen, J., Jiao, R. (1996a), 'The separation of Am from lanthanides by purified Cyanex 301 extraction', *Separation Science and Technology*, 31, 2723.

Zhu, Y., Chen, J., Jiao, R. (1996b), 'Extraction of Am(III) and Eu(III) from nitrate solution with purified cyanex 301, *Solvent Extraction and Ion Exchange*, 14, 61.

Emerging separation techniques:
supercritical fluid and ionic liquid extraction
techniques for nuclear fuel reprocessing
and radioactive waste treatment

C. M. WAI, University of Idaho, USA

Abstract: Minimizing liquid waste generation in the nuclear fuel cycle is of great importance to the future of nuclear energy. Separation techniques utilizing green solvents, supercritical fluid carbon dioxide and ionic liquids, for dissolution and extraction of uranium dioxide and fission products relevant to nuclear waste management are described in this chapter. An industrial demonstration of the supercritical fluid technology for recovering enriched uranium from the incinerator ash produced by the light water reactor fuel fabrication process by Areva NP in Richland, Washington is a good example of the new trend for treating nuclear wastes. Prospects and advantages of these emerging green techniques for nuclear fuel reprocessing and radioactive waste treatment are discussed.

Key words: green extraction techniques, supercritical fluid, ionic liquid, nuclear waste, spent fuel.

14.1   Introduction

With the threat of global warming, developing environmentally sustainable energy sources to replace traditional fossil fuels is of ultimate importance for the survival of our civilization. Nuclear power is free of carbon emission. Currently, nuclear energy contributes to about 20% of the electricity generated in the USA compared to 80% of that in France. One public concern regarding expanding use of nuclear energy for power generation in many countries including the USA is the economic and environmental issues associated with managing the wastes produced by nuclear power generation. Traditional methods of treating nuclear wastes and reprocessing spent fuel require aqueous acids and organic solvents for dissolution and separation of radioactive elements with the unavoidable consequence of generating large volumes of liquid wastes. Minimizing waste generation in the nuclear fuel cycle is obviously of great importance to the future of nuclear energy. Searching new technologies for managing nuclear wastes in an environmentally sustainable way has become an active research area in

recent years. This chapter presents two emerging techniques utilizing environmentally sustainable solvents, namely supercritical fluid carbon dioxide and room temperature ionic liquids, for separation of actinides, lanthanides and fission products relevant to nuclear waste management and spent fuel reprocessing.

Supercritical fluid carbon dioxide (sc-CO_2) and ionic liquids (ILs) are considered green solvents for chemical reactions and separations (Phelps *et al.* 1996, Welton 1999). Research in sc-CO_2 dissolution and extraction of metal species started in the early 1990s (Laintz *et al.* 1991, 1992). Even in the early stage of the technology development, it was realized that one potential application of this new extraction technique would be in the area of nuclear waste treatment, because supercritical fluid extraction does not require conventional liquid solvents. Two decades later, supercritical fluid extraction technology has emerged as an acceptable green technique for treating nuclear wastes. One example is a recent announcement by AREVA NP to construct a supercritical fluid extraction plant for recovering enriched uranium from the incinerator ash waste produced by the light water nuclear reactor fuel fabrication process (Smith and Thomas 2008). The AREVA NP project currently in progress in Richland, Washington represents the first industrial effort of adopting a non-traditional green technology for nuclear waste management. Some information regarding the AREVA's supercritical fluid extraction technology will be described later in Section 14.4.

Ionic liquids have unique properties including non-flammable nature, near zero vapor pressure and high solubilities for a variety of compounds (Welton 1999, Dietz and Dzielawa 2001). These properties make ILs attractive for replacing volatile organic solvents traditionally used in various liquid-liquid extractions. In addition, ILs like sc-CO_2 show good radiation stability (Visser and Rogers 2003, Dietz and Dzielawa 2001, Mekki *et al.* 2006) an attractive property for their utilization as media for processing radioactive materials. Both sc-CO_2 and IL-based separation techniques are emerging as potential alternatives for replacing the conventional aqueous acids and organic solvent-based techniques for managing nuclear wastes.

14.2   Supercritical fluid extraction of lanthanides and actinides

Carbon dioxide is widely used for supercritical fluid extraction studies because of its moderate critical constants (P_c = 73 atm and T_c = 31 °C), chemical inertness, and low cost (Phelps *et al.* 1996). Above the critical point, CO_2 becomes a fluid that has both gas-like and liquid-like properties as illustrated in Fig. 14.1. Supercritical fluid CO_2 has mechanical properties
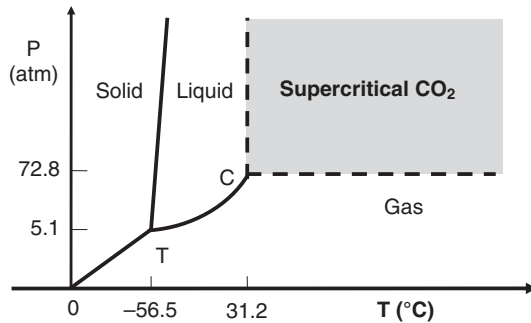
Supercritical fluids have both gas-like and liquid-like properties

	Density (g/mL)	Diffusion coeff. (cm^2/s)	Viscosity (g/cm s)
Gas	$(0.6\text{-}2)\times10^{-3}$	$(1\text{--}4)\times10^{-1}$	$(1\text{--}3)\times10^{-4}$
S.F.	$0.2\text{--}0.9$	$10^{-3}\text{--}10^{-4}$	$(1\text{--}3)\times10^{-4}$
Liquid	$0.6\text{--}2.0$	$(0.2\text{--}2)\times10^{-5}$	$(0.2\text{--}3)\times10^{-2}$

14.1 Phase diagram of CO_2 and some properties of sc-CO_2.

like a gas and yet has solvation strength like a liquid. Therefore, it is capable of penetrating into small pores of solid materials and dissolving organic compounds from the solid matrix. After extraction, the fluid phase can be vented as CO_2 gas by reduction of pressure causing precipitation of the extracted solutes. In principle, no liquid waste is produced by this extraction technique according to the idealized operation.

One important factor which determines the efficiency of supercritical fluid extraction is the solubility of the target compound in the fluid phase (Darr and Poliakoff, 1999). Because CO_2 is a linear molecule with no dipole moment, sc-CO_2 is a good solvent for dissolving non-polar organic compounds, but is ineffective for dissolving highly polar compounds or ions. Metal ions are not soluble in sc-CO_2. Searching for methods of dissolving metal ions in sc-CO_2 was the focus of the initial research started in the author's laboratory at the University of Idaho two decades ago. In 1991, Laintz *et al.* (1991) noticed that complexes formed by transition metal ions with a fluorinated dithiocarbamate chelating agent bis(trifluoroethyl) dithiocarbamate (FDDC) exhibited unusually high solubilities (by 2–3 orders of magnitude) relative to their non-fluorinated analogs. Based on this information, the authors demonstrated that copper ions (Cu^{2+}) in aqueous solutions can be effectively extracted into sc-CO_2 with the aid of FDDC (Laintz *et al.* 1992). The idea of using fluorinated chelating agents for dissolution of metal ions in sc-CO_2 was actually inspired by the fact that perfluorinated alkanes were considered at that time as blood substitutes because of their high solubilities for oxygen and carbon dioxide. The reverse is apparently true for dissolution of fluorinated compounds in sc-CO_2.

Today, fluorine-containing compounds are generally referred to as "CO_2-philic" because of their high solubilities in sc-CO_2. The successful demonstration of Cu^{2+} extraction immediately led to the investigation of extracting lanthanides and uranium in sc-CO_2 using fluorinated ligands because of its potential relevance to nuclear waste management. Several reports appeared after 1992 demonstrating that trivalent lanthanide ions and uranyl ions dissolved in water or spiked in solid materials could be effectively extracted by sc-CO_2 using fluorinated β-diketonates as extractants (Lin *et al.* 1993, Lin and Wai, 1994, Lin *et al.* 1994). Among a number of fluorinated β-diketonates tested for sc-CO_2 extractions, thenoyltrifluoroacetone (Htta) was more often used than the others because it is a solid at room temperature and is easier to handle experimentally (Wai and Wang 1997). After these initial reports, dissolution of uranium oxides directly in sc-CO_2 with fluorinated β-diketones was investigated (Wai and Waller, 2000). Direct dissolution of solid UO_3 in sc-CO_2 with Htta occurs according to the following equation:

$$UO_3(s) + 2\ Htta \rightarrow UO_2(tta)_2 \cdot H_2O \qquad\qquad 14.1$$

The dissolution of UO_3 proceeds with a much higher efficiency if tri-n-butylphosphate (TBP) is present with Htta in sc-CO_2. The enhance efficiency is attributed to the fact that TBP is a stronger Lewis base which can replace water in $UO_2(tta)_2 \cdot H_2O$ to form a more soluble adduct complex $UO_2(tta)_2 \cdot TBP$ as shown in equation (14.2).

$$UO_3(s) + 2\ Htta + TBP \rightarrow UO_2(tta)_2 \cdot TBP + H_2O \qquad\qquad 14.2$$
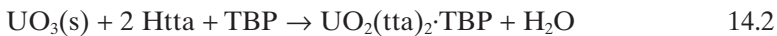
The solubility of $UO_2(tta)_2 \cdot TBP$ in sc-CO_2 is reasonably high to be potentially useful for reprocessing consideration. For example, at a fixed temperature of $40\,°C$ its solubility in sc-CO_2 is 7.5×10^{-3} mol/L at 200 atm and increases to about 1.5×10^{-2} mol/L at 300 atm. Reaction (14.2) occurs efficiently for UO_3 because uranium is in the +6 oxidation state, which leads to the formation of the uranyl-tta-TBP adduct complex with no need of an oxidation step. However, this reaction does not occur with UO_2 because uranium is in the +4 oxidation state, which does not form a stable complex with tta and TBP. A CO_2-soluble oxidizing agent such as H_2O_2 has been shown to promote the dissolution of UO_2 in sc-CO_2 with Htta and TBP but the efficiency is limited (Trofimov *et al.* 2001). Research in extraction of actinides in sc-CO_2 using fluorinated β-diketones and organophosphorus reagents may still find applications in nuclear waste treatments. For example, a report in 2003 showed that plutonium and americium in soil could be effectively removed by sc-CO_2 augmented with Htta and TBP (Fox and Mincher 2003). The solubilities of uranium, plutonium, neptunium, and americium β-diketonates and their adducts with organophosphorus reagents in sc-CO_2 were also reported (Murzin *et al.* 2002).

A significant development in supercritical fluid extraction of uranium was made in 1995 by Lin *et al.* (1995) who reported that uranyl ions in nitric acid solutions could be extracted into sc-CO_2 with the aid of TBP, a well-known ligand for uranium extraction in the conventional PUREX (Plutonium Uranium Extraction) process. TBP happens to be highly soluble in sc-CO_2. An earlier report showed that about 10% by mole of TBP could be dissolved in sc-CO_2 under normal extraction conditions (Page *et al.* 1993). Actually, TBP becomes miscible with sc-CO_2 above a certain pressure at a given temperature according to a later report (Joung *et al.* 1999). The efficiency of extracting uranium by the sc-CO_2/TBP process depends on the nitric acid concentration and follows closely the same trend as the traditional solvent extraction process using dodecane and TBP as shown in Fig. 14.2 (Lin *et al.* 1995). The extracted uranium species in sc-CO_2 was identified as $UO_2(NO_3)_2(TBP)_2$ similar to the uranyl complex extracted from nitric
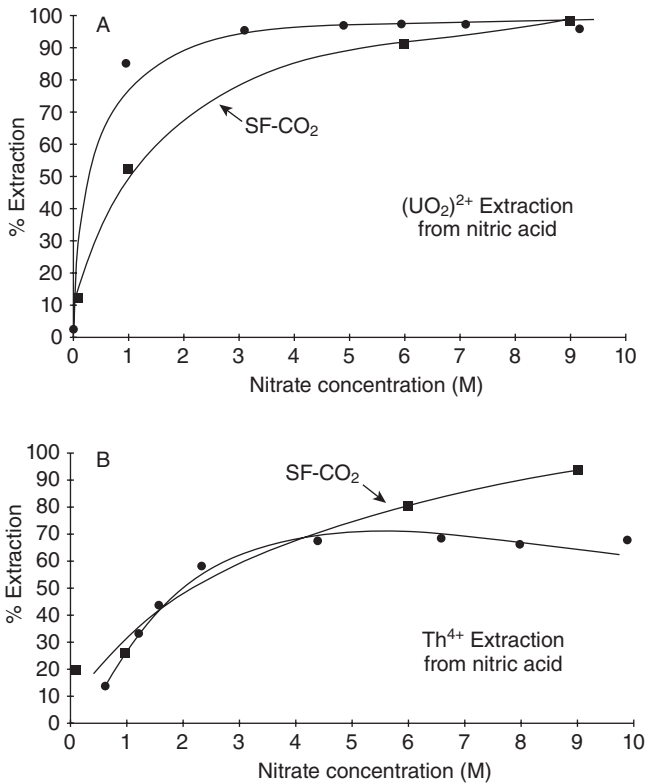
14.2 Extraction of U(VI) and Th(IV) from nitric acid solutions with sc-CO_2 containing TBP. Solvent extraction data with 19% TBP in dodecane are given for comparison. From Lin *et al.* 1995. Reproduced by permission of The American Chemical Society.
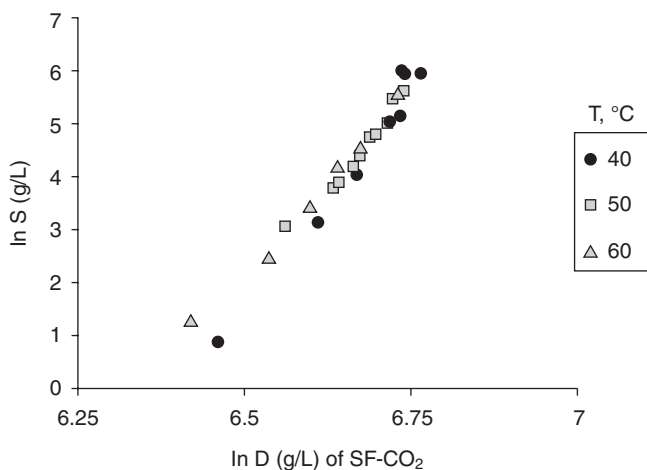
14.3 Solubility of $UO_2(NO_3)_2(TBP)_2$ in sc-CO_2. From Carrott *et al.* 1998. Reproduced by permission of The Royal Society of Chemistry.

acid into dodecane with TBP (Carrott *et al.* 1998). To evaluate the solubility of the uranyl complex in sc-CO_2, a high-pressure fiber-optic cell was designed to measure the absorption spectrum of the complex *in situ* in the fluid phase (Carrott and Wai 1998). The solubility of $UO_2(NO_3)_2(TBP)_2$ in sc-CO_2 measured by the spectroscopic method is surprisingly high. At 40 °C and 200 atm, the solubility of the uranyl complex in the fluid phase reaches 0.45 moles per liter, a concentration comparable to that used in the conventional PUREX process (Wai 2001). When the solubility of the uranyl complex in sc-CO_2 is plotted against the density of the fluid phase, a linear relationship is observed as shown in Fig. 14.3. The results given in Fig. 14.3 demonstrate the solvation strength of the supercritical fluid is tunable with respect to density. Consequently, the solubility of $UO_2(NO_3)_2(TBP)_2$ in sc-CO_2 can be predicted based on the relationship log S = a log φ + b, where S is the solubility in g/L, φ is the density also in g/L, and a and b are constants. The tunable solvation property is unique for sc-CO_2 and suggests a possibility of selective dissolution or separation of metal complexes in sc-CO_2 by manipulation of density (i.e., temperature and pressure) of the fluid phase. Conventional liquid solvents are basically not compressible and the solvation strength cannot be altered at a given temperature by varying pressure except perhaps at extremely high pressures. Other studies of uranium extraction using sc-CO_2 and TBP were reported by Meguro *et al.* (1998a, 1998b). In another study, Iso *et al.* (2000) showed that the distribution of Pu(IV) between 3 M nitric acid and sc-CO_2 containing TBP depends on pressure at a given temperature (60 °C) and follows the equation log D = a log φ + b, where D is the distribution coefficient, φ is the density of the
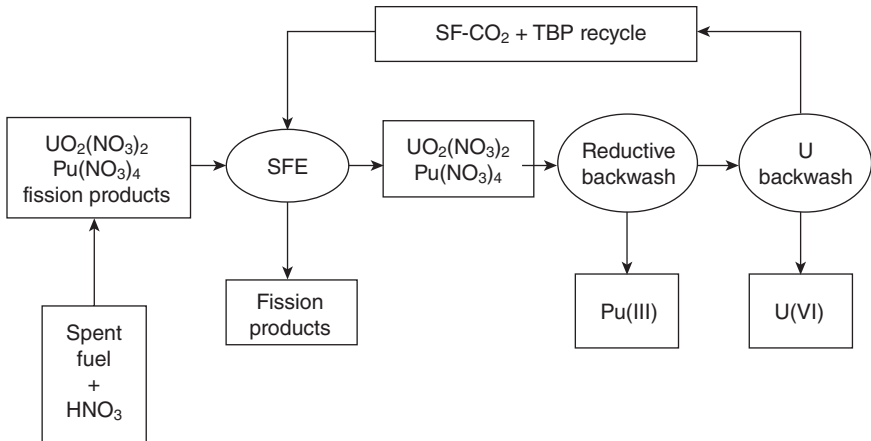
14.4 Schematic diagram of the supercritical fluid-PUREX process proposed by Smart *et al.* 1998. Reproduced by permission of The Royal Society of Chemistry.

fluid and a and b are constants. The D values as well as the constants a and b for U(VI) in the same system are different from those of Pu(IV) suggesting some degree of separation of Pu(IV) and U(VI) can be achieved by adjusting the pressure of the sc-CO_2 extraction process. These studies provide a basis for using sc-CO_2 to replace the organic solvents used in the PUREX process.

Based on the information available in 1998, Smart *et al.* proposed a supercritical fluid-PUREX process for reprocessing spent nuclear fuel as illustrated in Fig. 14.4 (Smart *et al.* 1998). In this process, sc-CO_2 is employed to replace the organic solvent conventionally used in the PUREX process. The advantages of the supercritical fluid-PUREX process include conceivably higher mass transport properties, faster extraction rates, and tunable distribution coefficients of uranium and other actinides. However, since nitric acid is used to dissolve spent fuel in the supercritical fluid-PUREX process, it would still produce acidic liquid waste like the PUREX process. After the proposed application by Smart *et al.* (1998), research in finding a dry process for dissolution of uranium dioxide in sc-CO_2 intensified (Wai 2006a).

14.3 Direct dissolution of uranium oxides in supercritical carbon dioxide

In the PUREX process, UO_2 is first dissolved in a nitric acid solution (3–6 M) to form uranyl ions followed by TBP extraction of the uranyl ions using an organic solvent such as dodecane. Nitric acid oxidizes uranium in

UO_2 from the +4 oxidation state to +6 oxidation state in the form of $(UO_2)^{2+}$ which is subsequently extracted into the organic phase with TBP as $UO_2(NO_3)_2(TBP)_2$. Therefore, nitric acid serves two purposes in this process: (1) it acts as an oxidizing agent converting UO_2 to uranyl $(UO_2)^{2+}$ ions and (2) it provides nitrate ions to neutralize the charges carried by uranyl ions leading to the formation of extractable $UO_2(NO_3)_2(TBP)_2$. In the early sc-CO_2 experiments for extracting uranyl from nitric acid solutions it was noted that HNO_3 can be carried into the fluid phase in the presence of TBP (Wai *et al.* 1999c). This is true also in the PUREX process (Chaiko and Vandegrift 1988). After the extraction, the aqueous phase remained separated from the sc-CO_2 phase but the concentration of HNO_3 in the aqueous phase was significantly reduced. The possibility of using TBP as a carrier for dissolving HNO_3 in sc-CO_2 was investigated by several groups including one group at Nagoya University in Japan (Tomioka *et al.* 2001) and another at the University of Idaho (Samsonov *et al.* 2001). According to the Lewis acid-base complex formation principle, the P=O group in TBP is an electron donor (Lewis base) which can be bound to protons of Lewis acids such as HNO_3 or H_2O through hydrogen bonding. When TBP is mixed with concentrated nitric acid (15.5 M) by rigorous shaking, HNO_3 can dissolve in the TBP phase forming a complex of the general form $TBP(HNO_3)_x(H_2O)_y$ which is immiscible with water. The values of x and y in the complex can vary depending on the relative amounts of TBP and the concentrated nitric acid used in the preparation of the complex. Experimentally, the values of x and y in the complex can be determined by acid-base titration and by Karl Fischer titration, respectively. As shown in Table 14.1, the complex has the composition $TBP(HNO_3)_{1.8}(H_2O)_{0.6}$ if it is prepared by mixing equal volumes of TBP and concentrated nitric acid (15.5 M). If the ratio of TBP to the acid is 5:1 (e.g. 5 mL TBP to 1 mL of the concentrated nitric acid) in the preparation, the TBP phase has the composition $TBP(HNO_3)_{0.7}(H_2O)_{0.7}$. Nuclear magnetic resonance (NMR) studies indicate that the protons of HNO_3 and H_2O in the complex probably undergo rapid exchange resulting in one single peak which shifts upfield with increasing x/y ratio (Enokida

Table 14.1 Composition of TBP-HNO_3-H_2O complexes. From Enokida *et al.* 2003

TBP volume	HNO_3 volume[a]	Mole ratio[b] TBP/HNO_3/H_2O
5 mL	0.815 mL	1:0.7:0.7
5 mL	1.30 mL	1:1.0:0.4
5 mL	5.00 mL	1:1.8:0.6

a. 15.5 M nitric acid.
b. Based on Karl-Fisher analysis and acid-base titration of the TBP phase.

et al. 2003). When the TBP-HNO$_3$ complex is added to a low dielectric constant solvent such as chloroform, the solution becomes cloudy due to formation of very fine droplets of nitric acid. This is attributed to an anti-solvent effect because nitric acid has a very low solubility in chloroform. The same phenomenon occurs when the TBP(HNO$_3$)$_{1.8}$(H$_2$O)$_{0.6}$ complex is added to sc-CO$_2$. This anti-solvent effect provides a mechanism of dispersing find droplets of nitric acid in the supercritical fluid phase for dissolution of uranium oxides. The concentration of HNO$_3$ in the small water droplets is probably very high, significantly higher than the 3–6 M nitric acid used in the PUREX process. The small acid droplets perhaps can exist in the sc-CO$_2$ phase like reverse micelles surrounded by TBP. Water-in-sc-CO$_2$ microemulsions (reverse micelles) have been extensively studied using CO$_2$ soluble surfactants (Ji *et al.* 1998a, Wai 2002). The microemulsions are dynamic in nature and they are able to extract uranium from soil and dissolve the uranyl ions in the water core of the CO$_2$ microemulsion (Campbell *et al.* 2001).

The TBP-nitric acid complex is soluble in sc-CO$_2$ and capable of dissolving uranium oxides in contact with the fluid phase. Figure 14.5 shows the amounts of UO$_2$ and UO$_3$ solids dissolved in sc-CO$_2$ containing the TBP(HNO$_3$)$_{0.7}$(H$_2$O)$_{0.7}$ complex with respect to time in a continuous flow system (Samsonov *et al.* 2001). The sc-CO$_2$ solution containing the TBP-nitric acid complex was prepared by bubbling liquid CO$_2$ through a cell containing the complex placed upstream of the dissolution cell. As shown in Fig. 14.5, UO$_3$ is easier to dissolve than UO$_2$ in the sc-CO$_2$ containing the
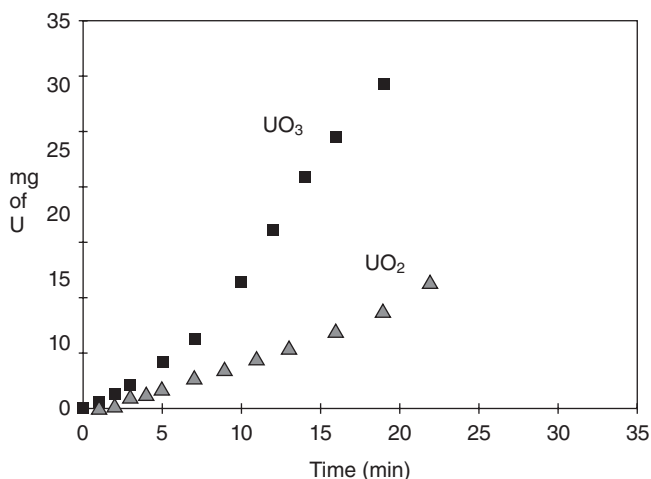
14.5 Direct dissolution of UO$_2$ and UO$_3$ solids in sc-CO$_2$ with TBP(HNO$_3$)$_{0.7}$(H$_2$O)$_{0.7}$. From Samsonov *et al.* 2001. Reproduced by permission of The Royal Society of Chemistry.

extractant because UO_3 is already in the +6 oxidation state. The dissolution of UO_3 in sc-CO_2 with the TBP-nitric acid complex may be expressed by the following equation:

$$UO_3(solid) + 2 \ TBP{\cdot}HNO_3 \rightarrow UO_2(NO_3)_2(TBP)_2 + H_2O \qquad 14.3$$

For the dissolution of UO_2 in sc-CO_2, the reaction may be expressed by Equation (14.4).

$$3 \ UO_2(solid) + 8 \ TBP{\cdot}HNO_3 \rightarrow 3 \ UO_2(NO_3)_2(TBP)_2$$
$$+ 2 \ TBP + 2 \ NO + 4 \ H_2O \qquad 14.4$$
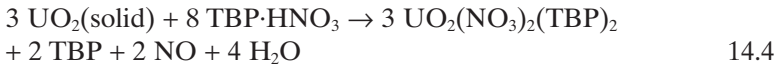
If $TBP(HNO_3)_{1.8}(H_2O)_{0.6}$ is used as the extractant, the rate of dissolution of UO_2 in sc-CO_2 is more rapid because of a higher HNO_3 concentration provided by the complex. After the dissolution, no aqueous phase is formed in the extraction cell because small amounts of water formed during the dissolution process can be carried out of the system by sc-CO_2 and TBP. The alkali metals, the alkaline earth metals, and many transition metals cannot be extracted by the TBP-HNO_3 complex in sc-CO_2.

One advantage of the sc-CO_2 dissolution method compared with the conventional PUREX process is that the former process combines dissolution and extraction in one step with no aqueous waste and organic solvent involved. In the PUREX process two steps are involved in the dissolution and extraction of spent fuel, i.e. UO_2 is first dissolves in a nitric acid solution followed by extraction of uranyl ions from the acid solution into an organic solvent with TBP under ambient pressure. The possibility of selective dissolution of lanthanides and actinides in the sc-CO_2 process has not been explored but is conceivable based on the tunable solvation property of the fluid. Furthermore, the sc-CO_2 dissolution process is carried out in a closed system, therefore volatile fission products can be concentrated in the sc-CO_2 stream and removed on-line with a suitable sorbent with minimal release into ambient atmosphere. Better control of volatile fission products may be another advantage of the sc-CO_2 process for reprocessing spent nuclear fuel. In the conventional PUREX process, volatile fission products including iodine-129 is released in the off-gas after dissolution of the spent fuel.

A conceptual illustration of a dry sc-CO_2 dissolution process for reprocessing spent nuclear fuel is given in Fig. 14.6 (Wai 2002). Using a TBP-HNO_3 complex, lanthanides, uranium and transuranic elements would be dissolved in the sc-CO_2 phase leaving fission products such as Sr and Cs behind in the residue. After isolation of $UO_2(NO_3)_2(TBP)_2$ from the sc-CO_2 phase, the un-used TBP-HNO_3 and CO_2 can be recycled. Figure 14.6 also includes a hypothetical ligand regeneration step in which $UO_2(NO_3)_2(TBP)_2$ would be converted to UO_2 with the regeneration of TBP-HNO_3. The proposed sc-CO_2 reprocessing process presents an idea which requires exten-
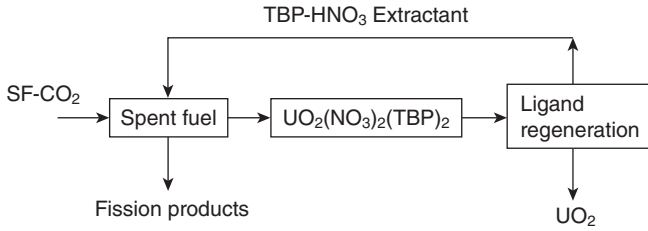
14.6 A conceptual illustration of reprocessing spent nuclear fuel in sc-CO_2 using a TBP-HNO_3 Lewis acid-base complex such as TBP$(HNO_3)_{1.8}(H_2O)_{0.6}$.

Table 14.2 Extraction of Sr^{2+}, Ca^{2+}, and Mg^{2+} from water by supercritical CO_2 containing DC18C6 and pentadecafluoro-n-octanoic acid at 60 °C and 100 atm. From Wai *et al.* 1999a

Mole ratio			% Extraction		
Sr^{2+}:DC18C6:PFOA-H			Sr^{2+}	Ca^{2+}	Mg^{2+}
1	10	0	1	0	0
1	0	10	4 ± 1	1 ± 1	1 ± 1
1	5	10	36 ± 2	1 ± 1	1 ± 1
1	10	10	52 ± 2	2 ± 1	1 ± 1
1	10	50	98 ± 2	7 ± 2	2 ± 1

The aqueous solution contained a mixture of Sr^{2+}, Ca^{2+}, and Mg^{2+} with a concentration of 5.6×10^{-5} M each; pH of water under equilibrium with SF-CO_2 = 2.9; 20 min static followed by 20 min dynamic flushing at a flow rate of 2 mL/min. PFOA-H = $CF_3(CF_2)_6COOH$. From Wai *et al.* 1999a. Reproduced by permission of The Royal Society of Chemistry.

sive research to turn it into a reality. Nevertheless, it points to a future direction for reprocessing spent nuclear fuel in an environmentally sustainable way (Wai 2006b).

Extractions of fission products such as ^{90}Sr and ^{137}Cs by sc-CO_2 have also been evaluated using selective ligands such as crown ethers (Wai *et al.* 1999a, 1999b). Table 14.2 shows the extraction of Sr^{2+} from water by sc-CO_2 with dicyclohexano-18-crown-6 (DC18C6), a CO_2 soluble ligand which is known to be selective for Sr^{2+} in conventional solvent extraction processes. However, the Sr^{2+}-DC18C6 complex is not soluble in sc-CO_2. One method of making the Sr^{2+}-DC18C6 soluble in sc-CO_2 is to use a fluorinated counter anion which would neutralize the charge of the complex and make the resulting ion-pair soluble in the fluid phase. Fluorinated counter anions such as ammonium or potassium salts of pentadecafluoro-n-octonoic acid and perfluoro-1-octane sulfonic acid are effective for extracting Sr^{2+} and Cs^+

using crown ether ligands in sc-CO_2. Selective extraction of Sr^{2+} over Ca^{2+} and Mg^{2+} in water by sc-CO_2 containing DC18C6 and pentadecafluoro-n-octonoic acid $CF_3(CF_2)_6COOH$ can be achieved as shown by the results given in Table 14.2 (Wai *et al.* 1999a). Selective extraction of Cs^+ by sc-CO_2 with dicyclohexano-21-crown-7 and perfluoro-1-octanesulfonate has also been demonstrated (Wai *et al.* 1999b). These studies may provide valuable information for designing ligands for selective extraction of fission products in sc-CO_2 that may be critical for future development of sc-CO_2-based processes for reprocessing spent fuel.

14.4   Current industrial demonstrations of supercritical fluid extraction technology for nuclear waste treatment and for reprocessing spent fuel

In the fuel fabrication process for light water nuclear power reactors, enriched uranium hexafluoride (UF_6) is converted to UO_2 as illustrated in Fig. 14. 7. Disposable solid waste generated by the process is reduced by a factor of 1/25 through a carefully controlled incineration process. The incinerator ash contains approximately 10% by weight of enriched uranium (about 3.5% ^{235}U). Some gadolinium (Gd) which is added to the fuel as a neutron absorber is also present in the waste ash. In 2003, AREVA NP started looking into the possibility of using sc-CO_2 as a medium for recovering enriched uranium from the incinerator ash waste generated by the fuel fabrication process in collaboration with the University of Idaho. With the aid of the TBP-HNO_3 complex described in the previous section, enriched uranium and gadolinium in the incinerator ash can be effectively extracted

Uranium recovery   Waste treatment

Incoming UF_6 vaporization UO_6 powder   Powder   Fual rod/   Transport to
UF_6 cylinders   production   processing/   bundle assembly/ nudear reactors
                                                       pellet   quality check
                                                       manufacturing
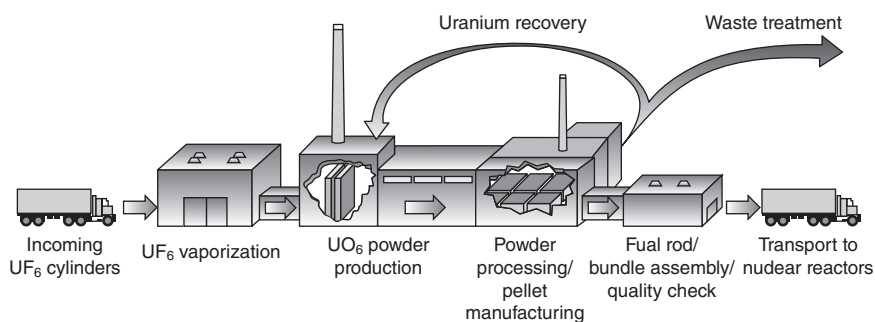
14.7 Illustration of a typical light water reactor fuel fabrication facility (Source: US Nuclear Regulatory Commission. "Light Water Reactor Low-Enriched Uranium Fuel," Fuel Fabrication. ONLINE. 2009. Nuclear Regulatory Commission. Available: http://www.nrc.gov/materials/fuel-cycle-fac/fuel-fab.html [5 Aug. 2009].

Countercurrent column stripping and separation
of Gd^{3+} and $(UO2)^{2+}$ in supercritical fluid CO_2
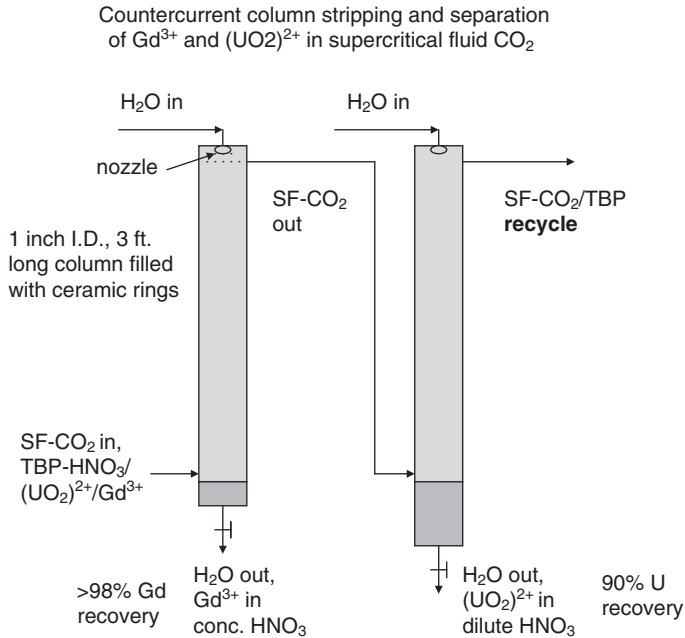
14.8 Illustration of AREVA's supercritical fluid countercurrent stripping process for recovering enriched uranium from incinerator ash.

into the sc-CO_2 phase. Separation of uranium and gadolinium is achieved down-stream from the extractor using a counter-current stripping method as illustrated in Fig. 14.8. Water is introduced into the stripping column from the top via a nozzle. Separation of gadolinium and uranium is based on the fact that $UO_2(NO_3)_2(TBP)_2$ and $Gd(NO_3)_3(TBP)_x$ exist in the sc-CO_2 phase at different HNO_3 concentrations. $Gd(NO_3)_3(TBP)_x$ can be stripped from the sc-CO_2 phase at a higher HNO_3 concentration than $UO_2(NO_3)_2(TBP)_2$. Therefore, with a small amount of water adding to the first stripping column, greater than 98% of Gd^{3+} is removed from the sc-CO_2 phase. After removing Gd^{3+}, the fluid is fed into a second counter-current column to strip UO_2^{2+} from the fluid with additional water. TBP and some uranium remaining in the sc-CO_2 phase are recycled for repeated extraction of the ash. The whole process is in a closed loop system to minimize any discharges to the environment. The AREVA's supercritical fluid extraction plant is currently under construction in Richland, Washington with a capacity of processing approximately 120 kg of the ash for every eight-hour shift. The AREVA uranium recovery project is the first application of the supercritical fluid technology for treating a nuclear waste by the nuclear industry. The new technology offers a cleaner, cheaper method to recover and recycle a valu-

able commodity (enriched uranium) from a material that previously was considered waste.

Another industrial demonstration of the sc-CO$_2$ extraction technology was conducted in Japan by Mitsubishi Heavy Industries, Japan Nuclear Cycle Corp. and Nagoya University testing the feasibility of reprocessing spent nuclear fuel using this green solvent (Shimada *et al.* 2002). The process is called "Super-DIREX" process which stands for supercritical fluid for direction extraction. The main purpose of this project is to evaluate the feasibility of direct dissolution of uranium and plutonium in irradiated uranium oxides and in spent fuel by sc-CO$_2$ containing the TBP(HNO$_3$)$_{1.8}$(TBP)$_{0.6}$ complex. After dissolution, uranium and plutonium are stripped from the sc-CO$_2$ phase with water. Recovery of UO$_2$ from the strip solution follows the conventional PUREX process. The details of the Super-DIREX project are not fully known. The nitric acid concentration in the acid droplets surrounded by TBP (like reverse micelles) is estimated to be greater than 12 mol/L (Sawada *et al.* 2005). A recent report by Sawada *et al.* (2009) described the distribution coefficients of U(VI) and some simulated fission products measured between aqueous phase of high nitrate concentrations (4–15 mol/L) and dodecane with the purpose of understanding the extraction behavior of uranium and fission products in the Super-DIREX process. Reprocessing spent nuclear fuel in sc-CO$_2$ is obviously a complicated process and requires many efforts in chemical and engineering studies to evaluate its feasibility. Nevertheless, the Super-DIREX project should provide some valuable information regarding the chemistry of uranium, plutonium and fission products in the sc-CO$_2$ dissolution process and safe handling of highly radioactive materials in a pressurized system.

14.5   Ionic liquid and supercritical fluid coupled extraction of lanthanides and actinides

Ionic liquids (ILs) are salts with low melting points composed of an organic cation and an anion of various forms (Binnemans 2007). The properties of ILs with respect to miscibility with water, solubility of metal salts, polarity, viscosity, etc., can be changed by choice of the anion and the cation. One type of room temperature ILs widely used for current studies is based on the 1-alkyl-3-methylimidazolium cation (bmin) with different forms of anion. With a fluorinated anion, the bmim-based ILs can be water immiscible (hydrophobic). The bmin-based ionic liquid with bis(trifluoromethylsulfonyl)imide anion (Tf$_2$N$^-$) is of particular interest for extraction of metal ions due to their water stability, relative low viscosity, high conductivity, good electrochemical and thermal stability (Mekki *et al.*, 2006). The chemical structure of the ionic liquid [bmin][Tf$_2$N$^-$] is given in Fig. 14.9. Aqueous metal ions are usually not soluble in this type of IL but

with the aid of hydrophobic ligands or chelating agents, metal ions may become soluble in the IL phase. Extraction of uranyl ions, trivalent lanthanides and actinides from nitric acid solutions into the ILs has been investigated using a variety of ligands including TBP, octyl(phenyl)-N,N-diisobutylcarbamoylmethyl phosphine oxide (CMPO), β-diketone, and acidic dialkylorganophosphorous (Binnemans 2007). In general, cation exchange processes have been attributed to the observed metal extraction mechanism for IL systems, in which transfer of positively charged metal ions into the IL phase is accompanied by a simultaneous loss of cations to the aqueous phase (Visser *et al.* 2003, Jensen *et al.* 2003). After extraction of metal ions into the ILs, recovering the dissolved metal can be accomplished by back-extraction with an organic solvent. Using electrochemical methods for recovering metal species in ILs has also been investigated (Rao *et al.* 2008).

It is known that sc-CO_2 dissolves effectively in ILs whereas the solubility of the latter in the former is negligible. Therefore, sc-CO_2 provides an effective medium for removing solutes from ILs. Mekki *et al.* have recently demonstrated that Cu^{2+} ions and trivalent lanthanides (La^{3+} and Eu^{3+}) can be extracted from aqueous solutions into an imidazolium-based ionic liquid (1-butyl-3-methylimidazolium, or bmin) with Tf_2N^- counter anions using β-diketones as extractants (Mekki *et al.* 2005, 2006). The metal-β-diketonates in the ionic liquid phase can be effectively transferred to sc-CO_2 at 50 °C and 150 atm. The efficiency of extracting lanthanide-β-diketonates from the IL to sc-CO_2 is typically greater than 98% under the specified conditions. The reports by Mekki *et al.* (2005, 2006) suggest that sc-CO_2 may be an effective medium for stripping metal species dissolved in an ionic liquid phase without carrying over the ionic liquid to the CO_2 phase. Therefore, a two-step extraction process involving three phases (water, ionic liquid, and sc-CO_2) may provide an alternative for removing radioactive materials from aqueous solutions to the CO_2 phase (Fig. 14.9). The advantages of this new IL-sc-CO_2 coupled extraction technique include: (1) radionuclides from the aqueous wastes can be transferred to and concentrated in an ionic liquid under ambient temperature and pressure, and (2) back extraction of the radionuclides from the IL phase to the sc-CO_2 phase may be selective because the solvation strength of sc-CO_2 is tunable, and (3) no loss of the IL occurs in the back-extraction process and no organic solvent is introduced into the ionic liquid phase. Actually, due to its self cleaning nature, sc-CO_2 could help removing undesirable organic residues from the IL phase. After the back-extraction step, the IL can be reused and the CO_2 recycled after precipitation of the solutes by pressure reduction.

Transport of uranyl ions $(UO_2)^{2+}$ from aqueous nitric acid solutions to [bmin][Tf_2N^-] using TBP as a complexing agent followed by sc-CO_2 stripping of the uranyl complex from the ionic liquid phase to the supercritical
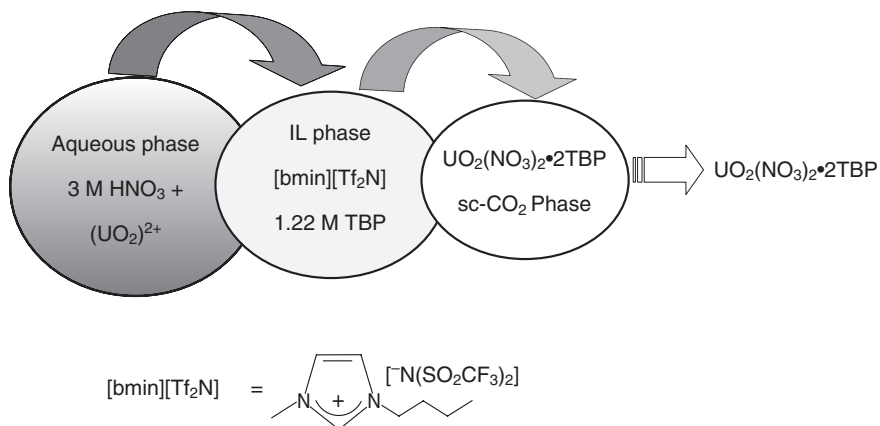
14.9 Extraction of uranium from nitric acid solution using ionic liquid and supercritical CO$_2$ in conjunction – a two-loop extraction system involving three phases.

fluid phase has been reported recently (Wang *et al.* 2009). The uranyl species involved in this three-phase system were studied using spectroscopic techniques. The efficiency of extracting $(UO_2)^{2+}$ in 3 M nitric acid to [bmin][Tf$_2$N$^-$] with 1.1 M TBP is greater than 95% at room temperature under ambient pressure at an acid to IL phase ratio of 1:1 by volume. The uranyl species extracted into the IL phase showed a UV-Vis absorption spectrum similar to that of $UO_2(NO_3)_2(TBP)_2$ but with some noticeable differences. The uranyl species in the IL phase can be effectively extracted into sc-CO$_2$ phase (>98%) at 40 °C and 150 atm. The rate of supercritical fluid extraction of $UO_2(NO_3)_2(TBP)_2$ from the IL phase appears to follow a zero-order rate equation. The absorption spectrum of the uranyl species extracted into the supercritical fluid phase is similar to that of $UO_2(NO_3)_2(TBP)_2$ known in the literature. The uranyl compound in sc-CO$_2$ was trapped in a hexane solution after depressurizing the system and the absorption spectrum is identical to that of $UO_2(NO_3)_2(TBP)_2$ observed from a standard solution prepared from synthesized $UO_2(NO_3)_2(TBP)_2$ crystals. These studies have provided a basis for developing a new process of extraction and separation of lanthanides and actinides from acidic solutions using a hyphenated IL-sc-CO$_2$ method. Separation of lanthanides and actinides after the sc-CO$_2$ extraction step could be achieved using the counter-current method described in the Areva NP project in the previous section. Separation of uranium from transuranic elements may also be possible using the counter-current method although no experimental results have been reported in the literature yet.

The hyphenated IL-sc-CO_2 extraction/separation technique may find applications in reprocessing spent fuel. In a recent report, Billard *et al.* demonstrated that uranium dioxide can be dissolved directly in [bmin] [Tf_2N^-] containing nitric acid (Billard *et al.* 2007). The IL can dissolve about 12,000 ppm of water without forming a separate aqueous phase (Billard and Gaillard, 2009). Our recent study also shows that uranium dioxide and lanthanide oxides can be dissolved directly in [bmin][Tf_2N^-] containing the $TBP(HNO_3)_{1.8}(H_2O)_{0.6}$ without forming a second aqueous phase. These new developments suggest the possibility of dissolving spent fuel directly in the IL without an aqueous nitric acid dissolution step. Therefore no aqueous waste would be produced and the dissolution can be done at room temperature under ambient pressure. Recovery of uranium from the IL may be achieved using the sc-CO_2 back-extraction method or by other techniques. For example, using electrochemical techniques for recovering uranium from the IL phase is another option.

14.6   Future trends

Supercritical fluid-based technologies for nuclear waste management have developed rapidly over the past two decades. A simple laboratory study in 1991 for testing solubility of metal chelates in supercritical fluid carbon dioxide has emerged as a new technology for nuclear waste management today. The AREVA NP's supercritical fluid extraction project for recovering enriched uranium from the incinerator ash generated by the light water nuclear reactor fuel fabrication process is driven by economic incentive and environmental consideration. The supercritical fluid extraction process would recover a valuable commodity (enriched uranium) from the incinerator ash and at the same time alleviate the cost and procedure that would otherwise be required to dispose of the waste. It perhaps can be called a new green technology for treating nuclear wastes in a profitable way. The success of the AREVA process would likely encourage the nuclear industry to consider this type of new green technology for treating other types of nuclear wastes and for reprocessing of spent nuclear fuel. The Super-DIREX demonstration project conducted by Mitsubishi Heavy Industries is one indication of the industry's interest in this new technology. Basic information regarding complexation and solvation of actinides, lanthanides, and fission products in sc-CO_2 and their partitions between CO_2 and aqueous acids or ionic liquids under pressure is needed to support future development of supercritical fluid-based technologies for nuclear fuel reprocessing and waste management. Engineering and materials studies with respect to safe handling of high-pressure systems for supercritical fluid operations are also needed to support the new technology development.

The current industrial demonstrations are all based on the use of phosphorus-containing reagents for extraction and separation of uranium. Phosphorus and fluorine-containing regents used in many supercritical fluid metal extraction studies are not environmentally friendly. Developing novel ligands based on the "CHON" principle is one approach which would make the current supercritical fluid extraction technology more environmentally sustainable. The CHON ligands contain only carbon, hydrogen, oxygen, and nitrogen. They can be finally disposed by incineration without creating serious environmental problems. One type of CHON ligand under the general name of oxa-diamides has been tested for supercritical fluid extraction of lanthanides and actinides (Tian *et al.* 2008). This type of new green ligand with multi-dentate electron donating groups may also be more effective and selective for complexation with lanthanides and actinides of different oxidation states. Research along this direction is needed for future development of supercritical fluid-based technologies for nuclear applications.

Room temperature ionic liquid dissolution of lanthanides and actinides in combination with supercritical fluid extraction appears to provide another promising alternative for nuclear waste management. Uranium in acid solutions can be dissolved in an IL at room temperature and under ambient pressure. Direct dissolution of uranium oxides in ILs would make this process attractive for reprocessing of spent nuclear fuel. Separation and recovery of uranium from the IL can be achieved by back-extraction with sc-CO_2. The hyphenated ionic liquid-supercritical fluid extraction technique would reduce the cost of high-pressure operation required by the sc-CO_2 process alone. It may also provide selectivity for lanthanides and actinides in the IL dissolution process and the supercritical fluid back-extraction process. The unusual nature of ILs may induce unique salvation, complexation, and extraction features which are largely unknown at the present time (Billard and Gaillard, 2009). The chemical behavior of actinides, lanthanides, and fission products in ILs and their distributions between IL and sc-CO_2 should be thoroughly investigated to support development of the hyphenated extraction techniques.

The need for renewable and emission free energy sources is obvious and urgent in order to alleviate the threat of global warming. Nuclear energy is carbon emission free and has been used for power generation for half a century. The bottleneck of public acceptance of nuclear energy is the main problem associated with nuclear waste disposal. Using green solvents such as supercritical carbon dioxide and room temperature ionic liquids to replace traditional aqueous acids and organic solvents for dissolution, extraction, and separation of uranium and other radioactive nuclides in the wastes generated by the nuclear fuel cycle appears to be a promising

approach to minimizing nuclear waste problems. These emerging separation techniques will probably play a significant role in managing nuclear wastes in the 21st century.

14.7   References

Billard, I. & Gaillard, C. 2009. Actinide and lanthanide speciation in imidazolium-based ionic liquids. *Radiochimica Acta*, 97:355–359.

Billard, I., Gaillard, C. & Henning, C. 2007. Dissolution of UO_2, UO_3 and of some lanthanide oxides in $BuminTf_2N$: effect of acid and water and formation of $UO_2(NO_3)^-$. *Dalton Transactions*, 4212–4221.

Binnemans, K. 2007. Lanthanides and actinides in ionic liquids. *Chemical Review*, 107:2592–2614.

Campbell, M.L., Apodaca, D.L., Yates, M.Z., McCleskey, T.M. & Birnbaum, E.R. 2001. Metal extraction from heterogeneous surfaces using carbon dioxide micro-emulsions. *Langmuir*, 17:5458–5463.

Carrott, M.J. & Wai, C.M. 1998. UV-vis spectroscopic measurement of solubilities in supercritical CO_2 using high pressure fiber optic cells. *Analytical Chemistry*, 70:2421–2425.

Carrott, M.J., Waller, B.E., Smart, N.G. & Wai, C.M. 1998. High solubility of $UO_2(NO_3)_2$2TBP complex in supercritical CO_2. *Chemical Communications*, 373–374.

Chaiko, D.J. & Vadegrift, G.F. 1988. A thermodynamic model of nitric acid extraction by tri-n-butyl phosphate. *Nuclear Technology*, 82:52–59.

Darr, J. & Poliakoff, M. 1999. New directions in inorganic and metal-organic coordination chemistry in supercritical fluids. *Chemical Review*, 99:495–541.

Dietz, M.L. & Dzielawa, J.A. 2001. Ion exchange as a mode of cation transfer into room-temperature ionic liquids containing crown ethers: implications for the "greenness" of ionic liquids as diluents in liquid-liquid extraction. *Chemical Communications*, 2124–2125.

Enokida, Y., Tomioka, O., Lee, S.C., Rustenholtz, A. & Wai, C.M. 2003. Characterization of tri-n-butylphosphate-nitric acid complex – a CO_2-soluble extractant for dissolution of UO_2. *Industrial & Engineering Chemistry Research*, 42:5037–5041.

Fox, R.V. & Mincher, B.J. 2003. Supercritical fluid extraction of plutonium and americium from soil using β-diketone and tributyl phosphate complexants. Chapter 4 in *ACS Symposium Series 860, Supercritical Carbon Dioxide Separations and Processes*, Editors A.S. Gopalan, C.M. Wai, H.K. Jacobs, American Chemical Society, Washington, DC, p. 36–49.

Iso, S., Uno, S., Meguro, Y., Sasaki, T. & Yoshida, Z. 2000. Pressure dependence of extraction behavior of plutonium (IV) and uranium(VI) from nitric acid solution to supercritical carbon dioxide containing tributylphosphate. *Progress in Nuclear Energy*, 37(1–4):423–428.

Jensen, M.P., Neuefeind, J., Beitz, J.V., Skanthakumar, S. & Soderholm, L. 2003. Mechanisms of metal ion transfer into room-temperature ionic liquids: the role of anion exchange. *Journal of the American Chemical Society*, 125:15466–15473.

Ji, M., Chen, X., Wai, C.M. & Fulton, J.L. 1999. Synthesizing and dispersing silver nanoparticles in a water-in-supercritical carbon dioxide microemulsion. *Journal of the American Chemical Society*, 121:2631–2632.

Joung, S.N., Kim, S.J. & Yoo, K.P. 1999. Single-phase limit for mixtures of tri-n-butylphosphate + CO_2 and bis(2-ethylhexyl)phosphoric acid + CO_2. *Journal of Chemical & Engineering Data*, 44:1034–1036.

Laintz, K.E., Wai, C.M., Yonker, C.R. & Smith, R.D. 1991. Solubility of fluorinated metal dithiocarbamates in supercritical carbon dioxide. *Journal of Supercritical Fluids*, 4:194–198.

Laintz, K.E., Wai, C.M., Yonker, C.R. & Smith, R.D. 1992. Extraction of metal ions from liquid and solid materials by supercritical carbon dioxide. *Analytical Chemistry*, 64:2875–2878.

Lin, Y. & Wai, C.M. 1994. Supercritical fluid extraction of lanthanides with fluorinated beta-diketones and tributyl phosphate. *Analytical Chemistry*, 66:1971–1975.

Lin, Y., Brauer, R.D., Laintz, K.E. & Wai, C.M. 1993. Supercritical fluid extraction of lanthanides and actinides from solid materials with a fluorinated beta-diketone. *Analytical Chemistry*, 65:2549–2552.

Lin, Y., Wai, C.M., Jean, F.M. & Brauer, R.D. 1994. Supercritical fluid extraction of thorium and uranium ions from solid and liquid materials with fluorinated beta-diketones and tributyl phosphate. *Environmetal Science & Technology*, 28:1190–1193.

Lin, Y., Smart, N.G. & Wai, C.M. 1995. Supercritical fluid extraction of uranium and thoriumfrom nitric acid solutions with organophorous reagents. *Environmental Science & Technology*, 29:2706–2708.

Meguro, Y., Iso, S., Sasaki, T. & Yoshida, Z. 1998a. Solubility of organophosphorus metal extractants in supercritical carbon dioxide. *Analytical Chemistry*, 70:774–779.

Meguro, Y., Iso, S. & Yoshida, Z. 1998b. Correlation between extraction equilibrium of uranium (VI) and density of CO_2 medium in a HNO_3/supercritical CO_2-tributyl phosphate system. *Analytical Chemistry*, 70:1262–1267.

Mekki, S., Wai, C.M., Billard, I., Moutiers, G., Yen, C.H., Wang, J.S., Ouadi, A., Gaillard, C. & Hesemann, P. 2005. Cu(II) extraction by supercritical fluid carbon dioxide from a room temperature ionic liquid using fluorinated β-diketones. *Green Chemistry*, 7:421–423.

Mekki, S., Wai, C.M., Billard, I., Moutiers, G., Burt, J., Yoon, B., Wang, J.S., Gaillard, C., Ouadi, A. & Hesemann, P. 2006. Extraction of lanthanides from aqueous solutions by using room temperature ionic liquid and supercritical carbon dioxide in conjunction. *Chemistry-A European Journal*, 12:1760–1766.

Murzin, A.A., Babain, V.A., Shadrin, A.Ui., Smirnov, I.V., Lumpov, A.A., Gorshkov, N.I., Miroslavov, A.E. & Muradymov, M.Z. 2002. Supercritical fluid extraction of actinide complexes: II. SFE of actinide β-diketonates. *Radiochemistry*, 44(5):423–427.

Page, S.H., Sumpter, S.R., Goats, S.R., Lee, M.L., Dixon, D.J. & Johnston, K.P. 1993. Tri-n-butylphosphate/CO_2 and acetone/CO_2 phase behaviors and utilities in capillary supercritical-fluid chromatography. *Journal of Supercritical Fluids*, 6:95–101.

Phelps, C.L., Smart, N.G. & Wai, C.M. 1996. Past, present and possible future applications of supercritical fluid extraction technology. *Journal of Chemical Education*, 73(12):1163–1168.

Rao, P.R.V., Venkatesan, K.A. & Srinivasan, T.G. 2008. Studies on applications of room temperature ionic liquids, *Progress in Nuclear Energy*, 50(12):449–455.

Samsonov, M.D., Wai, C.M., Lee, S.C., Kulyako, Y. & Smart, N.G. 2001. Dissolution of uraniuim dioxide in supercritical fluid carbon dioxide. *Chemical Communications*, 1868–1869.

Sawada, K., Uruga, K., Koyama, T. & Enokida, Y. 2005. Stoichiometric relation for extraction of uranium from UO_2 powder using TBP complex with HNO_3 and H_2O in supercritical CO_2. *Journal of Nuclear Science and Technology*, 42(3):301–304.

Sawada, K., Enokida, Y., Kamiya, M., Koyama, T. & Aoki, K. 2009. Distribution coefficients of U(VI), nitric acid and FP elements in extractions from concentrated aqueous solutions of nitrates by 30% tri-n-butylphosphate solution. *Journal of Nuclear Science and Technology*, 46(1):83–89.

Shimada, T., Ogumo, S., Ishihara, N., Kosaka, Y. & Mori, Y. 2002. A study on the technique of spent fuel reprocessing with supercritical fluid direct extraction (Super-Direx method). *Journal of Nuclear Science and Technology*, Supplement 3:757–760.

Smart, N.G., Wai, C.M. & Phelps, C. 1998. Supercritical Solutions. *Chemistry in Britain*, 34(8): 34–36.

Smith, T. & Thomas, J. 2008. Radioactive waste not wasted with new green chemistry technology. *Radwaste Solutions*, September/October issue, 32–35.

Tian, G., Liao, W., Rao, L. & Wai, C.M. 2008. Extraction of trivalent lanthanides with oxa-diamides in supercritical fluid carbon dioxide. *Industrial and Engineering Chemistry Research*, 47:2803–2807.

Tomioka, O., Meguro, Y., Iso, S., Yoshida, Z., Enokida, Y. & Yamamoto, I. 2001. Dissolution behavior of uranium oxides with supercritical CO_2 using HNO_3-TBP complex as a reactant. *Journal of Nuclear Science & Technology*, 38:1097–1102.

Trofimov, T.I., Samsonov, M.D., Lee, S.C., Smart, N.G. & Wai, C.M. 2001. Ultrasound enhancement of dissolution kinetics of uranium oxides in supercritical fluid carbon dioxide. *Chemical Technology and Biotechnology*, 76:1223–1226.

Visser, A.E. & Rogers, R.D. 2003. Room-temperature ionic liquids: new solvents for f-element separations and associated solution chemistry. *Journal of Solid State Chemistry*, 171:109–112.

Visser, A.E., Jensen, M.P., Laszak, I., Nash, K.L., Choppin, G.R. & Rogers, R.D. 2003. Uranyl coordination environment in hydrophobic ionic liquids: an *in situ* investigation. *Inorganic Chemistry*, 42(7):2197–2199.

Wai, C.M. 2001. Supercritical fluid extraction technology for nuclear waste management. Chapter 5.1 in *Hazardous and Radioactive Waste Treatment Technologies Handbook*, Editor C.H. Oh, CRC Press, Boca Raton, Florida, p. 5.1, 3–20.

Wai, C.M. 2002. Metal Processing in supercritical carbon dioxide. Chapter 10 in *Supercritical Fluid Technologies in Materials Science and Engineering: Synthesis, Properties, and Application*, Editor Y.P. Sun, Marcel Dekker, New York, NY, p. 351–386.

Wai, C.M. 2006a. Reprocessing spent nuclear fuel with supercritical carbon dioxide. Chapter 4 in *ACS Symposium Series 933, Separation for the Nuclear Fuel Cycle in the 21th Century*. Editors G.J. Lumetta, K.L. Nash, S.B. Clark, J.E. Friese, American Chemical Society, Washington, DC, p. 57–67.

Wai, C.M. 2006b. Supercritical fluid extraction of radionuclides – a green technology for nuclear waste management. Chapter 9 in *ACS Symposium Series 943, Nuclear*

Waste Management: Accomplishments of the Environmental Management Science Program, Editors P.W. Wang & T. Zachry, American Chemical Society, Washington, DC, p. 161–170.

Wai, C.M. & Waller, B. 2000. Dissolution of metal species in supercritical fluids – principles and applications. *Industrial and Engineering Chemistry Research*, 39:3837–3841.

Wai, C.M. & Wang, S. 1997. Supercritical fluid extraction: metals as complexes. *Journal of Chromatography A*, 785:369–383.

Wai, C.M., Kulyako, Y., Yak, H.K., Chen, X. & Lee, S.J. 1999a. Selective extraction of strontium with supercritical fluid carbon dioxide. *Chemical Communications*, 2533–2535.

Wai, C.M., Kulyako, Y. & Myasoedov, M. 1999b. Supercritical carbon dioxide extraction of cesium from aqueous solutions in the presence of macrocyclic and fluorinated compounds. *Mendeleev Communications*, 180:181–183.

Wai, C.M., Lin, Y., Ji, M., Toews, K.L. & Smart, N.G. 1999c. Extraction and separation of uranium and lanthanides with supercritical fluids. Chapter 23 in ACS Symposium Series 716, *Metal-Ion Separation and Preconcentration-Progress and Opportunities*, Editors A.H. Bond, M.L. Dietz & R.D. Rogers, American Chemical Society, Washington DC, p. 390–400.

Wang, J.S., Sheaff, C.N., Yoon, B., R. Addleman, S. & Wai, C.M. 2009. Extraction of uranium from aqueous solutions using ionic liquid and supercritical carbon dioxide in conjunction. *Chemistry-A European Journal*, 15:4458–4463.

Welton, T. 1999. Room-temperature ionic liquids. Solvents for synthesis and catalysis. *Chemical Review*, 99:2071-2084.

15

Development of biological treatment processes for the separation and recovery of radioactive wastes

E. M. N. CHIRWA, University of Pretoria, South Africa

Abstract: Due to the impact of the rapidly growing demand for energy worldwide, as well as concerns over global warming, there has been a resurgence of interest in nuclear energy in the developed world. However, further deployment of this otherwise cleaner source of energy in other lesser-developed regions is hindered by concerns over accumulation of radioactive waste from nuclear reactor operation and fuel processing. This chapter discusses emerging biological technologies for treating radioactive waste, focusing on biological reduction and recovery processes that may in future improve the viability of this energy source. The processes discussed include biological reduction of uranium (VI), biosorption of fission products and isotopic biofractionation processes. These technologies offer a possibly cost-effective and environmentally friendly alternative to physical-chemical processes currently used for treating radioactive waste in the nuclear-power industry.

Key words: nuclear waste minimization, uranium (VI) reduction, Cr(VI) reduction, radioisotope bioseparation, cationic species biosorption, fission product recovery.

15.1 Introduction

Due to the impact of the rapidly growing demand for energy, as well as concerns over global warming, there has been a resurgence of interest in nuclear energy in the developed world. Nuclear energy is one of the few economically viable base-load electricity generation technologies, which avoids the production of about eight percent of the present level of CO_2 emissions in the energy sector (Mourogov *et al.*, 2002). Currently, there are about 438 nuclear power plants in operation in 31 countries around the world providing about 14 percent of the world's primary energy needs (IAEA, 2009). The world's nuclear generating capacity currently stands at about 372 GWe, with the United States of America and France as the major producers, 27 and 17 percent, respectively (Fig. 15.1).

Electricity consumption in developing countries, such as South Africa, has been steadily increasing since the 1980s and, currently, the electricity

436
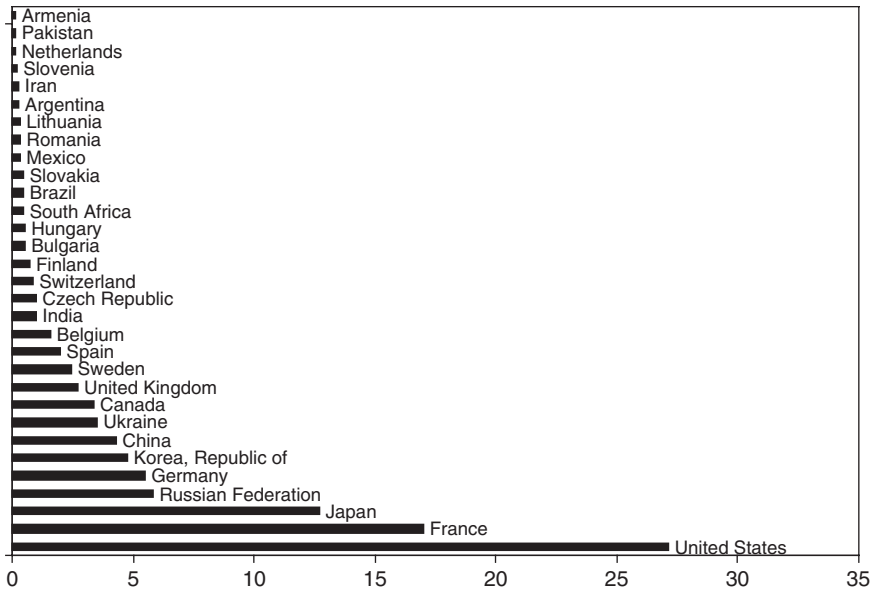
15.1 Global nuclear power generating capacity (%) per country (IAEA, 2009).

consumption/capita is estimated at about 5039.7 kWh. It is predicted that by the year 2025 electricity demand will exceed supply (Musango *et al.*, 2009). To accommodate future expansion in the domestic and industrial electricity consumption, there is need to develop safer, more efficient, and environmentally friendly technologies to replace the current fossil-fuel based power generation technologies.

In the developed world, most nuclear power plants in operation today have reached or are nearing their design life. Most of these power plants were constructed in the 1960s and 1970s. These need to be replaced by new, environmentally sustainable power generation technologies with improved safety features. An example of these new generation reactor systems is the Pebble Bed Reactor (PBR) technology, a Generation IV reactor technology that utilizes graphite as the neutron moderator. In this latter system, the reactor core is cooled by an inert gas such as helium instead of water (Koster *et al.*, 2003). Because the reactor can be allowed to operate at higher temperatures than the conventional water cooled reactors, the efficiency of the system is greatly enhanced. The drawback is that impurities in the containment material (graphite) are difficult to treat due to the inert nature of the graphite. This results in the accumulation of large volumes of low radiation level waste beyond the capacity of designated waste storage areas.

Potential radioactive pollution to the environment does not only concern nuclear power plants. Other activities such as radioisotope manufacturing

and biomedical research also release large amounts of potentially harmful radioisotopes. Most of the radioactive pollutants from the latter activities are organic in nature and are amenable to biological degradation (Cerniglia *et al.*, 1984; Bouwer and Zehnder, 1993). However, due to the toxic nature of the waste stream, an additional effort is required to isolate specialized bacteria that are resistant to the toxic effects of the released compounds and that are capable of breaking the complex structures of the organic compounds (Tikilili and Chirwa, 2009).

The following section provides a concise review of the waste compounds originating from nuclear power generation and other radioisotope releasing activities and how these could be treated for beneficial use. Biochemical processes that have yielded positive results are presented as part of the review and their impact on the future of power generation is evaluated.

15.2   Classification of waste

Several categories of radioactive waste are produced in the nuclear industry, ranging from highly radioactive waste to low radiation level waste. A detailed categorization of the radioactive waste is provided by the United States Nuclear Regulatory Commission (http://www.nrc.gov/waste), the main categories are summarized below.

15.2.1 Low level waste (LLW)

Low level waste (LLW) is generated from hospitals and industry, as well as the nuclear fuel cycle. It comprises paper, rags, tools, clothing, and filters, etc., which contain small amounts of mostly short-lived radioactivity. It does not require shielding during handling and transport and is suitable for shallow land burial. To reduce its volume, it is often compacted or incinerated before disposal. The bulk of graphitic waste from Generation IV fast reactors could fall into this category. In this case, the limitation is space requirements rather than shielding and treatability.

15.2.2 Intermediate level waste (ILW)

Intermediate level waste (ILW) contains higher amounts of radioactivity and some require shielding. It typically comprises resins, chemical sludges and metal fuel cladding, as well as contaminated materials from reactor decommissioning. It may be solidified in concrete or bitumen for disposal. Generally, short-lived waste (mainly from reactors) is buried in a shallow repository, whereas long-lived waste, for example waste from fuel reprocessing, could be buried deep underground.

15.2.3 High level waste (HLW)

High level waste (HLW) arises from the use of uranium fuel in a nuclear reactor and nuclear weapons processing. It contains the fission products and transuranic elements generated in the reactor core. It is highly radioactive and "hot". In the parlance of the nuclear industry, it is regarded as the "ash" from "burning" uranium. HLW accounts for over 95% of the total radioactivity produced in the process of nuclear electricity generation. However, the proportion of LLW is higher in the new generation HTGRs due to emphasis on safety. This reversal of waste volume ratios has resulted in a new problem of waste volume that puts emphasis on environmental compatibility in deference to safety.

15.2.4 Transuranic waste (TRU)

As defined by United States of America's regulations, transuranic (TRU) waste is without regard to source or form, waste that is contaminated with alpha-emitting transuranium radionuclides with half-lives greater than 20 years, and concentrations greater than 100 nCi/g but not including high level waste. In the US it arises mainly from weapons production, and consists of clothing, tools, rags, residues, debris and other such items contaminated with small amounts of radioactive elements mostly plutonium. These elements have an atomic number greater than uranium thus are transuranic (beyond uranium). Because of the long half-lives of these elements, this waste is not disposed of as either low level or intermediate level waste. It does not have the very high radioactivity of high level waste or its high heat generation. The US currently permanently disposes of transuranic waste of military origin at the Waste Isolation Pilot Plant.

A typical example of waste volumes produced in the power generation industry is shown for the Low Enriched Uranium Once Through (LEU-OT) and Mixed-Oxide Once Through (MOX-OT) fuel processing cycles (Tables 15.1 and 15.2). In the tables, it is shown that the majority of waste in the nuclear power generation industry originates from the uranium mining and milling operations.

The majority of radioactive organic waste is produced in the enrichment and reprocessing operations. All values in the tables are reported in cubic meters per Gigawatt electricity-year (m³/GWe-yr).

15.3   Waste from high temperature fast reactors

In high temperature gas-cooled reactors (HTGR), also known as fast reactors, graphite is utilized as the moderator of the nuclear reaction. The graphite is either used as part of the structural materials for the reactor

Table 15.1 Characteristics of waste generated from a Low Enriched Uranium Once Through (LEU-OT) processing cycle (m³/GWe-yr)

Steps	SF	ILW	LLW	Tailings	Comments
Mining and milling	–	–	–	65,000	In terms of radiation doses and numbers of people affected, uranium mining has been one of the most hazardous steps in the nuclear fuel chain, disproportionately impacting indigenous communities.
Conversion	–	–	32–112	–	Besides airborne and waterborne uranium, hazards include chemicals such as hydrofluoric acid, nitric acid, and fluorine gas.
Enrichment	–	–	3–40	–	Typically buried at dump sites with a high risk of leaching radionuclides into the groundwater. Waste is contaminated with polychlorinated biphenyls (PCBs), chlorine, ammonia, nitrates, zinc and arsenic.
Fuel fabrication	–	–	3–9	–	Because fuel fabrication does not involve the production of liquid waste, its effects are mainly restricted to workers and are on the same order as for workers in the reprocessing sector.
Reprocessing and vitrification	not applicable	not applicable	not applicable	not applicable	Wastes from reprocessing, together with spent fuel, contain more radioactivity than any other waste in the fuel cycle. Phenolic and chlorinated compounds are produced in large amounts due to the use of decontamination reagents such as CCl_4 together with phenolic tar (Gad Allah, 2008).
Reactor operations	–	22–33	86–130	–	Boiling water reactors have considerable emissions of radioactive noble gases.
Spent fuel storage and encapsulation	–	2	0.2	–	Considerable quantities of "low-level" waste are created due to fission products leaking into the spent fuel pools from cracks in the fuel cladding (Choi *et al*., 1997).
Spent fuel final disposal	26	–	–	–	Insufficient treatment can cause continued exposure to environment and local population.
Decommissioning	–	9	333	–	Most of the radioactivity from reactor decommissioning waste is in a relatively small volume of intensely radioactive material.
Totals	**26**	**33–44**	**457–624**	**65,000**	

Table 15.2 Characteristics of waste generated from a Mixed-Oxide Once Through (MOX-OT) processing cycle (m³/GWe-yr)

Steps	SF	HLW	ILW	LLW	Tailings	Comments
Mining and milling	–	–	–	–	50,060	Mill tailings account for over 95% of the total volume of the radioactive waste from MOX-OT processing cycle. This does not include mine wastes. Many tailings sites all over the world remain unremediated and/or neglected and pollute ground and surface water with radioactive and non-radioactive toxic substances.
Conversion	–	–	–	25–86	–	Besides airborne and waterborne uranium, hazards include chemicals such as hydrofluoric acid, nitric acid, and fluorine gas.
Enrichment	–	–	–	3–25	–	Typically buried at dump sites with a high risk of leaching radionuclides into the groundwater. Waste is contaminated with polychlorinated biphenyls (PCBs), chlorine, ammonia, nitrates, zinc and arsenic.
Fuel fabrication	–	–	13	7.4–12.5	–	Because fuel fabrication does not involve the production of liquid waste, its effects are mainly restricted to workers and are on the same order as for workers in the reprocessing sector.
Reprocessing and vitrification	–	2–4	17–39	8016–8037	–	As in LUE-OT system, wastes from reprocessing, together with spent fuel, contain result in the highest risk. The waste is high inorganic content. There is a particularly high risk of further contamination through accidents of storage facilities at the reprocessing plant.
Reactor operations	–	–	22–33	86–130	–	Boiling water reactors have considerable emissions of radioactive noble gases.
Spent fuel storage and encapsulation	–	–	0.3	0.03	–	As in the LUE-OT system, large quantities of "low-level" waste are created due to fission products leaking into the spent fuel pools from cracks in the fuel cladding. Fisson products are trapped in resins in filters, which then become "low-level" waste in the United States and intermediate level waste in Europe.
Spent fuel final disposal	26	–	–	–	–	Insufficient treatment can cause continued exposure to environment and local population.
Decommissioning	–	–	10.1	315	–	Most of the radioactivity from reactor decommissioning waste is in a relatively small volume of intensely radioactive material.
Totals	**26**	**2–4**	**62–95**	**8452–8615**	**50,060**	

Table 15.3 Carbon-14 production mechanisms and cross-sections

Target isotope	Mechanism	Thermal cross-section (barns)	Isotopic abundance (%)
^{14}N	$^{14}N(n, p)^{14}C$	1.81	99.6349
^{12}C	$^{12}C(n, \gamma)^{14}C$	n/k	n/k
^{13}C	$^{13}C(n, \gamma)^{14}C$	0.0009	1.103
^{17}O	$^{17}O(n, \alpha)^{14}C$	0.235	0.0383

Source: International Union of Pure and Applied Chemistry (IUPAC), 1984.
n/k: Not known.

core vessel or as fuel containment elements in the form of pebbles. The graphite used from natural sources contains non-carbon impurities within the carbon matrix. Among these impurities are oxygen and nitrogen from entrapped air, cobalt, chromium, calcium, iron, and sulfur (Khripunov *et al.*, 2006). Upon exposure to high neutron flux, most of the impregnated impurities are expected to transmute to unstable radioactive forms. For example, experimental exposure of graphite in nuclear reactors have shown that the stable forms of oxygen, nitrogen, and C-12 are converted to radiocarbon-14 (C-14) as shown in Table 15.3.

The radioactive fission products are created within the fuel grains and migrate through grain boundaries and then through microscopic cracks in the graphic matrix (Fig. 15.2). Most of the fission products are entrained in the matrix – a small proportion escapes through the outer layers into the gas phase. The challenge of reprocessing involves the separation of the metallic radionuclides from the graphite matrix and reducing the amount of C-14. Impurities in the fuel itself include: (1) metallic fission products (Mo, Tc, Ru, Rh, and Pd) which occur in the grain boundaries as immiscible micron to nanometre-sized metallic precipitates (ε-particles); (2) fission products that occur as oxide precipitates of Rb, Cs, Ba, and Zr, and (3) fission products that form solid complexes with the UO_2 fuel matrix, such as Sr, Zr, Nb, and the rare earth elements (Kleykamp, 1985; Shoesmith 2000; Buck *et al.*, 2004; Bruno and Ewing, 2006).

15.4   Treatment options

Currently available treatment options utilize mostly physical or chemical processes to separate the toxic component of the waste for further treatment. This is done to achieve one or all of the four targets for handling of waste, i.e. waste minimization, toxicity reduction, volume reduction, and/or
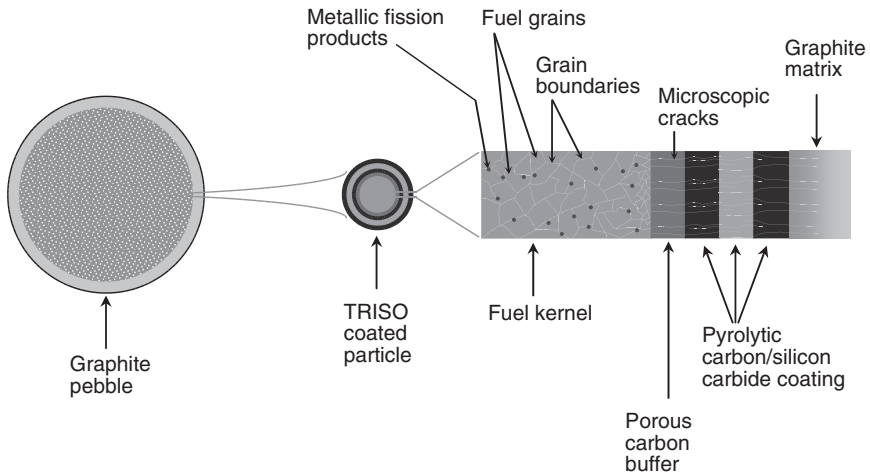
15.2 Propagation of fission products and impurities in a graphite regulated high temperature (gas) cooled reactor fuel element.

security (deterrence of proliferation). These targets can be achieved through physical, chemical, or biological means described below.

15.4.1 Physical and chemical treatment technologies

Physical chemical processes utilize chemicals or chemical properties of surfaces to chemically reduce or physically extract the radionuclides based on chemical charge or size. Processes that have been tried include the use of specialized ion exchange resins, chemical oxidation and adsorption columns. Mechanisms and materials employed include the following.

Adsorption

This is the most widely used among the available processes. It is primarily used for the removal of soluble organics with activated carbon serving as the adsorbent. Removal of organics on the adsorbent surfaces is mostly predicted by the Freundlich Isotherm:

$$y = kc^{1/n} \qquad\qquad 15.1$$

where y = adsorbent capacity, mass pollutant/mass carbon, c = concentration of the pollutant in waste (mass/volume), and k and n = empirical constants.

Other non-linear models are also available that are applicable under particular conditions.

Ion exchange

Several ion exchange resins have been tested for the removal of metallic elements and radiocarbon-14 from waste streams. Although sometimes proven successful, the regeneration of the resin for reuse is often a problem. For this reason, there has been limited efforts to develop this technology.

Stripping

Air stripping is applied for the removal of volatile substances from water. Henry's law is used in the design of stripping systems. The gas:liquid ratio required to remove a semi-volatile pollutant from liquid is estimated by:

$$\frac{Q_g}{Q_L} = \frac{C_{in} - C_{out}}{(H)C_{in}}$$

15.2

where Q_g = the flow rate of the stripping gas (volume/time), Q_L = the flow rate of the liquid carrying the waste, C_{in} and C_{out} = the influent and effluent concentration across the control volume (mass/volume), and H = Henry's constant for the pollutant (dimensionless).

Membrane processes

The emerging technology of nanopore membranes holds promise for the future as one of the processes that could be used for separation of radio-isotopes from water or gas streams. Membrane processes are normally easy to operate and offer the additional advantages of immediate capture of the pollutant for cleaning and recycling. An additional advantage is that membrane reactors tend to be portable and can be built to occupy the smallest land footprint possible.

15.4.2 Biological treatment technologies

The prospect of biological treatment is relatively new. Biological treatment is based on the principle of emulating the natural occurring processes to treat waste. During three billion years of existence, microorganisms have evolved mechanisms to survive in hostile environments and to adapt to changes in the environment (Bush, 2003). Environmental engineers around the world have undertaken to find ways to tap into the mysteries of nature by diligently studying the action of microorganisms as they adapt to extreme conditions.

One of the most conserved mechanisms in the living cell is the biochemical pathway for electron-transport through the cytoplasmic membrane to conserve energy through the oxidation of an electron donor and reduction of an electron acceptor such as oxygen. This process has been conserved over billions of years, such that, to this day, all life on earth depends on variants of this pathway (Bush, 2003; Thomas *et al.*, 1985; Nealson, 1999; Kalckar, 1974). Most biochemical processes for degradation and/or detoxification of compounds are linked to this process.

Lately, microorganisms have been isolated that are capable of reducing the toxic forms of heavy metal and transitional metal elements in transuranic waste (TRU) to less mobile precipitable forms (Lloyd, 2003). Other researchers have found microbial cultures with the capability to resist high radiation doses (Battista, 1997; White *et al.*, 1999). However, most of the resistant microbial species have not yet demonstrated the capability to degrade priority compounds such as polycyclic phenolics and polychlorinated compounds. But recent research shows promise that this scenario is soon to change. For example, recent studies have shown that microorganisms may not only resist radiation, but may to a certain degree utilize the radiation for metabolic advantage. One example was illustrated in a recent study in which cultures of melanizing fungi from the cold regions utilized ionizing radiation to derive metabolic energy (Dadachova *et al.*, 2007).

One aspect that has puzzled scientists in nuclear microbiology is the apparent capability of some species of bacteria to biologically separate different isotopes of the same element (Whiticar, 1999). This process has been observed for the lighter elements such as H and D and for some heavy metals such as selenium (Se(IV)/Se(II), sulfur S(-II), and C-14 (Habitch and Canfield, 1997; Habitch *et al.*, 1998; Herbel *et al.*, 2000). This process, if engineered correctly, could be used to separate different isotopes of a compound from a mixture for further processing. For example, the capability to separate the radioactive carbon-14 isotope from carbon-12 in irradiated graphite could result in cleaner graphite suitable for recycling (Molokwane and Chirwa, 2009).

15.5   Biological removal of metal oxyions

Most radioactive species in the actinide family are released in the waste streams as oxyions of the elements. The oxyionic forms are seen when the high oxidation states are present. Metals in the pentavalent and hexavalent states (V to VI, respectively) have high affinity for oxygen. The waste streams can also contain the oxyanions of the transition metals such as chromium and cobalt. The most common of these is hexavalent chromium Cr(VI) in the oxygen combined form of chromate (CrO_4^{2-}) and dichromate ($Cr_2O_7^{2-}$).

15.5.1 Biological reduction of actinides

Recent studies have shown that certain species of bacteria are capable of reducing the toxic oxyions of the actinide and transition metals to less toxic and less mobile forms. For example, U(VI) can be reduced to U(IV) by sulfate reducing bacteria such as *Desulfovibrio vulgaris* (ATCC 29579), *Desulfovibrio desulfuricans* (ATCC 29577), and *Geobacter metallireducens* (Lovley *et al.*, 1991; Lovley *et al.*, 1993; Payne *et al.*, 2004). U(VI) reduction in these species was demonstrated to be dissimilatory respiratory with the bacteria deriving metabolic energy through the U(VI) reduction pathway (Lovley *et al.*, 1993). Notably, U(VI) reduction by the above species of bacteria required incubation of the cultures under strictly anaerobic conditions. This is because the *Desulfovibrio* species favour reducing environments [ORP = −300 to −0.400 V] (Boonchayaanant *et al.*, 2007).

Lately, U(VI) reduction by bacteria under micro-aerobic conditions has been demonstrated (Chabalala and Chirwa, 2010a). In this case, a non-purified consortium from the mine soil was used to reduce U(VI) [UO_2^{2+}] to the less toxic and less mobile tertravalent state [U(IV)]. Three pure isolates were used, i.e., *Pantoea* sp, *Pseudomonas* sp. and *Enterobacter* sp., to reduce U(VI) under a pH range of 5 to 6 (Chabalala and Chirwa, 2010b). Figure 15.3 shows an example of the action of U(VI) reduction by the three species of bacteria while acting as pure cultures.

The significance of the above results is that the new cultures reduced uranium under conditions supporting the facultative range of bacteria. Such a culture could be less expensive to maintain. Additionally, by avoiding the formation of toxic sulfur precipitates, the culture could achieve more sustainable long-term operation and the separation of the product for reuse could be less expensive.

15.5.2 Reduction of transitional metal elements

Biological reduction of transitional metals such as chromium, copper and ferric iron has been shown to be enzymatically mediated in bacteria. The reduction process can be achieved under both aerobic and anaerobic conditions. Metal reduction under anaerobic conditions can in some cases be linked to the membrane respiratory pathway with energy released through the transfer of electrons to the metal (Fig. 15.4) (Suzuki *et al.*, 1992; Chirwa and Wang, 2000). However, under aerobic conditions, the metal reduction process is predominantly cometabolic, i.e., no energy is conserved for cellular metabolic processes. In fact, in some cases, the metal reduction process drew reducing equivalents that could have been used for cellular metabolic processes such as synthesis and maintenance (Chirwa and Wang, 1997). In such cases, the metal reduction process is inhibitory to cell growth.
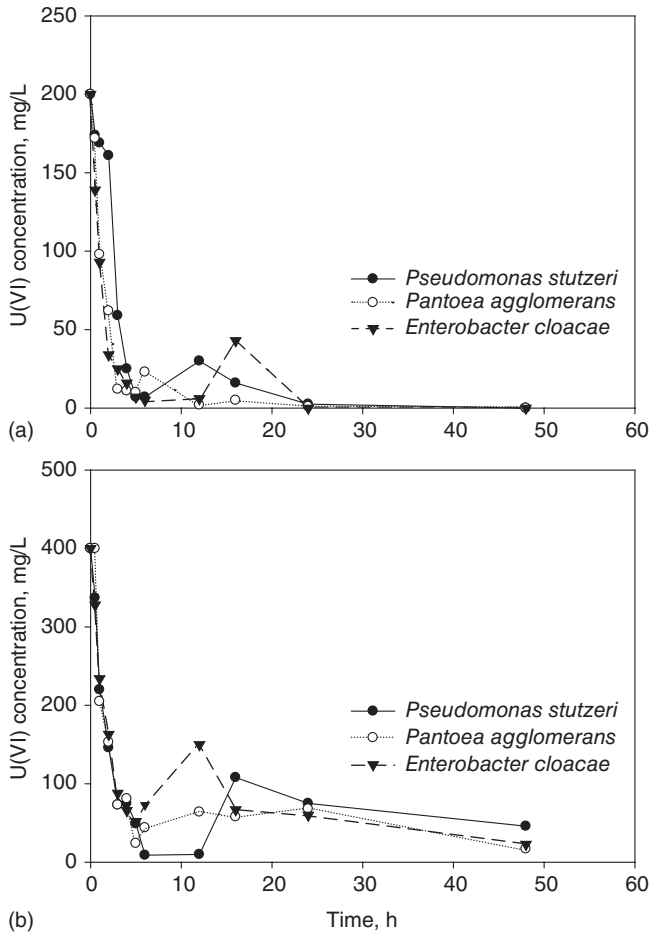
15.3 Uranium (VI) reduction for the three pure cultures of bacteria *Pseudomonas stutzeri*, *Pantoea agglomerans* and *Enterobacter cloacae* under initial concentration of (a) approximately 200 mg/L, and (b) approximately 400 mg/L (Adapted from Chabalala and Chirwa, 2010b).

Another aspect of metal reduction demonstrated by other researchers is the deactivation of viable cells by some metallic species. It was demonstrated by Shen and Wang (1993) while studying Cr(VI) reduction, that the cells of the gram-negative Cr(VI) reducing species – *Escherichia coli* ATCC 33456 – could be inactivated proportionally to the amount of Cr(VI) reduced by the species. Through a simple mass balance analysis, the researchers could estimate the metal reducing capacity of the bacteria by the metal species:

$$M^{n+}_{o} - M^{n+} = R_M(X_o - X) \qquad 15.3$$
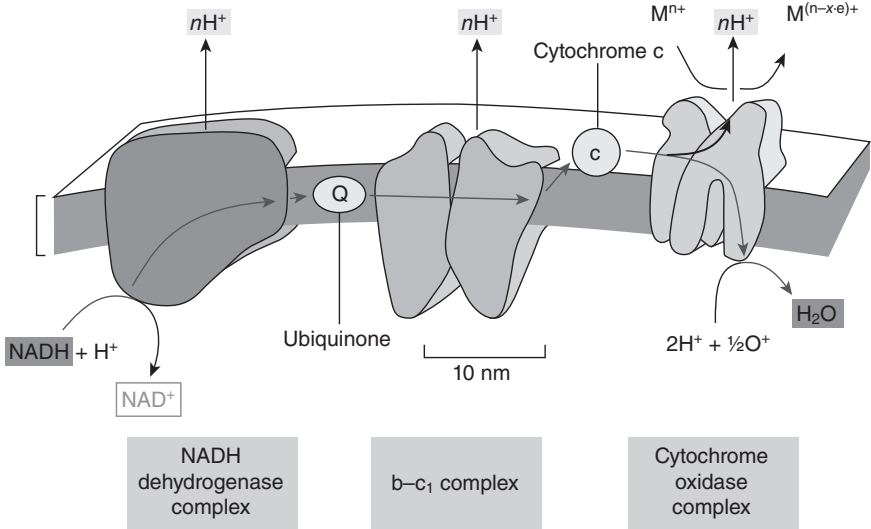
15.4 Electron flow pathway resulting in reduction of a metal species. The n-valent metal is reduced to an (n-*x*·e) valent species by receiving *x*·e electrons from electron donors in the system (updated from Alberts *et al.*, 1994).

where M^{n+}_o = initial metal concentration (ML^{-3})
M^{n+} = metal concentration (ML^{-3}) at any time t
X_o = initial viable cell concentration (ML^{-3})
X = viable cell concentration (ML^{-3}) at any time t
R_M = finite metal reduction capacity of the cells (MM^{-1})

Conversely, the amount of metal reducing viable biomass in system can be estimated by rearranging Equation 15.3 (Equation 15.4):

$$X = X_o - \frac{M^{n+}_o - M^{n+}}{R_M}$$

15.4

The concept of finite metal reducing capacity in bacterial cells has been confirmed in several species of metal reducing bacteria and the culture consortium of bacteria (Shen and Wang, 1994, Mazierski, 1994; Wang and Shen, 1997; Chirwa and Wang, 2000, for example). An example of the characteristic saturation of metal reduction rate is shown in a study by Molokwane *et al.* (2008) in which the metal reducing capacity of a consortium culture was limited at a concentration higher than 200 mg/L (Fig. 15.5).

Application of the metal reduction capacity term on biomass in the system yields the Monod-like metal reduction kinetics as shown in Equation 15.5 below:
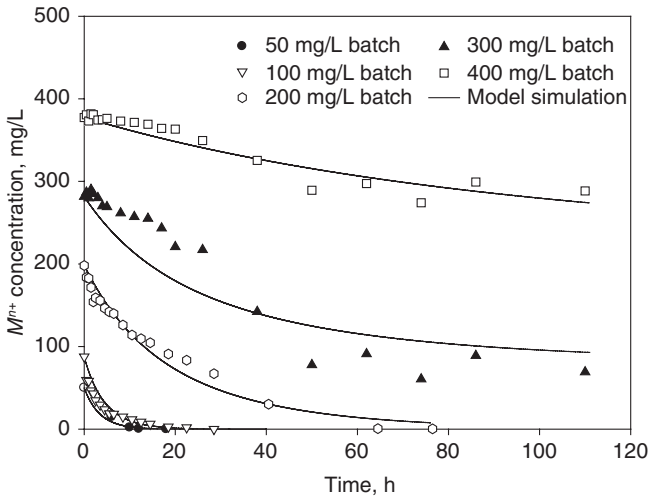
15.5 Typical metal reduction taken from actual experimental data using Cr^{6+} showing the characteristic limited capacity of cells at higher initial metal concentration in batch (adapted from Molokwane *et al.*, 2008).

$$-\frac{dM^{n+}}{dt} = \left(\frac{k_{mM}}{1 + M^{n+}_o/K_I}\right)\left(\frac{M^{n+}}{K_M + M^{n+}}\right)\left(X_o - \frac{M^{n+}_o - M^{n+}}{R_M}\right) \qquad 15.5$$

where k_{mM} = maximum reduction rate coefficient for the specific metal species M^{n+} (T^{-1}), K_M = half velocity concentration for the specific metal species (ML^{-3}), K_I = coefficient of non-competitive inhibition (ML^{-3}), and R_M = the metal reducing capacity of the cells (mass of metal reduced/mass of viable cells inactivated, MM^{-1}). In a continuous flow system, the biomass term is allocated dynamically since the biomass in the system will change with time. Changes will depend on the operational conditions of the system (i.e., the type and availability of carbon and energy sources for the cells, toxicity exposure conditions, and space availability).

15.5.2 *In situ* bioremediation process

Most transuranic waste is stored in specially engineered facilities above the ground. The chances of environmental contamination from such facilities are slight. However, most of the voluminous ILW and LLW can be packed and stored underground. The underground storage facilities pose a high risk of groundwater contamination. Where contamination has actually occurred, a pump-and-treat process is applied and the contaminated water is treated chemically before returning the treated water to the aquifer. For toxic metals, chemical agents may be applied followed by precipitation to reclaim

the metals (Mukhopadhyay *et al.*, 2007). The chemical reduction process utilizes toxic reducing agents that produce toxic sludge requiring further treatment before disposal into natural waters. Biological processes have been proposed for the pump-and-treat process, but this does not eliminate the problem of disposal of the product of the precipitation stage.

In situ bioremediation techniques using permeable reactive barriers (PRBs) offer another alternative of treatment whereby the toxic compound is treated without need for extraction. This is especially effective for treatment of organic compounds as they are completely mineralized by microorganisms to carbon dioxide (CO_2) and water (H_2O). A wide range of toxic recalcitrant organic compounds have been treated this way including methyl-tert-butyl-ether (MTBE), polynuclear hydrocarbons (PAHs), and petrochemical pollutants (i.e., benzene, toluene, ethylbenzene, xylene and polychlorinated biphenyls) (Doherty *et al.*, 2006; Liu *et al.*, 2006).

Several techniques for installing a biological barrier have been attempted such as construction of semi-porous walls which require a fair amount of excavation, injection of nutrients to encourage the growth of certain types of native species in the environment (a form of bioaugmentation), and inoculation of a region down gradient of a pollutant with specialized cultures of bacteria. Molecular *in situ* bioremediation, the process of introducing new genetic material in native species, has not been put into practice anywhere apart from small-scale experimental projects on petrochemical pollution (Liu *et al.*, 2006).

The main limitation of *in situ* bioremediation for treatment of metals such as uranium is that the element is not destroyed but rather trapped in the aquifer matrix in a reduced state. Should the conditions in the soil change one day in the future, the metal may be remobilized to its chemically toxic and mobile state and migrate down gradient to further contaminate groundwater and surface water resources. The alternative is to let the reduced form migrate without precipitating in the aquifer medium. This can then be removed by a pump-and-treat method as described above.

15.5.3 Types of permeable reactive barriers

Double layer system

Discussed here are PRBs specifically designed to utilize microorganisms in the treatment processes. A typical design comprises a double-layer with an aeration zone followed by the bioremediation zone. One such system was evaluated against the removal of methyl-tert-butyl-ether (MTBE) contaminated groundwater (Fig. 15.6) (Liu *et al.*, 2006). The aeration in this case was achieved chemically by the oxidation of calcium peroxide (CaO_2) to release oxygen into the medium. Other growth nutrients were added
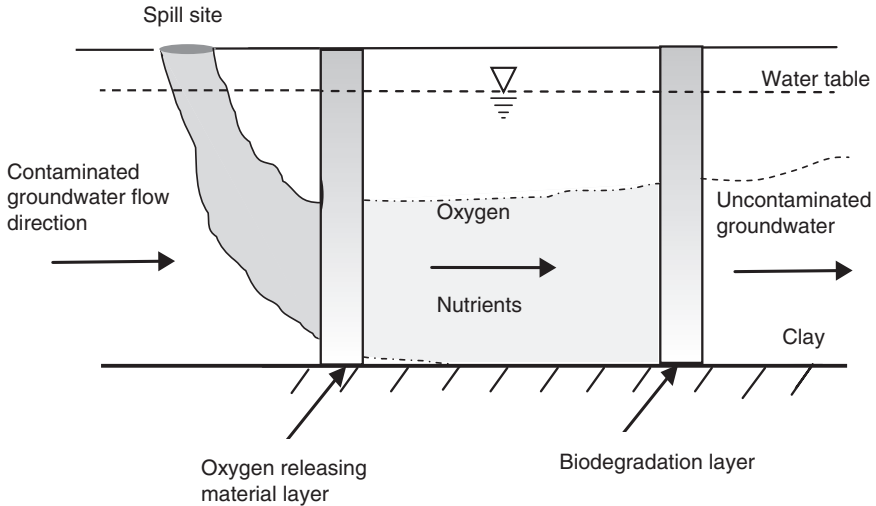
15.6 A two-layered biological barrier with first layer containing an oxygen releasing material and the second layer containing nutrients.

to encourage the growth of MTBE degrading organisms in the second layer.

Notably, inorganic salts such as potassium dihydrogen phosphate (KH_2PO_4) and ammonium sulphate ($(NH_4)_2SO_4$) can act as buffers against pH changes caused by the oxidation of CaO_2 into carbonates (CO_3^{2-}). Thus, nutrients added in the second layer must include the phosphate buffer for the proper functioning of the barrier.

Another documented application is the treatment of petrochemical pollutants (i.e., benzene, toluene, ethylbenzene, xylene and polyaromatic hydrocarbons), heavy metals (i.e., lead, arsenic, etc.), and cyanide in the system designed by Doherty *et al*. (2006) using a modified ash system. The BPRB system was implemented at an abandoned gas manufacturing plant after 150 years of operation.

Specific application of the biological permeable reactive barrier (BPRB) system for the removal of Cr(VI) in groundwater has not been attempted. This has been both due to the unavailability of microorganisms capable of growing under nutrient deficient conditions and lack of information on the fate of the reduced chromium species in the barrier.

Continuous trench and funnel-and-gate systems

The two models presented below have been used for physical-chemical treatment of pollutants. The continuous trench allows open access to water in multidirectional flow (Fig. 15.7a). In this system, the user is not interested
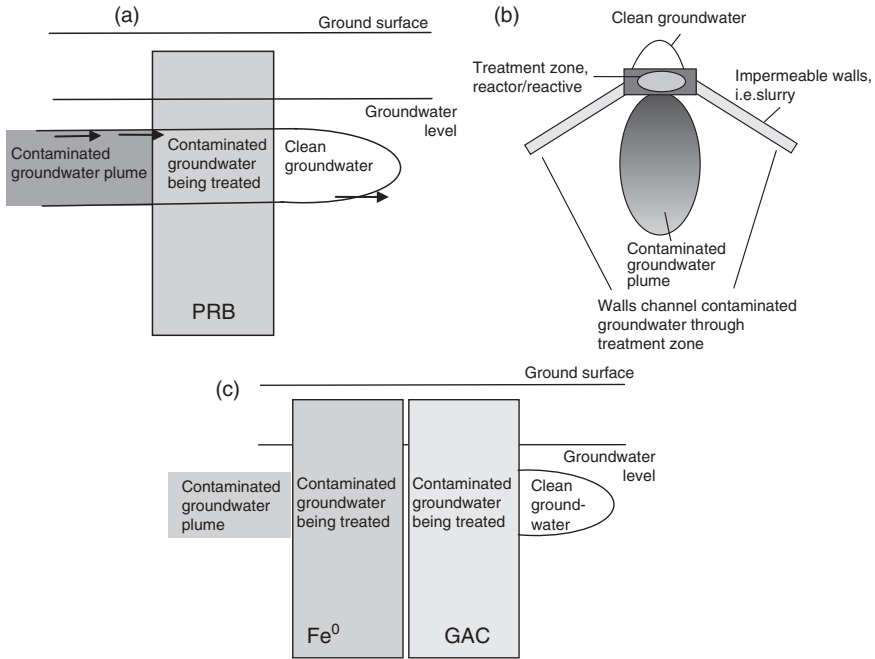
15.7 Conventional designs of permeable reactive barriers: (a) elevation view of a continuous trench or wall, (b) plan view of a funnel and gate, and (c) elevation view of a multi barrier.

in collecting the product of treatment for further processing. The alternative – funnel-and-gate system – offers the user the option of collecting flow from a localized position for further processing (Fig. 15.7b).

The flow in the continuous trench system, which is perpendicular to groundwater flow direction, needs to be slightly larger than the cross sectional area of the contaminated groundwater in order to capture the contaminants in both vertical and horizontal directions (Gavaskar *et al.*, 2000). The funnel-and-gate system is composed of impermeable walls and at least one reactive zone. The funnel structure could be sheet piles or slurry walls where the function of the funnel is to intercept the contaminated groundwater and lead it to the treatment zone. Phillips (2009) has elaborated on the designs of different reactive barriers, including but not limited to: the thickness of the PRB to provide sufficient residence time for the contaminants within the treatment zone to be completely treated.

Other complex designs have been tried including the multi-sequenced permeable reactive barriers (MS-PRBs) for multiple contaminants. MS-PRBs use multiple reactive materials in more than one reactive zone as shown in Fig. 15.7c (Dries *et al.*, 2004).

For the purpose of treating nuclear and radioactive waste around waste storage sites, the cheapest option could be the inoculated barrier system. All reactive barriers in the context of heavy metal treatment, unless heavily engineered and expensively constructed (which defeats the purpose), are mainly – if not only – suitable as temporary containment barriers to be operated until the pollutant source is completely removed or a more permanent solution for continuous remediation is found.

15.6   Biosorption and recovery

The biosorption process is designed to remove metallic species, especially those originating from the nuclear reaction process in power plants, for further processing and recovery. The majority of these are the products of nuclear fission of uranium to form lighter elements. During the first several hundred years after the fuel is removed from a reactor, fission products are considered the most hazardous elements to living organisms in the environment. Among these, radiostrontium (Sr-90) is one of the most abundant radioactive components of nuclear waste (Watson *et al.*, 1989). Strontium can be highly mobile in both soils and groundwater systems (Dewiere *et al.*, 2004) and it has a half-life of 28 years.

Due to its chemical similarity with calcium, it is easily incorporated into bone material in mammals. When incorporated in the organisms in this manner, it continues to irradiate localized tissues with the eventual development of bone sarcoma and leukaemia (Chen, 1997). The main disadvantages of using conventional adsorbents, such as zeolites and synthetic organic ion exchangers, for strontium removal from radioactive waste are: their decreasing efficiency at higher pH, and inhibited performance at high sodium concentration (Chaalal and Islam, 2001). Microbial adsorbents, on the other hand, have been shown to possess high capacities for the selective uptake of a range of metals and radionuclides from dilute metal-bearing solutions (Beveridge, 1989; Mullen *et al.*, 1989; Chubar *et al.*, 2008).

In the following sub-sections, the biologically mediated reactions at the surface of cells are explained and the operational conditions for the bioadsorbents and effects of co-occurrence with other cationic species are examined. Sulfate reducing bacteria are used as an example due to their demonstrated ability in adsorbing a range of metals including palladium (II) and calcium (II).

15.6.1 Biosorption processes

Biosorption of Sr^{2+} was observed under equilibrium conditions in 2 L bench scale anaerobic bioreactors (2 L). The initial Sr^{2+} concentration in the

Table 15.4 Langmuir and Freundlich model parameters for the equilibrium sorption of Sr^{2+} by a SRB biomass (1 g/L)

Langmuir model			Freundlich model		
q_{max} (mg/g)	b	R^2	k	n	R^2
444	0.011	0.993	17.2	1.95	0.986

experiments was varied between 75 and 1000 mg/L, while the sulfate reducing bacteria (SRB) cell density was kept constant at 1 mg/L. The suspensions were agitated for 3 hours and then samples were withdrawn for residual Sr^{2+} concentration analysis.

Sr^{2+} concentration was measured in the medium, and a desorption process was conducted to determine the amount sorbed on cells. Based on the amounts in the medium and the amount recovered from cells, it was observed that adsorption on the cells followed the Langmuir model. This suggests that Sr^{2+} removal occurred until equilibrium was reached, as opposed to precipitation reactions where the data cannot be fitted within a simple Langmuir model.

Straightforward precipitation follows a multi-layer model including surface precipitates. The SRB cells were then demonstrated conclusively to adsorb Sr^{2+} sorbent. The sorption capacity of the cells (q_{max}) was relatively high (444 mg/g), a value much higher than values obtained from other cell types (Shaukat *et al.*, 2005; Dabbagh *et al.*, 2007, Chegrouche *et al.*, 2009) and purified cultures of sulfate reducing bacteria (Vijayaraghavan and Yun, 2008).

The solution to the classical Langmuir model is shown in Equation 15.6 and the Freundlich isotherm in Equation 15.7 with the optimum values obtained for the sulfate reducing consortium shown in Table 15.4.

$$\frac{1}{q} = \frac{1}{q_{max}} + \frac{1}{C_{eq}} \cdot \frac{1}{bq_{max}} \qquad 15.6$$

$$log(q) = log(k) + \frac{1}{n} log(C_{eq}) \qquad 15.7$$

where: q = sorption uptake (MM^{-1}), q_{max} = maximum sorbate uptake (MM^{-1}), b = coefficient related to the affinity between the sorbent and sorbate, C_{eq} = equilibrium concentration of the sorbate remaining in the solution (ML^{-3}), k = constant corresponding to the binding capacity and n = coefficient related to the affinity between the sorbent and sorbate.
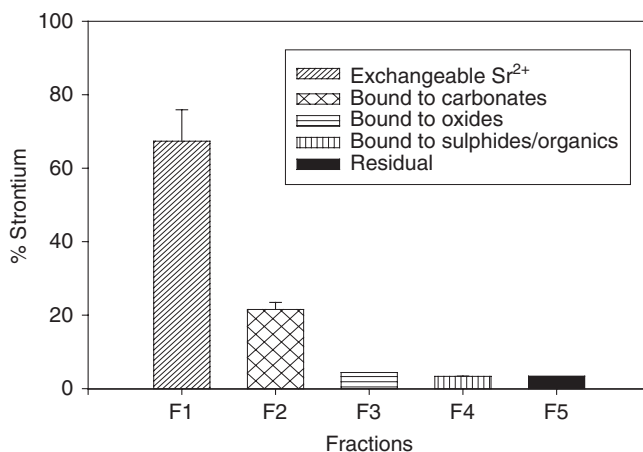
15.8 Partitioning of strontium species in the solid fraction after exposure to an SRB consortium.

15.6.2 Mechanisms

The study using SRBs showed that SRB cells could achieve up to 68% removal of strontium from the medium (Ngwenya and Chirwa, 2011). Most of the solid phase Sr^{2+} species were easily desorbed from biomass using $MgCl_2$ (Fig. 15.8). Metal species in the desorbed fraction gave an indication of the amount of Sr^{2+} that is bound on the biomass surface by relatively weak electrostatic interactions which are easily released by the ion-exchange process (Dahl *et al.*, 2008). The elevated concentrations of Sr^{2+} in the desorbed fraction may be due to the release from the complexing agents on the microbial cell surface.

These experiments showed that the SRB cells were excellent cation exchangers. The significance of these findings was that Sr^{2+} and other divalent cationic fission products could be extracted from water using bacteria under natural biological conditions. Separation of bacteria from water is relatively easy and cost effective. The bacteria could then be treated with an eluant to reverse the process thereby recovering the metals. The bacteria could then be returned into the biosorption reactors.

15.6.3 Fate of metal species in biosorbent cultures

The fate of strontium species in the microbial culture was determined by scanning electron micrographs (SEM) of SRB biomass previously exposed to medium containing Sr^{2+}. Precipitates on the cells surfaces were analyzed by an energy dispersive x-ray (EDX) spectrometer using a Cd^{109} radioisotope source and a Si(Li) semiconductor detector of resolution 170 eV for
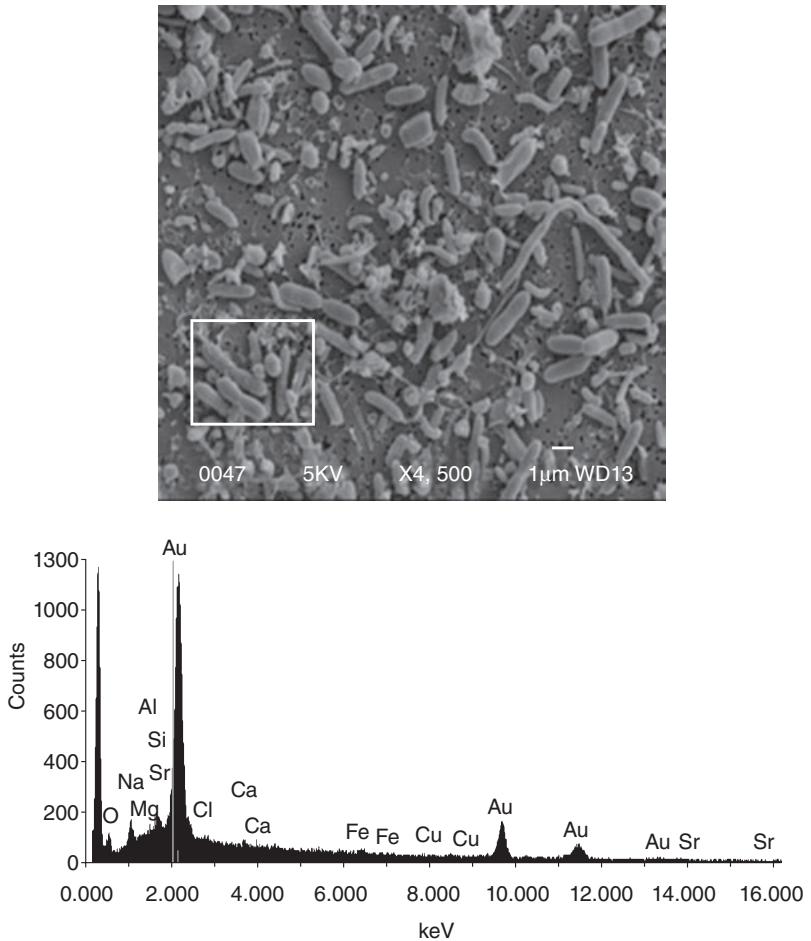
15.9 SEM image and EDX analysis of control. Elemental analysis: Sr = 0%, Mg = 4.58%, Al = 2.62%, Si = 8.44%, S = 18.18%, Ca= 15.52%, Fe = 15.53% and P = 35.12% (Ngwenya and Chirwa, 2011).

5.9 keV Mn K_α x-ray. The analysis revealed whitish crystallization on the surface of the cells. The composition of the precipitate as observed by the SEM was indeterminate (Figs 15.9 and 15.10). Speciation analysis of bacteria-free controls revealed that the solutions were undersaturated with respect to insoluble Sr species. This was consistent with the observation of adsorption as the dominant mechanism for metal removal from solution.

For the small part that precipitated, EDX analysis showed that about 65% was Sr^{2+} compounds (Fig. 15.10). In spite of the positive identification of Sr in the precipitate around the cells, the EDX scans clearly show that amount of precipitated Sr around the cells was indeed very low to insignifi-
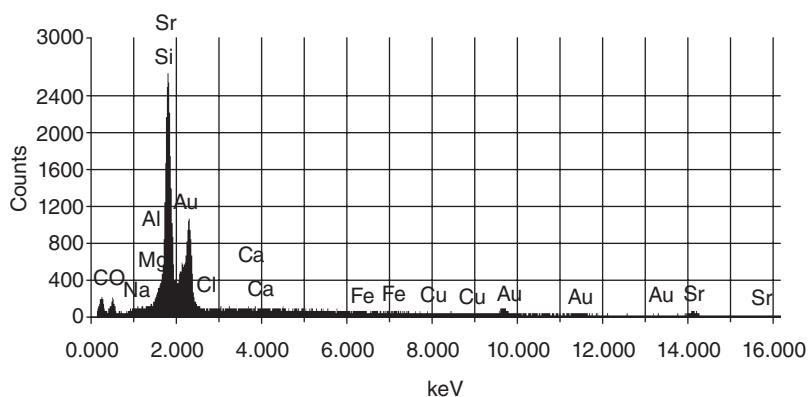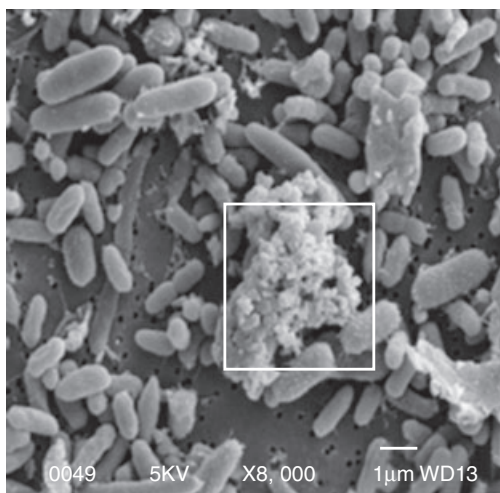
15.10 SEM image and EDX analysis of an area of SRB cells that was exposed to 100 mg L^{-1} Sr^{2+}. Elemental analysis: Sr = 65.27%, S = 33.45%, Na = 0.34%, Cl = 0.4%, Fe = 0.36% and Ca = 0.18% (Ngwenya and Chirwa, 2011).

cant. The low levels of precipitates as well as Sr peaks in the control sample after EDX analysis confirms that the observed Sr^{2+} in the precipitate is produced by the interaction with the bacteria. The low levels in both samples suggest that the production of Sr precipitates is transient in nature, that the accumulation of the precipitate is limited by the sorption rate to reaction sites on the cell. The findings on the fate of Sr in the SRB consortium culture are in agreement with other reports where functional groups on the cell surface of bacteria facilitated bulk metal binding from aqueous solution (Sherbet, 1978). However, further studies still need to be conducted to clarify the observed findings.

15.7   Biofilm processes

Microorganisms in nature and in reactor systems rarely grow as separate cells. The microorganisms form complex communities either in the form of agglomerations called flocs or as biofilm on the surfaces of inanimate objects and other organisms. The performance of a microbial culture is not only a function of its capability to degrade or transform a pollutant but also the configuration of the community in which it resides. There are complex interrelationships that occur within the microstructure that affects the availability of substrates, symbiotic existence through toxicity shielding of more susceptible species, and transfer of metabolites to organisms that could otherwise not grow on the only primary substrate in the bulk liquid. The biofilm itself is often a complex structure constructed by the bacteria. The formation of the biofilm especially in the initial stages is believed to be an active process coupled to the cell's central metabolism (Kjelleberg and Hermanson, 1984; Paul, 1984). Within the biofilm, complex processes take place such as nutrient cycling, mass transport resistance, cell and substrate diffusion, and biofilm loss at the surface that make prediction of the performance of the culture in the biofilm mathematically challenging.

15.7.1 Biofilm architecture

In pure culture biofilms, 80% of the biofilm weight is occupied by exopolysaccharides (EPS) (Nelson *et al.*, 1996). In continuous-flow systems, shear forces at the liquid/biofilm surface cause cell detachment and loss of EPS. Viable cells in the biofilm matrix must continuously replace the displaced biofilm materials thereby drawing on the cell's energy resources. Additionally, cell attachment plays an important role in the cell division cycle inside the biofilm. For example, Meadows (1971) observed that *Pseudomonas fluorescens* and *Aeromonas liquifaciens* cells undergo cell division only during their most stable attachment phase (when lying longitudinal to the solid surface). In more dramatic cases such as the prosthecate bacterium *Caulobacter crescentus*, cell division occurs only during the attachment phase of the cells life cycle (Neidhardt *et al.*, 1990). In *Caulobacter*, the prosthecate (stalked) form undergoes cell division giving rise to a swarm cell equipped with a flagellum while the other daughter cell remains attached to the surface with a single prostheca (stalk). The life cycle is completed by differentiation of swarm cells to prosthecates, followed by attachment and cell division.

   Scientists and mathematicians have found biofilms too complex to analyze and model especially when working with mixed-culture communities. Biofilm systems in laboratory studies are often oversimplified by using systems with defined chemical and microbial species composition. Attempts

to use data from natural systems to develop the models have been unsuccessful because of the variability and complexity of the natural aquatic environments. Recently, biofilm studies using microsensors have unravelled the existence of closed-cycles, such as the cycle of sulfate oxidation coupled with sulfate reduction, within biofilms or sediments (Kühl and Jørgensen, 1992). Models based only on bulk liquid and effluent characteristics often underestimate the overall performance of biofilm systems. The internal metabolic cycles in the biofilms, though hidden from the external observer, determine the final structure of the microbial community thereby affecting the long-term performance of the biofilm (Santegoeds *et al.*, 1998).

Furthermore, bacterial attachment and conglomeration play an important role in the survival of cells under hostile conditions. For example, attached cells may feed on adsorbed substrates on the surfaces of the immobile phase under starvation concentration levels (Zobell, 1943). In toxic environments, biofilm communities may be exposed to lower levels of toxicity either due to the masking effect of less susceptible species or due to heterogeneities within the biofilm microenvironment (Chen and Stewart, 1996; Nichols, 1989). Several researchers have proposed mass transport resistance as the main mechanism limiting penetration of toxic substances into biofilms (Xu *et al.*, 1998; Chen and Stewart, 1996; Hodges and Gordon, 1991; Hoyle *et al.*, 1992).

In engineering attached growth bioreactors, the biofilm is allowed to grow thick. This results in a complex dynamic at the surface with a high rate of cell shading and sloughing of the biomass. Inside a thick biofilm, tunnelling and honeycombing occurs which makes the prediction of the actual surface area for interfacial diffusion impossible. For this and the above reasons, biofilm models are regarded as mere approximations of the possible operating conditions.

15.7.2 Mass transport rate kinetics

The removal of substrates and other materials from solution in a fixed-film system involves complex physical and chemical processes which include: film transport, pore surface transport, adsorption reaction, and growth of biofilm and suspended biomass (Thacker *et al.*, 1981; Weber and Chakravorti, 1974). Expressions derived from biofilm kinetics are best solved by simplification by using empirical approaches. The mechanism of substrate removal by fixed-biofilm is shown in the simplified model of biofilm-on-inert-media in Fig. 15.11. The complexity of resolving mathematical equations expressed by the biofilm model lies in recognizing the critical features, namely:

(i) *The moving boundary problem*
    The biofilm thickness (L_f) can change while substrate diffuses into the biofilm during transient-state when the rate of substrate utilization is
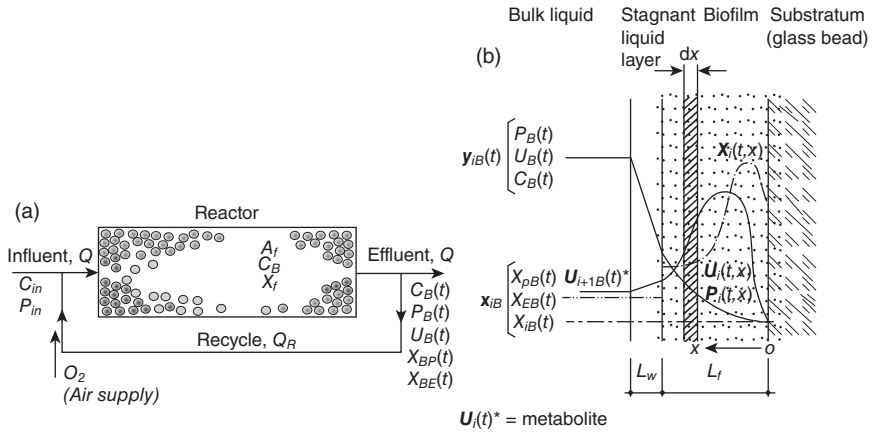
15.11 Conceptual mixed-culture biofilm model for (a) control volume space, and (b) biofilm environment.

not constant. The moving boundary problem is analogous to the problem of heat transfer during freezing and melting of ice in thermodynamics (the "Stefan" problem, Danckwerts, 1950), and the diffusion of oxygen in absorbing tissue (Crack and Gupta, 1972); and

(ii) *Diffusion with nonlinear reaction*

At any particular time, the rate of substrate diffusion across the liquid/biofilm interface as described by *Fick's law*, is equal to the rate of substrate utilization in the biofilm governed by the nonlinear Monod kinetics.

Figure 15.11 represents removal of dissolved species y in a multispecies biofilm contain microbial cells x_i, where x and y are vectors of cell types and dissolved species. In the above example, an organic compound P is used as primary carbon source to support a culture containing metal reducers X_E and the organics degrader X_p. In this particular system, metabolites U are produced inside the biofilm to feed the metal reducers. The metal reducers are assumed to be unable to grow on the primary supplied carbon source P.

Bulk liquid mass balance

The generic solution of the above system is provided by a diffusion-reaction model in which metal removal from the bulk liquid may be mass transport limited during high biomass output and reaction rate limited during inhibited growth. The mass balance across the bulk liquid compartment (Fig. 15.11a) is given by the following equation:

$$\frac{\partial(\hat{\mathbf{u}}_B V_B)}{\partial t} = Q(\hat{\mathbf{u}}_{in} - \hat{\mathbf{u}}_B) - \mathbf{r}_{\hat{\mathbf{u}}} \cdot V_B - \mathbf{j}_{\hat{\mathbf{u}}} \cdot A_f \qquad 15.8$$

$$\frac{\partial(\hat{\mathbf{x}}_B V_B)}{\partial t} = -Q\hat{\mathbf{x}}_B + \mathbf{r}_{\hat{\mathbf{x}}B} V_B + \lambda(u) \cdot \hat{\mathbf{x}}_f L_f A_f - b_x \hat{\mathbf{x}}_B V_B \qquad 15.9$$

where $\mathbf{r}_{\hat{\mathbf{u}}}$ = dissolved species removal rate $(ML^{-3}T^{-1})$; $\mathbf{j}_{\hat{\mathbf{u}}} = D_{wi}\partial\hat{\mathbf{u}}_i/\partial z$, dissolved species flux rate $(ML^{-2}T^{-1})$; $\hat{\mathbf{u}} = \{P, U, C\}$, is the vector for dissolved species concentration, where P = phenol concentration (ML^{-3}), U = metabolites concentration (ML^{-3}), and C = metal pollutant concentration (ML^{-3}); $\mathbf{r}_{\hat{\mathbf{x}}_B}$ = cell growth rate in the bulk liquid $(ML^{-2}T^{-1})$; $\hat{\mathbf{x}} = \{X_p, X_E, X_I\}$, is the vector of biomass concentrations, where X_p = viable cell concentration (ML^{-3}) of organic compound degraders, X_E = viable cell concentration (ML^{-3}) of toxic metal reducers, and X_I = inert cell concentration (ML^{-3}); $b_x = \{b_{xp}, b_{xE}\}$, is the vector of cell death coefficients (T^{-1}) for the respective cell types; and $\lambda = \{\lambda_p, \lambda_E, \lambda_I\}$, is a vector of cell detachment rate coefficients (T^{-1}). The reaction rate and cell growth terms can be formulated based on the enzymatic removal of substrates as shown in the derivation of Equation 15.5 and the Monod kinetics, respectively.

Biofilm mass balance

The removal of the dissolved species and cell growth is represented by a set of diffusion-reaction partial differential equations (PDEs). The PDEs represent a mass balance across an infinitesimal biofilm section (δz) parallel to the substratum surface (Fig. 15.11b):

$$\frac{\partial(\hat{\mathbf{u}})}{\partial t} = \varepsilon(t) \cdot \frac{\partial(\mathbf{j}_{\hat{\mathbf{u}}})}{\partial z} + \mathbf{r}_{\hat{\mathbf{u}}f} \qquad 15.10$$

$$\frac{\partial(\hat{\mathbf{x}})}{\partial t} = \varepsilon(t) \cdot \frac{\partial(\mathbf{j}_{\hat{\mathbf{x}}})}{\partial z} + \mathbf{r}_{\hat{\mathbf{x}}f} \qquad 15.11$$

where: $\mathbf{j}_{\hat{\mathbf{x}}} = D_{w\hat{\mathbf{x}}}\partial(\hat{\mathbf{x}})/\partial z$, mass flux rate of biomass $(ML^{-2}T^{-1})$, $\mathbf{r}_{\hat{\mathbf{u}}f}$ = the vector of removal rates of dissolved species in the biofilm $(ML^{-3}T^{-1})$, $\mathbf{r}_{\hat{\mathbf{x}}f}$ = the vector of biomass production rates in the biofilm zone $(ML^{-3}T^{-1})$, and ε = is a biofilm porosity constant (V_{fvoids}/V_{ftotal}). The movement of cells across the biofilm is induced by physical displacement due to growth whereas dissolved species are transported by diffusion. Thus, the values of the j terms for cells are expected to be lower (by orders of magnitude) than the j terms for dissolved species in the biofilm.

Boundary conditions

The outer and inner boundary conditions for dissolved species $\hat{\mathbf{u}}$ and biomass $\hat{\mathbf{x}}$ are defined by:

$$\mathbf{j}_{\hat{\mathbf{u}}} = k_{L\hat{\mathbf{u}}} \cdot (\hat{\mathbf{u}}_B(t) - \hat{\mathbf{u}}_{fs}(t, L_f)), \quad z = L_f, \text{ outer boundary} \qquad 15.12$$

$$\mathbf{j}_{\hat{\mathbf{x}}} = \bar{\lambda}(u) \cdot \hat{\mathbf{x}}_f \cdot L_f, \qquad\qquad z = L_f, \text{ outer boundary} \qquad 15.13$$

$$\mathbf{j}_{\hat{\mathbf{u}}} = 0, \qquad\qquad\qquad z = 0, \text{ inner boundary} \qquad 15.14$$

$$\mathbf{j}_{\hat{\mathbf{x}}} = 0, \qquad\qquad\qquad z = 0, \text{ inner boundary} \qquad 15.15$$

where $k_{L\hat{\mathbf{u}}} = D_{w\hat{\mathbf{u}}}/L_w$, is the mass transfer rate coefficient (L^2T^{-1}), and $\hat{\mathbf{u}}_{fs} =$ dissolved species concentration at the liquid/biofilm interface (ML^{-3}).

Simulation and parameter optimization

The system described above is an oversimplification of the actual biofilm processes in nature. However, the example serves to illustrate how complex the solution for such a simplified version could be. In the old days before fast and efficient computers, solving such problems manually was unthinkable. Lately, computer speed has increased exponentially and memory is no longer a limiting factor. Innovative tools for simulation of the PDE system and heuristic approaches for estimating parameters are now available. For example, Nkhalambayausi-Chirwa and Wang (2005) applied a custom PDE solver to solve the model equations for simultaneous Cr^{+6} reduction and phenol degradation in a dual species biofilm reactor. The PDE solver utilized the (fourth-order) Runge-Kutta method with spatial discretization using the (second-order) Crank-Nicholson and Backward Euler finite difference methods for the biofilm spatial profiles. The solution of the biofilm PDE system of equations is shown as a solid line in the effluent from a biofilm reactor showing the prediction of the metal reduction process in the biofilm (Figs 15.12 and 15.13).

Parameter optimization

The parameters in the biofilm model in the example above were estimated using a heuristic procedure – Genetic Search Algorithm (GSA). The first version of this algorithm was implemented in the C programming language using subroutines adopted from Hunter (1998). The GSA uses the inverse of the mean residual sum of squares (MRSS) computed as the global variance (σ^2) as a fitness function during parameter optimization using the principles of evolution and natural selection (KrishnaKumar, 1993). The global variance is the main objective function for GSA computed as:

$$\sigma^2 = \frac{1}{n-q} \sum_{i=1}^{n} (y^{obs} - y)^2 \qquad\qquad 15.16$$

where σ = average deviation of the model from measured values, y^{obs} = observed variables, y = simulated variables, n = number of observations, and q = degrees of freedom representing number of parameters being evaluated.
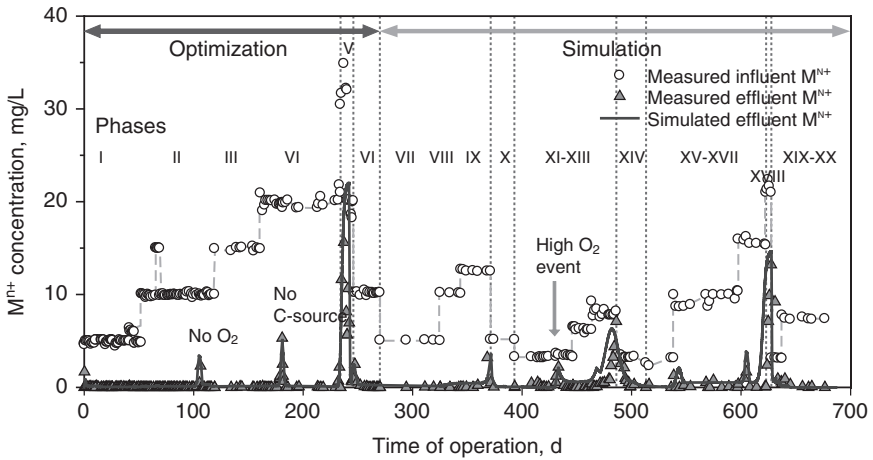
15.12 Simulation of the reduced metal M^{n+} (Cr^{6+}) in a dual species biofilm culture under a range of hydraulic loading conditions: 24 h HRT (Phase I–VI); 11.7 h HRT (Phase VII–X); 6 h HRT (Phase XI–XIV); 17.9 h HRT (Phase XV–XVIII).
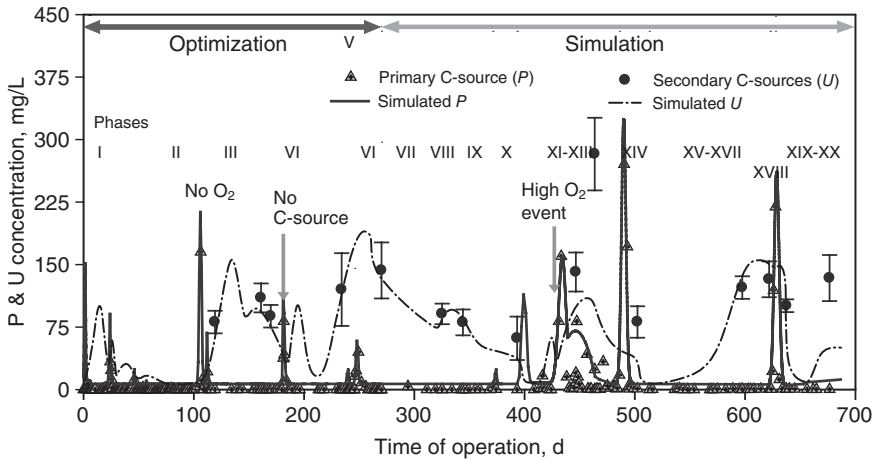
15.13 Simulation of the carbon source (P) and metabolite (U) concentration in a dual species biofilm culture under a range of hydraulic loading conditions: 24 h HRT (Phase I–VI); 11.7 h HRT (Phase VII–X); 6 h HRT (Phase XI–XIV); 17.9 h HRT (Phase XV–XVIII).

In Figs 15.12 and 15.13, parameters were estimated from the data obtained from the operation of the reactor at 24 hours hydraulic retention time (HRT) (Phase I–VI). The rest of the phases (VII–XVIII) were simulated using the optimized parameters. The results show high confidence in the optimization routine as the model accurately tracked the trends in effluent concentrations for both the electron donor (P) and the electron sink (M).

15.7.3 Application of biofilm process

The applications of mathematical models to complex biofilm process resembling natural systems are very rare. Most of the reports are based on laboratory-scale pure cultures. Black-box approaches are normally used to evaluate performance of actual systems. The above quoted example by Nkhalambayausi-Chirwa and Wang (2005) was one of the few efforts to mechanistically model a mixed culture system.

The efforts to understand the fundamental nature of biofilm systems are worthwhile since these offer unique solutions to contaminant treatment. For instance, cells growing in biofilm cultures have been observed to perform better than the same species suspended in medium (Semprini and McCarty, 1981). One reason offered for the better performance of cells in the biofilm environment is the effect of shielding from high toxicity levels. It is estimated in most biofilm systems that the bulk liquid concentration is much higher than the concentration in the deeper layers of the biofilm. Other complex interactions are also known to exist within the biofilm system. Cultures grown in a cooperative system where some species of microorganisms require a product from other species for survival (Nkhalambayausi-Chirwa and Wang, 2005). The mass transport conditions and balanced retention of substrates are required to sustain a culture for a specific purpose.

Biofilm systems have demonstrated the potential to package complex treatment systems into a small space to achieve removal of multiple substrates. These systems are especially useful when relatively sensitive species of bacteria are used to treat toxic waste. It is envisaged in this report that biofilm systems will in future form a significant part of the treatment and recovery regime for nuclear and radioactive waste.

15.8   Future trends

The problem of radiation pollution in the environment is expected to increase as industries in the world experience pressure to reduce their carbon atmospheric contributions. The dilemma is that production of goods will only increase with population growth. Most countries are considering nuclear energy as the interim solution to the growing energy crisis. This will

require environmental engineers and scientists to delve deeper into research on environmentally friendly processes to counter the pollution effects to avoid leaving a pollution legacy for the future generations. Advanced microbial cultures will be sought to treat a wider variety of recalcitrant pollutants. Discussions on the possibility of genetically engineering specialized cultures for the purpose are not new in the environmental engineering fraternity. However, the application of ideas bears a large ethical burden as it is forbidden in almost all countries in the world to introduce genetically engineered organisms into the environment. Less aggressive methods for dealing with the problem without violating ethics include *in situ* bioaugmentation and molecular bioaugmentation to a certain extent.

15.8.1 *In situ* bioaugmentation

This entails identifying indigenous species of bacteria within the vicinity of the contaminated site and determining the critical carbon sources and nutrients that could be supplied to encourage the growth of the target species. When the selected nutrients are introduced into the environment, either by injection into boreholes or by spreading on the ground, the target species will out-compete other species and will be able to degrade the contaminants. The potential problem with this form of bioaugmentation is that the nutrients may be viewed as pollutants in their own right especially at the beginning of the bioaugmentation process when microbial loading is very low. The nutrients such as NO_3^- and SO_4^{2-} have undesirable pollution effects on receiving water bodies such as eutrophication of streams receiving the base flow from the remediated areas.

15.8.2 Molecular bioaugmentation

The molecular bioaugmentation process utilizes genetic carriers such as transposons and plasmids to shuttle genetic information for toxic metal remediation into native species in the environment or species already adapted to the target environment. Several species of bacteria are capable of picking up and retaining circular fragments of DNA called Broad-Host-Range Plasmids which may be engineered to carry specific genes for the degradation of xenobiotic compounds and transformation of toxic metals (Weightman *et al.*, 1984; Vincze and Bowra, 2006). The same process can be applied using genetically engineered linear DNA called transposons. Although studies have been conducted using these techniques in laboratory microcosms, the application in actual environments has not been attempted (Hill *et al.*, 1994). In the future, it is foreseeable that these methods will find wide application for the new pollutant varieties that may be untreatable by conventional methods.

15.8.3 Biofractionation and bioseparation of elements

A very little understood application of bioseparation involves using microorganisms to discriminate radioisotopes by size. So far, this application has remained conceptual due to limited understanding on the structure and function of organisms that are suspected to achieve biofractionation (Molokwane and Chirwa, 2009). In the latter study, Molokwane and Chirwa observed with a modest degree of certainty that microbial cells previously isolated from a high radiation-exposed facility accumulated C-14 while growing on a C-14/C-12 carbon matrix from powdered nuclear graphite. The experiment was conducted in a closed loop chemostat system equipped with biofilters for collection of suspended matter for analysis. The observed metabolic activity in the cells indicated that the process was possible under very low dissolved oxygen, suggesting that the microorganisms preferred inorganic forms of carbon as the primary carbon source. Bacteria that utilize inorganic carbon sources such as CO_2 and HCO_3^- as primary carbon sources – known as autotrophic organisms – favour anaerobic conditions for growth. However, in this preliminary study, the amount of C-14 remaining in solution which could be required to draw a mass balance on C-14 in the system was not measured. These preliminary results on C-12/C-14 bioseparation hold promise for future HTGR nuclear reactors that produce large amounts of low radiation level waste as expired nuclear graphite. Success in the above process is also important for the decontamination and recovery of nuclear graphite from decommissioned plants for reuse in new reactors.

15.9   Sources of further information and advice

Chow B.G. and Jones G.S. (1999) *Managing Wastes With and Without Plutonium Separation* (Santa Monica, Calif.: RAND, 1999). The reprocessing LLW figure also uses data from Groupe Radioecologie Nord Cotentin, *Inventaire des rejets radioactifs des installations nucléaires*, vol. 1, July 1999, p. 19.

International Union of Pure and Applied Chemistry (IUPAC), 1984.

Makhijani A., Hu H. and Yih K. (1995). *Nuclear Wastelands: A Global Guide to Nuclear Weapons Production and Its Health and Environmental Effects*, Cambridge, Mass.: MIT Press, Massachusetts USA.

United States Nuclear Regulatory Commission (*http://www.nrc.gov/waste*).

15.10 References

Alberts, B., Bray, D., Lewis, J., Raff, M., Roberts, K. and Watson, J.D. (1994). *Molecular Biology of the Cell*, Garland Publishing, New York, NY.

Battista, J.R. (1997). Against all odds: the survival strategies of *Deinococcus radio-durans*. *Annual Review of Microbiology*, 51, 203–224.

Beveridge, T.J. (1989). Role of cellular design in bacterial metal accumulation and mineralization. *Annual Review of Microbiology*, 43, 147–171.

Boonchayaanant, B., Kitanidis, P.K. and Criddle, C.S. (2007). Growth and cometa-bolic reduction kinetics of a uranium- and sulfate-reducing *Desulfovibrio/Clos-tridia* mixed culture: Temperature effects. *Biotechnology and Bioengineering*, 99 (5), 1107–1119.

Bouwer, E.J. and Zehnder, A.J.B. (1993). Bioremediation of organic compound – putting microbial metabolism to work. *Trends in Biotechnology*, 11 (8), 360–367.

Bruno, J. and Ewing, R.C. (2006). Spent Nuclear Fuel. *Elements*, 2, 343–349.

Buck, E.C., Hanson, B.D. and McNamara, B.K. (2004) The geochemical behaviour of Tc, Np and Pu in spent nuclear fuel in an oxidizing environment. In: R. Gieré and P. Stille (eds.), *Energy, Waste, and the Environment: a Geochemical Perspective. The Geological Society of London Special Publication*, 236, 65–88.

Bush, M.B. (2003). *Ecology of a Changing Planet*, 3rd Edition, Prentice Hall, New Jersey, USA.

Cerniglia, C.E., Lambert, K.J., Miller, D.W. and Freeman, J.P. (1984). Transformation of 1- and 2-methylnaphthalene by *Cuninghamella elegans*. *Applied and Environ-mental Microbiology*, 47 (1), 111–118.

Chaalal, O. and Islam, M.R. (2001). Integrated management of radioactive strontium contamination in aqueous stream systems. *Journal of Environmental Manage-ment*, 61 (1), 51–59.

Chabalala, S. and Chirwa, E.M.N. (2010a). Uranium(VI) reduction and removal by high performing purified anaerobic cultures from mine soil. *Chemosphere*, 78 (1), 52–55.

Chabalala, S. and Chirwa, E.M.N. (2010b). Removal of uranium(VI) under aerobic and anaerobic conditions using an indigenous mine consortium. *Minerals Engi-neering*, 23 (6), 526–531.

Chen, J.-P. (1997). Batch and continuous adsorption of strontium by plant root tissues. *Bioresource Technology*, 60, 185–189.

Chen, X. and Stewart, P.S. (1996). Chlorine penetration into artificial biofilm is limited by a reaction-diffusion interaction. *Environmental Science and Technol-ogy*, 30 (6), 2078–2083.

Chegrouche, S., Mellah, A. and Barkat, M. (2009). Removal of strontium from aqueous solutions by adsorption onto activated carbon: kinetic and thermody-namic studies. *Desalination*, 235 (1–3), 306–318.

Chirwa, E.M.N. and Wang, Y.T. (1997). Chromium(VI) reduction by *Pseudomonas fluorescens* LB300 in fixed-film bioreactor. *Journal of Environmental Engineering*, 123 (8), 760–766.

Chirwa, E.M.N. and Wang, Y.T. (2000). Simultaneous Cr(VI) reduction and phenol degradation in an anaerobic consortium of bacteria. *Water Research*, 34 (8), 2376–2384.

Choi, H.B., Rhee, B.W. and Park, H.S. (1997). Physics study on direct use of spent pressurized water reactor fuel in CANDU(DUPIC). *Nuclear Science Engineering*, 126, 80–93.

Chubar, N., Behrends, T. and Van Cappellen, P. (2008). Biosorption of metals (Cu^{2+}, Zn^{2+}) and anions (F^-, $H_2PO_4^-$) by viable and autoclaved cells of the Gram-negative

bacterium *Shewanella putrefaciens*. *Colloids and Surfaces B: Biointerfaces*, 65 (1), 126–133.

Crack, J. and Gupta, R.S. (1972). A moving boundary problem arising from the diffusion of oxygen in absorbing tissue. *Journal of the Institute of Mathematics and its Application*, 10, 19–33.

Dabbagh, R., Ghafourian, H., Baghvand, A., Nabi, G.R., Riahi, H. and Ahmadi Faghih, M.A. (2007). Bioaccumulation and biosorption of stable strontium and Sr-90 by *Oscillatoria homogenea* cyanobacterium. *Journal of Radioanalytical and Nuclear Chemistry*, 221 (1), 53–59.

Dadachova, E., Bryan, R.A., Huang, X., Moadel, T., Schweitzer, A.D., Aisen, P., Nosanchuk, J.D. and Casadevall, A. (2007). Ionizing radiation changes the electronic properties of melanin and enhances the growth of melanized fungi. *PLoS One*, May 23, 2007.

Dahl, O., Nurmesniemi, H. and Poykio, R. (2008). Sequential extraction partitioning of metals, sulfur, and phosphorus in bottom ash from a coal-fired power plant. *International Journal of Environmental Analytical Chemistry*, 88 (1), 61–73.

Danckwerts, P.V. (1950). Unsteady-state diffusion or heat conduction with moving boundary. *Transactions Faraday Society*, 46, 701–712.

Dewiere, L., Bugai, D., Grenier, C., Kashparov, V. and Ahamdach, N. (2004). Sr-90 migration to the geosphere from a waste burial in the Chernobyl Exclusion Zone. *Journal of Environmental Radioactivity*, 40, 139–150.

Doherty, R., Phillips, D.H., McGeough, K.L., Walsh, K.P. and Kalin, R.M. (2006). Development of modified flyash as a permeable reactive barrier medium for a former manufactured gas plant site. *Northern Ireland. Environmental Geology*, 50, 37–46.

Dries, J., Bastiaens, L., Vos, J., Simons, Q., De Smet, M. and Diels, L. (2004). Comparison of different multi-barrier concepts designed for treatment of groundwater containing mixed pollutants. In: A. Boshoff and B. Bone (eds.), *Permeable Reactive Barriers*. *International Symposium on Permeable Reactive Barriers*, March 14, 2004, Queens University Belfast Northern Ireland, 298 (2005), 45–51.

Gad Allah, A.A. (2008). Safety aspects of radioactive waste management in different nuclear fuel cycle policies, a comparative study. *Proceedings of the 3rd Environmental Physics Conference*, 19–23 February 2008, Aswan, Egypt.

Gavaskar, A., Gupta, N., Sass, B., Janosy, R. and Hicks, J. (2000). *Design Guidelines for Applications of Permeable Reactive Barriers for Groundwater Remediation*, Battelle, Columbus, OH, Report No. AFRL-ML-WP-TR-2000-4546, NTIS: ADA380005, pp. 399.

Habicht, K.S. and Canfield, D.E. (1997). Sulfur isotope fractionation during bacterial sulfate reduction in organic-rich sediments. *Geochimica et Cosmochimica Acta*, 62 (24), 5351–5361.

Habicht, K.S., Canfield, D.E. and Rethmeier, J. (1998). Sulfur isotope fractionation during bacterial reduction and disproportionation of thiosulfate and sulfite. *Geochimica et Cosmochimica Acta*, 62 (15), 2585–2595.

Herbel, M.J., Johnson, T.M., Oremland, R.S. and Bullen T.D. (2000). Fractionation of selenium isotopes during bacterial respiratory reduction of selenium oxyanions, *Geochimica et Cosmochimica Acta*, 64 (21), 3701–3709.

Hill, K.E., Fry, J.C. and Weightman, A.J. (1994). Gene transfer in the aquatic environment: persistence and mobilization of the catabolic recombinant plasmid pDlO in the epilithon. *Microbiology*, 140, 1555–1563.

Hodges, N.A. and Gordon, C.A. (1991). Protection of *Pseudomonas aeruginosa* against ciprofloxacin and β-lactams by homologous alginate. *Antimicrobial Agents and Chemotherapy*, 35 (11), 2450–2452.

Hoyle, B.D., Alcantora, J. and Costerton, J.W. (1992). *Pseudomonas aeruginosa* biofilm as a diffusion barrier to piperacillin. *Antimicrobial Agents and Chemotherapy*, 36 (9), 2054–2056.

Hunter, A. (1998). Crossing over genetic algorithms: The sugal generalised GA. *Journal of Heuristics*, 52, 179–192.

IAEA (2009). *Nuclear Technology Review*. International Atomic Energy Agency Scientific and Technical Publication Series, Vienna.

Kalckar, H.M. (1974). Origins of the concept oxidative phosphorylation. *Molecular and Cellular Biochemistry*, 5 (1–2), 55–63.

Khripunov V.I., Kurbatov D.K. and Subbotin M.L. (2006). *C-14 Production in CTR Materials and Blankets*. Proceedings of the 21st Fusion Energy Conference (FEC2006), 16–21 October 2006, Chengdu, China. SE/p2-3. Available online at http://www-pub.iaea.org/MTCD/Meetings/FEC2006/se_p2-3.pdf. Last accessed on 28/05/07.

Kjelleberg, S. and Hermanson, M. (1984). Starvation-induced effects on bacterial surface characteristics. *Applied and Environmental Microbiology*, 48 (3), 497–503.

Kleykamp, H. (1985). The chemical state of the fission products in oxide fuels. *Journal of Nuclear Materials,* 131 (2–3), 221–246.

Koster, A., Matzner, H.D. and Nicholsi, D.R. (2003). PBMR design for the future. *Nuclear Engineering and Design*, 222 (2–3), 231–245.

KrishnaKumar, K. (1993). Genetic algorithms – a robust optimization tool. *Proceedings of the 31st Aerospace Sciences Meeting and Exhibit*, January 11–14, 1993, Reno, Nevada.

Kühl, M. and Jørgensen, B.B. (1992). Microsensor measurements of sulfate reduction and sulfate oxidation in compact microbial communities of aerobic biofilms. *Applied and Environmental Microbiology*, 58 (4), 1164–1174.

Liu, S.-J., Jiang, B., Huang, G.-Q. and Li, X.-G. (2006). Laboratory column study for remediation of MTBE-contaminated groundwater using a biological two-layer permeable barrier. *Water Research*, 40 (18), 3401–3408.

Lloyd, J.R. (2003). Microbial reduction of metals and radionuclides. *FEMS Microbiology Reviews*, 27, 411–425.

Lovley, D.R., Phillips, E.J.P., Gorby, Y.A. and Landa, E.R. (1991). Microbial reduction of uranium. *Nature* (London), 350, 413–416.

Lovley, D.R., Widman, P.K., Woodward, J.C. and Phillips, E.J. (1993). Reduction of uranium by cytochrome c_3 of *Desulfovibrio vulgaris*. *Applied and Environmental Microbiology*, 59 (11), 3572–3576.

Mazierski, J. (1994). Effect of chromium (VI) on the growth of denitrifying bacteria. *Water Research*, 28 (9), 1981–1985.

Meadows, P.S. (1971). The attachment of bacteria to solid surfaces. *Archiv für Mikrobiologie*, 75 (4), 374–381.

Molokwane, P.E. and Chirwa, E.M. (2009). Development of a carbon-14 bioseparation technique for cleanup of nuclear graphite. In: *Proceedings of 11th International Conference on Environmental Remediation and Radioactive Waste Management* (ICEM'07). Part A, pp. 113–117, 2–6 September 2007, Bruges, Belgium.

Molokwane, P.E., Meli, K.C. and Nkhalambayausi-Chirwa, E.M. (2008). Chromium (VI) reduction in activated sludge bacteria exposed to high chromium loading: Brits culture (South Africa). *Water Research*, 42 (17), 4538–4548.

Mourogov, V., Fukuda, K. and Kagramanian, V. (2002). The need for innovative nuclear reactor and fuel cycle systems: Strategy for development and future prospects. *Progress in Nuclear Energy*, 40 (3–4), 285–299.

Mukhopadhyay, B., Sundquist, J. and Schmitz, J.R. (2007). Removal of Cr(VI) from Cr-contaminated groundwater through electrochemical addition of Fe(II). *Journal of Environmental Management*, 82 (1), 66–76.

Mullen, M.D., Wolf, D.C., Ferris, F.G., Beveridge, T.J., Flemming, C.A. and Bailey, G.W. (1989). Bacterial sorption of heavy metals. *Applied and Environmental Microbiology*, 55 (12), 3143–3149.

Musango, J.K., Brent, A.C. and Bassi, A. (2009). South African energy model: a system dynamics approach. *International Conference of System Dynamics Society*. Albuquerque, New Mexico, 26–31 July, 2009. pp 1–32.

Nealson, K.H. (1999). Post-Viking microbiology: new approaches, new data, new insights. Origins of life and evolution of the biosphere. *Journal of the International Society for the Study of the Origin of Life*, 29 (1), 73–93.

Neidhardt, F.C., Ingraham, J.L. and Schaechter, M. (1990). In: *Physiology of the Bacterial Cell: A molecular approach*, pp. 442–462. Sinauer Associates, Inc. Publishers, Sunderland, MA.

Nelson, Y.M., Lion, L.W., Shuler, M.L. and Ghiorse, W.C. (1996). Modeling oligotrophic biofilm formation and lead adsorption to biofilm components. *Environmental Science and Technology*, 30 (6), 2027–2035.

Ngwenya, N. and Chirwa E.M.N. (2011). Biological removal of cationic fission products from nuclear wastewater. *Water Science and Technology*, 63 (1), 124–128.

Nichols, W.W. (1989). Susceptibility of biofilms to toxic compounds. In: W.G. Characklis and P.A. Wilderer (eds.), *Structure and Function of Biofilms*, pp. 321–331. John Wiley and Sons, Inc., New York, N.Y.

Nkhalambayausi-Chirwa, E.M. and Wang, Y.-T. (2005). Modeling Cr(VI) reduction and phenol degradation in a coculture biofilm reactor. *ASCE Journal of Environmental Engineering*, 131 (11), 1495–1506.

Paul, J.H. (1984). Effects of antimetabolites on the adhesion of an estuarine Vibrio sp. to polystyrene. *Applied and Environmental Microbiology*, 48 (5), 924–929.

Payne, R.B., Casalot, L., Rivere, T., Terry, J.H., Larsen, L., Giles, B.J. and Wall, J.D. (2004). Interaction between uranium and the cytochrome c_3 of *Desulfovibrio desulfuricans* strain G20. *Archives of Microbiology*, 181 (6), 398–406.

Phillips, D.H. (2009). Permeable reactive barriers: A sustainable technology for cleaning contaminated groundwater in developing countries. *Desalination*, 248, 352–359.

Santegoeds, C.M., Ferdelman, T.G., Muyzer, G. and DE Beer, D. (1998). Structural and functional dynamics of sulfate-reducing populations in bacterial biofilms. *Applied and Environmental Microbiology*, 64 (10), 3731–3739.

Semprini, L. and McCarty, P.L. (1981). Comparison between model simulations and field results for in-situ biorestoration of chlorinated aliphatics: Part 1. *Ground Water*, 29 (3), 365–374.

Shaukat, M.S., Sarwar, M.I. and Qadee, R. (2005). Adsorption of strontium ions from aqueous solution on Pakistani coal. *Journal of Radioanalytical and Nuclear Chemistry*, 265 (1), 73–79.

Shen, H. and Wang, Y.T. (1993). Characterization of enzymatic reduction of hexavalent chromium by *Escherichia coli* ATCC 33456. *Applied Environmental Microbiology*, 59 (11), 3771–3777.

Shen, H. and Wang Y.T. (1994). Modeling hexavalent chromium reduction in *Escherichia coli* ATCC 33456. *Biotechnology and Bioengineering*, 43 (4), 293–300.

Sherbet, G.V. (1978). *The biophysical characterization of the cell surface*. London, New York, San Francisco: Academic Press. pp. 1–298.

Shoesmith, D.W. (2000) Fuel corrosion processes under waste disposal conditions. *Journal of Nuclear Materials*, 282 (1), 1–31.

Suzuki, T., Miyata, N., Horitsu, H., Kawai, K., Takamizawa, K., Tai, Y. and Okazaki, M. (1992). NAD(P)H-dependent chromium (VI) reductase of *Pseudomonas ambigua* G-1: a Cr(V) intermediate is formed during the reduction of Cr(VI) to Cr(III). *Journal of Bacteriology*, 174 (16), 5340–5345.

Thacker, W.E., Snoeyink, V.L. and Crittenden, J.C. (1981) *Modeling of Activated Carbon and Coal Gasification Char Adsorbents in single-solute and Bisolute Systems*, research report 161, UILU-WRC-81–0161, Water Research Center, University of Illinois, Urbana, IL.

Thomas, P.G., Quinn, P.J. and Williams, W.P. (1985). The origin of photosystem-I mediated electron transport stimulation in heat-stressed chloroplasts. *Planta*, 167 (1), 133–139.

Tikilili, P.V. and Chirwa, E. (2009). Microbial degradation of polycyclic aromatic hydrocarbons and characterization of bacteria. In proceedings: *Nuclear Physics Methods and Accelerators in Biology and Medicine*. American Institute of Physics, Melville, NY, pp. 253–254.

Vijayaraghavan, K. and Yun, Y.-S. (2008). Bacterial biosorbents and biosorption. *Biotechnology Advances*, 26, 266–291.

Vincze, E. and Bowra, S. (2006). Transformation of Rhizobia with broad-host-range plasmids by using a Freeze-Thaw method. *Applied and Environmental Microbiology*, 72 (3), 2290–2293.

Wang, Y.T. and Shen, H. (1997). Modelling Cr(VI) reduction by pure bacterial cultures. *Water Research*, 41 (4), 727–732.

Watson, J.S., Scott, C.D. and Faison, B.D. (1989). Adsorption of Sr by immobilized microorganisms. *Applied Biochemistry and Biotechnology*, 20/21, 699–709.

Weber, T.W. and Chakravorti, R.K. (1974). Pure and solid diffusion models for fixed bed adsorbers. *Journal of the American Institute of Chemical Engineers*, 20, 228–238.

Weightman, A.J., Don, R.H., Lehrbach, P.R. and Timmis, K.N. (1984). The identification and cloning of genes encoding haloaromatic catabolic enzymes and the construction of hybrid pathways for substrate mineralization. In *Genetic Control of Environmental Pollutants*, pp. 47–80. Edited by Omenn, G.S. and Hollaender, A. New York and London: Plenum Press.

White, O., Eisen, J.A., Heidelberg, J.F., Hickey, E.K., Peterson, J.D., Dodson, R.J., Haft, D.H., Gwinn, M.L., Nelson, W.C., Richardson, D.L., Moffat, K.S., Qin, H., Jiang, L., Pamphile, W., Crosby, M., Shen, M., Vamathevan, J.J., Lam, P., McDonald, L., Utterback, T., Zalewski, C., Makarova, K.S., Aravind, L., Daly, M.J., Minton, K.W., Fleischmann, R.D., Ketchum, K.A., Nelson, K.E., Salzberg, S., Smith, H.O., Venter, J.C. and Fraser, C.M. (1999). Genome sequence of the radioresistant bacterium *Deinococcus radiodurans* R1. *Science*, 286 (5444), 1571–1577.

Whiticar, M.J. (1999). Carbon and hydrogen isotope systematics of bacterial formation and oxidation of methane. *Chemical Geology*, 161 (1–3), 291–314.

Xu, K.D., Stewart, P.S., Xia, F., Huang, C.-T. and McFeters, G. (1998). Spatial physiological heterogeneity in *Pseudomonas aeruginosa* biofilm is determined by oxygen availability. *Applied and Environmental Microbiology*, 64 (10), 4035–4039.

ZoBell, C.E. (1943). The effect of solid surfaces upon bacterial activity. *Journal of Bacteriology*, 46 (1), 39–56.

15.11 Engineering dimensions (units)

L — length (distance)

ML^{-3} — mass per unit volume, e.g., g/m^3

$ML^{-2}T^{-1}$ — mass per unit area per unit time, e.g., $g/m^2/d$

$ML^{-3}T^{-1}$ — mass per unit volume per unit time, e.g., $g/m^3/d$

MM^{-1} — mass per unit mass, e.g., U(VI) reduced/g of cells

T — time, t

T^{-1} — per unit time

Index